BRAIN CONNECTIVITY
Volume 4, Number 9, 2014

DOI: 10.1089/brain.2014.1501.abstracts

Abstracts

Fourth Biennial Conference on Resting State Brain Connectivity

September 11–13, 2014

Boston/Cambridge, Massachusetts, USA

Poster Session 1: Thursday, 11 September 2014

Theme 1: Technical Advances and Methodological Issues

P1A Subthalamic Nucleus in the Stop Network: Evidence from resting state functional connectivity MRI

S.A Anteraper[1], C. Triantafyllou[2], M.R. Geddes[3], A.T. Mattfeld[3], J. Gabrieli[3], and S. Whitfield-Gabrieli[3]

[1]A.A. Martinos Imaging Center at McGovern Institute for Brain Research, Massachusetts Institute of Technology, Cambridge, USA; [2]A.A. Martinos Center for Biomedical Imaging, MGH, Dept. of Radiology, Harvard Medical School, Charlestown, USA; [3]Massachusetts Institute of Technology, Department of Brain and Cognitive Sciences, Cambridge, USA

Background: Multiple cortical regions comprise the stop network including inferior frontal cortex (IFC), bilateral insula and supplementary motor area [1]. There is a paucity of evidence from functional connectivity MRI (fcMRI) supporting the putative role of subthalamic nucleus (STN) in inhibitory control due to the technical limitations of imaging a small subcortical structure. Resting state fcMRI of STN using a small sample has been reported [2], but because of the lack of whole-brain coverage, inferior prefrontal regions were not investigated. Given the relationship between STN and the stop network [3], we hypothesized that functional connectivity exists between IFC and STN.
Methods: 51 normal volunteers were imaged using a 3T Siemens Tim Trio (Siemens Healthcare, Erlangen, Germany) with the product 32 Channel (32 Ch) coil. High-resolution (2 mm^3) resting-state scans were acquired using single-shot gradient echo EPI, TR/TE/FA = 6000 ms/30 ms/90°. Prior to connectivity analysis, data were realigned, slice-time corrected, normalized, spatially smoothed with a 3-mm kernel using SPM8 (Wellcome Trust Centre for Neuroimaging, London, UK). Connectivity analyses were carried out using CONN [4] toolbox. Source regions of interest for STN were chosen as 2 mm seeds based on the peak coordinates from (http://www.nitrc.org/projects/atag). Band pass filtering was executed at 0.008–0.09 Hz. Physiological sources of noise (signals from white matter and cerebrospinal fluid) were regressed out together with movement related covariates and motion outliers (scan-to-scan threshold of 0.5 mm translation and 0.5° rotation). Correlation coefficients were converted to normally distributed scores using Fisher's r-to-z transform to allow for second-level analyses.
Results: In addition to bilateral insula and basal ganglia regions (lateral globus pallidus, and putamen), both left and right STN seeds revealed significant functional connectivity with IFC and premotor regions (Fig.1) at the group level (N = 51; whole-brain $p < 0.005$, cluster-level $p_{FDR\text{-}corr} < 0.05$).
Conclusions: Using the synergistic combination of 32 Ch head coil and high-resolution fcMRI, we provide evidence for the inclusion of STN in the stop network. Specifically, the functional connectivity of IFC with STN as demonstrated in this study indicates the STN-IFC ''hyperdirect'' pathway for inhibitory control. Since STN is a target for deep brain stimulation for clinical populations such as Parkinson's disease, enhanced understanding of the functional connectivity of STN can shed light on some of the therapeutic benefits and the possibility of adverse neuropsychiatric manifestations [5] associated with the intervention.
References: [1] Rae et al., 2014. Neuroimage 86:381–91. [2] Brunenberg et al., 2012. PloS one 7(6): e39061. [3] Aron et al., 2014. Trends Cogn Sci. 18(4):177–185. [4] Whitfield-Gabrieli et al., 2012. Brain connectivity 2(3): 125–141. [5] Volkman et al., 2010. Nature reviews. Neurology 6(9):487–98.

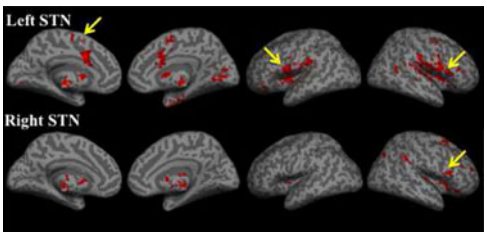

P2A Analysis of depression and the effect of ketamine in depression patients by use of ROIs designed from genetic expression analysis

P. R. Baldwin[1], T. Lal[2], K. Collins[3], S. Mathew[1], J. Murrough[3], R. Salas[1]

[1]Baylor College of Medicine, Menninger Department of Psychiatry and Behavioral Science, Houston TX, [2]University of Houston, Cullen College of Engineering, Houston TX, [3]Icahn School of Medicine at Mount Sinai, New York City

Background: Major depressive disorder affects one in 15 adults and can be associated with pathological brain functional connectivity. Seed based functional connectivity methods, however, assume regions of interest a priori and may overlook critical regions. We use genetic expression data to ascertain key ROIs in resting state seed based analysis, and justify these choices across a two site fMRI study.
Methods:
Gene Lists: Led by Fritz Henn, two lines of rats have been bred to exhibit learned helplessness (L) or exhibit resistance (N) to depression. The genetic prevalence of these lines resulted in two lists of genes. Our software finds that most (300 of 500) of the genes have a sagittal experiment associated to it in the Allen Brain Atlas. The coarse grained expression volumes for each set of these genes are then averaged; the differences between the L

and N lists are subtracted and compared to normal variability to arrive at significances. This analysis indicates that Habenula (Hb), Brodmann area 25 (BA25), Medial vestibular cortex (MVC), Nucleus Accumbens (Acc) and Precentral Gyrus (PCG), and septum verum are indicated in depression.

Resting state functional connectivity: We took resting state fMRI readings at two different sites in a depressed population and matched controls. At Mount Sinai: 17 controls, as well as 44 depressed subjects, with 8 of those subjects measured once before and once after administration of ketamine. At Baylor COM, 20 controls, 36 depressed, with 10 subjects scanned twice. The seed based, resting state software, CONN was employed, using as ROIs the regions suggested above as well as several areas such as dorsal raphe nucleus (DR), which have been otherwise implicated in depression.

Results: The brain ROIs that were suggested by the above genetic expression analysis figure prominently in the connectivities that most distinguish controls from the depressed cohort at each site, as well as the differences in connectivities due to the ketamine treatment. The BA25 to medial prefrontal cortex connectivity especially changed for pre-post ketamine, although the most consistent change across sites was Putamen/Acc and contralateral Striatum/ Putamen. Distinguishing controls from the depressed cohort was primarily given by the Caudate/Hb and Dor Raphe/Striatum connectivities.

Conclusions: The complimentary use of genetic expression results in the design of ROIs for seed based studies. These ROIs figure prominently in those connectivities that distinguish controls from the depressed cohort, as well as those areas affected by ketamine. We hope to develop this genetic expression analysis as use in intelligent design of ROIs.

P3A A comparison of existing volumetric and new retrospective slicewise motion metrics: current methods do not reliably identify corruption

E.B. Beall, M.J. Lowe

Imaging Institute, Cleveland Clinic, Cleveland, OH, USA

Background: Head motion remains a major problem for functional BOLD-weighted imaging. Existing correction and characterization methods rely on the assumption that motion is volume-synchronized, a known limitation. We have developed a method to obtain both in- and out-of-plane motion of every slice (SLOMOCO), and using BOLD data with known motion, we validate this method and compare volumetric and slicewise metrics. We show that volumetric metrics perform little better than chance, while slicewise metrics have good sensitivity and specificity to known motion events. The level of inaccuracy we have seen in volumetric methods strongly implies that motion artifact removal methods based on volumetrics (e.g. scrubbing) results in little to no reduction in motion sensitivity while penalizing BOLD sensitivity.

Methods: Known motion BOLD 2D EPI data was acquired in 8 cadavers with a motion-injection pulse sequence (SimPACE), using a predetermined sequence of motion impulses on each of 6 degrees of freedom (DOF), injected on every fourth volume (e.g. motion events were separated by 3 clean volumes). Part of motion sequence consisted of individual slice motion on $1/4^{th}$ of a volume (realistic motion), part consisted of volumetric motion (unrealistic motion). The resulting BOLD data was used to generate commonly used signal-based metrics: global signal (GS), variance of signal (VARS), and derivative of VARS (DVARS) [Power NI 11]. Data was passed to volume registration and the resulting volumetric parameters converted to common parameter-based metrics: total displacement (TD)[Jiang HBM 95], framewise displacement (FD), and volumetric translations (VTD) [Van Dijk NI 2012]. Data was passed to SLOMOCO [Beall and Lowe, accepted with revisions, NI 2014] and the resulting slicewise parameters converted to each metric, denoted by SLM. The original motion injection vector was converted to each metric, denoted by TRU for truth. SLM and TRU were converted to volumetric by taking the max across slices in each volume. True/False positive rate (TPR/FPR) was computed using the detected and known indices of motion, using thresholds obtained from the literature[Power 11, Van Dijk 12].

	% Corrupted	*TPR*	*FPR*
	BOLD signal-based		
GS	52	58.3	50
VARS	49	50	48.7
DVARS	98	100	97.4
	volumetric motion parameter-based		
TD	2	8.3	0
FD	0	0	0
VTD	24	66.7	10.5
	truth, slicewise injection vector-based		
TD-TRU	24	100	0
FD-TRU	48	100	31.6
VTD-TRU	38	75	26.3
	SLOMOCO-based		
TD-SLM	24	100	0
FD-SLM	48	100	31.6
VTD-SLM	46	100	28.9

Results: The SLOMOCO-derived parameters were observed to correlate significantly across all 6 DOF ($r > 0.75$ with 5000 timepoints, $p <$ machine precision). All volumetric and most slicewise metrics performed poorly, except TD-TRU and TD-SLM. BOLD signal-based metrics performed at chance or worse, while parameter-based metrics had weak sensitivity to slicewise motion. Note sensitivity could be improved for some metrics, but at a cost in specificity.

Conclusions: For accurate identification of motion, it is critical to use slicewise motion parameters with a trigonometrically-derived metric (TD), which is now possible. While this is a synthetic scenario, 1 mm/deg of ¼ volume is not unrealistic. Performance of existing metrics was unexpectedly poor, with major implications for all BOLD fMRI studies. Based on these results, slicewise motion methods are strongly preferred to traditional volumetric based methods. The authors gratefully acknowledge support from NIH grant 5P50NS038667-14 for MRI acquisition of cadaver tissue.

P4A Size matters: the influence of the size of the posterior cingulate cortex seed on the correlation values of the voxels of the medial prefrontal cortex

R.F. Casseb[1,2], G. C. Beltramini[1], M. Albuquerque[2], G. Castellano[1], M.C. França Jr[2]

[1]Neurophysics Group - Unicamp, Campinas, São Paulo, Brazil, [2]Neurology Dept. - Unicamp, Campinas, São Paulo, Brazil

Background: Resting State MR imaging (rs-fMRI) has been employed in a great variety of studies and has been extensively

discussed in the scenario of brain activity without external stimuli. However, there is still no consensus about some of its practical features, such as the size of the seed used to perform the seed-based analysis. This problem has already been mentioned in other works, but, to the best of our knowledge, has not been further investigated. The aim of this work was to investigate the influence of seed size (positioned on the posterior cingulate cortex (PCC)) on the correlation values of the voxels of the medial prefrontal cortex (MPFC).

Methods: Rs-fMRI data were acquired in a 3T scanner (Philips Achieva). Thirty-three healthy subjects were instructed to stay for 10 min with their eyes closed, to remain awake and to avoid engaging in any specific thoughts. A spherical seed with different radii (3, 6, 9, 12, 15, 18, 21, 24, 27 and 30 mm) was centered at the PCC ((0−51 18) - MNI coordinates) and an average PCC signal time series was generated to be correlated with all brain voxels. The correlation maps created with this procedure were multiplied by a binarized mask of the MPFC. Analyses were then performed in the resulting images with SPM8 and WFU PickAltas. Four parameters were evaluated: (I) the amount of voxels with correlation values greater than 0.4; (II) the sum of the correlation values above 0.4; (III) the average of the correlation values greater above 0.4; and (IV) the maximum correlation value.

Results: The largest amount of voxels above the correlation threshold (parameter (I)) was reached for a seed with radius of 10.4 ± 5.6 mm (average over subjects). The maximum values of the other parameters ((II), (III) and (IV)) were associated with radii of 10.4 ± 5.6 mm, 12.5 ± 7.1 mm and 12.6 ± 6.9 mm, respectively.

Conclusions: The size of the seed positioned in the PCC impacts on the correlation values between the PCC and the MPFC voxels. These regions were selected because they are part of the Default Mode Network, a structure that seems to play an important role in the organization of the brain. Our results suggest that if we are to make considerations about the relationship between these regions (assessed by functional connectivity), the seed size must be taken into account. We may also infer that the PCC seed loses its ''representativeness'' for both too small and too large radii: in the first case due to low signal-to-noise ratio, and in the latter, because the ''characteristic profile'' of this signal is diluted in the pool of signals included in the average time series of the seed. This work only considered the size of spherical seeds, but other options should be also tested, e.g.: the box shaped seed, the seeds based on atlases divisions of the brain, the seeds created based on z-score neighborhood of the central voxel and so on.

P5A Impact of head motion on ICA-derived functional connectivity measures

E. Damaraju[1,2], E.A. Allen[1,3], and V.D. Calhoun[1,2]

[1]The Mind Research Network, Albuquerque, NM, USA, [2]The University of New Mexico, Dept. of Electrical and Computer Engineering, Albuquerque, NM, USA, [3]K.G. Jebsen Center for Research on Neuropsychiatric Disorders, University of Bergen, Norway

Background: Several recent neuroimaging studies have demonstrated that a small but significant bias is introduced by subject head movement in resting state functional connectivity (FC) measures. To date, most of these studies have focused on seed-based connectivity approaches. Here we carefully investigate the impact of head motion on FC measures computed between network time courses (TCs) obtained using independent component analyses (ICA).

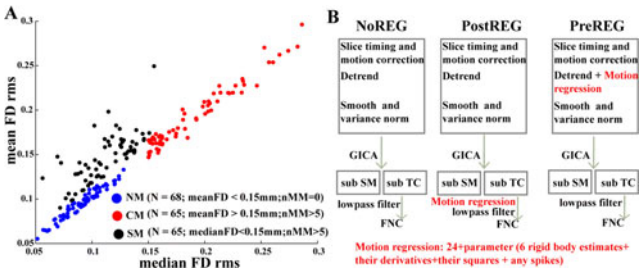

Methods: In this study, we selected a dataset of 199 subjects that show three different types of head motion categorized into: little to non-movers (NM); continuous movers (CM); spikey movers (SM) who large, but infrequent macro movements (MM) (Fig 1A). Five minute resting-state scans were acquired with TR = 2 sec. Data were processed as depicted in Fig 1B to yield a ''NoREG'' ICA decomposition (no regression of motion covariates performed), ''PostREG'' (regression of motion parameters was performed post-ICA, on the ICA TCs), and ''PreREG'' (regression of motion parameters performed *prior* to ICA). The aggregate spatial maps from ICA were matched to a reference set, and 19 intrinsic connectivity networks (ICNs) common to both decompositions were identified. Functional network connectivity (FNC) was then computed as the pairwise correlations between component TCs. To identify potential motion related bias, we calculated the slopes between the distances between nodes (Euclidean distance between component peaks) and the difference in FNC (ΔFNC). Slopes were calculated for each subject and evaluated for significance with one-sample t-tests.

Results: Our results are shown in Fig 2. For ''PreREG – NoREG'' and ''PreREG – PostREG'' comparisons, we found significant positive linear relationships between the distance between nodes and the observed ΔFNC, suggesting that PreREG removed some of the FC bias introduced by motion. Not surprisingly, the positive slopes were largest for the CM group. Additionally, ''PostREG – NoREG'' differences did not show a relationship with the distance between nodes (slopes were not different from zero), suggesting less compensation for motion bias.

Conclusions: Preliminary results suggest motion regression prior to ICA reduces some motion related bias in ICA-based connectivity measures. However pre ICA regression might have other consequences (such as on spatial maps) as regression models seem inadequate for bad movers and over compensate for subjects that move little.

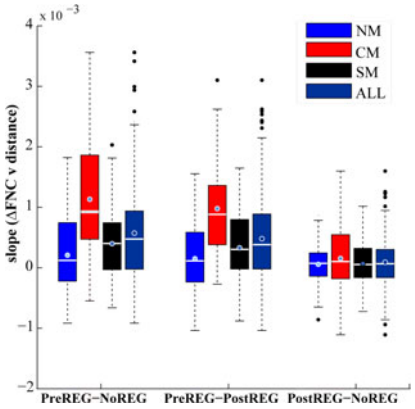

P6A Tracking functional pathways in the human brain using resting state functional magnetic resonance imaging

Z. Ding[1,2], X. Wu[1], R. Xu[1], V.L. Morgan[1], A.W. Anderson[1], J.C. Gore[1]

[1]Vanderbilt University Institute of Imaging Science, Nashville, TN, USA, [2]Deaprtment of Electrical Engineering and Computer Science, Nashville, TN, USA

Background: We have recently proposed a concept of spatio-temporal correlation tensors on the basis of spatio-temporal analyses of resting state BOLD (blood oxygenation level dependent) signals, which may be used to characterize functional structure in the human brain. In this work, we propose robust techniques that allow visualization of major functional pathways in the brain, explore biophysical mechanisms that provide tissue contrast, and demonstrate an application of using functional tensors to track functional pathways in the human language circuitry.

Methods: MRI of normal volunteers was performed on a 3T Philips Achieva scanner (Best, Netherlands) with a 32-channel phased-array coil. Informed consent was obtained from each volunteer according to a protocol approved by local Institutional Review Board. BOLD signals were acquired using a multi-echo T2*-weighted gradient echo, echo-planar imaging sequence with TR = 3 s, TE = 11/31/51/71 ms, 3 × 3 × 3 mm thick, and 200 dynamics. Subjects were instructed to close eyes and not to perform any tasks.

Construction of spatial-temporal correlation tensors: The BOLD signals were corrected for slice timing, head motion and global time course, and then filtered to retain frequency of 0.01–0.08 Hz. For each brain voxel Vi, a volume of interest (VOI) was defined, and Pearson's linear correlation coefficient (Cij) was calculated between the time course at Vi and each Vj in the VOI. The vector connecting Vi and Vj was normalized into unit vector **n**ij, with which a diadic tensor **D**ij was obtained (x, y and z are the three elements of **n**ij):

$$\mathbf{D}_{ij} = \begin{pmatrix} \mathbf{n}_{ij,x}\mathbf{n}_{ij,x} & \mathbf{n}_{ij,x}\mathbf{n}_{ij,y} & \mathbf{n}_{ij,x}\mathbf{n}_{ij,z} \\ \mathbf{n}_{ij,y}\mathbf{n}_{ij,x} & \mathbf{n}_{ij,y}\mathbf{n}_{ij,y} & \mathbf{n}_{ij,y}\mathbf{n}_{ij,z} \\ \mathbf{n}_{ij,z}\mathbf{n}_{ij,x} & \mathbf{n}_{ij,z}\mathbf{n}_{ij,y} & \mathbf{n}_{ij,z}\mathbf{n}_{ij,z} \end{pmatrix} \quad [1]$$

$$\mathbf{T}_i = \sum_j C_{ij}\mathbf{D}_{ij} \quad [2]$$

Resting state spatio-temporal correlation tensor **T**i at voxel Vi was defined to be the sum of all diadic tensors Dij (Eq. 1) in the VOI weighted by Cij (Eq. 2). To demonstrate a potential use of functional tensor**s**, pathways between Broca's and Wernicke's areas were tracked from reconstructed spatio-temporal correlation tensors using streamline tracking.

Results: Maps of spatio-temporal correlation tensors are shown in Fig. 1. The map at TE = 31 ms exhibits best directional consistency with that in the DTI map. While the map from M0 image only contains random blobs, the map from R2* image shows similar patterns to that at TE = 31 ms. Reconstructed pathways between the Broca's and Wernicke's areas are shown in the lower left panel, which appear to be consistent with known functional neuroanatomy.

Conclusions: This study shows that resting state signals obtained using conventional BOLD-sensitive acquisitions in brain white matter possess anisotropic correlations. We found that R2* but not M0 image exhibits DTI-consistent patterns in white matter regions, suggesting local hemodynamic effects may drive the patterns observed. The spatio-temporal correlation tensor may be used to characterize a local functional structure, which offers the potential of directly mapping structure-function relations in the brain.

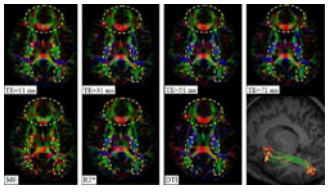

FIG. 1. Maps of spatio-temporal correlation and diffusion tensors, and reconstructed functional pathways.

P7A Removal of motion-corrupted resting state functional MRI data using dynamic system identification and interpolation of motion-free data

B. Erem[1], A. Akhondi-Asl[1], O. Afacan[1], S.K. Warfield[1]

[1]Boston Children's Hospital and Harvard Medical School, Boston, Massachusetts, USA

Background: When resting state fMRI data are motion-free (*i.e.,* the patient or subject remains motionless during imaging), there are well-accepted methods for preprocessing the data and extracting functional networks. However, in the presence of motion, these data may be corrupted, and thus the usual process may be insufficient. Methods that perform temporal preprocessing (*e.g.,* slice timing correction, filtering, regression, etc) on motion-corrupted data are fundamentally flawed, as this causes the motion-corrupted data to have some amount of influence on the rest of the volumes. Instead, we propose a method for replacing the motion-corrupted data, prior to standard preprocessing, such that it is dynamically consistent with the regular data. Thus the method that we propose completely removes the influence of motion-corrupted data from the analysis.

Methods: We solve an optimization problem to identify low-order linear dynamical systems (Ayazoglu *et al.*, IEEE CDC, 2012), based on low-rank matrix approximation. We interpolate the motion-free fMRI data, replacing motion-corrupted data. Then standard preprocessing is performed and networks are extracted. In our experiments, we compared these networks to those extracted using the naïve approach (*i.e.,* using the original data as though all time instances were motion-free).

Results: We applied the naïve approach and our method to 158 volumes of resting state fMRI data, of which 90 volumes were acquired during motion. Figure 1 shows maps of correlations with the posterior cingulate cortex (PCC). The connectivity of

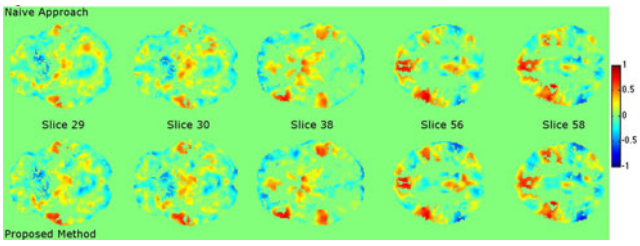

FIG. 1.

the PCC with several key areas is better preserved with our method, as compared to the naïve approach.
Conclusions: Our initial results demonstrate the promise of our approach, which completely discards motion-corrupted data prior to standard preprocessing. In future work we will compare our approach to ''scrubbing'' (Power *et al.*, Neuroimage, 2012), which discards data after preprocessing, and may retain some of the corrupted data.

P8A Combining task-evoked and spontaneous activity mapping for pre-operative fMRI

Michael D. Fox*[1,2,3], Tianyi Qian*[2,4], Joseph R. Madsen[5], Danhong Wang[2], Manling Ge[6], Huan-cong Zuo[7], Bo Hong[4], Hesheng Liu[2]

[1]Berenson-Allen Center for Noninvasive Brain Stimulation, Department of Neurology, Beth Israel Deaconess Medical Center and Harvard Medical School, Boston, MA, USA. [2]Athinoula A. Martinos Center for Biomedical Imaging, Massachusetts General Hospital, Harvard Medical School, Boston, MA, USA. [3]Department of Neurology, Massachusetts General Hospital, Harvard Medical School, Boston, MA, USA. [4]Department of Biomedical Engineering, School of Medicine, Tsinghua University, Beijing, China. [5]Department of Neurosurgery, Boston Children's Hospital, Harvard Medical School, Boston, MA, USA. [6]Key Laboratory of Electromagnetic Field and Electrical Apparatus Reliability, Department of Biomedical Engineering, Hebei University of Technology, Tianjin, China. [7]Second Affiliated Hospital of Tsinghua University, Beijing, China.
**These authors contributed equally to this work*

Background: Noninvasive localization of brain function is used to understand and treat brain disease, particularly pre-operative fMRI mapping prior to neurosurgical intervention. This mapping traditionally relies on brain responses evoked by a task, however mapping based on correlations in spontaneous brain activity has also been demonstrated. Here we test the hypotheses that task-based and spontaneous activity mapping provide complimentary information for pre-operative localization, can be combined to improve mapping accuracy, and can be performed using the same conventional pre-operative fMRI data.
Methods: Eight patients with epilepsy underwent routine pre-operative fMRI scans, implantation of electrode grids, and precise electrical cortical stimulation mapping of the somatomotor cortex. fMRI maps generated using traditional approaches were compared to those generated using a novel algorithm that separates task-based and underlying spontaneous activity, generates maps based on each type of data, and combines the maps in a weighted fashion. Accuracy was quantified and compared using receiver operating characteristic (ROC) curves and electrical cortical stimulation as a gold standard.
Results: Our novel combo-mapping algorithm improved signal to noise, sensitivity, and specificity of pre-operative fMRI in all eight patients. The algorithm performed significantly better than either task-based or spontaneous activity mapping alone and also outperformed several alternative processing approaches designed to improve localization.
Conclusions: Combing task-based and spontaneous activity mapping using the method presented here significantly improves localization of function with fMRI in pre-operative patients. Because the method requires no additional scan time or modification to conventional pre-operative data acquisition protocols we anticipate it may see widespread clinical utility.

P9A Effect of low-frequency physiological noise correction on the reproducibility of resting-state functional connectivity measurements

A. M. Golestani, J. J. Chen

Rotman Research Institute, University of Toronto

Background: Reproducibility is one of the most important attributes of a potential imaging biomarker such as resting-state functional connectivity (rs-fcMRI). Variations in physiological signals such as cardiac rate (CRV), respiratory volume (RVT) and end-tidal CO_2 ($PETCO_2$) have confounding effects on rs-fcMRI [1–3], and previous studies investigated the effect of correcting for RVT and CRV on rs-fcMRI by qualitatively comparing connectivity maps before and after correction [1,2]. However, the effect of correction on the reproducibility of rs-fcMRI is unknown, and low-frequency physiological noise correction is not typically included in the fcMRI analysis. The objective of this study is to quantitatively investigate the effect of simultaneous correction for the CRV, RVT and $PETCO_2$ variation on rs-fcMRI reproducibility.
Methods: We imaged 5 healthy subjects (2 male, age 21 to 36) using a Siemens TIM Trio 3 T MRI scanner. Two sets of rs-fMRI images were acquired using GRE_EPI (TR/TE = 2000/30 ms, FA = 90, 26 slices, $3.44 \times 3.44 \times 4.6\,mm^3$ voxels, 360 frames). RVT and $PETCO_2$ signals were derived from BioPac recordings, and the cardiac signal was recorded using a finger oximeter. Default processing steps include motion correction, brain extraction, spatial smoothing (10 mm FWHM), high-pass filtering (> 0.01 Hz) and regression of six motion parameters. Time-locked physiological artifacts were removed using RETROICOR [4]. This is the extent of processing for ''Not-corrected''. For the data with physiological correction (''Corrected''), CRV was estimated from the time interval between consecutive R waveforms [2], RVT as the breathing depth divided by breathing period [1] and $PETCO_2$ as the exhaled CO_2 peak in each breath. Voxel-wise brain response functions to the three physiological signals were simultaneously estimated using a linear Gaussian model [2]. $PETCO_2$, CRV and RVT signals were convolved with the corresponding per-voxel estimated response functions and then regressed out. The posterior-cingulate was used in a seed-based connectivity analysis for the default-mode network (DMN) and the correlation values were averaged within the DMN [5]. Intra-class correlation (ICC) and coefficient of variation (CV) between the two runs were calculated for ''Corrected'' and ''Not-corrected'' datasets.
Results: We found the intra-subject CVs for ''Corrected'' (gray) to be consistently lower than for ''Not-corrected'' (black) ($p < 0.07$). ICC for ''Not-corrected'' and ''Corrected'' methods are 0.56 and 0.82, respectively.

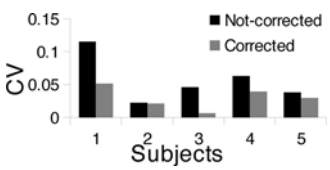

Conclusions: We demonstrate that simultaneous $PETCO_2$, CRV and RVT correction dramatically improves the reproducibility of fcMRI in the default-mode network. Our work suggests that this type of correction may be essential and should be included in the typical fcMRI analysis pipeline.

References: [1] Birn RM, Neuroimage 62 (2012) 864–870. [2] Chang C, et al., Neuroimage 44 (2009) 857–869. [3] Wise R, et al., Neuroimage 21 (2004) 1652–1664. [4] Glover GH, et al., Magn Reson Med. 44(1) (2000) 162–167. [5] Yeo BT, et al., J Neurophysiol 106(3) (2011) 1125–1165.

P10A Resting state frequency signatures across regions

D.A. Handwerker[1], J. Gonzalez-Castillo[1], C. Chang[2], P.A. Bandettini[1]

[1]Section on Functional Imaging Methods, NIMH, NIH, Bethesda, MD, USA; [2]Advanced MRI Section, NINDS, NIH, Bethesda, MD, USA

Background: Resting state networks, such as motor, visual, and default mode networks, have been observed across many studies. Although these networks are consistently identified, there is still little understanding about what aspects of fMRI signal fluctuations distinguish the networks. We examine how the frequency of time series can vary across pre-defined regions of interest. Using 60 minute runs, we reduce noise in our power spectra and other frequency measures and identify subtle differences across regions.

Methods: We collected 60 minutes of fMRI data (TR = 1 s, Voxel Size = 3.75 × 3.75 × 4 mm, 3T) from 12 subjects (one excluded due to high motion). Preprocessing included regressing out physiological noise from cardiac and respiratory traces, motion estimates, and local white matter and ventricle signals (Jo et al, 2010) and 0.01–0.25 Hz bandpass filtering. Subject data were warped into a MNI space and divided into regions-of-interest based on the Craddock Atlas (Craddock et al., 2012). 130 ROIs with sufficient voxels across subjects were assigned to 12 functional networks based on Laird et. al. 2011. The principal singular vector across all voxels in each ROI was used as the representative time series. Power spectra for each ROI and coherence estimates across ROIs were calculated and averaged across the pre-defined network labels.

Results: There was large variation across subjects for within ROI power spectra. Still, some within-subject differences were consistent across the population. Differences of in power spectra between 4 representative pairs of networks are shown. Consistent low frequency differences across subjects were visible in 16 of 66 pairs of networks.

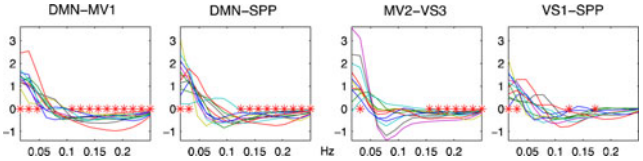

DMN = Default mode network (Laird component 13), MV1&2 = motor/visuospatial (Laird components 6&7) SPP = Speed production network (Laird component 17), VS1&3 = visual (Lair components 10&12). * marks frequency bins where power for 11 subjects are greater in one region.

Conclusions: While the information that distinguishes networks is not solely within frequency power, these results show some consistent differences across networks. Such frequency differences may be one part of resting dynamics that distinguish networks.

Craddock et. al. (2012) Hum Brain Mapp 33, pp1914–1928; Jo et. al.(2010) Neuroimage 52 pp571–582.; Laird, et. al. (2011). J Cogn Neurosci 23, pp4022–4037.

P11A Frequency-dependency of the default-mode network

A. Hoffmann[1], R. Sladky[1], M. Spies[2], D. Pfabigan[3], M. Küblböck[1], A. Höflich[2], K. Paul[3], A. Hummer[1], G.S. Kranz[2], C. Lamm[3], R. Lanzenberger[2], C. Windischberger[1]

[1]MR Center of Excellence, Center for Med. Physics and Biomed. Engrg,, Med. University of Vienna, Vienna, Austria, [2]Department of Psychiatry and Psychotherapy, Medical University of Vienna, Vienna, Austria, [3]Social, Cognitive and Affective Neuroscience Unit, Faculty of Psychology, University of Vienna, Vienna, Austria

Background: The default-mode network (DMN) has become a promising research area in the ongoing quest of finding biomarkers for brain-related disorders and in deepening the understanding of them. Functional connectivity maps of the DMN can be obtained from resting-state fMRI (rs-fMRI) data by correlating slow oscillations of a seed region in the posterior cingulate cortex with those of the rest of the brain. The BOLD signal is commonly filtered at 0.009 Hz to 0.08 Hz (Biswal, 1995), however, this notion has been challenged recently and it was proposed that the DMN can also be found in frequency ranges well above 0.08 Hz (van Oort, 2013; Niazy, 2013). This work further investigates the presence of the DMN at different frequency bands.

Methods: Dataset A: 3T rs-fMRI; 27 subjects; length: 1 hour. Dataset B: 7T rs-fMRI; 27 subjects; length: 6 minutes. Both datasets underwent the same pre-processing, i.e. slice-timing, realignment and normalization; smoothing; nuisance/global mean signal regression, bandpass-filtering, motion-scrubbing and seed voxel correlation. Bandpass-filtering frequency ranges: 0.009 Hz-0.08 Hz (reference) as well as: (A) 0.0003–0.01 Hz, (B) 0.01–0.05 Hz, (C) 0.05–0.1 Hz, (D) 0.1–0.15 Hz, (E) 0.15–0.2 Hz and (F) 0.2–0.25 Hz.

Results: For the 3T data, significant ($p < 0.05$ FWE) correlations with the ventromedial prefrontal cortex (vmPFC) and dorsomedial prefrontal cortex (dmPFC) were found only in the frequency bands (B), (C) and (reference), as well as (D) for 7T. Significant connections to the hippocampal formation were found only at (B) only on 7T. Correlations with the temporal lobes exclusively showed up in the much longer 3T scan at (B). The inferior parietal lobules (IPL) remained significant for all probed frequency

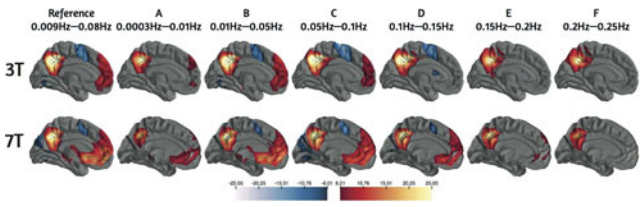

ranges above 0.01 Hz in both datasets, however, with fewer super threshold voxels above 0.15 Hz for 3T and above 0.1 Hz for 7T.
Conclusions: Even with a high signal-to-noise ratio, using state of the art pre-processing methods, and very long scan length, the most influential frequency components of the DMN have been shown to reside between 0.01 and 0.1 Hz and partly up to 0.15 Hz.

P12A Discrete functional parcellation of the cortex with clustering methods and MRF

N. Honnorat[1], H. Eavani[1], T. D. Satterthwaite[2], R. E. Gur[2], R. C. Gur[2], C. Davatzikos[1]

[1]University of Pennsylvania, CBICA, Philadelphia PA, USA; [2]University of Pennsylvania, BBL, Philadelphia PA, USA

Background: Most functional connectivity analyses require a prior dimensionality reduction of the rs-fMRI data. A promising approach consists of parcellating the brain into functionally coherent spatial regions. This approach has the advantage of extracting data-driven biologically meaningful functional units that cover the brain entirely. Several clustering, segmentation and graph-based methods were proposed for this task. Their reliability was assessed by measuring the reproducibility of the parcels obtained. The present study compares the reproducibility of two common clustering methods: Ward hierarchical clustering and spectral clustering (Shen et al., 2010; NeuroImage) and a novel discrete Markov Random Field (MRF) framework (Honnorat et al., 2013; PRNI) for the cortical parcellation of rs-fMRI scans of a large neurodevelopmental study.
Methods: The methods were compared using the Philadelphia Neurodevelopmental Cohort (Satterthwaite et al., 2014; NeuroImage). The scans were registered to FreeSurfers fsaverage5 cortical template (for each hemisphere separately), where the subjects time-series were projected, motion corrected and band-pass filtered. 859 low-motion scans were selected and divided into three age groups of similar size, each group being divided into five sets of scans that were concatenated. The concatenated scans were parcellated and the reproducibility was measured by comparing two-by-two the parcellations of a same age group using the adjusted Rand index (Hubert & Arabie, 1985; J of Classification). The discrete MRF method was applied first. Then, the clustering methods were used while controlling for the same number of parcels. All the experiments were reproduced at four different resolutions / number of parcels.
Results: Figure 1 presents a parcellation and the reproducibility results. According to the two-group t-tests reported, the discrete MRF framework significantly outperforms the clustering methods for all the resolutions.
Conclusions: In this study, the reproducibility of two common clustering methods and a novel discrete MRF framework designed for the functional parcellation of the cortex were compared on a large neurodevelopmental dataset. The parcellations generated by the discrete MRF framework were significantly more reproducible.

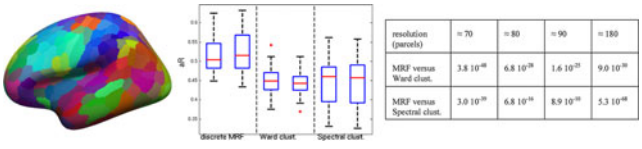

resolution (parcels)	≈ 70	≈ 80	≈ 90	≈ 180
MRF versus Ward clust.	$3.8\ 10^{-48}$	$6.8\ 10^{-39}$	$1.6\ 10^{-35}$	$9.0\ 10^{-30}$
MRF versus Spectral clust.	$3.0\ 10^{-39}$	$6.8\ 10^{-16}$	$8.9\ 10^{-16}$	$5.3\ 10^{-68}$

FIG. 1. Left, one parcellation. Middle adjusted Rand measures (for all the resolutions together, but each hemisphere separately). Right, p-value obtained at each resolution (approximate number of parcels).

P13A Investigation of the dynamics of inter-network brain connectivity from multiband EPI acquisition of resting state fMRI data

J. Jang[1], J Gabriel Castrillon[2], C. Preibisch[1,2], V. Riedl[1,2], A.M. Wohlschläger[1,2]

[1]TUM-Neuroimaging Center, Technische Universität München, Munich, Bayern, Germany, [2]Neuroradiology, Klinikum Rechts der Isar, Technische Universität München, Munich, Bayern, Germany

Background: Recent developments in fMRI acquisition yield data with higher spatial and/or temporal resolutions. However, the impact of the different multiband factors on functional connectivity dynamics has not yet been investigated. In this study, we evaluate the fluctuations of functional connectivity (FC) between intrinsic connectivity networks (ICN) in the resting state by applying a sliding time window approach based on several multiband factors.
Methods: 19 healthy subjects (11 female, age 24.6 ± 4.1 years) were scanned on a Philips Ingenia 3 T scanner using a 32 channel head coil with a multiband EPI sequence (Gyrotools, Zürich). r-fMRI data were acquired for 7 min using four protocols with different multiband factors (m), repetition times (TR) and number of volumes (n): m = 1, TR = 2 sec, n = 210; m = 2, TR = 1 sec, n = 420; m = 3, TR = 0.7 sec, n = 610; m = 4, TR = 0.52 sec, n = 810. Data was preprocessed using SPM8, and group-level spatial independent component analyses (ICA) were performed using the GIFT toolbox with two different approaches: (1) Separate ICA for each multiband factor, (2) One ICA over all multiband factors with a number of scans of m = 1 for all m. Dynamic FC was estimated from Pearson correlation (Fisher-Z transformed) with a sliding window of width 40 sec, which slid in steps of 1TR. Finally, the interquartile range (IQR) and power spectral density (PSD) were computed for correlation coefficients across all window segments.
Results: Default mode, occipital and auditory networks could be consistently detected in all ICAs, although differing in number and spatial extent. For both analysis approaches, clear impact on dynamics depending on multiband factor was revealed. IQR were decreased and Spectra were shifted to lower frequencies as m-factors increased.
Conclusions: One joined ICA improves comparability between different m-factors, while separate ICA is in practice probably the more realistic approach. Our results prove that both approaches reflect the impact of different multiband factors on network connectivity dynamics in the resting state. In the presented setup m = 2 constitutes the best compromise between information gain through higher resolution, and loss through reduction in signal-to-noise with increasing m-factor.

Table 1. The Number of Revealed Independent Components, and Subject Averages of IQR (mean ± std), and the Normalized Frequency (Hz) of the Peak of PSD (mean ± std) Over all Consistently Detected Networks

		Separate ICA		*One ICA*	
m	*Number of ICs*	*IQR*	*PSD*	*IQR*	*PSD*
1	15	0.5371 ± 0.0539	0.0353 ± 0.0126	0.5428 ± 0.0498	0.0303 ± 0.0131
2	20	0.4806 ± 0.0502	0.0160 ± 0.0068	0.4544 ± 0.0671	0.0181 ± 0.0060
3	13	0.4380 ± 0.0389	0.0101 ± 0.0051	0.3714 ± 0.1126	0.0169 ± 0.0027
4	3	0.3951 ± 0.0647	0.0075 ± 0.0075	0.2139 ± 0.1558	0.0145 ± 0.0065

P14A Resting state functional connectivity in the default mode network: preliminary evaluation of multicentre test-retest reproducibility

J. Jovicich[1], L. Minati[1,2], R. Marchitelli[1], G.B. Frisoni[3,4], The Pharmacog Consortium

[1]Center for Mind/Brain Sciences, University of Trento, Rovereto, Italy, [2]Scientific Department, Fondazione IRCCS Istituto Neurologico Carlo Besta, Milano, Italy, [3]LENITEM Laboratory Q1 of Epidemiology, Neuroimaging, and Telemedicine IRCCS Istituto Centro San Giovanni di Dio-FBF, Brescia, Italy, [4]Memory Clinic and LANVIE - Laboratory of Neuroimaging of Aging, University Hospitals and University of Geneva, Geneva, Switzerland

Background: PharmaCog [1] is a longitudinal multicentre European study aimed at evaluating biomarkers of disease progression in amnestic mild cognitive impairment patients. Candidate markers include functional connectivity (FC) assessed through resting-state fMRI [2]. We present preliminary findings on test-retest reproducibility of default mode network (DMN) FC, obtained through atlas-based regions-of-interest (ROIs), seed-based and independent-component analysis (SBA, ICA).
Methods: Five healthy elderly volunteers (50–80 years) were recruited at each of 13 clinical 3T MRI sites over 6 countries with heterogeneous scanners scanned twice at least a week apart. A harmonized acquisition protocol included 3D MPRAGE and resting state fMRI (TE = 30 ms, TR = 2.7 ms, $3 \times 3 \times 3$ mm3 voxels, 200 volumes). Standard preprocessing and physiological filtering was performed. The temporal signal-to-noise ratio (tSNR) was calculated in native space, with all other measurements performed in MNI space. Pair-wise correlations between DMN nodes were determined using prior ROIs [3]. SBA for the precuneus-posterior cingulate was performed, alongside ICA with 10 components, repeated once pooling together all sites, and once separately for each site.
Results: tSNR was significantly different across these sites, and there were significant inter-site differences in FC from ROI, SBA and ICA measurements. For ICA, inter-site differences were reduced performing group ICA over all sites together. Despite these differences, the test-retest reproducibility of all FC parameters under consideration did not show statistically significant differences across sites.
Conclusions: Our preliminary results highlight that there are important differences in tSNR and FC measures across sites, even when a harmonized scanning protocol is utilized. Across-session test-retest reproducibility, however, appears consistent across sites. While inter-site comparisons in FC parameters should be avoided, pooling longitudinal FC data across sites may be feasible.

[1] http://www.alzheimer-europe.org/FR/Research/PharmaCog. [2] Hedden et al., J Neurosc. 2009, 29:12686–12694. [3] Rosazza and Minati, NeurolSci 2010, 32:773–85.

Pharmacog is funded by the EU-FP7 for the Innovative Medicine Initiative (grant n°115009).

P15A Fine structure of regional network organization revealed by local PCA of resting state data

P. Kohn, J. Czarapata, M. Gregory, S. Kippenhan, N. Turner, K.F. Berman

Section on Integrative Neuroimaging, Clinical Brain Disorders Branch, National Institute of Mental Health, Bethesda, MD, USA

Background: Methods for parcellating the brain that are based on inter-regional or inter-voxel covariance can provide organization of brain modules into neurobiologically meaningful systems. While many current parcellation methods assign each voxel to a single cluster, functional features of a given voxel actually reflect a weighted sum of many neurons, each of which may perform a different function on the same inputs and project its outputs to different brain modules. Although the resolution of current neuroimaging technologies cannot resolve this fine structure, a more complete accounting can be achieved by assigning each voxel a set of weights for network-level membership. We propose a new method in which each voxel is not assumed to have the same system membership across subjects; rather, each subject is given an independent set of system weights to account for the expected inter-subject variability at this scale. Resulting single subject weight maps can be tested at the group level to determine the statistical significance of the spatial overlap across subjects, used for group comparisons, or used to define subject specific sub-region masks for analysis of task-based fMRI, VBM, DTI, or PET ligand data.
Methods: Whole brain eyes-open rest data were acquired from 31 healthy adults (3T GE MR750, 32 channels, $96 \times 96 \times 40$ matrix, 3 mm slices, ASSET x2). Functional scans were motion corrected, aligned to the subject's anatomic scan, normalized to MNI space, and bandpass filtered ($0.008 < f < 0.1$ Hz). Signal due to nuisance regressors as determined by anatomic CompCor (Chai, 2012) and time points associated with motion were removed prior to filtering. Each unsmoothed voxel in region-of-interest masks (PickAtlas) was taken as a seed to produce a Pearson's correlation image with the rest of the brain. These correlation images were transformed to Z values, rescaled to equalize total variance between subjects, and entered into a PCA analysis (3 dpc). The PCA components were used to weight the

seed voxels in each subject to best explain the variance in their connectivity patterns. The seed weights can be interpreted as a measure of network membership. A second-level t-test of these weight maps across subjects was used to identify significant overlaps in seed voxel network membership at the group level.
Results: The method was tested on regions including the striatum, hippocampus, insula and intraparietal sulcus. The results show statistically significant, spatially localized sub-regional structure at the group level that is in line with previous work. In other regions it reveals distinctive and significant ($p < 0.05$ FDR) spatial organization that was not detected by simple voxel and ROI seed based correlation analyses on these same data.
Conclusions: The described method provides a means to identify and statistically test network-level organization within a region, and may have the potential to offer new information about pathophysiology, developmental trajectories, genotypic variation, and other active areas of neuroimaging investigation.

P16A Dynamic mapping of resting-state network coherence at multiple frequencies

H.-L. Lee[1], J. Assländer[1], P. LeVan[1], J. Hennig[1]

[1]*Medical Center Freiburg, Freiburg, Baden-Württemberg, Germany*

Background: Time–frequency analysis of rs-fMRI data has gained huge interests. Using wavelet transform coherence (WTC) we can obtain multi-resolution results with progressive window lengths and have greater flexibility to assess temporal-spectral relation between brain regions. In this study we used ICA and WTC on MREG resting-state data to look at connectivity and centrality of brain regions at different frequencies.
Methods: Experimental setup: 11 healthy volunteers, 3.0 T Siemens Trio scanner, 32-channel head coil, MREG sequence (TR = 100 ms), total scan time = 6 min 50 sec. Routine fMRI preprocessing was done in SPM. Spatial ICA ($c = 60$) was used to extract components (nodes) from the data. Neuro-physiological relevant components were manually selected. Time-frequency WTC of all selected nodes' time-series corresponding to nodes in PCC and right post-central gyrus were calculated. Degree centrality weighted by both coherence magnitude and phase were averaged across time and subject.
Results: 37 functionally related components were identified after ICA. Figure 1 shows sample frames of the dynamic coherence maps (averaged over the respective frequency bands) of a representative subject. Maps were visualized in HSV-color-coded images, where *hue* represents the phase difference between the individual node and the seed node, and *value* represents the magnitude of coherence. Figure 2 shows the averaged centrality spectra for both cases. Centrality of PCC has a significant drop between 0.05 ~ 1 Hz.
Conclusions: We demonstrated dynamic coherence maps corresponding to PCC and motor cortex. In these two cases the variations in coherence phase, as well as the averaged centrality, are both stronger at lower frequencies.

*This work was supported by European Research Council Advanced Grant agreement 232908 ''OVOC'' and DFG Cluster of Excellence EXC-1086 ''Brain Links-Brain Tools''.

P17A Functional crosstalk between object- and space-encoding brain regions during scene viewing

D. Linsley[1], S. MacEvoy[1]

[1]*Boston College, Chestnut Hill, MA, USA*

Background: Behavioral data suggest that scene recognition draws heavily upon analysis of scenes' spatial properties, particularly their layout (e.g. Greene & Oliva, 2009). At the same time, scene recognition is strongly influenced by the kinds of objects scenes contain (e.g. Davenport & Potter, 2004). We

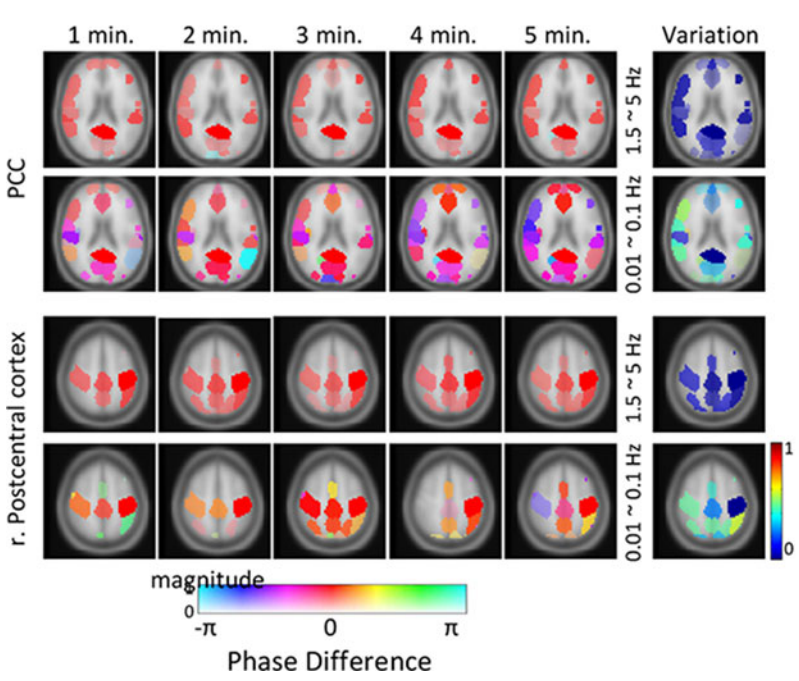

(Left) **FIG. 1.** Coherence maps corresponding to different time points.

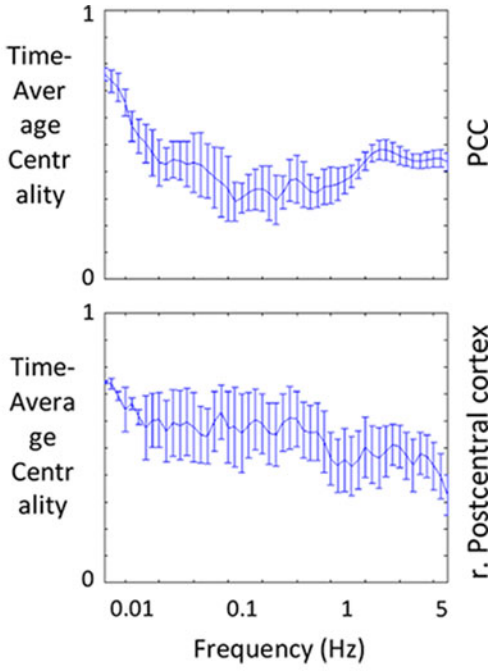

(Right) **FIG. 2.** Averaged degree centrality across time and subject.

recently used multivariate analysis (MVPA) of fMRI data (Linsley and MacEvoy, *Cerebral Cortex* 2014) to show that these two routes to scene recognition converge in parahippocampal place area (PPA), an area of ventral-temporal cortex sensitive to scenes' spatial properties (e.g. Kravitz et al., 2011). Along pattern dimensions in PPA representing scene spatial properties, extremely small and large scenes were encoded as more similar to their category average when category-informative objects were intact versus masked. The source of this object-triggered ''centripetal''-bias of encoded spatial properties however remains unclear. In the present study, we applied a novel information-based functional connectivity analysis (iFCA) to identify brain regions mediating the generation of centripetal bias in PPA encoded spatial properties.
Methods: Cortical volumes of 12 human participants were collected with fMRI during presentation of images of bathrooms varying in size, with extremely small and extremely large exemplars randomly containing either masked or visible category-informative objects (e.g. toilet, shower, sink). Volumes were processed with iFCA, in which an iterative whole-brain MVPA searchlight procedure identified voxel clusters containing latent representations of object-masking state. For each such cluster, mediation analysis captured the extent to which its trial scores, measured along its object-masking state (i.e. masked or visible) pattern dimension, explained the trial-wise variability of PPA encoded spatial properties.
Results: A functional network containing regions of the visual system and default-mode network (DMN) mediated centripetal bias in PPA. Consistent with PPA resting-state connectivity (e.g. Baldassano et al., 2013), regions in the DMN were preferentially connected to anterior PPA ($_{A}$PPA) while the visual system was connected to posterior PPA ($_{P}$PPA). The strength of these connections was asymmetric only in $_{P}$PPA, with the strongest mediation produced by lateral occipital complex, a region implicated in processing scene objects (e.g. MacEvoy et al., 2011). The connectivity gradient observed in PPA coincided with significantly stronger object-triggered centripetal bias in $_{A}$PPA versus $_{P}$PPA.
Conclusions: We have demonstrated that encoded spatial properties in PPA are impacted by its functional interactions with connected visual and DMN regions. Curiously, the organization of these connections along the anteroposterior axis of PPA corresponds with increased centripetal bias in portions of PPA preferentially connected to the DMN. Together, these results help explain previously observed object-induced biases in PPA spatial representation and characterize a functional network supporting scene recognition.

P18A Spatio-Temporal Dynamics of Low Frequency Oscillations in Resting-state fMRI

D. Mastrovito[1], S. Hanson[1], C. Hanson[1]

[1]*Rutgers University, Newark, NJ, USA*

Background: Resting-state fMRI has been shown to capture intrinsic fluctuations in brain activity. These fluctuations are thought to mediate long distance neuronal synchronization and have a characteristic power spectrum dominated by low frequency oscillations (<.1 Hz). Using techniques such as correlation-based functional connectivity analysis, studies have identified structure in resting-state time series related to functional networks. However, functional connectivity analysis assumes temporal stationarity of the MRI time series and provides no indication of asymptotic convergence. Evidence suggests that functional connectivity changes over time, however few studies have attempted to characterize the spatio-temporal dynamics of resting-state functional connectivity. Those that have, employed techniques such as PCA or ICA that force constraints such as orthogonality or statistical independence on the data that may not be true of the underlying signals. The current study explores the dynamics of resting-state functional connectivity employing multidimensional scaling and state-of-the-art high temporal resolution multiband resting-state functional magnetic resonance imaging (rsFMRI).
Methods: Multiband resting state data from the Enhanced Nathan Kline Institute-Rockland Sample (TR = 645 msec; voxel size = 3 mm isotropic; duration = 10 minutes), was obtained from the 1000 Functional Connectomes Project. 63 lateralized regions of interest (ROIs) from the Montreal Neurological Institute (MNI) 2 mm atlas were selected based on their high power in the low frequency band between .02 and .1 Hz as indicated by Fourier analysis. Temporal dynamics of the relationships between each of the 63 ROIs were explored using continuous wavelet transform. Additionally, using these ROIs, sliding window correlations were used as an input similarity measure to map the ROIs into a 3 dimensional non-parametric multidimensional scaling (MDS-Kruskal-Shepard) space.
Results: A solution recovering 3 dimensions was able to account for 90 percent of the variation in the time series and provided a spatial visualization of the resting state network as it evolved over time. The resultant visualization of the ROI dynamics showed a highly structured interplay between ROIs with periodic local collapse of ROIs towards the center of the space and subsequent expansion.
Conclusions: Consistent across individuals, a pronounced periodic grouping effect was identified and visualized over time in the 3 dimensional MDS space. The function of intrinsic brain activity is not understood, but many have proposed that the purpose of low-frequency oscillations are to establish large-scale synchronous states of high and low excitability across broad networks. The pattern of activity observed is consistent with this idea and is shown for the first time in resting-state fMRI.

This material is based upon work supported by the National Science Foundation Graduate Research Fellowship under grant number DGE-1313667.

P19A Application of independent vector analysis for resting state fMRI can better preserve subject specific features

Andrew Michael[1,2], Mathew Anderson[3], Robyn Miller[1], Tülay Adalı[3], Vince Calhoun[2,4]

[1]*Geisinger Health Systems, Danville, PA, USA,* [2]*The Mind Research Network, Albuquerque, NM, USA,* [3]*University of Maryland Baltimore County, Baltimore, MD, USA,* [4]*University of New Mexico, Albuquerque, NM, USA*

Background: In resting state fMRI (rsfMRI) fluctuations of the BOLD signal are captured while the research participant does not engage in an explicitly assigned task. It is reasonable to expect that a higher degree of inter subject variability can exist in rsfMRI compared to task fMRI. Unlike in task fMRI, rsfMRI cannot be modeled using an *a priori* task time course. Analyses of rsfMRI data are achieved through various blind source separation techniques, but a comprehensive performance evaluation of these techniques under varying degrees of subject variability has not been performed. In this work we compare the estimation accuracies of widely applied group independent component analysis (GICA) and a novel technique called independent vector analysis

(IVA). Using simulated data we performed numerous simplistic and realistic experiments to characterize the performance of these techniques and checked accuracies across all estimated components of the decomposition in both spatial and temporal domains.
Methods: GICA and IVA are extensions of ICA and enable users to derive consistently covarying fMRI components across a group of subjects. In GICA, subject specific fMRI data are combined through temporal concatenation to first estimate group level components. Subject specific spatial maps (SM) and time courses (TC) are obtained through a back-reconstruction step. In IVA subject data are not mixed together but kept distinct and the back reconstruction step is not required. IVA maximizes an objective function that considers both the independence of within subject SMs and the dependence of similar SMs across subjects. SimTB (http://mialab.mrn.org/software/gift) was used to simulate fMRI datasets under the assumption of spatiotemporal separability of fMRI data. Different types of fMRI datasets were simulated by systematically varying the spatial properties of the SMs across subjects. TCs were generated randomly and were kept independent between components and subjects (to allow maximum variability in the time domain). Correlation between ground truth and estimated components was used as the primary metric of estimation accuracy.
Results: (1) At low levels of SM variability or when just one SM is varied, both GICA and IVA perform well. (2) At higher levels of SM variability or when multiple SMs are varied, IVA continues to perform well but GICA estimates are composites of ground truth. (3) Both GICA and IVA remove spatial correlations of overlapping SMs and introduce artificial correlations in their TCs. (4) If number of components is over estimated, IVA continues to perform well but GICA introduces artifacts. (5) In the absence or presence of SMs unique to one subject, GICA produces errors in TCs whereas IVA estimates are accurate.
Conclusions: Our results indicate that compared to GICA, IVA better preserves subject variability, can produce more accurate results for functional network connectivity analyses and performs better while overestimating the number of components.

P20A Why Timecourse Normalization is Crucial in Dual Regression For Assessing Functional Connectivity

L.D. Nickerson[1], S.M. Smith[2], C.F. Beckmann[2,3]

[1]*McLean Hospital & Harvard University, Belmont, MA, USA*
[2]*FMRIB, Oxford University, Headington, Oxford, UK*
[3]*Radboud University Medical Center & Donders Institute, Radboud University, Nijmegen, The Netherlands*

Background: Group independent component analysis (GICA) with dual regression (DR) is a powerful tool for assessing group differences in resting state functional connectivity (RSFC). Within this framework, magnitude information about the BOLD signals is preserved. The magnitude, or amplitude, of the BOLD signal oscillations in some resting state networks (RSNs) has been shown to be related to task load, to predict task-evoked responses, and to be reliably decreased during fixation versus eyes closed rest and during sedation, suggesting that RSN amplitude conveys meaningful information regarding RSFC. More importantly, whether or not one is interested in amplitude effects, ignoring amplitude information in the RSFC analysis could lead to spurious group differences. We show here how to address this important issue within the GICA-DR framework.

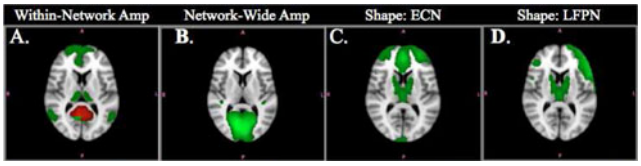

FIG. 1. Amplitude effects: A) within-network: voxels in ROI (red) have greater TC amp than voxels in green, and B) network-wide (Group B amp > Group A amp). Shape differences: C) Basal ganglia connected to ECN in Group A and D) LFPN in Group B.

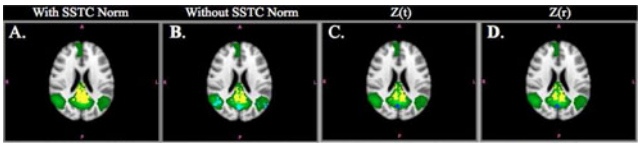

FIG. 2. Only SSMs with SSTC normalization accurately identify within-network amplitude group differences. All other SSMs show group differences outside of the ROI. A) SSMs with SSTC normalization, B) raw SSMs without SSTC normalization, C) Z(t), and D) Z(r) statistic maps (red-yellow: Group B > Group A, blue-light blue: Group A > Group B, $p < 0.05$).

Methods: Simulated data (n = 36) were created using ground truth timecourses (TCs) and RSN maps corresponding to real spatial and temporal signals from real RSNs. Group differences in shape and amplitude (amp) were introduced into half of the datasets (Group B; n = 18; Fig. 1). Within-network amp: voxels in a ROI (red) had 1.5*ground truth TC of voxels in the rest of the DMN (green) for each simulated dataset. Network-wide amp: in Group B, all voxels in the medial visual network (MVN) were assigned a TC equal to 1.1*ground truth TC. Shape difference: basal ganglia were connected only to ECN for Group A and only to LFPN for Group B. Simulated data were analyzed using the DR procedure: 1) ground truth RSNs were regressed against each FMRI dataset to identify subject-specific timecourses (SSTCs), 2) SSTCs were regressed against each FMRI dataset to give subject-specific summary statistic maps (SSMs). Inference was done on SSMs obtained with and without normalization of SSTCs to unit variance and SSMs of Z(t) and Fisher Z-transformed correlation coefficients (Z(r)) using FSL's *randomise*.
Results: Fig 2: Group differences identified using each SSM type.
Conclusions: Only DR *with* SSTC normalization accurately reflects within-network amplitude differences (Fig 2A) while also localizing network-wide amplitude and shape differences (not shown). Z(t) and Z(r), and SSMs *without* normalization, show spurious differences outside the ROI (Fig 2B-D), because of different sensitivity to TC variance and scale, respectively, than SSMs with normalization. Thus, these SSMs should not be used for inference. Further analyses are necessary to disentangle synchrony and amplitude effects on RSFC.

P21A On large DCMs for resting state fMRI

A. Razi[1,2], M. L. Seghier[1], G. Rees[1], and K. J. Friston[1]

[1]*Wellcome Trust Centre for Neuroimaging, UCL, London, U. K*
[2]*N.E.D. University of Engineering & Technology, Karachi, Pakistan*

Background: Stochastic dynamic causal modelling (DCM) (Friston 2003, Li 2012) allows for unknown (random) fluctuations to drive the neuronal system but has to estimate both hidden states

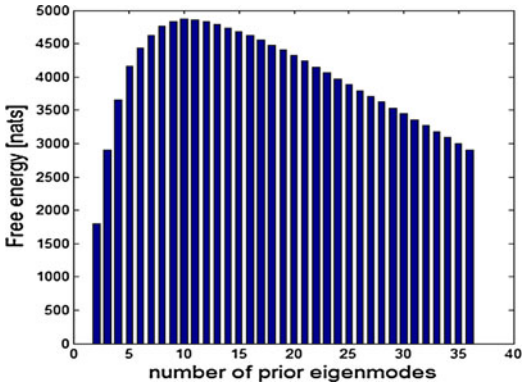

FIG. 1. Stochastic DCM

and parameters; hence it is practically not possible to invert large stochastic models with many nodes. Recently we introduced a new DCM scheme (Friston 2014) based upon a deterministic model that generates predicted crossed spectra - referred to as spectral DCM (spDCM). Compared to stochastic DCM (sDCM), the inversion of spDCM is computationally efficient taking about 10 s per iteration for a 10 nodes graph, with convergence achieved usually between 16 to 64 iterations. Here we show that using prior constraints that bound the number of free parameters (Seghier 2013), the Bayesian inversion of large graphs (nodes > 32) can be made computationally very efficient. Our simple solution uses a smaller number of prior modes to reduce the dimensionality of the problem in an informed way.

Methods: We used the open access Oxford dataset from the FC1000 project using a subset of 10 adults. Scanning was performed using a 3T Siemens Trio (for scanning parameters see Filippini 2009). Data were realigned, normalized to MNI space, and spatially smoothed using a 6 mm (FWHM) Gaussian kernel. To identify key nodes, resting state fluctuations were modelled using a GLM comprising a discrete cosine basis set with frequencies ranging from 0.0078–0.1 Hz (Kahan 2014), plus nuisance regressors (movement parameters and a time series from the lateral ventricle). We used the 36 ROI coordinates from (Raichle 2009) representing seven resting-state networks: Default mode, dorsal attention, executive control, salience, sensorimotor, visual and auditory networks. The regional responses were summarized using the principal eigenvariate of each region (defined as an 8 mm-radius sphere). Effective connectivity was computed using both schemes (sDCM and spDCM).

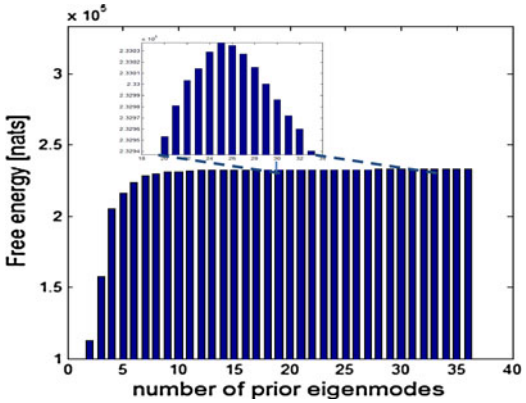

FIG. 2. Spectral DCM

Results: In Fig.1, the plot shows the average free energy (log evidence) over 10 participants over number of modes m relative to the free energy at $m = 1$ using sDCM. The plot shows that free energy first increases and then systematically decreases with increasing number of modes (peak at $m = 10$). Fig. 2 shows results when the inversion was performed using spDCM. We again see a similar trend but this time the free energy reached a plateau at around $m = 10$ modes.

Conclusions: By replacing connections between many *nodes* with connections between a small number of *modes*, effective connectivity of large graphical models can be estimated with spDCM. The ability to estimate large models of resting-state data with DCM provides the opportunity to use graph theory that rests upon the statistics on large number of edges (Rubinov 2010).

P22A Two Intrinsic Functional Connectivity Visualization Mobile Applications: iBraiN and iBraiNEEG

G.M. Rojas[1], J.A. Fuentes[1], M. Gálvez[2], D.S. Margulies[3]

[1]*Laboratory for Advanced Medical Image Processing,*
[2]*Department of Radiology, Clínica las Condes, Santiago, Chile,*
[3]*Max Planck Institute for Human Cognitive and Brain Sciences, Leipzig, Germany*

Background: Visualization of complex neuroimaging data such as functional connectivity and his relation to EEG is a challenge. Different visualization solutions to view complex image data have been proposed. Some authors described 2-D and 3-D neuroimaging visualization methods for tractography and functional connectivity data. Others described an anaglyph method to view neuroradiological 3-D images. EEG is the standard diagnostic method for epilepsy, and the relation of EEG electrodes position and functional connectivity data could be of interest. Here we describe 2 Android applications: i) visualize the 7 standard functional connectivity networks, ii) shows the position of EEG 10-20 electrodes in relation to functional connectivity networks.

Methods: Using MNI152 2 mm standard MPRAGE image we created a mesh model (Gray Scale Model Maker, 3D Slicer software). A 7 Yeo Network Liberal Mask was used to create the mesh model of the 7 standard Yeo Networks (Model Maker, 3D Slicer software). Laplacian HC algorithm (MeshLab) was used to smooth the mesh of the networks and the brain. Android applications were created with javascript and software tools: Unity 4.02 f (graphic engine), Sublime text3 tools, Blender (mesh, materials), Gimp (textures). The position of EEG 10-20 standard electrodes was published by same author.

Results: We created two applications: i) **iBraiN (i**ntrinsic **Brai**n **N**etworks**)**: The user view a 3D transparent brain with 7 standard functional connectivity networks (Fig 1). The user could rotate the brain using onscreen controls. Tapping each network the name of it was shown in the screen. Tapping with 2 fingers in each network that connectivity network was shown in a transparent brain. ii) **iBraiNEEG (i**ntrinsic **Brai**n **N**etworks and

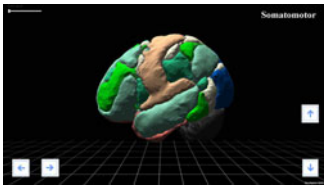

FIG. 1.

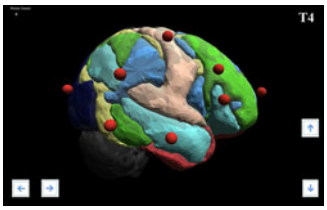

FIG. 2.

EEG electrodes): The user view a similar brain as previous with EEG 10-20 electrodes as spheres over the brain (Fig 2). Tapping each electrode, its name appears on screen.
Conclusions: The application iBraiN has potential use as an academic tool, because it shows the position in the cortex in a 3D environment of the different regions of each functional network. iBraiNEEG is an application tool that helps to analyze EEG data in relation to functional connectivity networks.

P23A Network signatures of resting state in high-density EEG

S. Saperstein[1], R. Sekuler[2], J. W. Bohland[1]

[1]Boston University, Boston, MA, USA, [2]Brandeis University, Waltham, MA, USA

Background: The analysis of resting state functional connectivity using fMRI has gained widespread acceptance, but such approaches remain underdeveloped in EEG. EEG provides a much finer temporal resolution than fMRI and thus offers tremendous opportunities for studying the dynamics of brain states at rest. A bottleneck in the study of these dynamics in EEG is a lack of established sensor network signatures for the ''default mode'' or other prominent networks emerging from the fMRI literature. Here we develop an approach to characterize network signatures of brain states during periods of rest, in comparison to periods of focused task performance.
Methods: Nine healthy normal subjects participated in experiments conducted using a 128-channel high density, high impedance EEG system, consisting of a pre-task resting period, a task period, and then a post-task resting period. The resulting time series were manually quality controlled, and band-pass filtered, then split into epochs one-second in duration. The maximum values (across a range of lags) of pairwise cross-correlations between electrodes, for each epoch, were compared to an empirically created null distribution [1]. The resulting percentile ranks of the correlations were used as edge strengths, encoding a measure of functional connectivity between electrodes. Mann-Whitney U-tests identified pairs of electrodes that were significantly more correlated during resting periods than during the task, and the consistency of these rest-enhanced networks across resting periods was tested using a hypergeometric test. Vectors encoding functional connection strengths (for each edge) or node degrees (for each electrode) over each epoch formed the input to a *k*-means cluster analysis in a network generalization of microstate analysis [2]. The resulting clusters were used to compare the occupancy of network microstates common to both rest periods, across a range of values for *k*.
Results: The overlap of rest-enriched networks between pre- and post-task rest periods in individual subjects was highly significant across a range of *p*-value thresholds from the Mann-Whitney U-tests. Network microstates derived from *k*-means clustering of network edge weights tended to recur preferentially during the pre- and post-task resting periods in each subject, while a set of relatively unique network states occurred during task performance. Repeating the analysis based on node degrees again showed a high degree of similarity between rest periods, and in each case, these patterns were found consistently across a range of values for *k*.
Conclusions: This work furthers methodologies for network-based analysis of EEG. Our approach identifies common sensor correlation patterns that occur preferentially during rest. These results should be validated across additional subjects and experimental tasks, but they hold promise for examining resting state dynamics with high temporal precision as well as examining interactions between interleaved periods of task and rest.

1. Kramer MA, Eden UT, Cash SS, Kolaczyk ED. *Phys Rev E*, 79:061916, 2009.
2. Pascual-Marqui RD, Michel CM, Lehmann D. *IEEE Trans Biomed Eng*, 42:658, 1995.

P24A Evaluation of dynamic analysis methods for characterization of time-varying functional connectivity

Sadia Shakil[1], Shella D. Keilholz[2], Chin-Hui Lee[1]

[1]Electrical and Computer Engineering, Georgia Institute of Technology, Atlanta, GA, USA, [2]Biomedical Engineering, Emory University/ Georgia Institute of Technology, Atlanta, GA, USA

Background: Dynamic analysis of resting-state MRI data can provide new insight into psychiatric disorders and normal cognition, but the effects of the analysis methods used on the results obtained has barely been explored. It is known that apparent variability in connectivity can arise from properties of the BOLD signal itself, since similar changes can be observed in phase scrambled or mismatched signals[1,2]. In this study, we examine model networks with known transitions to test the impact of analysis factors on the detection and classification of network states.
Methods: Three simulated networks consisting of seven nodes with time series taken from a voxel of resting-state fMRI downloaded from[4] with TR of 645 ms were formed. Network configurations were changed every 20*TR to 200*TR s by altering the correlation between each node pair. Sliding window correlations between all pairs of nodes were computed, and clustered in 5 clusters (states)[3] using k-means clustering. Windows of 25, 50, 100[1], and 200 seconds were used.
Results: The length of the sliding window impacted analysis as expected, with shorter windows improving localization to short-lived states and vice versa, which is shown in actual vs. sliding window correlation plots for different window lengths in Figure 1.

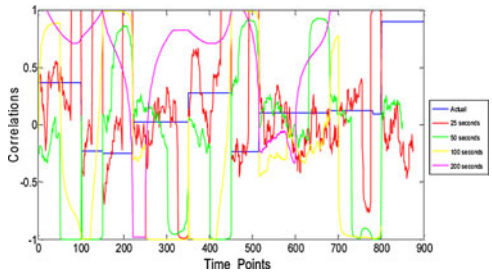

FIG. 1. Actual correlation vs. sliding window correlations for different window lengths

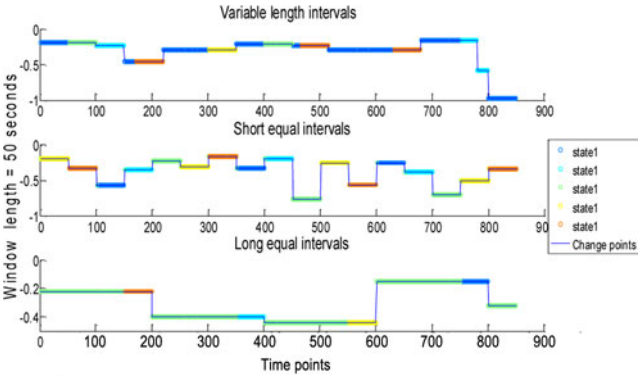

FIG. 2. State distribution of 3 simulated networks.

The state distribution for the networks with variable-length (top), short (middle) and long (bottom) periods between transitions obtained with a 50 second window is plotted in Figure 2. Transitions in a configuration are shown by discontinuities and distinct colors indicate different states.

Conclusions: Sliding window correlation can be sensitive to changes in network configuration but short-lived states can be lost with longer window sizes. Clustering based on the correlation time courses provides the best results when network configurations are strongly separated.

References: 1. Keilholz, S.D., et al., Dynamic Properties of Functional Connectivity in the Rodent. Brain Connectivity, 2013. 3(1): p. 31–40; 2. Handwerker, D.A., et al., The continuing challenge of understanding and modeling hemodynamic variation in fMRI. Neuroimage, 2012. 62(2): p. 1017–23; 3. Allen EA, et al., Tracking Whole-Brain Connectivity Dynamics in the Resting State. Cerebral Cortex, 2014. 24(3): p. 663–76; http://fcon_1000.projects.nitrc.org/indi/pro/eNKI_RS_TRT/FrontPage.html

P25A Shrinkage prediction of seed-voxel brain connectivity using resting state fMRI

H. Shou[1], A. Eloyan[1], M.B. Nebel[2,3], A.F. Mejia[1], J. J. Pekar[2,4], S.H. Mostofsky[2,3], B. Caffo[1], M.A. Lindquist[1], C. Crainiceanu[1]

[1]Department of Biostatistics, Johns Hopkins University, Baltimore, MD, USA, [2]Kennedy Krieger Institute, Baltimore, MD, USA, [3]Johns Hopkins School of Medicine, Baltimore, MD, USA, [4]Department of Radiology, Johns Hopkins University, Baltimore, MD, USA

Background: Seed-based correlation analysis of resting state fMRI (rs-fMRI) is commonly used for understanding brain networks and cognitive process (Biswal et al., 1995; Greicius et al., 2003; Fox et al., 2005; Margulies et al., 2007). The correlation map between brain voxels and seed regions are crucial for connectivity analysis, but its reliability is overlooked in many studies. We propose a shrinkage method that improves the estimation of subject-level correlation map. The method is evaluated on multiple seed regions, and is compared with several conventional approaches.

Methods: We reanalyze the scan-rescan rs-fMRI data sets from 20 healthy adults (Landman et al., 2010), where two 7-min scans were acquired from each subject. Images were registered to MNI template, spatially smoothed (6-mm kernel) and temporally filtered (.01–0.1 Hz). 12 seed regions including precentral gyrus and cuneus are selected using ''Type II Eve Atlas'' (Oishi et al., 2009). For each seed region, the correlation map $W_{ij}(v)$ for subject $i = 1, 2, \ldots, 20$ at session $j = 1,2$ is calculated as the Pearson correlation between the time series of brain voxel $v = 1, 2, \ldots, 293712$ and the average time series in the seed region. $W_{ij}(v)$ is then Fisher's z-transformed to $V_{ij}(v)$. Given subject i_0 and its transformed correlation map at session 1 $V_{i_0 1}(v)$, a conventional estimator of $V_{i_0 2}(v)$ could be $V_{i_0 1}(v)$ itself, or the average of all session 1 data from the 20 subjects. The shrinkage estimator is a weighted average of these two conventional estimators, through a voxel-wise shrinkage coefficient $\gamma(v)$. $\gamma(v)$ is defined as the ratio between the signal versus the total variability in the $V_{ij}(v)$, and can be estimated using two easy-to-implement approaches. The pointwise approach estimates $\gamma(v)$ voxel by voxel and the local approach accounts for the spatial correlation in the neighborhood of each voxel. All estimators are then transformed back to the originally correlation space.

Results: The methods are evaluated by computing the mean square error (MSE) between the estimators and $W_{i_0 2}(v)$. For correlation analysis with precentral gyrus, the shrinkage estimator achieves an average of 30% reduction in MSE over 20 subjects, compared with merely using session 1 data. The improvement is even larger for other seed regions in the visual system. Surprisingly, the group correlation map also provides a better prediction of a subject's connectivity than the individual's own data. It even outperforms the shrinkage estimator when sample size is small.

Conclusions: For imaging data with large scan-rescan variability, the shrinkage estimators that borrow strength from the population average show better within-subject prediction properties than subjects previous scans alone. It demonstrates potential impact in brain region clustering, segmentation or inference that are based on the calculation of correlation maps, and is important to the development of reliable imaging biomarkers.

P26A Evidence of decrease of the network mean degree when healthy volunteers go from resting state to language task

L. C. T. Herrera, H. F. B. Ozelo, A. Alessio, M. S. Oliveira, M. Cordeiro, R. J. M. Covolan, G. Castellano

Neurophysics Group, Gleb Wataghin Physics Institute, University of Campinas (UNICAMP), Brazil

Background: The purpose of this work was to find differences in brain networks when two states of the brain are compared. For this, functional networks were built (Basset D.S. 2006, Wang J. 2010) using preprocessed and low-frequency (0.01–0.1 Hz) filtered fMRI data. One session was done during resting state (RS) and another during a language task (LT). Two hypotheses were tested: 1) Existence of network metrics that reflect differences for these two functional networks; 2) Existence of network metrics for LT that reflect brain hemisphere dominance for language, if this dominance exists.

Methods: Twelve healthy subjects (mean age 35 ± 10, 6 men) participated in this study. The study was approved by the Ethics Committee of UNICAMP. Volunteers took part in two fMRI sessions (one RS and one LT). Functional networks, corresponding to each session (RS/LT) were built, using undirected and unweighted graphs. For each network the following parameters were computed (Rubinov 2010) : 1) Mean degree; 2) Cluster coefficient; 3) Characteristic path length. Left/right brain hemisphere networks for LT were compared to each other, and this result was compared to the corresponding fMRI activation result (computed using a general linear model (GLM) with SPM8), to see if the dominance shown in fMRI activation maps reflected somehow in network parameters.

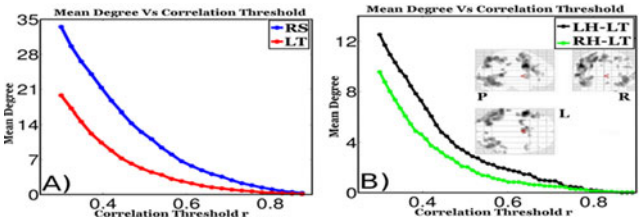

Results: Fig. 1A shows the behavior of network mean degree as a function of correlation threshold for one volunteer. It shows that the number of connections for the RS network is higher compared with the LT network. This result holds for 8 of the 12 volunteers ($p < 0.05$). Fig. 1B shows a higher number of connections for the left hemisphere (LH) LT network compared to the right hemisphere (RH) LT network of one volunteer; it also presents the outcome of the fMRI GLM analysis, that shows a LH dominance for LT. The fMRI GLM analysis showed left hemisphere dominance for 8 (of 12) volunteers. From these, 6 showed a qualitative LH LT mean degree higher than the RH LT mean degree, but only for 3 of them results were significant ($p < 0.05$).
Conclusions: The decrease of network mean degree in the LT compared to the RS session seems to reflect the well-known synchronization of neurons at rest and desynchronization while performing a task, which shows as an amplitude decrease of certain frequency bands of the EEG signal (Kuebler 2001). In the present case, when the brain performs the task, the correlation among different regions decrease, and so does the number of nodes in the corresponding networks. We also found that 6 out of 8 volunteers that showed LH dominance for LT with standard fMRI analysis could also be detected comparing the mean degree of the corresponding LH and RH networks.

P27A Hippocampal connectivity to posterior cingulate cortex reliably predicts memory across sessions and age groups

Alexandra Touroutoglou[1,2], Joseph Andreano[1,2], Lisa Feldman Barrett[1,2,3] and Bradford C. Dickerson[1,2,4]

[1]Athinoula A. Martinos Center for Biomedical Imaging, Charlestown, MA, USA [2]Psychiatric Neuroimaging Division, Massachusetts General Hospital/Harvard Medical School, Charlestown, MA, USA [3]Department of Psychology, Northeastern University, Boston, MA, USA [4]Frontotemporal Disorders Unit, Massachusetts General Hospital/Harvard Medical School, Charlestown, MA, USA

Background: Despite the optimistic results of initial intrinsic connectivity reliability studies, no study to our knowledge has sought to investigate whether intrinsic connectivity-behavioral relationships are stable over time. The possibility that these relationships may be stable traits could be addressed by using data from one point in time to predict relationships at a different time point within the same individuals. In this study, we investigated the stability of such brain-behavior relationships at two timepoints, approximately 1 week apart, testing the hypothesis that intrinsic connectivity at one point in time would predict behavior at a later point in time, and vice versa.
Methods: We focused on an individual differences brain-behavior finding previously reported by our laboratory (Wang et al. (2010a): episodic memory performance of older adults was predicted by the strength of hippocampal to posterior cingulate/precuneus cortex (PCC) connectivity. We analyzed behavioral and resting state scan data on forty-one young adults (mean age = 28.07, SD = 9.51; 23 females) collected at two timepoints, approximately 1 week apart. To examine memory performance, we computed sensitivity on a paired associate recognition task. To examine the intrinsic functional connectivity strength between the hippocampus and PCC, we used seed-based resting state functional connectivity MRI analysis. Using a series of linear regression analyses, we next examined the relationship between hippocampal connectivity to PCC and memory performance at two timepoints.
Results: Our results showed that the same relationship observed in Wang et al. (2010)'s study generalizes to an independent sample of participants of a different age, and further that the relationship within this sample is reliable over two points in time, such that connectivity at either timepoint predicts memory performance during the other timepoint.
Conclusions: These findings provide the first evidence that the relationship between large-scale intrinsic network connectivity and episodic memory performance is a stable trait that varies between individuals. Critically, intrinsic connectivity between the hippocampus and PCC significantly predicts performance on a learning and memory task one week later. Our results thus suggest that the connectivity between hippocampus and PCC relates to a trait-level characteristic which predicts associative learning ability, rather than a transient state.

P28A Role of remote synchronization and symmetry in indirect interactions in functional correlations between distant cortical regions

V. Vuksanović and P. Hövel

Institute für Theoretische Physik, Technische Universität Berlin, Germany, Bernstein Center for Computational Neuroscience Berlin, Humboldt-Universität zu Berlin, Germany

Background: Mechanisms generating functional connectivity between distant cortical regions are largely unknown. Here, we use a modeling approach in conjunction with experimental data to investigate dynamical aspects of large-scale functional connectivity in the human brain with reference to remote synchronization and symmetry in the network interactions.
Methods: We model (neural and BOLD) activity of cortical regions as sets of self-sustained oscillators, oscillating in gamma frequency band and embedded into topology of complex brain functional connections. Additionally, using element-wise product of the binarized functional and anatomical connectivity matrices, we consider only those functionally connected regions that are also connected via direct neural links. Consequently, we derive functional interactions combining connectivity maps from fMRI and DW-MRI experiments.
Results: In the simulated functional networks, we first identified pairs of remotely synchronized ($\rho > 0.8$) nodes i.e. functionally connected nodes without direct anatomical link. We then showed that remote synchrony arises from the symmetry in indirect connections, which is quantified by the number of shared neighbors. An increasing size of a joint neighborhood positively correlates with a higher level of synchrony. In addition, the desirable patterns of the pair-wise synchrony i.e. those that match experimental findings are revealed by globally meta-stable states.
Conclusions: Our results indicate that functional connectivity observed between spatially distant cortical regions can be

explained by remote synchronization arising from the symmetry of cortical functional interactions. This symmetry is quantified by the overlap of the neighborhoods of pairs of nodes. The level of synchrony between remote nodes strongly correlates with the corresponding number of shared connections. This is an important network property as some of the spatially close and anatomically connected cortical regions fail to synchronize their activity if they do not share a sufficient number of links.

NeuroImage (2014) (available online: DOI:10.1016/j.neuroimage.2014.04.039)

P29A Detecting Intrinsic Brain Activity Using Whole Brain 3D-VASO Imaging

X. Miao[1], H. Gu[2], L. Yan[3], H. Lu[4], D.J. Wang[3], X.J. Zhou[5], Y. Zhuo[1], Y. Yang[2]

[1]State Key Lab of Brain and Cognitive Science, CAS, Beijing, China; [2]Neuroimaging Research Branch, NIDA, NIH, Baltimore, MD, USA; [3]Dept. of Neurology, UCLA, Los Angeles, CA, USA; [4]UT Southwestern Med. Center, Dallas, TX, USA; [5]Center for Magnetic Resonance Research, Univ. of Illinois at Chicago, Chicago, IL, USA

Background: Knowledge about intrinsic brain activities has been mostly acquired from resting-state BOLD imaging, although BOLD signal represents the combined effects of cerebral blood volume, flow and metabolism (CBV, CBF and $CMRO_2$) and therefore is difficult to interpret without knowing the complex interplay of these parameters. Furthermore, BOLD signal has relatively poor spatial specificity, compared to CBV and CBF. As such, imaging based on a single physiological parameter may overcome these drawbacks of BOLD. Here, we demonstrate that intrinsic brain activity can be reliably detected by spontaneous fluctuations of CBV-weighted signal using 3D vascular space occupancy (VASO) imaging.
Methods: VASO and BOLD resting-state data of 18 healthy participants were collected. The acquisition parameters of a 3D-GRASE VASO sequence were: matrix size = $64 \times 64 \times 22$, TR/TE/TI = 2500/14.6/742 ms, GRAPPA factor along ky = 3, and total acquisition time = 8 min and 30 s. For comparison, a gradient-echo EPI sequence was used for BOLD imaging acquisition, with most acquisition parameters the same as the VASO. To identify resting functional networks, a group independent component analysis (gICA) was applied to both VASO and BOLD resting data, using the MELODIC in the FSL.
Results: The gICA identified eight meaningful resting functional networks of VASO and BOLD: sensorimotor, auditory, primary visual, higher visual, default-mode, salience, left and right executive-control networks, as shown in Fig.1. Spatial correlation between the VASO- and BOLD-based functional networks revealed a high degree of similarity (mean correlation of 0.45).
Conclusions: We developed a novel 3D-VASO technique for detecting intrinsic brain activities based on CBV fluctuations. Initial results demonstrated that brain networks that often observed in BOLD can be detected reliably by the VASO technique. Since VASO signal has better spatial specificity and less sensitive to susceptibility artifacts than BOLD, the 3D-VASO resting-state fMRI may become an attractive technique for assessing brain activities in regions that precluded by traditional BOLD techniques.
Acknowledgment: This work was supported by the Intramural Research Program of the National Institute on Drug Abuse, NIH.

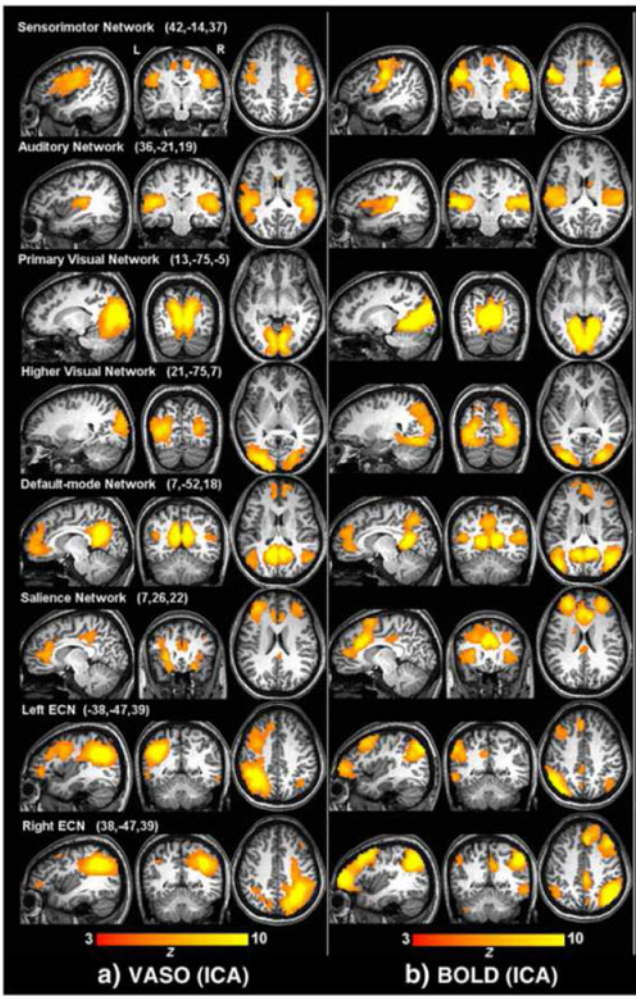

FIG. 1. Brain networks detected by the independent component analysis of the VASO (a) and BOLD (b) data.

P30A Intrinsic functional interactions between the thalamus and cortical networks in human

R. Yuan[1], X. Di[1], P. Taylor[2,3], S. Gohel[1], Y.H. Tsai[4], B.B. Biswal[1]

[1]New Jersey Institute of Technology, Newark, USA, [2]University of Cape Town, South Africa, [3]African Institute for Mathematical Sciences, Muizenberg, Western Cape, South Africa, [4]Chang Gung Memorial Hospital at Chiayi, and Chang-Gung University, Taoyuan, Taiwan

Background: An increasing number of studies have indicated that the thalamus is involved in controlling corticocortical information and cortical communication with the rest of the brain. More than simply relaying information to cortex, this thalamocortical system might be much more complex than it has been thought. By designating to grossly defined cortical segmentation, eg cortical lobes, previous studies [1,2]demonstrated functional connectivity and white matter fiber connections between non-overlapped thalamic sub-regions and grossly defined cortical lobes. In the current study, we used resting-state fMRI to investigate the human thalamocortical system with respect to brain networks.

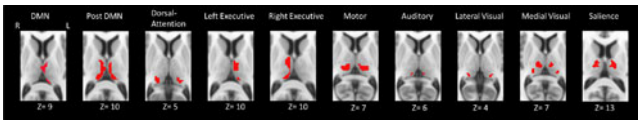

Methods: Resting state fMRI datasets with 198 subjects were downloaded from 1000 Functional Connectomes Project [3]. The functional images were motion corrected, and corregistered to subject's anatomical images. Then functional images were normalized into MNI space. No smoothing was performed. The thalamus ROI was defined by the Harvard-Oxford structural atlases. Seed-based analysis was used to map thalamocortical functional connectivity (FC) between each voxel of the thalamus and the whole brain. Then the independent component analysis was performed on the FC maps to determine distinct connectivity maps between the thalamus and functionally independent brain networks. Using these group-level brain network maps in a spatial regression model against each voxel's correlation map, we estimated the subject-specific thalamic maps for each functional network. These maps were then used to statistically model the thalamic subdivisions with regarding the set of brain networks.
Results: We identified sub-regions of the thalamus with each corresponding brain network as well as functional overlaps between certain networks. The functional overlaps were examined within the context of cortical network relations.
Conclusions: This study demonstrated the thalamocortical relationship in terms of brain networks, including overlaps in the thalamus with implications for functional modulation. This result also suggested that the function of the thalamus should no longer be neglected in functional network studies.
References: 1, Behrens, Nature neuroscience 6, no. 7: 750–757, 2003. 2. Zhang, Journal of neurophysiology, no. 4 (2008): 1740. 3, Biswal BB, PNAS 107(10):4734–9, 2010.

Theme 2: Structural Brain Connectivity/ Multi-modal Approaches/Animal Models

P31A Alterations of the resting state functional connectivity in the GPR88 knockout mice

Tanzil M. Arefin[1,2,3,4], A. Mechling[2,3,4], S. B. Hamida[4], Thomas Bienert[2], Hsu-Lei Lee[2], Dominik V. Elverfeldt[2], Jürgen Hennig[2], Brigitte Kieffer[4,5], and Laura-Adela Harsan[2]

[1]Bernstein Center Freiburg, Germany, [2]Dept. of Diagnostic Radiology, University Hospital, Freiburg, Germany, [3]Faculty of Biology, University of Freiburg, Germany, [4]IGBMC, Strasbourg, France, [5]Douglas Research Center, Canada

Background: The orphan G protein coupled receptor (GPCR) 'GPR88' is densely expressed not only in the striatum and amygdala, but also in olfactory tubercle, and less intensively in inferior olive nucleus[1]. Recently GPR88 gene has drawn an increasing attention in the clinical and pre-clinical research because of its modulated expression in several psychiatric disorder-related treatment[2,3]. However, the neurobiological function of GPR88 and the impact of its modified expression on brain functional connectivity (FC) are so far unknown. In this context, the goal of our study was to investigate the role of GPR88 in brain functional communication, GPR88 knock-out (GPR88 −/−) mice.
Methods: 8 weeks old wild type (n = 15) and GPR88−/− (n = 15) male (74.9% C57B/6J, 25% 129/SvPas, 0.05% FVB/N, 0.05% SJL/J) mice were imaged using a 7T small bore animal scanner and a mouse head adapted cryogenic surface coil (Bruker, Germany). rsfMRI data was acquired[4] with single shot GE-EPI sequences (TE/TR = 10 ms/1700 ms). Group ICA using the MATLAB tool GIFT[5] was carried out to identify the functional clusters of the GPR88−/− mice. Partial positive correlation and graph theory[6] were used to test the connectional relationship of the identified functional clusters, to identify the brain functional hubs and therefore to get an inclusive portrait of GPR88−/− mouse brain FC.
Results: Several findings point toward a remodeling of the mouse brain connectivity in the absence of GPR88. Firstly, less and different brain regions were identified as FC hubs in the GPR88 −/− group (Fig.1, 4 hubs: from left to right: 1. CPu, NAc, 2. S1Sh, S1HL, 3. RSG, SC, 4. Auditory cortex, S2 [Abbrevaitons[7]]) when compared to the WT group (Fig.2, 8 hubs: from top left to bottom right: 1. RSA, V2ML; 2. RSA, RSG; 3. V1, AuD; 4. Visualcortex, S1; 5. Subiculum; 6. RSG, SC; 7. Hippocampus; 8. M1, M2, cg1 [Abbrevaitons[7]]). Secondly, significant group differences were identified in the connectivity of striatum (CPu) and amygdala (Fig.3). Additionally, higher number of functional modules was identified in the GPR88 -/- brains (7), compared with the WT group (5), indicating higher degree of functional network segregation.
Conclusions: This study demonstrates the potential of rsfMRI to noninvasively probe the brain functional networks in genetically modified mice. Here we have shown preliminary data indicating a remodeling of functional networks in GPR88 −/− mice. Further

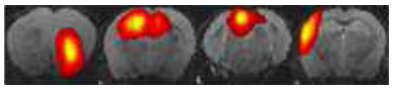

FIG. 1. Hubs specific to the KO.

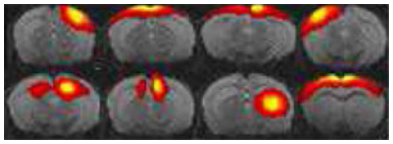

FIG. 2. Hubs specific to the WT.

FIG. 3. Significant group differences (CTRL vs KO) in the FC of the CPu and amygdala.

study involving parallel behavioral investigations will expand our understanding about the implication of GPR88 gene on the development of neurological or psychiatric disorders.

References: [1]Mizushima et al., Genomics, 2000, [2]Conti B. et al., Mol Psychiatry, 2007, [3]Befort K. et al., Eur. J. Neurosci, 2008, [4]A. Mechling et al., Neuroimage 2014, [5]Calhoun et al., 2001, [6]Rubinov and Sporns, Neuroimage, 2010, [7]Paxinos Mouse Brain Atlas.

P32A Functional connectivity of the dorsal and median raphe nuclei at rest

Vincent Beliveau[1], Doug N. Greve[2,3], Claus Svarer[1], Vibe G. Frokjaer[1], Gitte M. Knudsen[1], Patrick M. Fisher[1]

[1]Neurobiology Research Unit, Copenhagen, Denmark, [2]Athinoula A. Martinos Center for Biomedical Imaging, Boston, MA, USA, [3]Harvard Medical School, Boston, MA, USA

Background: Serotonin (5-hydroxytryptamine, 5-HT) is a key neurotransmitter that modulates a broad range of functions and is implicated in the pathophysiology of neuropsychiatric disorders including mood, anxiety and sleep disorders. Serotonergic functions are however still not fully understood and further knowledge can be gained by the study of functional connectivity (FC) of serotonergic nuclei using resting-state functional magnetic resonance imaging (rs-fMRI). The dorsal raphe (DR) and median raphe (MR) nuclei contain the serotonergic neurons that project throughout brain and thus provide a target for a seed-based probe of serotonergic FC. Here we estimated DR and MR rs-fMRI using a multimodal neuroimaging approach including a subject-specific automated DR/MR delineation procedure based on high-resolution serotonin transporter (SERT) positron emission tomography (PET) scans applied to rs-fMRI scans.
Methods: Forty-nine healthy women completed 1) a 10 min rs-fMRI scan acquired on a Verio 3T MRI scanner and 2) a 90 minute high-resolution [^{11}C]DASB PET scan to measure SERT binding as part of a broader study protocol. Using voxel-level PET time activity curves, we developed a novel algorithm to automatically delineate subject-specific DR and MR regions based on known anatomical constraints. These regions were applied to the rs-fMRI data from which we extracted time series to use as seeds in a FC analysis in cortical and subcortical spaces using the software package Freesurfer.
Results: The DR and MR seeds produced similar FC maps. For both seeds, we observed significant positive FC within raphe/brainstem, rostral anterior cingulate (rACC), basal ganglia (putamen, caudate, pallidum), thalamus, hippocampus, amygdala, insula and cerebellum. Negative FC was observed within the pre- and postcentral gyrus (Pr-PoG) for the DR but not for the MR.
Conclusions: For both DR and MR, FC was observed within regions highly innervated by serotonergic projections, supporting that these FC maps represent a serotonin-related resting state network (RSN). The observed FC maps overlapped with the previously described basal ganglia (BG) RSN, but extended to additional cortical and subcortical regions, suggesting that this BG RSN may effectively be part of a broader RSN related to serotonin. DR is also known to be implicated in the inhibition of nociceptive inputs to the somatosensory cortex and the negative FC observed within the Pr-PoG for DR supports a role for this function at rest. Preliminary analysis suggests good reproducibility both for the DR and MR seeds and observed FC maps but this requires additional investigation. In conclusion, these findings provide a novel method for estimating serotonergic brain functions, which can benefit the investigation of related neuropsychiatric illnesses.

P33A The functional dissociation between the language and the cognitive control systems persists in subcortical and cerebellar regions

Idan Blank[1] and Evelina Fedorenko[1,2]

[1]Department of Brain and Cognitive Sciences, MIT, Cambridge, MA, USA; [2]Department of Psychiatry, MGH, Charlestown, MA, USA

Background: The relationship between language and other high-level cognitive systems has been long debated. Recent fMRI studies have shown that frontal and temporal regions that respond robustly to linguistic stimuli show little response to a wide range of non-linguistic, cognitive tasks. In contrast, frontal and parietal regions of the cognitive control (CC) system do respond to such tasks, increasing activity as cognitive demands increase. Evidence that these two large-scale systems dissociate in their patterns of resting state BOLD signal fluctuations further suggests that they support distinct cognitive processes. Here, we used fMRI to test whether the language and CC systems include subcortical and cerebellar components in addition to their cortical components, and whether such components exhibit a similar functional dissociation.
Methods: In 18 adults, we studied candidate components of the language and CC systems in ten bilateral pairs of subcortical regions and the cerebellum. First, within each region, we functionally localized sub-regions of interest that responded to a previously validated language task (''language ROIs'') or to a working memory task (''CC ROIs''). Then, we examined the resting state functional correlations between BOLD signal fluctuations in these ROIs and in (functionally-localized) cortical language and CC ROIs.
Results: Most subcortical and cerebellar regions contained robustly localizable language ROIs, except for the right caudate and thalamus. Similarly, most regions contained robustly localizable CC ROIs, except for the left posterior cingulate, left hippocampus and bilateral amygdala. Overlap across language and CC ROIs was minimal. Resting state data from these ROIs revealed four functional correlation profiles: (1) in the right insula, bilateral anterior and middle cingulate and cerebellum, language ROIs were more correlated with the cortical language system than with the cortical CC system (''language-bias''), while CC ROIs showed the opposite pattern (''CC-bias''); (2) in the bilateral posterior cingulate, hippocampus and amygdala, language ROIs showed a language-bias but CC ROIs (when localizable) did not show a CC-bias; (3) in the bilateral thalamus and left insula, language ROIs (when localizable) did not show a language-bias but CC ROIs did show a CC-bias; and (4) in the basal ganglia, no language- or CC-bias was observed.

Conclusions: Most excitingly, several regions had both ROIs that showed a language-bias and ROIs that showed a CC-bias, similar to e.g. Broca's area, which contains functionally distinct language and CC ROIs with opposite functional correlation patterns. The precise functional contributions of such ROIs remain to be determined, as do the contributions of ROIs that respond to either the language or CC localizer tasks but do not show a language- or CC-bias, respectively. Regardless of their specific contributions, our data clearly demonstrate that many subcortical regions and the cerebellum are functionally heterogeneous and include components that belong to different, large-scale brain systems, thus contributing to high-level cognition in a number of distinct ways.

P34A Characterizing Network Connectivity with Infraslow Fluctuations of the High Gamma Band Using Electrocorticography

K. Casimo[1], J.D. Wander[2], F. Darvas[3], T.J. Grabowski[1,4], J.G. Ojemann[1,3], K.E. Weaver[4]

[1]Program in Neurobiology and Behavior, Depts. of [2]Bioengineering, [3]Neurological Surgery, [4]Radiology, University of Washington, Seattle, WA, USA

Background: Resting state fMRI (rsfMRI) estimates of functional connectivity (fc) have yielded tremendous insight into the organization and natural physiology of the brain's intrinsic architecture. Despite the wide-spread application of rsfMRI, the electrophysiological dynamics underlying spontaneous, infraslow (<0.1 Hz) fluctuations of the BOLD signal interactions across a network has received considerably less attention. Previous studies using surface-based MEG/EEG have focused on spontaneous activity within higher frequency ranges including alpha (8–12 Hz) and beta (12–30 Hz.) bands. However, paralleling rsfMRI studies to a greater degree, a few electrocorticographic (ECoG) investigations have revealed a modulation function within the infraslow (<1 Hz) range of the high gamma (HG; 70–200 Hz) range. Infraslow HG (ifsHG) amplitude fluctuations have been previously used to identify the default mode network (DMN) over several hours of ECoG data. In an effort to characterize the electrophysiological dynamics of ifsHG interactions across nodes of the DMN, we have begun to apply various computational approaches to short (8 min) resting-state periods of spontaneous ECoG data.
Methods: This is an ongoing study with active data collection. Here we include data from three epilepsy patients undergoing long-term seizure ECoG monitoring. Eight minutes of resting state ECoG data was acquired, inspected for epileptiform discharges, re-referenced for the common-average, and band-pass filtered for HG. Signals were then subjected to a secondary band-pass within the infraslow range (0.1–1 Hz). DMN electrodes were selected based on spatial overlap with a DMN fc map generated by combining a standard posterior cingulate (PPC) seed point analysis to preoperatively rsfMRI. Pairwise correlations, which capture tightly coupled signals and pairwise phase-locking values (PLVs) which are sensitive to a consistent phase relationship, were estimated for the ifsHG envelope across all channel pairs within a recording montage.
Results & Conclusions: Pairwise correlations and PLVs were higher for pairs of electrodes that were both in DMN regions as defined by preoperative fMRI, though neither feature captured all of the electrodes in DMN regions. Pairwise correlation detected some pairs where only one or neither electrode was in the DMN. Both measures detected electrodes in DMN regions for all three subjects. Concurrent and overlapping pairwise correlation and PLV of the ifsHG fluctuations suggests an additional level of computation between nodes of a network during the resting state. Future directions include analysis of additional signal features, including linear and non-linear coupling measures. Contrasting various computational approaches to time-varying ECoG signals from across nodes of a network may yield insight into the electrophysiological mechanisms contributing to resting state interactions.

P35A Functional connectivity mapping in mouse model of Huntington disease

Kai-Hsiang Chuang[1], Wei-Tang Chang[1], Hui Chien Tay[1], Porshin Ng[1], Lynn YC Ho[1], Michael R. Hayden[2,3], Mahmoud A. Pouladi[2,3]

*[1]Singapore Bioimaging Consortium, A*STAR, Singapore, [2]Translational Laboratory of Genetic Medicine, A*STAR, Singapore, [3]Department of Medicine, National University of Singapore, Singapore*

Background: Resting-state functional connectivity MRI has been widely applied in neurodegenerative diseases and psychiatric disorders. Mouse models of these diseases provide further understanding of disease mechanisms and relevant treatment effects. Recent finding in Huntington disease suggests that axonal dysfunction may be a driving mechanism of the huntingtin gene defects. Here we applied our recently established method for imaging resting-state functional connectivity in mouse brain to the YAC128 mouse model of Huntington disease (Nasrallah, Neuroimage 2014).
Methods: YAC128 transgenic mice of FVB background which expresses full length of human huntingtin gene was used. Mice were sedated by medetomidine using a protocol optimized for mouse resting-state fMRI and scanned on a 9.4 T MRI (Agilent Technologies, USA). fMRI of both resting state and forepaw stimulation (6 Hz, 0.5 mA) was performed. GE-EPI of TR/TE = 2000/15 ms, slices = 15, voxel = $0.31 \times 0.31 \times 0.5$ mm3 was used. Structural data was acquired by FSE. Resting state fMRI data was regressed with signal from ventricle and skin to remove physiological noises and other artifacts. Bandpass filter at 0.01 and 0.1 Hz was applied and spatial smoothing was done with Gaussian kernel of 1 pixel FHWM. Signal in ventricle was regressed out to reduce. Connectivity maps were generated by correlation ($r>0.25$, cluster threshold = 4 voxels) using seed points in the primary somatosensory cortex (SI) and caudate putamen (CPu).
Results: Compared to wild-type mice, YAC128 mice showed lower bilateral connectivity in both the SI and CPu. Especially, the 48 weeks old YAC128 mice show further reduction compared to the age-matched wild-type and the younger YAC128 mice of 22 weeks old.
Conclusions: The preliminary study indicates that bilateral connectivity is impaired in the Huntington mice. This could be associated with their behavior deficits on motor function. The results also correlated with the reduced FA in corpus callosum (Hong, ISMRM 2014). However, a caveat of the disease study is the potential change in vasculature and neurovascular coupling, which confound the BOLD signal measure. Further examination of the cerebral blood flow and neurovascular in the disease mice is ongoing.

P36A Long-term effects in rat resting state networks following postnatal morphine exposure

D. Bajic[1,2], M.M. Craig[1], D. Borsook[1,2], L. Becerra[1,2]

[1]Department of Anesthesiology, Perioperative and Pain Medicine, Boston Children's Hospital, Boston, Massachusetts; [2]Department of Anaesthesia, Harvard Medical School, Boston, Massachusetts

Background: Exposure to prolonged morphine treatment during development is associated with increased incidence of opioid tolerance and dependence. This suggests that neonatal chronic morphine treatment risks altering normal brain network development. Currently, the long-term consequences of neonatal morphine treatment on functional brain networks are not known. We hypothesized that functional activity in resting state networks following chronic morphine administration in adulthood will differ depending on previous exposure to opioids in postnatal period.
Methods: The study was approved by Boston Children's Hospital IACUC. Rats received twice-daily injections of either morphine (10 mg/kg, N = 12, MMA Group) or equal volume of saline (N = 7, SMA Group) subcutaneously for 13 ½ days (postnatal day (PD) 1–14). Morphine group underwent a weaning period of 10 days to prevent withdrawal. Subsequently in adulthood, both groups received an additional two weeks of morphine treatment (PD55–70) following which they underwent high field functional magnetic resonance imaging (fMRI). Imaging: A 7T Bruker Biospec MRI was used for this study, animals were anesthetized with isoflurane (0.5–1%). Animals underwent an anatomical scan (RARE : 256^2 in-plane resolution FOV:3 cm, 0.6 mm 40 slices, TR/TE = 5.3/33 ms), and a functional scan (EPI: 64^2 in-plane resolution, FOV: 3 cm, 1 mm slices, TR/TE = 1 s/21.5 ms, 600 volumes). Analysis was performed with fsl. Preprocessing steps included brain extraction, motion correction, high pass filtering-100 s and spatial smoothing 0.7 mm. We used independent component analysis (ICA) to determine total group components and subsequently used dual regression to determine differences in connectivity between the groups. A rat brain template from our lab was used for registration and group comparison. Group ICA results were compared to published RSN rat templates (Becerra et al. Neuroimage 2011) for network identification.
Results: We identified 6 published rat brain networks (Becerra et al. PloSe One 2011): default mode (DMN), sensorimotor (SMN), interoception (ICN), cerebellar, basal ganglia and autonomic networks. We observed significant differences in connectivity in DMN, SMN, and ICN. The DMN displayed increased connectivity with orbito frontal (OFC), anterior cingulate, primary sensory, nucleus accumbens (NAc) and PAG. The SMN displayed increased connectivity with OFC, NAc, Caudate Putamen, hippocampus and thalamus. The ICN only displayed decreased connectivity with primary motor, septal nucleus, retrosplenial, and hippocampus.
Conclusions: These results suggest exposure to morphine in neonates produced brain alterations in adulthood when re-exposed to morphine. Several brain networks associated with analgesic pathways displayed hyperconnectivity with intrinsic brain networks. The interoception network only presented reductions in connectivity.
Support: NIH K08 DA035972-01 and Trailblazer Award Department of Anesthesia at Boston Children's Hospital (Bajic), NIDA K24 (Borsook).

P37A Cross-frequency coupling mechanisms in the ongoing resting-state

E. Florin, S. Baillet

Montreal Neurological Institute, Montreal, Quebec, Canada

Background: Even after 20 years of research little is known about the electro-physiological correlates of structured BOLD fluctuations during rest. In the present study, we propose and demonstrate with MEG source imaging a possible electrophysiological mechanism underlying resting-state BOLD fluctuations and probe this mechanism based on visual stimulation.
Methods: We recorded 26 healthy subjects with MEG. 12 subjects were only measured at rest (5–30 minutes) and the other 14 were presented with a visual stimulation consisting of inwards moving circles (Hoogenboom et al., 2006). Before and after visual stimulation 5 minutes of rest were recorded.

A forward solution and the constrained minimum norm imaging kernel were computed with Brainstorm. For each source time-series we determined the strongest phase-amplitude coupling (PAC) between 2–30 Hz and 80–150 Hz. At the troughs and peaks of the low-frequency phase the gamma-amplitude was extracted and a new time-series generated. Based on these time series the resting state networks were obtained with singular value decomposition.
Results: The resting state analysis revealed the expected networks that are consistent with the resting-state networks described in the literature using fMRI. We found no significant difference in PAC value for the resting period before and after the visual stimulation, indicating a consistent mechanism during rest. However, once the visual stimulation starts the PAC value significantly increases. Still, the low-frequency corresponding to the highest PAC of the rest period and the low-frequency that couples strongest to the evoked visual gamma response were identical.
Conclusions: Our results suggest that the mechanisms that reveal the brain's resting-state networks with fMRI are based on the cross-frequency coupling between a low-frequency phase and high-gamma amplitude. The PAC is a constant mechanism even if interleaved with visual stimulation and it has a predictive value for the evoked gamma response during visual stimulation.

P38A Injury alters the intrinsic functional connectivity of spinal cord grey matter in monkeys

L.M. Chen[1,2], A. Mishra[1,2], F. Wang[1,2], J.C. Gore[1,2]

[1]Vanderbilt University Institute of Imaging Science, Nashville, TN, USA, [2]Department of Radiology and Radiological Sciences, Vanderbilt University Medical Center, Nashville, TN, USA

Background: The objectives of this study are to establish whether distinct functional connectivity patterns can be detected within spinal grey matter in non-human primates, and whether traumatic injury alters connectivity between regions in the spinal cord.
Methods: Five squirrel monkeys underwent MRI scanning repeatedly under light isoflurane anesthesia at 9.4T. MR images of spinal cords were acquired with a saddle-shape surface transmit-receive coil. Parallel high-resolution axial images ($0.25 \times 0.25 \times 3\ mm^3$ resolution) were acquired with off-resonance saturating pre-pulses (sensitive to magnetization transfer) to differentiate grey and white

matter. Resting state BOLD-sensitive fMRI (rsfMRI) images ($0.5 \times 0.5 \times 3\ mm^3$ resolution) were obtained using a multi-slice gradient echo sequence (TE/TR = 6.5/24 ms, single volume acquisition time = 1.54 s). Pre-processing of rsfMRI signals included standard procedures and regression of the muscle and CSF signal using the PCA component that accounts for major (at least 70%) of the cumulative variance. Five seed regions of interest (ROIs) were manually placed, at the four horns and in the white matter in each slice, and the inter-voxel correlations to each seed ROI were quantified. Two monkeys subsequently underwent surgery to produce unilateral dorsal column lesions at the C4-C5 spinal cord level, and both exhibited behavioral deficits on food reaching and retrieval within the first 2 weeks after surgery. The location and extent of the spinal cord lesions were later validated histologically.

Results: We found in normal monkeys; 1) across-slice ventral and dorsal horns showed high resting state functional connectivity, and correlation strength reduced as a function of distance from the seed along the cord; 2) horns were more strongly inter-connected than to white matter structures; 3) inter-regional correlation patterns were reproducible across imaging runs, session within each monkey and across animals. In two spinal cord lesioned animals, we found; 1) significantly reduced connectivity within the spinal cord segments below the lesion (two 3 mm thick slices); 2) dorsal to ventral horn connectivity on the lesion side was significantly weaker than that of contralateral normal side.

Conclusions: Our data demonstrate that distinct functional networks may be identified in normal grey matter in the spinal cord using resting state fMRI methods, and these networks are altered following traumatic injury.

P39A Correlations between DTI structural connectivity and EEG functional connectivity coherence measures in autistic and neurotypical populations

M.C. Baker[1], D. Patel[1], T. Monday[1], J. Hou[1], R.C. Anderson[1], E. Hames[1]

[1]*Texas Tech University, Lubbock, TX, USA*

Background: Autism has been hypothesized to be a disorder in which, among other things, connective pathways within the brain are different from those in neurotypicals, with both under- and over- connectivity reported in the literature. Diffusion tensor imaging (DTI) has been used to measure structural connectivity via fractional anisotropy (FA) and mean diffusivity (MD). EEG coherence between channel pairs has been used to determine functional connectivity between brain regions. The objective of this study was to compare DTI structural metrics (FA and MD) and EEG functional coherence to determine how the two measures correlate, and how the correlations differ in individuals with autism compared with neurotypical populations.

Methods: This study consisted of 10 participants, five neurotypical (NT) controls and five autistic (ASD), between the ages of 13 and 18. EEG coherence was measured during an executive attention task using a EGI 64-channel HydroCel Geodesic Sensor Net. EEG coherence pairs were selected to provide anterior, posterior, and far coherence measures in both hemispheres. DTI data were acquired using a Siemens Skyra 3T system. Acquired diffusion data were preprocessed using a MATLAB toolbox named 'Pipeline for Analyzing braiN Diffusion imAges' (PANDA). Regions of interest (ROIs) defined in the whole brain regions were created by overlying the TBSS-generated skeleton from the Johns Hopkins University DTI-based probabilistic tractography atlas. Average FA and MD values were determined for each region. Statistical tests (ANOVA and t-tests) were used to determine FA regions, MD regions, and EEG coherence pairs that were different between autistic and neurotypicals. Correlations were calculated between EEG coherence for all channel pairs and FA and MD structural connectivity measures for all regions of interest.

Results: Overall, EEG coherence was found to be higher in controls than in autistics across all frequency bands, with the exception of some left frontal-temporal and central parietal regions. FA was typically higher and MD lower in controls compared to autistics. When EEG coherence values for alpha and beta bands were correlated with FA values, autistics showed positive correlations between left and right EEG coherence values and FA values for left and right fiber tracts, while controls showed negative correlations.

Conclusions: Our data indicated that controls had greater connectivity than autistics, as determined by both functional and structural measures. In autistics, the structural and functional measures were more likely to have a positive correlation, while in controls the measures were more likely to be negatively correlated. This suggests that autistics and controls might have different ways of accessing and transmitting information during a task that requires specific functional connections.

P40A Temporal variation of correlations between EEG low frequency fluctuations and MREG

T. Hiltunen[1], V. Korhonen[1], T. Starck[1], V. Kiviniemi[1]

[1]*Oulu University Hospital, Oulu, Finland*

Background: Infra-slow (< 0.1 Hz) EEG fluctuation areas correlate to BOLD signal fluctuations in resting state network (RSN) distributions. The same BOLD RSNs have shown spatiotemporal variation and in this study we wanted to explore if this variation exists also in the EEG vs BOLD signal correlation.

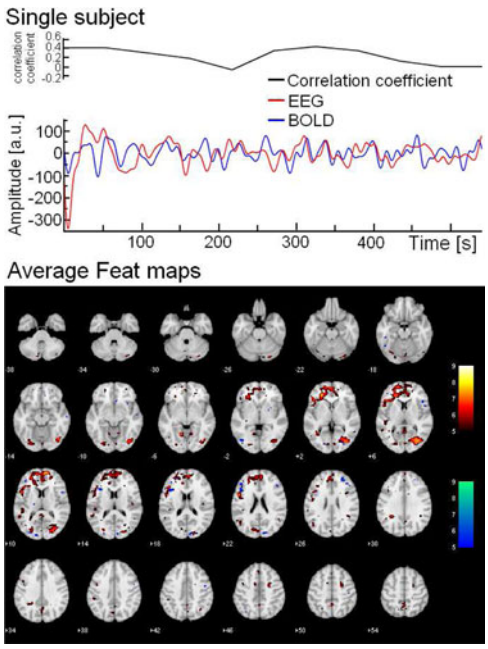

Methods: We performed resting state fMRI-EEG study to 9 healthy volunteers. FMRI was done with 3T SKYRA using MREG sequence (TR 100 ms). Group PICA was performed and DMN_{vmpf} component was selected for further analyses. EEG was recorded with 32-channel MR compatible system. Scanning artefacts were removed and ICA (32 comp) was calculated. Components were down-sampled to 10 Hz and bandpass filtered to 0.009–0.08 Hz. After that they were divided to 2 min time windows with 50% overlap. Correlation maps between EEG IC time series and MREG DMN_{vmpf} were calculated using to MREG DMN_{vmpf} highest correlating EEG ICs as Feat regressors. Also correlation coefficients (cc) were calculated.
Results: Correlation coefficients varied in 2 min time windows (upmost signal in figure) and average correlation Feat maps showed higher correlations in DMN_{vmpf} area when using the highest correlation 2 min time window (red-yellow in figure) than when using the lowest correlation 2 min time window (blue-green in figure).
Conclusions: EEG (0.009–0.08 Hz) correlations to MREG DMN_{vmpf} shows marked spatiotemporal variability.

P41A Identification of Brain Networks participating in the Transition from the Default Resting State to an Emotionally Willed Movement

C. Karmonik[1], A. Verma[2], S.H. Fung[3] T, R.G. Grossman[1]

Departments of [1]Neurosurgery, [2]Neurology and [3]Radiology, Houston Methodist, Houston, TX, USA

Background: Investigation of the mechanisms of switching from a brain at rest to goal-directed behavior can be used to identify and quantify the interaction strength of brain regions that participate in the generation of willed activity.
Methods: With subjects (n = 9) in the resting state for 60 seconds, 10 images of faces were presented. Subjects could remove a face eliciting an unpleasant emotional response by squeezing a ball for 10 seconds (right hand). Separate BOLD fMRI activation maps for pleasant and unpleasant faces (5 unpleasant faces) were calculated and brain region with higher activation for unpleasant faces were identified ($p < 0.05$). Differences in 2D and 3D interaction networks created using graph-theoretical analysis were quantified ($p < 0.05$). 3D printing technology was investigated for improving visualization of 3D networks.
Results: Statistically significant larger activation for responding to unpleasant faces existed predominately in the left hemisphere (figure 1): in the motor cortex, inferior parietal lobe, frontal gyrus, insula, thalamus and caudate. Bilateral activation was found in the supplementary motor area and in the anterior cingulate. Statistically significant larger activation for responding to pleasant faces was distributed more bilaterally in the frontal gyrus, in the precuneus, the posterior cingulate gyrus, the middle temporal gyrus, the thalamus and parahippocampal gyrus. Interaction networks for the response to the unpleasant faces showed higher density, eigenvalues and eccentricity than for the pleasant faces. Average interaction path length was shorter when responding to unpleasant faces. 3D printouts of interaction networks helped visualize complexity of 3D network graphs.
Conclusions: The initiation of a willed movement in response to an unpleasant stimulus relative to a pleasant stimulus predominantly engages areas in the left hemisphere (in right-handed subjects) including emotional and executive regions. Corresponding interaction networks demonstrated a stronger centrality and connectivity expressed by higher values for the largest eigenvalue and average path length.

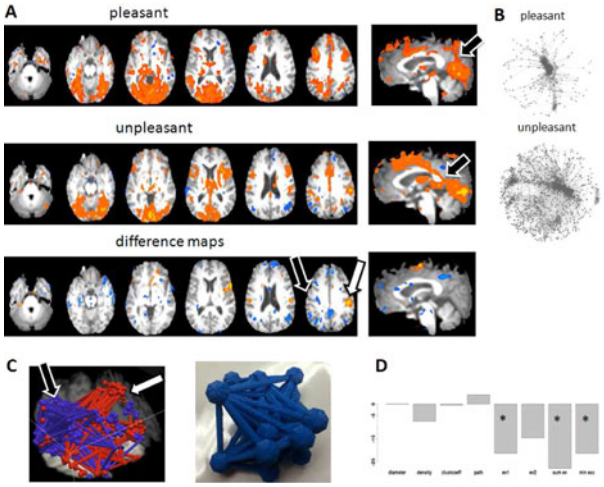

FIG. 1. **A:** BOLD fMRI activation maps when responding to pleasant and unpleasant faces. Of note is a band of activity between sensory input (visual cortex) and precuneus (filled arrow) for the response to the pleasant stimuli and a shift of this band connecting the motor area to the visual cortex for the unpleasant stimulus. **B:** 2D visualization of interaction networks for subject #1 revealing a small-world nature for both stimuli with a more compact appearance for the unpleasant faces. **C:** 3D visualization of interaction networks overlaid on anatomy on left (blue: response to pleasant faces, red: response to unpleasant faces) and 3D printout of 3D interaction network on right for response to unpleasant faces as well as photo of 3D printout. **D:** Difference (in percent) in values for selected network parameters (path: average path length, ev: eigenvalue, min ecc: minimum eccentricity). Except average path length, values for all parameters are reduced for the pleasant relative to the unpleasant faces.

P42A Dynamic resting state functional connectivity in awake and anesthetized rodents

Zhifeng Liang[1], Xiao Liu[2], Nanyin Zhang[1]

[1]Department of Biomedical Engineering and The Huck Institutes of Life Sciences, The Pennsylvania State University, University Park, PA 16802 [2]Laboratory of Functional and Molecular Imaging, National Institutes of Health, Bethesda, MD 20892

Background: It has been increasingly recognized that resting-state functional connectivity (RSFC) is dynamic in nature. Methods like sliding window correlation and single volume co-activation have been utilized to reveal dynamic properties of RSFC in humans. However, dynamic RSFC in animals is much less explored.
Methods: Resting-state fMRI data of 42 male Long-Evans rats were acquired at a 4.7 T Bruker scanner at the awake condition. 16 rats were also imaged under the anesthetized condition (1.5% isoflurane). Functional images were preprocessed with conventional procedures. The regionally averaged time series of infralimbic cortex (IL) were extracted, and 15% frames with the highest seed signal intensity were averaged to generate mean maps. In addition, these frames were clustered into 3 co-activation patterns

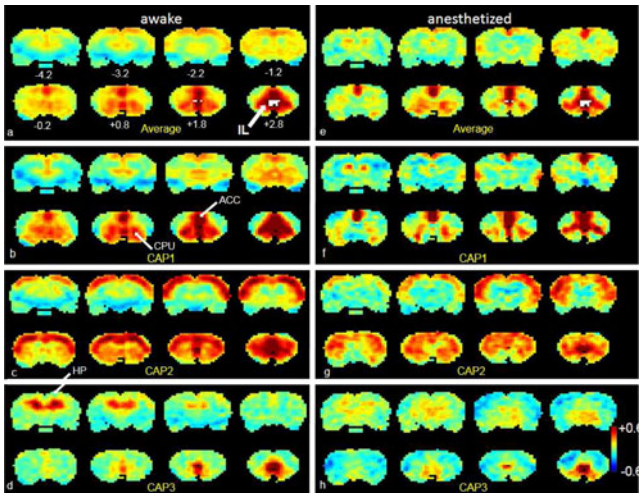

FIG. 1. Distinct spatial CAPs of IL. Left (a-d), awake. Right (e-h), anesthetized. a,e, average d map. b-d, f-h, CAPs. Colorbar in standard deviation (SD).

(CAPs) based on their spatial similarity using k-means clustering. To evaluate the temporal evolution properties of these CAPs, the averaged map of each CAP was used as a template to calculate the spatial correlation with individual frames. The spatial correlation (SC) was thresholded at 0.2 ($p < 10^{-6}$). The time 0 ($t = 0$) was defined at SC peaks, and 5 frames before and 6 frames after $t = 0$ were selected and those frames were together considered as one epoch for a CAP.

Results: The averages of top 15% frames closely resembled the results of conventional seed-based functional connectivity for IL maps in both awake and anesthetized conditions. Importantly, each CAP showed distinct spatial patterns that were not prominent in averaged maps (Fig. 1). In addition, the differences between awake and anesthetized conditions were more apparent in individual CAPs than in the averaged maps. For example, co-activation in hippocampus was significantly stronger in awake than anesthetized states (Fig. 1.d and h), and this difference was not as appreciable in the averaged maps. For temporal dynamics, epochs of all CAPs showed consistent temporal evolution in the scale of 10 s.

Conclusions: The results validated the single-volume co-activation method in rats. CAPs revealed subtle differences between awake and anesthetized states, which were not apparent in averaged maps. Importantly, those CAPs also have consistent temporal patterns.

P43A Temporoparietal junction connectivity is modulated by attentional state

C.J. Lynch[1], X. You[1], M. Norr[1], E.M. Gordon[1], C. Vaidya[1,2]

[1]*Department of Psychology, Georgetown University, Washington, DC*
[2]*Children's Research Institute, Children's National Medical Center, Washington, DC*

Background: Adaptive behavior requires flexible reorienting of attention in response to changing demands in our environment. Such reorienting is posited to engage the ventral attention system, particularly the right temporoparietal junction (rTPJ), which activates in response to unexpected but relevant stimuli for the task at hand. How rTPJ connectivity is modulated in response to unexpected relevant events remains unclear. We examined these changes in rTPJ connectivity as participants transitioned three attentional states, 1) a resting-state reflecting no attention demands; 2) a selective attention task with unexpected irrelevant stimuli (IR); and 3) a selective attention task with unexpected behaviorally relevant stimuli (BR). Task-conditions were regressed from the IR and BR task-runs, to facilitate comparability with the resting-state run. Further, we examined whether modulation of rTPJ connectivity across the three attentional states predicted individual differences in attentional function in everyday life.

Methods: Fifty adults underwent fMRI at 3T on a Siemens Tim Trio completing a resting-state scan followed by IR and BR task runs. Subjects completed the Adult ADHD Self-Report Scale v1.0 (ASRS) during a separate visit. For both task runs, subjects monitored for a centrally presented target triangle. On the IR run, task irrelevant distractor stimuli flashed in the periphery of the display. On the BR runs, subjects monitored for a target distractor, in addition to the central task. Thus, the two runs were identical, except for the behavioral relevance of distractors. Data were preprocessed and analyzed using SPM8. Functional data were slice time corrected, realigned, normalized to the Montreal Neuropsychological Institute (MNI) template, and spatially smoothed. Data were bandpassed filtered (0.01-.01 Hz), and head motion and mean WM/CSF signals regressed out. For the IR and BR task runs, task conditions were additional regressors of no interest. Seed-based rTPJ (Fox et al., 2006, MNI: 63, −41, 36) connectivity maps were generated for each subject for each of the three fMRI runs and then compared using a repeated measures ANOVA. A step-wise multiple regression analysis examined whether the slope (Rest < IR < BR) of rTPJ connectivity (z-values) to regions identified by the ANOVA across the three attentional states predicted scores on the inattention scale of the ASRS.

Results: The ANOVA revealed that rTPJ connectivity with ventral attention regions, including the ventral prefrontal and insular cortex, and dorsal parietal regions, including the right posterior parietal cortex (rPPC) and left intraparietal sulcus, were modulated by attentional state ($p < 0.05$, monte carlo correction). Regression analyses revealed that slope of the rTPJ-rPPC connection across attentional states was most predictive of inattention scores ($r = -0.39$, $p < 0.007$).

Conclusions: These findings suggest that rTPJ connectivity is indeed sensitive to differing attentional demands (i.e. the relevance of unexpected events) and, critically, the observed pattern of network modulation is behaviorally meaningful. This may provide preliminary insight into potential mechanisms by which the rTPJ selectively encodes relevance of unexpected stimuli. Furthermore, this work highlights a novel method for examining connectivity of large-scale functional systems across resting and evoked brain states.

P44A Effects of childhood maltreatment on brain connectivity of the fiber-stream networks

K. Ohashi[1,2], C.M. Anderson[1,2,3], E. Bolger[1], C.E. McGreenery[1], H. McCormack[1], A. Khan[1,2], G. Vitaliano[1,2], M.H. Teicher[1,2]

[1]*Developmental Biopsychiatry Research Program, McLean Hospital, Belmont, MA*
[2]*Department of Psychiatry, Harvard Medical School, Boston, MA, USA*
[3]*Brain Imaging Center, McLean Hospital, Belmont, MA, USA*

Background: Childhood maltreatment is a major risk factor for mood, anxiety and substance abuse disorders. Previous studies

have shown alterations in specific brain regions for individuals with history of maltreatment. However, beyond specific brain regions and circuits, the effects of maltreatment on brain networks are not yet understood. The aim of this study was to test the hypothesis that exposure to childhood maltreatment alters the connectivity network of white matter pathways assessed by graph theory using diffusion tensor imaging and tractography.
Methods: Two hundred sixty three healthy unmedicated subjects (102 M/161 F; 18–25 years; 22.4 ± 2.3, mean $\pm$ SD) were neuroimaged and analyzed using DTI and fiber tractography. History of exposure to maltreatment was retrospectively assessed by Maltreatment and Abuse Chronology of Exposure (MACE) scale and Traumatic Antecedent semi-structured interviews. Cerebral cortex was parcellated into 90 regions. Numbers of fiber-streams interconnecting all pairs of regions were calculated to construct a white matter connectivity network. Each cortical region and number of fiber-streams interconnecting regions were defined as nodes and edges. Network measures were calculated for all individuals and compared between groups of subjects with exposure to maltreatment versus subjects without. Global/local efficiency, cost, strength, pathlength and clustering coefficient were calculated for the whole brain network. Relative importance of each node was assessed by determining their degree/strength, betweenness, local clustering coefficient, closeness and eigenvector centrality. Analyses were adjusted for effects of gender, age, parental education and household finances.
Results: Global efficiency ($p < 0.02$), cost ($p < 0.02$) and network strength ($p < 0.06$) were significantly smaller and path length was significantly greater ($p < 0.04$) in subjects with histories of maltreatment (corrected for multiple comparisons). The most marked reductions in nodal centrality measures were observed in right putamen ($p < 0.01$: corrected) and in the left orbital part of inferior frontal gyrus ($p < 0.0007$, uncorrected). Additional uncorrected differences were observed in temporal regions and other components of frontal cortex and basal ganglia.
Conclusions: Childhood maltreatment has global effects on the connectivity network of the white matter fiber-stream pathways. Frontal, basal ganglia and temporal regions were most severely affected. This may indicate altered information processing in these regions leading to enhanced risk for mental disorders.

P45A Decoupling of structural and functional brain connectivity in older adults with white matter hyperintensities

Y.D. Reijmer[1], A.P. Schultz[2], M.E. Gurol[1], R.A. Sperling[2], S.M. Greenberg[1], A. Viswanathan[1], T. Hedden[2]

[1]J. Philip Kistler Stroke Research Center,
[2]Athinoula A. Martinos Center for Biomedical Imaging, Massachusetts General Hospital, Boston, MA, USA

Background: Aging is associated with disturbances in large-scale functional networks. These functional impairments are assumed to arise from disconnectivity of underlying white matter tracts. Here we probed whether the degree of functional connectivity between major nodes of the default mode network (DMN) was specifically related to structural connectivity of the connected white matter tract in a sample of clinically normal older adults. We additionally examined whether coupling between structural and functional connectivity was impacted by white matter hyperintensity (WMH) burden.
Methods: One hundred twenty-five individuals (mean age 74 ± 6 years, 63% female) underwent a resting-state fMRI scan, a diffusion weighted MRI scan, a FLAIR scan, and cognitive testing. Functional connectivity between the posterior cingulate cortex (PCC) and medial prefrontal frontal cortex (MPFC) of the DMN was calculated by correlating the average fMRI time series between the two regions. Fiber tractography was used to reconstruct the cingulum bundle connecting these two DMN regions and the mean fractional anisotropy (FA) and mean diffusivity (MD) of the tract was computed. The inferior longitudinal fasciculus (ILF), a tract not connected to the PCC or MPFC, served as a control tract. WMH volume was classified using the Fazekas visual rating scale and individuals were classified as having low (score 0 or 1) or high WMH (score 2 or 3) burden. Analyses were adjusted for age and sex.
Results: Individuals with high WMH burden ($n = 61$) were older, had lower resting-state functional connectivity, lower tract FA, and higher tract MD than elderly with low WMH load ($n = 64$). Within the low WMH group, functional connectivity between the PCC and MPFC was specifically correlated with FA and MD of the cingulum bundle (FA: $r = 0.36$; $p = 0.003$; MD: $r = -0.53$; $p < 0.001$), and not with FA/MD of a non-connecting tract (ILF: $r < 0.12$; $p > 0.34$). However, the relationship between cingulum microstructure and PCC/MPFC functional connectivity was absent in elderly with high WMH burden (FA: $r = 0.09$; $p = 0.52$; MD: $r = 0.02$; $p = 0.86$; MD $\times$ WMH burden interaction $p = 0.01$). In this group, functional and structural connectivity were independently related to information processing speed and executive functioning ($p < 0.05$).
Conclusions: We observed a location specific relationship between functional connectivity of two major DMN nodes and structural connectivity of the cingulum bundle in older individuals. However, the coupling between structural integrity and functional connectivity was not observed in the context of high WMH burden.

P46A Structural and functional connectivity fingerprints for face, body, scene, and object perception

Z.M. Saygin, N.G. Kanwisher

McGovern Institute for Brain Research and Department of Brain and Cognitive Sciences, Massachusetts Institute of Technology, Cambridge, MA 02139

A fundamental hypothesis in neuroscience is that connectivity mirrors function at a fine spatial grain across the cortex. Previous research supports this hypothesis for the human brain, by demonstrating that the degree of voxelwise face-selectivity in the fusiform gyrus of individual subjects can be predicted from that voxel's connections to the rest of the brain (its unique connectivity fingerprint), measured through diffusion-weighted imaging (DWI; Saygin et al. 2012). Here we asked whether resting-state functional connectivity (fcMRI) can also predict face-selectivity in the fusiform gyrus, and whether structural or functional connectivity fingerprints also predict other visual selectivities in multiple extrastriate cortices. We found that both fcMRI and DWI connectivity predicted face selectivity in the fusiform more accurately than did a group analysis of face selectivity from other subjects. Prediction accuracies from DWI connectivity were slightly but significantly better than predictions from fcMRI connectivity for the fusiform gyrus. A direct comparison of the subset of connections that best predicted face-selectivity revealed that DWI and fcMRI connectivity fingerprints for function were generally quite similar, especially for the top predictors, although differences existed among weaker predictors. We performed similar comparisons of DWI and fcMRI connectivity fingerprints for other extrastriate regions and for body, object, and scene

perception. These data provide converging evidence from both DWI and fcMRI that i) connectivity and function are tightly linked at a voxelwise scale in extrastriate cortex in humans, and ii) functionally-selective voxels can be predicted from either diffusion or resting functional data alone. These results also raise the possibility that connectivity fingerprints direct the functional specialization of cortex in development. Finally, this work has practical relevance for researchers and clinicians, by providing a method to infer functional brain maps from structural images alone in individuals who cannot be functionally scanned (e.g. comatose subjects, or sleeping infants).

P47A Automatic Annotation of 3D Axoplasmic Reticula for Neuron Segmentation

A. Sinha[1], W. G. Roncal[1,2], N. Kasthuri[3,4], J. W. Lichtman[3,4], R. Burns[1]

[1]Department of Computer Science, The Johns Hopkins University, Baltimore, MD, USA, [2]The Johns Hopkins University Applied Physics Laboratory, Laurel, MD, USA, [3]Department of Molecular and Cellular Biology, Harvard University, Cambridge, MA, USA, [4]Center for Brain Science, Harvard University, Cambridge, MA, USA

Background: A connectome is a high resolution wiring diagram, or graph, of the brain, where each neuron is a node, and each synapse is an edge. Connectomes are expected to elucidate the structure and function of the brain, potentially leading to advances in understanding and curing diseases, learning, and technology. One major problem in accurately estimating human connectomes is the presence of approximately 100 billion neurons, and 100 trillion synapses in a single human brain. It is difficult to automatically annotate neurons because of the large diversity in their shape and size. Several automatic segmentation methods have been proposed to segment neurons; however, these methods are error prone, and often result in process fragmentation and graphs with very high error.
Methods: We present a method to automatically annotate thin tubular neuronal structures called axoplasmic reticula (AR), which are present in axons, as well as similar structures found in dendrites. We apply a bilateral filter followed by a Laplacian filter to isolate AR in each 2D image slice of the Kasthuri11cc dataset, a color-corrected cube of high-resolution neural EM data. Then, we use a region growing technique based on biological priors (e.g., shape, size, color) to annotate AR, which appear as small dark spots in our images. After annotating each slice, we find 3D connected components to obtain strands of AR. We can use these 3D annotations to merge, and therefore rectify, segmentations obtained from automatic methods by considering the overlap of AR strands with fragmented processes. Processes that are connected by a strand can be merged.
Results: Based on limited gold standard, we are able to annotate AR on a single slice with about 87% precision, and 52% recall. However, since AR are subcellular structures, the more salient performance measure is to check whether our 3D AR annotations remain within a single process or neuron object. We evaluated our 3D annotations in the AC4 region of our dataset which contains true segmentations from the ISBI 2013 Segmentation Challenge. We measured AR *purity*, which is a measure of the number of true neuron labels touched by each AR object. An AR object spanning exactly one neuron label will have a purity value of 1. Since our aim is to merge processes through multiple slices, we focus our analysis on the 70% of AR annotations that span more than one slice. We found the average purity of all multi-slice AR objects to be 0.995, and the average purity of AR objects spanning at least 10 slices to be 0.999. We are now working on tracking these AR objects to produce longer strands. This will enable us to detect AR spanning more slices, and therefore, merge more fragmented processes.
Conclusions: Our results show that our AR annotations are highly precise, and can be reliably used to merge automatic segmentations of neural EM data. This will help us build more precise connectomes, which in turn will give us more reliable information about structural brain connectivity.

P48A Hemispheric specialization in men and women using graph theory: a resting-state functional connectivity MRI study in highly educated healthy adults

M. Termenon[1,2], A. Jaillard[3,4], S. Achard[1–3,5], C. Delon-Martin[1–3]

[1]Inserm, U836, F-38000 Grenoble, France; [2]Univ. Grenoble Alpes, GIN, F-38000 Grenoble, France; [3]University Hospital of Grenoble, F-38000 Grenoble, France; [4]Univ. Grenoble Alpes, IRMaGe, F-38000 Grenoble, France; [5]GIPSA-Lab, F-38000 Grenoble, France

Background: Neuropsychological findings often have found asymmetries in relation to the kind of material being processed, the left hemisphere associated with more verbal materials and the right with non-verbal materials (Gazzaniga 2000). Topological organization of human brain networks at rest can be explored using graph theory analysis (Achard *et al.*, J Neurosci, 2006). Recent reports in children and young adults showed hemisphere and sex-related differences in detected hubs (Tian et al., Neuroimage, 2011; Nielsen *et al.*, PloS One, 2013). However no significant difference was detected among global network parameters. The aim of this study was to test the effect of hemispheric lateralization, sex and age in highly educated healthy adults using metrics derived from graph analysis of resting state networks.
Methods: Forty one healthy adults (age range 22–62 years, 19 males, 3- to 10-year post-baccalaureate) were included in this study that was approved by local ethical committee. Participants underwent a 13 minutes resting-state fMRI acquisition session (400 volumes, TR = 2 s, spatial resolution $3 \times 3 \times 3.85\,mm^3$, 36 slices, 3T Philips MR scanner). Subjects were instructed to let their mind wandering and to keep their eyes open. Preprocessing included motion correction, compensation for time shift between slices and elastic registration using DARTEL onto the ICBM152 template (SPM12b software: http://www.fil.ion.ucl.ac.uk/spm/). Graph analysis was performed using the method described in Achard *et al.* Time-series corresponding to the grey-matter voxels of 89 ROIs from the AAL template were extracted. After wavelet decomposition of the time-series, the individual graphs were computed selecting the 10% of the highest correlated connections in the [0.03–0.06 Hz] frequency band. Then, three graph metrics were computed at node level: global efficiency (Eglob), node degree (k) and betweenness centrality (BC). Finally age, sex, and hemispheric side effects were assessed using GLM repeated measures analyses (SPSS software v20).
Results: Multivariate analysis showed a significant effect of hemispheric side ($p < 0.0001$) and age ($p = 0.005$) with a sex by side interaction ($p = 0.014$): compared to females, males show higher connectivity in the right hemisphere and a lower connectivity in the left hemisphere. Univariate analyses showed: (i) significantly higher graph metrics in the right than in the left hemisphere ($p_k < 0.0001$; $p_{Eglob} < 0.0001$; $p_{BC} = 0.005$); (ii)

significant side by sex interaction for degree ($p_k = 0.004$) and global efficiency ($p_{Eglob} = 0.009$), but not for betweenness centrality ($p_{BC} = 0.358$); (iii) No significant effect was found for age at the single metric level.
Conclusions: The right hemisphere appears to present more connections than the left hemisphere in highly educated healthy adults. Moreover, the differences in hemispheric graph metrics relative to sex suggest men and women may have distinct hemispheric specialization. Our results are consistent with previous findings in children and young adults (Tian et al., Neuroimage, 2011; Nielsen *et al.*, PloS One, 2013), supporting the classical idea of greater language abilities in women and better aptitude in men for visuospatial skills. The mild effect of age has to be put into perspective with the age range (20 to 62) and the high level of education of our sample. These lateralization and demographic differences should be considered when using resting-state functional connectivity MRI methods in clinical studies.

This work is supported by a grant from the Rhône-Alpes Région.

P49A Functional Networks Observed with Scale-Free and Oscillatory Cortical Activity

H. Wen[1], Z. Liu[1,2]

[1]*School of Electrical and Computer Engineering,*
[2]*Weldon School of Biomedical Engineering, Purdue University, West Lafayette, Indiana, United States*

Background: Electrophysiological recordings sample the full dynamics of neural activity and can be used to reveal much richer temporal patterns than are attainable with fMRI. Notably, brain electrical signals often exhibit a varying mixture of broadband arrhythmic and narrowband rhythmic patterns. These patterns, known as scale-free and oscillatory activities respectively, are increasingly thought to originate from distinct mechanisms and indicate distinct features of underlying structural networks. We aim to separate scale-free and oscillatory activities and then investigate their differential contributions to large-scale fluctuations and correlations observed with resting electrocorticogram (ECoG).
Methods: We used a new method (Wen and Liu, 2014) to separate scale-free and oscillatory components in the time-dependent power spectrum of 5-min ECoG signals collected from 128 locations covering the entire lateral surface of the left macaque cortex (publicly available from Richen Brain Science Institute). We assessed the temporal fluctuations of the separated scale-free and oscillatory spectral components for all frequencies and locations. We also assessed and compared the inter-regional correlational patterns of such separated scale-free and oscillatory activities.
Results: In the frequency domain, the scale-free component followed a power-law distribution, whereas the oscillatory components were confined to specific frequencies (Fig. 1). The scale-free activity was the major contributor to the mean power, whereas the oscillatory activity was the major contributor to the temporal fluctuation of the power. Moreover, the inter-regional correlation of the scale-free activity was wide spread with even global reach, whereas the oscillatory activity was correlated in a spatially specific manner, revealing a finer degree of details regarding neuronal interactions.
Conclusions: The capability of separating and characterizing the scale-free and oscillatory activities opens a new window of opportunities to study the brain's functional networks. The reported findings also shed light on the potentially different neuronal origins of global and regional correlational patterns previously observed with resting state fMRI.
Reference: Wen H. and Liu Z., IEEE TBME, submitted, 2014

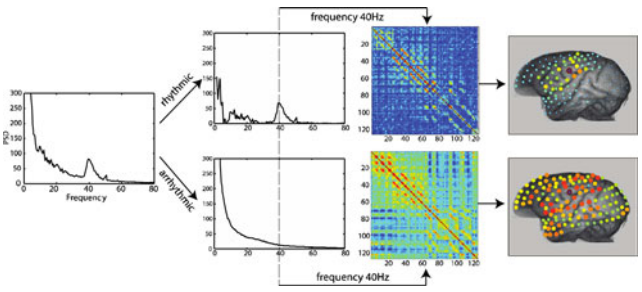

FIG. 1. From left to right are shown the raw ECoG spectrum, the separated spectra of rhythmic and arrhythmic signals, their corresponding correlation matrices and patterns.

P50A MNET : a multimodal network analysis toolbox for the brain

M. Yoon[1,2], B. Park[3], H.C.T. Do[1,2], C. Pae[1,2], J.D. Lee[1,2], H.J. Park[1,2]

[1]*Brain Korea 21 PLUS Project for Medical Science, Yonsei University College of Medicine, Seoul, Korea;* [2]*Department of Nuclear Medicine, Yonsei University College of Medicine, Seoul, Korea;* [3]*Department of Anesthesiology, David Geffen School of Medicine at UCLA, Los Angeles, California, USA*

Background: In the current research on brain network, common approaches to define functional brain networks are based on statistical dependency between regional time series on functional MRI (fMRI) and electroencephalography (EEG), while structural brain networks are based on the existence or the number of fibers on diffusion tensor imaging (DTI). Currently, combining multimodal brain networks is receiving a great attention since each can serve different but modality-unique information. In order to take different advantages from the three imaging modalities, our group has developed a Multimodal NETwork analysis toolbox, named as ''MNET'', which enables to analyze and combine brain network data of the three different types in a fully automatic analyzing pipeline.
Methods: MNET offers various analyses tools based on the graph theory; e.g.) defining network node and calculating edge and topological properties for each modality (fMRI, EEG, and DTI). To define unique and homogeneous nodes from the continuous medium of the cortex, MNET provides several advanced methods to define network nodes from existing atlas map using spatial ICA (Kim et al., 2013) or Anatomical-constrained Hierarchical Modularity Optimization (Park et al., 2013). Edge weights are based on cross-correlation on fMRI/EEG and on number of fibers passing through the nodes on DTI. MNET constructs DTI-based network using fiber tractography in DoDTI (http://neuroimage.yonsei.ac.kr/dodti). MNET can serve both univariate and multivariate approaches to identify canonical subnetworks as well as those topological properties for each modality (e.g. graph-ICA and modularity optimization). Graph-ICA can be used to decompose networks into edge-sharing independent subnetworks (Park et al., 2014). Finally MNET provides methods for combining, analyzing, and visualizing three network modalities.
Results: MNET provides statistical analysis modules for each network in the group level study. Users can assign design matrix and contrasts for statistical evaluations of nodes, edges,

topological properties and multivariate components based on generalized linear model. MNET also provides various interactive and integrative visualization techniques; 2D-circular and 3D-rendering of edge weights, node degrees, colored adjacency matrices, and hierarchical edge bundle display.

Conclusions: Our group has developed a multimodal network analysis toolbox, MNET, which can fully serve to analyze and integrate functional and structural brain networks defined using fMRI, EEG, and DTI. This toolbox can be usefully applied in diverse researches using multimodal brain networks.

Theme 3: Applications in Neurological and Psychiatric Diseases

P51A Hyper-Connectivity in the Default Mode Network (DMN) of Asymptomatic High School Football Athletes as a Result of Repetitive Subconcussive Head Trauma

K Abbas[1], T.E. Shenk[1], V.N. Poole[1], L.J. Leverenez[1], E.A. Nauman[1], T.M. Talavage[1], M.E. Robinson[1,2]

[1]*Purdue University, West Lafayette, IN, USA,* [2]*VA Boston Healthcare System, Boston, MA, USA*

Background: Football athletes can experience hundreds of hits to the head during a single season, which may be particularly dangerous even in the absence of observable symptoms. Recent research suggests that repetitive head-trauma could lead to long-term neurodegeneration. In this study, we compare the resting state fMRI (rs-fMRI) of asymptomatic high school football athletes—who experienced repetitive hits to the head during the season and were not diagnosed with concussion—with non-exposed healthy peers. We hypothesize that football athletes would deviate from their non-contact athlete peers as a chronic effect of sub-concussive head trauma.
Methods: Two groups of high school male athletes (age 14–18) were recruited for this study: 22 football athletes and 10 non-collision sport controls. The controls participated in two imaging sessions (Baseline and Follow-up). Football athletes participated in 3–6 imaging sessions (87 total); one prior (*Pre*), at least one during (*In*), and one after the end (*Post*) of their competition season. In-season sessions were grouped by month so no player was represented more than once. AFNI was used to compute regional (116 AAL regions) connectivity to the seed ROI, a 12 mm radius sphere placed at posterior cingulate/precuneus. To compensate for monthly group sizes (N = 8–15), N-Choose-7 subsets were used to compare Fisher Transformed regional correlation coefficients between controls and football athletes.
Results: Football athletes are significantly hyper-connected relative to controls before and during much of the season (Fig 1). Hyper-connectivity is reduced during months (1 and 4) with highest head collision activity.
Conclusions: Findings suggest chronic differences between football and non-collision high school athletes, affected by the type and number of hits to the head recently experienced. In months 1 (two-a-days) and 4 (playoffs), football athletes experience a more intense hit burden that was associated with appearing more similar to their non-collision peers. This transient drop may indicate a slow-acting compensatory mechanism.

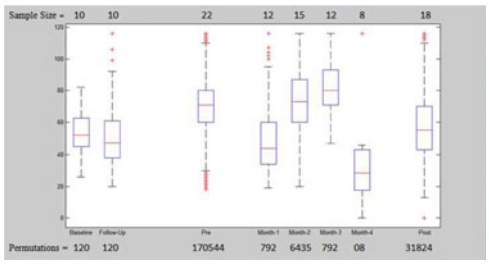

FIG. 1. The number of significant DMN connections for each session, using all possible permutation of subjects, choosing 7 at a time.

P53A Occipital networks in the blind and visually impaired

C.M. Bauer[1], B.B. Koo[2], L. Zajac[2], G. Heidary[3], L.B. Merabet[1]

[1]*Massachusetts Eye and Ear Infirmary, Boston, MA, USA,* [2]*Boston University School of Medicine – Center for Biomedical Imaging, Boston, MA, USA,* [3]*Boston Children's Hospital, Boston, MA, USA*

Background: The occipital cortex in the ocular blind has been shown to take over other non-visual roles. This may be due in part to altered white matter connectivity. On the other hand, individuals with visual deficits due to non-ocular causes (i.e. cortical/cerebral visual impairment – CVI) may show deleterious

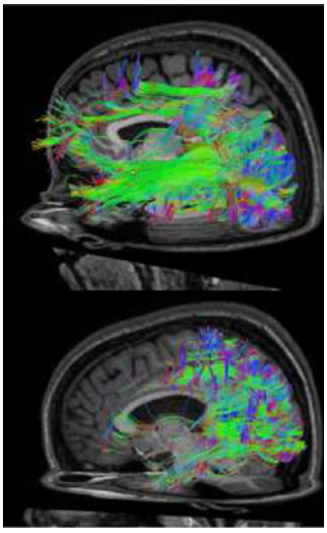

FIG. 1. HARDI reconstruction of a representative sighted control (top) and CVI subject (bottom). Notice the significant lack of long-range projections in the CVI subject.

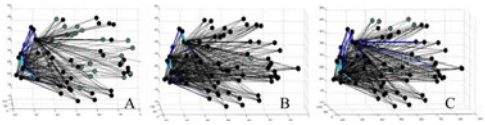

FIG. 2. Connection strength and node degree of occipital seeds to the whole brain for cortical visual impairment **(A)**, ocular blind **(B)**, and sighted controls **(C)**. The occipital network shows significant differences between the three groups for both connection strength (lines) and node degree (spheres). Strength of connection and node degree is represented in thirds, whereby the weakest is represented by black, the middle third by dark blue, and the strongest by cyan. Notice that in the CVI subjects, the connection strength is comparable in the posterior regions, but is weak for long-range connections to frontal cortex compared to ocular blind and sighted controls, while the ocular blind shows weaker node degree in frontal regions than either CVI or sighted controls.

alterations in white matter connectivity, particularly involving higher order visual pathways of the dorsal and ventral streams.
Methods: A HARDI MRI protocol was used to acquire data from 2 CVI subjects as well as 7 early ocular blind (EB) and 9 sighted controls (SC) for comparison. HARDI images were acquired using an 8-channel head coil on a 3 Tesla Philips Achieva system using a single shot EPI sequence (64 diffusion directions, B_{max} 3000 s/mm^2, B_{min} 0 s/mm$^{2)}$. HARDI volumes were corrected for eddy current artifacts and were skull-stripped prior to orientation distribution function (ODF) calculation and subsequent white matter fiber tracking and reconstruction. The brain was parcellated into 68 discrete regions in HARDI space. In house MATLAB software was used to generate connectivity matrices using fibers from occipital seeds to the whole brain were assessed for number of fibers, quantitative anisotropy (QA), node degree and strength, and path length.
Results: Reconstruction of white matter projections using HARDI revealed striking increase in extrageniculostriate fibers in CVI subjects ($N_{avg\ fibers}$ = 438.38) compared to ocular blind ($N_{avg\ fibers}$ = 285.32) and sighted controls ($N_{avg\ fibers}$ = 247.70). As is evident from Figure 1, these projections in the CVI subject are mainly short-range, with a relative absence of long-range projections. Figure 2 indicates that there are significant differences in occipital networks in subjects visually impaired due to ocular blindness or cortical/cerebral causes.
Conclusions: These results begin to provide a neuroanatomical basis for the compensatory changes observed in the occipital cortex in ocular blind as well as for the deleterious changes observed in CVI.

P54A Functional connectivity biomarkers of depression risk: Resting state activity in relation to mood and stress among healthy youth

D.J. Walder[1,2], J.D. Coplan[3], C.Y. Tang[4], V. Wang[4], E.F. Walker[5], J. Kaufman[6], B. Yaffe[2], Y. Ehrlich[2], L.H. Ospina[2]

[1]Brooklyn College of The City University of New York (CUNY), Brooklyn, NY, USA, [2]The Graduate Center of CUNY, New York, NY, USA, [3]SUNY Downstate Medical Center, Brooklyn, NY, USA, [4]Mount Sinai School of Medicine, New York, NY, USA, [5]Emory University, Atlanta, GA, USA, [6]Yale University School of Medicine, New Haven, CT

Background: Depression is marked by impaired functional brain connectivity, including within the default mode network (DMN)[1]. Little is known, however, about such biomarkers among youth[2], individuals who may be at heightened risk (e.g., siblings of depressed patients[3]), individuals early in the course of depression[4] or individuals prior to illness onset. Moreover, few studies examined functional brain connectivity in relation to behavioral measures that have been linked with heightened depression risk (see[5]). The current study aimed to fill this gap, in a pilot sample of non-treatment seeking youth, by examining resting state functional magnetic resonance imaging (rsfMRI) activity in DMN and attentional network (AN) in relation to mood symptoms and stressful experiences.
Methods: Participants included 8 (3 F/5 M) youth ages 13–21 years (Mean = 18.13; SD = 1.08) without a history of clinical depression, recruited from the general community. Youth were administered a structured clinical interview, completed mood and stress questionnaires, and underwent neuroimaging procedures (using a Siemens Verio 3T). Independent component analysis was used to identify 20 unique networks of resting state activity using MELODIC (Beckmann and Smith, 2004) as implemented in FSL. The DMN, consisting of anterior and posterior cingulate cortex (ACC, PCC) and bilateral parietal cortices (PC), has been consistently reported in the literature[6,7]. General linear modeling and permutation-based inference testing (RANDOMISE) were used to test for symptom and stress correlates of DMN, using alpha level of .05.
Results: In this cohort without a history of clinical depression, preliminary findings indicated that measures of depressive and anxiety symptoms, stressful life events and daily hassles were significantly associated with DMN and bilateral AN connectivity, after adjusting for age. Analyses did not correct for multiple comparisons given the early exploratory stage of the study.
Conclusions: Results suggest DMN and AN activity may serve as biomarkers of risk for depression among healthy youth, by virtue of the association of functional connectivity with clinical and behavioral indicators of depression risk (mood symptoms, stressful life events, daily hassles). Additional data collection is currently underway towards expanding the study sample. This preliminary report holds potential to elucidate biological precursors to depression that may, in turn, inform novel approaches to preventive intervention.

References

[1] Sheline et al., Proc Natl Acad Sci U S A 2009; [2] Connolly et al., Biol Psychiatry 2013.
[3] Liu et al., J Affect Disord 2013; [4] Bluhm et al., Psychiatry Clin Neurosci 2009. [5] Felder et al., BMC Psychiatry 2012; [6] Greicius et al., Proc Natl Acad Sci USA 2003; [7] Damoiseaux et al., Proc Natl Acad Sci USA 2006.

P55A Resting-State Networks in Autism Spectrum Disorder

D.J. Bos[1], T.R. van Raalten[1], B. Oranje[1], A.R. Smits[1], N.A. Kobussen[1], J. van Belle[1], S.A.R.B. Rombouts[2,3,4], S. Durston[1]

[1]NICHE Lab, Department of Psychiatry, Rudolf Magnus Institute for Neurosciences, University Medical Center Utrecht, The Netherlands. [2]Department of Radiology, Leiden University Medical Center, The Netherlands. [3]Institute of Psychology, Leiden University, The Netherlands, [4]Leiden Institute for Brain and Cognition (LIBC), Leiden University Medical Center, The Netherlands

Background: Autism Spectrum Disorder (ASD) has been associated with a complex pattern of increases and decreases in resting-state functional connectivity [1]. The developmental

disconnection hypothesis of ASD poses that shorter connections become overly well established with development in this disorder, at the cost of long-range connections [2]. Here, we investigated resting-state connectivity in young boys with ASD and typically developing children. We hypothesized that ASD would be associated with reduced connectivity between networks, and increased connectivity within networks, reflecting poorer integration and segregation [3] of functional networks in ASD.
Methods: Resting-state fMRI was acquired from 27 boys with ASD and 29 age and IQ-matched typically developing boys between 6 and 16 years of age. Functional connectivity networks were identified using Independent Component Analysis (ICA), implemented in the GIFT-toolbox. Ten higher-order cognitive and default-mode resting-state networks of interest were selected for group analysis. Group comparisons were conducted using permutation testing, with and without voxel-wise correction for grey matter density. Results were all FWE-corrected for multiple comparisons, using threshold-free cluster enhancement.
Results: We found reduced connectivity between higher-order cognitive resting-state networks in ASD. No between-group differences in within-network connectivity were detected, however, connectivity was reduced in small clusters in the right superior frontal and supramarginal gyrus just outside network boundaries. Furthermore an interaction effect with age was found in the DMN: insula connectivity increased with age in ASD, whereas it decreased in typically developing children.
Conclusion: Our results show both reduced connectivity outside network boundaries and developmentally increased connectivity within networks. These results are supportive of the suggested atypical functional integration of resting-state networks in ASD. However, the global architecture of resting-state networks appeared to be intact in children with ASD, which argues against recent suggestions that changes in connectivity in ASD may be most prominent during development.

P56A Increased corticostriatal functional and structural connectivity in Anorexia Nervosa

J. Cha[1], J.E. Steinglass[1], J. Posner[1]

[1]Columbia University, College of Physicians and Surgeons, Department of Psychiatry and the New York State Psychiatric Institute, New York, New York, USA

Background: Anorexia nervosa (AN) is a serious disorder with a mortality rate among the highest of any psychiatric illness[1]. It has been proposed that abnormal corticostriatal loop (CStr)[2,3] may play a role in pathogenesis of AN; however, the connectivity of this system in AN has yet to be examined. In the current study, we aimed to investigate (i) the functional and structural connectivity of the CStr loop in AN and (ii) whether anomalies of the CStr are associated with obsessional symptoms in AN.
Methods: We recruited 20 individuals with AN and 20 healthy control participants (HC). We acquired MRI on GE 1.5T scanner: a T1-weighted structural MRI, two 5-min resting-state MRI, and two diffusion MRI. *Resting-state FMRI (Rs-fMRI):* Rs-fMRI was preprocessed in SPM (Friston et al., 1994) and the conn toolbox[5] to investigate intrinsic functional connectivity of the CStr system. We examined temporal correlation between a seed striatal region (inferior and superior NAcc)[6] and target cortical regions. *Diffusion MRI (dMRI)-tractography:* After performing preprocessing on dMRI[7] and a multi-fiber probabilistic model fitting[8], we estimated fiber tracts using probabilistic tracking in FSL. We calculated the number of streamlines from the seed mask (the NAcc) arriving at the cortical target regions, proportional to the total number of samples (25,000 per voxel). These measures thus represent ROI-to-ROI structural connectivity.
Results: We found abnormally increased CStr functional and structural connectivity in participants with AN, compared with HC. AN showed greater intrinsic functional connectivity between the NAcc and the medial OFC (corrected $P<0.01$; left hemisphere), and greater probabilistic tractography between the NAcc and the lateral, medial OFC/rostral ACC ($P<0.011$; right hemisphere). Effects remained significant after controlling for age and BMI. Probabilistic tractography measures correlated with symptom severity of eating disorder (Eating Disorder Examination-Self-Report Questionnaire: Eating Concern, $r=0.63$, $P=0.003$; Restraint, $r=0.63$, $P=0.003$) in AN.
Conclusions: Our results demonstrate an aberrant CStr circuit in AN; the anomalies of this circuit significantly differentiates AN from the HC and are associated with severity of the eating disorder symptoms.

P57A Prospective Target Selection Based on Structural Connectivity Pattern for Subcallosal Cingulate Deep Brain Stimulation

K. Choi[1], P. Riva-Posse[1], P. E. Holtzheimer[2], C. McIntyre[3], R. Gross[1], S. J. Garlow[1], J. K. Rajendra[1], H. S. Mayberg[1]

[1]Emory University, Atlanta, GA, USA, [2]Geisel School of Medicine at Dartmouth, Hanover, NH, USA, [3]Case Western Reserve University, Cleveland, OH, USA

Background: Deep brain stimulation (DBS) of subcallosal cingulate white matter (SCC-WM) has shown considerable promise for treatment resistance depression (TRD)[(1,2)]. Its proposed mechanisms of action include electrical modulation of a network of brain regions involved in mood regulation[(3)]. Structural connectivity analysis of SCC-WM DBS has been shown that SCC is a critical hub for mood regulation network[(4)] and small differences in stimulation location can generate substantial differences in the directly activated pathways[(5)]. Moreover, we has been demonstrated the necessary pathways for effective stimulation (Figure 1)[(6)]. These pathways can be characterized in individual patients prospectively using DBS models coupled to structural connectivity analysis. We hypothesized that prospective precise targeting of this specific combination of WM tracts by diffusion tractography would improve DBS response over the standard approach.
Methods: 10 patients with TRD had pre-operative MRI, including 60 directions DTI with both A-P and P-A phase encoding direction for distortion correction (2 mm isotropic, 4 b0s). Deterministic tractography (TrackVis) from sphere ROI (2.5 mm radius) in SCC was used to find optimal target location in each subject prior to surgery based on structural connectivity patterns of necessary pathways (Figure 2). Later, probabilistic tractography was used to validate the structural connectivity pattern that matched to previous retrospective findings[(6)].
Results: DBS surgical targeting guided by pre-defined structural connectivity pattern improves the clinical response rate (50% decreases in standard depression rating scale scores) from 41% (7/17)[(2)] where targeting was performed using anatomy alone, to 70% (7/10) in this new cohort. Probabilistic tractography analysis of responders (n = 7) confirmed same structural connectivity pattern to previous findings (n = 12) (forceps minor, uncinate fasciculus, cingulum, and medial frontal-striatal/subcortical fibers) (Figure 3).

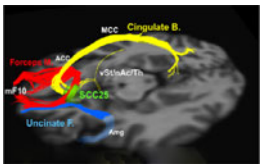

FIG. 1. Necessary Pathways.

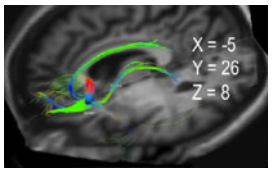

FIG. 2. Prospective targeting.

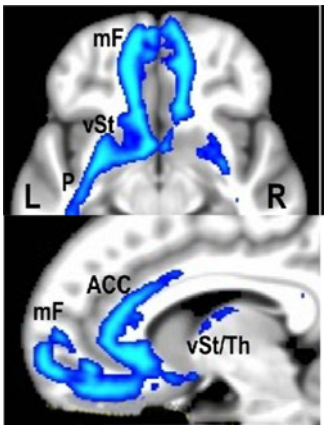

FIG. 3. Probabilistic SC pattern.

Conclusions: Structural connectivity pattern based prospective targeting can improve SCC-WM DBS outcomes over standard anatomical guidelines, ensuring that the necessary combinations of tracts are targeted during DBS lead implantation.

References

[1] Mayberg, et al. Neuron. 2005, 45(5), 651–660. [2] Holtzheimer, et al. Arch Gen Psychiatry. 2012, 69(2), 150–158. [3] Mayberg, et al. J Clin. Invest. 2009, 119(4), 717–725. [4] Gutman, et al. Biol. Psychiatry. 2009, 65(4), 276–282. [5] Lusan, Choi et al. Brain Stimul. 2013, 6(5), 737–739. [6] Choi, Riva-Pose, et al. Biol. Psychiatry. In press

P58A Change in Amygdala Circuitry with Treatment in Adolescent Depression

K.R. Cullen[1], M. Westlund[2], B. Klimes-Dougan[1,2], B.A. Muller[1], A. Houri[1], L.E. Eberly[3], K.O. Lim[1]

[1]*Dept. Psychiatry, Univ. of Minnesota (UMN) Medical Sch., Minneapolis, MN, USA*
[2]*Psychology Dept., UMN, Minneapolis, MN, USA;*
[3]*Biostatistics, School of Public Health, UMN, Minneapolis, MN, USA*

Background: Abnormal resting-state functional connectivity (RSFC) involving fronto-limbic circuitry has been implicated in major depressive disorder (MDD). Less is known about whether these abnormal circuits are malleable with treatment. We recently found abnormal amygdala RSFC in 41 un-medicated adolescents with MDD versus 31 healthy controls (HC). The purpose of this study was to measure change in amygdala RSFC in response to a standard MDD treatment.

Methods: All adolescents underwent clinical evaluation and MRI scanning at baseline. Brain imaging was conducted at UMN on a 3 Tesla TIM Trio Siemens scanner. The resting scan consisted of 180 whole brain EPI volumes (TR = 2000 ms; TE = 30 ms; FOV = 256 mm; voxel size 3.4 × 3.4 × 4 mm; 34 slices; 64 × 64 matrix); participants were instructed to stay awake with their eyes closed (6 min). A field map and a T1 were collected. Processing steps included brain extraction, motion correction, RETROICOR, linear de-trend, geometric distortion correction, nuisance regression (white matter, cerebrospinal fluid, and the six motion parameters), and data scrubbing. A seed-based, whole-brain approach was used to examine amygdala RSFC (cluster threshold $p < 0.05$. $z > 2.3$). We compared amygdala maps between groups, correcting for age and sex (cluster z threshold 2.3, $p < 0.05$.) Of the original sample of 41 adolescents, 12 patients returned for a second scan after completing 8 weeks of treatment (9 antidepressant medication, 3 psychotherapy). Participants repeated scanning procedures and self-reported their depression symptoms (Beck Depression Inventory-II [BDI-II].) Treatment response was defined as a drop in BDI-II score of at least 10. RSFC values from baseline analysis clusters were extracted from each individual's pre-and post-treatment amygdala RSFC maps in order to examine change with treatment.

Results: Adolescents with MDD showed lower baseline amygdala-hippocampal RSFC, but greater amygdala-precuneus RSFC than HC. Instead of the expected ''normalization'' pattern for treatment responders (n = 8), amygdala-precuneus RSFC decreased with treatment only in non-responders (n = 4), while RSFC in this circuit stayed the same or increased in responders. In contrast, amygdala-hippocampal RSFC increased significantly after treatment across the whole group (''normalization'') but this change was observed in both responders and non-responders (overall treatment effect).

Conclusions: Baseline differences in amygdala RSFC changed with treatment. Some neural changes followed ''normalization'' pattern, whereas others represented an enhancement of a previous abnormality. Aberrant amygdala-precuneus RSFC could serve a compensatory role that is enhanced when treatment is beneficial. Limitations included small sample size and lack of uniformity in the treatment intervention.

P59A Functional overconnectivity accompanied by anatomical white matter compromise of the imitation network in children with autism

M. Datko[1,2], I. Fishman[1], Y. Cabrera[1], R. Carper[1], R.-A. Müller[1]

[1]*San Diego State University, San Diego, CA;*
[2]*University of California San Diego, La Jolla, CA*

Background: The increasing prevalence of autism spectrum disorder (ASD), a neurodevelopmental disorder characterized by sociocommunicative impairments, presents a growing public health challenge. Converging evidence indicates disrupted neural connectivity and atypical brain network organization in ASD, but studies attempting to integrate both functional and structural connectivity measures are very scarce. Such multimodal approaches may provide critical insights into the interplay between functional connectivity within a network and the state of white matter connections comprising that network.

We tested for (a) altered functional and structural connectivity within a network associated with imitation, a social cognition domain putatively impaired in ASD; (b) links between clinical symptoms, functional connectivity of this imitation network, and white matter microstructure within pathways connecting network nodes.

Methods: Forty children and adolescents with ASD, ages 7–18 years, and 40 typically developing (TD) controls, matched for age, handedness and non-verbal IQ, completed resting-state functional magnetic resonance imaging (rs-fMRI) and diffusion weighted imaging scans. Whole-brain intrinsic functional connectivity (iFC) analyses were conducted using seed regions consistently activated by imitation tasks, as determined in a recent ALE meta-analysis. Structural connectivity was analyzed using probabilistic tractography and measures derived from the diffusion tensor. Seed and target regions for tractography were

derived from a subset of regions used for the FC analyses, with inclusion of nearby white matter. Robust intrahemispheric pathways consistent with known anatomy were identified between 3 region pairs in each hemisphere. DTI indices were extracted from these tracts. Head motion from functional and diffusion scans were used as statistical covariates.
Results: Direct group comparisons of FC maps revealed a pattern of predominant overconnectivity in the imitation network in ASD, with all overconnected clusters (ASD > TD) falling outside the imitation network, consistent with the notion of impaired network differentiation in ASD. Structurally, higher radial, axial and mean diffusivity was found in tracts connecting major nodes of the imitation network, including inferior frontal gyrus to lateral dorsal premotor, and to medial premotor cortices, bilaterally. Further, volumes of these tracts were significantly correlated with the FC values (z scores) of the left inferior frontal gyrus in the TD, but not in the ASD group.
Conclusions: These multimodal imaging data have revealed aberrant WM microstructure in tracts directly connecting brain regions that are abnormally functionally connected in ASD, reflecting reduced anatomical and functional network integration and differentiation. Our study shows that multimodal investigation may reveal complementary aspects of aberrant connectivity in ASD.

P60A Epileptic Source Localization using Functional Connectivity Analysis of rfMRI

D. Devakumar[1], K. Malathi[2], Jeeva J.B[2]

[1]Department of Nuclear Medicine, Christian Medical College, Vellore, India, [2]Division of Biomedical Engineering, VIT University, Vellore, India.

Background: Identification of the epileptic focus plays an important role in ensuring seizure free outcome after the surgery. The epileptogenic origin can be identified by analyzing the Functional Connectivity (FC) of the brain from RS-fMRI.
Methods: Retrospective functional and structural MR volumes of age matched six focal epileptic subjects and thirty healthy controls (data from 1000 functional connectomes project) were analyzed through this study. The pre-processed volumes were parcellated into 116 Regions of Interest (ROI). Pearson's correlation coefficient was calculated for the time series extracted from each pair of ROIs to form whole brain connectivity matrix. An average healthy control connectivity matrix was formed by averaging the connectivity matrices of 30 healthy controls. Difference matrix was obtained for each of the six epileptic subjects by subtracting the epileptic subject's connectivity matrix from the average healthy control connectivity matrix. The pair of ROI with maximum deficit in connectivity was identified by applying a high threshold to the difference matrix. Within the identified pair, ROI with minimum average functional connectivity was identified as the epileptic focus. The functional connectivity map of the identified ROI in each epileptic subjects were compared with the healthy controls using two sample t-test to identify the location of the epileptic focus within the ROI.
Results: The identified epileptogenic zone by FC analysis and the clinical diagnosis by iEEG for each epileptic subject are given in Table-1. The identified epileptogenic zone superimposed on T1 template for epileptic subject 19001 is shown in fig-1 as an example. The epileptogenic zone identified by FC analysis correlated with the location identified by iEEG.
Conclusions: The possibility of using whole brain functional connectivity analysis for estimating the functionally deficit areas and consequently identifying the epileptic focus was tested with the retrospective data of six focal epileptic subjects with promising results.

Table 1. Comparison of FC Analysis Results with iEEG diagnosis

Subject ID	*Epileptogenic zone from iEEG*	*Epileptogenic zone from FC*
19001	Left Occipital Lobe	Left Superior Occipital Lobe
19002	Right Temporal Lobe	Right Mid Temporal
19003	Left Fronto-temporal	Left Medial Orbitofrontal
19004	Right Medial Temporal Lobe	Right Heschl's Gyrus
19005	Right Medial Temporal Lobe	Right Heschl's Gyrus
19006	Right	Right Frontal Pole

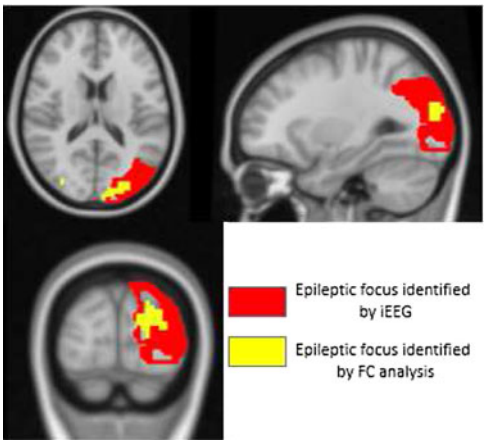

FIG. 1. Epileptic focus identified in subject ID 19001.

P61A Asymmetric Development of Dorsal and Ventral Attention Networks In the Human Brain

K. Farrant and L.Q. Uddin

Department of Psychology, University of Miami, Coral Gables FL

Background: Two neural systems for goal-directed and stimulus-driven attention have been described in the adult human brain; the dorsal attention network centered in the frontal eye fields (FEF) and intraparietal sulcus (IPS), and the ventral attention network anchored in the temporoparietal junction (TPJ) and ventral frontal cortex (VFC) (Corbetta and Shulman, 2002). There is an abundance of literature demonstrating that the long-range cortical connections within large-scale brain networks are stronger in adults than in children (e.g. Dosenbach et al., 2010). Surprisingly, at present very little is known regarding the processes governing typical development of attention networks in the brain.
Methods: Using resting state functional MRI data collected from 30 typically developing children and 30 adults obtained from the Autism Brain Imaging Data Exchange (Di Martino, 2014) we compared functional connectivity of two key regions of interest from the dorsal and ventral attention networks. Whole-brain resting-state fMRI (3T Allegra, 33 slices, slice thickness 4 mm,

TR 2 s, flip angle = 90°, FOV 240 mm, TE 15 ms, 180 volumes) data were used. Functional images were preprocessed using FSL's FEAT. We used white matter (WM) and cerebrospinal fluid (CSF) mean time-series as nuisance regressors in the general linear model (GLM) to reduce the influence of physiological noise (Margulies, 2007). Four separate GLMs were constructed, each using one of the ROI time-series as regressors of interest along with the nuisance regressors for WM and CSF. Group-level analyses was conducted individually for each ROI. When comparing the two groups for each ROI, we conducted a two-sample t-test implemented using FSL's FLAME. Corrections for multiple comparisons were carried out at the cluster level for each of our ROIs using Gaussian random field theory (min $Z > 2.3$; cluster significance: $P < 0.05$, corrected).

Results: We found that functional connectivity of both dorsal attention network nodes (FEF, IPS) and one ventral attention node (TPJ) is stronger in adults than in children. In contrast, functional connectivity of VFC within the ventral attention network is greater in children than in adults. The VFC region is in close anatomical proximity to an anterior insula region that has recently been implicated in causally influencing other large-scale brain networks such as the central executive network and the default mode network.

Conclusion: This asymmetric pattern of development of attention networks may be a neural signature of the shift from over-representation of bottom-up attention mechanisms to greater top-down attentional capacities with development.

P62A Effects of cannabis and THC on reward circuitry in patients with schizophrenia and cannabis use disorder

A.S. Fischer[1], S. Whitfield-Gabrieli[2], R.M. Roth[1], M.F. Brunette[1], A.I. Green[1]

[1]Department of Psychiatry, Geisel School of Medicine at Dartmouth, Lebanon, NH, [2]Department of Brain and Cognitive Sciences, Massachusetts Institute of Technology, Cambridge, MA

Background: Cannabis use disorder (CUD) occurs commonly in patients with schizophrenia (SCZ) and substantially worsens the disease course in these patients. Available treatments for SCZ are rarely successful in limiting cannabis use. Development of effective treatments will be facilitated by a more complete understanding of the basis of their cannabis use. We have proposed that patients with SCZ may use cannabis to ameliorate brain reward circuit (BRC) dysfunction. In the present study we used resting state functional connectivity (rs-fc) to assess the integrity of the BRC in patients with SCZ and co-occurring CUD as compared to controls. We also investigated rs-fc after patients smoked cannabis or ingested a delta-9-tetrahydrocannabinol (THC) pill.

Methods: Participants included 12 patients with SCZ and co-occurring CUD (abstinent from cannabis for ≥ 7 days) and 12 control subjects. Patients and controls completed fMRI resting scans at baseline, and patients were assessed again (in a double-blind design) after either smoking a 3.6% THC cannabis cigarette ($n = 6$) or swallowing a 15 mg THC pill ($n = 6$). Controls were also tested a second time, with no intervention. Seed-to-voxel resting state functional connectivity (rs-fc) of BRC was analyzed using bilateral anatomically defined nucleus accumbens (NAc) seed regions. In patients, plasma THC level, symptom severity (PANSS), marijuana craving (MCQ) and withdrawal (CWS) were assessed at baseline and following pharmacological intervention.

Results: At baseline, patients showed decreased rs-fc between NAc and other BRC regions (amygdala, hippocampus, orbitofrontal and anterior cingulate cortices) relative to controls. Both smoked cannabis and THC pill ingestion increased connectivity within the BRC. Plasma THC after cannabis or THC administration was positively correlated with BRC connectivity. No changes in symptom severity, marijuana craving or withdrawal were detected.

Conclusion: To our knowledge, this is the first study to use rs-fc to study the BRC in patients with SCZ and co-occurring CUD. Our findings indicate that BRC rs-fc is reduced in these patients, and that both cannabis and THC increase BRC connectivity. Moreover, the study supports the use of rs-fc to identify BRC abnormalities and, potentially, to track the effect of pharmacologic agents on this circuitry. If confirmed by subsequent study, our findings suggest that THC might be tested as a potential adjunctive treatment for cannabis use in SCZ.

P63A Emergence of resting state functional connectivity across face selective cortical regions in congenital late sight-onset blind individuals

T. Gandhi[1], P. Swami[2], A. Kalia[1], V. Mahajan[4], M. Meng[5], S. Gorlin[3], S. Ganesh[6], S. Whitfield-Gabrieli[1], P. Sinha[1]

[1]Massachusetts Institute of Technology, USA; [2]Indian Institute of Technology, Delhi, INDIA; [3]Choicestream, USA; [4]Mahajn Imaging Centre, New Delhi, INDIA
[5]Dartmouth College, NH, USA; [6]Shroff Charity Eye Hospital, Daryaganj, New Delhi, INDIA

Can individuals who have been blind for the first several years of life acquire the ability to visually distinguish faces from non-faces after sight restoring surgery? What kinds of neural changes underlie the very initial stages of such development? Is there any possibility to improve the neural activity across face-selective cortical regions late in life, and if so, how rapidly does it emerge? Is it spatially and topographically similar in organization to that found in the normally developed brain?

We report here results from an unusual opportunity to address these questions by studying congenitally blind individuals whose sight we were able to restore post-adolescence. Our behavioral tests reveal the development of face/non-face discrimination skills over the span of a few months after sight onset. We complemented these assessments with fMRI studies. In order to examine the development functional connection across face selective cortical network, we selected the right fusiform face area (rFFA) seed as the region of interest and apply the seed based correlations across brain regions in the resting state fMRI blood oxygenation level-dependent time series signals. The experiment was conducted as close to the surgery date as possible and repeated several times in the subsequent months, depending on each subject's availability.

In this report, we are including results of two congenital cataract blind children (12 years and 18 years, male), who had only light perception before surgery. We followed up these two kids two months and 18 months after sight onset. In order to show the contrast with age matched control subjects, we have included one fifteen-year male subject. In this resting state functional connectivity analysis, we have used the rFFA seed (the rFFA seed is generated from face localizer study) from the last time point of experimental subject's data in three longitudinal time point of observation. We find strong evidence of brain plasticity in these subjects. There is a rapid emergence of spatially localized, functionally specific responses in higher visual cortical areas after surgery. Taken together, these findings have important implications for our understanding of brain plasticity as well as the development of object representations in the brain.

P64A Effective connectivity during the processing of intelligible speech in Chinese: a Granger causality analysis study

Y. Yan[1], J.-H. Gao[1], J. Ge[1]

[1]*Center for MRI Research, Peking University, Beijing, China*

Background: How does information flow among brain regions during speech comprehension? Little is known about this cortical dynamics in a tonal language in which the lexical tone carries semantic information, such as Chinese. Using analysis of multivariate Granger causality, we investigated the effective connectivity of the classical language areas in left hemisphere and the tone processing related brain area in the right hemisphere during the speech comprehension of Chinese.
Methods: Twenty-eight native speakers in Chinese were scanned (on a 3T Siemens Trio system using a standard head coil) while presented with intelligible and unintelligible Mandarin Chinese speech in blocks, spoken by a male and a female. Subjects were instructed only to judge the gender of the speakers (which can be judged easily in time-reversed, unintelligible speech). Four brain regions were identified in the whole-brain SPM analysis based on contrast of intelligible > unintelligible: left anterior superior temporal sulcus/gyrus (aSTG), left posterior superior/middle temporal gyrus (pSTG), left inferior frontal gyrus (IFG) and right superior temporal pole (rSTP). The analysis of Granger causality was based on a variation of direct directed transfer function (dDTF) approach for fMRI data (Deshpande et al., 2009), and computed from a multivariate autoregressive model of the times series in the selected ROIs. The raw time series from the selected ROIs were normalized across runs and subjects and concatenated across all runs and subjects to form a single vector per ROI for analysis. Clustering coefficient and eccentricity of the resulted causality graph were also calculated.
Results: The dDTF values reflects the magnitude of causal influence between the ROIs are shown in Figure 1. The graph analysis of clustering coefficient (Table 1) and eccentricity showed that pSTG was a predominantly node to drive other ROIs, and aSTG was the major information driven node in the intelligible network. Similar results were also found in unintelligibility network, only that aSTG and rSTP were both driven node.
Conclusions: Our study revealed the different roles played by the anterior and posterior regions of temporal cortices during the processing of intelligible speech in Chinese.

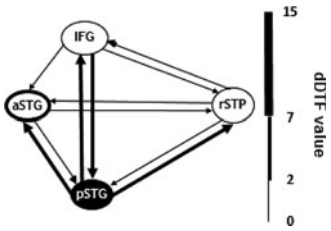

FIG. 1. The network for intelligible speech. The significant links ($P < 0.05$) are represented and the dDTF-value of the connections are idicated by the width of the arrows. pSTG was the major node with the maximum eccentricity (shown as dark oval). aSTG was predominantly information driven (shown with dark circle) while pSTG was a strong driver.

TABLE 1. CLUSTER-IN AND CLUSTER-OUT FOR ALL ROIS

		aSTG	*pSTG*	*IFG*	*rSTP*
Intelligible	C_{in}	20.9	12.7	9.6	16.3
	C_{out}	6.4	31.1	15.7	6.3
Unintelligible	C_{in}	13.2	5.4	2.4	13.0
	C_{out}	1.6	20.0	4.5	8.0

P65A Aberrant large-scale networks differentiate unipolar from bipolar depression

R. Goya-Maldonado[1], K. Weber[1], S. Trost[1], E. Diekhof[2], M. Keil[1], P. Dechent[3], O. Gruber[1]

[1]*Center for Translational Research and Systems Neuroscience and Psychiatry, University Medical Center, Goettingen, Germany,* [2]*Biocenter Grindel and Zoological Museum, Department of Human Biology, University of Hamburg, Hamburg, Germany,* [3]*MR-Research in Neurology and Psychiatry, Department of Cognitive Neurology, University Medical Center, Goettingen, Germany*

Background: Misdiagnosing bipolar depression can lead to mistreatment and deleterious consequences. Even nowadays misdiagnosis happens in about 60% of the cases. Sophisticated imaging methods could be applied to support the differential diagnosis of depression. Therefore, our objective was to differentiate symptomatic unipolar and bipolar patients by the topology of key large-scale networks. According to the triple network model of psychopathology, we studied the cingulo-opercular (CO), frontoparietal (FP), and default mode (DM) networks. We also aimed to investigate whether topological changes in functional connectivity (FC) were trait or phase-related to disorder severity.
Methods: Recurrent patients (20 unipolar and 20 bipolar) presenting similar total scores from clinical scales (MADRS and BDI) and 20 age/gender matched controls were included in the analysis. Whole-brain resting-state fMRI (Siemens Magnetom TRIO 3T, 33 slices, 64×64 matrix, 3 mm thickness, 0.6 mm spacing, TR 2 s, flip angle 70°, FOV 192 mm, TE 30 ms, 160 volumes) was performed. With spm8 preprocessed functional images were used to extract residuals of nuisance factors (6 mov, WM, CSF) and those used to identify CO, FP and DM components with fsl ICA. Back transformation was performed for each component with individual timecourses (Butterworth 0.01–0.1 Hz) GLM followed by Fisher's r-to-z transformation. Images were then used for second-level analysis and group comparison (FWE $p < .05$). Masks were created based on topological differences for each component. Extracted values from individual beta weights were correlated with individual clinical parameters (r Pearson $p < .05$).
Results: By the CO network, unipolars presented significantly reduced FC in the anterior cingulate cortex (ACC), pregenual and subgenual ACC, posterior cingulate cortex (PCC), and inferior parietal cortex bilaterally in relation to bipolars and controls. By the DMN, unipolars exhibited increased FC in the precuneus and hippocampus bilaterally in relation to bipolars and controls. By the FP, bipolars displayed significantly increased FC mainly in the left ventrolateral and dorsolateral prefrontal cortex in relation to unipolars and controls. Topological changes significantly correlated to the number of depressive episodes but not to symptom scores.
Conclusions: Groups displaying similar symptomatology were clearly distinguished by unique changes in large-scale networks. Bipolar patients were characterized by increased FC in the FP network. Unipolar patients presented increased FC in the DM

network. Together with the CO impairment, DM regions were seen as a fingerprint to unipolar depression. These changes seem to predict the vulnerability to depressive episodes.

P66A Topological and functional connectivity disturbances precede the onset of Huntington disease

D.L. Harrington[1,2], M. Rubinov[3], S. Durgerian[4], L. Mourany[5], C. Reece[5], K. Koenig[5], M.J. Lowe[5], J.D. Long[6], J.S. Paulsen[6], E. Bullmore[3], S.M. Rao[5]

[1]VA San Diego Healthcare System, San Diego, CA, USA, [2]University of California, San Diego, La Jolla, CA, USA, [3]University of Cambridge, Cambridge, UK, [4]Medical College of Wisconsin, Milwaukee, WI, USA, [5]Cleveland Clinic, Cleveland, OH, USA, [6]The University of Iowa, Iowa City, IA, USA

Background: Huntington disease (HD) is an autosomal dominant neurodegenerative disorder resulting from CAG repeat expansion in the HTT gene. A formal diagnosis of HD is made at the appearance of unequivocal motor signs, yet subtle motor, cognitive, and psychiatric symptoms are detected decades before diagnosis during the prodromal phase (prHD). Behavioral variables improve the prediction of disease onset and track disease progression beyond that of genetic factors, but striatal volume is a notably robust marker. Tissue loss in the striatum, however, does not adequately capture the functional topography of disease progression. To address this limitation, we used resting-state fMRI (rs-fMRI) to identify functional connectivity changes in prHD by means of two analytic approaches, network topology and functional connectivity analyses.
Methods: The sample consisted of 16 gene-negative controls (offspring of a parent with HD, but no CAG expansion), and 48 prHD subjects who were stratified into Low, Medium, and High groups (n = 16 each) based on the CAP score [(Age) × (CAG repeats – 33.66], a proxy of genetic burden. To analyze rs-fMRI scans, cortical and subcortical structures were parcellated into 300 nodes using a spatially constrained clustering method. For topological analyses, group differences were examined for density, global efficiency, average clustering coefficient, and rich club organization. For functional connectivity analyses, anatomical sources of altered whole-brain connectivity were identified by comparing the Negative group and each prHD group on the fitted z-scores of correlation coefficients for all edges connecting the 300 nodes using the network based statistic. From this analysis, a subset of nodes was identified that showed multiple aberrant connections in prHD. Whole-brain functional connectivity (sum of z-scores) of these nodes was then compared between the groups. Functional connectivity indices that were altered in prHD were correlated with measures of executive functioning.
Results: Network topology results: Significant group differences were found in global efficiency and rich club organization, which correlated with CAP scores, but not cognitive variables. Functional connectivity results: Disturbances were characterized by connections in which functional connectivity was weaker (red) or stronger (blue) in the prHD group than in the Negative group (fig.). A striking increase in the number of nodes exhibiting aberrant connectivity occurred as genetic burden increased. For nodes with multiple aberrant connections, whole-brain connectivity was weakened in the thalamus, anterior cingulate (AC), inferior frontal gyrus, insula, and hippocampus in all prHD groups, and strengthened in the inferior parietal lobule (IPL) as a function of CAP scores. AC, thalamus, and IPL connectivity correlated with executive functions.
Conclusions: Our results provide novel evidence for a progressive disruption in whole-brain communication and central-hub functioning as genetic burden increases in prHD. Anatomically, connectivity within frontal cortex weakens with greater genetic exposure, presumably due to disruptions in striatal pathways, and is enhanced in posterior cortex, notably the IPL, a center for attentional control. Supported by NINDS (U01NS082083)

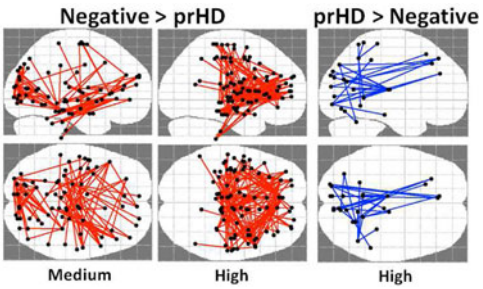

P67A Characterizing chronic stage acquired brain injury using a white matter distance-based energetic cost measure of fMRI resting-state cortical connectivity

T.J. Herron[1] and A.U. Turken[1]

[1]US Dept. of Veterans Affairs, Northern Healthcare System, Martinez, CA, USA

Background: Acquired brain injury recovery is often characterized by alterations in brain function. We analyzed the difference between stroke patients' whole cortex connectivity vs. corresponding aged controls by applying an energetic cost (EC) measure to rs-fMRI connectivity data. We hypothesized that cortical connectivity is spatially efficient [Karbowski, Front Neur Circ, 8:9, 2014]; thus acquired brain injury should increase EC values over and above simple increases in network activity as a response to injury.
Methods: All rs-fMRI data are processed to obtain Pearson correlation coefficients using standard methods including COMPCOR noise removal and several head motion correction techniques [Power, Neuroimg, 84, 2014]. Use of a minimum white matter (WM) distance metric improves EC values, which are mean distance-weighted correlations, along the midline and in perisylvian areas compared to using a Euclidean metric. **Exp. 1** We used NYU Test-Retest rs-fMRI data (25 subjects, 3 sessions each) to test the cross-session reliability compared to subject specificity of EC in contrast to standard rs-fMRI power (ALFF) and topological graph-theoretic measures (GTM). We also looked at measures' sensitivity to image sampling density and sampling diameter. **Exp. 2** We used NKI-Rockland rs-fMRI data (86 healthy subjects) to see how well EC measures correlate with demographic, health and cognitive measures to further test EC's likely usefulness in characterizing brain injury. **Exp. 3** We applied EC, ALFF and GTM to data from 14 patients with left hemisphere, mainly perisylvian, strokes in order to detect potential right hemisphere connectivity cost greater than in 17 older controls.
Results: 1) ALFF had the highest subject variance to session variance ratio (1.74), followed by mean minimal path length (L, 1.58) followed by EC (1.4x, Euclidean or WM metric). Also, L is affected the most by both sample spacing and sampling diameter, followed by EC (primarily diameter) and then ALFF (diameter only). **2)** EC measures, in particular mean correlation normalized ones, covaried positively with age (r = 0.50), socioeconomic standing (r = 0.38), and trended with blood pulse rate and diastolic blood pressure (r ~ 0.2x). Unnormalized measures covaried negatively with being female (r = −0.33). There were no

substantial correlations of EC, GTM, or ALFF with cognitive tests (WASI & D-KEFS). **3)** In the 14 stroke patients, the contralateral (right) hemisphere rs-fMRI data showed a trend to higher non-normalized EC ($p = 0.06$) and lower mean efficiency (E, $p = 0.06$) than in controls with other GTM measures and ALFF showing less difference. EC did not correlate with lesion volume ($r = -0.05$), however (nor did E).
Conclusions: EC measures have reasonably good reliability and appear to have potential for application as part of a set of rs-fMRI tools to characterize acquired brain injury. The opinions herein are those of the authors, not the U.S. Government or Dept. of Veterans Affairs. Support was provided by US Veterans Affairs Research Service.

P68A Intrinsic network connectivity differentially predicts sub-components of executive attention in patients with schizophrenia and bipolar disorder

M.H. Hunter[1,2,3], V.P. Clark[1,3], V.D. Calhoun[3,4], C. Wootton[2,3], Y. Chen[2,3,5], J.C. Edgar[5], M.X. Huang[6], B. Howell[2,3], J.M. Cañive[2,3]

[1]Dept. Psychology, The University of New Mexico (UNM), Albuquerque (ABQ), NM, USA, [2]New Mexico VA Hospital, ABQ, NM, USA, [3]The Mind Research Network, ABQ, NM, USA, [4]Dept. Electrical and Computer Engineering, UNM, ABQ, NM, USA. [5]The Children's Hospital of Philadelphia, Philadelphia, PA, USA. [6]The University of California, Dept. Radiology, San Diego, CA, USA

Background: Current evidence suggests that psychosis is a clinical dimension associated with overlapping symptomology and cognitive dysfunction in schizophrenia (SZ) and bipolar disorder (BD). Anomalies within and between intrinsic connectivity of the default-mode and task-related networks may contribute to the frequently observed deficits in executive attention. The objective of this study was to characterize dimensions of executive attention and their relation to intrinsic connectivity in SZ and BD.
Methods: Performance on the Wisconsin card sorting task (WCST) and the Conner's continuous performance task II (C-CPT) were obtained in 41 chronic patients with SZ, 22 euthymic patients with BD, and 44 demographically-matched healthy controls (HC). Resting-state functional magnetic resonance imaging (fMRI) measures were obtained within 8 days (on average) of the neuropsychological assessment. Principle component analysis (PCA) with Varimax rotation modeled the factor structures of WCST and C-CPT performance, separately. Group independent component analysis (ICA) decomposed fMRI scans into 75 networks. Twelve resting-state networks were identified with significant voxel-wise functional connectivity in anatomical regions of interest. To compare WCST & C-CPT normalized factor scores and ICA-generated spatial maps, 3-way ANCOVAs were computed (using $p < 0.05$, FWE-corrected). Multiple regressions tested their relationships. Measures of functional connectivity *between* networks (FNC) were also compared between groups, and partial correlations assessed their relationships with factor scores, controlling for age and gender.
Results: PCA revealed 2 factors for the WCST, comprising problem-solving (69% variance explained) and inefficient sorting (14%). Four factors were observed for the C-CPT, comprising focused attention (33%), impulsivity (15%), vigilance (13%) and sustained-attention (12%). Compared to HCs, patients with SZ performed worse on problem-solving and focused attention; patients with BD were worse only on sustained attention (p's < 0.01). Increases in voxel-wise functional connectivity within the superior temporal gyrus (STG), anterior cingulate (ACC) and basal ganglia (BG) were observed in SZ versus HCs and BD. STG connectivity predicted problem-solving and focused attention within SZ and BD, respectively; ACC connectivity predicted sustained attention and vigilance in BD. Increased FNC was observed between STG and BG in the patient groups, but correlated with problem-solving only in patients with SZ.
Conclusions: Overall, results are consistent with the reappraisal of SZ and BD as distinct diagnostic entities, with shared abnormalities in network connectivity compared to HCs. However, there were also differences across patient groups, particularly connectivity *within* STG and ACC. Such distinctions were also found in their relation to impairments in executive attention, suggesting that patterns of intrinsic connectivity can be used to reveal group differences that translate to unique neurocognitive profiles.

P69A Single-session effects of electroconvulsive therapy on the dynamics of functional inter-network connectivity in major depressive disorder: a resting-state fMRI study

J. Jang[1], C. Sorg[1,2,3], D. Schwerthöfer[3], J. Bäuml[3], V. Riedl[1,2], A.M. Wohlschläger[1,2]

[1]TUM-Neuroimaging Center, Technische Universität München, Munich, Bayern, Germany, Department of [2]Neuroradiology and [3]Psychiatry, Klinikum Rechts der Isar, Technische Universität München, Munich, Bayern, Germany

Background: Electroconvulsive therapy (ECT) remains the gold-standard treatment for severe, treatment-resistant major depressive disorder (MDD), although the underlying mechanisms remain unclear. MDD is associated with increased functional connectivity in specific neural networks, however the temporal variability of connectivity dynamics have not been taken into account. In this study, we used a sliding time window approach to investigate functional connectivity between intrinsic connectivity networks (interFC) of the brain before and after ECT treatment. We focused on session effects of single-ECT.
Methods: 10 patients with treatment-resistant major depression were treated by ECT (12 single-ECT in 6 weeks) and assessed by about 6 resting-state fMRI sessions before and after the whole therapy (morning and afternoon, each) serving as reference, and once during first phase of treatment (before and after single-ECT at the same day i.e. morning and afternoon). r-fMRI data were acquired

TABLE 1. SUBJECT AVERAGES OF STANDARD DEVIATION OF CORRELATION COEFFICIENTS (MEAN ± STD) FOR SIGNIFICANT INTERFC DYNAMICS CHANGES AFTER SINGLE-ECT FROM ANCOVA

	Single ECT Application		*Before vs. After*	
Networks	*Before*	*After*	*Direction*	*p-value*
pDMN – fLfp	0.2968 ± 0.0785	0.3499 ± 0.1041	Before < After	0.0228
pDMN – pLfp	0.2842 ± 0.0650	0.3101 ± 0.0769	Before < After	0.0384

on a Philips 3T Achieva, and preprocessed using SPM8. Group-level spatial independent component analyses (ICA) were performed using the GIFT toolbox for morning and afternoon measurements, respectively. Dynamic interFC between 6 time courses was estimated: frontal and posterior default mode network (fDMN, pDMN), frontal (f) and parietal (p) parts of left and right fronto-parietal networks (Lfp, Rfp). We computed covariance matrices (Pearson correlation, Fisher transformed) from windowed segments of width 40 TRs, slid in steps of 1 TR. Finally, standard deviations of correlation coefficients across all time windows were computed.
Results: We performed an analysis of covariance (ANCOVA) to estimate between-group differences in standard deviation of correlation coefficients before and after single-ECT, while controlling for the effects from morning and afternoon by including the reference scans. This revealed significantly increased variation in functional connectivity dynamics between pDMN and Lfp after single-ECT.
Conclusions: Our results provide first evidence for alterations in functional connectivity dynamics caused by single-ECT in depressive patients, which specifically centered on the left fronto-parietal central executive and posterior default mode network. Our results contribute to the understanding of the specific mode of action of ECT, which after several applications stabilizes in altered functional connectivity especially of the left dorsolateral prefrontal cortex.

P70A Functional connectivity at rest in amnestic mild cognitive impairment-A functional magnetic resonance study

Himanshu Joshi[1,4], John P John[1,2,4], Srikala Bharath[1], Rakesh B[2,3], Shilpa S.[1], Jitendra Saini[3], Mathew Varghese[1]

[1]Departments of Psychiatry, [2]Department of Clinical Neuroscience, [3]Neuroimaging and Interventional Radiology, and [4]Multimodal Brain Image Analysis Laboratory (MBIAL), National Institute of Mental Health and Neurosciences, Bangalore, Karnataka, INDIA

Background: Amnestic Mild Cognitive Impairment (aMCI) represents the transition between healthy aging and Alzheimer's dementia wherein gradual impairment of cognitive abilities, especially memory sets in. Dysfunctional connectivity in various brain networks is known to underlie impairment of cognitive functions mediated by those circuits. We aimed at examining functional connectivity within selected resting state networks (RSNs) in patients with aMCI in comparison to healthy elderly subjects using functional magnetic resonance imaging (fMRI).
Methods: The study samples comprised of 15 patients with aMCI individuals [age = 70.93 (s.d. = 8.37) years] recruited from the Geriatric Clinic and Services, NIMHANS and 15 healthy elderly subjects [age = 66.26(s.d. = 8.06) years] Between-group comparisons of connectivity in individual RSNs were carried out using Multivariate Exploratory Linear Optimised Decomposition into Independent Components (MELODIC) followed by dual regression with age, gender, and number of years of formal education as co-variates.
Results: The aMCI group was found to have reduced functional connectivity in the default mode (DMN) and basal ganglia (BGN) networks, and increased connectivity in insular salience, executive, precuneus, frontal salience and secondary visual networks using a *family-wise error* (*FWE*) *correction* at $p < 0.05$.
Conclusions: The results of the study demonstrate that dysfunctional connectivity in multiple RSNs is present even during the MCI stage before transition to dementia. Therefore, RSN dysconnectivity may have potential utility as a screening tool to detect incipient dementia. The increased connectivity in certain networks might reflect the brain's efforts at compensating for the attenuated connectivity in the DMN and BGN.

P71A Temporal dynamics of neural network dysfunction in Major Depressive Disorder

R.H. Kaiser[1,2], S. Whitfield-Gabrieli[3], F. Goer[2], M. Beltzer[2], D.A. Pizzagalli[1,2]

[1]Harvard Medical School, Boston, MA, USA, [2]McLean Hospital, Belmont, MA, USA, [3]Massachusetts Institute of Technology, Cambridge, MA, USA

Background: Theoretical models propose that the ruminative, self-focused cognitive style characteristic of Major Depressive Disorder (MDD) stems from dysfunction in the coordinated activity of large-scale neural networks involved in goal-directed control of attention and behavior (''frontoparietal control network'', FPN), and internally- or externally-oriented attention (''default mode network'', DMN, and ''dorsal attention network'', DAN). However, studies testing such models have yielded mixed results. Two possible reasons for inconsistencies are investigated in the present study. First, previous studies have often relied on analytic techniques, e.g., global signal regression, that can bias network relationships. Second, previous studies have failed to investigate variability in the activity within a network over time, e.g., *switching*; or in connectivity within or between networks over time, e.g., *stationarity*; both of which can influence estimates of average network functioning. The present study aimed to address these gaps by applying a novel set of analytic tools to the investigation of network dysfunction in MDD.
Methods: Thirty adults with MDD and 30 adults with no history of psychiatric illness (Controls) participated in a resting-state fMRI study. First, seed-to-voxel analyses were conducted to examine group differences in network organization, using *a priori* seed regions of interest that represent ''hubs'' of FPN (e.g., dorsolateral prefrontal cortex (dlPFC)); DMN (e.g., posterior cingulate cortex (PCC)); and DAN (e.g., middle temporal gyrus (MTG)). Second, within-participant DMN and DAN ROIs were extracted and activation was computed across each network at each timepoint; comparison of the relative activation of these networks over time provided an estimate of switching. Third, a sliding-window procedure was performed to compute a series of seed-to-voxel correlations; variance in correlation values over time provided an estimate of stationarity.
Results: Analyses revealed within-network abnormalities in MDD, including DMN hyperconnectivity; FPN hypoconnectivity; and DAN hypoconnectivity. The MDD group also exhibited aberrant between-network relationships, including hyperconnectivity of FPN-DMN; and hypoconnectivity of FPN-DAN. Analyses that explored group differences in network switching or stationarity indicated that, relative to controls, individuals with MDD showed anomalies in the relative recruitment of DAN and DMN, and in the variability in connectivity within and between FPN, DAN, and DMN.
Conclusions: Together, these initial findings indicate that excessive coupling between brain systems involved in top-down control of attention and those involved in internal mentation, along with weakened control of attention to the external world, are critical network abnormalities in MDD. In addition, these results suggest that evolving and novel analytic techniques for investigating neural network functioning may shed new light on network anomalies and resolve conflicting findings reported in previous studies.

P72A Altered Interhemispheric Resting-State Connectivity in Autism

D.N. Kennedy[1], T.V. Mitchell[1], S.M. Hodge[1], D. Cochran[1], J.A. Frazier[1]

[1]Department of Psychiatry, University of Massachusetts Medical School, Worcester, MA, USA

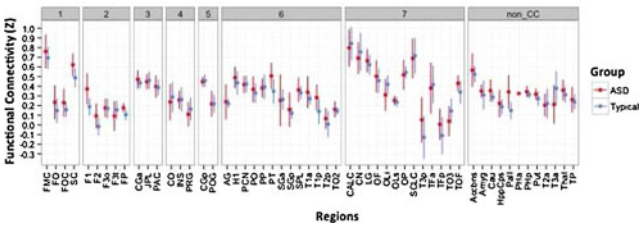

Background: Autism is a pervasive and high-incidence developmental disorder the underlying neurobiology of which remains poorly understood. The corpus callosum (CC), the primary site of information transfer between the cerebral hemispheres, has reduced area and volume and anomalies of microstructure in individuals with ASD compared to neurotypical individuals. Little is known about how CC anomalies contribute to ASD symptomatology.
Methods: We studied 8 adolescent males (Age 13–17) with ASD and 10 matched typically developing adolescent males. MRI imaging at 3T included a high-resolution volumetric structural scan and a 6-minute resting-state fMRI scan. Structural images were analyzed with FreeSurfer to generate a set of anatomical ROIs. Resting state analysis included motion correction, intensity normalization and band-pass temporal filtering (.05 - .001 Hz), regression of nuisance covariates. For each seed region we generate the correlation of the time signal with its contralateral region.
Results: A number of regions demonstrated significant differences in their interhemispheric resting state correlation when comparing the subjects with ASD to neurotypical subjects. Regional differences were most pronounced in: superior frontal gyrus (F1), pallidum (PAL), subcallosal cortex (SC) and planum temporal (PT); all with ASD resting-state correlation greater than controls.
Conclusions: This study follows-up prior literature that has established the incidence of structural differences in the corpus callosum in subjects with Autism. By identifying the concomitant alterations in resting state interhemispheric correlation, which may relate to altered interhemispheric connectivity, we have a potential mechanism by which such structural alterations can alter behavior in these subjects.

P73A Sex Differences in the Clinical Expression and Resting State Brain Co-Activity in Bipolar Disorder

Sara Kimmich[1,3,5], Sanja Kovacevic, PhD[3], and Lisa T. Eyler, PhD[2,3,4,5]

[1]UCSD Department of Cognitive Science [2]UCSD Department of Psychiatry
[3]Veterans Medical Research Center [4]Veterans Affairs Hospital
[5]UC San Diego

The course and expression of bipolar disorder (BD) clearly differs between women and men. Women more often have a seasonal pattern of mood disturbance, and are more likely to experience rapid cycling than men. Men are more likely to have a comorbid substance use disorder, while women more frequently have comorbid anxiety disorders. Previous studies have observed sex effects in connectivity of the default mode network (DMN) of healthy individuals, but more research is needed to see whether a similar effects holds among BD patients. This study investigates 1)how sex differences in DMN activity among BD I patients compared to individuals without BD, and 2)how sex differences may relate to clinical or cognitive differences in BD. We compared 27 euthymic patients with bipolar I disorder to 28 age and gender comparable healthy participants using functional magnetic resonance image during a period of eyes open rest. Averaged functional activity between the nodes of the DMN (medial prefrontal cortex, posterior cingulate, and bilateral angular gyrus) revealed that BD females tend to have greater co-activity within the default mode network than male BDs, contrasting with the pattern of greater connectivity among male healthy participants compared to females ($p = .01$). Negative psychotic symptoms were more pronounced in male than female bipolar participants ($p = .07$). There was a significant negative correlation of average DMN connectivity with negative symptoms ($r(28) = -.44$, $p = .05$). These results suggest subtle sex differences in the inter-relationship of resting brain activity within the DMN that may relate to clinical differences between men and women with bipolar disorder, including severity of negative psychotic symptoms.

P74A Functional connectivity from the primary motor cortex to the posterior cingulate is dependent on genetic burden in prodromal HD

K.A. Koenig[1], M.J. Lowe[1], J. Lin[1], D.L. Harrington[2], K.E. Sakaie[1], J.S. Paulsen[3], and S.M. Rao[1]

[1]Cleveland Clinic, Cleveland, OH, USA, [2]VA San Diego Healthcare System, San Diego, CA, USA, [3]The University of Iowa, Iowa City, IA, USA

Background: Changes in cognition, motor function, and neuroimaging measures have been observed in individuals in the preclinical stages of Huntington's disease (preHD). Resting state functional connectivity MRI (rs-fMRI) has identified disruptions in intrinsic brain connectivity in preHD, though findings have been mixed. The current study uses a seed-based approach to examine rs-fMRI in preHD as a function of genetic burden. Specifically, we investigate the relationship between CAP score and the strength of connectivity to the left primary motor cortex (M1), a region that has previously shown functional and structural changes in preHD.
Methods: In an IRB-approved protocol, 48 preHD participants were scanned at 3T in a 12-ch receive head coil. For each participant, a measure of genetic burden, CAP score, was calculated from age and CAG repeat length. Scans included a T1-MPRAGE ($1 \times 1 \times 1.2$), a rs-fMRI scan at $2 \times 2 \times 4$ mm voxels, 1954 Hz/pix BW, 31 axial slices, TR/TE/FA = 2800/29/80, and a Time Reproduction Task (TRT) fMRI scan at $2 \times 2 \times 4.5$ mm voxels, 1954 Hz/pix BW, 31 axial slices, TR/TE/FA = 2800/29/80°. Activation during the TRT task was used to identify the area of highest activation in left M1 (Figure 1.A). Postprocessing of rs-MRI data and creation of the left M1 whole brain rs-fMRI map are described in Koenig et al., AJNR, 2013. Left M1 rs-fMRI maps were transformed to common space and the strength of connectivity at a given voxel for each of the 48 participants was entered into a partial correlation with CAP score, using age as a covariate. The result is a whole-brain voxel-wise map showing the relationship between the strength of connectivity to left M1 and CAP score across the preHD subjects.

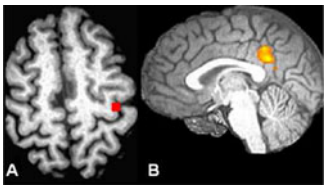

Results: Connectivity from left M1 to the posterior cingulate cortex (PCC) was the only region to show a significant correlation with CAP score (Figure 1.B, $p < 0.01$, cluster size 1500). Mean connectivity to the PCC ROI was calculated for each subject and entered into a partial correlation with CAP score ($r = 0.60$, $p = 1 \times 10^{-5}$). Mean connectivity was also correlated with performance on a measure of executive function, the Trails Making Test ($r = 0.34$, $p = 0.018$).
Conclusions: As genetic burden increases, connectivity from left M1 to the PCC becomes stronger. Though the PCC has multiple functions, it is a critical node of the default mode network. It is possible that connectivity between typically anti-correlated networks begins to strengthen as those in the prodromal stage move closer to disease onset. Further, this change in connectivity is related to a measure of executive function. This research was supported by a grant from the CHDI (A2015) and a grant from the NINDS (RO1 NS054893).

P75A Default mode and task positive subnetworks across age

M.A. Kriegsman[1], N. Kovacevic[2], A.R. McIntosh[2], C. Grady[2], H.A. Abdi[1]

[1]The University of Texas at Dallas, Richardson, Texas, USA, [2]Rotman Research Institute, Baycrest, Toronto, Ontario, Canada

Background: The default mode network (DMN) and task positive network (TPN) are negatively correlated functional networks. The strength of the negative correlation between DMN and TPN is positively associated with cognitive performance, and both diminish with age. Thus, the interplay between DMN and TPN is important for successful cognitive performance and may be subject to insult (e.g., in aging). Also, DMN subnetworks have recently been observed, and may be uniquely altered across age.
Methods: Functional connectivity was computed from fMRI BOLD time series of 96 cortical regions-of-interest (ROIs) over a concatenation of visual tasks in $N = 46$ adults (range 22 to 85 years of age), and analyzed by DISTATIS. DISTATIS is a principal component analysis-based (multivariate) method for multiple distance data tables. Data were arranged as an array, with one connectivity matrix per participant. Connectivity matrices were double centered (to bring each participant to the same center), normalized (to give each participant comparable importance), and analyzed as in STATIS. DISTATIS gave factor maps of the rows (maps of connectivity among ROIs) from an overall perspective and from each age group's perspective. Cluster analysis on factor maps revealed subnetwork structure. Inference tests were performed by bootstrap resampling—resampling subjects with replacement.
Results: To begin, clusters were identified within DMN (alone) and within TPN (alone). Analysis of all cortical ROIs revealed that these DMN and TPN clusters formed subnetworks—some within DMN, some within TPN, and some interconnecting DMN and TPN. Also, overall cortical connectivity was strongly divided in two: one contained the core DMN and TPN ROIs, and the other contained remaining ROIs. Unexpectedly, the Young age group contained two sub-populations, one (called Young A) that looked like the older groups, and one (called Young B) that differed from all other groups. Young B exhibited unusual organization of DMN clusters. For example, only in Young B, precuneus and angular gyrus (core DMN ROIs) did not cluster. Moreover, only in Young B, overall cortical connectivity was divided into (not two but) three, and ROIs from the DMN and TPN did not cluster together.
Conclusions: DMN and TPN subnetworks did not reflect boundaries between DMN and TPN. Instead, many subnetworks contained a mixture of DMN and TPN ROIs. More broadly, among all cortical ROIs, DMN and TPN subnetworks clustered together and opposed remaining ROIs, suggesting a higher-order organization between DMN/TPN and other networks. This organization did not hold for the Young B group. Instead, Young B exhibited unique network structure, both in select DMN subnetworks and in overall cortical connectivity. In sum, DMN and TPN are not only competing networks, but are also intimately interconnected and may together constitute a broader functional unit.

P76A Functional connectivity and recognition of familiar faces in Alzheimer's disease

S. Kurth[1], M.A. Bahri[1], E. Moyse[3], C. Bastin[1], E. Salmon[1,2]

[1]Cyclotron Research Center, University of Liège, Belgium, [2]Memory Clinic, CHU Liège, Belgium, [3]Department of Psychology: Cognition and Behaviour, University of Liège, Belgium

Background: Previous studies have reported that Alzheimer patients experience difficulties to recognize their own face on recent photographs. To date, few studies have explored the neural correlates of own face recognition abilities in Alzheimer patients, whereas, in healthy adults, neuroimaging studies related these abilities to a bilateral fronto-parieto-occipital network. The aim of our study was to explore the relationship between functional cerebral connectivity of key regions within this network and face recognition abilities.
Methods: 20 moderate Alzheimer patients (Mean age: 74.2 ± 6.2, MMSE: 19.1 ± 5.7) and 20 healthy elderly matched controls (Mean age: 74.3 ± 6.0, MMSE: 28.9 ± 1.1) had to complete a behavioral face recognition task where they discriminated between their own face, the face of a close relative and unknown faces on the basis of photographs from different life periods (from age 20 to current age). The patient group also underwent a resting-state fMRI acquisition. Behavioral results were analyzed by using non-parametric statistic tests. Regarding fMRI, group independent component analyses (ICA) was used to identify brain networks in Alzheimer patients. Seed to voxel analyses were then performed to measure connectivity of a given seed region and other regions of the brain using regions of interest (ROIs) from the literature. Correlations between connectivity maps and behavioral recognition scores were then performed.
Results: At the behavioral level, Mann-Whitney tests revealed that patients had significantly poorer performance than their healthy elderly matched controls for recognizing their own face and the face of a relative on photographs. More particularly, difficulties were evidenced when patients had to recognize themselves on photographs taken at recent periods of their life (65 years and more). fMRI results showed highly significant negative correlations between each recognition score (self recognition, recent self recognition and relatives recognition) and connectivity between the medial prefrontal cortex and the right superior frontal gyrus.
Conclusions: These results suggest that the higher the connectivity between the medial-prefrontal cortex and the right superior-frontal gyrus, the lower the self and relatives face recognition scores. In previous studies, the superior frontal region has been linked to control processes rather than face recognition processes and these results might thus reflect less segregation and more interference between networks in Alzheimer's disease. In other words, the association between increased connectivity and poorer recognition scores found in our study could reflect functional de-differentiation of specific brain regions in Alzheimer patients.

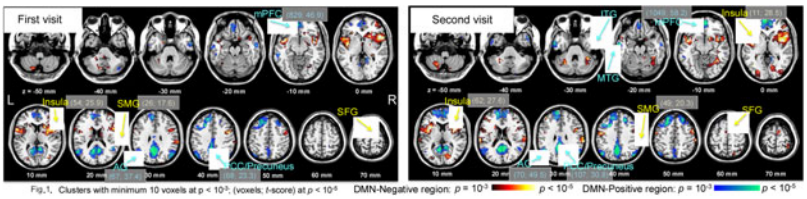

P77A Non-Resting-State fMRI Data Analysis via Default-Mode Networks: Feasibility Study

D.Y. Kim, J.H. Lee

Department of Brain and Cognitive Engineering, Korea University, Seoul, Korea

Background: Analysis of functional magnetic resonance imaging (fMRI) data acquired with task-instruction, but without distinct task paradigm (i.e. onset and duration of tasks) is not straightforward to identify task-associated brain regions. For example, in real-time fMRI (rtfMRI) neurofeedback (NF) setting, participants were often asked to freely engage to task by modulating regional neuronal activity as guided via visual NF information. To circumvent this issue and to enable identification of modulated neuronal networks, we present a novel scheme based on functional connectivity (FC) analysis. In this scheme, temporal pattern of so-called, ''default-mode networks (DMN)'', which is believed to be negatively correlated networks with task when participants perform cognitively demanding tasks, was used a reference signal of task-negative FC networks. We hypothesized that the DMN-negative (i.e. DMNn) FC networks would reveal task-positive networks in the rtfMRI-NF data and this would qualitatively be justified using rtfMRI-NF data obtained from heavy cigarette smokers.
Methods: Heavy cigarette smokers (n = 7; age = 26.0 ± 2.2; Edinburg handedness score = 84.0 ± 8.7) participated in rtfMRI-NF experiments to learn to resist the urge to smoke during two visits in one-week interval. Neuronal activity levels in brain regions known to be associated with cigarette resistance were provided to them as NF information. Participants were asked to increase their cigarette resistance and opacity of the smoking video clip was controlled in real-time as NF information for them using the neuronal activity levels in these regions. A group independent component analysis was adopted to extract spatially independent FC networks of the rtfMRI-NF data including DMN into independent components (ICs) using the GIFT toolbox (mialab.mrn.org). Then, DMNn as well as DMN-positive (DMNp) FC networks were obtained using DMN IC time course as reference signal via partial correlation coefficients by removing non-neuronal artifacts. Group inference was performed from one-sample *t*-test using Fisher's *r*-to-*z* scores.
Results: A total of 10 ICs were extracted and DMN was separated in one of these ICs. Fig. 1 shows the DMNn and DMNp networks at each visit. It is notable that effect sizes of potentially cigarette resistance related regions such as the insula as well as DMN regions strengthened from the first visit to second visit.
Conclusions: In this study, we presented a feasibility of our proposed scheme to identify task-associated FC networks from DMNn FC networks when specific task-paradigm was not available such as in our rtfMRI-NF data. Future investigation is warranted to justify the identified modulated brain regions via quantitative evaluations and craving levels.

P78A Investigating local changes of EEG and fMRI spectral power in multiple sleep stages

Y.H. Li[1], Y.J. Hong[1], Y.T. Ko[1], P.J. Tsai[2], P.C. Hung[1], C.W. Wu[1]

[1]Graduate Institute of Biomedical Engineering, National Central University, Taoyuan, Taiwan, [2]Department of Biomedical Imaging and Radiological Sciences, National Yang-Ming University, Taipei, Taiwan

Background: Based on recent advances in spontaneous synchronizations, the fMRI spectrum demonstrates its sensitivity to clinical abnormalities. However, unlike EEG, mechanisms of BOLD frequency features remain unclear. The general assumption is that BOLD signal reflects the neural activity linearly through single hemodynamic response function. In this project, we bypassed the assumption and observed both EEG and fMRI spectra under multiple sleep stages across brain channels/regions.
Methods: Nine healthy volunteers participated this study in a 3T Tim Trio MR scanner with a 32-channel MR-compatible EEG system. While sleeping, the fMRI signal was acquired with GE-EPI (TR = 2.5, TE = 35 ms, 35 slices with thickness of 3.4 mm, MTX = 64*64) for at most 2-hr simultaneous EEG-fMRI recordings in the midnight. Gradient and BCG artifacts were corrected for EEG data and the fMRI data underwent the standard preprocessing. Then we analyzed the spectrum from both motor cortex and the frontal region across 3 sleep stages.
Results: Figure 1 shows the spectral changes of EEG and fMRI in 3 stages. In Motor, the low-frequency fMRI power was greatly enhanced in stages 2, but EEG located in stage 3. Similar mismatch was also found in frontal, deviant from motor outcomes.
Conclusions: We presented that (1) regional specificity existed in the spectral change across sleep stages, and (2) linearity assumption across modalities may fail in sleep.

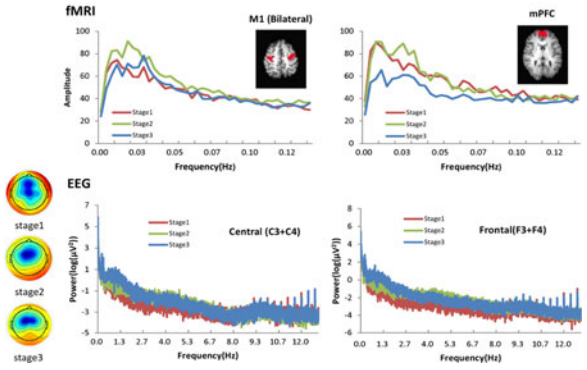

FIG. 1. Spectrum of fMRI (top) and EEG (bottom) across 3 NREM sleep stages. The red regions in MR image denote the selected ROI (M1 & mPFC), matching EEG channels from central and frontal regions.

P79A Effects of type and timing of childhood maltreatment on volume of ICA-based functional connectivity networks

S.B. Lowen[1,2], C.M. Anderson[1,2], E. Bolger[1], C.E. McGreenery[1], H. McCormack[1], M.H. Teicher[1]

[1]*Developmental Biopsychiatry Research Program, McLean Hospital, Belmont, MA, USA*
[2]*Brain Imaging Center, McLean Hospital, Belmont, MA, USA*

Background: Childhood maltreatment is a major risk factor for mood, anxiety, substance abuse, personality and psychotic disorders. Several studies have identified reproducible structural and/or functional alterations in a variety of regions including hippocampus, prefrontal and sensory cortex in adults with histories of childhood maltreatment. Studies also suggest that there are sensitive periods when specific regions are maximally vulnerable to the effects of childhood abuse, and that some regions may be particularly vulnerable to specific types of abuse. The aim of this study was to assess whether type and timing of recollected exposure was associated with alterations in volume of functional connectivity networks assessed using independent component analysis (ICA).
Methods: Resting state fMRI data was collected on 185 healthy, unmedicated subjects (71 M/114 F, 20–25 years of age). Data was preprocessed, aligned to MNI152 space, and resampled to 4 mm isotropic voxels. Group concatenation ICA with D = 40 was performed using Melodic, followed by dual regression using an in-house program, yielding subject-specific spatial maps; voxels exceeding a threshold of 10 were counted, yielding 185*40 component volumes. Exposure to ten types of childhood abuse was evaluated retrospectively with the Maltreatment and Abuse Chronology of Exposure (MACE) scale. Predictive modeling with cross-validation (using 11 different machine learning algorithms) was used to assess whether specific types and time periods of maltreatment were consistently identified across models as the most important predictors of volume.
Results: The primary predictors of default mode network volume were exposure to physical neglect, witnessing inter-parental violence, and parental and peer physical abuse (PA). Peak periods of sensitivity were at 3–6, 10, and 16 years of age. In contrast, volume of the executive control network was predicted more strongly by exposure to parental PA than any other type of maltreatment, and was particularly vulnerable at 15 years of age. Volume of the right attention network was most strongly predicted by exposure to peer emotional abuse between 10–13 years of age.
Conclusions: These findings support the hypothesis that exposure to early life stress affects brain network organization and highlights the possibility that the potential consequences are dependent on type of maltreatment and developmental stage at time of exposure. This may help explain why maltreatment is a risk factor for many different forms of psychopathology.

P80A Centrotemporal Spike Networks in Children with BECTS

T. Maloney[1], J. Tenney[1], J.P. Szaflarski[2], K.C. Hibbard[1], J. Vannest[1]

[1]*Cincinnati Children's Hospital Medical Center, Cincinnati, Ohio, U.S.A.,* [2]*University of Alabama at Birmingham, Birmingham, Alabama, U.S.A*

Background: Benign Epilepsy with Centrotemporal Spikes (BECTS) is one of the most common forms of pediatric epilepsy that is characterized by usually infrequent seizures but frequent centrotemporal spikes (CTS). Previous studies have shown subtle cognitive deficits in BECTS patients and there is still uncertainty as to what characteristics of CTS, if any, affect patients' cognitive outcomes. EEG source localization suggests that the CTS arise from activity in the centrotemporal regions but it is less clear how CTS may influence the brain's wider functional networks.
Methods: The analysis examined 6 BECTS patients (ages 8–10, 5 F), all right-handed native English speakers who had right sided CTS during a 10 to 15 minute resting state fMRI scan. EEG was acquired simultaneously to the fMRI; after removal of scanning and ballistocardiographic artifacts EEG was reviewed by an epileptologist who marked left, right and bilateral (symmetric) CTS. The timing of the right sided CTS was used in a group event related independent component analysis (eICA) (Masterton et al., 2012). The eICA method allows for the detection of functional networks related to the event of interest without placing constraints on the shape and onset of the hemodynamic response. The ICA was implemented in MELODIC, a part of FSL (FMRIB's Software Library), where the number of ICs were automatically chosen (Minka 2000, Beckmann 2004) and IC maps were thresholded with a probability $p > .5$ using a mixture model fit to the intensity histogram (Beckmann 2004). A dual regression analysis was performed on the eICA components to get spatial maps and timecourses for each subject that relate to the group results.
Results: The eICA analysis identified 16 components at the group level related to right CTS. Five of the components showed patterns and time courses that are indicative of motion or some other physiological noise, leaving 11 components that were related to the right CTS. Of the 11 components, 7 show involvement of the centrotemporal regions but they also indicate engagement of bilateral temporal, parietal, occipital and subcortical regions; with varying time courses relative to CTS.
Conclusions: These results suggest that there is a much wider network involved in CTS generation and/or maintenance that is not restricted to the centrotemporal region. Further analysis will help determine whether differences in the CTS networks explain the effect of CTS on patients' cognitive outcomes.

P81A Fetal functional connectivity and infant behavior: A preliminary report

J. H. Manning[1, 2], L. G. Grove[1, 2], J. D. Sakhardande[1], T. A. Ricard[1], P. Srivastava[1], M. E. Thomason[1, 2, 3]

[1]*Merrill Palmer Skillman Institute, Wayne State University, Detroit, MI;* [2]*Department of Pediatrics, Wayne State University School of Medicine, Detroit, MI, 48202 USA;* [3]*Perinatology Research Branch, NICHD/NIH/DHHS, Detroit, Michigan, 48202 USA*

Background: A tremendous amount of variability in early infant cognitive development may be explained by neural functioning in the fetal period. The opportunity both to quantify emerging neural circuitry and to prospectively link *in utero* brain networks to infant behaviors exists for the first time. Here we present the first longitudinal analysis of third trimester neural networks and infant behavior at 4-months-of-age (4 m).
Methods: Women in their third trimester of pregnancy were recruited during obstetrical visits in the Detroit Medical Center. All pregnancies were singleton, uncomplicated pregnancies.

Fetal functional connectivity (FC) was evaluated using resting-state functional MRI in seven fetuses (Gestational Age: mean = 35.591 weeks, SD = 4.488 days, range = 15 days). Seed-based connectivity was performed from primary visual (V1), auditory (A1), and motor-face (M1) regions. Later, when infants were 4 months-of-age, parents completed the Infant/ Toddler Sensory Profile (ITSP), describing the infants' development. ITSP auditory, visual, and tactile processing scores were compared to fetal FC measures using regression analyses. Results were considered significant at $p \leq 0.001$; $k \geq 10$.

Results: Connectivity between M1 and supplementary motor area was associated with increased sensitivity to face and head tactile input at 4 m. In contrast, connectivity between M1 and right ventrolateral prefrontal cortex (VLPFC) was associated with decreased sensitivity to tactile input at 4 m. Connectivity between V1 and the left hippocampus and right middle frontal gyrus were associated with behavioral sensitivity to bright lights at 4 m. However, connectivity between V1 and the right angular gyrus was associated with decreased light sensitivity at 4 m. Connectivity between A1 and left VLPFC was associated with increased ability to ignore nuisance sounds at 4 m. In contrast, connectivity between A1 and anterior cingulate cortex was associated with greater attention to continuous ambient sounds at 4 m.

Conclusions: We were able to establish that FC from regions-of-interest in the third trimester of gestation were be linked to infant behavior, as reported by parents, 4 months following birth. This was demonstrated in tactile, visual, and auditory behaviors from associated brain regions (M1, V1, and A1). Our study was limited by small sample size but continued data collection is underway to increase study numbers. Understanding typical *in utero* developmental course can provide insight in to the effect of insult, injury, or anomalous developmental trajectories. We were able to show, for the first time, that individual variability in infant behavior can be linked to covariation in brain functional *in utero*.

P82A Copy number deletions in schizophrenia: the relationship between mutation load, cognition, and functional connectivy of resting-state networks

A.K. Martin[1], G. Robinson[2], D. Reutens[3], B. Mowry[1]

[1]University of Queensland, Queensland Brain Institute, Brisbane, Queensland, Australia
[2]University of Queensland, School of Psychology, Brisbane, Queensland, Australia
[3]University of Queensland, Centre for Advanced Imaging, Queensland, Australia

Background: Total deletion burden has been implicated in schizophrenia risk and has been associated with reduced cognitive functioning. Previous studies have investigated total brain volumes but have not looked at functional connectivity in key resting-state brain networks implicated in cognition and schizophrenia risk.

Methods: Thirty-three chronic schizophrenia patients from a large genome-wide association study had resting-state fMRI and intelligence testing using an abbreviated IQ test. A seed-to-voxel analysis of the default mode and cognitive control networks was performed and correlated with IQ scores.

Results: Total deletion burden was negatively associated with IQ performance. Functional connectivity analysis identified correlations between deletion burden and both hyper- and hypoconnectivity within the default-mode network (posterior cingulate cortex and medial prefrontal cortex) and hypoconnectivity within the cognitive control network (right dorsolateral prefrontal cortex). Correlation analysis between measures of IQ and the regions of structural and functional connectivity differences found that greater functional connectivity in both the cognitive control network and default mode network was positively correlated with IQ. Greater functional connectivity between the default mode and cognitive control network was negatively associated with IQ.

Conclusions: Total deletion burden in schizophrenia is associated with reduced cognitive performance, which correlated with functional connectivity in a cognitive control and default mode network. Deletions may be affecting the efficiency of connections between regions important for cognition in patients with schizophrenia.

P83A A Biomarker Signal: Context-Dependent fMRI Connectivity Analysis of Clinical Trial Measures in AD

D.G. McLaren[1,2,3], R.A. Sperling[1,3,4], A. Atri[1,2,3]

[1]Massachusetts General Hospital, Boston, MA, USA; [2]Edith Nourse Rogers Memorial Veterans Hospital, Bedford, MA, USA; [3]Harvard Medical School, Boston, MA, USA; [4]Brigham and Women's Hospital, Boston, MA, USA

Background: With promising therapies for Alzheimer's disease (AD) entering clinical trials, fMRI has potential as a biomarker of trait or state to identify individuals who may be at higher risk or who are showing early neurophysiological changes in cognitive networks, and as a biomarker of rate, effect or efficacy to provide an early biological signal to prognosticate, gauge clinical progression or treatment response. The majority of fMRI studies in patients with AD have nevertheless focused on regional task-related activity rather than how functional connectivity during performance of a cognitive task can be related to disease stage, treatment or a clinical outcome measure. Importantly, this study assesses the patterns of associative-memory-related fMRI functional connectivity in AD associated with performance on cognitively demanding neuropsychological tests and clinical measures.

Methods: Twenty-four subjects with mild AD dementia (ages 54–82, nine females) participated in a face-name paired-associate encoding memory study. Generalized psychophysiological interactions (gPPI) were used to estimate the connectivity between the hippocampus and the whole brain during episodic memory encoding of novel and repeated face-name pairs. The dynamic flexibility of connectivity between these two conditions was correlated with standard AD clinical trial measures.

Results: The analysis revealed connectivity-behavior relationships that were distributed and task-specific within and across intrinsic networks. Importantly, these spatially distributed performance patterns were unique for each measure. In general, out-of-network behavioral associations with encoding novel greater than repeated face-name pairs hippocampal-connectivity were observed in the default-mode network, while correlations with encoding repeated greater than novel face-name pairs hippocampal-connectivity were observed in the executive control network. Psychophysiological interactions revealed significantly more extensive and robust associations between hippocampal-whole brain connectivity and performance on memory and clinical measures than previously revealed by standard activity-behavior analysis.

Conclusions: The patterns of robust correlations of whole brain connectivity and behavioral measures identified here may serve as ''coordinated state'' candidates for clinical interventions that affect the dynamic range of connectivity between seed and target regions. While these observations support the promise of gPPI as

a potential AD biomarker for clinical performance and stage, they require further development and validation through longitudinal pharmacological studies. The findings provide further support for the validity of an associative face-name encoding paradigm to probe the functional integrity of the distributed memory network in AD.

P84A Aberrant functional connectivity of resting state networks associated with trait anxiety

S. Modi[1], M. Kumar[1], C. P. Jeenger[1], P. Kumar[1], S. Khushu[1]

[1]*NMR Research Centre, Institute of Nuclear Medicine and Allied Sciences (INMAS), Delhi, India*

Background: Trait anxiety, a personality dimension, has been characterized by functional consequences such as increased distractibility, attentional bias in favour of threat-related information and hyper-responsive amygdala etc. The present study was aimed to investigate the possible associated alterations in the functional integrity of Resting State Networks (RSNs) associated with trait anxiety of the healthy subjects.
Methods: Twenty nine right-handed healthy individuals screened for current or past medical and psychiatric illness using the Hindi version of the Diagnostic Interview for Genetic Studies participated in the study. Resting state fMRI (Rs-fMRI) was carried out on a 3 Tesla whole-body MRI system using echo-planar T2*-weighted sequence. Each volume consisted of 30 interleaved 5-mm thick slices without interslice gap (TE = 30 ms, TR = 2000 ms, FOV = 240 mm, flip angle = 90°, voxel size = $3.75 \times 3.75 \times 5\ mm^3$). Total scanning time was 410 seconds (205 brain volumes), during which the subjects were asked to keep their eyes closed but being awake. After the rs-fMRI session, participants' trait anxiety levels were assessed using Spielbergers State-Trait Anxiety Inventory (STAI-Y2). Participant's current depression levels were noted using Beck Depression Inventory (BDI). The Rs-fMRI data was analysed using independent component analysis and a dual regression approach using FSL (www.fmrib. ox.ac.uk/fsl).
Results: Subjects were median split into two groups based on their STAI-Y2 scores: low anxiety group (STAI-Y2 score between 21 and 35), high anxiety group (STAI-Y2 score above 35). BDI scores were taken as covariates of no interest. Out of the twelve RSNs identified, high anxious subjects showed significantly reduced functional connectivity in regions of default mode network (posterior cingulate gyrus, middle and superior temporal gyrus, planum polare, supramarginal gyrus, temporal pole, angular gyrus and lateral occipital gyrus) and perceptual systems including medial visual network (Lingual gyrus, intracalcarine cortex, precuneus, cuneal, parahippocampal gyrus, supracalcarine cortex, Postcentral Gyrus, Superior Parietal Lobule, and Supramarginal Gyrus), auditory network (Heschl's gyrus, Planum Temporale, middle and superior temporal gyrus) and another network involving temporal, parieto-occipital and frontal regions (Postcentral Gyrus, Superior Parietal Lobule, anterior Supramarginal Gyrus and posterior parahippocampal gyrus) (Fig. 1).
Conclusion: Reduction in resting state connectivity in regions of the perceptual networks might underlie the perceptual, attentional and working memory deficits associated with trait anxiety. Our results might supply a novel insight into biological underpinnings of sub-clinical trait anxiety.

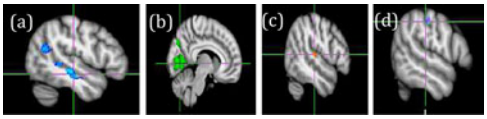

FIG. 1. Reduced connectivity in regions of (a) Default-mode network, (b) Medial visual network, (c) Auditory network and (d) Temporo-parietal-frontal network in high anxious subjects (FWE corrected $p < 0.05$)

P85A Cortical-subcortical circuits underlying parallel behavioural control systems

L.S. Morris[1,2,3], P. Kundu[1], M.A. Irvine[2], T.W. Robbins[1,3], E.T. Bullmore[2], V. Voon[2]

[1]*Behavioural and Clinical Neuroscience Institute, Cambridge, UK,* [2]*Department of Psychiatry, University of Cambridge, UK,* [3]*Department of Psychology, Cambridge, UK*

Background: Distinct yet overlapping cortical-subcortical circuits orchestrate an individuals' ability to flexibly navigate a dynamic environment. Three parallel cortical-subcortical loops, involving dorsolateral prefrontal cortex (dlPFC), supplementary motor areas (SMA) and ventromedial prefrontal/orbitofrontal cortex (vmPFC/OFC), are responsible for cognitive, sensorimotor and limbic processes, respectively. The striatum can be similarly dissected, with the ventral striatum (VS) typically being involved with more limbic, and the putamen with more motoric processes. Recruiting these circuits are two coexisting yet dissociable behavioural control systems; goal-directed and habitual. Crucial to flexible goal-directed control is adaptive reinforcement-driven learning, as well as the ability to shift attention away from previously relevant stimuli. These processes can be tested with reversal-learning (RL) and extradimensional (ED) set-shifting tasks, respectively. The current study aimed firstly to map the intrinsic cortical-subcortical circuitry, then to determine the extent to which these connections play a role in the described neurocognitive systems.
Methods: Resting-state functional MRI (rsfMRI) was collected from 66 healthy volunteers. Traditionally, single-echo planar sequences are used to acquire rsfMRI data. However, these are highly vulnerable to major movement-related artifacts, resulting in much spurious noise. To avoid this poor signal:noise ratio, we employed a unique multi-echo planar sequence allowing a more precise distinction between neuronal (BOLD-like) and non-neuronal (non-BOLD-like) components. Averaged BOLD time-courses within cortical seed regions were correlated with every other voxel in the brain to produce seed-based functional connectivity maps. These were then correlated with performances on three tasks: a sequential choice task designed to distinguish goal-directed (model-based) from habitual (model-free) learning strategies; a probabilistic RL task; and an ED set-shifting task.
Results: Prominent borders were apparent between connectivity of the dlPFC, vmPFC and SMA, which almost exclusively correlated with the activity within the dorsal caudate, ventral striatum and putamen, respectively. Medial and lateral OFC were examined separately due to distinctions of their anatomical connectivity and function. The medial OFC (mOFC) was exclusively functionally connected with VS. While more model-based learning was associated with mOFC and VS connectivity, more model-free learning was associated with SMA and posterior putamen connectivity. Reward-related acquisition learning was associated with connectivity between vmPFC and VS, whereas reversal-learning errors were associated with mOFC and

VS connectivity. Interestingly, loss-related reversal errors were negatively correlated with mOFC and VS connectivity. Furthermore, ED shift errors were associated with dlPFC and VS connectivity.
Conclusions: We highlight that while some of these systems are working in parallel, they remain functionally independent and neuroanatomically dissociable.

P86A To what extent do abnormal default mode network cerebellar activations coincide with mTBI impairments?

D.E. Nathan[1,2], P.H. Yeh[1,3], J.L. Graner[1], W. Liu[1,2], T.R. Oakes[1] and G. Riedy[1]

[1]Dept. Neuroimaging, National Intrepid Center of Excellence, Walter Reed National Military Medical Center, Bethesda, MD, USA, [2]NorthTide Group LLC, Dulles, VA, USA, [3]Henry M. Jackson Foundation, Bethesda, MD, USA

Background: The cerebellum has been typically associated with motor control and coordination. However, there is a growing body of evidence which suggests the presence of cerebellar involvement in cognitive networks, visual spatial processing, executive function and emotional processing. An understanding of how information is relayed to, and from the cerebellum with respect to emotional, cognitive and functional networks warrants more research. This relationship between cerebellar and cortical networks may elucidate the disruptive effects of mild traumatic brain injury (mTBI), which at this moment remain elusive in standard clinical imaging modalities. The goal of this study is to explore the extent of differences in resting state default mode network cerebellar connectivity between mTBI subjects and healthy controls.
Methods: Resting state default mode network maps were obtained using dual-regression independent component analysis (ICA). This is a data driven approach and the group data sets were decomposed into 25 independent components. The final group maps were corrected at a p-value < 0.0001 and a cluster size greater than 200 voxels (8 mm^3 each). Regions of interest were defined using the Harvard cortical, Harvard subcortical and probabilistic cerebellar atlases. An independent samples *t-test* and ANOVA with a significance level of $p < 0.05$ were used to identify regions of significant difference between groups. Partial linear regression analysis was used to assess the correlations between DMN activation in the cerebellum with neuropsychological assessments. The results were thresholded using $R^2 \geq \pm\ 0.70$, and a corrected p-value < 0.005.
Results: The results from the resting state DMN maps showed the presence of significantly higher co-activity within the left cerebellum lobule VII, left cerebellum lobule IV, right cerebellar tonsil, right cerebellar inferior semi-lunar lobule and right Culmen, of mTBI subjects. This is a unique finding that has not been traditionally reported in resting state default mode network analysis. The analysis of neuropsychological data showed correlations ($R^2 > 0.70$, $p < 0.005$) between areas of the cerebellum with behavioral measures of working memory, executive function and visual spatial processing.
Conclusions: The results from this study suggest that the cerebellum has a larger role during cognitive-related processes and could be part of a network involved with memory-related functions, through connections via regions of the thalamus and brain stem that in turn project to cortical regions such as the frontal and temporal lobes. The results from the partial correlations analysis also suggest a relationship between visual attention measure and frontal regions of the brain and cerebellum. However, more testing with a larger sample size is needed to determine the generalizability of these findings and practicality as a biomarker of mTBI.

P87A Network modeling of resting state connectivity points towards the bottom up theories of schizophrenia

F. Orliac[3], N. Delcroix[5], M. Naveau[6], P. Delamillieure[1,2,3], M. Joliot[4]

[1]CHU de Caen, Service de Psychiatrie Adultes, Centre Esquirol Caen, F-14000, France; [2]Université de Caen Basse-Normandie, UFR de médecine, Caen, F-14000, France; [3]UMR 6301 CNRS-CEA-Univ. Caen, France; [4]GIN, UMR 5296 CNRS CEA Université de Bordeaux, France; [5]GIP Cyceron, UMS 3408, Caen, France; [6]Jülich Supercomputing Centre, Forschungszentrum, Jülich, Germany

Background: The dysconnectivity theory of schizophrenia proposes that schizophrenic symptoms arise from abnormalities in neuronal synchrony. Based on large-scale network functional connectivity (FC) analysis of fMRI resting state data, we search for those abnormalities and their relations to clinical variables.
Methods: We analyzed intra- and between-network FC strength of 34 resting-states networks (RNs) in 29 Schizophrenia Patients (SP) and 29 Healthy Controls (HC) using resting-state FMRI data. Each RN reference map (Naveau et al., Neuroinformatics, 2012) was used to generate subject-specific versions of the spatial maps, and associated time series, using dual regression (Beckmann et al., OHBM, 2009). For each subject FC between time series of the each RN pair was computed using Pearson's correlation; from these graphs we extracted individual subject RN degree of centrality (DC) and intra-network connectivity strength (INCS). Group differences were tested on DC, INCS (MANOVA, $p < 0.05$) and FCs (ANOVA, $p < 0.05$ Bonferonni-Holmes corrected, $N = 155$). Non-parametric Spearman test was used to assess the correlation of FC values with the 3 clinical variables: the Positive And Negative Syndrome Scale (PANSS-P and PANSS-N) and the hallucinatory status (No Hallucinations (NH), Auditory Hallucinations (AH), or Auditory and Visual Hallucinations (AVH)).
Results: Our results showed significant MANOVAs weaker DC ($p = 0.0013$) and INCS ($p = 0.0016$) in the SP group. Post-hoc analysis demonstrated that alterations affect the four RNs encompassing the occipital lobe and a right fronto-parietal RN. Among the 10 pairs showing significant lower FC in the SP compared to the HC group 7 were in between a visual RNs and one of the 3 cross-modal binding networks. Three of these pairs showed FC decrease associated with positive (PANSS-P), and one pair with negative symptoms severity (PANSS-N). Moreover, FC between one of the 4 visual networks and a multimodal sensory network was significantly lower in AVH compared to NH patients. Surprisingly, FC between a posterior component of the default mode network (described as subtending mental imaging process) and a visual associative network was found higher in SP compared to HC. FC values of this pair were positively correlated with the positive symptoms, and FC was significantly more important in AVH patient group than each of the two other groups (NH and AH).
Conclusions: Sensory networks, and more precisely visual and cross-modal binding networks seem more functionally altered than high-level cognitive networks in schizophrenia. Negative symptoms, positive symptoms and hallucinations seem related to abnormalities in visual processing and crossmodal binding, which is in line with bottom-up model of schizophrenia.

P88A Resting-state connectivity changes in women with breast cancer

S.J. Peltier[1,2], M.G. Berman[3], M.K. Askren[4], B. Misic[5], M.S. Jung[6], A.R. McIntosh[5], L. Ossher[7], M. Zhang[8], P.A. Reuter-Lorenz[7], B. Cimprich[6]

[1]Functional MRI Laboratory, [6]Nursing, [7]Psychology, [8]Biostatistics, University of Michigan, Ann Arbor, MI, USA; [3]Psychology, University of South Carolina, Columbia, SC, USA; [4]Radiology, University of Washington, Seattle, WA, USA; [5]Rotman Research Institute, University of Toronto, Toronto, Canada

Background: This study investigates resting-state network correlations in women treated for breast cancer and age-matched healthy controls. Univariate connectivity changes between timepoints and a multivariate partial-least squares analysis were examined.
Methods: 30 women were enrolled: patients with breast cancer undergoing treatment with chemotherapy (n = 10) or radiation (n = 10); and 10 age-matched healthy controls. Subjects were scanned at baseline (prior to therapy, time 1) and 5 months later (time 2, which corresponded to 1 month after chemotherapy; and 3 months after radiotherapy). FMRI data was acquired on a 3.0 T scanner using a spiral-in sequence (TR/TE/FA/FOV = 1.5 s/30 ms/90/24 cm, 64 × 64 matrix, 5 mm slice thickness, 25 slices). T1 overlays and whole-brain SPGRs were also collected. Subjects were instructed to look at a fixation cross during the resting state acquisition (8 min duration).

Data preprocessing included: RETROICOR physiological noise removal, slice timing correction, motion correction, normalization to MNI space, and spatial smoothing (4 mm FWHM). Nuisance regressors (first principal component of head motion, and the global mean) were removed prior to low-pass filtering (< 0.08 Hz). verage AAL template ROI timecourses were extracted and the correlation between every pair of ROI timecourses was calculated and z-scored. Univariate t-tests were used to examine significant differences versus time and group. Partial Least Squares (PLS) was used to find the combination of group and time saliences (i.e., contrast weights) that explain the most covariance in the data. Permutation testing was used for reliability.
Results: Changes in connectivity z-scores were observed, with significant timepoint differences in the chemotherapy and the radiation therapy group as compared to the control group. Unique regional correlations were observed for each patient group. The PLS analysis also showed significant time by group interactions. The principal latent variable was expressed in all groups, but was accentuated for the patient groups. The chemotherapy group showed the largest difference in functional connectivity from time 1 to time 2.
Conclusions: Univariate and multivariate analyses both exhibited differential patterns of resting-state connectivity across therapy groups and time in subjects with breast cancer. This may form the basis for improved diagnostic and monitoring techniques for cognitive changes associated with breast cancer and its treatment.

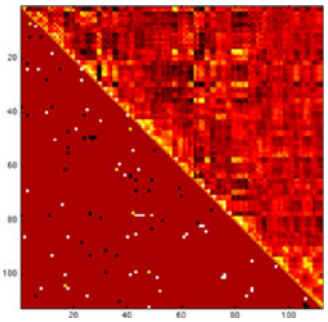

FIG. 1. AAL correlation results. (Upper triangle) Average control z map, time 1(Lower triangle) Significant time 2 – time 1 differences vs. controls for chemo (black), radiation (white), overlap(yellow) ; p < 0.01.

P89A Telomere Length is Associated with Altered Amygdala Resting State Functional Connectivity

N.S. Philip[1,2], S.L. Carpenter[1], L.H. Sweet[3], H.T. Kao[4], B. Porton[4], L.H. Price[2], L.L. Carpenter[2] and A.R. Tyrka[2]

[1]Center for Neurorestoration and Neurotechnology, Providence VA Medical Center; Alpert Medical School of Brown University, Providence RI USA [2]Laboratory for Clinical and Translational Neurosciences; Alpert Medical School of Brown University, Providence RI USA [3]Department of Psychology, University of Georgia, Athens GA USA [4]Laboratory for Molecular Psychiatry, Brown University, Providence RI USA

Background: Recent studies have demonstrated that various psychiatric illnesses and exposures can affect resting state networks; our group has recently demonstrated that childhood trauma impacts resting state functional connectivity (RSFC) within and between resting state networks (RSN), including the default mode, executive and emotional processing networks. Recent evidence has also demonstrated the importance of telomeres in mediating apoptosis, as telomere shortening leads to cell senescence. One potential etiology of trauma's impact on RSNs may be via induction of early cell death mediated by pathogenic telomere shortening. This study sought to explore the relationship between telomere length (TL) and amygdala RSFC.
Methods: 21 unmedicated healthy participants, without medical or psychiatric disorders, were scanned during 8 minutes of resting state acquisition using 3T MRI. After image preprocessing and motion correction, whole-brain RSFC was evaluated by seeding the left and right amygdala. TL was measured in leukocyte DNA via quantitative polymerase chain reaction, and was evaluated as a predictor of whole brain RSFC with the amygdala. Whole-brain results were corrected for family-wise error with statistical significance set at 2-tailed p < .05.
Results: Amygdala RSFC matched expected spatial patterns. When evaluating the right amygdala, greater TL was associated with decreased RSFC with the left middle frontal gyrus (inclusive of Brodmann areas 6 and 8; corrected p < .01) and increased RSFC with the bilateral precuneus (corrected p < .025). When evaluating the left amygdala, the association between TL and reduced RSFC with the left Brodmann 6 and 8 did not reach statistical significance (corrected p = .12).
Conclusions: These results indicate that TL may be associated with changes in RSFC between the amygdala and regions critical for visual attention, motor planning and self-monitoring. A shift from external to internal-based threat processing may represent reallocation of internal priorities, perhaps mediated by, or at least correlated with, cellular aging. Although it is unclear whether peripheral TL length reflects CNS cellular aging, these results suggest the possibility that TL changes might modulate important brain connections, and that future studies are needed to further investigate the relationship between brain connectivity and metrics of cellular aging.

P90A Foreign Language Learning Experience Enhances Inter-hemispheric Functional Connectivity

Z. Qi[1], Y. Wang[1], Q. Liu[1], C. de los Angeles[1], S. Whitfield-Gabrieli[1], J. D. E. Gabrieli[1]

[1]*Massachusettes Institute of Technology, Cambridge, MA, USA*

Background: Foreign language learning is one of the most challenging educational activities during adulthood. For native English speakers of Mandarin learners, the tonal feature and logographic writing system add extra difficulty to adapt to a profoundly distinctive language. Previous fMRI research suggested Mandarin processing is less left lateralized, compared to Western languages in native speakers. Moreover, second-language learning literature provides mixed findings regarding the plasticity of lateralization. The extent of left lateralization is reported to be associated with second-language proficiency, the type of language being processed, and multilingualism (e.g. Wong et al., 2007; Hull & Vaid, 2007; Hosoda et al., 2013). Nevertheless, how language-learning experience modulates the organization of the functional language network remains poorly understood. Therefore, resting-state connectivity provides a unique approach to study learning-induced plasticity in a task-free context.
Methods: Twenty-three native speakers of American English (mean age = 23.2 years, 8 females) participated in an intensive 4-week Mandarin course in a naturalistic classroom setting. Resting-state MRI images were obtained before and after language training in a 6.2-min scan (TR = 2.5 sec, 37 slices with $3.5 \times 3.5 \times 3.5$ mm voxels). Images were slice-time corrected, realigned, normalized in MNI space, and smoothed with a 6-mm kernel. The head motion artifact outliers were modeled in the first-level general linear model. Functional connectivity was analyzed using a seed-driven approach with CONN. Given the functional importance of the Broca's area in language, we chose Broca's area (BA 44/45) and its right-hemisphere homologue as the two seeds for analysis.
Results: The inter-hemispheric connectivity significantly increased after language training. We observed enhanced connectivity from the Broca's area seed to its right-hemisphere homologue (BA 44/45), right insular (BA 13), and the right superior temporal gyrus (BA 22). Symmetric increase of connectivity was also observed with the right BA 44/45 as the seed connecting with the left pars triangularis (BA 45), the left insular (BA 13), and the left temporal areas (BA 20, 21, and 22). The extent of connectivity increase between Broca's area and the right IFG was positively correlated with learners' Mandarin proficiency at the end of training ($r = 0.67$). All results were corrected for multiple comparisons using FDR methods with the clusterwise threshold of $p < 0.05$, and the voxelwise threshold of $p < 0.05$.
Conclusions: Our results unveil that foreign language learning experience strongly enhanced the functional connectivity between the classic language network in the left hemisphere and its right homologue. The increase of inter-hemispheric coherence induced by language training suggests critical roles of right hemisphere and inter-hemispheric communication in learning a foreign language.

P91A Reduced intra- and inter-hemispheric resting state functional connectivity in chronic cocaine smokers

S. Ray[1], S. Gohel[2], B. Biswal[2]

[1]*Rutgers Univesity Center of Alcohol Studies, Piscataway, NJ, USA,* [2]*New Jersey Institute of Technology, Newark, NJ, USA*

Background: According to the functional magnetic resonance imaging (fMRI) studies, chronic cocaine use is associated with changes in frontal lobe functioning. Resting-state fMRI techniques have demonstrated reduced (Kelly, 2011; Munier, 2012) as well as increased (Camchong, 2011) resting state functional connectivity (RSFC) in frontal brain region in cocaine users relative to control participants. To begin to address the discrepancies in the literature involving the relationship between RSFC between brain regions and cocaine use measure, we first examined RSFC between brain regions in non-treatment-seeking chronic smokers of cocaine and healthy control participants. We then examined the relationship between functional connectivity between brain regions and duration of cocaine use in cocaine smokers.
Methods: Twenty (29–53 yrs; 15 M; 5 F) non-treatment seeking chronic cocaine smokers abstinent from cocaine use for 72 hrs and 17 (25–53 yrs; 13 M; 4 F) healthy volunteers completed a resting state scan and an anatomical MPRAGE scan. During the resting state scan, participants were instructed to lie quietly without any movements and visually fixate on a cross for six min. Imaging data processing included motion correction, brain extraction, band pass filtering between 0.01/0.1 Hz. Pre-processed fMRI data were transformed into MNI 3 mm standard space. Group independent component analysis (ICA) was performed on this fMRI data and 20 ICs were estimated. Of these 20 ICs, 9 ICs were found to represent known resting state networks and were divided into 61 distinct regions of interest (ROIs). For each of the 61 ROIs, time series were extracted and pair-wise correlation was computed for each of the ROI pairs. These correlation values representing functional connectivity strength were converted into Fishers z-values. Unpaired t-tests were conducted to compare these connectivity strength values between cocaine smokers and controls. For each of the ROI pairs that significantly differed from the control participants in connectivity strength, correlations were computed between connectivity strength and cocaine use duration for the cocaine group.
Results: Significant differences were detected between cocaine smokers and controls in the inter-hemispheric and intra-hemispheric connectivity of different ROI pairs. Healthy controls showed significantly higher connectivity compared to cocaine smokers across these ROI pairs. Connectivity between left medial frontal gyrus and left precuneus, left cingulate gyrus, right cingulate gyrus, left medial frontal gyrus and left middle frontal gyrus; between right superior temporal gyrus and left pyramis; and between left cuneus and right culmen significantly correlated with duration of cocaine use.
Conclusions: Chronic cocaine smokers showed a decreased RSFC within intra-hemispheric frontal brain regions, intra-hemispheric frontal-limbic as well as inter-hemispheric frontal-limbic brain regions compared to controls. This is the first study to indicate that connectivity strength within frontal and frontal-limbic brain regions are positively related to years of cocaine use. Future studies may address whether these alterations in functional connectivity contribute to impaired decision making and judgment. This research was supported by NIDA K01DA029047.

P92A Does traumatic brain injury lead to a functionally split brain? A study of resting state networks following traumatic brain injury

A. Rigon[1], M.C. Duff[1,2,3], M.W. Voss[1,4]

[1]*Neuroscience Graduate Program, University of Iowa, IC, IA;* [2]*Department of Neurology, University of Iowa, IC, IA;* [3]*Department of Communication Science and Disorder, University of Iowa, IC, IA,* [4]*Department of Psychology, University of Iowa, IC, IA*

Background: Traumatic brain injury (TBI) often has long term debilitating sequelae in cognitive, social and affective domains. Understanding how TBI impacts functional and structural integrity of brain networks that underlie these domains is key to guiding future approaches to TBI rehabilitation. The objectives of the current study are 1) to investigate the presence of differences in functional connectivity (FC) of resting state networks (RSNs) between patients with chronic TBI ranging from mild to severe and demographically matched normal comparison participants (NC) and 2) to examine how these observed differences correlate with white matter (WM) damage.
Methods: We conducted network seed-based FC analyses by using RSNs derived from the Smith et al., 2009 meta-analysis as seeds. In particular, we focused on two externally oriented networks (EONs), the Frontal Executive network (FEN) and the Emotional Salience network (ESN), and one internally oriented network (ION), the Default Mode Network (DMN). Initial network seed-based analyses suggested differences in laterality between subject groups. Therefore, follow-up analyses examined this further by dividing each network seed into a left and right lateralized seed. Standard RSN processing was performed with a custom toolbox, including ICA-based denoising and motion scrubbing. Finally, we performed diffusion tensor imaging (DTI) analyses to explore how FC differences correlate with structural WM connectivity.
Results: When compared with NC, TBI patients displayed significantly less FC between lateralized seeds and both homologous and non-homologous regions in the opposite hemisphere for EONs but not for the ION. Region of interest (ROI) correlation analyses confirmed the presence of significantly higher correlations between left and right seeds in NCs for the FEN and ESN ($p < .01$), but not for the DMN ($p = .98$). In addition, TBI patients showed higher FC between the bilateral DMN seed and both the precuneus (PCUN) and the hippocampus. DTI analyses of the TBI sample also revealed that greater global fractional anisotropy (FA) values were associated with less FC between DMN and the PCUN ($r = -.52$; $p < .01$).
Conclusions: For the first time, the current study reveals that TBI patients show less inter-hemispheric FC between the FEN and ESN, traditionally linked with the allocation of cognitive resources to external stimuli, but not between nodes of the DMN, which has been shown to be involved in internally directed cognition. As TBI patients often report difficulties interacting with the outside environment (e.g., attention impairment, sensory overload, etc.), future studies should explore how lack of inter-hemispheric FC in EONs correlates with behavioral performance on tasks that require attending to the external environment.

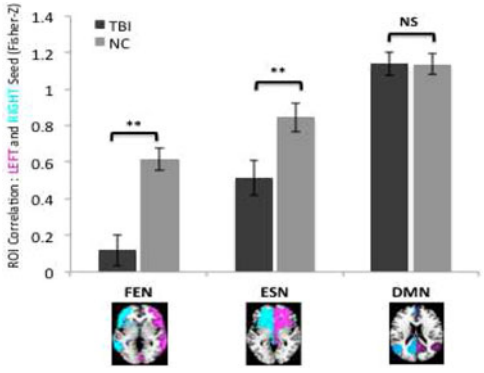

P93A Can graph-theory parcellation schemes based on resting state functional connectivity inform us about depression disease and vulnerability status?

Z. Samara[1], E.A.T. Evers[1], H.B.M. Uylings[2,3], G. Rajkowska[4], J.G. Ramaekers[1], P. Stiers[1]

[1]Department of Neuropsychology & Psychopharmacology, Faculty of Psychology & Neuroscience, Maastricht University, Maastricht, NL, [2]Department of Anatomy & Neuroscience, VU University Medical Center, Graduate School Neurosciences Amsterdam, Amsterdam, NL, [3]Departrment of Psychiatry & Neuropsychology, School for Mental Health and Neuroscience, Maastricht University, NL, [4]Department of Psychiatry and Human Behavior, University of Mississippi Medical Center, Jackson, MS 39216-4505, USA

Background: The orbitomedial prefrontal cortex (OMPFC) is involved in goal-directed decision making, reward processing and the experience of emotion. Recent work (Kahnt et al., 2012; Samara et al., *submitted*) demonstrates that functional connectivity-based parcellation of the OMPFC is feasible despite the presence of susceptibility artefacts in this part of the brain. Furthermore, a graph-theory parcellation approach which delineates individual-optimized modules, gives rise to neuro-anatomically meaningful results both at the level of individual cortical fields and at the level of the higher-order connectional organization within the OMPFC (Samara et al., *submitted*). However, it remains unknown whether this parcellation scheme can be used to identify differences between patients and controls in systems-level diseases such as major depressive disorder (MDD).
Methods: We used the left-hemisphere OMPF parcellation map delineated in our previous study as a template to examine connectivity differences between 35 patients with MDD (BDI > 20), 36 participants with familial MDD history and 38 controls. A 6-min resting state scan (eyes open) of each participant was parcellated using the Louvain module-detection algorithm. Individual modules were assigned to the previously established template by means of both their spatial proximity and their connectional similarity.
Results: Data are currently under analysis and will be presented at the conference. The functional connectivity profiles of clusters at the ventromedial PFC, the ventral anterior insula, dorsolateral PFC, dorsal ACC and medial and lateral orbital cortex are compared between the three groups.
Conclusions: This approach, if successful, would constitute an important step forward in the application of resting state connectivity methods for the diagnosis and treatment of depression.

P94A Resting state connectivity in high functioning autism and ADHD using EEG coherence: A preliminary study

A. K Saunders[1], J. P Hamm[1], I. J Kirk[1], K. E Waldie[1]

[1]the University of Auckland, Auckland, New Zealand

Background: Abnormal resting state brain activity may be a defining feature of neurodevelopmental disorders such as attention deficit hyperactivity disorder (ADHD) (Murias, Swanson & Srinivasan, 2007) and autism spectrum disorder (ASD) (Murias, Webb, Greenson & Dawson, 2007). Imaging studies reveal that connectivity of posterior regions to prefrontal cortex is atypical in people with ASD (Langen, Leemans, Johnston et al., 2012). In addition, EEG research has demonstrated elevated coherence in

the alpha band, and reduced coherence in the theta band in ASD (Mantini, Perrucci, Del Gratta, Romani & Corbetta, 2007). Abnormal structural and functional connectivity has also been implicated in ADHD (Konrad & Eickhoff, 2010). More specifically, EEG research has found subjects with ADHD show elevated coherence in the lower alpha band and reduced coherence in the upper alpha band (Murias, Swanson & Srinivasan, 2007). The current pilot study uses EEG coherence measures in ADHD and ASD populations to investigate resting state connectivity. The current study will add to a larger research effort to investigate brain based differences in ASD and common coexisting conditions.

Methods: Resting state EEG analysis was conducted on 12 adult participants aged between 17 and 32 years (high functioning autism ($n=4$); ADHD ($n=4$); neurotypical controls ($n=4$)). Subjects were fitted with a 128-channel Geodesic electrode net and instructed to look at a fixation cross centered on a blank computer screen for two minutes, then close their eyes for two minutes. Electroencephalogram (EEG) was registered continuously from all electrodes and the signal amplified (1000 X) and filtered through a 0.1–100 Hz analogue bandpass filter using the Electrical Geodesics, Inc., preamplifier system (300 input impedance). Initial coherence analysis was performed in the theta (4–7 Hz) and alpha (8–12 Hz) bands between frontal and temporal electrodes, and within temporal, parietal and occipital electrodes.

Results: Consistent with previous work, people with ASD had larger EEG coherence, relative to controls, in the theta band particularly within temporal and parietal regions. Frontal to parietal and temporal coherence was higher in controls in the alpha band. Relative to controls and people with ASD, early data suggest higher theta coherence in parietal and occipital lobes in people diagnosed ADHD.

Conclusions: The current pilot study is consistent with existing research that demonstrates atypical resting state connectivity in ASD and ADHD compared to neurotypical controls. Current preliminary analysis serve as a basis for further research. Given that ASD and ADHD co-occur 50–70% of the time (Ghaziuddin & Zayfar, 2008) it is important to investigate the shared underlying brain basis of both conditions. Future analysis will investigate the brain basis of the conditions when they occur together in one individual versus alone.

P95A Modulation of the Default-Mode-Network in the mouse brain using functional connectivity MRI

D. Shah[1], E. Jonckers[1], I. Blockx[1], F. Kara[1], S. Rossner[2], M. Verhoye[1], A. Van der Linden[1]

[1]Bio-Imaging Lab, University of Antwerp, Antwerp, Belgium, [2]Paul Flechsig Institute for Brain Research, Leipzig, Germany

Background: The Default-Mode-Network (DMN) is a resting-state network affected in many human brain disorders. Investigating DMN alterations in mouse models of disease allows to explore disease-specific mechanisms, perform treatment studies and subsequently enables pathology-specific readouts in the clinic. Considering the lack of DMN studies in mouse models and the potential differences between the human and murine DMN, it is imperative to first understand how DMN functional connectivity (FC) can be modulated in mice. The present study explores the inference of the mouse DMN by investigating DMN FC under medetomidine sedation, under cholinergic and serotonergic modulation and in the TG2576 mouse model of amyloidosis[1].

Methods: RsfMRI was performed on a 9.4 T MRI system using a gradient echo EPI sequence. All mice (N = 15/group) were sedated using medetomidine[2]. The effect of medetomidine sedation (0.3 mg/kg) was evaluated in 2 groups of C57BL/6 mice at 20 min and 50 min post-injection. Additional groups of C57BL/6 mice were s.c. injected with saline (10 ml/kg), a cholinergic antagonist (scopolamine, 3 mg/kg) or agonist (milameline, 1 mg/kg) and a serotonergic antagonist (WAY100135, 3 mg/kg) or agonist (8OHDPAT, 1 mg/kg). Finally, DMN FC was evaluated in TG2576 and wild-type mice (18 months old). All rsfMRI data were analyzed with a region-of-interest analysis.

Results: The mouse DMN could only be discerned at 50 min after the medetomidine injection. At 20 min post-injection the DMN showed decreased FC with the hippocampus and temporal association cortex. Scopolamine and milameline induced an overall decrease and increase of DMN FC, respectively. WAY100135 decreased DMN FC in the orbitofrontal cortex and hippocampus. 8OHDPAT had no effect on DMN FC. The TG2576 mice showed decreased DMN FC that overlapped with the cholinergic and serotonergic modulations i.e. in the cingulate cortex, hippocampus, thalamus and temporal association cortex.

Conclusions: Different sedative conditions differently influence DMN FC, suggesting a role in consciousness. Modulating cholinergic and serotonergic neurotransmission disrupts DMN FC, proposing a similar effect in diseases involving these systems. This was confirmed in the TG2576 mice showing corresponding DMN FC deficits. Altogether, this study takes the first step to a greater understanding of the mouse DMN.

References: [1] Hsiao et al., (1996) Science 274:99–102, [2] Jonckers et al (2011) Plos One 6

Acknowledgements: This research was supported by the EU 7th Framework Programme (INMiND), by Molecular Imaging of Brain Pathophysiology (BRAINPATH) within the Marie Curie (IAPP) program, by the Institute for the Promotion of Innovation by Science and Technology (IWT) in Flanders and by the UA doctoral grant BOF-DOCPRO 2013.

P96A Abnormal Cerebellum Functional Connectivity in Schizophrenia

A.K. Shinn[1,2], J.T. Baker[1,2], K.E. Lewandowski[1,2], D. Öngür[1,2]

[1]McLean Hospital, Belmont, MA, USA, [2]Harvard Medical School, Boston, MA, USA

Background: Schizophrenia (SZ) is a devastating illness associated with disturbances in multiple domains. Growing evidence suggests that cerebellar abnormalities play a major role in the pathophysiology of SZ. However, it is unclear what specific cortico-cerebellar networks are altered in SZ. Here, we ystematically investigated cerebellum functional connectivity (FC) using a seed-based approach, utilizing the cortical parcellation map of Yeo et al. (2011) as the basis for our FC seeds.

Methods: Participants were 44 patients with schizophrenia spectrum disorders (SZ) and 28 healthy controls (HC). Using a Siemens Trio 3-Tesla MRI scanner, we acquired T2-weighted functional scan (interleaved EPI sequence, 42 oblique slices, flip angle 82°, TE/TR = 24/2500 ms, 3.5 mm isotropic voxels, matrix 128×128, 224 mm^2 FOV, 240 volumes over 600 s). Participants were scanned at rest, and instructed to stay awake, keep their eyes open, and think of nothing in particular.

We used FSL v5.0.6 for image analyses. After discarding the first 4 volumes, images were slice-time and motion corrected, smoothed with a 6 mm Gaussian kernel, band-pass filtered ($0.009\ Hz < f < 0.08\ Hz$), and affine registered to standard MNI space.

We used the 17 network (N) cortical parcellation map of Yeo et al. (2011) as the basis for our FC seeds. We excluded the Visual Peripheral (N1) and Visual Central (N2) networks due to potential confounding by signal from visual cortical regions, located immediately adjacent to cerebellum. Consistent with Baker et al. (2014), we also combined N9 (temporal pole) and N10 (orbitofrontal cortex) into a single Limbic network. Thus we analyzed 14 total networks. With the exception of the already small Control C (N11) and Default Mode C (N15) networks, we eroded each of the network maps by one voxel layer using a 3D kernel. The BOLD time course from each of the 14 network seeds was extracted and entered into GLM, with signal from white matter, CSF, and motion correction parameters regressed. Data from first-level analyses were entered into a mixed-effects group analysis. Given our goal to investigate between-group FC differences in the cerebellum, we restricted our analysis to the cerebellum, using the cerebellum atlas in FSL as a pre-threshold mask. We set our voxel threshold to $p < 0.01$, correcting for multiple comparisons with a $p < 0.05$ cluster threshold.

Results: In this preliminary analysis, we found SZ to have *reduced* cortico-cerebellar FC in Ventral Attention (N7), Salience (N8), Control A (N12), and Control B (N13) networks, and *greater* cortico-cerebellar FC in Default Mode A (N14), B (N15), and D (N17) networks, compared to HC. SZ did not differ from HC in the cortico-cerebellar FC of Somatomotor (N3, N4), Dorsal Attention (N5, N6), Limbic (N9-10), Control C (N11), and Default Mode A (N16) networks.

Conclusions: Our findings suggest that cerebellar FC abnormalities in SZ mirror the cortical FC abnormalities that have been described by others in SZ.

P97A Placebo effect on resting-state subgenual cingulate functional connectivity in Major Depressive Disorder

M. Sikora[1], M. Peciña[1], E. Avery[1], B. J. Mickey[1,2], J. Zubieta[1,2]

[1]Molecular and Behavioral Neuroscience Institute, [2]Department of Psychiatry and Radiology, Medical School, University of Michigan, Ann Arbor, MI, USA

Background: High placebo rates have been consistently observed in antidepressant (AD) clinical trials (Rutherford & Roose, 2013). Yet, our understanding of the neurobiology of placebo responses and how they contribute to recovery from Major Depressive Disorder (MDD) is lacking. Activity in the subgenual anterior cingulate (sgACC) has shown promise in predicting treatment outcome in MDD; decreases in sgACC activity have been associated with various AD treatments (Mayberg et al., 2005). Here, we examined, for the first time, the effects of placebo administration with positive expectations on sgACC resting-state functional connectivity (sgACC-rsFC) in patients with MDD. Based on previous evidence on the mechanisms involved in recovery from depression (Ressler & Mayberg, 2007), we hypothesized that placebo administration will be associated with decreases in rsFC between the sgACC and subcortical (e.g. amygdala (AMY)) regions and increases with cortical regions (e.g. dorsolateral prefrontal cortex (DLPFC)).

Methods: 24 un-medicated subjects underwent a clinical placebo trial in which subjects were randomized to two different conditions: 1-week of inactive placebo pills with disclosure that it represents an inactive agent (inactive condition) and 1-week of active placebo pills with expectations of mood improvement (active condition). After the placebo trial, subjects underwent a 10-week open label treatment with an AD. Depression severity was measured with the QIDS-SR16 at screening, the start and completion of each condition, and biweekly throughout the 10-week AD trial. Eight-minute rsfMRI session was performed after each condition. Spatially averaged time series obtained from the ROI (sgACC: −10, 28, −12; radius 5 mm) were correlated with each voxel to produce sgACC-rsFC correlation maps. Final z-maps were produced through Fisher's r-to-z transformation. The following Pearson correlations were conducted: baseline sgACC-rsFC and depression severity (QIDS at screening); inactive-active sgACC-rsFC maps with behavioral placebo (ΔQIDS Active – ΔQIDS Inactive) and behavioral AD response (QIDS at week 0 – QIDS at week 10) with depression severity as a covariate.

Results: Significant decreases in depressive symptoms were found after the 1-week active placebo (ΔQIDS-SR16: baseline 14 ± 5; post-placebo $= 12 \pm 5$; $t = 2.7$, $p = 0.01$) compared to the 1-week inactive placebo (baseline $= 13 \pm 6$; post-placebo $= 13 \pm 5$; $t = .7$, $p = 0.5$). The functional connectivity maps revealed no main effect of placebo administration on sgACC-rsFC. However, greater placebo responses were associated with decreases in sgACC-rsFC with the AMY (22, 0, −26, 320 mm^3, $Z = 3.98$, $p < 0.001$) and increases with the DLPFC (-52, 8, 40, 213 mm^3, $Z = 3.75$, $p < 0.001$). The same functional connectivity pattern was observed between behavioral AD response (placebo-induced decreases in sgACC-AMY rsFC (-22, −6, −26, 99 mm^3, $Z = 3.57$, $p < 0.001$) and increases in sgACC-DLPFC rsFC (−32, 20, 28, 344 mm^3, $Z = 3.71$, $p < 0.001$).

Conclusions: Our data suggest that placebo with expectation of AD effects influence sgACC-rsFC, which seems to underlie the biological mechanisms involved in recovery from depression during placebo treatment. Response to one week of placebo and 10-weeks of AD treatment decreases rsFC between the sgACC and subcortical areas, while increasing rsFC with cognitive areas.

P98A Reduced frontostriatal functional connectivity in schizophrenia revealed by eigenvector centrality mapping

K.C. Skatun[1,2], L.T. Westlye[1,3], O.A. Andreassen[1,2]

[1]NORMENT, KG Jebsen Center for Psychosis Research, Division of Mental Health and Addiction, Oslo University Hospital, Oslo, Norway, [2]Institute of Clinical Medicine, University of Oslo, Oslo, Norway, [3]Department of Psychology, University of Oslo, Oslo, Norway

Background: Schizophrenia and bipolar disorder are common, severe mental disorders with overlapping symptomatology. Imaging methods have shown functional brain network abnormalities in both patient groups. Eigenvector centrality mapping is a novel graph theoretic measure, which is sensitive to global connectivity by identifying prominent regions in the network-hierarchy of the brain. To the best of our knowledge this method has not yet been used to investigate differences between patients with schizophrenia, bipolar disorder, and healthy controls.

Methods: We analyzed resting state functional magnetic resonance images from 53 patients with schizophrenia spectrum disorder, 34 patients with bipolar disorder, and 196 healthy control subjects. Eigenvector centrality mapping was calculated voxel-wise in the brain for each individual, and between-group differences were assessed by non-parametric threshold-free cluster enhancement permutation testing. Mean values of the areas revealing group differences were extracted and submitted to an ANCOVA with age and sex as covariates for pairwise comparisons. The same areas were further used as seed regions in subsequent analysis to investigate aberrant functional connectivity with other areas in the brain.

Results: There was a significant effect of diagnosis in the left and right putamen. Pairwise comparisons showed a significantly decreased eigenvector centrality in schizophrenia patients and, to a lesser degree, bipolar disorder patients, compared to healthy controls. No differences were found between the patient groups. Connectivity analysis showed that both the left and right putamen had a decreased connectivity with the frontal lobe in schizophrenia patient group compared to healthy controls.
Conclusions: Eigenvector centrality mapping revealed a reduction in the global centrality of the putamen in schizophrenia and bipolar disorder, indicating an overlapping and less central role of this region in patients. Patients with schizophrenia also showed a reduced connectivity between the putamen and frontal cortex, indicating pathology in the frontostriatal pathway.

P99A A disenchanting attempt to use resting state fMRI as a diagnostic biomarker of major depression in a clinically realistic sample

B. Sundermann[1], S. Feder[1], H. Wersching[2], A. Teuber[2], H. Kugel[1], W. Heindel[1], K. Berger[2], B. Pfleiderer[1]

[1]University Hospital Münster, Department of Clinical Radiology, Münster, NRW, Germany, [2]University of Münster, Institute for Epidemiology and Social Medicine, Münster, NRW, Germany

Background: Multivariate classification of resting state fMRI (rs-fMRI) data has been introduced as a potential biomarker in major depression (MDD). Purpose of this analysis was to assess the diagnostic applicability of linear support vector machines (SVMs) in a larger dataset with a heterogeneous population-based control group.
Methods: Analyses are based on rs-fMRI data at 3 T from the BiDirect Study (funded by the German Ministry of Education and Research BMBF, grants 01ER0816 and 01ER1205). For this methodological optimization project multiple statistically independent non-overlapping samples representing age- and gender-matched pairs of patients with clinically diagnosed MDD and community-dwelling control subjects without MDD (but reflecting other sources of morbidity in the general population) were drawn from the complete baseline dataset: A subset of 360 subjects (MDD: n = 180, 50.84 ± SD 7.13 y; controls: n = 180, 51.20 ± SD 7.59 y) served for cross-validated training and performance estimation of SVM-classifiers (two-class problem MDD vs. controls, C-SVC from libsvm, linear kernel, C = {0.001, 0.01, 0.1, 1, 10, 100, 1000}). As features for classification we used pairwise z-transformed correlation coefficients representing functional connectivity (FC) among 38 meta-analytically identified regions of interest with known alterations of spontaneous brain activity at rest in MDD. Classification performance was explored using the whole set of features as well as reduced sets using four different feature selection techniques (t-test- and SVM-based filters, SVM recursive feature elimination, minimum redundancy / maximum relevance criterion each selecting the 20% most important features).
Results: Overall classification accuracies ranged from 45.9% to 53.6% (chance level 50.0%) with sensitivities from 45.0% to 73.3% and specificities from 33.9% to 53.9% with a typical sensitivity-specificity-tradeoff.
Conclusions: Multivariate classification of rs-fMRI in a large clinically defined MDD sample and population controls using linear SVMs with different feature selection techniques did not yield clinically meaningful diagnostic performance for binary classification (MDD vs. no MDD). We therefore refrained from validation in a second, equally-sized independent validation dataset. Thus classification methods seemingly established in small homogenous samples do not translate to a clinically realistic setting. We therefore hypothesize that such approaches crucially need to take the heterogeneity of clinical populations into account and have to focus on specific clinical questions. As a limitation, other, particularly non-linear classification techniques have not been tested.

P100A Default and salience network intrinsic connectivity in behaviorally inhibited children at risk for anxiety

B.C. Taber-Thomas[1], S. Morales[1], K.E. Perez-Edgar[1]

[1]Child Study Center, Department of Psychology, Penn State University, University Park, PA

Background: Behaviorally inhibited (BI) temperament in childhood is associated with perturbed social information processing, such as biased attention to negative stimuli (Perez-Edgar et al., 2010) and avoidance of negative emotion (Pine, 1999), as well as increased risk for social anxiety (Hirshfeld et al., 1992). One mechanism that may underlie perturbed information processing in children at risk for anxiety is altered intrinsic functional connectivity (iFC; Buckner et al., 2013). Anxious adults exhibit increased iFC in the default mode (PCC-mPFC) and salience (insula-ACC) networks, but iFC in well-established intrinsic networks has not been examined in children at risk for anxiety. Here we collected resting state fMRI data from BI (n = 13) and non-BI (n = 20) children to study the relationship between BI and iFC in mid-childhood (ages 9–12).
Methods: Data were collected on a Siemens Magnetom Trio 3T scanner (6 minute run; 180 volumes; TR = 2s; TE = 30 ms; flip = 70; FOV = 220 × 135 mm; voxel = 2.3 × 2.3 × 5). Preprocessing was performed in SPM8 and the CONN toolbox (Whitfield-Gabrieli & Nieto-Castanon, 2012). Whole-brain seed based functional connectivity analyses were then performed in the CONN toolbox with results cluster-level FDR-corrected to $p < 0.05$. Salience network seeds were placed in left and right insula (xyz = +/-36 14 6; 5 mm radius), and a DMN task-negative seed placed in mPFC (xyz = −1 47−4; 5 mm radius).
Results: For the BI versus non-BI group (i) left and right insula connectivity was greater to vmPFC but less to the typical salience node of dorsal ACC and (ii) mPFC connectivity was greater to PCC and right dlPFC.
Conclusions: This suggests that a bias in salience network iFC toward self-referential and affective processing (vmPFC) may be an underlying neural mechanism for perturbations to social information processing and risk for anxiety in BI. Moreover, results suggest that mPFC, a central node in default self-referential networks, may play an increased role in coordinating intrinsic functional connectivity in BI.

P101A Surface-based homologous inter-hemispheric connectivity: reliability, validation and relationship with callosal atrophy in multiple sclerosis

S.M. Tobyne[1], D. Boratyn[1], J.L. Johnson[4], D.N. Greve[2,3], E.C. Klawiter[1,3]

Department of [1]Neurology, [2]Radiology, Massachusetts General Hospital, Boston, MA; [3]Harvard Medical School, Cambridge, MA; [4]Augustana College, Sioux Falls, SD

Background: Inter-hemispheric communication depends mainly upon the corpus callosum (CC), the largest white matter structure in the brain. CC axonal integrity is integral to efficient intrinsic connectivity between the hemispheres. This study further developed existing voxel-mirrored homologous connectivity (VMHC) techniques for mapping the integrity of inter-hemispheric homotopy by leveraging a surface-based technique for precise hemispheric alignment of reconstructed cortical surfaces.
Methods: Scan-rescan anatomical and resting state (RS) data for 21 healthy controls (HC) (mean age 37.76 yrs, SD = 9.35, 11 male) from two separate sessions were used for development and validation. The reconstructed cortical surface was used to precisely cross-register both hemispheres into a symmetrical surface template. Surface-based VMHC (sVMHC) was calculated by sampling preprocessed RS data onto the template and calculating pairwise Pearson's correlations between all homologous vertices. Z-scores were used to compute intraclass correlation coefficients (ICC) between the scan-rescan pairs. A dataset of 992 HC was used for large-scale validation and exploration. sVMHC was calculated for all 992 subjects and the coefficient of variation (CoV) was calculated to identify regions of high variability. Lastly, a dataset of 20 multiple sclerosis (MS) (mean disease duration 8.48 years; median EDSS = 2.0, range 1–6.5) and 35 age- and gender matched HC subjects was used to investigate the relationship between CC atrophy and sVMHC. A semi-automated scheme was used to calculate the mid-sagittal area of the CC for each subject. CC area and sVMHC were compared using a Spearman's correlation and group comparisons were conducted using a Mann-Whitney U-test.
Results: sVMHC results revealed several clusters of high sVMHC within primary somatosensory and occipital cortex, as well as cingulate sulcus, ventromedial prefrontal cortex, posterior insula, angular gyrus, precuneus, posterior cingulate, and superior temporal gyrus. Mean ICC values were 0.3 (range 0.03–0.55) for structural and 0.39 (range 0.25–0.59) for functional parcellation schemes. CoV values from the large-scale validation dataset were highest in the anterior insula, orbitofrontal and temporal pole. CC area and mean sVMHC were significantly decreased in the MS group ($p < 0.001$, respectively) and significantly correlated (rho = 0.397, $p = 0.002$).
Conclusions: sVMHC provides a reliable and reproducible metric for assessing functional homotopy. Reliability measures showed overall strong reproducibility and minimal variability between subjects. Reliability was lowest in areas most sensitive to susceptibility artifacts. Results demonstrated improved spatial localization compared to volume-based VMHC methods. A novel relationship between sVMHC and CC atrophy in MS was revealed and has the potential to be a sensitive early biomarker for CC integrity.

P102A Multi-echo atlas of seed-based functional connectivity

V. Voon[1], M. Irvine[1], P. Vertes[1], P. Bandettini[2], E.T. Bullmore[1], P. Kundu[1,2]

[1]*Department of Psychiatry, University of Cambridge, Cambridge, UK*
[2]*National Institute of Mental Health, National Institutes of Health, Bethesda, MD, USA*

Background: Seed-based functional connectivity is measured as correlation between denoised fMRI time series. We use multi-echo independent coefficients regression (ME-ICR), which interprets independent components analysis (ICA) as a transformation into approximately independent coefficients (Kundu, PNAS, 2013) to allow: classifying BOLD/non-BOLD based on component-level TE-dependence (κ); denoising by non-BOLD component rejection; correlation between BOLD coefficient vectors of voxels; BOLD DOF regularization within Fisher *R-Z* transform. We show a connectivity atlas for seed regions of cortex and subcortex, with power analysis at $N = 10, 25, 50, 75, 100$.
Methods: 139 subjects were scanned with multi-echo EPI (TR = 2.47s;FA = 78°; $3.75 \times 3.75 \times 4.4\,mm^3$; 32 oblique slices, TE = 12,28,44,60 ms) [2], and MPRAGE. *Preprocessing* ME-ICA v2.5 implemented slice/volume realignment, nonlinear co-registration (AFNI *Qwarp*), T_2* weighted combination, BOLD/non-BOLD ME-PCA dimensionality reduction and ME-ICA decomposition and component separation [1]. *Subject-level ME-ICR* ICA mixing matrix was fit to T_2* weighted ME data and concatenated maps of "high-κ" BOLD components produced the coefficient vector dataset. Seed and target coefficient Pearson correlation values were converted to Z_{corr} scores using Fisher *R-Z* transform. *Group ME-ICR* Subject-level ME-ICR coefficient datasets were input to AFNI *3dGroupInCorr* producing 1-sample T-test group connectivity seed maps. *T*-values were converted to Z_T.
Results: Group ICR maps (Fig 1a) show that maps conform well to anatomy, show cortical and subcortical connectivity, do not show anticorrelation and agree with task activation. Power gain with N (Fig 1b) ($Z_T = 3\sigma$ OFC-hippocampus connectivity at $N = 25$; 6σ at $N \sim 75$; higher N does not proportionally add power).
Conclusions: Group ME-ICR enables high-quality whole-brain functional connectivity analysis for hypotheses regarding individual brain regions, producing well-localized connectivity maps with stable behavior across varying *N*.

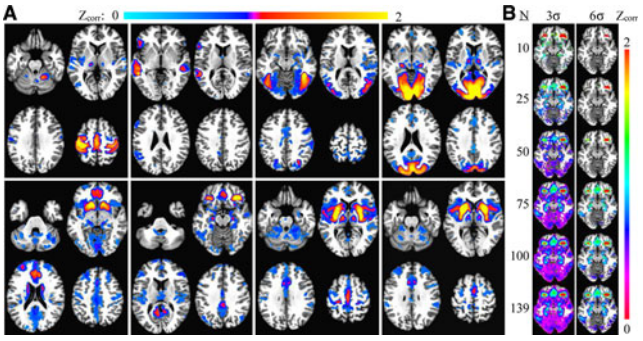

FIG. 1. Underlay is high-resolution MNI template **(a)** Group ICR maps of seeds (clockwise) in MNI coordinates. Overlay is mean Z_{corr} thresholded by $Z_T \geq 6[\sigma]$: right hand area (−33, −29, 57), Wernicke's area (−53, −41, 2), fusiform face area (43, −44, −18), primary visual (−5, −96, −4), ant. putamen (−24, 10, 1), pos. putamen (−29, −8, 4,), orbitofrontal cortex (36, 34, −16), ventral striatum (−13, 20, 5). **(b)** Orbitofrontal connectivity at 3σ and 6σ, for varying N. Note stable 6σ connectivity for $N \geq 75$.

P103A Differences and the Relationship in DMN Intrinsic Activity and Functional Connectivity in Mild AD and aMCI

M. Weiler[1], B.M. de Campos[1], M.H. Nogueira[1], C.V.L. Teixeira[1], B.P. Damasceno[2], F. Cendes[1], M.L.F. Balthazar[1,2]

[1]*Neuroimaging Laboratory, Department of Neurology, University of Campinas (Unicamp), Brazil;* [2] *Unit for Neuropsychology and Neurolinguistics, Department of Neurology, University of Campinas (Unicamp), Brazil*

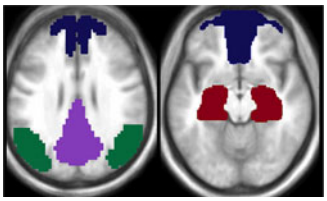

Background: There is evidence that the Default Mode Network (DMN) functional connectivity is impaired in Alzheimer's disease (AD) and few studies also reported a decrease in DMN intrinsic activity, measured by the amplitude of low frequency fluctuations (ALFF). In this study, we analyzed the relationship between DMN intrinsic activity and functional connectivity, as well as their possible implications on cognition in patients with mild AD and amnestic mild cognitive impairment (aMCI) and healthy controls. In addition, we evaluated the differences both in connectivity and ALFF values between these groups.
Methods: We recruited 29 controls, 20 aMCI and 32 mild AD patients. To identify the DMN, functional connectivity was calculated by placing a seed in the posterior cingulate cortex (PCC). Within the DMN mask obtained (Fig), we calculated regional average ALFF of each DMN sub-area: temporal (in green), PCC (in purple) and frontal (in blue).
Results: Compared to controls, aMCI patients showed decreased ALFF in the temporal sub-area; compared to AD, higher values in the PCC but lower in the temporal area. The mild AD group had lower ALFF in the PCC compared to controls. There was no difference between the connectivity in the aMCI group compared to the other groups, but AD patients showed decreased connectivity in the frontal and PCC sub-areas. Also, PCC ALFF correlated to functional connectivity in nearly all sub regions. Cognitive tests correlated to connectivity values but not to ALFF.
Conclusions: Alterations in the ALFF values of s the PCC disrupts the DMN functional organization (and thus causes cognitive problems), due to the correlation between ALFF and functional connectivity. The cognitive decline observed in mild AD patients is modestly associated with disrupted functional connectivity, rather than the intrinsic activity of such regions, which gives evidence that AD is, among other physiopathological features, a disconnection syndrome.

P104A Single-dose serotonergic stimulation shows widespread effects on functional brain connectivity

B.L. Klaassens[1,2], H. van Gorsel[3], N. Mahani[1], J. van der Grond[2], M. van Buchem[2], B. Whitcher[4], B.T. Wyman[4], J.M.A. van Gerven[3], S.A.R.B. Rombouts[1,2]

[1]*Leiden Institute for Brain and Cognition, Leiden, The Netherlands;*
[2]*Leiden University Medical Center, Leiden, The Netherlands;*
[3]*Centre for Human Drug Research, Leiden, The Netherlands;*
[4]*Pfizer Inc., Groton, CT, USA*

Background: The selective serotonin reuptake inhibitor (SSRI) sertraline alters the concentration of synaptic serotonin (5-hydroxytryptamine), and is commonly prescribed as a treatment for depression and anxiety disorders. SSRIs influence task-related activation in the limbic system (hippocampus, amygdala, cingulate gyrus, thalamus) and prefrontal circuitry. Also, SSRI treatment alters resting state functional connectivity in depressed and healthy subjects. However, little is known of the effects of single-dose SSRI administration on large-scale functional brain networks.
Methods: Twelve healthy young volunteers (mean age 23.0 ± 3.8, range 19–28; gender ratio 1:1) were included in this single center, double blind, placebo-controlled, crossover study with sertraline 75 mg. To cover the maximum concentration of sertraline (Tmax: 5.5–9.5 hrs.), five resting state fMRI (RS-fMRI) scans were acquired during study days, one at baseline and four after administering sertraline or placebo (at 3, 5, 7 and 9 hrs. post dosing). After preprocessing, RS-fMRI networks were extracted using a dual regression analysis with FSL using 10 standard network templates with confound regressors of white matter and CSF. Within-group comparisons (sertraline vs. placebo) of voxel-wise functional connectivity with these 10 networks were examined using a multivariate model with heart rate and respiration as confound regressors ($p < 0.005$, corrected).
Results: The following connections showed a decrease in functional connectivity after sertraline compared to placebo: 1) precuneus, cingulate cortex and prefrontal cortex with the default mode network; 2) medial prefrontal cortex and the limbic system (including the cingulate gyrus, thalamus, amygdala and hippocampus) with the executive control network; 3) occipital regions with the visual networks; 4) cingulate gyrus and central gyri with the sensorimotor network. Increased connectivity was limited to small parts of the central gyrus and the cingulate cortex with the auditory network.
Conclusions: A single dose of the SSRI sertraline induced widespread decreases of functional connectivity with multiple resting state networks. Effects in the default mode network, limbic system, frontal circuitry and executive control network are mostly in agreement with earlier studies. New findings were the lowering of connectivity within visual networks and the alterations in functional connectivity with the sensorimotor and auditory network. However, these results are consistent with the existence of a widespread serotonergic neural system relating to various brain functions as cognition, perception and action.

P105A Stress in the spontaneous brain activity: a resting state fMRI study of individual variability and vulnerability

Diane Yan[1], Omar Singleton[1], Sara W. Lazar[1]

[1]*Massachusetts General Hospital, Harvard Medical School, Boston, MA, USA*

Background: Stress is a risk factor for, or consequence of, many psychiatric disorders. Because stress is a complicated process that involves multiple psychological, neurological and endocrine systems, there is intrinsic individual variability in these systems that contribute to the individual variability in perceived stress.
Methods: The present study was designed under the framework of the research domain criteria (RDoC) proposed by NIMH, aimed to investigate the neural correlates of perceived stress as well as their interrelationships with self-related psychological processes such as mindfulness and various components of self-compassion. Resting state fMRI, morning saliva cortisol and self-report data were collected from 40 young healthy adults.
Results: Results suggest that the individual variability in perceived stress is positively correlated with the individual variability in amygdala spontaneous activity while negatively correlated with the individual variability in the spontaneous brain activity of the PCC/precuneus cluster. Individual variability in negative self-processes such as self-judgment, over-identification and isolation contributes to the variability in amygdala spontaneous activity which eventually contributes to stress, whereas mindfulness as a positive self-process is antagonistic to these negative self-processes and may act as a protective factor against perceived stress.

Conclusions: Findings from the present study highlight the interrelationships between stress and the amygdala with self-related psychological processes and the spontaneous activity in the PCC/precuneus cluster which are critical regions in the ''default mode network''. These findings expand our understanding about the stress system and are informative for designing proper intervention strategies for stress-related disorders.

P106A Identifying cortical brain connections using cortical morphological pattern and structural connectivity in pure subcortical vascular dementia and Alzheimer's disease

J.J. Yang[1], H.K. Kwon[1], H.J. Kim[2], S.W. Seo[2], D.L. Na[2], J.M. Lee[1]

[1]Department of Biomedical Engineering, Hanyang University, Seoul, south Korea, [2]Department of Neurology, Samsung Medical Center, Sungkyunkwan University School of Medicine, Seoul, Korea

Background: Alzheimer's disease (AD) is pathologically characterized by the formation of neurofibrillary tangles and neuritic plaques, in contrast, subcortical vascular dementia (SVaD) pathology demonstrated by white matter hyper-intensities and lacunes might cause subcortical axonal damage and interruption of critical pathways, leading to secondary neuronal cell body damage, and finally gray matter atrophy. Although recent research has shown that the topography of cortical thinning of SVaD was different from that of AD, it remains unclear whether cortical thinning related to actual anatomical connectivity between brain regions in these patients. We propose a novel method for identifying cortical brain connections in association with the cortical morphological patterns and structural connectivity.
Methods: 41 of patients with Pittsburgh compound B (PiB)-negative SVaD and 56 of those with PiB-positive AD were recruited. Similarity map was constructed to represent the correlation of regional mean cortical thickness between a pair of ROIs using structural magnetic resonance imaging (MRI) and whole brain white matter network was constructed based on the fiber-tract bundles and mean fractional anisotropy (FA) using diffusion tensor imaging (DTI). Proposed cortical brain connectivity matrix was reconstructed based on a correlation between every edge by the similarity matrix and white matter connectivity matrix and followed by a graph theoretical analysis.
Results: We examined whether morphometric correlations of regional mean cortical thickness across individuals reflect anatomical connectivity, as axonally connected regions. The results showed were significantly different, suggesting that morphometric correlation network cannot be regarded as a structural connectivity for an alternative structural network in the specific pathology. Our cortical brain connectivity yield more informative results since it provides both structural connections associated with the identified similarity of cortical morphology.
Conclusions: We believe that the proposed cortical brain connection based on cortical morphological pattern and structural connectivity reflect that indeed specific symptoms in PiB-negative SVaD and PiB-positive AD.

P107A Local efficiency is sensitive to social functioning and Autism Spectrum Disorder

X. You[1], M. Norr[1], E. Murphy[1], W.D. Gaillard[2], L. Kenworthy[2] and C.J. Vaidya[1, 2]

[1]Department of Psychology, Georgetown University, Washington, DC; [2]Children's Research Institute, Children's National Medical Center, Washington DC

Background: Current views about atypical functional connectivity in Autism Spectrum Disorders (ASD) are primarily based upon either task-evoked activation findings or task-free (i.e., resting state) findings with apriori focus on selective networks (e.g., default mode). Here, we examined whether a voxel-wise graph theory metric of the efficiency of information processing at the *local* node level differs between ASD and typically developing control children and whether it is sensitive to individual differences in social functioning (measured by the Social Responsiveness Scale – SRS). *Local efficiency* is the inverse shortest path length for the local nodes to the rest of all other nodes in the network, thus allowing examination of regional differences in information processing/transferring. We hypothesized that local efficiency ought to differ in ASD children in regions that show activation differences during social-emotional tasks such as ventromedial prefrontal cortex (vmPFC), insula, and superior temporal gyrus (STG). Further, if those regions relate to social functions that are affected in ASD, then local efficiency in those regions ought to predict everyday social behavior regardless of diagnosis.
Methods: Forty-six 9–13 year old children, 23 ASD and 23 age, gender and IQ matched controls underwent 5 min resting state fMRI (3 mm isotropic resolution, TR 2000 ms, TE 30 ms, flip angle 90°, FOV 192×192 mm) with eyes open. Images were slicetime corrected, motion corrected with scrubbing (120 volumes kept) following Power et al (2012; Neuroimage vol 63(2):999), normalized and resliced to 4 mm, band pass filtered (0.01–0.08 Hz), smoothed with 4 mm FWHM, and physiological noise removed. Time course of each voxel was correlated to every other voxel and thresholded at $p = .001$ FDR corrected ($r > .32$). Local efficiency maps were computed using the brain connectivity toolbox (https: //sites.google.com/site/bctnet/measures/list); the images were down-sampled to 8 mm voxel size for computational efficiency. Group difference was examined for local efficiency maps using SPM8 with age and mean framewise displacement regressed out at $p < .05$ corrected for multiple comparisons (monte-carlo). In addition, in regions showing group differences, we examined whether the magnitude of local efficiency correlated with total raw scores on the SRS across the two groups with age and motion regressed out, in a step-wise multiple regression analysis.
Results: Local efficiency (i.e. efficiency of information transferring to global brain networks at this local node) was lower in ASD than controls in vMPFC, left ventral striatum extending into insula, right middle frontal gyrus, left posterior STG, middle cingulum extending to precuneus, and left superior parietal lobule. Local efficiency in vMPFC and left ventral striatum-insula predicted SRS scores: the lower the local efficiency, the worse the social function.
Conclusions: The present results contrast with those of Redcay et al (2013; Frontiers in Neuroscience, vol 7, 573), who found no differences in local efficiency between ASD and control adolescents. Perhaps, our voxel-wise analysis was more sensitive in detecting group differences as opposed to their regions of interest analysis. Low communication efficiency in spontaneous neural activity in regions underlying social-emotional perception in ASD may underlie the observed activation differences during tasks evoking those functions. The present results suggest that local efficiency in vMPFC and ventral striatum-insula could be a useful neural correlate of social functioning, a dimension that is affected in multiple psychiatric disorders.

P108A Thalamic dysfunction in cocaine dependence – a framework for functional connectivity analysis

Sheng Zhang,[1] Sien Hu,[1] Sarah R. Bednarski,[1] Emily Erdman,[1] Chiang-shan R. Li[1,2,3]

[1]*Department of Psychiatry, Yale University School of Medicine, New Haven, CT 06519*
[2]*Inter-departmental Neuroscience Program, Yale University, New Haven, CT 06520*
[3]*Department of Neurobiology, Yale University School of Medicine, New Haven, CT 06520*

Background: Recent studies started to elucidate altered resting state cerebral functional connectivities in individuals with cocaine dependence (CD), highlighting the effects of cocaine use on both the activities and connectivities of the thalamus. Both reduced and increased activations of the thalamus were observed in CD compared to healthy controls (HC) in a variety of behavioral tasks, suggesting functional heterogeneity and different etiological relevance of thalamic subclusters. In the current study, we developed a framework to employ resting state fMRI and identify altered functional subclusters of the thalamus in cocaine dependence.
Methods: Resting state fMRI data (3T, 10 minutes, eye closed) of 66 CD and 66 age/gender matched HC were analyzed. We performed for individual subjects linear regressions between the averaged time course of each of the 116 AAL masks and the time courses of each individual voxel of the thalamus. The correlation coefficients were converted to z scores by Fisher's z transform, and a two-sample t-test was applied to the ''z maps'' to identify altered functional connectivity between each thalamic voxel and each of the 116 masks in CD as compared to HC. We then used the 116 connectivity effect sizes (t values) of each thalamic voxel to functionally segment the thalamus with K-means clustering.
Results: The results showed the thalamus being divided into 4 functional subclusters, in the area of the mediodorsal nucleus (MD), ventral anterior/ventral lateral nucleus (VA/VL), ventral lateral posterior/ventral posterior lateral nucleus (VLP/VPL), and pulvinar nucleus (PUL), each in association with a different pattern of functional connectivity. For instance, MD and VA/VL but not the other two clusters showed reduced connections to putamen and ACC, specifying the thalamic subregions with this altered pattern of connectivity (Gu et al., 2012; Verdejo-Garcia et al., 2012). Furthermore, the connection strengths between the MD and putamen negatively correlated with the average amount of cocaine per use in the past month for males but not for females.
Conclusions: These findings suggest a distinct pattern of altered functional connectivity of thalamic subnuclei in cocaine dependence. The proposed analytic framework may provide new insight to using resting state and task related fMRI data to delineate circuit level deficits in cocaine dependence and other neuropsychiatric conditions.

P109A Theta burst stimulation of the precuneus induces resting state functional changes in the left temporal pole

C. Mastropasqua[1], B. Sonia[2], M. Bozzali[1], M. Mancini[3], C. Caltagirone[2], M. Cercignani[1,4], G. Koch[2]

[1]*Neuroimaging Laboratory - IRCCS Santa Lucia, Roma, Italy* [2]*Department of Clinical and Behavioural Neurology - IRCCS Santa Lucia, Rome, Italy* [3]*Department of Engineering, Università degli Studi di Roma Tre, Rome, Italy* [4]*Brighton and Sussex Medical School, Clinical Imaging Sciences Centre, University of Sussex, UK*

Background: Recent works seem to indicate that it is possible to probe functional connectivity (FC) changes assessed by Resting State (RS)-fMRI by applying repetitive transcranial magnetic stimulation over specific key areas (1–3). We observed that continuous theta burst stimulation (cTBS) over the precuneus (PC) induces behavioral changes in memory functions (4). The aim of this study is to investigate the effects of cTBS of the PC by analyzing changes in FC RS-fMRI. We hypothesized that cTBS of the PC would selectively induce remote changes in interconnected areas that are involved in memory processes.
Methods: 21 healthy subjects (M/F = 10/11; mean (SD) age = 27.3 (4.32) underwent MRI at 3.0 T. The acquisition protocol included: 1) baseline T2*-weighted-EPI sensitized-to-BOLD (TR = 2470 ms, TE = 30 ms, 38 axial slices); 2) PC cTBS; 3) first follow-up (fup1) and 4) second follow-up (fup2) RS-fMRI. Each subject underwent the same paradigm receiving either cTBS or a sham stimulation on 2 separate sessions. T1-weighted-images MPRAGE (TR = 1338 ms, TE = 2.4 ms) and diffusion weighted EPI (TR = 7 s, TE = 85 ms, number of diffusion directions = 61; max b factor = 1000 smm-2) were also acquired as anatomical reference. Three-pulse bursts at 50 Hz repeated every 200 ms for 40 s were delivered over the PC with MagStim Super Rapid magnetic stimulator. The RS-fMRI data were preprocessed using SPM8 and band-pass filtered to remove high frequency variations. Seed-based analysis was performed to identify changes in FC of the stimulated area. Moreover, two other regions close to the stimulated one were used as control sites. The spheres were centered in the most significant peak of 3 different networks extracted with ICA: PC network (5), DMN and visual network. Second level analysis was performed using 6-way-Flexible-factorial design in order to compare different conditions. Results were considered significant for $p < 0.05$ FWE-corrected.
Results: We found that cTBS induced a decreased correlation between the PC and left temporal pole in both fup1 and fup2 ($p < 0.003$ FWE-corrected) with respect to baseline data. No significant change was found when looking at fup1 and fup2 after sham. Moreover, we did not find any significant results when looking at changes in functional connections between the spheres extracted from DMN and visual network.
Conclusion: Our study demonstrates that cTBS applied on PC induces selective changes in FC between the stimulated PC and the temporal cortex. These results are supported not only by unchanged correlation after sham stimulation but also by the absence of any altered correlation between two controls sites close to the stimulated one. It is interesting to note that our results were restricted to the correlation between the PC and the antero-inferior part of the temporal lobe that is known to be involved in semantic memory processes (6), thus underlining the potential role of PC cTBS on the modification of neuronal circuits involved in memory functioning. Moreover it has to be consider that the alteration of FC between the PC and temporal pole could be due to their structural connection through the inferior portion of the cingulm. Further analyses have to be carried out using DTI tractography in order to understand if structural properties (such as fractional anisotropy and mean diffusivity) of this tract could be predictive of subjective changes of FC after cTBS.

1) Mastropasqua et al. (2014); 2) Liston et al. (2014); 3) Gratton et al. (2013); 4) Bonni et al. (2014); 5) van den Heuvel et al. (2009); 6) Chan et al. (2001).

Poster Session 2: Friday, 12 September 2014

Theme 1: Technical Advances and Methodological Issues

P1B Differential effect of ICA denoising on gradient-echo and spin-echo BOLD fcMRI

T. Aso, S. Urayama, H. Fukuyama

Human Brain Research Center, Kyoto University School of Medicine, Kyoto, Japan

Background: Functional connectivity MRI (fcMRI) has been largely based on gradient echo (GE) BOLD contrast. In spite of a better spatial specificity of spin echo (SE) fMRI, its feasibility in fcMRI has not been verified. In the present study we applied an automated ICA-based denoising to fcMRI datasets acquired using typical GE/SE-BOLD pulse sequences and compared its effect on the seed-based connectivity maps.
Methods: Every subject went through two GE- and four SE-BOLD runs, each lasting 6 min, in a 3T scanner. For Experiment #1, data were acquired on 20 healthy subjects with an 8-channel head coil. Seven sagittal slices (4 mm + 50% gap) covered the midline structure at TR/TE = 1000/85 ms with 6/8 phase partial Fourier and 3×3 mm resolution. For Experiment #2, 5 subjects were scanned using an 32-channel coil at TE = 80 ms and a multiband factor of 3. Twenty-four axial slices mostly covered the entire cerebrum at $3.5 \times 3.5 \times 4$ mm voxel size with other parameters the same as Exp. #1.

For the denoising procedure we followed Smith, PNAS 2012. Individual datasets were fed into MELODIC ICA before spatial normalization and without spatial smoothing. The ICs were classified as artifacts by temporal frequency power > 0.2 Hz, excessive involvement outside the gray matter and excessive slice dependency. The thresholds were chosen to minimize false-positive in artifact detection. The seed-based correlation mapping was done before and after the ICA denoising, following a classic method (Fox, PNAS 2005). The posterior cingulate was used as the seed region and the signals from the deep white matter and CSF were used as regressor of no interest.
Results: By the ICA denoising, more ICs were classified as artifact in SE- than GE-BOLD (65% vs. 43%). In both experiments, remote connectivity between the PCC and MPF by GE-BOLD significantly decreased by the denoising process (see Bar plot from Exp. #1). On the contrary, in SE-BOLD, the denoising even reversed the negative MPF connectivity in the raw data, resulting in a similar correlation map with that from GE-BOLD (Figure, left, from Exp. #2). Large draining veins showed opposite correlation between GE and SE.

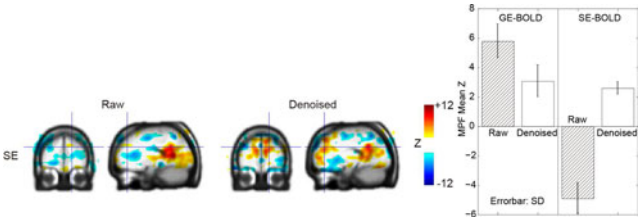

Conclusions: The artifact contamination in random fluctuation has opposite effects in terms of MPF-PCC remote connectivity in the two BOLD fcMRI. The similarity in the resulting maps suggests the efficiency of the ICA denoising method used. Difference in radius-dependent intravascular contribution might account for the discrepancy.

P2B Resting state functional connectivity in the human spinal cord at 7 Tesla

R.L. Barry[1,2], S.A. Smith[1,2], A.N. Dula[1,2], J.C. Gore[1,2]

[1]Vanderbilt University Institute of Imaging Science, Nashville, TN, USA, [2]Department of Radiology and Radiological Sciences, Vanderbilt University Medical Center, Nashville, TN, USA

Background: Low-frequency correlations between blood oxygenation level dependent (BOLD) signal fluctuations in the resting brain have been studied extensively to characterize functional connectivity within the cortex. However, to date there have been no conclusive studies using resting state acquisitions to detect functional connectivity in the spinal cord. Here we describe our use of high-resolution functional magnetic resonance imaging (fMRI) at 7 Tesla to detect and characterize reproducible resting state BOLD signals within gray matter of the human cervical spinal cord.
Methods: Experiments were performed on a Philips Achieva 7 Tesla scanner with a custom-designed 16-channel receive coil for spinal cord imaging. Twenty-two healthy volunteers (11 male) with no history of spinal cord injury were scanned under a protocol approved by the institutional review board. A 3D multi-shot gradient-echo sequence was used to reduce T_2* blurring and geometric distortions. Robust data-driven methods were applied to de-noise functional data, which were then band-pass filtered in preparation for analyses of functional connectivity. Gray and white matter masks were created for each anatomical slice and subdivided into quadrants to identify left and right ventral and dorsal horns, as well as surrounding white matter regions. Each mask was eroded to mitigate partial volume effects, and time series of voxels were averaged within each cluster.
Results: Robust correlations were found between different subregions of spinal gray matter both within slices and also between slices. Figure 1 summarizes group-level functional connectivity between sub-regions of spinal gray matter and white matter within slices. The most significant correlations were between left and right ventral (motor) horns ($p < 0.01$, corrected) followed by left and right dorsal (sensory) horns ($p < 0.01$, corrected). No significant correlations ($p > 0.05$) were observed between spinal gray and white matter regions, suggesting that observed gray matter correlations cannot be simply attributed to spatially correlated physiological noise but instead represent genuine connectivity.
Conclusions: We present the first conclusive evidence that resting state fMRI at ultra-high field (7 Tesla) can non-invasively detect and assess functional connectivity in the human spinal

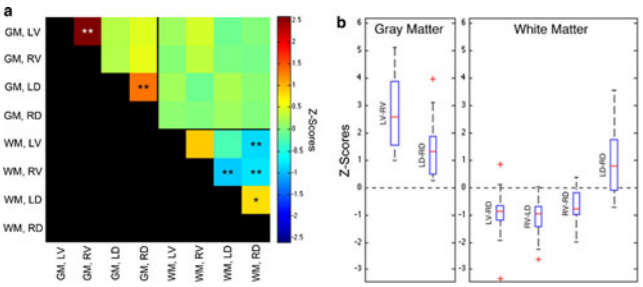

FIG. 1. Group-level functional connectivity between regions of spinal gray matter (GM) and surrounding white matter (WM) within slices. (**a**) In GM, positive correlations are observed between left (LV) and right (RV) ventral horns, as well as left (LD) and right (RD) dorsal horns. Weaker positive and negative correlations are observed within WM (* = $p < 0.05$; ** = $p < 0.01$; Bonferroni corrected). No significant correlations are observed between spinal cord GM and WM. (**b**) Box-and-whisker plots showing the median and upper and lower quartiles of the six statistically significant results.

cord. This work is significant because it provides new opportunities to study basic aspects of spinal cord function both in normal development and in clinical disorders of the central nervous system, and investigate long-range connectivity between the cerebrum, cerebellum, and spinal cord.

P3B A method for assessing the similarity between resting state networks

J.C.W. Billings[1], A. Medda[2], G. Thompson[3], W. Pan, S. Shakil[4], J. Grooms[3], S Keilholz[3]

[1]Emory University, Graduate Division of Biological and Biomedical Sciences – Program in Neuroscience; [2]Georgia Tech Research Institute, Aerospace & Acoustics Technologies; [3]Georgia Institute of Technology and Emory University, Biomedical Engineering; [4]Georgia Institute of Technology, Electrical Engineering, GA, USA

Background: Resting-state networks (RSN) networks may be defined over a range of temporal intervals to identify dynamic patterns of functional connectivity (dFC). The repetition of RSNs across time is taken to be the repetition of a favored micro-state of the regions under investigation. However, it is often challenging to rigorously identify how similar are sets of RSNs are to one and other. To this end, we have investigated the implementation of 'variation of information' (VI), an entropy-based measure, for the assessment of RSN similarity.
Methods: BOLD data (GE-EPI, TR = 0.5 s, $0.3 \times 0.3 \times 1.0$ mm resolution, 1000 images) from a single coronal slice of the rat brain (bregma 1.8 mm) were acquired. Data were binned into time intervals of 50 seconds with 25 seconds of overlap between epoch. An additional 200 images of scrambled data were added to the series' end for contrast. The voxel time-series from each epoch were then hierarchically clustered together (Euclidean distance, and average linkage metric) to produce 19 separate sets of RSN's. The variation of information was then assessed between each set according to the following algorithm:

$$VI(C, C') - [H(C) - I(C, C')] + [H(C') - I(C, C')] \quad (1)$$

Here C and C' are two separate hierarchical clusters, H(C) is the entropy of cluster C, and I(C, C') is the mutual information between clusters C and C'. The two terms on the RHS indicate, from left to right, the amount of information about clustering C lost, and the amount of information in C' left to uncover, when reorganizing the voxels from clustering C to clustering C'. A VI of 0 is a perfect overlap. Finally, the VI metrics were used as the distance measure to compute the hierarchy of similarity between clusterings.
Results: Box A shows the VI between clusterings (axis are cluster labels), while B shows the between-cluster hierarchy formed from the data in A (ordinate shows cluster labels, abscissa linkage distances). Notice how the type of organization presented in the individual clusterings (1,5,10,15,18), go from highly noisy and stratified to more anatomically organized. These analytical methods naturally group such RSN types.
Conclusions: These results demonstrate the feasibility and usefulness of VI for dFC.

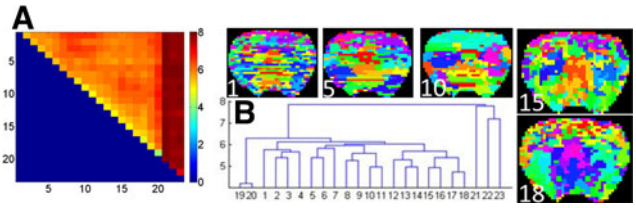

P4B Functional connectivity based parcellation of posterior cingulate cortex

J.H. Cha[1], H.J. Jo[2], D.K. Lee[1], J.M. Lee[1]

[1]Department of Biomedical Engineering, Hanyang University, Seoul, South Korea
[2]Section on Functional Imaging Methods, Laboratory of Brain and Cognition, National Institute of Mental Health, National Institutes of Health, Bethesda, MD, USA

Background: The posterior cingulate cortex (PCC) has been shown to be associated various brain networks simultaneously and may serve various functions. We examined functional connectivity patterns of each voxel within the PCC using resting-state (RS) fMRI and then defined the human PCC sub-regions using voxel-wise parcellation with similarity of functional connectivity patterns.
Methods: We performed our analyses using the part of the 1000 Functional Connectomes Projects (23 subjects (male, age: 21.4 ± 2.12)). Preprocessing was carried out using AFNI software. The first five volumes were discarded. The slice-timing and motion corrected functional images were performed using ANATICOR with PESTICA. And then, the functional images were band-pass filtered ($0.009 < f < 0.08$) and performed spatial smoothing (6 mm FWHM). Finally, the images normalized in MNI152 template using nonlinear transformation. PCC were defined using the Harvard-Oxford probabilistic atlas (Fig (a)). We applied k-means algorithm to parcellate PCC region into several sub-regions. The basic approach of parcellation is that the voxels with similar functional connectivity patterns across the whole gray matter voxel are combined into a same cluster. To explore the functional connectivity of each cluster, we defined maximum probabilistic map of clusters (Fig (b)). Then, we generated functional connectivity group maps using one-sample t-test (Fig (c)-(f)). ANCOVA was performed to determine the differences.
Results: PCC was mainly parcellated into 4 sub-regions using k-means algorithm. The mapping of these clusters revealed the presence of mainly four clusters along the dorsal and ventral PCC. The majority of functional connectivity patterns were similar

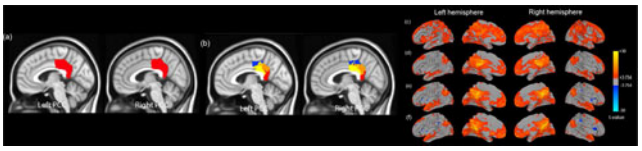

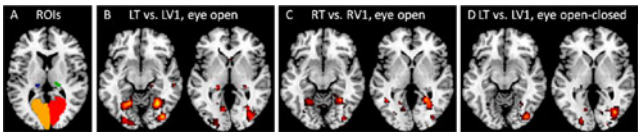

across sub-cluster within PCC. Nevertheless, the differences of functional connectivity between the clusters were existed.
Conclusions: Our major findings were as follows: i) PCC could be separated four sub-regions based on functional connectivity patterns as known previous cytoarchitecture studies (2 dorsal PCC and 2 ventral PCC); ii) In addition, these sub-regions differs functional connectivity between each clusters. Taken together, our finding suggests that the PCC is complex connectivity and it divided into 2 regions. Besides it also divided into four regions more detailed.

P5B Modulatory interactions between the thalamus and visual cortex in resting-state are modulated by eye open/closed conditions

Xin Di, Rui Yuan, Bharat B. Biswal

Dept. of Biomedical Engineering, New Jersey Institute of Technology, Newark, NJ, USA

Background: Physiophysiological interaction (PPI) has been used to study modulatory interactions in resting-state, i.e. the modulations of connectivity between two regions by a third region (1, 2), however, it is not clear whether modulatory interactions are modulated by subject's mental states. We studied modulatory interactions between the thalamus and visual cortex in resting-state in eye-open and eye-closed conditions, and hypothesized that modulatory interactions would only take place in the eye-open condition.
Methods: Resting-state fMRI data of 47 subjects with separate eye-open and eye-closed scans (3) were analyzed using SPM8. The functional images were motion corrected, and corregistered to subject's anatomical images. The anatomical images were segmented, and the deformation field images were used to normalize the functional images into MNI space. The functional images were smoothed using an 8 mm Gaussian kernel.

Left and right visual related thalamus (LT and RT) were defined using the 6th region of the Oxford thalamic connectivity atlas (4) (Fig A). Left and right V1 (LV1 and RV1) were defined as the calcarine sulcus of the AAL template (5). The first eigen-variable of the four ROIs were extracted, and PPI were calculated between the LT and LV1, and between the RT and RV1, respectively. GLM of PPI effects were built for each subject and each condition, including two time series of the two ROIs, their PPI effect, two regressors representing the WM and CSF signals, and 24 regressors of head motion parameters. One sample t-test and paired t-test were performed for group level inference. Results were thresholded at $p < 0.01$, and cluster level FDR corrected at $p < 0.05$.
Results: Consistent with our hypothesis, significant modulatory interactions were only observed in the eye-open condition. Bilateral visual regions which were mainly located in the middle occipital gyrus and fusiform gyrus showed positive PPI effects with both the LT and LV1 (Fig B), and the RT and RV1 (Fig C). Paired t-test between conditions showed that the right middle occipital region revealed higher PPI effects with the LT and LV1 in the eye open condition than in the eye closed condition.
Conclusions: In addition to previous findings showing modulations of eye open/closed conditions on fluctuations of the visual cortex and connectivity between the thalamus and visual cortex (3, 6), the current results suggested that the activation of the thalamus may boost communications between the primary visual cortex and higher visual areas. Most importantly, the modulatory interactions only took place when the subjects' eye were open, suggesting their functional significance in visual processing.
References: 1, Di & Biswal 2013. PloS One, 8(8), e71163. 2, Di & Biswal 2014. PeerJ, 2, e367. 3, Liu et al., 2013. Neuroinformatics, 11(4), 469–76. 4, Behrens et al., 2003. Nat Neurosci 6(7), 750–7. 5, Tzourio-Mazoyer et al., 2002. NeuroImage, 15(1), 273–89. 6, Zou et al., 2009. Hum Brain Mapp, 30(9), 3066–78.

P6B Hub crosslinks in resting state fMRI

H.C.T. Do[1,2], M. Yoon[1,2], J.I. Kim[1,2], H.J. Park[1,2]

[1]Department of Nuclear Medicine and Radiology, and Severance Biomedical Science Institute, Yonsei University College of Medicine, Seoul, KOREA
[2]Brain Korea 21 PLUS Project for Medical Science, Yonsei University College of Medicine, Seoul, KOREA

Background: Graph theoretical analysis on human brain networks is commonly used as a tool to gain access in the organization of functional structures in the brain arising from patterns of structural or functional connectivity between brain regions.

To investigate the synchronized dynamics of brain networks, the mathematical framework for hypergraph theory has been utilized. Hyperedges (or crosslinks) are synchronized patterns of interactions among brain regions, which co-vary in time.

In this study, we carried out identification and analysis of hub edges in resting state fMRI, which can be regarded as important communication pathways in the brain network.
Methods: Resting state fMRI data from 12 healthy subjects (all right-handed) have been acquired for 8 sessions (each approximately 5.5 mins) at different time periods within a day (Park et al., Neuroimage 2012) and preprocessed using our in-house program MNET. Mean time series of MRI signals from 138 brain regions according to the Harvard Oxford Atlas for subsequent analysis have been extracted. In order to construct the temporal networks, we extracted 40 time points (60 sec. time window for each timepoint) by concatenating the sessions and applying a sliding window. For the functional networks, we calculated z-transformed correlation coefficients among BOLD time series of ROIs. For the co-variation of edges, we constructed an edge-edge correlation matrix by another calculation of Pearson correlation coefficient across the time windows for every subject. The group averaged edge-edge correlation matrix was thresholded and was used to extract co-varying connected components, i.e. hyperedges. From these hyperedges, we estimated the hub crosslinks by means of eigenvector centrality. We also examined co-evolution of hyperedges to investigate the asymmetry of hemispheres during resting state.
Results: Hub crosslinks revealed typical resting state subnetworks including a default mode subnetwork and a salient subnetwork. The co-evolution of hyperedges in the left hemisphere was found to be higher compared to the right hemisphere.
Conclusions: In this study, the main important pathways of synchronized edges defined as hub crosslinks are well suited in the identification of functional modules. These hyper edges may be associated with the graph-ICA results (Park et al., PLoS ONE

2014). Further studies foucs on how these hub crosslinks interact with each other and what this arrangement can tell us about the brain organization in terms of recruiting or dimissing of hub crosslinks in particular for the execution of certain tasks.

P7B Resting-state brain networks predict working memory and sustained attention across individuals

Emily S. Finn[1], Monica D. Rosenberg[2], Xilin Shen[3], Dustin Scheinost[3], Xenophon Papademetris[3], Marvin M. Chun[1,2,4], R. Todd Constable[1,3]

[1]Interdepartmental Neuroscience Program; [2]Dept. of Psychology; [3]Dept. of Diagnostic Radiology; [4]Dept. of Neurobiology; Yale University, New Haven, CT, USA

Background: A variety of brain regions are involved in working memory and sustained attention tasks. While activity/connectivity during performance of such tasks has been well characterized, relatively few studies have looked for correlates of individual differences in these cognitive abilities in data acquired at rest. Here, we used task-based fMRI to detect the functional networks associated with accuracy on a continuous working memory task. We then probed these networks in data obtained at rest to determine if their intrinsic strength predicts performance across individuals.
Methods: While undergoing high-resolution fMRI (voxel size = 2.5 mm^3; TR = 1 s), 22 healthy subjects performed n-back tasks of varying difficulty: 1-back (baseline), 2-back (increased working memory load) and degraded 1-back (stimuli with added salt-and-pepper noise; increased perceptual load). Stimuli were face photographs. Subjects also underwent two 6-minute resting-state runs. We used a novel whole-brain functional parcellation scheme to calculate connectivity matrices for each subject during five states: each of the three task loads, all tasks combined, and rest. We used rank correlation to identify connections (''edges'') associated with sensitivity (*d'*) during the task. We then examined the predictive power of these networks at rest by summing the z-scores of all edges involved in the network in the resting-state matrices and correlating the summed network strength with *d'* across subjects. We also conducted leave-one-subject-out cross-validation to test our method's ability to predict the behavior of novel subjects.
Results: For all three task loads, as well as all tasks combined, we identified networks in the range of 400–700 edges ($\sim$1.5% of a total possible 36,000 edges) that were significantly ($p < 0.01$) correlated with accuracy, both positively and inversely, during the task. Summing the strength of these networks at rest yielded highly accurate predictions of task accuracy ($|r| = 0.6$–0.8; $p < 0.005$). Leave-one-subject-out cross-validation proved that performance of a previously unseen subject could be predicted using that subject's resting-state data. While predictive networks involved intricate connections between disparate regions, some anatomical trends could be detected. Cerebellar connectivity emerged as important to both high and low performance, as well as connectivity of task-relevant regions such as the supplementary motor area and fusiform gyrus. However, predictive power was considerably higher using distributed networks rather than single nodes, underscoring the need for a comprehensive, whole-brain approach.
Conclusions: Results indicate that it is possible to predict an individual's performance on working memory tasks from resting-state data. This suggests that networks associated with accuracy and attention on such tasks are at least partially intrinsic — i.e., present in the absence of any explicit task, and reflective of individual cognitive abilities.

P8B Comparing Scrubbing Strategies and how they Affect Graph Theoretical Measures in Resting State fMRI

N.K. Aurich[1], A.M. Marques da Silva[1,2], A.R. Franco[1,2]

[1]Graduate Program in Electrical Engineering, PUCRS, Porto Alegre, Rio Grande do Sul, Brazil, [2]Brain Institute (InsCer), PUCRS, Porto Alegre, Rio Grande do Sul

Background: Graph theory (GT) is increasingly being applied to neuroimaging data to study the human brain connectome, at the structural and functional level [S. Achard and E. Bullmore, 2007]. However, measures from GT, such as global efficiency (GE), characteristic path length (CPL), average clustering coefficient (ACC) and average local efficiency (ALE) can alter simply based on the quality of the data and not just the mental state and/or diagnosis of the subject undergoing a resting state fMRI scan [H. Cao et al. 2013, C.G. Yan et al. 2013]. In fMRI data there are several sources of noise, including head motion, which has been show to have a great impact on GT measurements [C.G. Yan et al. 2013]. In order to correct possible artifacts in measures of connectivity, a method (scrubbing) [J. D. Power et. al 2011] was applied. Typically, scrubbing has been performed based on motion parameters, where time-points with excessive motion are censored. However, these motion parameters do not measure several other sources of noise that affect fMRI data, including those related to hardware imperfections and physiological noise. There are other measurements that seed to find outliers within the functional data [R. W. Cox, 2002], which identifies time-points that exceed a typical range. The aim of this paper is to evaluate how the choice of scrubbing method (head motion or outlier measurements) affects GT measurements.
Methods: A subset of healthy controls (N = 102) from the 1000 Functional Connectome Project was used in this analysis. [B. B. Biswal et al. 2010]. All functional data were preprocessed through conventional resting state preprocessing steps using AFNI [R. W. Cox, 1996], including regressing noise measurements (WM, CSF and 6 motion parameters). Data were processed through two different scrubbing methods: Method 1 (censoring excessive head motion) and Method 2 (censoring data outliers), whereas the default parameters from ANFI were chosen. Data were then subdivided into 200 nodes [R. C. Craddock, 2012] and GT measurements were performed with the Brain Connectivity Toolbox [M. Rubinov and O. Sporns 2010]. The connectivity matrix was thresholded at three different levels (L): 0.2, 0.3, and 0.5.
Results: For each GT measure and thresholding levels, pairwise t-tests were performed to compare the two scrubbing methods. Significant statistical difference ($p < 0.01$) was found in 7 out of 12 pairs of measures, with the exception of ACC at L = 0.2, ACC and ALE at L = 0.3, and CPL at L = 0.5. Statistical difference ($p < 0.05$) of ACC was shown at L = 0.5. Additionally, the correlation between the GT measures and average motion estimation, for both scrubbing methods, was calculated. Scrubbing method 1 showed a higher correlation compared to method 2, for all nine correlation contrasts.
Conclusions: More than half of GT measures were strongly affected by changing the scrubbing method, where ACC was less affected. This is worrisome, since a minor change, choosing scrubbing method, can substantially affect GT measures. Additionally, results have shown that scrubbing method with data outliers reduces motion related variation within data more than using motion estimation.

P9B Which graph theory metrics best convey information about on-going cognition?

J Gonzalez-Castillo, L.C. Buchanan, C.W. Hoy, D.A. Handwerker, P.A. Bandettini

Section on Functional Imaging Methods, NIMH, NIH, Bethesda, MD, USA

Background: Previous studies [1,2] have shown how patterns of whole-brain functional connectivity can be used to differentiate cognitive states. Nevertheless, the large dimensionality of the feature space associated with the human brain connectome makes analysis and interpretation challenging. Discovering meaningful ways to compress such vast amounts of information, while maintaining classification power, would ease computational hurdles and help uncover the primary drivers of distinct mental states. Here, we evaluate if graph theory network metrics can help dramatically reduce the dimensionality of the data without negatively affecting classification accuracy. We also rank graph theory metrics in terms of their informative value for discriminating cognitive states. In that manner, we find a subset of metrics that convey the most cognitively relevant information about the network structure of the brain.
Methods: We collected 25 mins of fMRI data (TR = 1.5 s, voxel size = 8 mm3, 7T) on 22 subjects as they perform and transition between 4 tasks: rest, math, 2-back, and visual attention. Each task was performed continuously for 3 mins during 2 different blocks within the scan. Time-series for 150 ROIs from the Craddock Atlas [3] were extracted after pre-processing; and subsequently segmented into 90 s non-overlapping windows aligned with task blocks. For each window, we computed 20 graph theory metrics using the Brain Connectivity Toolbox [4]. Some metrics were computed at the whole brain level, while others were computed for each ROI. Metrics were then sorted based on how well they discriminate between tasks. Finally, vectors with an increasing number of metrics entered a k-means clustering algorithm (k = 4). Agreement between k-means results and the window groupings according to task was quantified using the Adjusted Rand Index [5].
Results: (1) The discriminative values of the evaluated set of metrics varied substantially across metrics. (2) Locally computed metrics (e.g., per ROI) are more informative than global metrics when attempting discrimination between cognitive states. (3) Optimal combinations of metrics produced moderate accuracy when classifying windows according to task (see figure on the left). These accuracy levels are lower than those obtained with classification algorithms based on whole-brain connectivity matrices for the same set of ROIs and tasks [2].
Conclusions: We show how only a subset of graph theory metrics conveys cognitively relevant information about how the brain functionally re-organizes in order to perform different tasks. Optimally combining these metrics helped us achieve moderate classification accuracies when attempting to discriminate between cognitive states established by the task paradigm.
[1] Shrier et al. 2012 Cer Cortex; [2] Gonzalez-Castillo et al. OHBM 2013; [3] Craddock et al. 2012 Hum. Brain Mapp.; [4] Rubinov et al. 2010 NeuroImage. [5] Hubert et al. 1989 J. Classification.

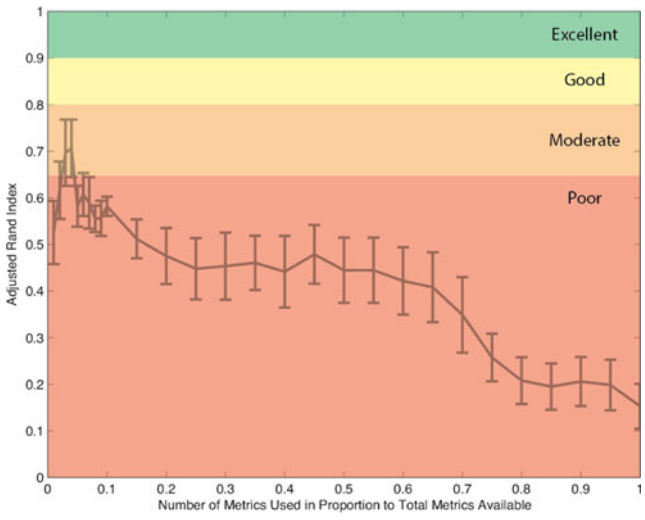

P10B The Virtues of Exploration: A Philosophical Framework for Resting State Connectivity and Data-Driven Connectomics Approaches

Philipp Haueis

Max Planck Research Group for Neuroanatomy & Connectivity, Max Planck Institute for Human Cognitive and Brain Sciences, Leipzig

Background: History and philosophy of science (HPS) scholars have argued that exploratory experiments allow researchers to systematically map a phenomenon without testing specific hypotheses or theories about its behavior. While former HPS studies have specified the criteria for exploratory experiments in physics, molecular biology, or genetics, an application of these criteria to neuroscience has been missing so far. The following philosophical analysis attempts such an application to resting state connectivity and large-scale connectomics approaches. By thus making the prospects and issues of neuroscientific methodologies explicit, philosophy of science can actively contribute to ongoing research.
Methods: A survey of the HPS literature identified three criteria for successful exploratory experiments. (i) *Conceptual development:* By varying a large number of experimental parameters one-by-one, researchers identify the conditions necessary for applying a concept across experimental variations. (ii) *Identifying entities*: By combining independent manipulation techniques, exploratory experiments identify entities (e.g., DNA) by experimental, rather than theoretical criteria (e.g., that DNA is animal-specific, as early molecular biologists assumed). (iii) *Type of instrumentation*: The search for concepts and entities is facilitated by the use of high-throughput instruments (e.g., DNA micro-arrays) that monitor an entire system rather than test a specific hypothesis about one of its parts.
Results: Application of the three criteria showed that resting state functional connectivity studies fulfill criterion (i), because they use various instruments (EEG, PET, MEG, fMRI) referring to different neuronal events (neurons, ensembles or networks) via various correlational techniques (across/within conditions, subjects, time courses). So far, however, no necessary conditions for applying ''functional connectivity'' emerged from these variations. Non-invasive rsfMRI studies alone are insufficient to fulfill criterion (ii), because correlation measures do not unambiguously identify the causal source of BOLD signal changes. Further exploratory research could identify entities (e.g., cortico-cortical microcircuits) by combining connectivity analyses with intervention techniques (e.g., optogenetics). Furthermore, connectomics studies that map wiring diagrams with whole brain imaging techniques (rsfMRI, DWI) fulfill criterion (iii), because they record overall brain interactions rather than testing cognitive hypotheses about isolated brain areas.
Conclusions: Applying the criteria for exploratory experiments indicates that the virtue of resting state connectivity approaches lies in bottom-up description and conceptual development, rather than top-down hypothesis testing and explanation. Philosophers and

scientists often overlook, however, that building conceptual frameworks shapes later theoretical and explanatory activity. The absence cognitive hypotheses in exploratory resting state and connectomics approaches may thus contribute to building a new descriptive framework that captures human brain organization more adequately.

P11B Sensitivity of the default-mode network at 7T

A. Hoffmann[1], R. Sladky[1], M. Spies[2], D. Pfabigan[3], M. Küblböck[1], A. Höflich[2], E. Seidel[3], A. Hummer[1], C. Lamm[3], R. Lanzenberger[2], C. Windischberger[1]

[1]MR Center of Excellence, Center for Med. Physics and Biomed. Engrg, Med. University of Vienna, Vienna, Austria, [2]Department of Psychiatry and Psychotherapy, Medical University of Vienna, Vienna, Austria, [3]Social, Cognitive and Affective Neuroscience Unit, Faculty of Psychology, University of Vienna, Vienna, Austria

Background: The introduction of ultra high-field MR scanners brought about numerous benefits for functional MRI, including a higher signal-to-noise ratio (SNR) and faster acquisition times. Unfortunately, field inhomogeneities due to susceptibility differences are also increased at higher field strengths and thus signal dropouts due to intra-voxel dephasing effects are also increased. This work examines the sensitivity of resting-state fMRI (rs-fMRI) at ultra high-field (7T) in comparison to 3T at the example of the default-mode network (DMN).
Methods: The following table shows the key facts for the datasets used in this study.

Name	*Subj.*	*Age*	*TR*	*Vol.*	*Length*	*TE*	*Voxel size*	*MB*
3T-a	164	24.9 ± 4.96	1.8 s	192	5 min 46 s	38 ms	128 × 128 × 23	-
3T-b	133	24.8 ± 3.66	1.8 s	192	5 min 46 s	33 ms	128 × 128 × 54	3
7T-a	40	27.0 ± 6.04	1.4 s	247	5 min 46 s	23 ms	128 × 128 × 78	3

All subjects were healthy volunteers. The datasets underwent the same pre-processing, including slice-timing correction, realignment, normalization, smoothing (9 mm FWHM), nuisance signal regression, bandpass-filtering (0.009 Hz-0.08 Hz), motion-scrubbing and seed-voxel correlation with the posterior cingulate cortex (PCC, x/y/z = 0/-52/30 mm). For any number N ranging from 3 to 40, connectivity maps of N subjects were randomly chosen from either the 297 3T or the 40 7T datasets and subjected to one-sample t-tests. This procedure was then repeated 300 times to obtain robust estimates of sensitivity. Finally, the mean p-values from all repetitions were compared between 3T and 7T.
Results: Correlations of the PCC with the ventral parts of the DMN, that are commonly more prone to susceptibility-related effects and physiological artifacts, were found to be more significant at 7T, which is also illustrated in fig. 1 at the example of the subgenual cingulum (SGC). Here, the higher SNR at 7T allows achieving the same level of significance with fewer subjects, i.e. 15 instead of 26 subjects for the SGC. The dorsal part of the DMN, however, did not show any noteworthy changes in sensitivity.
Conclusions: Here we showed, at the example of the DMN, that the usage of ultra high-field scanners is beneficial for rs-fMRI studies that concern the ventral brain, a highly important area particular for studies on psychiatric diseases. This increase in ventral brain sensitivity may arise from scanning very thin slices, which is useful only at 7T because of the increased SNR.

P12B Exploring the feasibility of high-resolution functional connectivity through the perspective of physiological contribution ratio

A.L. Hsu[1], C.W. Wu[2], C.P. Lin[4], J.H. Chen[1]

[1]Institute of Biomedical Electronics and Bioinformatics, National Taiwan University, Taiwan, [2]Graduate Institute of Biomedical Engineering, National Central University, Taoyuan, Taiwan, [3]Institute of Neuroscience, National Yang-Ming University, Taiwan

Background: To reveal detailed spatial information, the high-resolution resting-state fMRI (rsfMRI) is preferred, but brain connectivity with high spatial resolution is rarely reported, which may be due to low physiological contribution ratio (PCR, the ratio of physiological fluctuations versus instrumental noise). Henceforth, we hypothesized that the PCR can be accessed via SNR ratios according to Glover's theory [1].
Methods: Five rsfMRI scans with different spatial resolutions of GE-EPI (TR = 3 s, TE = 41 ms, FA = 87°, 150 scans, BW = 1260 Hz/px) were scanned on 7 healthy participants in a 3T Trio system. The preprocess steps included realignment, field map correction, detrending and RETROICOR correction. Based on Glover's model, the PCR is proportional to the ratio of SNR_0/tSNR (Fig. 1 top-left corner). Then we compared the PCR in thalamus between all datasets. In addition, we also explored the impact of RETROICOR corrections on the physiological contribution in all datasets.
Results: Both SNRs increased with the voxel size, and the SNR_0/tSNR ratio changed from 0.98 to 1.23. With detrending, the PCR in thalamus ranged from 0.06 (highest resolution) to 0.74 (voxel size = 4 mm), indicating the instrumental noise dominance across all datasets. The bilateral connectivity in thalamus became prominent when PCR > **35%**; however, we failed to discover connectivity patterns when the voxel-size 2 mm. In addition, moderate effect of RETROICOR correction on the physiological contributions was also demonstrated, and it would not affect the connectivity outcomes.
Conclusions: (1) Through the estimation of physiological contribution ratio (PCR), we addressed a new strategy for quality check on rs-fMRI signal. (2) At the typical EPI resolutions ($3 \times 3 \times 3\ mm^3$), the PCR ratio was 49% of the thermal noise level, enabling to produce strong connectivity patterns. (3) With high spatial resolution (voxel size $\leq$ 2 mm), PCR would be disappointingly low, leading to the loss of functional connectivity.

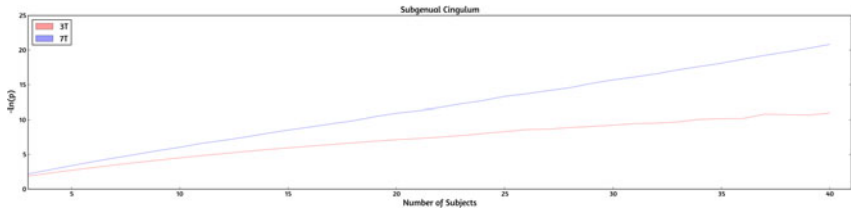

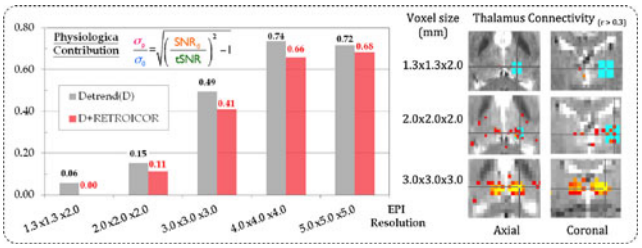

Reference: Krüger G and Glover GH. Magn Reson Med, 2001; 46(4), 631–637.

P13B Variability of the inter-hemispheric connectivity of homotopic hemispheric resting-state region pairs: Effects of handedness and sex in a cohort of 414 subjects

M. Joliot, E. Mellet, L. Petit, B. Mazoyer, N. Tzourio-Mazoyer

Groupe d'Imagerie Neurofonctionnelle, UMR5296 CNRS, CEA, Univ. Bordeaux, France

Background: Hemispheric Specialization (HS) is an essential feature of the human brain corresponding to the hosting by a given hemisphere of a given cognitive function (Hervé et al., 2013). HS is supported by both intra-hemispheric specialization and inter-hemispheric interactions. Inter-hemispheric connectivity, mandatory for cognitive functioning, is operated through the corpus callosum in an anatomical homotopic way at both cortical and cytoarchitectonic levels (Van der Knaap et al. 2011). Such callosal cooperation can be quantified by measuring intrinsic connectivity between homotopic regions, such connections exhibiting the strongest correlations (Stark et al. 2008). To our knowledge, there has been no evaluation of the variability of these functional connections, although they represent a central aspect of human brain connectivity. In the present work, we took advantage of the BIL&GIN, a database developed for the study of hemispheric specialization, balanced for gender and handedness, to investigate the variability of homotopic inter-hemispheric connectivity with gender, handedness, age.
Methods: For each of 414 healthy volunteers (215 women, 189 left-handers), 8 minutes resting state FMRI data (r-FMRI, TR = 2 s) covering whole cerebrum were acquired and pre-processed (Doucet et al. 2011). The averaged r-FMRI time-course was computed for each of the 384 regions of the homotopic atlas ''AICHA'' (Joliot et al. 2012) an inter-hemispheric functional correlation (FC) being calculated for each of the 192 pairs of homotopic regions (hROI). A MANOVA was computed with hROI as a within-subject factor, and age, sex, handedness and intra-cranial volume as between-subject factors. We examined main effects of age, sex and handedness and their interactions with the hROI factor, post-hoc analysis being conducted for uncovering the involved hROIs ($p < 0.05$ uncorrected).
Results: Significant main effects were found for age ($p < 0.001$) and sex ($p = 0.02$) but not for handedness ($p = 0.17$), FC values decreasing with age and being higher in men than in women. We found significant interaction between hROI and age ($p < 0.0001$), sex ($p < 0.0001$), and handedness ($p < 0.004$). Post-hoc analyses showed reduced FC values with age in the pre- and post-central (except in its upper part), superior and inferior temporal, insular, and lateral prefrontal cortices. Meanwhile, higher FC values in men were located in parietal and temporal areas, while higher FC values in left-handers encompassed inferior frontal gyrus, inferior part of the precentral gyrus and medial-temporal regions.
Conclusions: The present results are consistent with previous report of larger inter-hemispheric correlation in primary and associative unimodal areas (Stark et al. 2008). They provide new insight on the mechanisms supporting differences in lateralization of functions that have been reported with aging (Davis et al., 2012), gender, and handedness (Hervé et al., 2013).

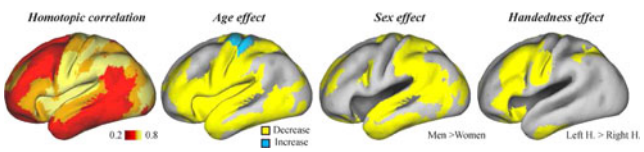

P14B Validity and Reliability of a Proposed New Standard for Resting fMRI Data

C. Kelly[1], K. Somandepalli[1], A. Di Martino[1], P. Velasco[2], M.P. Milham[3,4], F.X. Castellanos[1,4]

[1]Center for Neurodevelopmental Disorders, NYU Child Study Center, New York, NY, USA, [2]Center for Brain Imaging, New York University, New York, NY, USA, [3]Child Mind Institute, New York, NY, USA, [4]Nathan Kline Institute, Orangeburg, NY, USA

Background: Resting state fMRI (R-fMRI) and intrinsic functional connectivity (iFC) mapping have energized developmental and psychiatric neuroimaging, but concerns about the impact of motion and preprocessing strategies on findings have begun to stall progress. Multi-echo independent components regression (ME-ICR; Kundu et al., *PNAS*, 2013), offers a principled and objective approach to identifying and removing motion-related artifact and other nuisance signals from R-fMRI data. This method capitalizes on the principle that multiecho (ME) acquisitions can be used to isolate non-BOLD changes in signal intensity (related to nuisance sources) from changes in BOLD signals of interest, which exhibit a dependence on echo time (TE). Here, we describe steps toward investigating the applicability of ME-ICR in developing and clinical populations.
Methods: ME R-fMRI data were collected from >450 children (aged 7–18) and adults (19–55) with and without Attention-Deficit/Hyperactivity Disorder (ADHD). A subsample (~125) was scanned twice (>1 week apart). Our ultimate aim is to

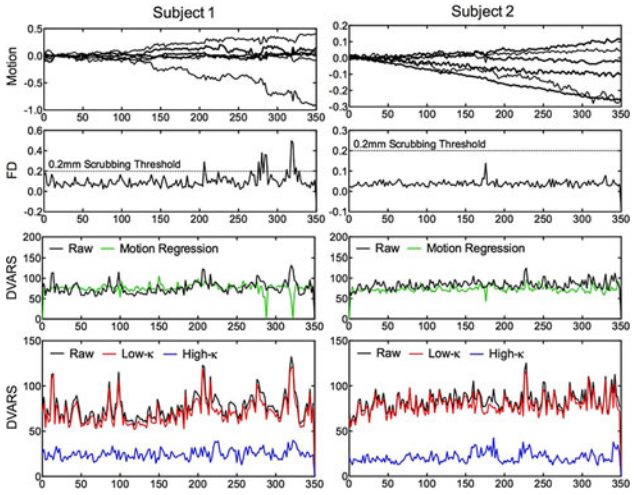

FIG. 1.

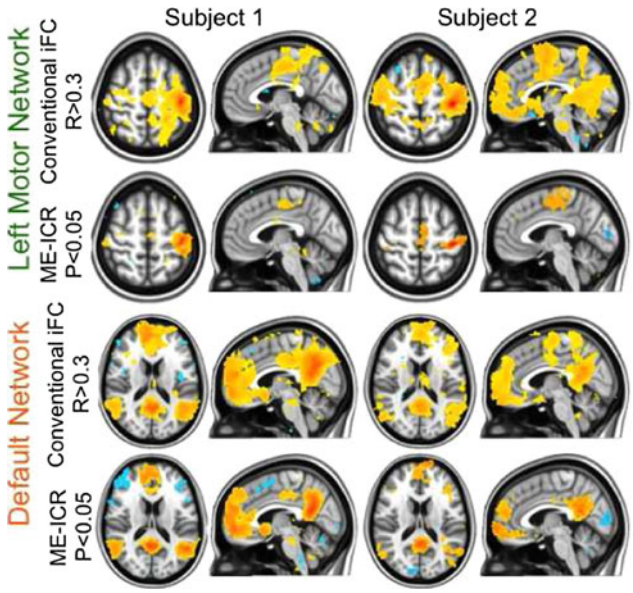

FIG. 2.

validate ME-ICR by examining its impact on (1) developmental trajectories of iFC, (2) group differences in iFC between ADHD and NT, and (3) test-retest reliability of iFC, relative to conventional analyses. A first step is to verify reasonable results are obtained with our sequence, which comprises 3 echo times (7.32, 12.12 and 32.93 msec), but was not specifically optimized for ME-ICA. Initially, data from two subjects (S1 = 14.5 yrs, male, ADHD; S2 = 9.5 yrs, male, NT) were analyzed using the AFNI script meica.py.

Results: Relative to conventional regression of motion parameters (Fig. 1, green trace), which does not effectively remove motion-related signals, ME-ICR yielded effectively denoised R-fMRI time series (Fig. 1, blue trace). We observed the same two-fold increase in tSNR, as well as the increase in specificity of iFC and valid individual-level statistical inference (Fig. 2) demonstrated by Kundu et al. (2013).

Conclusions: Preliminary analyses suggest our ME data will indeed serve as an initial test of the generalizability and clinical utility of ME-ICR. Eventual application to our full dataset will establish whether ME acquisition and analysis should constitute a new standard for R-fMRI studies, particularly in developing and clinical populations.

P15B Reduction of vascular confounds in fMRI group analysis results using modified RESCALE method

M. Küblböck[1], A. Hoffmann[1], A. Hahn[2], D. Pfabigan[3], A. Hummer[1], M. Woletz[1], R. Sladky[1], S. Ganger[2], E. Seidel[3], R. Lanzenberger[2], C. Lamm[3], C. Windischberger[1]

[1]MR Centre of Excellence, Center for Medical Physics and Biomedical Engineering, Medical University of Vienna, Vienna, Austria; [2]Department of Psychiatry and Psychotherapy, Medical University of Vienna, Vienna, Austria; [3]Faculty of Psychology, University of Vienna, Vienna, Austria

Background: Amplitudes of task-related signal changes in fMRI are dependent on local vascular features with vary across voxels and subjects. As a consequence, parameter estimates from GLM analyses will also vary according to the individual responsiveness, thereby increasing the inter-individual variance and thus reducing sensitivity. We have recently presented a method that is based on normalizing responsiveness using parameters obtained from fractional amplitudes of low-frequency fluctuation (fALFF) maps in resting-state fMRI scans, thereby increasing t-values in random- effect group analyses (RESCALE, Kalcher et al, NI, 2013). Here, we present a modified rescaling approach that improves the gain in sensitivity and shows that this method is successful in a variety of task-based fMRI paradigms.

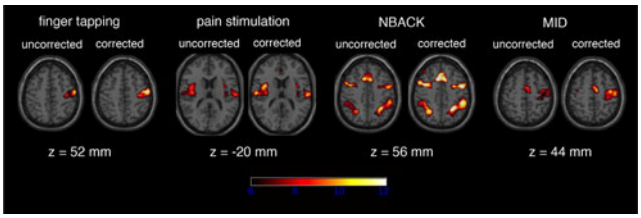

Methods: Measurements were performed using a 3T Trio Siemens Magnetom scanner, using a standard EPI sequence (TE/TR = 38 ms/1.8 s, voxel size = $1.48 \times 1.48 \times 3.0\,mm^3$). 23 healthy, right-handed subjects underwent a five-minute resting-state scan and performed four different tasks (electrical pain stimulation, monetary incentive delay, working memory task, right finger tapping). Standard preprocessing steps were applied. For each subject, voxel-wise fALFF maps were calculated from the resting-state data. Single-subject parameter estimates for all fMRI paradigms were calculated using SPM12b. Different to the original RESCALE method we varied the normalization quantile used for calculating the slope correction coefficient (SCC) over a wide range to find the optimal correction parameters.

Results: Application of the RESCALE method resulted in significant improvement of group analysis results for all four paradigms (see fig, FWE-corrected). Our modified SCC normalization approach yielded a strong increase in the number of activated voxel after correction compared to the original method: finger tapping: +34/ +82%; n-BACK: +19/ +42%, monetary incentive delay, MID: +24/ +59%, painful electrical stimulation: +17/ +41% (original/modified normalization).

Conclusions: RESCALE is an effective method for reducing inter-subject variability in task-based fMRI data. This correction approach has a wide range of potential applications for group analysis of both block- and event-related design fMRI experiments.

P16B Large functional connectivity network analysis of whole-brain high-resolution resting-state fMRI

A.C. Leitão[1], A.P. Francisco[1], R. Abreu[2], P. Figueiredo[2], L.L. Wald[3], M. Bianciardi[3], L.M. Silveira[1]

[1]INESC-ID/ Instituto Superior Técnico – Universidade de Lisboa, Portugal; [2]ISR/ Instituto Superior Técnico – Universidade de Lisboa, Portugal; [3]Athinoula A. Martinos Center for Biomedical Imaging, Charlestown, MA USA

Background: It has recently become possible to collect fMRI data from the whole-brain for the analysis of resting-state BOLD fluctuations at ultra-high-field (e.g. at 7T). The resulting high-resolution datasets cover a wider volume of the brain, including the cerebellum and the brainstem. In this work, we apply graph theory algorithms to investigate the brain functional connectivity (BFC) networks obtained from high dimensionality data based on full voxel-based correlation analysis. Using such techniques we can measure basic properties of the network's structure and

find functional modules of the brain. The high resolution enabled a much higher granularity than previous works.

Methods: Resting-state fMRI data were collected from a group of healthy volunteers on a 7T Siemens whole-body scanner equipped with custom-built 32-channel receive coils, using a 3× slice accelerated SMS EPI sequence (TE/TR = 32 ms/2500 ms, 210 volumes), with 1.1 mm isotropic voxels covering the whole-brain in 123 sagittal slices (FOV = 264 × 198 mm^2). Standard pre-processing was performed using FSL, including: slice scan time correction, motion correction, non-brain removal, spatial smoothing (FWHM = 1.5 mm Gaussian kernel) and high-pass temporal filtering (100 ms cut-off). BFC networks were obtained with vertices representing voxels and edges functional connections, computed as correlations between voxels' BOLD signals. Basic properties of the network's structure were extracted including degree distribution, connected components, average distance and clustering coefficient. A preliminary modularity analysis of the network was conducted in order to find brain functional modules.

Results: BFC graphs with over one million vertices were obtained. The unusually high dimensionality of the data required specialized algorithms to be implemented to enable construction and subsequent analysis of the networks. We found that these networks have: 1) a small-world topology (average minimum path is low compared with the number of vertices and the clustering coefficient is high compared with the coefficient of the equivalent random network); and 2) a scale-free organization (taking into account computed centrality measures distributions). The BFC modules obtained were consistent with those reported in previous works, although showing finer-grained modules.

Conclusions: We obtained large voxel-based BFC networks from whole-brain 1.1 mm isotropic resting-state fMRI data, and found small-world and scale-free properties as previously reported for smaller networks. We did find a much higher module granularity, which should be further investigated. A systematic analysis of the network modularity will be performed using appropriate methods that we have found to be efficient in such big networks, and compared with conventional analysis.

Acknowledgments: This work was partly supported by national funds through FCT – Fundação para a Ciência e Tecnologia, under projects PTDC/EEI-ELC/3246/2012 and PEst-OE/EEI/LA0021/2013.

P17B A novel, data-driven approach to whole-brain analysis of fMRI network activity

X. Liu[1], C. Chang[1], J.H. Duyn[1]

[1]*Advanced MRI, LFMI, NINDS, National Institutes of Health*

Background: Previous observations that many of the established resting-state networks (RSNs) can often be identified from a small sub-selection of time points from an fMRI data set has led to a method that decomposes a specific RSN into multiple co-activation patterns (CAPs) that may have distinct functional roles

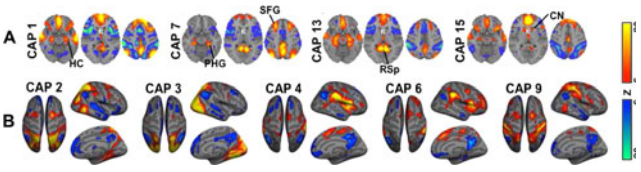

FIG. 1. CAPs in ''task-negative'' **(A)** and ''task-positive'' **(B)** regions of the brain

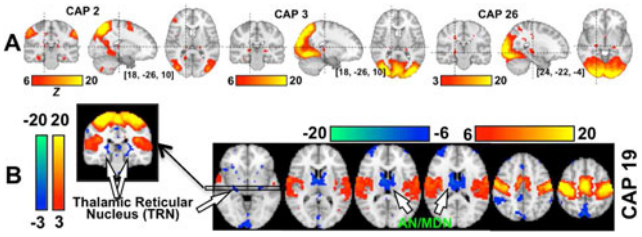

FIG. 2. Visual **(A)** and sensorimotor **(B)** CAPs with specific thalamocortical co-activations.

at different times. Here, we extend this method to a whole-brain data-driven approach and apply it to extract 30 CAPs that show information complementary to that available with conventional analysis methods, and furthermore offered a means to quantify population differences.

Methods: We analyzed resting-state data of 102 subjects from the ''fcon 1000 project''. After typical pre-processing steps, the fMRI voxel time series were demeaned and normalized by temporal standard deviation. Then, k-means clustering was applied to classify all fMRI volumes (time frames) into 30 groups based on their spatial similarity, and these volumes were then averaged within groups to extract 30 final CAPs.

Results: Many of the extracted CAPs were consistent with established functional connections. Four of 30 CAPs showed patterns resembled the default mode network (DMN) but with distinct differences at specific brain structures (Fig. 1A). Another group of 6 CAPs show co-deactivation in the DMN but co-activation in different sets of ''task-positive'' regions (Fig. 1B), suggesting a multiple-to-one anti-correlated relationship between these two sets of brain regions. Multiple CAPs showed very specific thalamo-cortical co-activations consistent with the established hierarchical organization in the various sensory systems. For example, a coactivation between LGN and V1 was observed, distinct from one between pulvinar and visual association areas (Fig. 2A); sensorimotor activation was accompanied by de-activation in the anterior and medial dorsal nuclei (AN/MDN) and the thalamic reticular nucleus (TRN) (Fig. 2B), consistent with the functional role of these thalamic nuclei in the control of brain's arousal level.

It was also found that CAP 23, covering a part of sensorimotor cortex, occurs much more frequently ($p < 0.01$, Bonferroni corrected) in males than in females (Fig. 3), indicating a means to derive quantitative information from data-driven RSN analysis.

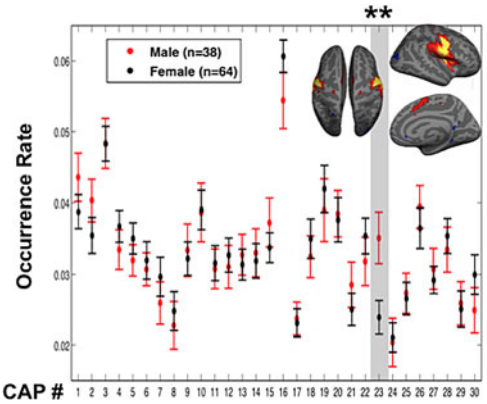

FIG. 3. Occurrence rates of CAPs in males and females.

Conclusions: A whole-brain, data-driven technique is proposed for the analysis of resting-state fMRI signals, which may have advantages over conventional methods regarding the information about the time-varying configurations of the brain.

P18B Choice of affine registration systematically alters apparent seed based synchrony

J. McGonigle[1], C. Orban[1], A.R. Lingford-Hughes[1]

[1]*Centre for Neuropsychopharmacology, Imperial College London, London, UK*

Background: The first step in a spatial transformation to a standard space is the calculation of an affine transform from a low-res functional image to a high-res structural. Prevalent algorithms for this are normalized mutual information (NMI) and correlation ratio (CR), implemented in SPM's *spm_coreg* and FSL's *FLIRT* respectively. Recently, boundary based registration (BBR) has been introduced, and made available in the FSL suite. As much past work has used CR it is important to be aware of possible systematic biases when comparing seed based studies in the literature with newer work.
Methods: Here we use open data from the 1000 Functional Connectomes release (Oxford dataset, n = 22), but the effect is seen using any data. Two pipelines were run, identical apart from their affine registration step. These included despiking, motion correction, CR registration (FLIRT with 6 d.o.f.) or BBR, nonlinear registration (ANTs), motion scrubbing, bandpass filtering and removal of nuisance variables (6 motion, local white matter, draining vessels, and ventricle CSF), and smoothing. An amygdala seed was used.
Results: Figure 1a shows the mean brain outlines at the end of the two pipelines. The CR based approach is systematically shifted inferiorly with respect to the BBR by 5.0 ± 0.9 mm (mean ± SD). On visual inspection the BBR pipeline is closely aligned with the underlying anatomy. Figure 1b shows the result of a comparison of the approaches at the group level, with the cooler colours in the white matter demonstrate that activity has been misplaced using the CR approach.
Conclusions: Wherever an atlas is used to define ROIs the interpretability of the results is closely dependent on the accuracy of the affine registration. Whole brain task analysis will not be affected beyond the slight misalignment with a high-res image. However, approaches using parcellations or seeds, including graph theory and meta-analysis based methods, may have been systematically biased to superior parts of regions when using CR approaches. This may create a difficulty in correctly comparing current and past work, especially where small regions have been sub-divided further into regions of a size on the same order of magnitude as the extent of the misalignment.

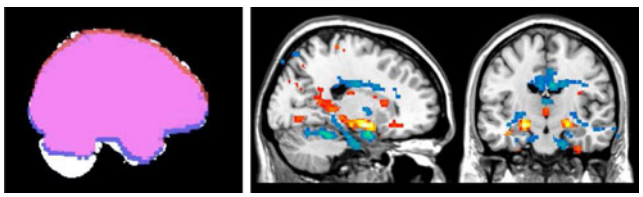

FIG. 1. **(a)** Mean brain masks. White = ground truth. Red = BBR pipeline. Blue = CR pipeline. Purple = overlap. **(b)** Warmer colours represent higher apparent synchrony with amygdala when using BBR, while cooler colours represent lower apparent connectivity.

P19B Meta-state analysis reveals reduced resting fMRI connectivity dynamism in schizophrenia across multiple multivariate analytic techniques

R.L. Miller[1], M. Yaesoubi[1,2], V.D. Calhoun[1,2]

[1]*The Mind Research Network, Albuquerque, NM, USA,* [2]*Department of Electrical and Computer Engineering, University of New Mexico, Albuquerque, NM, USA*

Background: Network connectivity remains a central focus of much resting-state fMRI research. Until very recently, most studies have assumed functional network connectivity (FNC) to be effectively stationary in the resting brain. Interest is growing however in the dynamical properties of network connectivity. Our approach models FNC matrices computed on successive windowed segments of network timecourses (wFNCs) as weighted sums of maximally temporally independent *basis connectivity patterns* (BCPs). This approach is motivated by a desire to understand network connectivity dynamics in terms of (not necessarily observable) correlation patterns that ''pipe in'' and fade out of observed time-varying FNCs in a relatively independent manner. To investigate possible dependencies of our results on the optimization objectives used in identifying BCPs from wFNCs, we also perform our dynamical analysis on maximally spatially independent correlation patterns and on mutually orthogonal correlation patterns ordered by explained wFNC variance.
Methods: This study was conducted on a large fMRI dataset (N = 314; 163 healthy (HC), 151 schizophrenia patients (SZ)). Data was preprocessed and decomposed into functional networks using group ICA. wFNCs were computed from subject-specific network timecourses, then decomposed into five BCPs according to three common data-driven techniques: temporal ICA, spatial ICA and PCA. The timecourses (TCs) associated to these BCPs were then discretized into signed quartiles (reassigned values in $\{\pm 1, \pm 2, \pm 3, \pm 4\}$ designating quartile position among same-sign TC values).
Results: For best comparability across decomposition techniques, we focus on the general dynamic behavior of *meta-states*. These are the length five vectors of discretized weights characterizing subject wFNCs at each time window. There are 8^5 possible such meta-states. We investigate several inter-related measures of generic dynamism in this discrete five-dimensional state space: the number of times that subjects *switch* meta-states, the *number* of distinct meta-states occupied, the L^2 *-span* of occupied meta-states, and the overall *distance* traveled in the state space. For all four of these measures, and with respect to each of the three decompositions employed here, schizophrenia was significantly negatively correlated with connectivity dynamism.
Conclusions: We find strong and consistent evidence for reduced connectivity dynamism in SZ patients using several higher-dimensional models of time-varying connectivity. These distinctive dynamical properties of SZ network connectivity cannot be assessed with conventional static FNC, and were not evident in previous lower-dimensional cluster-based studies of windowed FNCs.

P20B On the parcellation of the amygdala in studies of resting state functional connectivity

C. Orban[1], A. Santos Ribeiro[1], A.R. Lingford-Hughes[1], J. McGonigle[1]

[1]*Centre for Neuropsychopharmacology, Imperial College London, London, UK*

Background: Studies of resting state functional connectivity (RSFC) in humans typically define the amygdala either as a single structure, or alternatively as two to three distinct subregions inferred from the Juelich probabilistic atlas (Amunts et al., 2005; n = 10). While some studies have successfully shown distinct RSFC topology in two (Baur et al., 2013) and three subregion models (Roy et al., 2009), others continue to use the single region model over concerns of poor signal-to-noise ratio in the amygdala (Hahn et al., 2011). Furthermore, high field *in vivo* MRI reveals considerable anatomical variability in the boundaries of amygdala subdivisions (Solano-Castiella et al., 2011; n = 10). To inform future studies of amygdala RSFC in their choice of seed, we directly compare several histologically defined subregions versus a whole amygdala model, to detect RSFC across the brain.
Methods: 197 healthy participants (age 18–35) were analysed from the Cambridge_Buckner cohort within the 1000 Functional Connectomes dataset. Four Juelich atlas based subregions were compared with Freesurfer segmented whole amygdala seeds (AMYG): centromedial (CMA), superficial (SFA) and basolateral (BLA), centromedio-superficial (CSA), to determine differences in voxelwise RSFC. Separate general linear models were conducted in FSL's FEAT for each comparison. Preprocessing included despiking, motion correction, boundary based registration, non-linear registration (ANTs), motion scrubbing, bandpass filtering and removal of nuisance variables (6 motion, local white matter, draining vessels, and ventricle CSF), and smoothing (6 mm).
Results: The BLA and CMA seeds showed significantly greater RSFC with default mode and salience networks respectively, while the SFA and CSA seeds only showed greater RSFC to a cluster located in the right middle frontal gyrus, compared with the whole amygdala seed. In addition the CMA seed showed significantly greater RSFC in the ventral, and significantly less RSFC in the dorsal pallidum compared with the whole amygdala seed.
Conclusions: Researchers interested in examining amygdala anchored resting state networks in the context of clinical or experimental studies are faced with the challenge of defining their seed. Here we explicitly test whether, and where, smaller amygdala subregions provide greater sensitivity in detecting RSFC than the whole amygdala, thereby facilitating this decision. Furthermore we extend past work looking at distinct patterns of RSFC associated with these commonly used subregions by implementing several improvements in pre-processing approaches on a large dataset.

P21B A confound between static and dynamic connectivity

BP Rogers, DM Wilkes, JC Gore, Z Shi, VL Morgan

Vanderbilt University, TN, USA

Background: Recent work has suggested that functional connectivity in the brain varies minute-to-minute (e.g. Chang et al. 2010, Hutchison et al. 2013). This has often been measured using the standard deviation of the Pearson correlation coefficient. The variance of the estimated Pearson correlation has a strong relationship with its mean (Fisher 1915). The purpose of this study was to understand how this relationship affects the measurement of dynamic connectivity.
Methods: We used sliding window correlation coefficients to analyze both simulated time series and data from a sample of 12 people with temporal lobe epilepsy and 12 matched controls.
Results: Simulations showed that the measured standard deviation of the correlation coefficient r depended on the mean connectivity even when the degree of dynamic connectivity present was the same.

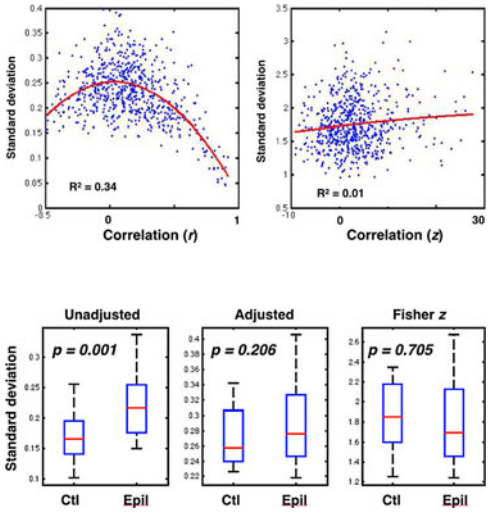

In real data, the standard deviation of r was quadratically related to its mean in a network relevant to epilepsy (Fig 1 left, $R^2 = 0.34$). This was not true for the standard deviation of the Fisher transformed correlation z (Fig 1 right, $R^2 = 0.01$).

Mean inter-hippocampal connectivity was lower in people with epilepsy (r = 0.39) than in controls (r = 0.61). The standard deviation of r was higher in epilepsy (Fig 2 left, p = 0.001). When this measure of dynamic connectivity was statistically adjusted for the mean r or when the Fisher transform was used (Fig 2 center and right) the difference between groups disappeared (p > 0.2). This suggests that the important difference in epilepsy was actually in the baseline level of connectivity, not in its dynamic variation.
Conclusion: When the mean connectivity differs between conditions or groups, differences in the standard deviation of the Pearson correlation coefficient r cannot be attributed to differences in connectivity dynamics without accounting for the mean connectivity. Changes in the standard deviation of the correlation coefficient are impossible to interpret in isolation.

P22B Pattern Approach for brain connectivity using K-means clustering of resting-state fMRI time series using 10-10 EEG related seeds

C. Montoya[1], G. Rojas[2], M. Galvez[3], J. Cisternas[4]

[1]Advanced Medical Image Processing Lab, Clínica Las Condes, Las Condes, Santiago, Chile, [2]Faculty of Engineering and Applied Sciences, Universidad de los Andes, Las Condes, Santiago, Chile

Background: Many resting state processing algorithms are in research now. New ones are related to k-means based clustering of the connectivity matrix. Here we show a new method that do the clustering of the resting state time data.
Methods: We processed resting state fMRI scans for 45 right handed healthy volunteers (age 18–30, 3T MRI, Cambridge-Buckner dataset, 1000 Functional Connectomes Project; http://fcon_1000.projects.nitrc.org). The data was motion-corrected, despiked, detrended and spatially-normalized using AFNI and FSL. We used 6 mm radius spherical seeds located in 65 EEG electrodes 10-10 system equivalent MNI coordinates (Rojas et al, 2012) to get resting state time series with each seed, and to

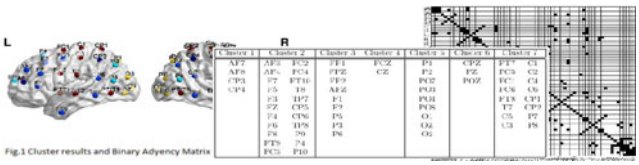

Fig.1 Cluster results and Binary Adyency Matrix

calculate participant-level whole brain connectivity maps. For seed based analysis, correlation matrix is created to look up how every pair of node is correlated and the compute of binary adjacency matrix used to calculate clusters coefficient. The method to find cluster groups is K-Means, an iterative process that partition the data in k disjoints clusters, defined k by the user previously, in this case seven clusters (quantity of standard functional connectivity networks, Yeo et al 2011) and starts with random centroids. The algorithm used for the iterative process is the Hartigan-Wong algorithm.

Results: For firsts analysis, Big Patient data was construct joining the 45 patient's time series creating a simulate patient that has the full data characteristic. ANOVA Test was used to find out the best cluster representation of the 10 times K-Means application. For this first results we could find that both Adjacency Matrix (by visual inspection).

Binary and K-Means has symmetrical seeds in contralateral hemisphere (for example FP1-FP2, AF3-AF4). Other cluster intra-connections has been detected, for example Central-Parietal area connects with Central and Parietal Areas or Frontal-Parietal zone connects with Frontal zone and Parietal zone.

Conclusions: This method shows that using 10-10 EEG related seed for RS-fMRI, it is possible to find how the brain connectivity can be cluster supported by different methods as the popular data mining K-Means analysis.

P23B Structural and resting state functional connectivity mapping in patients with implanted deep brain stimulation electrodes using low-power MRI

S.N. Sarkar[1], R.R. Rojas[1], F.A. Barrios[1,5], L.C. Shih[2], R.L. Alterman[3], E. Papavassiliou[3], D.B. Hackney[1] and M.D. Fox[2,4]

Departments of [1]Radiology, [2]Neurology and [3]Surgery, Beth Israel Deaconess Medical Center and [4]Massachusetts General Hospital, Harvard Medical School, Boston, MA, USA and [5]National Autonomous University of Mexico, Queretaro, Mexico

Background: MRI can be performed in patients with implanted electrodes for deep brain stimulation (DBS), but must adhere to strict safety guidelines regarding the amount of radiofrequency power or energy that can be delivered to brain tissue. Connectivity imaging including diffusion tensor imaging (DTI) and resting state functional connectivity MRI (rs-fcMRI) could help evaluate electrode placement (1) and the effect of DBS on brain connectivity (2), but traditionally require energy well above the safety limit. Building on prior low-energy work (3), we developed and tested very low energy (<0.1 W/kg) MRI sequences for DTI and rs-fcMRI.

Methods: Ten Parkinson's disease patients with implanted electrodes were imaged in a 1.5 T MRI with vendor and FDA specified MRI hardware and custom low energy anatomical and DTI sequences. Four of these ten patients were also imaged with low energy rs-fcMRI sequences (single-shot gradient echo EPI, TR = 2 s, TE = 50 ms, Voxel = $4\times4\times5$ mm3, interleaved). DTI data was processed using NordicBrainEX and fractional anisotropy (FA) values were compared to FA values obtained on the same patients with high-energy DTI obtained pre-operatively. Rs-fcMRI data was processed using the ''conn'' toolbox (5) and the default mode network was identified using canonical seed regions (4,5). The default mode network pattern was compared to that obtained from a large cohort of normal subjects.

Results: Low energy DTI and rs-fcMRI data were collected in patients with implanted electrodes within current safety limits and without adverse consequences. White matter fiber topography from low energy sequences was similar to pre-operative high energy sequences in thalamic and subthalamic regions (STN). Mean STN FA values were within 10% (0.41 pre, and 0.38, post-DBS, $P<0.05$). Low energy rs-fcMRI results were noisy, however the default mode network was identified and matched well with the known pattern seen in normal subjects.

Conclusions: Anatomical and functional connectivity mapping with MRI can be performed in patients with implanted DBS electrodes while adhering to current safety guidelines. Low-power DTI results were similar to high-power results obtained pre-operatively while low-power rs-fcMRI results reproduced the well-known topography of the default mode network.

References: (1) Henderson: Front. Integr. Neurosci 24 April 2012. (2) Kahan et al: Brain Feb 2014;1–15. (3) Sarkar et al: Radiology 2011;259:550. (4) Fox et al: Nat Rev Neurosci 2007;700–711. (5) Whitfield-Gabrieli et al: Neuroimage 2011;225–232.

P24B Connectome-Wide Associations Studies for Brain-Phenotype Relationships

Z. Shehzad[1,2,3], C. Kelly[4], P.T. Reiss[4,7,2], R.C. Craddock[1,2], J.W. Emerson[6], F.X. Castellanos[4,2], and M.P. Milham[1,2]

[1]Center for the Developing Brain, Child Mind Institute, New York, NY; [2]Nathan S. Kline Institute for Psychiatric Research, Orangeburg, NY; [3]Department of Psychology, Yale University, New Haven, CT; [4]Department of Child and Adolescent Psychiatry, New York University, New York, NY; [6]Department of Statistics, Yale University, New Haven, CT; [7]Department of Population Health, New York University, New York, NY

Background: Connectome-wide association studies (CWAS) remain limited by statistical approaches that are computationally intensive, depend on a priori hypotheses, or require stringent correction for multiple comparisons. To address these issues, we previously proposed a data-driven framework (Shehzad et al., 2014) that provides a comprehensive, voxel-wise survey of brain-behavior relationships using multivariate distance matrix regression (MDMR; Anderson 2001). The approach identifies voxels whose whole-brain connectivity patterns vary significantly with a phenotypic variable. Here, we introduce the R software package *connectir* for applying CWAS to resting-state fMRI data (http://connectir.projects.nitrc.org).

Methods: We examined 104 healthy adults (18–65 years old; 33 males) with Full Scale IQ from the NKI Rockland Sample. First, we used the command *connectir_subdist* to measure each voxel's temporal correlation with every other voxel in the brain (i.e., to generate its voxelwise connectivity map), at a resolution of $4\times4\times4$ mm. Then, using *connectir_subdist*, we compared each voxel's connectivity map between subjects using one minus the Pearson correlation (the default distance), as well as several other distance measures for comparison. Next, we used *connectir_mdmr* to apply MDMR and assess the association between IQ and individual differences in each voxel's connectivity map. Statistical significance was assessed using permutation tests. Finally, we

examined the relationship between these findings and those of a standard GLM using *connectir_glm.*

Results: We identified significant connectivity-phenotype relationships ($p < 0.05$) for IQ in areas that overlapped with prior literature (e.g., pre-frontal cortex). These results were robust to varying brain resolution (i.e., voxelwise results are highly similar to results as few as 50 parcellations). Compared with other distance measures (Chebychev, Kendall Tau, Lin's Concordance, and Spearman Rank), we found that the Pearson, Euclidean, and Mahalanobois distances yielded more significant results. We also demonstrated the ability of CWAS to guide subsequent seed-based correlation analyses.

Conclusions: The CWAS tools applied here are available in the *connectir* package, which includes accessible R functions and user-friendly command-line tools. Our approach reflects a shift from testing for associations in the connectome one connection at a time to connectivity patterns. As an example of its utility, we identified regions with connectome-wide associations related to IQ and obtained a set of findings not previously attainable with traditional univariate approaches. Future work will apply a derived distribution for significance testing in MDMR instead of computationally intensive permutation tests and provide additional utilities for manipulating distance matrices.

P25B A systematic examination of test retest reliability for R-fMRI metrics in childhood

K. Somandepalli[1], C. Kelly[1], F.X. Castellanos[1,2], X.N. Zuo[3], M.P. Milham[2,4], A. Di Martino[1]

[1]NYU Langone Medical Center, New York, NY, USA, [2]Nathan Kline Institute, Orangeburg, New York, NY, USA, [3]Key Laboratory of Behavioral Science, Institute of Psychology, Chinese Academy of Sciences, Beijing, China, [4]Child Mind Institute, New York, NY, USA

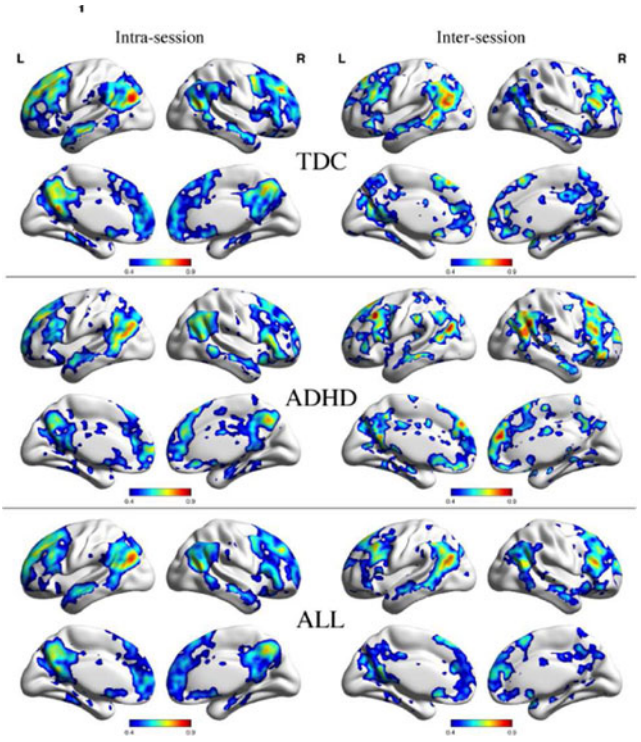

FIG. 1. ICC maps for PCC correlation analyses.

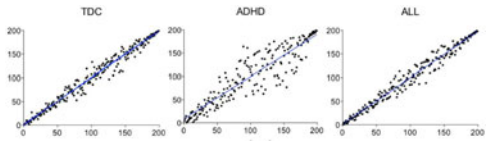

FIG. 2. Scatterplots for rank-ordered ROI-wise fALFF (x-axis: session1, y-axis: session2).

Background: Resting-state fMRI is increasingly used to characterize brain function in typical and clinical populations. This calls for measures that are reliable over time [Shehzad et al., 2009]. Moderate to high test-retest reliability (TRT) has been reported by several studies considering motion, scanner characteristics and other confounding factors [Yan et al, 2013; Patriat et al., 2013] mostly in healthy adults. Here, we aim to examine TRT for an array of R-fMRI metrics in children with and without ADHD.

Methods: We examined short-term TRT in 72 typically developing children (TDC; 36 males, 11.7 ± 3.1 yrs) and 54 with ADHD (37 males, 12.5 ± 2.8). We acquired a structural image, followed by a first 6-min resting echo-planar imaging (EPI) scan (TR = 2000 ms; TE = 33 ms; flip angle = 90, 33 slices; voxels = $3 \times 3 \times 4$ mm; Siemens-Allegra 3T) with eyes open. A second resting scan was collected within 45 min. Forty-nine children (29 TDC, 15 males, 10.4 ± 2; 20 ADHD, 15 males, 9.8 ± 2) completed a second session after 1–44 weeks (mean = 15), allowing for examination of long-term TRT. After standard preprocessing, rest scans were corrected for Friston-24 motion parameters, and signals from CSF and WM masks, and were registered to the first T1 scan and MNI152 space. We examined TRT for seed-based functional connectivity (Posterior Cingulate Cortex-PCC), Fractional Amplitude of Low frequency Fluctuations (fALFF), Voxel-Mirrored Homotopic Connectivity (VMHC) and Regional Homogeneity (ReHo), voxel- & ROI-wise. To quantify TRT reliability we computed Intraclass Correlation Coefficients (ICC), correlations between sessions and Kendall's rank correlation coefficient (tau).

Results: Moderate ($ICC > 0.5$) to high reliability was observed for all voxelwise measures (Fig. 1). Although short- & long-term ICC ranges were similar, short-term reliability was more spatially extended. We found high long-term consistency for all ROI-wise measures with Pearson's $r > 0.85$ & Kendall's Tau $\tau > 0.75$ (Fig. 2). We will further investigate differences in ICC between ADHD and TDC groups in detail.

Conclusions: R-fMRI metrics show moderate to high reliability in children albeit with regional variation. TRT reliability is not strongly contingent on diagnostic status; additional analyses will characterize this in detail.

P26B Denoising fMRI resting state data using systemic evolving regressors

Y. Tong[1,2], B. de B. Frederick[1,2]

[1]Brain Imaging Center, Mclean Hospital, 115 Mill Street, Belmont, MA 02478, USA
[2]Department of Psychiatry, Harvard University Medical School, Boston, MA 02115, USA

Background: fMRI signals are known to be affected by various physiological processes, including physiological low frequency oscillations (pLFOs), respiration, and cardiac pulsation. Among them, the pLFO signal has the greatest effect due to its strong spectral density in the lower frequency range, which overlaps with the neuronal signals of interest in resting state network

analyses. Moreover, since the pLFO's origins and function are not clear, it is challenging to identify and remove this signal. In our previous research, we found that 1) the pLFOs were closely associated with cerebral blood flow (Tong and Frederick, 2010); 2) they are present in most voxels, with varying magnitude; 3) their waveforms evolve in a way that suggests they are associated with blood traveling through the brain, and 4) they can be extracted from the BOLD data itself (Frederick, et al., 2012). We have recently developed a new, robust recursive analytical procedure to extract these evolving signals from the fMRI data itself. In this study, we used these extracted pLFO temporal traces as noise regressors to clean resting state fMRI data.

Methods: fMRI resting state studies were conducted in 11 healthy participants. All MR data was acquired on a Siemens TIM Trio 3T scanner (Siemens Medical Systems, Malvern, PA) using a 32-channel phased array head matrix coil. Multiband EPI (University of Minnesota sequence cmrr_mbep2d_bold R008) (Feinberg et al., 2010) sequence was applied with TR = 400 ms. The resting state scans lasted 360 s. Ultrafast acquisition was used to help remove respiration and cardiac signals. For each subject, we applied our method to identify 10–20 evolving pLFO regressors, and used GLM to remove the corresponding regressor for each voxel. We then used Multivariate Exploratory Linear Optimized Decomposition into Independent Components (MELODIC) ICA from FSL (Beckmann et al., 2005; Beckmann and Smith, 2004) on the ''cleaned'' data and compared the results with those of the original data.

Results: The RSN results from ''clean'' data are spatially more localized. The resulting ICs associated with well-known RSNs, including DMN, motor network, explained more variance in the ''cleaned'' data set. The temporal correlations calculated between different ICs (from the cleaned data) are much smaller than those calculated from original data, meaning pLFOs with high temporal correlation are being removed effectively.

Conclusions: In this study, we show a novel method to extract and remove dynamic pLFOs from resting state BOLD fMRI data. The method does not require extra physiological monitoring, and is not constricted by TR. The noise regressors were derived from the fMRI data itself. We demonstrated that it significantly improves the results of ICA on resting state data.

P27B Enhancement of BOLD complexity after a long work

P.J. Tsai[1], C.W. Wu[2], C.P. Lin[3]

[1]Department of Biomedical Imaging and Radiological Sciences, National Yang-Ming University, Taipei, Taiwan, [2]Graduate Institute of Biomedical Engineering, National Central University, Taoyuan, Taiwan, [3]Institute of Neuroscience, National Yang-Ming University, Taipei, Taiwan

Background: Brain oscillation is a complex system and its complexity could be time-variant. In fMRI analysis, we generally assumed that during the acquisition time the complexity remains at the same level, but the real situation remains to be studied. In this study, we proposed that using multi-scale entropy (MSE) to detect whether the brain operates in a time-invariant complex system, or the complex oscillations are regulated by task. To achieve this goal, we investigated the alternation of MSE before, during and after the finger-tapping task to understand the modulation of task engagement.

Methods: We recruited 5 healthy participants and measured their BOLD oscillations in 4 sessions by 3T Trio system. We

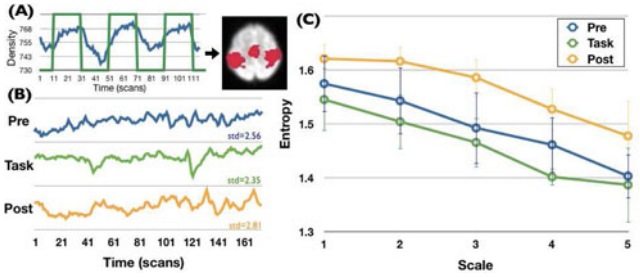

asked participants keep performing finger tapping for 6 minutes (Task) and applied 6-min resting state measurement before (Pre) and after (Post) the continuous task session. Additional block-designed motor task was used to define task-relative regions (Fig. A). Time-courses from the motor network were extracted for MSE calculation based on sample entropy algorithm in *Pre*, *Task* and *Post* sessions. MSE calculation from fMRI signals using parameters of pattern length m of 1, similarity factor r = 0.35 and scale factor 1 to 5, according to Yang's previous study.

Results: The raw time courses and entropy curves of motor region in *Pre*, *Task* and *Post* are showed in Fig. B and C. Compared with *Pre* and *Post* sessions, the entropy curves in *Task* had lowest level of complexity. After the motor task, the complexity dramatically enhanced, exceeding the *Pre* state ($p < 0.05$).

Conclusions: Our findings indicated that while task engaging, brain regions showed low complexity (more regularity), but the complexity is greatly enhanced after task. The complexity level could be an indication of fatigue effect or restorative function. In short, we found that MSE is sensitive to manipulations of cognitive or physiological conditions, with potential to be the diagnostic index for the resting-state fMRI signals.

P28B Multifaceted characterization of functional gradients in the intrinsic brain

T. Xu[1,2,3], A. Opitz[1,3], C. Craddock[1,3], X.N. Zuo[2], M. Milham[1,3]

[1]Nathan Kline Institute for Psychiatric Research (NKI), Orangeburg, NY, USA, [2]Institute of Psychology, Chinese Academic of Sciences, China, [3]Child Mind Institute, New York, NY, USA

Background: Recent R-fMRI studies have proposed that borders between functional brain areas occur at transitions between whole brain functional connectivity patterns. Here, we evaluate the utility of a broad array of local and global measures of R-fMRI for revealing functional gradients and assessing their test-retest reliability. In particular, we will focus on: fractional amplitude of low frequency fluctuation (fALFF), regional homogeneity (ReHo) or local functional homogeneity, degree centrality (DC), eigenvector centrality (EC) and maps of the spatial similarity of whole brain connectivity.

Methods: We made use of the public Nathan Kline Institute-Rockland Sample test-retest R-fMRI dataset (n = 22, 19–60 years old). Two scans, TR = 2500 ms (5 min) and TR = 645 ms (10 min), were acquired for each participant in each of two sessions that were at least a week apart. Data were preprocessed using the Connectome Computation System (CCS: Zuo et al., 2013). We computed the vertex-wise fALFF, ReHo, DC, EC, and spatial similarity of connectivity. Putative functional boundaries were identified by calculating the spatial gradient at each vertex. The magnitude of the gradient represents the speed of transition from each vertex to its 6 neighbors. A linear mixed model was applied to

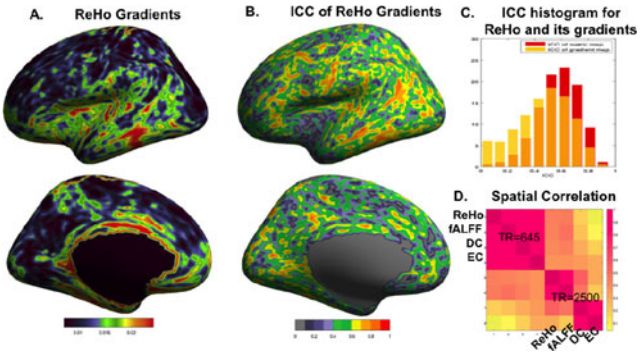

the gradient maps to estimate intra-class correlation (ICC) and hence test-retest reliability.

Results: The ICC distributions for the gradient maps tended to be lower than for the derivatives themselves. Nonetheless, they appeared to contain distinct information, and maximum ICC values approached 0.95 (median: 0.48) for various gradients with the 645 scan and 0.90 (median: 0.34) for the 2500 (Figure C). For the 2500 ms sequence, local (fALFF, ReHo) and global (DC, EC) measures differed though less ($r = 0.21–0.88$) so for the 645 sequence ($r = 0.89–0.97$). Differences in sequences are likely more reflective of the longer sampling duration and higher sampling rate (Figure D).

Conclusions: The present work suggests the value of a variety of metrics for defining functional gradients from intrinsic brain activity. A subset of the gradients defined for each of the measures exhibited moderate to high test-retest reliability and the location of these gradients varied across measures. This suggests that the observed reliability is not solely a function of large structural features (i.e. sulci) and that many different measures are necessary for mapping functional transition zones. Future work will focus on optimizing gradient definition approaches based on reliability and their application to examinations of brain-behavior relationships.

P29B Neuropsychiatric biomarkers hidden in global signal: focus on schizophrenia and bipolar illness

G.J. Yang[1], J.D. Murray[2], G. Repovs[3], M.W. Cole[4], A. Savic[1,5], M.F. Glasser[6], C. Pittenger[1], J.H. Krystal[1], X-J. Wang[2], G.D. Pearlson[1], D.C. Glahn[1], A. Anticevic[1]

[1]Yale University, New Haven, CT, U.S.A., [2]New York University, New York, NY, U.S.A., [3]University of Ljubljana, Ljubljana, Slovenia, [4]Rutgers University, Newark, NJ, U.S.A., [5]University of Zagreb, Zagreb, Croatia, [6]Washington University in St. Louis, MO, U.S.A.

Background: Schizophrenia patients (SCZ) show widespread dysconnectivity observed via neuroimaging. We hypothesized that abnormal cortical computations in SCZ may produce measurable changes in the averaged time course over all brain voxels (global signal, GS) obtained through resting-state fMRI (rs-fMRI). We therefore obtained rs-fMRI of SCZ and matched healthy comparison subjects (HCS), as well as data from a sample of patients diagnosed with bipolar disorder to determine diagnostic specificity of our results.

Methods: Power and variance analyses were conducted on cortical gray matter (CGm) BOLD signal from rs-fMRI studies of two independent SCZ groups ($N = 90$ & $N = 71$) and one group of bipolar patients ($N = 73$), along with matched HCS ($N = 220$), with and without GS regression (GSR). Whole brain voxel-wise variance and restricted global brain connectivity (rGBC) analyses of prefrontal cortex were performed with and without GSR. A validated computational model of resting state BOLD activity was adapted to inform empirical findings.

Results: SCZ CGm was significantly increased ($p < 0.01$) in power and variance compared to HCS; effects correlated with symptom severity. Between-group power/variance differences were reduced ($p < 0.03$) by GSR. GSR significantly altered between-group inferences for SCZ in rGBC analyses. SCZ showed increased local voxel-wise variance independent of GSR. Modeling simulations reproduced increases in local and GS variance as a function of varying synaptic parameters: recurrent local coupling (w) and/or global coupling (G). Findings for SCZ were absent in bipolar patients.

Conclusions: The abnormally increased variance in SCZ cortical signal and the GSR-mediated attenuation of this increase indicates increased variance in the GS component of the signal, a finding specific to SCZ. GSR also impacted group comparisons in data-driven analyses in complex ways. Reproduction of empirical findings *in silico* establishes groundwork for potential pharmacological interventions impacting model-derived synaptic parameters.

P30B Detecting differences between eyes closed and open resting-states using ASL and BOLD fMRI

Qihong Zou[1,2], Binke Yuan[3,4], Hong Gu[2], Dongqiang Liu[3,4], Danny JJ Wang[5], Jia-Hong Gao[1,6], Yihong Yang[2], Yu-Feng Zang[3,4]

[1]MRI Research Center and Beijing City Key Lab for Medical Physics and Engineering, Peking University, Beijing, China; [2]Neuroimaging Research Branch, National Institute on Drug Abuse, National Institutes of Health, Baltimore, MD, USA [3]Center for Cognition and Brain Disorders, Affiliated Hospital, Hangzhou Normal University, Hangzhou, Zhejiang, China; [4]Zhejiang Key Laboratory for Research in Assessment of Cognitive Impairments, Hangzhou, Zhejiang, China; [5]Department of Neurology, University of California, Los Angeles, CA, USA; [6]McGovern Institute for Brain Research, Peking University, Beijing, China

Background and purpose: Recent resting-state functional MRI studies have been increasingly focused on multi-contrast techniques, such as BOLD and ASL fMRI. However, little is known about the similarity of results from the two techniques. Eyes closed (EC) and eyes open (EO) are two physiological resting-states with different levels of brain activity. Here we aimed to investigate whether and how BOLD and ASL could differentiate between EC and EO and whether those findings would be reliable between research centers.

Methods: Forty-eight healthy subjects participated at National Institute on Drug Abuse (NIDA), NIH, while thirty-four healthy subjects participated at Hangzhou Normal University (HNU). NIDA data were collected on a 3-T Siemens scanner. A pCASL technique was adopted for static and dynamic CBF measurement. HNU data were acquired using a 3-T GE scanner. The static CBF images were acquired with 3D pCASL sequence. Conventional BOLD data were acquired at both centers. For pCASL data, quantitative CBF-mean maps were generated. For BOLD data, we calculated voxel-wise BOLD-ALFF. Similarly, CBF-ALFF was calculated only for NIDA data. Differences between EC and EO were obtained by paired *t*-tests.

Results: Using NIDA data, BOLD-ALFF was significantly higher under EC than EO in the primary somatosensory cortices,

primary auditory cortices, and supplementary motor areas, while lower under EC than EO in the occipital cortex. CBF-mean in the primary visual cortex was lower under EC than EO, while CBF-ALFF was higher in the bilateral primary auditory cortices under EC. The two sets of brain regions that detected by CBF-mean and BOLD-ALFF overlapped at the PVC with only 29 voxels, while the regions detected by CBF-ALFF were generally a subset of those detected by BOLD-ALFF. Using HNU data, similar state differences were observed. Both NIDA and HNU datasets consistently showed higher CBF-mean under EO than EC in the primary visual cortex and overlapped BOLD-ALFF differences in the primary somatosensory cortices, primary auditory cortices, supplementary motor areas, and occipital cortex.
Conclusions: Convergent state differences detected by both BOLD and ASL fMRI were located at the visual cortex with only a small volume. The convergent and divergent state differences from CBF-mean and BOLD-ALFF, which were consistent between the two centers, indicate that the two categories of indices detect brain activity from different aspects and suggest combinations of these two techniques in future studies.

Theme 2: Structural Brain Connectivity/Multi-modal Approaches/Animal

P31B Comparing and parcellating voxel-scale multimodal human brain connectivity

C. Baldassano[1], A. Esteva[1], D.M. Beck[2], L. Fei-Fei[1]

[1]Stanford University, Stanford, CA, USA, [2]University of Illinois, Urbana, IL, USA

Background: Advances in neuroimaging techniques now allow us to map functional and anatomical connections throughout the whole brain at high resolution. However, most studies downsample connectivity data into a small number of predefined parcels, preventing analysis of fine-scale connectivity structure and potentially introducing atlas-dependent confounds. Work on building data-driven parcels has relied on greedy clustering algorithms, which can provide only approximate parcellations.
Methods: Using data from the Human Connectome Project, we constructed high-resolution 60,000 by 60,000 connectivity matrices from both resting-state correlations and diffusion tractography, and compared between the two modalities. We explored the underlying structure of these matrices by clustering the cortex into spatially contiguous parcels using a new nonparametric generative clustering model, which is more accurate than previous methods and can select the number of clusters in a data-driven way.
Results: We found that the correlation between functional and tractography measures previously reported for coarse regions extends to the individual voxel scale ($r = 0.25$), but varies depending on cortical location (Fig. 1). We clustered each matrix under our generative model, yielding two related but distinct parcellations (Fig. 2, top). These clusters better capture connectivity structure than those from existing algorithms, explaining $\sim 80\%$ of the variance in the full connectivity matrices with parcel connectivity matrices that are $\sim 100{,}000$ times smaller. Some clusters correspond to existing functionally-defined regions (such as retrosplenial cortex, RSC), while others reveal interesting structural features, such as eccentricity rings in early visual cortex, and connectivity differences within the Parahippocampal Place Area (PPA) (Fig. 2, bottom).
Conclusions: We have shown how whole-brain multimodal connectivity measures are related at the scale of individual voxels, and have developed the most precise connectivity-based parcellation to date. We are currently investigating the use of these parcellations as general-purpose atlases for analyses such as whole-brain decoding.

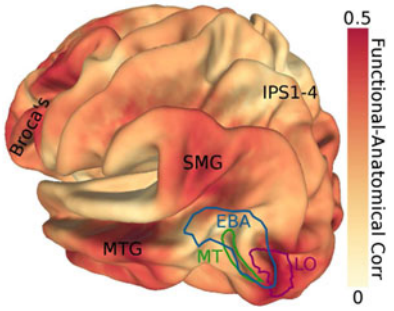

FIG. 1. Functional correlations are well predicted by tractography in areas LO1/2 and language regions including supramarginal gyrus, middle temporal gyrus, and Broca's area, but functional and anatomical measures diverge in visual areas such as the extrastriate body area (EBA), MT, and IPS1-4.

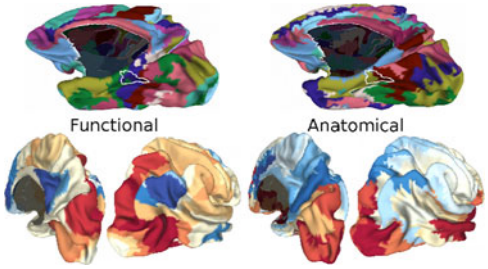

FIG. 2. Functional and anatomical parcellations (top), showing that the PPA spans multiple parcels (white outline). The posterior PPA parcels are more connected to occipital regions (bottom, in red), while the anterior parcels are more connected to medial parietal regions and angular gyrus (in blue).

P32B Temporo-parietal source localisation and functional connections of the N250 emotion-related potential evoked by social and non-social stimuli

J. Athilingam[1], J. Jones-Rounds[2], D.J. Post[3], B.L. Ganzel[2,4], M.K. Belmonte[5]

[1]University of California San Francisco, USA, [2]Cornell University, Ithaca, New York, USA, [3]University of Illinois at Chicago, USA, [4]Binghamton University, Binghamton, New York, USA, [5]The Groden Center, Providence, Rhode Island, USA

Background: Emotion recognition is a crucial component of social interaction that subserves the interpretation and comprehension of another actor's mental state. The temporo-parietal junction, in particular, has been identified as an essential node within brain networks subserving social perspective-taking, at the interface between perceptual and cognitive-affective processes. The current study aimed to factor out the process of emotion recognition from facial encoding by recording event-related potentials during recognition of emotions in both social (face) and non-social (object) stimuli, to localise this emotion-related activity, and to assay its functional connectivity with other loci.
Methods: In 22 normal young adults, event-related potentials were examined for the effect of task set (simple discrimination vs. emotion recognition), stimulus type (face vs. object), and valence (emotional vs. neutral). Stimuli were presented for 1000 ms with a response window of 5000 ms and a 500 ± 50 ms jittered inter-trial interval. EEG was recorded from 128 active electrodes at 512 hz with a bandpass of 0.01 to 200 hz, then digitally re-referenced to the left mastoid and filtered to 0.1 to 100 hz. Gross artefacts were removed using the ADJUST toolbox for EEGLAB and independent component analysis was performed on the entire continuous recording to reject artefactual components. Independent components were extracted from epoched EEG, their dipoles localised and clustered across subjects, and projected to the scalp surface. Relationships between dipole clusters were assayed via a Granger causality measure.
Results: The paradigm evoked N170, N250, P300 and late positive (LPP) potentials. P300 and LPP were augmented by emotional content regardless of stimulus type, suggesting that emotion processing and recognition are indeed processes distinct from facial encoding. The LPP also seemed modulated by attention as its amplitude was greater during the emotion recognition task than during discrimination. The N250, scalp maximal at fronto-central electrode locations, was associated with difficulty of emotion recognition and was generated near the temporo-parietal junction, a major node which receives information from nearby superior temporal N170 generators and occipital visual sources and from lateral prefrontal cortex, and which forwards information on to medial prefrontal cortex.
Conclusions: These results provide the first examination of the neural correlates of emotion processing from non-social stimuli, show that the emotion-related anterior scalp N250 is in fact generated posteriorly near temporo-parietal junction, and outline the functional sources and sinks of emotion-related perceptual and cognitive information.

P33B Pupil diameter relates to time-varying BOLD functional connectivity

A. Breeden[1], M. Norr[1], G. Siegle[2], C.J. Vaidya[1]

[1]Dept. of Psychology, Georgetown University, Washington, DC, USA, [2]Dept. of Psychiatry, University of Pittsburgh School of Medicine, Pittsburgh, PA, USA

Background: A recent advancement in the study of resting state networks (RSNs) is the recognition that their functional connectivity is not static. RSNs' functional connectivity is modulated by cognitive state (Gordon et al., 2014), and can fluctuate across the course of resting state scans (Chang & Glover, 2010). While these fluctuations have the potential to help elucidate the dynamic nature of large-scale brain networks, their source remains unclear. Previous studies using simultaneous resting state fMRI and EEG/physiological measurement have shown that some RSNs' fluctuations in functional connectivity across the resting state may be attributable to vigilance/autonomic nervous system states (Chang et al., 2013a, Chang et al., 2013b). We thus concurrently measured resting state functional connectivity and resting pupil diameter, a measure of arousal that may index the locus-coeruleus norepinephrine (LC-NE) system (Murphy et al., 2014), to determine which, if any, RSNs' functional connectivity would co-vary with arousal.
Methods: Fifteen 18–27 year old adults were scanned at rest for 12 minutes with controlled (low) room and screen luminance. Functional images were acquired on a 3T Siemens Tim Trio and preprocessed and analyzed using SPM8. Volumes were slice time corrected, realigned, coregistered with each participant's structural scan, normalized and spatially smoothed. Each voxel's time series was band-passed filtered to exclude frequencies outside of .01-.1 Hz, and head motion and mean white-matter and CSF signals regressed out. Pupil diameter was recorded at 60 Hz during functional image acquisition with an MRI-integrated infrared camera over the right eye. Pupil data were preprocessed using methods described in (Siegle et al., 2003), including: noise and blink correction by interpolating through time points which displayed a greater than expected rate of change, and convolving pupillary time courses with a hemodynamic response function, and band pass filtering to exclude frequencies outside of .01-.1 Hz. For each participant, sliding window analyses (window size = 35 TRs, 87.5 s) were used to correlate time varying changes in functional connectivity between all nodes of canonical RSNs defined by Power et al., 2011 with fluctuations in pupil diameter. One sample T-tests were run on Z-transformed single-subject data from the aforementioned analyses to find RSNs related to pupil diameter across the entire sample.
Results: Pupil diameter significantly related to functional connectivity strength in several resting state networks. Across time, there were positive associations between pupil diameter ($p < .05$) and functional connectivity in the fronto-parietal control network, the cingulo-opercular network, and the visual network. There were negative associations ($p < .05$) between pupil diameter and functional connectivity in the default mode network and the dorsal-motor network. Of all examined RSNs, the strength of the fronto-parietal control network related most strongly to pupil diameter.
Conclusions: Fluctuations in functional connectivity across the resting state were partially attributable to changes in arousal state indexed by pupil diameter. Given recent evidence that pupil diameter is sensitive to changes in the LC-NE system, this raises the interesting possibility that neuromodulatory changes accompanying different arousal states may relate to dynamic changes in resting state networks, especially attention related networks like the fronto-parietal control and cingulo-opercular networks.

P34B Electrophysiological and behavioral contributions to the resting-state fMRI signal

C. Chang[1], D.A. Leopold[2], M.L. Schölvinck[3], J.H. Duyn[1]

[1]Advanced MRI Section, NIH, Bethesda, MD, USA; [2]Section on Cognitive Neurophysiology and Imaging, NIH, Bethesda, MD, USA; [3]Ernst Strungmann Institute (ESI) for Neuroscience in Cooperation with Max Planck Society, Frankfurt am Main, Germany

Background: Despite the widespread use of resting-state fMRI, the neural basis of spontaneous BOLD signal fluctuations is not fully understood. Here, we investigate the differential contributions of high- and low-frequency local field potential (LFP) power fluctuations to the spontaneous fMRI signal, as well as their relationship to the behavioral state of the animal as assessed by videos of eye opening/closure.

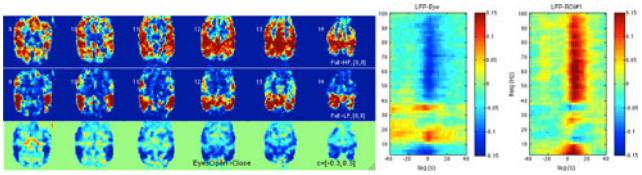

FIG. 1. (Left) Regions of significant low-frequency (top) and high-frequency (middle) LFP contributions to fMRI data, assessed by F-tests. Bottom row shows correlation between fMRI and the eye signal. **FIG. 2 (Right).** Cross-correlation between the LFP power at each frequency with the binary eye open/close signals (left), and with the fMRI signal from an ROI having significant correlations with LFP (right).

Methods: Simultaneous electrophysiological and fMRI data of awake macaques in the resting state were analyzed. LFP was measured from a single site in V1. Regressors for low (3–7.5 Hz; ''LF'') and high (40–80 Hz; ''HF'') frequency bands of the LFP were constructed by computing, within each fMRI TR, the mean power of the LFP signals in these bands. A binary ''eye signal'' indicating whether the eyes were open (=1) or closed (=0) was constructed from the behavioral data. Both LFP and eye regressors were convolved with a standard HRF prior to comparison with fMRI.
Results: Fig. 1 shows the spatial dependence of low- and high-frequency LFP correlations with fMRI, indicating distinct spatial signatures. The eye signal also showed correlations with fMRI (Fig. 1, bottom), overlapping substantially with LFP-fMRI correlations. Yet, the partial R^2 of LFP and eye signals were both significant in accounting for fMRI variance in overlapping regions of Fig. 1 ($p < 1e\text{-}4$), suggesting both joint and unique contributions from eye activity and LFP to resting-state fMRI. Strikingly, the LFP-eye relationship occurred in nearly identical frequency bands as those of LFP-fMRI (Fig. 2).
Conclusions: LFP correlations with fMRI were spatially specific: HF power correlated most strongly within a network of visual cortex regions, while LF was correlated farther away from the recording site, consistent with findings that LF may reflect longer-range cortical processes. Behavioral data suggest that the states of open and closed eyes are also predictive of LFP and fMRI signal changes, contributing to their observed correlation.

P35B Altered hippocampal connectivity in wild sea lions exposed to a naturally occurring neurotoxin: a resting state BOLD analysis

P. Cook[1], L. Libby[2], A. Rouse[3], C. Reichmuth[3], B. Van Bonn[4], C. Ranganath[2], F. Gulland[5]

[1]Center for Neuropolicy, Emory University, Atlanta, GA, USA, [2]University of California Davis, USA, [3]University of California Santa Cruz, [4]Shedd Aquarium, Chicago, IL, USA, [5]The Marine Mammal Center, Sausalito, CA, USA

Background: Each year, hundreds of wild sea lions strand (come to shore in distress) in Central California due to neurological symptoms resulting from exposure to algal neurotoxin domoic acid. Domoic acid is a glutamate agonist with high affinity for AMPA and kainite receptor sites, and has been shown to cause gross damage to the hippocampal formation and a persistent epileptic-like state. We have previously characterized hippocampal damage using structural MRI in this population of wild sea lions, and have identified behavioral impairments tracking with lesion severity. However, no work has been done to explore more subtle, network-level disruptions in these exposed animals. Understanding the neurological and behavioral effects of this toxin is crucial for making informed rehabilitation and conservation decisions regarding affected sea lions. Here we report findings from a resting-state study examining connectivity between hippocampal, subcortical, and cortical seed regions.
Methods: Eleven wild sea lions undergoing rehabilitation were imaged in a 1.5 T Siemens MRI scanner at Animal Scan veterinary imaging center in Redwood City, CA. Four were deterimined to have gross hippocampal lesions, while seven ''control'' animals were judged neurologically normal. Each animal received a structural scan as part of a veterinary work-up, to which we appended a 10 minute ''resting state'' BOLD sequence. All animals were imaged under general anesthesia (isoflurane gas). Given small sample size, whole-brain analysis of group averages was underpowered. We placed anatomically defined seed regions bilaterally in anterior and posterior hippocampus for each animal, and identified four bilateral extra-hippocampal regions that showed relatively high connectivity with the hippocampus at the group level (lateral frontal, medial superior occipital, lateral parietal, and ventral caudate). We then computed correlation coefficients between the hippocampal seeds and between the hippocampal and extra-hippocampal seeds for each animal, and compared coefficients between the animals with hippocampal lesions and the controls using a Mann Wilcoxon rank order test.
Results: Animals with hippocampal lesions from domoic acid exposure showed increased intra-hippocampal connectivity and decreased hippocampal-cortical connectivity in comparison to controls, across nearly all seed comparisons. Hippocampal-caudate connectivity was marginally higher in the animals with hippocampal lesions.
Conclusions: These findings suggest disrupted hippocampal-cortical connectivity and increased intra-hippocampal and hippocampal-subcortical connectivity in wild sea lions with toxic exposure to domoic acid. This is in line with resting state fMRI findings in humans with medial temporal lobe epilepsy, and indicates that behavioral impairment in exposed wild sea lions may be rooted in neurological disruption outside of the hippocampus proper.

P36B Large EEG data analysis for estimating microstates at rest in sensor and source spaces

A. Custo[1], D. Van de Ville[3,4], M.I. Tomescu[1], C.M. Michel[1,2]

[1]Functional Brain Mapping Laboratory, Department of Fundamental Neurosciences, University of Geneva, Geneva, Switzerland, [2]University Hospital, Geneva, Switzerland, [3]Department of Radiology and Medical Informatics, University of Geneva, Switzerland, [4]Institute of Bioengineering, Ecole Polytechnique Fédérale de Lausanne, Lausanne, Switzerland

Background: In recent years the analysis of brain activity at rest has become common practice. What once was considered background noise is now believed to contain useful information in the form of low power oscillatory activity of several areas of the brain in specific spatial patterns.

EEG analysis of brain activity at rest is well suited to study the fast temporal dynamics of the resting state networks, but the low SNR characterizing electrophysiological signal at rest hinders an effective analysis.
Methods: We propose a paradigm to analyze rest EEG in the sensors and source space. The process takes advantage of a large multi-center dataset (62 healthy subjects recorded, 48 with EEG and 14 with EEG-fMRI) and uses a new method for microstates group analysis combining k-means clustering and cross

validation optimal criterion. For the source-space analysis we use a new method (TESS) developed especially to compute the sources of low-SNR spontaneous EEG.
Conclusions: Through a better understanding of the coupling between the rest microstates and their generators we will be able to integrate the insight offered by the numerous fMRI RSN studies and thus have a more complete picture of the dynamic activity of the brain at rest.

P37B The Influence of Participant and Task Characteristics on the Relation between Functional and Structural Connectivity

Jaclyn H. Ford[1], Elizabeth A. Kensinger[1]

[1]*Boston College, Chestnut Hill, Massachusetts, USA*

Background: Over the last decade, researchers have become increasingly interested in understanding both the structural networks representing white matter integrity of neural tracts and functional networks reflecting the ability of multiple brain regions to interact with one another. Although structural changes and functional connectivity changes have often been measured independently, examining the relation between these two measures is critical to understanding the specific function of neural connections and the ways in which such functions may differ across tasks and individuals. Recent studies suggest that there is not a direct one-to-one mapping between structural and functional connectivity, perhaps reflecting the ability for cognitive goals to moderate activity levels along paths involving more than one node. We have recently demonstrated that healthy aging influences this relation, and that this influence exists during retrieval of positive event retrieval only (Ford & Kensinger, *in press*, *Frontiers in Human Neuroscience*), however it is unclear which cognitive or emotional mechanisms may underlie this interaction. The current analysis examines the effect of these relations on memory performance (i.e., accuracy and retrieval time) and responses to emotional stimuli (i.e., ratings of emotional valence and arousal). We also investigate the role of individual differences in cognitive ability (via standardized test scores) on these interactions in older adults.
Methods: The current study examined the effect of aging (treated as a continuous variable) on functional connectivity during retrieval of emotional information and structural integrity (measured using fractional anisotropy, FA). As prior studies have suggested that prefrontal regions may guide emotional memory and regulate emotions via functional connections with the amygdala, the current analysis focused on functional and structural connectivity between the left ventral prefrontal cortex and amygdala. Prior to scanning, participants encoded positive, negative, and neutral images paired with neutral titles. After a thirty-minute delay, while undergoing fMRI, participants viewed the neutral titles and indicated whether the title had been presented with an image during study.
Results: Aging was associated with a significant increase in the relation between measures of structural integrity (FA) along the uncinate fasciculus and functional connectivity between the left ventral prefrontal cortex and amygdala. Preliminary results highlight a significant age-by-FA interaction in arousal ratings, such that increased structural integrity was associated with decreased negative arousal ratings in older adults, but increased ratings in young adults. Interestingly, there was also a significant age-by-FA interaction in standardized tests of long-term memory, such that increased structural integrity was associated with improved memory performance in young adults only.
Conclusions: These findings provide initial evidence that both cognitive and emotional changes may occur in healthy aging that contribute to altered relations between structural and functional connectivity measures. Specifically, this interaction may be driven by age related differences in emotion regulation, a finding that is consistent with theories that older adults may utilize structural pathways differently than young adults to satisfy shifting goals and motivations. Alternatively, this interaction may reflect an age-related decrease in the ability to utilize this pathway to enhance memory performance.

P38B 'Resting-state' Functional Connectivity Networks with Underlying Structural White Matter Tracts in the Healthy Elderly

M. Gorges[1], H.-P. Müller[1], V. Rasche[2], A.C. Ludolph[1], J. Kassubek[1]

[1]*Department of Neurology, University of Ulm, Ulm, Germany,* [2]*Experimental Cardio-vascular Imaging, Core Facility Small Animal MRI, University of Ulm, Ulm, Germany*

Background: Functional connectivity magnetic resonance imaging (fcMRI) has emerged as an investigation tool for mapping intrinsic connectivity networks (ICNs). Anatomical connections as assessable by diffusion tensor imaging (DTI) form one structural groundwork for the identified ICNs. This study aimed at the analysis of well-defined ICNs at single subject and at group level in the healthy elderly brain together with the complementary structural anatomy.
Methods: Twelve healthy subjects (68 ± 7 years) underwent fcMRI and DTI investigations at a 3T scanner (with fcMRI parameters 200 vol., 36 slices, 64×64 pixels, slice thickness 3.5 mm, pixel size 3.5 mm × 3.5 mm, TR = 2.2 s, TE = 30 ms and DTI GD = 31, 72 slices, 128×128 pixels, slice thickness 2 mm, pixel size 2.0 mm × 2.0 mm, TR = 12.7 s, TE = 95 ms, b = 1000 s/mm^2, respectively). The data were analyzed using the *Tensor Imaging and Fiber Tracking* (TIFT) software package. The utilized algorithm for fcMRI data processing comprised: 1) quality control, 2) resampling on a cubic 1 mm grid, 3) stereotaxic MNI normalization, 4) spatial Gaussian filter (7 mm FWHM), 5) temporal linear detrending and temporal bandpass filtering (0.01–0.08 Hz), 6) seed-based correlation by using a single-voxel as seed, 7) Fisher's r- to z-transformation, and 8) arithmetically averaging in order to obtain the final ICNs. DTI was analyzed according to previously published methods and streamline fiber tracking was performed on averaged DTI data sets.
Results: Our findings demonstrated robust ICNs in the healthy elderly at the single subject and at the group level together with the complementary fiber tractography. The following ten ICNs and structural connectivity maps were identified: the default mode network and the cingulum bundle, the left and right frontoparietal control ICNs and the inferior longitudinal fasciculus, the motor ICN and the corticospinal tracts, the visuospatial ICN and the optic radiation, the dorsal attention system and callosal radiations (segment II), the ventral attention ICN and callosal radiations (segment I), the basal ganglia thalamic ICN and thalamic radiation, the brainstem ICN and the corticopontine pathway, and the cerebellar ICN and the superior cerebellar peduncle.
Conclusions: With the complementary analysis approach of iFC and DTI in a single software environment (TIFT), it was shown that comprehensive analyses between functional network mapping and structural network mapping could be performed. This study on brain connectivity in healthy elderly subjects demonstrated a methodological framework for future investigations aiming at contrasting pathological (neurodegenerative) conditions with healthy controls on the basis of multiparametric brain connectivity mapping.

P39B EEG correlates of cognition during the resting state

R. Hardstone[1], B.A. Diaz[1], S.-S. Poil[1], H.D. Mansvelder[1], K. Linkenkaer-Hansen[1]

[1]*Department of Integrative Neurophysiology, Center for Neurogenomics and Cognitive Research (CNCR), Neuroscience Campus Amsterdam (NCA), VU University Amsterdam, Amsterdam, Netherlands*

Background: The human brain generates complex patterns of activity and cognition during wakeful rest, yet their relationship remains elusive. Despite great advances in characterizing resting-state neurophysiology, linking (electro)physiology to the rich inner experiences during the resting-state has received scant attention. To assess such experiences, we developed the Amsterdam Resting-State Questionnaire (ARSQ) of 54 items for rating feelings and thoughts experienced during wakeful rest. Using factor analysis, the ARSQ can be reduced to ten factors of resting-state cognition (Discontinuity of Mind, Theory of Mind, Self, Planning, Sleepiness, Comfort, and Somatic Awareness, Health Concern, Visual Thought, Verbal Thought). Here, we investigate relationships between cognition and brain activity during the resting state using the ARSQ and electroencephalography (EEG).
Methods: We recorded >111 subjects using 128-channel EEG during a five minutes eyes-closed rest session. The ARSQ was used to explore cognitive content of the participants directly after the session. EEG data were analyzed using the Neurophysiological Biomarker Toolbox (NBT, http://www.nbtwiki.net/), which is dedicated to the computation of a wide range of classical and novel biomarkers, and correlated these with the average factor sum scores derived from the ARSQ data.
Results: We found significant ($p < .05$) negative correlations between alpha power [8–13 Hz] in fronto-parietal regions and the factor ''Self'' as well as significant positive correlations between normalized central delta-amplitude [1–4 Hz] and the factor ''Sleepiness''.
Conclusions: Our results show that the ARSQ could prove useful for shedding light on functional implications of genetic or disease related variation by successfully combining electrophysiological and cognitive measures. Future analyses with novel EEG-biomarkers and measures of functional connectivity may reveal an even more detailed view on the link between electrophysiology and cognition.

P40B Reproducibility of Resting-State fMRI Data in Rats across Three Months

Li-Ming Hsu[1], Jennifer A. Stark[1], Julia K. Brynildsen[1], Hong Gu[1], Hanbing Lu[1], Elliot A. Stein[1], and Yihong Yang[1]

[1]*Neuroimaging Research Branch, National Institute on Drug Abuse, Baltimore, Maryland, United States*

Background: There has been growing interest in resting-state fMRI (rs-fMRI) using animal models, following the demonstration of intrinsic brain activities in non-human primates and rodents [1, 2]. Since most animal fMRI scans are performed under anesthesia, individual differences in delivery of and responding to the anesthetics may lead to relatively large variations in physiology across animals and/or sessions. While the reproducibility of rs-fMRI measures in humans has been investigated extensively [3–5], its characteristics in animals are much less known. In this study, we investigate the reliability of rs-fMRI signal of rats in short (10 min), middle (2 weeks) and long (3 months) term-scan intervals.
Methods: Sixteen male 275 + 25 grams Spragur-Dawley rats were used. Animals were anesthetized with a combination of 2-0.5% isoflurane and 0.015 mg/kg/hr dexmedetomidine hydrochloride.

All MRI data were acquired using a Bruker Biospin 9.4T scanner. Three sessions were scanned, the second session (S2) and third session (S3) were acquired two weeks and three months later than the first session (S1), respectively. Each session contained the high-resolution anatomical images and two resting-state scans (rs-scan, TR = 1,000 ms), 10 min apart.

Motion correlation, spatial smoothing, detrend and temporally band-pass filtered (0.01 – 0.1 Hz) were used in preprocessing. All rs-scans were included in ICA analysis by MELODIC and dual regression approaching. A one-sample t-test was performed to obtain a robust functional connectivity map ($t > 20$).

We computed three ICCs for each connectivity component to investigate the reproducibility of rs-fMRI signal [6] : 1) the ICC

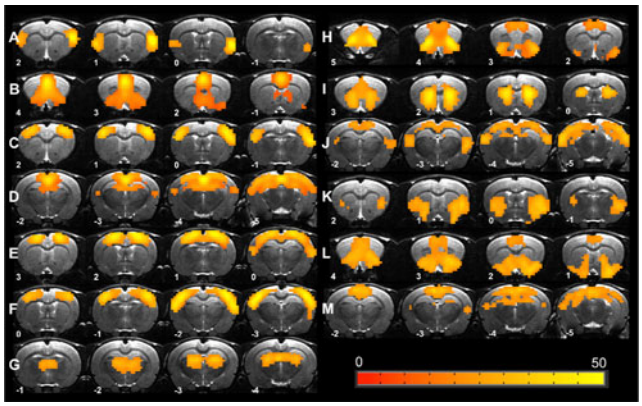

FIG. 1. Functional connectivity maps ($t > 15$) resulting from the group ICA of rs-fMRI data of 16 rats. Component maps, which appear to be anatomically meaningful (13 out of 15), are shown. **A)** Insular cortex (IC), **B)** cingulate and nucleus accumbens, **C)** motor cortex (MC), **D)** restrosplenial/dorsal hippocampal/parietal cortex, **E)** somatosensory cortex (SC), **F)** barrel cortex, **G)** thalamus(Thal), **H)** prelimbic and orbital cortex, **I)** caudate putamen (CPu), **J)** visual and auditory cortex, **K)** ventral lateral striatum, **L)** cingulate/olfactory tubercle(OT), **M)** restrosplenial cortex (RSC). Distance to bregma (in mm) is labeled at the bottom of each slice.

TABLE 1. ICC VALUES ACROSS COMPONENTS. THE MEAN ICC VALUE WAS CALCULATED ACROSS COMPONENTS

	A	*B*	*C*	*D*	*E*	*F*	*G*	*H*	*I*	*J*	*K*	*L*	*M*	*Mean*
ICC_1	0.87	0.70	0.70	0.70	0.47	0.59	0.61	0.66	0.59	0.61	0.64	0.68	0.37	0.63 SD: 0.12
ICC_2	0.58	0.72	0.55	0.62	0.72	0.66	0.40	0.61	0.49	0.44	0.63	0.54	0.44	0.57 SD: 0.11
ICC_3	0.23	−0.06	0.50	0.14	0.46	0.40	0.13	0.11	0.52	0.08	0.29	0.01	0.06	0.22 SD: 0.19

between rs-fMRI scan 1 and 2 (ICC1, 10 min apart); 2) the ICC between S1 and S2 (ICC2, 2 weeks apart); and c) the ICC between S1 and S3 (ICC3, 3 months apart).
Results: The ICC values for each component (Fig. 1) are listed in Table 1, in which ICC1 and ICC2 are generally higher than corresponding ICC3 in each component. The mean ICC across the 13 components also showed a significant decrease in the long-term stability.
Conclusions: Our data suggests that longitudinal experiments within weeks would have good reproducibility, but studies across months should be performed with caution. Reliability of preclinical rs-fMRI data may also depend on anesthesia procedures, requiring additional assessments on various anesthesia protocols for longitudinal preclinical rs-fMRI experiments.
References: 1. Vincent JL, et al. Nature 447:83–86 (2007). 2. Lu H, et al. Proc Natl Acad Sci U S A. 104:18265–18269 (2007). 3. Damoiseaux JS, et al. Proc Natl Acad Sci U S A. 10313848–13853 (2006). 4. Chen S, et al. Brain Res. 1239:141–51 (2008). 5. Zuo XN, et al. Neuroimage. 49:2163–2177 (2010). 6. Shrout PE, et al. Psychol Bull 86:420–428 (1979).
Acknowledgments: This work was supported by the Intramural Research Program of the National Institute on Drug Abuse, National Institutes of Health and FDA Center for Tobacco Products.

P41B Delineation of functional parts of the salience network concerning intrapersonal/extrapersonal aspects of awareness

S. Kinreich[1,3], I. Podlipsky[3], S. Jamshy[4], N. Intrator[4], T. Hendler[1,2,3]

[1]Department of Psychology, Tel Aviv University, Tel Aviv 6997801, Israel. [2]Department of Physiology, Sackler Faculty of Medicine, Tel Aviv University, Tel Aviv 6997801, Israel. [3]Functional Brain Center, Wohl Institute for Advanced Imaging, Tel-Aviv Sourasky Medical Center, Tel-Aviv 6423906, Israel. [4]School of Computer Science, Tel Aviv University, Tel Aviv 6997801, Israel

Background: The insula has been found to be involved in various functions including playing a role in externally oriented attention for the detection of prominent stimuli in order to guide other networks. Additional functions involve regulation of consciousness, functions linked to emotion or the regulation of the body's homeostasis. Yet, the distinct roles of its anterior and posterior parts remain unclear. The aim of the current study was to unveil the neural dynamics between the anterior and posterior parts of the insula as expressed during the mental transition from being fully awake to pre-sleep.
Methods: In order to induce the mental shift in a controlled manner, we employed a well-established relaxation protocol of EEG neurofeedback (NF) of the theta /alpha ratio. The time at which theta becomes greater than alpha has been named the theta/alpha ''crossover'' and has been assumed to mark the transition into deep relaxation/pre-sleep. We used this temporal electrophysiological marker along with heart rate parasympathetic indexing to identify successful sessions of transitioning into pre-sleep during the EEG-NF procedure. In addition, we applied simultaneous fMRI to identify the neural underpinnings of this shift in the mental state.
Results: The whole brain fMRI analysis was based on a contrast of successful versus unsuccessful pre-sleep sessions. We emphasize that the analysis was employed for distinct periods of pre- or post-crossover points and separately for alpha and theta modulation during the relaxation training. This analysis was followed by a regional estimate of activity and variance.
Conclusions: Our findings suggest that to initiate the mental transition into pre-sleep, it is critical to reduce activation in areas known to be involved in directing outward awareness and gating sensation (e.g. medial thalamus). In contrast, for sustainment of the pre-sleep state, opposite activation of anterior versus posterior salience networks was necessary. This opposition possibly represents the shifting from extra (anterior insula reducing activity) to intrapersonal (posterior insula increasing variance) neural processing, respectively. Revealing the underlying insula' dynamics of the transition from full awake towards falling asleep might serve brain-targeted diagnostics and therapeutic treatment for sleep disorders.

P42B Resting-state ECoG networks persist during loss of consciousness while losing their spectral signature

X. Liu[1], T. Yanagawa[2], D.A. Leopold[3], N. Fujii[2], J.H. Duyn[1]

[1]Advanced MRI, LFMI, NINDS, NIH, USA; [2]Laboratory for Adaptive Intelligence, BSI, RIKEN, Japan; [3]Laboratory of Neuropsychology, NIMH, NIH, USA

Background: Although the regional correlations between resting-state fMRI signals have been widely used for charting brain networks, their neural basis and functional role remain elusive. One intriguing issue is the general robustness of fMRI derived networks over a range of behavioral conditions, including those of reduced consciousness, which generally are characterized by distinct spectral changes of the electrophysiological activity. To investigate this, we analyzed a unique set of electrocortocography (ECoG) data recorded from nearly entire hemispheres of macaque monkeys under various conscious conditions.
Methods: ECoG signals were recorded from 4 macaques (Fig 1a) during eyes-closed wakefulness, sleep, ketamine/medetomidine anesthesia, and propofol anesthesia. The inter-electrode cross-correlation matrix was calculated based on either broadband power ($1 \sim 100$ Hz) or band-limited power (BLP) at various frequency bands (i.e., δ, θ, α, β, γ), after removal of the global signal. K-means clustering was applied to classify electrodes into multiple groups based on the similarity of their correlation profiles (the matrix's rows/columns), and the pattern of ECoG networks was extracted from the correlation profile

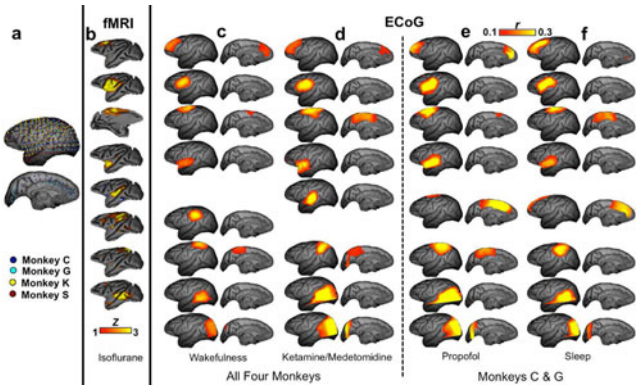

FIG. 1. A comparison between the fMRI-derived RSNs and covariation patterns of ECoG broadband power under four onditions.

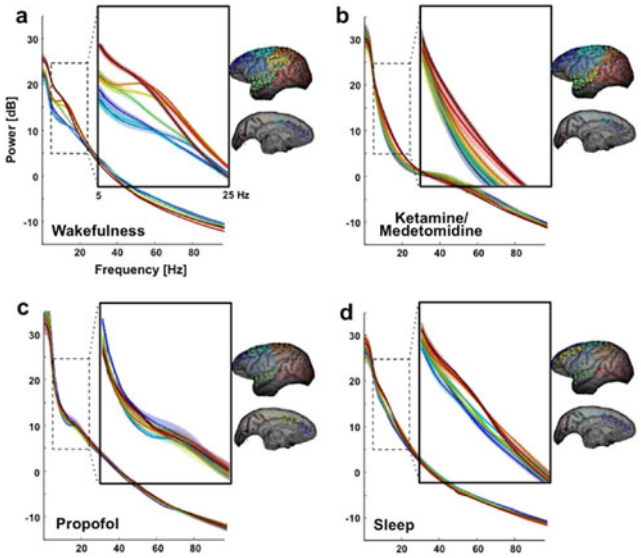

FIG. 2. Power spectra of the ECoG-derived networks under four conditions.

averaged within groups. Power spectra of the raw signals were also calculated for each electrode and then averaged according to network divisions.

Results: We found 8 distinct networks based on the correlations of ECoG broadband power. Their spatial patterns are strikingly similar to 8 of 11 fMRI RSNs of macaques reported previously (Fig. 1b). Despite significant changes in raw ECoG signals, these network patterns were largely preserved under the ketamine anesthesia, propofol anesthesia, and sleep (Fig. 1d-f). Analysis of the individual BLPs les to very similar results. Nevertheless, spectral averages within each network showed distinct differences, most notable in the α-β frequency range (Fig 2a). Interestingly, this spectral distinction vanished under all conditions of reduced consciousness, during which the entire cortex presented a uniform, state-specific spectrum (Fig 2b-d).

Conclusions: Resting-state fMRI networks reflect region-specific correlations in broadband power of electrophysiological signals. Despite the loss of spectral distinction between the networks with loss of consciousness, their spatial distinction persists. The results suggest that fMRI network distinction results from broadband neuro-electrical activity, rather than specific oscillatory processes with distinct spectral fingerprints.

P43B Insight into functional brain connectivity remodeling in mu-opioid receptor knock-out mice

A.E. Mechling[1,2], T. Arefin[1,3], H.-L. Lee[1], M. Reisert[1], J. Hennig[1], D. von Elverfeldt[1], B. Kieffer[4], L.-A. Harsan[1]

[1]Medical Physics, Dep. of Radiology, University Medical Center Freiburg, Germany, [2]Faculty of Biology, University of Freiburg, Germany, [3]Bernstein Center, University of Freiburg, Germany, [4]Douglas Institute, Montreal (Quebec), Canada/IGBMC, Illkirch, France

Background: In humans, the functional brain networks and their alterations in pathologies are intensively studied. However, the intrinsic connectional architecture of these networks in the mouse brain remains a significantly underexplored research area. The goal of the present study was to bridge this gap by adapting the rsfMRI techniques for studying the functional connectivity (FC) pattern in mu-opioid receptor (MOR) knock-out mice (Oprm1−/−), an extensively used model of drug addiction and reward [1].

Methods: Mouse brain resting-state fMRI was performed with a 7T small bore animal scanner (Biospec 70/20, Bruker, Germany) and a mouse head adapted cryogenic surface coil. Data was acquired from 12 weeks old wild type (n = 14) and Oprm1−/− (n = 14 [2]) male mice using single shot GE-EPI (TE/TR = 10 ms/1700 ms, 12 slices à 0.7 mm, 200 volumes) sedated with medetomidine. After preprocessing including motion correction, normalization/coregistration and smoothing (SPM8), spatial Group Independent Component Analysis (ICA) allowed for identification of elementary functional clusters of the Oprm1−/− mouse brain. Their connectional relationship was further tested with partial correlation and Graph theory providing a comprehensive picture of Oprm1−/− brain FC.

Results: An identical number of stable modules (n = 6) was revealed in Oprm1−/− and respective wild type (WT) animals by combined ICA, partial correlation and Graph Theory [3, 4]. Brains of mice genetically lacking Oprm1 revealed conserved topological features of small-worldness (high level of functional segregation along with effective integration of regions at the same time). Nevertheless, the evaluation of the connectional relationship of functional brain nodes shows a decreased ability of the Oprm1−/− brain to form strong inter-nodal associations. The average connectional strength as a measure of FC appears to be 31.7% lower than the strength assigned for the control brain nodes. Moreover, important areas of the limbic system, whose key role in reward processes has long been established, show strongly altered connectivity strength in mutant mice, eg hippocampus, amygdala or entorhinal cortex FC was significantly decreased in Oprm1−/− compared to WT mice. Additionally, habenula which raises increasing interest in the field of motivated behaviors and represents the densest site of MOR expression displays remarkably lower importance in mutant mice.

Conclusions: Genetic MOR inactivation induces alterations in mouse brain connectivity patterns involving modifications in the functional importance of specific brain areas. Remodeling features were shown by the identification of Oprm1−/− specific hub regions, demonstrating the importance of reward system pathways. This study on innate MOR deprived brain highlights a developmental process of FC remodeling, highlighting the possible role of MOR in psychiatric disorders involving reward and addiction.

References: [1] Le Merrer et al. (2009), Physiol Rev 89: 1379–1412, [2] Matthes et al. (1996) Nature 383(6603):819–23, [3] Hyvärinen et al. (2000), Neural Netw. 13(4–5):411–30, [4] Rubinov and Sporns (2010), Neuroimage 52(3):1059–69.

P44B The Anatomic Embedding of the Structural Connectome in the White Matter of the Human Brain

Julia P. Owen, Yishin Chang, Pratik Mukherjee

Department of Radiology and Biomedical Imaging, UCSF, San Francisco, CA, USA

Background: The edges of the structural connectome represent geometric trajectories through white matter (WM), but this anatomic embedding has been largely overlooked. Examining the physical embedding of edges is important, since many WM

diseases extend across anatomic boundaries other than only along particular edges. In this work, we use diffusion tractography to extract the direct WM pathway of each edge of the structural connectome. We define a new voxel-level metric, ''edge density'', as the sum of connectome edges that pass through a voxel. In the limit of a voxel-level parcellation of the gray-white interface for connectome reconstruction, this metric converges to the track density of Track Density Imaging.
Methods: We performed diffusion tractography between 82 cortical and subcortical regions, as defined by FreeSurfer. For every WM voxel, we measured the edge density (ED): the number of edges that pass through that voxel. With test-retest diffusion data from 10 healthy control subjects (five male, five female; mean age 26.7 ± 5.9 years; nine right-handed) with an average of 30.4 ± 2.7 days between scans, we are able to assess the reproducibility of mean ED in 27 supratentorial white matter regions of interest (ROIs) using intra-class correlation coefficient (ICC) and coefficient of variation (CV). We also decomposed ED into components representing specific connectomic criteria, e.g. edges connecting hubs or rich clubs. We explored the additional information added by incorporating edge weights into the ED calculation, using a degree-weighting and an edge-centrality weighting, and compare ED to fractional anisotropy (FA). In order to test the independence from the FreeSurfer atlas, we also computed mean ED using the Automatic Anatomic Labeling (AAL) atlas and the Harvard-Oxford (HO) cortical and subcortical atlas.
Results: We find variation in mean ED in the 27 white matter tracts showing that there are certain white matter pathways that contribute more to the connectome than others. This variation is greater than the mean FA variation. Most striking is that posterior tracts tend to have higher mean ED than anterior tracts. The ICC and CV values indicate that the tract mean ED is a reliable measure. The edges that connect to hubs are not evenly distributed across tracts; the superior fronto-occipital fasciculus, posterior limb of the internal capsule, and the corpus callosum have a high ratio of hub edges to non-hub edges. In contrast, the rich-club connections (connecting rich-club nodes) are fairly evenly distributed across tracts. Using the degree-weighting does not provide additional information to the mean ED measurements, but adding a edge-centrality weighting does diverge from the mean ED values. Lastly, we do not find a significant difference in tract ED when using the AAL or HO atlases.
Conclusions: This anatomic perspective on the connectome is complementary to the existing literature and could become a useful method to assess the effects of neuropsychiatric disorders, as well as the brain after injury or in the malformed brain.

P45B Local Activity Determines Functional Connectivity in the Resting Human Brain: A Simultaneous FDG-PET/fMRI Study

Valentin Riedl[1,2,4], Christian Sorg[1,3,4], Alexander Drzezga[5]

Departments of [1]Neuroradiology, [2]Nuclear Medicine, and [3]Psychiatry, and [4]Technische Universitaet Muenchen-Neuroimaging Center, Klinikum Rechts der Isar der Technischen Universitaet Muenchen, 81675 Muenchen, Germany, [5]Department of Nuclear Medicine, Uniklinik Koeln, 50937 Koeln, Germany

(The Journal of Neuroscience, April 30th, 2014)

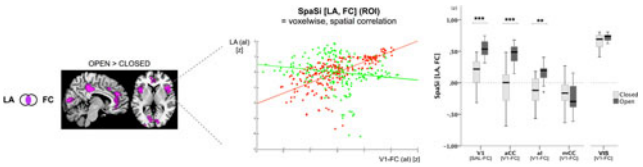

Background: Over the last decade, synchronized resting-state fluctuations of blood oxygenation level-dependent (BOLD) signals between remote brain areas [so-called BOLD resting-state functional connectivity (rs-FC)] have gained enormous relevance in systems and clinical neuroscience. However, the neural underpinnings of rs-FC are still incompletely understood.
Methods: Using simultaneous positron emission tomography/magnetic resonance imaging we here directly investigated the relationship between rs-FC and local neuronal activity in humans. Computational models suggest a mechanistic link between the dynamics of local neuronal activity and the functional coupling among distributed brain regions. Therefore, we hypothesized that the local activity (LA) of a region at rest determines its rs-FC. To test this hypothesis, we simultaneously measured both LA (glucose metabolism) and rs-FC (via synchronized BOLD fluctuations) during condi- tions of eyes closed or eyes open.
Results: During eyes open, LA increased in the visual system, and the salience network (i.e., cingulate and insular cortices) and the pattern of elevated LA coincided almost exactly with the spatial pattern of increased rs-FC (Figure: violet regions). Specifically, the voxelwise regional profile of LA in these areas strongly correlated with the regional pattern of rs-FC among the same regions (e.g., LA in primary visual cortex accounts for $\sim$50%, and LA in anterior cingulate accounts for $\sim$20% of rs-FC with the visual system), Figure: boxplots.
Conclusions: These data provide the first direct evidence in humans that local neuronal activity determines BOLD FC at rest. Beyond its relevance for the neuronal basis of coherent BOLD signal fluctuations, our procedure may translate into clinical research particularly to investigate potentially aberrant links between local dynamics and remote functional coupling in patients with neuropsychiatric disorders.

P46B Apparent dynamic changes in resting-state connectivity in somatosensory cortex

ZY Shi, A Mishra, LM Chen, DM Wilkes, VL Morgan, JC Gore, BP Rogers

Vanderbilt University, TN, USA

Background: Resting-state correlations in BOLD signals appear to vary over time and such dynamic changes may indicate changes in brain states. However, changes in estimated correlation may also arise from statistical sampling variations when using a sliding window correlational analysis. We investigated apparent dynamic changes by simulation of pairwise correlated signals to derive appropriate window sizes, and applied these to examine the behaviors of resting-state data from somatosensory (SI) networks in anesthetized squirrel monkeys at high field (9.4T).
Methods: Simulations: The variations of estimated correlation coefficients between stationary simulated signals (no dynamic variations in correlation) were obtained using the sliding window correlational analysis over a range of window sizes.

Non-human primates: We acquired resting-state data from sub-regions of SI in anesthetized squirrel monkeys and measured the dynamic behavior of functional connectivity between somatosensory cortex sub-regions 3a, 3b, 1 and a control.
Results: Simulations of stationary random signals show that the variance of correlation coefficients goes down as window size

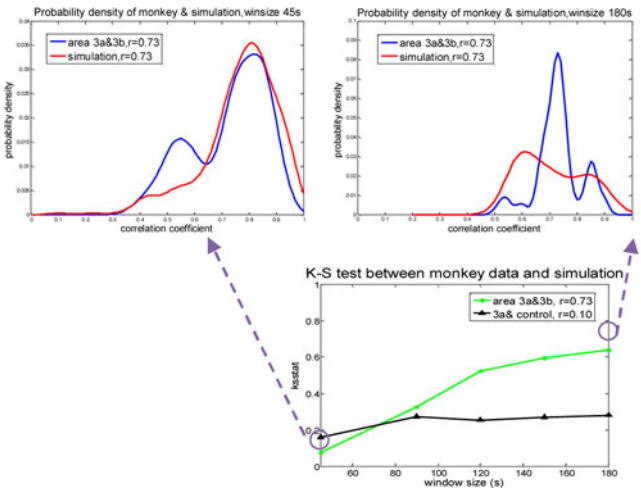

increases as expected; also, the variance decreases for stronger correlation coefficients. The behaviors of the correlation between stationary signals were similar to in vivo monkey data when using smaller window sizes, such as 45 s.

For example, figure 1 shows the probability density functions (pdf) of the cross-correlations between two sub-regions of SI for fMRI data obtained from one monkey, along with the pdf of two stationary simulated signals with the same mean correlation, for window sizes 45 s and 180 s, respectively. For statistical comparison, the Kolmogorov-Smirnov (K-S) test shows that correlations between functionally related regions 3a and 3b in the monkey data are distributed similarly to the correlations derived from simulated stationary data at short window sizes (smaller ks-value indicates less difference), but depart substantially at larger window sizes. The correlations between functionally unrelated regions 3a and control are distributed similarly to the stationary data from the simulation at all window sizes (Fig 2).

Conclusions: Sliding window estimates of variations in correlation between non-stationary signals may reveal dynamic changes but also may be confounded by statistical variations. Whether there are additional features within the real monkey fMRI data that are not present in simulated stationary data remains unclear, but exploration of additional statistical metrics is underway.

P47B Lesion to left hippocampus changes functional connectivity according to changes in structure

R. Siugzdaite[1,3], B. Descamps[2], N. Van Den Berge[3], P. Van Mierlo[3], G. Wu[4], W. Fias[5], R. Raedt[6], D. Marinazzo[1]

[1]Data analysis department, Faculty of Psychology, Ghent University, Ghent, Belgium, [2]Infinity, Ghent University, Ghent, Belgium, [3]MEDISIP, Ghent University, Ghent, Belgium, [4]Key Laboratory for NeuroInformation of Ministry of Education, School of Life Science and Technology, University of Electronic Science and Technology of China, Chengdu, China, [5]Faculty of Psychology, Ghent University, Ghent, Belgium, [6]Laboratory for Clinical and Experimental Neurophysiology, Neurobiology and Neuropsychology, Department of Neurology, Ghent University Hospital, Ghent, Belgium

Background: Resting-state functional connectivity (rsFC) not only reflects structural connectivity in default mode network (Greicius et al 2009), but also allows exploring interactions between remote regions. For this, several recent fMRI studies both in animals and in humans used it as a convenient and non-invasive tool to systematically investigate the connectional architecture of selected brain networks (Zhang et al 2010). The purpose of this study is to trace changes in rsFC after inducing a unilateral hippocampal lesion in rats.

Methods: Male Sprague Dawley rats (n = 20, 250–275 g) were anesthetized (induction 5% isoflurane, s.c. bolus medetomidine (0.05 mg/kg), followed by continuous s.c. infusion medetomidine (0.1 mg/kg/h)) and were inserted into the MR scanner (7T Bruker Pharmascan, Ettlingen, Germany). Anatomical (voxel size $0.156 \times 0.156 \times 0.156$ mm3) and resting state fMRI (voxel size $0.375 \times 0.375 \times 1.1$ mm3) data were acquired. Afterwards, kainic acid (0,4 μg/0,1 μl) was injected into the right hippocampus under isoflurane anesthesia (5% induction, 2% sustenance). This resulted in lesions to ipsilateral or bilateral hippocampus, and other cortexes. Four days and three months after the injection animals were scanned again using the protocol described above.

Results: The rsFC analysis found generally reduced functional connectivity between different areas, ipsilateral but also contralateral to the lesion. It is worth to mention that the connectivity pattern varied across rats based on structural changes due to the lesion.

Conclusions: We conclude that functional networks in resting state are a valuable tool to map brain dynamics when we act on some specific nodes via targeted lesions.

P48B Phase-amplitude coupling indicates independence of infraslow versus high frequency neural electrical activity regarding their relationship to resting state fMRI in rats

G.J. Thompson[1], W.J. Pan[1], J.C.W. Billings[1], J.K. Grooms[1], S. Shakil[2], D. Jaeger[3], S.D. Keilholz[1]

[1]Biomedical Engineering, Emory University and Georgia Institute of Technology, Atlanta, GA, USA, [2]Electrical and Computer Engineering, Georgia Institute of Technology, Atlanta, GA, USA, [3]Biology, Emory University, Atlanta, GA, USA

Background: Fluctuations in the resting state functional magnetic resonance imaging (fMRI) signal have been linked to electrical potential changes in the brain, both band-limited power of high frequency activity (> 1 Hz) but also to local field potentials (LFPs) in infraslow (< 1 Hz) frequencies. One testable hypothesis for the neural basis of resting state fMRI is that power fluctuations in higher frequency neural activity correspond to the phase of the infraslow neural activity, and this relates directly to the infraslow changes seen in resting state fMRI. To test this hypothesis, we used an invasive LFP/fMRI rat model and quantified coupling between infraslow phases and high frequency amplitudes.

Methods: Data were recorded from 10 anesthetized Sprague-Dawley rats under a simultaneous infraslow LFP/fMRI protocol, and from 10 different rats under similar conditions except on the bench without fMRI scanning performed. The anesthesia used was either ~2.0% isoflurane (iso, 8 rats in total) or subcutaneous dexmedetomidine infusion (dex, 11 rats in total) or both in series (1 rat). Infraslow (0–1 Hz) phases from LFP and fMRI were compared to amplitude changes in simultaneously recorded high frequency (1–50 Hz) LFP power. Correlation between fMRI and LFP was also calculated.

Results: The only consistent phase-amplitude coupling was seen under iso and was due to the neural suppression burst condition that existed (Figure 1). No consistent phase-amplitude coupling was seen under dex. In addition, while both infraslow and high frequency power from the LFP correlated with the fMRI, these correlations were statistically independent, indicating that the high and low frequencies had independent relationships with resting state fMRI.

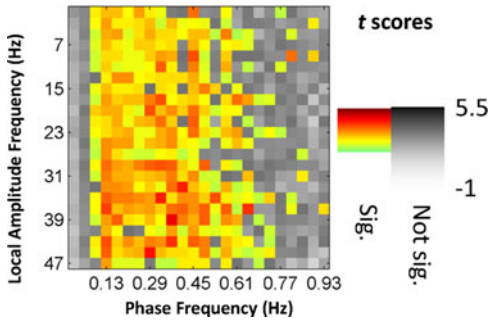

FIG. 1. Comodulogram of coupling between phase at 0–1 Hz (horizontal) and amplitude at 1–50 Hz (vertical) under iso. Hot colors are significant vs. shuffled data. The significant but non-specific coupling seen here is due to iso inducing a ''burst state'' of alternating activity and quiescence in the LFP. Phase-amplitude coupling under dex was either inconsistent or not statistically significant.

Conclusions: While we must be cautious, (as these results are from an animal model and under anesthetic conditions) these results do not support a hypothesis of power changes in high frequency neural activity driving the infraslow phase changes in resting state fMRI. Instead, these results suggest that infraslow and fast frequencies in the underlying neurophysiology may have independent effects on resting state fMRI observations. If this is true, future work may allow the resting state fMRI signal to be separated and additional information extracted from it about multiple underlying neural processes.

P49B Covariance between brain structural and functional metrics

Z. Yang[1], T. Xu[1], J Qiu[2], X-N. Zuo[1,2,3]

[1]Key Laboratory of Behavioral Sciences, Institute of Psychology, Chinese Academy of Sciences, Beijing, China, [2]Department of Psychology, Southwest University, Chongqing, China; [3]Center for Collaboration and Innovation in Brain and Learning Sciences, Beijing Normal University, Beijing, China

Background: Both anatomical structure and intrinsic activity of the human brain are essential sources of inter-individual variability in behaviors and cognitive functions. However, to what extent the variability in intrinsic connectivity networks (ICNs) can be explained by variability of anatomical structure is unclear. In this study, we used two large samples to investigate: (1) which matrices of brain structure and ICNs tend to covary across individuals, so that they comprise a multi-metric co-variance graph? (2) which functional metrics provide unique information that doesn't covary with anatomical metrics?
Methods: Dataset 1 (N = 110) was adopt from the human connectome project, and Dataset 2 (N = 345) was collected from college students from Southwest University, Chongqing, China. High resolution anatomical scans and resting state functional MRI scans were acquired for each subject in both datasets. Six metrics depicting the anatomical structure of the cerebral cortex, including cortical volume, area, thickness, curvature, and local gyrification index (LGI), were computed using Freesurfer. The ICNs were also characterized using six metrics: degree centrality (DC), eigenvector centrality (EC), regional homogeneity (ReHo), regional homogeneity calculated on cortical surface (2dReHo), amplitude of low frequency fluctuation (ALFF), and fractional ALFF (fALFF). These metrics were all projected to the cortical surface space. For Dataset 1, we performed independent component analysis (ICA) for each metric. The resultant component maps represented brain areas that share common variations across subjects. gRAICAR was applied to align the component maps obtained in different metrics according to their mixing matrix (indicating varying trends across subjects). The resultant co-variance graphs linked functional and structural metrics, indicating that, e.g., a brain network revealed by a structural metric has a highly similar cross-subject variation with another brain network shown in an ICN metric. We validated these findings using the Dataset 2 and calculated intraclass correlation coefficient (ICC). This cross-validation ruled out the co-variance graph due to spurious subjects.
Results: We ranked all co-variance graphs according to the ICC value. We found 7 co-variance graphs that had an ICC value above 0.8, but these graphs only linked anatomical metrics. We found 9 co-variance graphs that had an ICC value above 0.7 and linked structural and ICN metrics. We averaged the covariance matrices from 39 co-variance graphs that had an ICC > 0.4 to investigate the general dependency between multiple metrics for brain structure and ICNs. We found that the 6 structural metrics formed a dense cluster. The ALFF, DC, EC, ReHo, 2dReHo formed another cluster, while the fALFF showed the most different inter-individual variability from all other metrics.
Conclusions: We found inter-individual variations in a few ICN metrics can be explained by anatomical metrics in brain regions different from the ICNs. fALFF may carry unique information that are not well-explained by other metrics.

P50B Dissociable salience networks in the macaque brain anchored in right anterior insula

J. Zhang[1], A. Touroutoglou[2], E. Bliss-Moreau[3], D. Mantini[4,5,6], W. Vanduffel[2,4], B.C. Dickerson[2], L.F. Barrett[1,2]

[1]Northeastern University, Boston, MA, [2]Martinos Center for Biomedical Imaging, Massachusetts General Hospital and Harvard Medical School, Charlestown, MA [3]University of California at Davis and California National Primate Research Center, Davis, CA, [4]KU Leuven Medical School, Leuven, Belgium, [5]Oxford University, Oxford, UK, [6]ETH Zurich, Zurich, Switzerland

Background: Salience network (Seeley et al., 2007) is a resting state network that is heavily involved in affective processing and includes major nodes such as amygdala, anterior insula (AI) and anterior cingulate cortex (ACC). Research on the human salience network has demonstrated two separable networks anchored by ventral and dorsal AI (vAI and dAI), respectively implicated in attention and affective experience (Touroutoglou et al., 2012). In monkeys, despite a burgeoning number of resting state studies (Mantini et al., 2013; Belcher et al., 2013; Hutchison et al., 2011), it is still not known whether there is a salience network. We used a hypothesis-driven seed-based approach to investigate whether a salience network exists in the monkey brain and has similar dorsal and ventral extents, which may give us insights into how affect is experienced by monkeys.
Methods: Subjects were 4 rhesus monkeys (*Macaca mulatta*, 1 female, 4–6 kg, 4–7 y.o.) (Mantini et al., 2013). Each subject underwent twenty 10-min resting state scans in a 3T Siemens Trio scanner, during which subjects sat in a sphinx position while continuously fixating a point on a blank screen. Using SPM5, fMRI data were slice time corrected, motion corrected, linearly detrended, coregistered to the anatomical image, spatially normalized to F99 atlas space, and smoothed with a 2 mm fwhm Gaussian kernel. Regions of interest (ROIs) were

generated as 2 mm-radius spheres centered on right frontal insula (FI), vAI and dAI coordinates homologous to the respective human seeds (Seeley et al., 2007; Touroutoglou et al., 2012). At subject level, whole-brain connectivity was calculated for the average time course from each ROI and then converted to z-scores using Fisher's r-to-z transformation; at group level, correlation maps were produced by fixed-effect analysis (Mantini et al., 2011).
Results: Right FI seed reveals a monkey salience network consisting of dorsal ACC, bilateral AI and amygdalae. Right vAI and dAI have distinct connectivity patterns. The vAI seed is preferentially connected to dorsal ACC and pregenual ACC, ventral AI and bilateral amygdalae, closely resembling human vAI network. The dAI seed is preferentially connected to posterior cingulate, dorsal and ventral AI, putamen, and dorsolateral prefrontal cortex, lacking some of the parietal targets in human dAI network.
Conclusions: To our knowledge, this is the first study that clearly demonstrates the existence of salience network in the macaque brain at 3T. Importantly, we identified two distinct networks anchored by vAI and dAI seeds. Furthermore, while the vAI-seeded network closely resembles the human vAI network, the dAI-seeded network exhibits some different characteristics than the human dAI network. Our findings have implications for understanding affective experience in monkeys.

Theme 3: Applications in Neurological and Psychiatric Diseases

P51B Resting state functional connectivity abnormality in neonates at genetic risk for schizophrenia, bipolar, and mood disorders not otherwise specified

S. Alcauter[1], J.H. Gilmore[1], J.K. Smith[1], W. Lin[1], W. Gao[1]

[1]*University of North Carolina, Chapel Hill, NC, USA*

Background: Schizophrenia (SCZ) and different mood disorders, including bipolar disorder (BPD), are neurodevelopmental disorders with shared risk genes and overlapping symptoms[1]. Neuroimaging studies revealed both common and disorder-specific dysconnectivity patterns for these disorders. Reportedly, such abnormal connectivity patterns exist in people at genetic risk for these disorders well before symptom onset[2]. However, whether such genetic-risk-related connectivity abnormalities could be observed at the earliest stage of brain development-infancy, remains unknown. Answers to this question would dramatically improve our understanding of the effect of risk genes on the brain's early functional organization, which is critical for potential early identification of risk factors for future disorder onset. Based on a unique sample including neonates at genetic risk for SCZ, BPD, mood disorders not otherwise specified (MdD), and normal controls, this study aimed to answer this question and further explore whether the altered FC patterns could serve as effective biomarkers to discriminate neonates at different genetic risks.
Methods: Resting state functional MRI data from neonates at genetic risk for SCZ (n = 15), BPD (n = 20), MdD (n = 20) and normal controls (n = 20) was analyzed. Seed-based FC analyses of 17 regions of interest (ROIs) followed by voxel-wise ANOVA were conducted to detect differences among groups. The ROIs included the anterior cingulate, thalamus, amygdala, Wernicke's and Broca's area, anterior/posterior insula, dorsolateral prefrontal cortex (DLPFC), and hippocampus. Linear SVM analyses were subsequently conducted to test the classification power of the detected abnormal FC patterns between different risk groups based on leave-one-out cross-validation. Permutation tests (1000 permutations) were performed to test the significance of classification accuracies.
Results: Significant differences in FC among different neonate groups were detected for most ROIs. The classification test showed high accuracy for discrimination between at-risk neonates and controls (86.7%, $p < 0.001$). Further, high classification power was also observed when discriminating among the high-risk subgroups (SCZ-other at-risk groups: 96.4%, $p < 0.001$; BPD-other: 80%, $p = 0.001$; MdD-other: 90.9%, $p < 0.001$). More specifically, the right DLPFC showed the highest discriminative power between at-risk neonates and controls (80%, $p < 0.001$) while the left Broca's area, left amygdala and right hippocampus showed the highest power to discriminate SCZ, BPD and MdD, respectively, from other at-risk subjects (81.8%, $p < 0.001$ in the three cases).
Conclusions: Abnormal functional connectivity patterns associated with prefrontal, limbic, thalamic and language-related regions were observed, either commonly or uniquely, in neonates at genetic risk for SCZ, BPD, and MdD. Moreover, such abnormal FC patterns provide sensitive biomarkers to discriminate neonates at high-risk for SCZ, BPD, and MdD. These findings shed new light into our understanding of the influence of genetic risks on the earliest brain functional organization.
References: [1]Craddock N. Schizophr Bull 2006. [2]Weinberger DR. Arch Gen Psychiatry 1987.

P52B Between-Network Connections Supporting Attentional Control in Children with ADHD

A.D. Barber[1,2], L.A. Jacobson[1,2], J.L. Wexler[2], M.B. Nebel[1,2], B.S. Caffo[1,2], J.J. Pekar[1,2], S.H. Mostofsky[1,2]

Background: Intra-subject variability (ISV) is the most consistent behavioral deficit in Attention Deficit Hyperactivity Disorder (ADHD). ISV may be associated with networks involved in sustaining task control (cingulo-opercular network: CON) and self-reflective lapses of attention (default mode network: DMN). The current study examined whether connectivity supporting attentional control is atypical in children with ADHD.
Methods: 50 ADHD and 50 typically-developing (TD) children (ages 8–12 years) were matched for age, gender, handedness, socioeconomic status, and two IQ measures. The two groups did not significantly differ in scan motion. All children had a five-minute resting state scan. Preprocessing was performed in SPM8. Physiological noise (identified using CompCor), global signal, and absolute and differential motion were removed from each

voxel. Functional images were spatially-smoothed (6 mm FWHM) and temporally-filtered (bandpass 0.01–0.1 Hz). Behavioral measures (ISV, Tau of the Ex-Gaussian Reaction Time distribution and Omission Error Rate) were obtained from a Go/No-go task performed outside of the scanner. Mean time-courses were extracted and full-brain connectivity maps were created for five CON and three DMN seeds. For each subject, the five CON maps were averaged to make one mean CON map and the three DMN maps were averaged to make one mean DMN map. Second-level t-tests were performed in SPM8 to examine voxel-wise full-brain associations with the behavioral measures for the CON and DMN. Regions with differential brain-behavior associations between the two groups were significant at a voxel-wise level of $p < 0.01$ and a cluster-level of $p < 0.0083$ (i.e. $p < 0.05 / 6$ statistical maps (2 networks * 3 behavioral variables))) according to random field theory.
Results: Full-brain behavioral associations were found for a number of between-network CON-DMN connections. For all CON-DMN connections identified, between-network connectivity was associated with better attentional control for the ADHD group, but worse attentional control in the TD group. This was the case for CON-medial prefrontal cortex associations with ISV, DMN-dorsal medial frontal cortex (dMFC) associations with ISV and DMN-dMFC and DMN-inferior parietal associations with Tau. The opposite relationship was found for a connection between DMN and occipital cortex, a region of the dorsal attention network, and its association with ISV. For that region, greater anti-correlation was associated with better attentional control in TD children, while no association was found for children with ADHD. Follow-up analyses revealed that these associations were specific to attentional control and were not due to individual differences in working memory, IQ, motor control, age, or scan motion.
Conclusions: While CON-DMN anti-correlation is associated with improved attention in ADHD, other circuitry supports improved attention in TD children. Greater CON-DMN anti-correlation supported better attentional control in children with ADHD, but worse attentional control in TD children. On the other hand, greater DMN-occipital anti-correlation supported better attentional control in TD children.

P53B Frontoparietal network connectivity associates with executive functioning deficits in young adults at risk for depression

E.H. Beam[1,2,3], G. Coombs, III[1,2,3], E. Boeke[1,2], S. Crowell[3,4], M. Fava[6], A. Farabaugh[6], D.J. Holt[1,2,5], R.L. Buckner[1,2,3], A.J. Holmes[1,2,7]

[1]Department of Psychiatry, Massachusetts General Hospital, Boston, MA, United States, [2]Athinoula A. Martinos Center for Biomedical Imaging, Charlestown, MA, United States, [3]Department of Psychology, Center for Brain Science, Harvard University, Cambridge, MA, United States, [4]Georgia State University, Atlanta, GA, United States, [5]Department of Psychiatry, Harvard Medical School, Boston, MA, United States, [6]Depression and Clinical Research Program, Massachusetts General Hospital, Boston, MA, United States, [7]Department of Psychology, Yale University, New Haven, CT, United States

Background: The frontoparietal control network is believed to play a crucial role in support of goal-directed planning and adaptive behavioral adjustments to shifting environmental contingencies. In major depressive disorder, disrupted frontoparietal network connectivity associates with task-related impairments in both cognitive and emotional control. Young adults at risk for onset of depressive illness may also show a coupling between executive deficits and disrupted integrity of the frontoparietal network.
Methods: To explore the possibility that frontoparietal network function co-varies with illness risk, we examined the integrity of this circuitry in a sample of 76 participants at increased vulnerability for affective illness onset and 381 demographically matched healthy young adults. Frontoparietal network integrity was explored using resting-state functional connectivity. Assessments of psychopathology and executive impairment were administered to a subset of subjects (at-risk $n = 37$, comparison sample $n = 24$).
Results: After partialing out variance associated with gender, age, IQ, and SNR, young adults vulnerable to depression exhibited a selective disruption in connectivity strength between dorslateral prefrontal (dlPFC), superior frontal (supFC), and inferior parietal (IPL) regions of the frontoparietal control network. On the global network level, connectivity was elevated in the at-risk group compared to controls, while follow-up analyses revealed a right-hemisphere decrease in connectivity among at-risk individuals who had been diagnosed with depression. Subgroups of participants were further evaluated on assessments of executive impairment. Compared to healthy controls, young adults at risk for depression were significantly impaired in executive functions that included shifting and self monitoring. Within the at-risk sample, the level of impairment in shifting and self monitoring predicted a right-hemisphere decline in frontoparietal network connectivity. There was no relationship between frontoparietal connectivity and executive functioning in the comparison sample.
Conclusions: These collective findings suggest that disrupted frontoparietal network connectivity, and associated reductions in executive functions, may contribute to the onset of major depressive disorder.

P54B Predicting the network effects of central pain lesions using resting-state functional connectivity MRI

Aaron D. Boes[1,2], Samar S. Ayache[3,4], Jean-Pascal Lefaucheur[3,4], Alvaro Pascual Leone[2], Michael D. Fox[1,2,5]

[1]Department of Neurology, Massachusetts General Hospital, Harvard Medical School, Boston, MA, USA. [2]Berenson-Allen Center for Noninvasive Brain Stimulation, Division of Cognitive Neurology, Department of Neurology, Harvard Medical School and Beth Israel Deaconess Medical Center, Boston, MA, USA. [3]Université Paris-Est-Créteil, Faculté de Médecine, EA 4391, Créteil, France [4]Assistance Publique, Hôpitaux de Paris, Hôpital Henri Mondor, Service de Physiologie, Explorations Fonctionnelles, Créteil, France. [5]Athinoula A. Martinos Center for Biomedical Imaging, Charlestown, MA, USA

Background: The functional consequences of a focal brain lesion are not solely the manifestation of dysfunction at the site of lesion, but also result from lesion-induced alterations in activity in connected brain regions. Recently we developed a novel method for exploring the neural networks associated with brain lesions, termed lesion-based network analysis. Here, we apply this technique to lesions causing central post-stroke pain and test the hypothesis that these lesions have in common functional connectivity to the pain matrix, including the anterior cingulate cortex and anterior insula.
Methods: We report 8 new cases of central post-stroke pain. Lesions were mapped to a common brain atlas and sites of overlap in the lesion location were identified. Next, the size and shape of the brain lesion from each patient is input into a resting

state functional connectivity analysis from a large cohort of normal healthy subjects. The network of regions correlated with the lesion in the healthy brain serves as a prediction of regions most likely to be altered in the lesioned brain. The resulting networks are then overlaid to identify networks common to multiple lesions.

Results: Central post-stroke pain lesions were widely distributed, with a maximum overlap of three lesions in the posterolateral thalamus. Despite little overlap in the lesions themselves, lesion-based network analysis revealed that 7 of 8 lesions were positively correlated specifically with the anterior cingulate and anterior insula in the hypothesized pain matrix.

Conclusions: Lesion-based network analysis expands the lesion method from a tool looking only at the site of injury to one that also looks at the predicted distributed network effects of the brain lesion. As shown with central post-stroke pain, this method links lesions to clinical symptoms in a way not possible with traditional lesion analysis and is likely to find broad application in elucidating brain-behavior relationships.

P55B Evidence of distinct stages of functional connectivity changes in Alzheimer's disease

M.R. Brier[1], A.Z. Snyder[2], A. Mitra[2], J.C. Morris[1,3], B.M. Ances[1,2,3]

[1]Department of Neurology, [2]Department of Radiology, [3]Knight Alzheimer's Disease Research Center, Washington University in St Louis, St. Louis, MO, USA

Background: Alzheimer's disease (AD) is the most common form of dementia and is characterized by progressive memory loss and cognitive dysfunction. AD pathology is defined by amyloid plaques and tau neurofibrillary tangles. These processes have a complicated but defined progression. However, the exact relationship of AD pathology to neural dysfunction remains unclear. In recent years, functional disruptions have been described in brain regions not affected by frank neuropathology. This has motivated investigation of the topography of neural dysfunction with advancing AD. The current study uses resting-state functional connectivity (rs-fc) and algorithms from the machine learning literature to describe the topography of dysfunction parametric to AD stage. We demonstrate that AD is associated with a distinct and predictive topography but that topography varies across AD stages suggesting distinct stages of neural dysfunction.

Methods: We investigated rs-fc data from 244 participants including healthy older adults, AD patients with mild or moderate cognitive symptoms. These data were divided into two data sets: one set of mild AD patients and age-matched controls and another set of moderate AD patients and age-matched controls. We calculated the correlation in the blood oxygen level dependent (BOLD) signal between 36 brain regions from 7 functional networks and subject these data to principal components analysis (PCA) followed by linear discriminant analysis (LDA). A separate classifier was trained for each data set. We then extracted the feature weights from LDA to investigate the topography of important features at each stage.

Results: Leave-one-out cross validation demonstrated that each classifier performed well (accuracy above 80%), but failed to generalize to the other data set with accuracies indistinguishable from chance. Examination of the LDA feature weights revealed that the classifiers used in each data set used distinct information. For example, the posterior cingulate cortex, and area of intense amyloid deposition early in AD, was highly involved in separating mild AD from controls, but was not as important for distinguishing more advanced disease from controls. Interestingly, the cerebellum was predictive early in the disease but only when considering rs-fc with brain regions outside of its usual network. However, in the later disease stages functional connections to the cerebellum within and between networks were involved in predicting disease presence. Importantly, the cerebellum does not generally exhibit AD-related pathology until much later in the disease than those participants studied here.

Conclusions: We have presented data extracted from PCA-LDA of rs-fc data that demonstrate that AD-related neural dysfunction measured by functional connectivity progress through distinct stages. In particular, certain brain regions were predictive early in the disease but others became important later. Interestingly, we identified brain region that were predictive of AD stage but are known not to be affected by histopathology. These findings may suggest that predictive neural dysfunction can manifest independent of histopathologic spread.

P56B Integrating Functional Connectivity and Cognition to Understand Alzheimer's Disease

C. R. Chin Fatt[1], M. D. Devous[2], S. Whitfield-Gabrieli[3], H. Abdi[1]

[1]University of Texas at Dallas, Richardson, TX, USA, [2]University of Texas Southwestern Medical Center, Dallas, TX, USA, [3]Massachusetts Institute of Technology, Boston, MA, USA

Background: Resting state functional connectivity (*fc*MRI) of the Default Mode Network (DMN), Salience Network (SN), Executive Control (Left) Network (EN-L), and Executive Control (Right) Network (ECN-R), are impaired in Alzheimer's Disease (AD) and Mild Cognitive Impairment (MCI). In addition, cognitive measures such as CDR, CERAD neuropsychological battery (CERAD), and MMSE are sensitive to changes in cognition, distinguishing healthy controls from both MCI and AD. In this study we investigate how cognitive measures are related to *fc*MRI in the progression of AD.

Methods: Resting state fMRI measures were collected in 16 healthy controls (HC), 16 MCI, and 16 Early AD participants. Cognitive measures (CDR, MMSE, and CERAD) were selected using ROC analysis. The correlation between resting state functional connectivity and the selected cognitive measures were analyzed using multiple regression. These relationships were confirmed using two multivariate statistical methods: Barycentric Discriminant Analysis (BADA) and Multiple Factor Analysis (MFA).

Results: ROC analysis showed that CERAD was best at differentiating between HC, MCI, and early AD. Analysis of the CERAD sub scores, showed that modified Boston Naming task, constructional praxis recall, word list learning, word list recall and verbal fluency were significant ($p < .01$) at differentiating between cohorts. As a result, all further analysis was restricted to the subset of CERAD sub scores.

Functional connectivity—primarily in the DMN and ECN-R—was correlated with CERAD total score, and with a subset of the CERAD scores. Further modified Boston naming task and verbal fluency were the most sensitive scores of cognitive decline.

MFA analysis differentiated between the three cohorts using a combination of DMN, SN, ECN-L, ECN-R connectivity, and CDR and CERAD scores. This analysis showed that DMN is negatively correlated with SN, and ECN-R is negatively correlated with ECN-L, but CDR and CERAD were positively correlated as expected.

Conclusions: Cohort differences between HC, MCI and early AD were expressed as decrements in DMN and ECN-R connectivity that related to CERAD total score, as well as a subset of

CERAD sub scores. The relationships between DMN and ECN-R and cognitive measures are related to efficient compensation in the progression of AD. Cohort differences in SN and ECN-L connectivity that relate to cognitive measures were mainly reflected in inefficient compensation.

P57B Abnormal default mode network activation specific to negative, not positive or neutral, stimuli in currently depressed and recovered depressed individuals

T. Chou, J.M. Hooley

Harvard University, Cambridge, MA, USA

Background: Major depressive disorder (MDD) is characterized by a persistent negative mood and/or loss of interest or pleasure. People who are having their first depressive episode, those who are currently depressed (not first episode), those with late-life depression, those with treatment-resistant depression, and those who have recovered from depression all show either greater or less DMN functional connectivity at rest, compared to healthy controls (e.g., Bluhm et al., 2009; Bohr et al., 2012; Greicius et al., 2007; Li et al., 2013; Wu et al., 2013). However, based on Beck's (1967) cognitive model of depression, we know that maladaptive self-referential cognitions in depressed individuals only emerge when an individual's schemas are activated by potentially negative stimuli. Few researchers have looked at DMN activation at rest after different mood inductions. The present study's purpose was to investigate abnormal DMN functioning in depressed individuals after positive, neutral, and negative stimuli. Further, we wanted to know if people who have recovered from depression continue to show abnormal DMN functioning specifically after negative stimuli.
Methods: Data were analyzed from a previous collected neuroimaging dataset. Currently depressed ($n=8$), recovered depressed ($n=8$), and healthy individuals ($n=9$) heard critical, praising, and neutral comments from their mothers while being scanned (1.5 Tesla GE LX MRI scanner). Functional data was processed using SPM5 software. Individual contrast images (comparing rest after critical comments, praising, or neutral comments to the rest period at the beginning of the experiment) were entered into a flexible factorial analysis. We then completed region of interest (ROI) analyses at $p<0.005$ with our a priori regions defined by Buckner et al.'s (2008) identification of core regions in the DMN. To control for multiple statistical comparisons, we maintained a cluster-level false positive detection rate at $p<0.005$ with a cluster (k) extent empirically determined by Monte Carlo simulations in the AFNI program AlphaSim (Ward, http://afni.nimh.nih.gov/afni/docpdf/alphasim.pdf). We then ran linear regression analyses to understand if depressive symptom severity, rumination, and thought suppression predicted DMN activation.
Results: Depressed and remitted depressed participants demonstrated increased DMN activation relative to controls in the medial prefrontal cortex (predicted by brooding in remitted depressed participants), posterior cingulate cortex/retrosplenial (collectively predicted by depressive symptom severity, rumination, and thought suppression in depressed participants), and inferior parietal lobule (predicted by thought suppression in remitted depressed participants) for the rest periods following criticism, but not praise. Depressed participants also showed significant hippocampal formation activation relative to remitted depressed participants and controls. There was no difference in DMN activation after the praising or neutral comments.
Conclusions: The results suggest that abnormal DMN activation may emerge only after exposure to negative stimuli. Complex and negative thought processes are involved and further research is needed to understand the cognitions that are actually occurring during DMN hyperactivation. Both currently depressed and recovered depressed individuals showed abnormal DMN activation specific to the negative stimuli, suggesting that abnormal DMN functioning in response to negative stimuli may be a scar of depression.

P58B Association of resting state fronto-striatal network function with striatal presynaptic dopamine synthesis in humans

J.B. Czarapata, D.P. Eisenberg, M. Gregory, C. Hegarty, P.D. Kohn, K.F. Berman

Section on Integrative Neuroimaging, Clinical Brain Disorders Branch, National Institute of Mental Health, Intramural Research Program, NIH, DHHS, Bethesda, MD 20892–1365

Background: Striatal dopaminergic function is hypothesized to be a pivotal modulator of motivational and cognitive functions that rely on effective frontostriatal communication (Pochon et al., 2012). However, in vivo evidence for a link between normative variation in striatal dopaminergic tone and frontostriatal connectivity is lacking. Here, we tested for this link using both positron emission tomography (PET) to measure presynaptic dopamine synthesis and rs-fMRI to measure basal frontostriatal network coupling in the same healthy volunteers.
Methods: Subjects were 30 right-handed volunteers (mean age 33 ± 11; 18 males) without medical or neuropsychiatric illness. PET studies were conducted in a fasting state after carbidopa pretreatment and an intravenous bolus of 8–16 mCi 18F-Fluorodopa. Twenty seven images were acquired over 90 minutes and were attenuation and motion corrected. Two regions of interest (ROI's) – dorsal caudate and ventral striatum – and one cerebellar reference region were delineated on each individual's structural MRI and applied to their PET data. The Patlak-Gjedde graphical method was employed using PMOD software to calculate the specific uptake constant Ki for each ROI. rs-fMRI scans (3T, TR/TE = 2000/24) were acquired during two 6 min runs and were preprocessed in AFNI (Cox, 1996), including correction for pulse and respiration with RETROICOR (Glover et al., 2000). Time series taken from the same striatal ROIs in native space were used in a voxel-wise Pearson correlation analysis to generate correlation maps which were then normalized to MNI space, converted to z scores and entered into a group correlation analysis with striatal Ki values. Results were considered significant at $p<0.001$, uncorrected.
Results: rs-fMRI correlation maps featured expected frontostriatal networks, with relative prominence of dorso- and ventromedial frontal regions for dorsal caudate and ventral striatal ROIs, respectively. Individuals with greater ventral striatal Ki values showed diminished positive coupling between the ventral striatum and subgenaul anterior cingulate. Similarly, greater left dorsal caudate Ki values demonstrated diminished positive dorso-medial frontal gyrus coupling.
Conclusions: Our rs-fMRI correlation maps confirmed close functional relationships between frontal and striatal regions, as previously described (Salvador et al., 2005, Robinson et al., 2009). Furthermore, these data suggest that these relationships may be related to dopamine synthesis and stores. If replicated, these results may allow better elucidation of the neurobiological and neurochemical foundation of select fronto-striatal network function derived from resting-state fMRI.

P59B Development of Fronto-Occipital Connectivity in Congenitally Blind Children

B. Deen[1], H. Richardson[1], A. Fulton[2], R. Saxe[1], M. Bedny[1,3]

[1]Department of Brain and Cognitive Sciences, Massachusetts Institute of Technology, Cambridge, MA, USA, [2]Department of Ophthalmology, Boston Children's Hospital, Boston, MA, USA, [3]Department of Psychological and Brain Sciences, Johns Hopkins University, Baltimore, MD, USA

Background: The occipital cortex of congenitally blind individuals shows remarkable plasticity, taking on responses to tactile, auditory, and linguistic inputs. In blind adults, this plasticity is accompanied by an increase in functional connectivity between occipital and frontal cortex. However, the developmental origins of this effect are unknown. Is fronto-occipital functional connectivity present in all children early in development but suppressed by visual input in sighted individuals? Alternatively, are functional connections acquired de novo in the absence of visual input? Does fronto-occipital connectivity in blindness developmentally precede or follow occipital responses to nonvisual stimuli? To address these questions, we assessed the development of fronto-occipital connectivity in congenitally blind and sighted children, as well as the development of occipital responses to language in blind children.
Methods: Resting-state data were acquired from 16 blind children and young adults (age 4–25 years) and 20 age-matched blindfolded, sighted individuals, after excluding 6 participants due to excessive head motion. In addition to standard preprocessing, nuisance removal (using CompCorr) and scrubbing were performed. Functional connectivity was assessed using frontal and occipital seed regions that were found to have group differences in functional connectivity in an independent sample of blind and sighted adults. Additionally, fMRI data were acquired during an auditory language comprehension task, to assess plasticity of occipital responses in blind individuals.
Results: We found an age-group interaction in fronto-occipital correlations ($P < .01$), in a model with mean translation and rotation as nuisance covariates. This interaction reflected an increase with age in blind participants ($r = .38$, $P = .064$), and a decrease with age in sighted participants ($r = -.39$, $P < .05$). The age-group interaction and age effect in blind participants were also observed in a whole-brain analysis using an occipital seed region. Occipital responses to spoken language were observed in blind children as young as 4 years, before the emergence of connectivity with frontal cortex.
Conclusions: Fronto-occipital correlations in congenitally blind individuals develop gradually between the ages of 4 to 25 years. Occipital plasticity precedes the development of fronto-occipital correlations, and may play a role in shaping these functional connections through development.

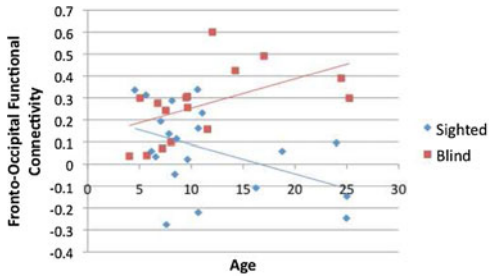

P60B Exercise increases neural synchrony power in children treated with cranial radiation for brain tumors

C. Dockstader[1,2], S. Gauvreau[1,2], J. Piscione[3], S. Laughlin[4], T. Cunningham[5], B. Timmons[6], Eric Bouffet[3], S. Doesburg[1,2], D.J. Mabbott[1,2,3]

[1]Neurosciences and Mental Health, Hospital for Sick Children; [2]Department of Psychology, Hospital for Sick Children; [3]Division of Haematology/Oncology, Hospital for Sick Children; [4]Diagnostic Imaging, Hospital for Sick Children; [5]Department of Applied Psychology and Human Development, University of Toronto; [6]Department of Psychology, McMaster University, Toronto, Ontario

Background: Children who have been treated with cranial radiation therapy (CRT) for posterior fossa (PF) brain tumors have altered brain function compared to healthy children. Aberrant neural function is highly correlated with impaired cognitive abilities in this patient group. MEG analysis of resting-state networks has proven to be a reliable measure of cognitive impairment in patients treated with CRT. The aim of the present study was to investigate the effect of three months of structured exercise intervention on resting state synchrony in children treated with CRT for PF brain tumors.
Methods: Before and after the three-month exercise program, a three minutes, eyes-open resting state Magnetoencephalography (MEG) recording, MRI structural scan, and neuropsychological assessment was collected from 21 children treated with CRT for malignant brain tumors of the Posterior Fossa at The Hospital for Sick Children (13 M/8 F, mean age = 12.41 yrs +/− 2.58 SD). MEG data were projected into anatomical space using Statistical Parametric Mapping and images from pre- and post-exercise conditions were averaged, separately. The pre-exercise data was subtracted from the post-exercise data for separate bandwidths in the theta (4–7 Hz), alpha (8–12 Hz), beta (13–29 Hz), and low (30–59 Hz) gamma ranges to determine source power changes in the strength and frequency of neural oscillations following intervention.
Results: MEG analyses showed increases in source power in peak locations corresponding to the default mode and motor networks. Specifically, we observed increased theta power in inferior parietal regions, increased alpha power in posterior cingulate and midfrontal gyrus, increased beta power in precuneus, and increased low gamma in posterior cingulate regions following exercise. Moreover, patients showed increases in power across the theta, alpha, beta, and gamma bands in widespread regions of the posterior part of the cortex following exercise.
Conclusions: Exercise behavior facilitates increased brain synchrony power in default mode and motor networks in children treated with CRT for brain tumors, particularly within the theta, alpha, and beta bandwidths. Moreover, the posterior regions, in which patients have received the most damage, appear to show particular responsivity to exercise across the frequency spectrum. Extensive changes in the frequency, strength and spatial composition of neural oscillations may underlie improvements in behavioral measures following exercise intervention in children treated with CRT for PF brain tumors. Changes in bandwidth power may be a sensitive index of enhanced brain function following exercise.

P61B Functional Network Correlates of Impaired Executive Function in Mild Cognitive Impairment

D.C. Farrar[1], M. Moss[2], R. Killiany[1,2]

[1]Center for Biomedical Imaging, [2]Dept. of Anatomy and Neurobiology, Boston University School of Medicine

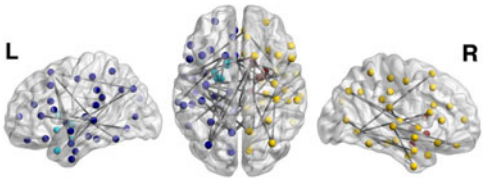

Background: Mild Cognitive Impairment (MCI) affects 16% of individuals aged 70 and older in the US. Most imaging investigations into the cognitive deficits associated with MCI have focused on memory function in patients with so-called MCI of the amnestic type. However, deficits in the executive function realm, such as impaired decision making ability, can be more devastating to an individual's quality of life than memory deficits.
Methods: Using data from the Alzheimer's Disease Neuroimaging Initiative (ADNI), we examined the resting state network connectivity of 30 individuals with an MCI-amnestic diagnosis. Fifteen of the subjects were classified as ''high executive functioning individuals'' and sixteen were classified as ''low executive functioning'' individuals, based on neuropsychological test performance. Regions of interest (ROIs) were identified based on MRI anatomical scans, and a Pearson correlation of all ROI pairs determined functionally connected regions of the resting state fMRI scans obtained from these individuals. We used the Network Based Statistic (NBS) algorithm on the populations to correct for multiple comparisons.
Results: We found a significant decrease in connectivity between the frontal-parietal-temporal network in the subjects with low executive function performance when compared to those with high executive function performance.
Conclusions: By examining the functional network connectivity of individuals with high performance on executive function tests compared to those with low performance on executive function tests, we were able to identify significant decreased network connectivity in the frontal, temporal and parietal regions in those with diminished executive abilities. These findings suggest that the network connections responsible for efficient brain function beyond the medial temporal lobes is compromised early in the processes leading to Alzheimer's disease.

P62B Mindfulness and resting state connectivity of amygdala

C.E. Fulwiler[1], N. Zhang[2], J.A. King[1]

[1]*University of Massachusetts Medical School, Worcester, MA, USA,* [2]*Pennsylvania State University, State College, PA, USA*

Background: Mindfulness based stress reduction training has been reported to reduce negative emotions. However, it's impact on the neural circuits subserving modulation of negative emotions is not well understood. We have explored the possibility that mindfulness may impact resting state functional connectivity (rsFC) of amygdala-prefrontal circuits which are known to be involved in emotion regulation. We hypothesized that rsFC in these networks, specifically the amygdala-prefrontal and amygdala-insula circuits, would be associated with trait mindfulness and would be modified by mindfulness training.
Methods: Participants (N = 10, 6 females) from Mindfulness-Based Stress Reduction classes (mean age 42.9 yrs, SD 8.53) were studied within 1 week pre/post the 8-week program. Exclusion criteria included taking psychotropic medications, using drugs of abuse, serious mental disorder, and head injury. Trait mindfulness was measured with the Kentucky Inventory of Mindfulness Scale (KIMS; Baer et al. 2006). fMRI sessions were composed of two 5-minute acquisition scanning runs. Correlational analysis for rsFC was conducted with left and right amygdala as separate seed regions. Trait mindfulness measures were correlated to RSFC involving right and left amygdala on a voxel-by-voxel basis across all subjects.
Results: Trait mindfulness (total KIMS score) was positively associated with rsFC of right amygdala-right dorsolateral prefrontal cortex ($R^2 = 0.472$). Of the mindfulness subscales, only the Aware subscale showed significant correlations with amygdala-insula rsFC: right ($R^2 = 0.468$) and left ($R^2 = 0.399$). Amygdala functional connectivity increased significantly after MBSR for right amygdala-right dorsolateral PFC and amygdala-insula bilaterally.
Conclusions: Both hypotheses were supported. Amygdala resting state functional connectivity with dorsolateral PFC and Insula was associated with trait mindfulness and increased following the 8-week mindfulness training. To our knowledge this is the first evidence that amygdala resting state functional connectivity is associated with trait mindfulness and is modified by MBSR. Taken together, both the association of FC with trait mindfulness and the pre-post change in FC following the 8-week MBSR program may suggest that mindfulness training produces greater top-down

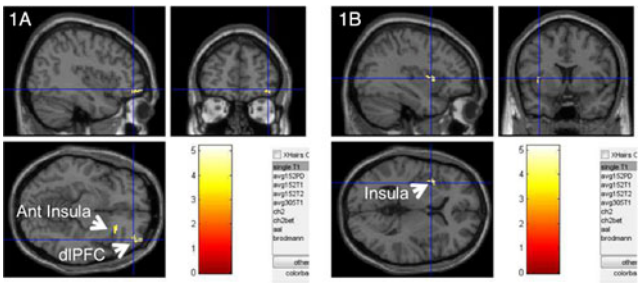

FIG. 1. Contrast map of amygdala connectivity between pre- and post-MBSR. Color voxels indicate significantly changed FC with amygdala seed (**A** right, **B** left; two-sample t-test, $p < 0.005$, uncorrected).

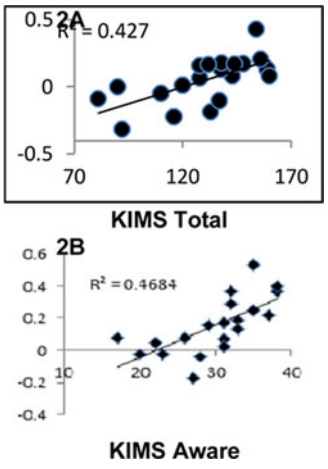

FIG. 2. Relationship between right amygdala FC and mindfulness traits. A: amygdala-dlPFC and total KIMS; B: amygdala-insula and KIMS Aware subscale.

control of emotional reactivity by enhancing prefrontal regulation of amygdala responses. These data are consistent with the hypothesis that a critical component of MBSR's impact is the enhancement of emotional regulation. Our findings also suggest that rsFC may prove valuable as a marker for the effects of mindfulness training on emotion regulation circuits.

P63B Anatomical connectivity of the prelemniscal radiations: Implications in Parkinson's disease

M. G. García-Gomar[1], F. Velasco[2], L. Concha[1]

[1]*Instituto de Neurobiología, Universidad Nacional Autónoma México (UNAM), Juriquilla, Querétaro, México,* [2]*Unidad de Neurocirugía Funcional, Estereotaxia y Radiocirugía, Hospital General de México, México, D.F., México*

Background: The subthalamic prelemniscal radiations (Raprl) have been proposed as a neurosurgical target for deep brain stimulation (DBS) for the treatment of Parkinson's disease (PD) and essential tremor since 1970's. It has been proven to be a superior target for ameliorating tremor and rigidity than any other target. Despite its clinical usefulness, the anatomic connectivity of the Raprl remains unknown and, therefore, the mechanisms of actions of DBS of this region are elusive. This work describes the different fiber populations that traverse through the Raprl in healthy humans using high angular resolution diffusion MRI and probabilistic tractography through crossing fibers.
Methods: The Institutional Review Board approved the protocol and all subjects signed a written informed consent according to the Declaration of Helsinki. Images from twelve healthy subjects were acquired from using a 3 Tesla Philips Achieva MRI scanner. T1, T2 and diffusion-weighted images (DWI) were acquired using 120 unique diffusion-gradient directions with a b value of 2000 s/mm^2 (voxel size of $2\times2\times2$ mm^3). Total scan time was around 1 hour per subject.

Eddy-current distortion correction of DWI was made by *fsl* (FMRIB, Oxford). Constrained spherical deconvolution (CSD) was performed, followed by the creation of track-density images (TDI) based on 1 million tracks seeded homogeneously throughout the white matter using MRtrix (Brain Research Institute, Melbourne Australia). Final resolution of the TDI was of $0.2\times0.2\times0.2$ mm^3; these images were crucial for the accurate visualization of the different subthalamic structures, which were manually segmented based on the Schaltenbrand-Wahren atlas. Next, we seeded the Raprl for probabilistic tractography and the resulting bundles were selected according to their targets, which were automatically parceled by *freesurfer* (FreeSurfer Software Suite, Harvard).
Results: Probabilistic tractography demonstrated connectivity of the Raprl with distinct cortical and subcortical structures. All subjects showed connectivity with motor and premotor cortex, orbitofrontal cortex, thalamus, globus pallidus (GP), cerebellum and pedunculopontine nucleus (PPN). In 80% of the subjects GP showed connectivity with the contralateral dorsal brainstem in a region that corresponds to the location of the contralateral PPN.
Conclusions: Probabilistic tractography based on TDI and CSD allows the visualization of Raprl. Previous reports have proposed an intimate relationship between tremor and cerebellar activity, which is supported by our findings, in which we show considerable connectivity between Raprl and the cerebellum. PD patients that have undergone DBS of this area show an improvement on gait that also occurs after unilateral GP- DBS, which could be explained by the intimate anatomic relation between Raprl and PPN.

P64B Connectivity of midline pre-frontal cortex during speech production in aphasic stroke and controls

F. Geranmayeh[1], R.J.S. Wise[1], R Leech[1]

[1]*Computational Cognitive and Clinical Neuroimaging Laboratory, Imperial College London, London, UK*

Background: Midline pre-frontal cortex is functionally and structurally heterogeneous. Amongst other functions it is activated in language tasks[1]. The aim of this study was to investigate the complex and dynamic pattern of activity in midline frontal cortex that may reflect activity in other brain networks; and investigate how these networks are engaged during speech production in healthy controls and after aphasic stroke.
Methods: Three groups of subjects were scanned during a "sparse" fMRI paradigm containing Speech, Count, Decision (non verbal task), and Rest; 24 healthy subjects (HV), 17 non-aphasic chronic stroke patients (Non_Aphasic), and 35 patients with chronic aphasic stroke (Aphasic). In addition resting state fMRI was obtained from a separate age-matched healthy control group, to define 10 Region of Interest (ROI) in the supplementary motor cortex/dorsal anterior cingulate/paracingulate (SMA/dACC). Univariate ROI analysis, group temporal concatenation independent component analysis (ICA), and dual regression were carried out.[2]
Results: A functionally defined ROI in midline (SMA/dACC) was identified based on the univariate contrast of Speech > Rest in the HV group. Compared to the Non-Aphasic group, the Aphasics showed reduced activity in this region during Speech > Rest ($P=0.02$) with a similar trend in Speech > Count ($P=0.08$).

We fractionated the midline prefrontal cortex into subregions based on an independent age-matched resting state dataset (ROI in Figure). Resulting subregions within SMA/dACC showed connectivity with multiple different brain networks. For example a dorsal subregion showed connectivity with left fronto-temporo-parietal network. This network showed significant activation in Speech > Count in all three groups.

Another subregion showed connectivity with the default mode network (DMN). This component showed a significant relative deactivation in Speech > Count in all three groups. Finally

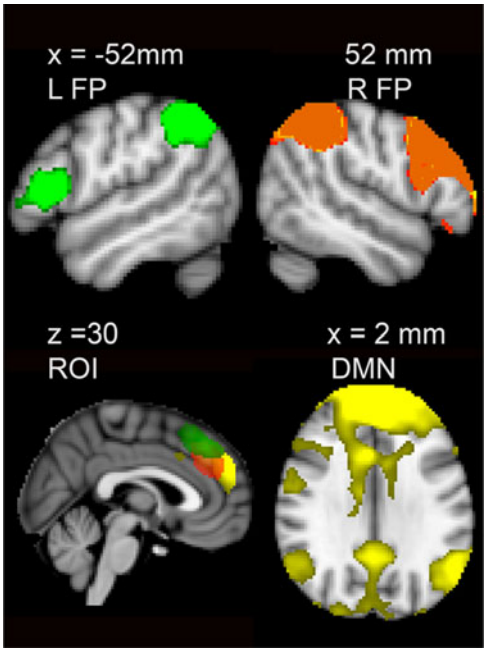

another subregion showed connectivity with a right fronto-parietal network that was significantly active during the Count and Decision trials reflecting attentional demands of these tasks. We explored the differential activation within these networks between the three groups.
Conclusions: Midline frontal cortex shows a complex pattern of connectivity with other brain systems with differential activations during speech production in healthy and lesioned brains.
Reference: Brain Lang. 2012;12:47–57. 2. J Neurosci 2012;32: 215–222.

P65B Resting state analysis of neural dynamics for music therapy with guided imagery and music

Y. Han[1,2], S.E. Lee[3], D. Kim[2], H.W. Park[2]

[1]Department of Biomedical Engineering, Gachon University, Incheon, Republic of Korea
[2]Department of Electrical Engineering, Korea Advanced Institute of Science and Technology, Daejeon, Republic of Korea
[3]Department of Music Therapy, Hansei University, Gunpo, Republic of Korea

Background: In the previous studies, we have demonstrated that guided imagery with music can be crucial in music psychotherapy for working emotions such as awareness, arousal, enhancement, reflection and transformation of emotions in therapeutic relationship. In this work, resting state fMRI (RS-fMRI) is used to analyze the importance of guided imagery.
Methods: For RS-fMRI, classical music and verbal instructions were presented to 24 healthy volunteers to examine functional connectivity established during music psychotherapy sessions composed of either (i) music (MU) only or (ii) guided imagery and music (GIM) sessions. To evaluate functional connectivity, we predefined ROI in auditory bran region (Broadmann 42) and mapped the Pearson correlation coefficient in each voxel of whole brain to calculate r-maps. R-maps of each subjects were normalized to Z-maps by using Fisher's Z transformation and two-sided one-sample t-test were performed for all Z-maps to detect the regions showing significant functional connectivity with the selected ROI.

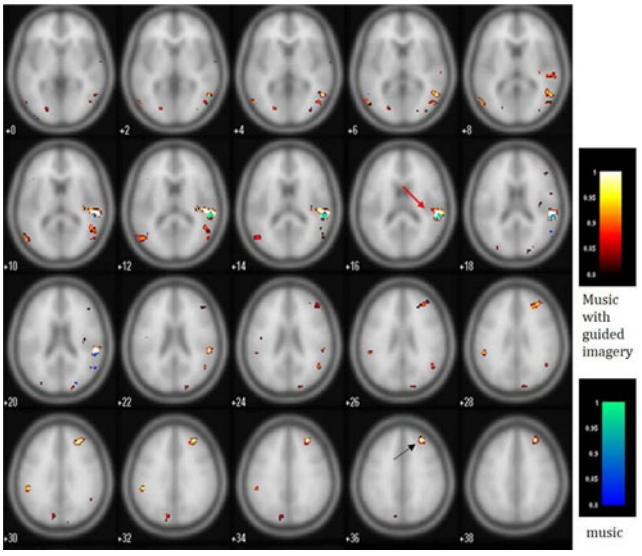

FIG. 1. Functional Connectivity.

Results: As presented in figure 1, where the functional connectivity established during GIM and MU experiments were mapped with red and blue color bars, respectively, the emotional working was amplified in case of GIM compared to MU. More specifically, functional areas related to emotional processing was highlighted in the GIM experiment (especially in the frontal areas as marked with a black arrow), while modest level of connectivity was observed for the MU experiment, focusing mainly in the auditory area (red arrow).
Conclusions: Findings based on RS-fMRI suggest that guided imagery and music as combined stimuli are effective approach in emotional work with personal episodic memories, indicating engagement of various neural regions functioning in emotions, various kinds of sensory modalities, integration of cross-modal sensory, episodic memory, and empathy.

P66B Exogenous testosterone modulates resting state functional connectivity in healthy young men

I.M. Haugen[1,2], J.M. Carré[2,3], H.A. Marusak[1,4], T.A. Ricard[1,2], J.H. Manning[1,4], M.E. Thomason[1,4,5]

[1]Merrill Palmer Skillman Institute, Wayne State University, Detroit, MI, USA; [2]Department of Psychology, Wayne State University, Detroit, MI, USA; [3]Department of Psychology, Nipissing University, North Bay, Ontario, CANADA; [4]Wayne State University School of Medicine, Detroit, MI, USA; [5]Perinatology Research Branch, NICHD/NIH/DHHS, Detroit, MI, USA

Background: Testosterone (T) is fundamental to social-emotional behavior, as is the amygdala. Previous work indicates that a single administration of T modulates amygdala reactivity and amygdala-orbitofrontal cortex (OFC) functional connectivity (FC) during processing of angry facial expressions. However, it remains unknown whether T also modulates amygdala-OFC connectivity at rest.
Methods: We used a novel two-step pharmacological challenge protocol to evaluate T's causal modulation of amygdala-OFC FC in 16 healthy young men ($M_{Age} = 26.81$). To control for baseline differences in T, we first administered a gonadotropin releasing hormone (GnRH) antagonist that temporarily suppressed T concentrations to a hypogonadal state. Next, participants received T (100 mg Androgel®) or placebo (counter-balanced within participants). Finally, we acquired resting state FC data approximately one hour after drug administration and compared conditions using seed-based connectivity analysis (SCA).
Results: Amygdala FC was greater for T vs. placebo across several medial prefrontal areas, including the OFC, and regions of the medial temporal lobe, including the hippocampus. Only one region showed the reverse effect: left premotor cortex showed an increase in FC with lower T.
Conclusions: Prior research shows that T degrades the reciprocal FC between the amygdala and the OFC, leading to dysregulation of the amygdala. Notably, all previous T administration studies have been conducted in women and have used protocols that increase T levels to well above the normal physiological level for that sex. Our finding that amygdala-OFC FC increases after T administration may point to a nonlinear relationship between T and FC within an amygdala-OFC circuitry. Within each sex's normal T range, amygdala-driven impulses may be well regulated; outside of that range, they become less regulated. The increase in amygdala-hippocampal FC is consistent with behavioral literature showing improved memory for emotionally salient stimuli with

increasing T levels. Increased OFC sensitivity to the amygdala's reactivity to emotional stimuli could help cue the hippocampus.

P67B Resting-state reorganization in Parkinson's Disease

S.G. Horovitz[1], P. Lauro[2], P. Malone[1], M. Hallett[1], S. Tinaz[1]

[1]Human Motor Control Section, NINDS, NIH, Bethesda, MD, USA, [2]Office of the Clinical Director, NINDS, NIH, Bethesda, MD, USA

Background: Parkinson's disease (PD) is characterized by and diagnosed based on its cardinal symptoms including bradykinesia, tremor, rigidity and loss of balance, and its response to levodopa medication. PD patients have difficulty with self-initiated and self-paced movements, as well as impairment in several cognitive domains including the allocation of attentional resources among others. Because of these deficits, comparison of task-related brain function between patients and healthy volunteers poses challenges. Either performance or effort can be matched, but not both. Resting state (rs) fMRI provides the opportunity to probe functional brain connectivity in the absence of task, thus eliminating effort- or performance-related variability. We hypothesized that the motor and cognitive deficits in PD are related and expected impaired functional integrity in the sensorimotor (SMN), cinguloopercular-task-set maintenance-(CON), and frontoparietal (FPN)-adaptive updating-networks.
Methods: Thirty PDs (average age = 61.2 ± 8.4, 11 females) and 30 HVs (average age = 61.4 ± 6.7, 10 females) were included in the functional MRI analysis. All subjects gave informed consent. The study was approved by an NIH IRB. Images included T1-weighted MPRAGE for registration, and a 6 min 50 sec rs-FMRI with eyes closed. All patients were scanned at least 12 hours after their dopaminergic medication. After standard data pre-processing in AFNI (including time shift, registration, motion correction, despiking, local WM removal, bandpass filtering), 86 nodes were defined based on Dosenbach et al. (2010) (FPN (n = 21), CON (n = 32), and SMN (n = 33)). Graph theoretical network analysis was performed using Brain Connectivity Toolbox. Figure shows the correlation matrices for each group.
Results: PD group showed lower node strength compared to HVs in several nodes including the left dorsal anterior insula (dAI), left temporoparietal junction (TPJ), and left posterior temporal areas in the CON, and right precentral gyrus and right posterior insula in the SMN. The clustering coefficient was also reduced in PDs mostly in the SMN nodes. Most CON and SMN nodes with lower node strength and clustering coefficient, as well as the left intraparietal sulcus in the FPN also demonstrated reduced local efficiency in the PD group. In addition, the left dAI, left TPJ and right putamen/posterior insula nodes in the CON and right orbitofrontal gyrus node in the FPN showed lower betweenness centrality in the PD group. The only metric that showed higher values in the PD group was the betweenness centrality in the left mid-insula and left precentral gyrus nodes in the SMN.
Conclusions: Overall, PD patients showed weaker functional connectivity, less efficient local information processing, and reduced ''bridging'' function in many nodes of the CON, FPN, and SMN. These deficits may underlie the difficulty in task-set maintenance and execution in PD.

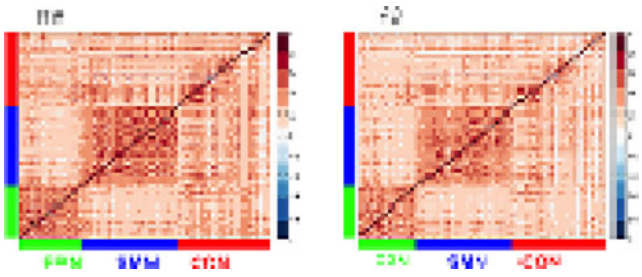

P68B Functional Organization of Language Networks in Children with Left Hemispherectomy

Anna Ivanova[1], Lucina Q. Uddin[1], and Stella de Bode[2]

[1]Department of Psychology, University of Miami, Coral Gables FL
[2]Reed Neurological Research Center, UCLA, Los Angeles, CA

Background: In rare cases of severe and intractable epilepsy, hemispherectomy is performed at a young age. Surprisingly, the remaining hemisphere is often capable of supporting many cognitive functions post surgery. The mechanisms by which this plasticity ensues are at present unknown. Here we examine functional connectivity of major large-scale brain networks in five children with hemispherectomy using resting state functional magnetic resonance imaging (rs-fMRI). We initially focus on language networks in the intact hemisphere, and qualitatively compare these and other functional systems with typical controls.
Methods: Resting state networks were analyzed using complementary approaches including seed-based functional connectivity and independent component analysis (ICA). First, seeds were selected based on automated meta-analyses of language processing conducted with Neurosynth (http://neurosynth.org/). A control group of 15 participants with intact hemispheres was used for qualitative comparison. Functional images were preprocessed using FSL's FEAT. We used white matter (WM) and cerebrospinal fluid (CSF) mean time-series as nuisance regressors in the general linear model (GLM) to reduce the influence of physiological noise. In addition, ICA denoising was used in the patient group.
Results: We found that in four of the five patients examined, a right hemisphere language network could be detected with seed-based functional connectivity analyses. This network strongly resembled the right hemisphere language network that could be detected in controls, and comprised inferior frontal, angular gyrus, superior temporal sulcus, and premotor regions. ICA revealed a right lateralized language network in all five patients.
Conclusion: Remarkably preserved patterns of functional connectivity are observed in language networks in the intact hemisphere of most hemispherectomy patients, suggesting possible dynamic reorganization capabilities in the developing brain. Collection of rs-fMRI at several time points post-surgery can provided a means for tracking recovery of function in these patients.

P69B Altered functional and structural connectivity in children with histories of early deprivation

J.W Jeong[1,2], A. Kumar[1,2], D.O. Kamson[2], W. Guy[2], H.T. Chugani[1,2], M.E Behen[1,2]

[1]Departments of Pediatrics and Neurology, School of Medicine, Wayne State University, Detroit, Michigan, USA, [2]Translational Imaging Laboratory, Children's Hospital of Michigan, Detroit, Michigan, USA

Background: Early social deprivation (ED) is associated with increased incidence of neurocognitive impairment. We have found abnormal white matter properties in frontal and temporal cortices as well as in the projections between these regions. This study combined resting state functional MRI (rs-fMRI) with diffusion tensor imaging (DTI) to investigate if functional abnormalities are associated with altered brain connectivity.
Methods: Twenty-six children with histories of ED (mean age: 10.4 ± 2.5 years, 11 males) and 25 nondeprived, nonadopted controls (NC; mean age:10.9 ± 2.5 years, 6 males) underwent rs-fMRI and DTI at a 3T scanner and neuropsychological evaluations. All ED children were raised from birth in international orphanages, and adopted in the USA. Exclusionary criteria included pre- or perinatal problems, focal neurological abnormality, and medical problems. BOLD time series were detrended, temporally filtered at < 0.08 Hz, and regressed out with rigid body realignment parameters, average white matter and ventricular system signals, and global signal. Independent component analysis with ball and stick model was applied for DTI tractography. A total of 116 cortical regions of interest were generated by fitting a deformable template, resulting in two 116×116 connectivity matrices in which the elements quantify the pair-wise connectivity scores (i.e., 1) correlation coefficients between low frequency time courses of any two given cortical regions and 2) fiber numbers connecting any two given cortical regions).
Results: DTI-group comparisons revealed that the ED group had *reduced* axonal connectivity for a number of frontal seeds: left middle orbital frontal to left anterior cingulum ($p = 0.007$), left rectal gyrus ($p = 0.04$), left insula ($p = 0.004$), left thalamus ($p = 0.008$), and right middle orbital frontal to left anterior cingulum ($p = 0.004$); right rectal gyrus to right temporal pole ($p = 0.002$), and left anterior cingulum ($p = 0.0001$). The ED group had *increased* axonal connectivity for a number of temporal seeds: right hippocampus to putamen ($p = 0.008$), amygdala to temporal pole, bilaterally (left, $p = 0.0007$; right, $p = 0.006$), and right middle temporal to right temporal pole ($p = 0.008$). Within (ED) group analyses revealed a significant correlation between time spent in the orphanage and functional connectivity from left hippocampus to putamen ($p = 0.009$). Analyses also revealed differential associations between frontal and temporal functional connections and neurocognitive and behavioral measures; *higher* temporal connectivity was associated with full scale IQ ($p < 0.001$), expressive language ($p = 0.03$), and verbal memory ($p = 0.02$); *lower* frontal connectivity was associated with increased likelihood of insecure attachment ($p = 0.004$) and poor behavioral regulation ($p = 0.008$).
Conclusions: Results revealed abnormal functional connectivity in frontal and temporal brain regions in children with histories of ED, which were differentially associated with behavioral functions. Abnormal functional connectivity in these networks may underlie the neurocognitive and behavioral consequences commonly identified in these children.

P70B Resting state fMRI functional connectivity in schizophrenia using an independent components analysis (ICA)-based approach

Himanshu Joshi[1,2], Harsha N Hallahalli[1#], John P. John[1,2,3]

[1]Multimodal Brain Image Analysis Laboratory (MBIAL), Departments of [2]Psychiatry and [3]Clinical Neuroscience, National Institute of Mental Health and Neurosciences, Bangalore, Karnataka, INDIA.; [#]Current affiliation: Department of Physiology, K.S. Hegde Medical Academy, Nitte University, Mangalore, Karnataka, India – 575018

Background: Schizophrenia is a neuropsychiatric disorder characterized by various symptom dimensions including positive (e.g., hallucinations, delusions), negative (e.g., avolition, apathy), disorganization (e.g., disorganized thought, emotions and behavior) and cognitive (e.g., executive dysfunction) symptoms.. Dysfunctional connectivity in various distributed brain networks is thought to constitute the core pathophysiology underlying these various symptom dimensions. We, therefore, aimed at examining functional connectivity within brain networks identified from the fMRI blood oxygen level dependent (BOLD) time series in the resting state[resting state networks (RSNs)] in patients with schizophrenia in comparison to healthy control subjects. In keeping with previous reports, we hypothesized that the RSN connectivity would be decreased in certain networks and increased in certain others.
Methods: The study samples comprised of 10 patients with paranoid schizophrenia [age = 33.1 (s.d. = 7.92) years] recruited from those attending the outpatient department of the National Institute of Mental Health and Neurosciences (NIMHANS), Bangalore, India and 10 healthy control subjects [age = 24(s.d. = 2.94) years]. Using Multivariate Exploratory Linear Optimised Decomposition into Independent Components (MELODIC), 17 RSN components were identified, referring to previously published works. Between-group comparisons of functional connectivity were then carried out using dual regression with age, gender, and number of years of formal education as co-variates.
Results: The schizophrenia group was found to have increased connectivity in left fronto parietal and cerebellar networks at *family-wise error* (*FWE*) *corrected* threshold of $p < 0.05$.
Conclusions: Increased connectivity in the left fronto-parietal and left cerebellar resting state networks might reflect the brain's efforts at compensating for the effects of a core neurochemical disturbance that underlies schizophrenia pathophysiology. The results of our study are in keeping with the findings of Shen et al. (2010), thus providing additional supportive evidence for the cognitive dysmetria hypothesis of schizophrenia. Thus, it may be concluded that dysconnectivity in RSNs may have potential utility as an investigative approach for improving our understanding of schizophrenia pathophysiology.

P71B Decreased local variance of resting-state functional MRI signal correlations in HIV patients may indicate cortical injury

K.J. Kallianpur[1], G.R. Kirk[2], C.M. Shikuma[1], T. Blumensath[3], A.L. Alexander[2]

[1]Hawaii Center for AIDS, Department of Medicine, University of Hawaii, Honolulu, HI, USA, [2]Waisman Laboratory for Brain Imaging and Behavior, University of Wisconsin, Madison, WI, USA, [3]ISVR, University of Southampton, Southampton, UK

Background: While structural imaging may capture local variations in the volume or thickness of gray matter structures, it is insensitive to functional integrity of brain tissue. Resting-state functional magnetic resonance imaging (rs-fMRI) may yield a measure of localized abnormalities in functional integration across the entire cortex at both the group and single-subject level. Within functional gray matter units and away from functional boundaries, nearby points are expected to show high correlations in rs-fMRI signal. Rs-fMRI has been infrequently used in HIV research although brain atrophy, including cortical thinning, is observed. Persistent HIV-associated neurocognitive impairment (HAND), even in HIV patients whose viral load is suppressed by

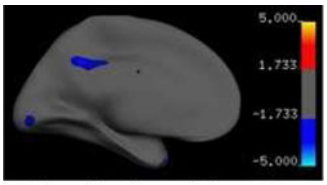

Reduced local correlation variance in HIV patients; map shows log(p).

long-term antiretroviral therapy (ART), remains an urgent problem. Using rs-fMRI to investigate local connectivity variance in HIV+ subjects compared to an HIV− group, we aimed to assess the utility of this measure for identifying regions of functional change in the cortex.

Methods: Cross-sectional rs-fMRI data from a cohort of HIV+ and HIV− individuals were analyzed. Subjects underwent neuropsychological (NP) testing. Six rs-fMRI scans were separately acquired at a single session for each of 22 healthy control volunteers. For each subject we computed a surface-based measure of local variance in correlations (Blumensath et al., *NeuroImage* 2013) across the cortical surface. We examined cortical gray matter only; white matter and ventricular voxels were excluded. Effects of head motion were reduced by a stringent 0.25 mm motion censoring threshold. HIV+ vs. HIV− group differences in local correlation variance were assessed, controlling for age. Corrections for multiple comparisons were performed by permutation testing. Ongoing work includes relating changes in the local correlation variance measure to NP test scores; and for the HIV+ subjects, to HIV clinical variables. Reproducibility of this measure is being evaluated using the 6 acquisitions for the control study subjects.

Results: We analyzed rs-fMRI data for 21 HIV+ patients (51.7 ± 7.6 years old; all stable on ART for ≥ 1 year; 81% with undetectable plasma viral load) and 21 HIV− individuals (54.3 ± 8.1 years old). Compared to the HIV− subjects, the HIV+ group exhibited significantly ($p < 0.01$) decreased local correlation variance in the posterior cingulate, precuneus, lingual, ventral anterior temporal and lateral temporal cortices.

Conclusions: The local connectivity measure used in our study holds potential for identifying areas of cortex whose functional properties have been altered relative to normative data. Decreased local variance of correlations in HIV disease may reflect hypersynchrony. This measure may indicate regional pathology and provide insight into HIV neuropathogenesis and HAND. More work is needed to improve data preprocessing methods that will optimize within-subject reproducibility of resting functional connectivity and thus improve specificity of the local correlation variance measure.

P72B Linked Structural and Functional Maturational Lag in ADHD

D. Kessler[1], M.A. Angstadt[1], Y. Fang[1], R.C. Welsh[1,2], C. Sripada[1]

[1]Department of Psychiatry and [2]Department of Radiology, University of Michigan, Ann Arbor, MI, USA

Background: A prominent neurodevelopmental hypothesis proposes that ADHD involves a lag in brain maturation. In order to investigate this hypothesis simultaneously across both brain structure and function, we used joint independent components analysis, a multivariate, multimodal method that identifies cohesive components that span modalities. We hypothesized that components associated with large-scale networks [in particular default mode network (DMN) and task positive network (TPNs)] and regions involved in cognitive and motoric regulation would exhibit both strong maturational effects and strong opposing ADHD effects.

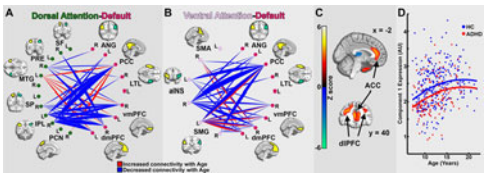

Detailed Examination of First Component. (A&B) Internetwork connectivity changes. Width of arc indicates quantity of affected edges. (C) Gray matter volume map reveals increased dlPFC and ACC. (D) Scatter shows component expression versus age.

Methods: For 421 participants from the ADHD-200 sample, we produced gray and white matter volume maps with voxel-based morphometry, as well as whole-brain functional connectomes derived from 1166 regions of interest throughout the brain. Joint independent component analysis was performed, and the resulting transmodal components were tested for differential expression as a function of disease and age.

Results: Two components significantly showed the predicted pattern of age effects that were lagged in individuals with ADHD. The first component showed (with increasing age) increased 1) intra DMN integration; 2) increased segregation between DMN and dorsal and ventral attention networks (two TPNs); and 3) increased gray matter volume in TPN regions responsible for regulatory control and decreases in striatal regions. The second had diffuse connectomic alterations and gray matter changes similar to the first.

Conclusions: We observed modality-spanning maturational lag in ADHD, specifically in the development of DMN interrelationships with attention networks. Our findings may shed light on the developmental etiology of ADHD.

P73B DC-EEG potential reflects blood brain barrier (BBB) integrity

V. Kiviniemi[1], J. Kortelainen[2], M. Isokangas[1], T. Siniluoto[1], E. Sonkajärvi[3], V. Korhonen[1,4], Tuija Hiltunen[1], T. Myllylä[4], T. Seppänen[2], O. Kuittinen[5]

[1]Radiology, Oulu Univ. Hospital (OUH), Finland, [2]Dept. Computer Science & Engineering, Oulu Univ. Finland [3]Anesthesiology, OUH, Finland [4]Dept. Optoelectronics, Oulu Univ. Finland [5]Oncology, OUH, Finland

Background: Slow oscillations in DC-EEG background has been shown to reflect potential over blood brain barrier. In this study we hypothetized that human blood-brain barrier integrity could be monitored using DC-EEG. To test the hypothesis we monitored the intra-arterial mannitol induced blood brain barrier disruption (BBBD) with multimodal set-up. BBBD is used in primary CNS lymphoma treatment because it increases chemotherapeutic penetrance to brain a 100 fold.

Methods: We measured Brain Products's DC-EEG continuously with fNIRS, NIBP and total anesthesia surveillance over the BBBD procedure in 8 measurements (2 patients both genders).

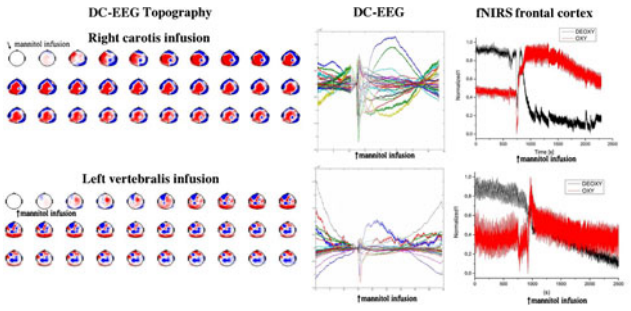

We compare DC-potential to pre-mannitol state and image topographic EEG power changes in the 10–20 EEG set-up.
Results: We were able to detect robust DC-EEG potential shift following i.a. mannitol infusion in each measurement. The topographic images indicate that the positive DC-shifts localize with the infused arterial territory. We were able to detect a localized DC-EEG and fNIRS shift in each measurement.

Figure above shows DC-potential topographical changes (30 s windows) in right internal carotid and left vertebral artery infusions on left panel. In the middle summed DC-EEG potentials over whole mannitol infusion period. Right panel shows fNIRS measurement data from forehead. Mannitol infusion marked with arrow.
Conclusions: We demonstrate that DC-EEG signal reflects human BBB integrity. The monitoring of BBB integrity is likely to have medical implications on ICU, neurological, neurosurgical patient monitoring.

P74B Default mode connectivity is mediated by genetic burden in prodromal HD

K.A. Koenig[1], M.J. Lowe[1], J. Lin[1], D.L. Harrington[2], K.E. Sakaie[1], J.S. Paulsen[3], and S.M. Rao[1]

[1]Cleveland Clinic, Cleveland, OH, USA, [2]VA San Diego Healthcare System, San Diego, CA, USA, [3]The University of Iowa, Iowa City, IA, USA

Background: Huntington's disease (HD) is an inherited neurodegenerative disorder. Individuals who meet the genetic criteria for HD but who do not yet show the motor symptoms required for formal diagnosis are considered to be in the prodromal phase (preHD). Changes in cognition and have been observed in preHD, but the neuronal bases are not well understood. One source of cognitive decline may be the default mode network (DMN), which is associated with cognitive decline in other diseases. The current work used a seed-based approach to examine rs-fMRI in the DMN in preHD and its relationship to genetic burden.
Methods: 16 gene-negative (mean age 42.6 ± 9.2, 4 males) and 48 preHD participants were scanned at 3T in a 12-ch receive head coil.

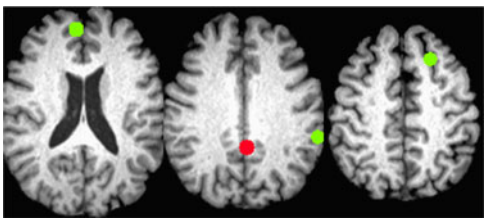

FIG. 1. PCC ROI (red) and regions in the DMN that showed significant differences in connectivity in preHD (green).

preHD subjects were stratified into three groups (n = 16 each) based on CAP score, a proxy of genetic burden: High genetic burden (HIGH, mean age 47.1 ± 12.6), low (LOW, mean age 32.6 ± 9.0), and medium (MED, mean age 38.3 ± 9.7). Scans included a T1-MPRAGE (1 × 1 × 1.2) and a rs-fMRI scan at 2 × 2 × 4 mm voxels, 1954 Hz/pix BW, 31 axial slices, TR/TE/FA = 2800/29/80. A 6 mm sphere was placed in a key region of the DMN, the posterior cingulate cortex (PCC), and then transferred to individual space. Postprocessing of rs-MRI data and whole brain map creation is described in Koenig et al., AJNR, 2013. rs-fMRI maps were transformed to common space, averaged, and thresholded at $p = 1 \times 10^{-4}$ (cluster size 260). ROIs were placed in each significant region at the point of peak connectivity to the PCC. Mean connectivity within each ROI was calculated for each subject and entered into a one-way ANCOVA using age as a covariate. Age-adjusted partial correlations were used to assess the relationship connectivity of the PCC and the CAP score.
Results: Three regions showed significant group differences in connectivity to the PCC (Figure 1), including the left superior frontal gyrus ($p = 0.021$, NEG < MED, LOW), the left inferior parietal lobule ($p = 0.02$, MED < LOW), and the right medial frontal gyrus ($p = 0.008$, LOW, HIGH < MED). In preHD subjects, CAP score was significantly related to the strength of connectivity from the PCC to the left superior frontal gyrus ($r = -0.343$, $p = 0.018$) and the right medial frontal gyrus ($r = -0.357$, $p = 0.014$).
Conclusions: The strength of connectivity from the PCC to the left inferior parietal lobule and right medial frontal gyrus show significant differences among those with differing levels of genetic burden. Differences in patterns of connectivity across the preHD groups suggests that changes in brain function may compensate for other functional or structural changes related to the disease process, and that connectivity within a given network may change in a non-linear fashion dependant on region and function. This research was supported by a grant from the CHDI (A2015) and a grant from the NINDS (RO1 NS054893).

P75B Empathy deficits in alcohol dependents: evidence from fMRI and functional connectivity analysis

Mukesh Kumar[1], Shilpi Modi[1], Janani Rajagopalan[1], Pawan Kumar[1], Subash Khushu[1]

[1]NMR Research Centre, Institute of Nuclear Medicine and Allied Sciences, Delhi, India

Background: The present study is aimed at exploring the functional connectivity underlying emotional empathy deficits in alcohol-dependents as compared to healthy controls using functional Magnetic Resonance Imaging (fMRI) and connectivity analysis of fMRI data.
Methods: 14 male alcoholic patients (mean age 34.25 ± 6.08; DSM-IV criteria) and 14 healthy males (mean age 28.15 ± 4.72) with no past history of alcohol or any other drug abuse underwent the fMRI study. At the time of study, alcoholics were abstinent from alcohol for 17.5 ± 4.5 days as verified by random administration of alcohol breath test and gamma glutamyl transferase levels. The evaluation of emotional empathy abilities was carried out using Inter-Personal Reactivity Index (IRI) questionnaires. fMRI was carried out on a 3 Tesla whole-body MRI system using echo-planar T2*-weighted sequence (projected using Nordic Neurolab). Block paradigm was used in which active phase consisted of natural photographs depicting the misery and suffering after any natural calamity and subject rated the photographs on a five point rating scale based on subjective intensity of emotions after viewing those photographs. Baseline consisted of

Table 1. Connectivity Table

*Connectivity in Alcoholic vs. Control contrast **				*Connectivity in Controls vs. Alcoholic contrast**			
	Seed region	*Target regions*	*K*		*Seed region*	*Target regions*	*K*
R	Amygdala	L Associative visual cortex (AVC)	121	R	Amygdala	R Somatosensory associative cortex (SAC)	111
R	Lingual gyrus	RAVC	218	R	Lingual gyrus	L SAC	172
R	IOG	R Secondary Visual cortex	118	R	IOG	R & L Cingulate Cortex	111
L	Hippocampus	R & L Cingulate cortex	132	L	Hippocampus	R & L AVC, R SAC	217
R	Fusiform gyrus	R & L Premotor cortex	164		Cerebellar vermis	R Anterior prefrontal, L Dorsal frontal cortex	113 107
R	Calcarine gyrus	R Fusiform gyrus, R AVC	350	L	IOG	L SAC, R Anterior prefrontal cortex	148
R	IFG	L SAC R AVC	404 91	R	MOG	L Cingulate cortex	116
R	Putaman	L Angular gyrus	136	L	ITG	R & L Secondary visual cortex, AVC	357 135

*R-Right, L- Left, IOG & MOG-Inferior and Middle Occipital gyrus, IFG- Inferior Frontal gyrus, ITG- Inferior Temporal gyrus.

mosaic photographs where no subject response was required. fMRI data was processed using SPM8 and the Functional Connectivity Toolbox "CONN 13p'' was used for deriving the functional connectivity between Seed regions (obtained from group analysis of fMRI data in both the groups) and all the target regions available in CONN.

Results: IRI showed reduced emotional empathy scores (sum of empathy concern and personal distress) in alcoholics (mean 26.25 ± 7.16 (SD) as compared to controls (mean 37.29 ± 6.70 (SD). fMRI result showed greater clusters of activation in controls as compared to alcoholics for empathy task. In controls, connectivity analysis showed greater connectivity between seed regions and higher order emotion processing centers whereas in alcoholics connectivity was greater between seed regions and the visual processing areas of the brain (Table 1).

Conclusion: Reduced functional connectivity between emotion processing areas might be responsible for lower/altered emotional empathy in alcoholics as compared to controls.

P76B Differential effect of normal aging and ischemic stroke in the deficit of low-frequency fluctuations of the default-mode network

Christian La[1], Pouria Mossahebi[1], Veena A. Nair[1], Justin Sattin[2], Marcus Chacon[2], Matthew Jensen[2], Elizabeth M. Meyerand[3,4], Vivek Prabhakaran[1,2]

Depts. of [1]Radiology, [2]Neurology, [3]Biomedical Engineering, [4]Medical Physics, University of Wisconsin-Madison, Madison, WI, USA

Background: The processes of normal aging and onset of diseases such as ischemic stroke impose re-organization of the cortical networks. Among these, the default-mode network (DMN) has consistently been implicated with decreases in both activation and connectivity strength, in particular in the slow-5 (0.01–0.27 Hz) range of resting-state frequencies. Here, we proposed to investigate a possible differentiation of the aging- vs. stroke-related deficits of the DMN, with a characterization of low-frequency fluctuation (LFF) of groupICA derived network sub-components' principal component.

Methods: We performed a mid-order groupICA on 127 eyes-closed rs-fMRI sessions from a group comprised of healthy young and old subjects, aging patients with risk factors for stroke, aging stroke patients in the acute stage and aging patients in the sub-acute stage, and have identified three sub-components of the DMN: posterior-DMN, anterior-DMN, and ventral-DMN. Of these, the posterior-DMN was the only component disrupted in both aging and stroke. An analysis of LFF of the posterior component was implemented with six univariate measures descriptive of the power spectra: peak oscillation amplitude, area under the curve (AUC), fractional ALFF, peak oscillation frequency, FWHMx, and skewness.

Results: Investigation of posterior-DMN co-activation yielded no dramatic differences between the deficits from ischemic stroke and normal aging, with both conditions exhibiting decreased co-activation over the posterior cingulate cortex. In contrast, our analysis of LFF presented a difference in the distribution of low-frequency oscillations among the assessed population groups. Two statistically significant observations were made: 1) a deviation in peak oscillation frequency with aging [fig., label 1], and 2) a reduction in cortical oscillation power as measured by peak oscillation amplitude [fig., label 2], AUC, and fractional ALFF in the sub-acute stroke patients. Oscillations in the slow-5 band were also revealed to be more susceptible to disruption from those processes than that of slow-4 (0.027–0.08 Hz).

Conclusions: Despite the high variability of the oscillations, our results suggest selective influences of aging on the low-frequency oscillations within the posterior-DMN component, particularly on the slow-5 oscillations. This suggests that an aging network may operate at a non-optimal frequency inhibiting the functioning of the network. In contrast, stroke patients in their sub-acute stage exhibited a global reduction of cortical oscillation power, potentially representative of their diseased brain state.

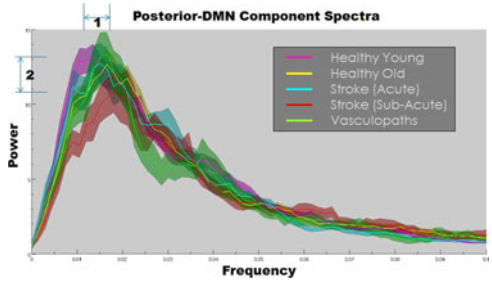

P77B Relation of functional connectivity to cognitive abilities in adolescents from socioeconomically diverse backgrounds

Julia A. Leonard[1], Amy S. Finn[1], Allyson P. Mackey[1], Carlo de los Angeles[1], Calvin A. Goetz[1], John D.E. Gabrieli[1], Susan Whitfield-Gabrieli[1]

[1]*Department of Brain and Cognitive Sciences, Massachusetts Institute of Technology, Cambridge, MA, U.S.A*

Background: A fundamental question in developmental cognitive neuroscience is how brain maturation supports the development of cognitive abilities and how the environment shapes this relationship. The present study explored this question with resting-state functional MRI in a socioeconomically diverse sample of teenagers.
Methods: Seventy-five students (mean age = 14.5, 37 male) who completed a statewide standardized test, participated in a resting state scan. All data was preprocessed with SPM and run through ART (Artifact Detection Tool) to detect outliers based on motion and global signal intensity. Outlier volumes were used as nuisance parameters within the first level general linear model. Connectivity analyses were conducted using the Conn functional connectivity toolbox (http://www.nitrc.org/projects/conn/). The aCompCor method of noise reduction was implemented. Seeds from the default mode network (DMN) and dorsal attention network (DAN) were chosen based on previous work (Fox et al., 2005).
Results: Students were separated into low-socioeconomic status (SES) and high-SES groups based on whether or not they received free or reduced lunch from the public school system. Although the DAN and DAN-DMN relationship did not differ between the SES groups, there was a trend for stronger connectivity within the DMN in the low-SES group ($t(73) = 1.8$, $p = .07$). Linking these data to behavior within the groups, we found that the strength of the DMN predicted standardized test scores in the low-SES group ($r = 0.297$, $p = .05$) but not in the high-SES group, while anti-correlations between the DAN-DMN predicted standardized test scores in the high-SES group ($r = -0.344$, $p = .05$), but not in the low-SES group.
Conclusions: These results reveal two main findings: (1) that resting state networks do not strongly differ by SES and (2) that different neural features predict academic success depending on one's SES background.
Citations

Fox, M. D., Snyder, A. Z., Vincent, J. L., Corbetta, M., Van Essen, D. C., & Raichle, M. E. (2005). The human brain is intrinsically organized into dynamic, anticorrelated functional networks. *Proc Natl Acad Sci U S A, 102*(27), 9673–9678.

P78B Disrupted network interactions in chronic cocaine dependents as revealed by modular network analysis of resting-state functional MRI

Xia Liang[1,2], Hong Gu[1], Betty Jo Salmeron[1], Yuzheng Hu[1], Yong He[2], Elliot Stein[1], and Yihong Yang[1]

[1]*Neuroimaging Research Branch, National Institute on Drug Abuse, Baltimore, Maryland, United States,* [2]*State Key Laboratory of Cognitive Neuroscience and Learning, Beijing Normal University, Beijing, Beijing, China*

Background: Functional neuroimaging studies on chronic cocaine dependents revealed their impairments in various brain circuits, including the striatum (ST) regions involved in reward, the regions in medial temporal lobe (MTL) implicated in memory and emotion, and the executive control network (ECN). In addition, two other brain networks, the default mode network (DMN) putatively involved in self-referential processes and the salience network (SN) implicated in interoceptive processing, have also shown addiction-related impairments. However, whether and how the network-level interactions are disrupted in chronic cocaine users is unknown.
Methods: 47 cocaine dependents (CD) and 47 healthy controls (HC) were recruited for resting fMRI scan. Following standard preprocessing, we constructed a binary voxel-wise brain network for each subject by thresholding the correlation matrix ($p < 0.001$, FDR-corrected). We performed modular analysis to identify the modules of interest on group networks averaged across each cohort. We then investigated cocaine-related alterations of intra-/inter-module connectivity at both module and nodal levels. At the module level, the intra-module (inter-module) connectivity was the sum of all connections within a module (between two modules). At the nodal level, we calculated the within-module degree and participation coefficient (PC) for each node as indices of their intra- and inter-module connectivity. We also assessed the relationships between intra-/inter-module connectivity and cocaine-using behaviors and Toronto Alexithymia Scale (TAS-20).
Results: In both HC and CD groups, modular analysis uncovered five modules that were of particular interest in this study, including the DMN, SN, ECN, MTL and ST. On the modular level, we found that compared with HCs, CDs exhibited significantly decreased inter-module connectivity between the DMN and SN modules ($p = 0.0002$), and between the DMN and MTL modules ($p = 0.0045$). On the nodal level, CDs showed decreased PC in bilateral insula and rostral anterior cingulate cortex. Finally, we found that the intra-module connectivity within SN module showed significantly negative correlation with difficulty of describing feelings (DDF), which is a sub-scale score of TAS-20.
Conclusions: Our results demonstrate that cocaine addiction is associated with disruptions of network-level interactions, including default mode, salience and emotional networks. We also observed that the cocaine addicts with higher difficulty in describing feelings tend to be less connected within SN, suggesting that the deficits in interoceptive function may be associated with the impaired SN system. Together, our results may provide novel insights into the neurobiological mechanisms of cocaine addiction.
Acknowledgment: This work was supported by the Intramural Research Program of the National Institute on Drug Abuse, NIH.

P79B Dsyregulation of antiparallel task-negative and task-positive network components in the course of neurodegeneration

M. Gorges[1*], J. Heimrath[1*], N. Birbaumer[2,3], J. Kassubek, A.C. Ludolph[1], D. Lulé[1]

[1]*Department of Neurology, University of Ulm, Ulm, Germany,* [2]*Institute of Medical Psychology and Behavioral Neurobiology, Eberhard-Karls-University of Tübingen, Tübingen, Germany,* [3]*Ospedale San Camillo, IRCCS, Venezia, Italy*
**contributed equally*

Background: Amyotrophic lateral sclerosis (ALS) is the most common adult onset motor neuron disease with cardinal symptoms of neurodegeneration of motor neurons. Structural and functional changes in cortical networks have been described in the course of ALS. This study aimed at investigating whether the inability to down-regulate task-negative networks is associated with inability to substantially upregulate task-positive networks. Both networks are considered as anti-correlated components of the same network.

Methods: Using different MRI techniques, we investigated task-negative and task-positive cerebral networks to determine influence of neurodegeneration on these anti-correlated networks. N = 12 ALS patients and N = 12 healthy controls participated in the study. Task-negative networks were determined by functional connectivity parameters in the default mode network (DMN) in resting state sequences (6 pre-defined spherical ROIs). Task-positive networks were measured in a functional MRI (fMRI) paradigm of imagery and observation tasks of different movements. Before fMRI measurement, subjects practiced imagery of movements until they performed it vividly (at least 4 on a Likert scale 0–6) and without any muscular activity. Motor impairment of the patients as a measure of neurodegeneration was assessed using the ALS functional rating scale revised (ALS-FRS). Cognitive and psychiatric measurements were performed.
Results: Patients had an increased activity in the task-negative network in the sense of increased functional connectivity in parahippocampal areas and inferior parietal lobe of the DMN compared to controls. There was a trend for reduced connectivity in the course of the neurodegeneration (ALS-FRS and connectivity of parahippocampal areas and inferior parietal lobe $r = 0.62$ and $p = 0.08$). Furthermore, an altered pattern was seen in the task-positive network for movement observation and imagery of movement for ALS patients, e.g. a reduced activity for imagery of movements in motor and premotor areas (BA 4, BA 6). Increased activity was seen for ALS patients in e.g. parietal areas (BA 40) for movement observation and it increased the higher the motor impairments were.
Conclusions: Increased connectivity in the DMN in parahippocampal and parietal areas might represent an inability to downregulate the task-negative network while reduced activity in task-positive networks, e.g. in primary motor pathways might represent an inability to upregulate this antiparallel network. In the course of neurodegeneration, other parts of the task-positive network pointed towards dysregulation of these networks, e.g. parietal areas for higher order motor processing were increasingly upregulated.

P80B Imaging of resting state pathological networks in various neuropsychiatric disorders

Sandhya M.[1,2], R.D. Bharath[1], Rajanikanth P.[1], Neeraj Upadhyay[1], A.K. Gupta[1]

Cognitive neuroscience centre [1], Dept of NIIR, NIMHANS, MSR-INS [2]Consultant neuro radiologist, MSR-INS, Bangalore, Karnataka, India

Background: The identification of spatiotemporal correlation patterns in these spontaneous fluctuations has been termed resting state functional connectivity (fcMRI) and the identification of various networks has the potential to greatly increase the translation of fMRI into clinical care. Our article reviews the various functional networks in variety of pathological states and their neuropsychiatric clinical applications. Our main objective is to map the pathological functional networks in order to understand the clinical entity better and how we can translate the findings into practical applications. The other highlight of this article is that the processing has been performed on individual cases and demonstrates the role of resting fmri as a powerful clinical tool.
Methods: The neurological cases included are patients with stammering (speech network), charles bonnet (visual network), hallucination, Tinnitus (auditory network), pathological laughter (emotional network), writers cramps (motor cortex) patient with tumour in motor cortex (correlation of structural lesion and functional network) and temporal lobe epilepsy (default mode network). Psychiatry disorders such as schizophrenia (executive network) and depression (cerebellar network) are also included. These are compared with healthy control subjects. Data acquisition using a 3T scanner (Skyra, Siemens, Erlangen, Germany). T1-weighted, three-dimensional, high-resolution imaging was performed to facilitate localization of fMRI activation.
Results: The networks considered are both normal networks and how their connectivity differs from healthy controls and also pathological networks which develop as part of disease. *In Charles bonnet hallucinations* hyper connectivity was noted in the extra striate and peri striate pathway and hypo connectivity in primary visual striate pathway. *In tinnitus* hyper connectivity was noted in the limbic and cerebellum. Hypo connectivity was noted in the auditory and cortical auditory pathway. *In writers cramps* hyper connectivity was noted in the motor cortex of affected hand and hypo connectivity in the unaffected hand. *In stuttering* hyper connectivity was noted in the sensorimotor and speech motor areas and hypo connectivity in the language reception area and sensory association area. *In mesial temporal sclerosis* the anterior DMN showed hyperconnectivity and posterior DMN showed hypoconnectivity. *In depression* hyper connectivty was noted in the paleocerebellum and hypoconnectivity in the neocerebellum *In schizophrenia* the DLPFC an ACC showed hyperconnectivity and hypoconnectivity was noted in the SMA and paracentral lobule. *In pathological laughter* hyper connectivity was noted in the involuntary laughter network and hypoconnectivity was noted in the voluntary network. *In case of brain tumour* ipsilateral motor cortex showed hypoconnectivity and hyper connectivity was noted in the contralateral motor cortex.
Conclusions: Resting fmri has an important role to evaluate various networks and map the abnormal functional networks on per case basis as has been highlighted in our article.

P81B Neural circuitry associated with mood dysregulation in response to stress: shared across psychiatric diagnoses and differs by sex

K. Mareckova[1,2], L. Holsen[1], R. Admon[1,3], K. Lancaster[1], S. Whitfield-Gabrieli[4], J. Goldstein[1]

[1]Brigham and Women's Hospital, Harvard Medical School (HMS), Boston, MA, USA; [2]CEITEC, Masaryk University, Brno, Czech Republic; [3]McLean Hospital, HMS, Boston, MA USA; [4]Massachusetts Institute of Technology, Boston, MA, USA

Background: The stress response engendered by negative valence stimuli is normally distributed in the population and implicated in every psychiatric disorder, in part, as dysregulated mood traits. Further, women are more likely to express mood dysregulation than men. Thus, in this study, we hypothesized that *neural circuitry activity and connectivity* associated with mood dysregulation would be shared across psychiatric diagnoses and healthy people and differ by sex. Stress response circuitry includes anterior hypothalamus (HYPO), amygdala (AMYG), hippocampus (HIPP), medial prefrontal, orbitofrontal and anterior cingulate cortices (mPFC, OFC, ACC), and periaqueductal gray (PAG). In this functional MRI (fMRI) study, we tested the hypothesis that lower mood would be associated with higher blood oxygen level dependent (BOLD) signal changes in these stress circuitry regions in response to a mild visual stress challenge and that the effect sizes would be larger in females. We further predicted that connectivity between hypothalamus and cortical and hippocampal regions would be stronger in subjects with lower mood, given the key role of hypothalamic nuclei in arousal under stress and the inhibitory control roles of the cortex and hippocampus.

Methods: 74 adults (39 females) from a community population of schizophrenia and bipolar psychoses, major depression, and healthy controls, underwent an fMRI task of a mild visual stress challenge, using negative, neutral, and fixation images adapted from the International Affective Picture System. Twenty (12 females) were diagnosed with psychoses, 20 (12 females) with recurrent major depressive disorder in remission, and 34 (15 females) were healthy controls. Mood-related symptoms and anxiety were systematically assessed by standard instruments and factor analyzed to create composite measures of mood and anxiety state and trait. fMRI occurred on a 3T Siemens scanner and was analyzed using SPM8. Contrasts comparing negative versus neutral stimuli were assessed for stress response circuitry regions. Mood and sex were entered as covariates to assess their impact on BOLD responses in stress circuitry regions. Task-related connectivity was assessed using generalized psychophysiological interaction (gPPI).
Results: Small volume corrections showed a positive relationship between mood and BOLD in left ($z = 3.4$, *FWE* $p = 0.006$) and right ($z = 2.63$, *FWE* $p = 0.05$) HYPO, left ($z = 3.37$, *FWE* $p = 0.03$) and right HIPP ($z = 3.62$, *FWE* $p = 0.01$), and left ($z = 3.57$, *FWE* $p = 0.04$) and right ($z = 3.49$, *FWE* $p = 0.05$) OFC, effect sizes that were larger in females vs. males. gPPI analysis using right and left HYPO as seeds showed connectivity between (1) left HYPO and left anterior insula ($z = 3.44$, *FWE* $p = 0.04$), (2) right HYPO and left OFC ($z = 3.72$, *FWE* $p = 0.03$), and (3) right HYPO and right HIPP ($z = 3.58$, *FWE* $p = 0.02$) increasing as a function of mood, and stronger among females. Results remained significant even after adjusting for diagnosis.
Conclusions: Brain response and connectivity in the neural circuitry associated with mood dysregulation in response to stress was shared across diagnoses and healthy individuals, with a greater BOLD response among women versus men. Lower mood was associated with larger stress-related increases in connectivity between the key subcortical stress-arousal region (HYPO) and inhibitory (such as OFC and HIPP) and integrative affective (insula) regions.

P82B Functional connectivity in chronic stroke compared with normal aging changes

V. Balaev[1], L. Mayorova[1,2], A. Petrushevsky[1,2], O. Martynova[1,3]

[1]Institute of Higher Nervous Activity and Neurophysiology RAS, Moscow, Russia, [2]Centre for Speech Pathology and Neurorehabilitation, Moscow, Russia, [3]National Research University ''Higher School of Economic'', Moscow, Russia

Background: Ischemic stroke affects not only the areas near the lesion but also intact regions. Functional connectivity (FC) of distinct resting state networks (RSN) in chronic stroke patients is able to reveal compensatory and/or suppression effects on various brain functions. In order to explore this issue we compared FC in post-stroke patients, young and older healthy adults.
Methods: Participants were 13 patients (age 57.6 ± 7.3) after ischemic stroke in the left middle cerebral artery, 13 older (age 66.6 ± 6.9) and 13 (age 28.3 ± 6.8) young healthy right-handed adult voluntaries. We used Siemens 1.5 T MRI scanner to acquire T2*-weighted EPI (180 volumes, TR = 2 s, TE = 50 ms, 32 slices, slice thickness - 3 mm, FoV-192 mm, matrix - 64×64). Data was preprocessed using SPM8. Seven resting state networks were defined by ICA (GIFT). Correlation coefficients (CC) between RSNs (Fig. 1) underwent Fisher's r-to-z transformation and were subjected to ANOVA, followed by post-hoc analysis.
Results: Default mode network (DMN) was higher correlated with sensorimotor (SSM) network in young than in older adults and stroke patients, nevertheless stroke patients demonstrated less connectivity between DMN and SSM compared with older adults. Remarkably, the intact right frontoparietal (RFP) network was significantly more correlated with frontal (FRO) and auditory (AUD) in post-stroke patients comparing with young and older participants. CC between RFP and default mode network (DMN) networks was significantly higher in young adults group relative to that for patients. Moreover, younger adults showed the greater CC of sensorimotor (SSM) network with visual (VIS) and DMN.
Conclusions: Considering the fact that frontoparietal networks are known to be essential for executive functions, the increased FC between RFP network and AUD as well as FRO networks could be related to compensatory mechanisms. Decreased FC within SSM, DMN and VIS in older subjects corresponds to dysregulation of sensorimotor processing in normal aging.

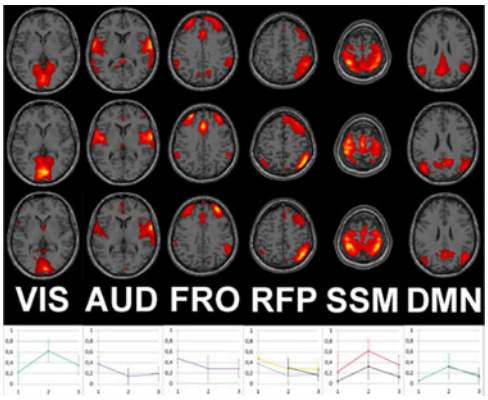

FIG. 1. Post-hoc of z scores between RSNs. VIS-red, AUD - blue, SSM - green, FRO - orange, RFP - purple and DMN - black line. 1 - post-stroke, 2-young, 3 raw- old subjects.

P83B Subchronic administration of reboxetine or amisulpride influences local and global resting state activity within the noradrenergic and dopaminergic pathway in healthy volunteers

C. D. Metzger[1,3,4], M. Wiegers[2], M. Walter[1,3], B. Abler[2], H. Graf[2]

[1]Department of Psychiatry and Psychotherapy, Centre for Behavioral Brain Sciences (CBBS), Otto-von-Guericke University, Magdeburg, Germany; [2]Department of Psychiatry, University of Ulm, Ulm, Germany; [3]Leibniz Institute for Neurobiology, Magdeburg, Germany; [4]Institute of Cognitive Neurology and Dementia Research, Magdeburg, Germany

Background: A variety of resting state data in psychiatric populations are currently acquired within big consortia, aiming to individualize diagnostics, treatment options and improve individual treatment outcome. While these studies provide rich insights regarding disease-relevant neuronal alterations in big sample sizes, most of the investigated psychiatric patients in clinical reality are treated with psychopharmacological medication. Our study therefore aimed to investigate the effects of noradrenergic and dopaminergic medication on local and global resting state behaviour in healthy volunteers, trying to identify mere drug effects rather than disease-related changes. We hypothesized, that the antidepressant and selective noradrenalin reuptake inhibitor reboxetine (REB) modulates the noradrenergic

pathway (NE-pathway), while the antipsychotic drug amisulpride (AMS) was hypothesized to act on the dopaminergic pathway (DA-pathway).
Methods: 20 healthy male volunteers were included in a randomized, double-blind, placebo-controlled cross-over design, taking either AMS, REB or placebo for one week, with a two-week wash-out phase between trials. After each trial, subjects completed an fMRI session including a 10 min eyes-closed resting state scan in a 3 Tesla Siemens scanner (FOV 192 mm, voxelsize $3\times3\times3.75$ including 0.75mm gap, TR 1500 ms, TE 35 ms, flip angle 90°). Drug intake was controlled by plasma levels. Resting state analysis was performed using DPARSF (Chao-Gan and Yu-Feng, 2010), the resting state fMRI data analysis toolkit (REST, Song et al. 2011) and SPM8 (Wellcome Department, London, UK). Whole brain functional connectivity (rsFC) was analyzed for the locus coeruleus (NE-pathway), the substantia nigra (DA-pathway), amygdala and nucleus accumbens (influenced by both noradrenergic and dopaminergic neurotransmission). The frequency amplitude of low frequency fluctuations (fALFF) was calculated on whole brain level as a marker of local resting state behaviour.
Results: REB altered local resting state behavior as measured by an increase in fALFF specifically in regions of the NE-pathway like the locus coeruleus. This change was linearly correlated with REB plasma levels. Moreover REB caused global changes in rsFC between regions within the NE-pathway, increasing rsFC between locus coeruleus, tectum, thalamus, amygdala and hippocampus. AMS increased fALFF in regions within the DA-pathway, like putamen. This change was linearly correlated with AMS plasma levels. Moreover AMS increased rsFC between regions within the DA-pathway like substantia nigra, nucleus accumbens, thalamus and amygdala (all $p<0.005$, corr.).
Conclusions: REB as a selective noradrenaline reuptake inhibitor specifically increased local fALFF and global rsFC between regions of the NE-pathway. AMS (acting pro-dopaminergic at low doses, Schoemaker et al. 1997) increased local and global resting state properties specifically of regions within the DA-pathway. These results provide help for the interpretation of 'big-data' in psychiatric populations (Castellanos et al. 2013).

P84B Functional Connectivity within Reward Network Regions is Associated with Sensitivity to Reward in Schizophrenia

L.V. Moran[1], L.E. Stoeckel[2], K. Wang[1], D. Ongur[1], D.A. Pizzagalli[1], A.E. Evins[2]

[1]McLean Hospital, Belmont, MA, [2]Dept. of Psychiatry, Massachusetts General Hospital, Boston, MA

Background: In studies of reward, individuals with schizophrenia demonstrate abnormal salience attribution to neutral/unrewarding stimuli. Because of evidence in schizophrenia of impaired modulation of large-scale networks by salience network hub anterior insula, we tested the hypothesis that insular functional connectivity with reward regions ventral striatum (VS) and ventromedial prefrontal cortex (vmPFC) is associated with reward sensitivity in schizophrenia.
Methods: Eighteen outpatients with schizophrenia and 11 controls completed resting state fMRI and a probabilistic reward task in which asymmetric reinforcement leads to a preferential response bias to the rewarded stimulus. Each subject completed the task and fMRI during two sessions while administered nicotine or placebo (drug currently blinded). Usable fMRI data was obtained from 11 subjects in each group. Z-transformed correlation coefficients between average time courses of ventral (vAIns) and dorsal anterior insular (dAIns) seeds and VS and vmPFC were calculated as connectivity measures. Response bias and z correlation maps were averaged across sessions.
Results: No significant group differences in response bias were observed ($p=0.7$). Subjects with schizophrenia had decreased connectivity between dAIns and vmPFC ($p=0.02$). Connectivity between dAIns and both VS and vmPFC was negatively correlated with response bias in schizophrenia ($r=-0.65$, $p=0.03$; $r=-0.72$, $p=0.01$), but not in controls (group differences in correlation coefficients: $z=-2.2$, $p=0.03$; $z=-2.4$, $p=0.01$).
Conclusions: Reward sensitivity was intact in clinically stable outpatients with schizophrenia. The finding of negative correlations between insular-reward region connectivity and response bias in schizophrenia, but not controls, suggests that reduced connectivity may be a compensatory mechanism associated with preserved reward sensitivity, possibly related to down-regulation of insula-mediated attribution of aberrant salience to unrewarded stimuli.

P85B Functional Hyper-Connectivity State in Parkinson's Disease Patients Without Cognitive Impairment: Disease-Specific Pathological Process or Adaptive Changes?

M. Gorges, H.-P. Müller, A.C. Ludolph, J. Kassubek

Department of Neurology, University of Ulm, Ulm, Germany

Background: Cognitive decline is one non-motor feature in Parkinson's disease (PD). In this study, we assessed functional connectivity (fcMRI) in PD patients after detailed classification of their cognitive state spanning the range of cognitively normal to PD associated dementia. Particularly, we aimed at contrasting PD patients without (PD-CU) and with (PD-CI) cognitive impairment against healthy controls in intrinsic connectivity networks (default mode, frontoparietal control, dorsal- and ventral attention, visuospatial, motor, basal ganglia-thalamic, brainstem, cerebellar).
Methods: Clinically and neuropsychologically confirmed PD-CU ($N=14$, median: 70 years) and PD-CI ($N=17$, 72 years) patients were compared with age matched healthy controls ($N=22$, 68 years). All subjects underwent fcMRI at a 3T scanner (Magnetom Allegra, 200 vol., 36 slices, 64×64 pixels, slice thickness 3.5 mm, pixel size 3.5 mm × 3.5 mm, TR = 2.2 s, TE = 30 ms). The data were analyzed using the *Tensor Imaging and Fiber Tracking* software package. The algorithm for fcMRI data processing comprised: 1) quality control and motion correction, 2) resampling to a cubic 1 mm grid, 3) MNI normalization, 4) spatial smoothing (7 mm FWHM), 5) temporal linear detrending and temporal filtering (0.01–0.08 Hz), 6) seed-based correlation and 7) Fisher's r- to z-transformation. Possible effects between groups were detected by using a voxel-wise *t*-test. Resulting *p*-values were corrected for multiple comparisons at <0.05 FDR followed by cluster-wise correction.
Results: All 10 ICNs were unambiguously identified for each group (PD-CI, PD-CU, controls). With an exception of the cerebellar and visuospatial intrinsic connectivity networks, all other networks revealed significant alterations in that intrinsic functional connectivity (iFC) was increased in PD-CU and decreased in PD-CI patients compared with controls. More specifically, increased connectivity preferentially presented in subcortical structures whereas decreased iFC was found in areas associated with the default mode network.
Conclusions: Besides the interpretation that anti-Parkinsonian treatment may contribute to increased iFC in PD-CU patients,

adaptive changes as an attempt to maintain cognitive performance may emerge also as a possible explanation. Another alternative possibility could be a loss of the inhibitory influence as part of the pathological process that result in an excessive pathological firing pattern in 'denial-of-service' fashion, i.e. brain areas excessively communicating are no longer responsible for functional interaction with other structures. In summary, increased iFC in PD-CU patients demonstrated that fcMRI may be a sensitive in-vivo measure of alterations in brain function before cognitive deficits have manifested.

P86B Developmental Changes in the Functional Connectivity of the Insular Cortex in Individuals with Autism Spectrum Disorder

T.Q. Nguyen[1,2], B. Baran[1,2], K.R.A. Van Dijk[1,3], S. Santangelo[2,4], D.S. Manoach[1,2], S. Whitfield-Gabrieli[5]

[1]Athinoula A. Martinos Center for Biomedical Imaging, Massachusetts General Hospital, Charlestown, MA, USA, [2]Department of Psychiatry, Massachusetts General Hospital, Harvard Medical School, Boston, MA, USA, [3]Department of Psychology, Center for Brain Science, Harvard University, Cambridge, MA, USA, [4]Department of Psychiatry, Maine Medical Center, Maine Medical Center Research Institute, Portland, ME, USA, [5]Department of Brain and Cognitive Sciences and McGovern Institute for Brain Research, Massachusetts Institute of Technology, Cambridge, MA, USA

Background: The insula plays a critical role in the processing of emotional and visceral sensory/motor information. Autism Spectrum Disorder (ASD) is associated with impairment in the understanding of sensations, intentions and emotions of self and others. The objective of the present study is to investigate developmental changes in the functional connectivity of the insular cortex in individuals with ASD with a well-matched sample of neurotypical controls (NT).
Methods: Participants were 38 high-functioning individuals with ASD (ages 8–21, mean = 13.9, SD = 3.8, 7 female) and 34 neurotypical controls (ages 8–25, mean = 14.8, SD = 4.5, 6 female), who were matched for age ($p = .41$), sex, and the number of motion artifacts ($p = .42$). The neuroimaging protocol included resting-state functional MRI (two 6-minute sessions) and structural MRI on a 3T Siemens Trio scanner. Artifact Detection Tools (ART) were used to mark time-points corrupted by motion (relative motion > 2 mm or signal intensity > 3 SD larger than global mean). Following standard preprocessing in SPM8, motion artifacts and physiological sources of noise were regressed out and functional connectivity was investigated using the ***Conn*** toolbox.
Results: A between-group comparison of seed-to-voxel connectivity with a bilateral insula seed (BA13) revealed a cluster in the right somatosensory cortex (peak: 42, −8, 60, 374 voxels). Connectivity between the bilateral insula and the right somatosensory cortex cluster was significantly stronger in the ASD group (Fisher's $z = .23 \pm .117$) than the NT group (Fisher's $z = .11 \pm .115$). Furthermore age correlated positively with connectivity between these two regions in the ASD group ($r = .41$, $p = .01$) but not in the NT group ($r = -.14$, $p = .42$). When participants with ASD were divided into three groups [children (8–12 yrs), adolescent (13–17 yrs), and adult (18–25 yrs)], the magnitude of the difference in the connectivity of the insula to the somatosensory cortex was most robust in the adults (partial-$\eta^2 = .491$) as compared to the adolescents (partial-$\eta^2 = .111$) and children (partial-$\eta^2 = .108$).
Conclusions: These preliminary findings suggest that ASD is characterized by hyperconnectivity of the insula and the somatosensory cortex. Further analyses will elucidate how the developmental trajectory of this hyperconnectivity relates to the nature and severity of ASD symptoms.

P87B Effects of HIV on Fronto-Striatal Connectivity in the Combination Anti-retroviral Therapy (cART) Era

M. Ortega[1], M.R. Brier[1], R. Paul[4], B.M. Ances[1,2,3]

[1]Dept. of Neurology, [3]Dept. of Radiology [3]Dept. of Biomedical Engineering, Washington University in Saint Louis, St. Louis, MO, USA, [4] Dept. of Psychology, University of Missouri, St. Louis, MO, USA

Background: The human immunodeficiency virus (HIV) can cause neuronal dysfunction leading to neurocognitive impairment. Currently, only neuropsychological (NP) tests are used to categorize neurocognitive impairment, but this method can be biased and often is time consuming. A non-invasive marker such as magnetic resonance imaging (MRI) may provide sensitivity and specificity to complement NP testing. HIV causes widespread atrophy not only within subcortical (caudate and putamen) but also cortical structures. However, few studies have investigated the potential functional changes in fronto-striatal connectivity in HIV infected (HIV+) individuals. We used resting state functional MRI (rsfcMRI) to investigate the effects of HIV on functional connectivity (fc) correlations between the subcortical and cortical areas using *a priori* subject-based regions of interest (ROIs). We then compared fc to NP results in these same individuals.
Methods: In this cross-sectional study, laboratory (current and nadir CD4 cell counts, and plasma HIV viral load) and demographic (age, education, and gender) values were obtained from 49 HIV− and 132 HIV+ (65% on cART therapy) individuals. Freesurfer anatomical and functional analysis streams were completed for all individuals. RsfcMRI was performed to assess fc between subcortical ROIs and the cortical ribbon. These ROIs have been shown to project to multiple resting networks including: default mode (DMN), ventral attention (VATT), control (CON), and motor (MOT). An analysis of covariance (ANCOVA) was used to test if age, degree of cognitive impairment, or laboratory measures (plasma CD4 cell and HIV viral counts) affected striatal-cortical connectivity.
Results: HIV− and HIV+ groups did not differ between education and gender. HIV+ individuals were older ($p = 0.003$) and had marginally lower NP scores than HIV− controls ($p = 0.08$). HIV+ individuals had significantly decreased striatal connectivity to the DMN ($p < 0.001$) and VATT ($p < 0.001$) networks compared to HIV− controls. Within the HIV+ group, individuals on cART had greater fc correlations from to the striatum to DMN ($p = 0.024$) and VATT ($p = 0.01$) than HIV+ individuals not on cART. Rs-fc measures between subcortical and cortical regions did not correlate with NP testing or laboratory values (plasma viral load nor CD4 cell counts).
Conclusions: Striatal fc may detect brain dysfunction, however, fc was not decreased across all brain networks. Specifically, the MOT and CON networks did not have an HIV effect, implying that fc networks are not uniformly affected. HIV+ individuals on cART had functional connectivity values closer to the HIV− levels, while HIV+ cART naïve individuals had the most diminished connectivity. Future longitudinal studies need to be performed to determine the impact of initiation of cART on fronto-striatal connections, as well as the pattern and sequelae of fc changes across the fronto-striatal networks and relationship to NP testing.

P88B Support vector prediction of aging using resting-state functional MRI connectivity

S. Peltier[1], J. Wiggins[2], L. Swain[3], Y. Kwak[4], B. Fling[4], C. Monk[2], R. Seidler[2,4], S.F. Taylor[5], R.C. Welsh[3,5]

[1]Functional MRI Laboratory, [2]Psychology, [3]Radiology, [4]Kinesiology, [5]Psychiatry, University of Michigan, Ann Arbor, MI, United States

Background: Multivariate techniques offer an alternative to standard univariate analysis in studying resting-state functional connectivity, and has recently been applied in fMRI using support vector machines (SVM) (LaConte 2005). Following recent work (Dosenbach 2010, Wang 2012), this study extends the investigation of predicting brain age using resting-state scans to the entire lifespan, using a large sample size from one site.
Methods: Data were acquired on a 3.0 T GE scanner. T2*-weighted data was acquired using a spiral-in sequence (TR/TE/FA/FOV = 2 s/30 ms/90/22 cm, 64 × 64 matrix, 3 mm slice thickness, 40 slices). Anatomical T1 overlays and whole-brain T1 SPGRs were also collected. 188 subjects in total were scanned: < 18 years old (n = 70), 18–50 years old (n = 64), > 50 years old, (n = 83). Subjects were instructed to keep their eyes open using a fixation cross during the resting state acquisition. All data was preprocessed using SPM8, including slice timing correction, realignment, anatomical coregistration and segmentation, normalization to MNI space, and spatial smoothing (5 mm FWHM). Nuisance regressors were removed prior to band-pass filtering and correlation, using the 160 ROIs defined in (Dosenbach 2010). Support vector machine learning was performed using the 3 dsvm toolbox in AFNI. Binary SVM classification was performed using a linear kernel and multistate classification, using young (< 18), middle (18–50), and old age (> 50) as labels. Support vector regression was performed using a linear kernel and epsilon width of 0.1. Leave-one-out cross-validation (LOOCV) was used to calculate accuracies and predicted values. For visualization, regression model weights were averaged across all LOOCV permutations, absolute value taken, and summed for all ROIs.
Results: SVM classification results in 92% accuracy for young vs. old, 87% for young vs. middle, 74% for middle vs. old. Support vector regression resulted in predicted brain age that tracked well with chronological age. The top weights in the regression model were located in the cingulo-opercular and default mode networks.
Conclusions: The default mode network was implicated as important in the aging process, agreeing with previous studies. Aging can be investigated using resting-state connectivity across the lifespan, forming the basis for examining age-dependent pathologies.

TABLE 1. TOP FIVE NODES HAVING THE HIGHEST SUMMED ABSOLUTE AVERAGE WEIGHTS IN THE REGRESSION MODEL

MNI coordinates			Relative		
x	*y*	*z*	weight	Label	Network
11	-12	6	1	Thalamus	cingulo-opercular
0	51	32	0.95	mPFC	default
-4	-31	-4	0.69	Post. cingulate	cingulo-opercular
-16	-76	33	0.69	Occipital	Occipital
8	-40	50	0.67	Precuneus	cingulo-opercular

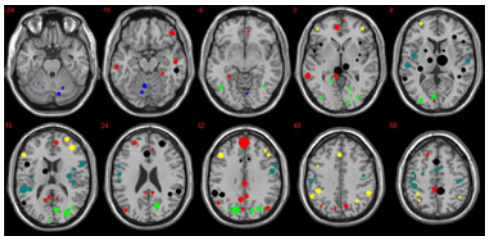

FIG. 1. Scaled regression weights for each ROI, on standard MNI anatomy. color corresponds to network identity (Black: Cingulo-opercular, Red: Default, Green: Occipital, Turquoise: Sensorimotor, Yellow: Fronto-parietal, Blue: Cerebellum).

P89B Decoupling between left vlPFC and parahippocampal gyrus during sacred value processing

M. Pincus, M. Prietula, G. Berns

Emory University, Atlanta, GA, United States

Background: Sacred values are beliefs and attitudes that people are unwilling to compromise. Our previous neuroimaging studies suggest sacred values are passively represented as deontological rules in the brain, evidenced by activation in the left ventrolateral prefrontal cortex (vlPFC)—a region consistently implicated in the retrieval of rules and associated with rigidity in the belief updating process. We reasoned that the passive retrieval of one's sacred beliefs, relative to non-sacred beliefs, may be associated with reduced connectivity between the vlPFC and evaluative processing regions in the brain, given that the strength and inflexible nature of sacred beliefs may obviate the need for elaborate evaluation. To test this question, we compared neural activation during the passive retrieval of sacred and non-sacred values and performed a psychophysiological interaction analysis using the left vlPFC as the seed region.
Methods: Participants were placed in the scanner and passively read value statements that ranged from mundane to sacred. Outside the scanner, participants were given the opportunity to submit a bid in a Becker-deGroot-Marshak auction for each value statement and their bid decisions were used to classify value statements as sacred or non-sacred. Using AFNI software, we performed a GLM on the whole brain to test whether regions involved in evaluative processing were significantly less active for sacred vs. non-sacred values. Using the left vlPFC as a seed region, we performed a psychophysiological interaction to test whether evaluative processing regions in the brain had significantly less connectivity with the left vlPFC during the retrieval of sacred vs. non-sacred values.
Results: We compared activation for sacred vs. non-sacred values in evaluative processing regions in the brain and found the left parahippocampal gyrus was significantly deactivated for sacred vs. non-sacred values ($t = -4.76$, $p < 0.005$). We performed a psychophysiological interaction analysis using the left vlPFC as the seed region and demonstrated that there was significant decoupling between activity in the left vlPFC and the left parahippocampal gyrus for sacred vs. non-sacred values ($t = -4.07$, $p < 0.005$).
Conclusions: The parahippocampal gyrus has been shown to be significantly activated across a range of tasks in which valenced stimuli are retrieved and evaluated implicitly and/or explicitly. Diminished activity in the left parahippocampal gyrus and

decoupling between this region and the left vlPFC during the retrieval of sacred vs. non-sacred values lends support to the hypothesis that sacred values are subject to minimal processing in evaluative networks. This finding suggests that sacred values remain inflexible and fixed in part because their retrieval is accompanied by diminished coupling with evaluative neural networks, precluding an opportunity to refine and modulate one's attitudes.

P90B Independent component analysis of passive listening reveals alterations in inter-network connectivity that correlate with emotional valence

E. Quattrocki Knight[1,2], Lisa Nickerson[1,2], Steven Lowen[1,2], Blaise de Frederick[1,2], Xiaoying Fan[1], Bruce Cohen[1,2]

[1]McLean Hospital, Belmont, MA, USA, [2]Harvard Medical School, Boston, MA, USA

Background: Although examinations of the resting state reveal that distributed brain regions organize into discrete, relatively reproducible networks, the myriad of different tasks accomplished by the brain suggest that these systems must dynamically respond to the ever-changing processing demands of the moment. Here, we have used a passive listening stimulation paradigm of emotionally salient sounds, devoid of cognitive or motor requirements, to examine whether interactions between these distributed networks differentially respond to the emotional salience of auditory stimuli. This study aimed to explore how the coupling between networks during auditory processing might adjust to contrasting emotionally salient sounds and whether emotional context alters inter-network correlations with known resting state networks.
Methods: Blood oxygenation level dependent (BOLD) signal activity was acquired on a Siemens 3.0 T Trio scanner during a passive listening of auditory stimuli (International Affective Digital Sound (IADS) library, Bradley, 2007) presented binaurally at 0.51 Hz using the Superlab 4® (Cedrus Corporation San Pedro, CA) software on a MacIntosh computer every 19.5 seconds. Other than passive listening, the subjects did not engage in any cognitive or motor task. The whole head BOLD fluctuations were then decomposed into a series of independent components using group independent component analysis (GIFT http://icatb.sourceforge.net). Dual regression was used to back reconstruct the subject specific timecourses and spatial maps for each component. Negative inverse covariance matrices were constructed to examine differences in the coupling between networks during two separate conditions (all pleasant sounds versus all unpleasant sounds).
Results: The initial ICA distinguished 50 separate components, including the previously identified resting state networks. Of these, 9 networks were selected, based on their hypothesized role in auditory and emotional processing for assessment of inter-component connectivity. Paired t-tests of the precision matrices indicate that the coupling between the auditory network, amygdala network, and the default mode network differs between the pleasant and unpleasant sessions.
Conclusions: Our findings suggest that inter-network changes in coupling might provide one possible mechanism for a differential response to contrasting emotionally valenced auditory stimuli. Additionally, subcortical networks, such as the amygdala network, may interact differently with both primary sensory cortex as well as the default mode network depending on the emotional context.

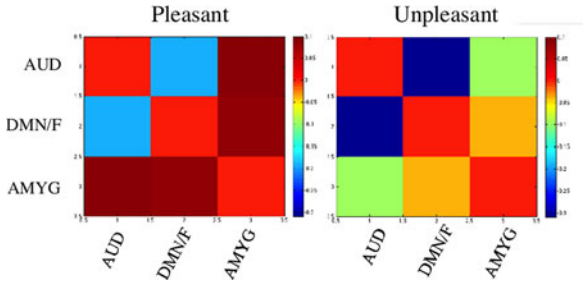

FIG. 1. Negative inverse covariance matrix of three components during the two conditions.

P91B Resting-State Functional Magnetic Resonance Imaging of Subconcussion

B.B. Reynolds[1], T. Chatlos[1], D.K. Broshek[1], M. Wintermark[1], S. Saliba[1], H.P. Goodkin[1], T.J. Druzgal[1]

[1]University of Virginia, Charlottesville, Virginia, USA

Background: The traumatic brain injury literature has started to describe subconcussion as an entity distinct from concussion. This differentiation is driven by concerns that cumulative head impact may correlate with short-term concussion risk and/or long-term development of neurodegenerative diseases, specifically chronic traumatic encephalopathy (CTE). The closest direct evidence for subconcussion has come from a small number of experiments in the neuropsychology and neuroimaging literature, studying athletes in high impact sports. Neuropsychology or neuroimaging studies of subconcussion have yet to describe significantly reliable findings in individual athletes. Concussion is hypothesized to reflect a diffuse injury of rotational acceleration forces that results in shear injury of axons at tissue interfaces. We hypothesize subconcussion to represent a similar mechanism, with more subtle effects per individual impact, but combining to have insidious consequences. The relatively diffuse, microscopic nature of injury limits the reliability of conventional imaging techniques, such as computed tomography and anatomic magnetic resonance imaging (MRI). However, resting state functional magnetic resonance imaging (rs-fMRI) represents a very promising method for measuring the physiologic signal of subconcussion in individual athletes.
Methods: In the fall of 2013, our research group collected rs-fMRI data from a cohort of football (N = 21) and lacrosse (N = 30) players, both in a pre-season scan and again in an immediate post-season scan. In each rs-fMRI scan, we calculated measures of global brain connectivity – specifically using methods more indifferent to the spatial distribution of findings than typical region of interest analyses. Standard mass univariate analyses were used to compare the pre-season and post-season brain connectivity metrics. In addition, support vector machine (SVM) learning classification was performed on the connectivity metrics, to test if the SVM could distinguish pre-season from post-season scans in individual athletes.
Results: For the football players, the total SVM classification accuracy was 78.6% ($p = 0.001$) across all individual scans. The classifier correctly identified 16 of 21 preseason scans and 17 of 21 postseason scans; classification accuracy for the preseason scans was 76.2% ($p = 0.004$) and for the postseason scans was 81.0% ($p = 0.003$). The overall sensitivity was 80.0% and specificity was 77.3%. The SVM model for the football players performs well above chance in distinguishing preseason from postseason rs-fMRI connectivity metrics.

For the lacrosse players, the total SVM classification accuracy was 51.7% (p = 0.383) across all individual scans. The classifier correctly identified 16 of 30 preseason scans and 15 of 30 postseason scans; classification accuracy for the preseason scans was 53.3% (p = 0.388) and for the postseason scans was 50.0% (p = 0.507). The overall sensitivity was 51.6% and specificity was 51.7%. The SVM model for the lacrosse players performs no different from chance in distinguishing preseason from postseason connectivity metrics.

Conclusions: Our preliminary data presents a compelling argument that rs-fMRI is capable of demonstrating physiologic effects of subconcussion in individual athletes.

P92B Incorporation of multiple processing strategies increases the diagnostic utility of resting state BOLD acquisitions

M. E. Robinson[1], R. E. McGlinchey[1,2], W. P. Milberg[1,2], D. H. Salat[1,2,3]

[1]VA Boston Healthcare System, Boston, MA, USA, [2]Harvard Medical School, Boston, MA, USA, [3]A. A. Martinos Center for Biomedical Imaging, Boston, MA, USA

Background: It is well established that resting state functional connectivity measurements can be a sensitive tool for understanding brain network activity in healthy populations, and much promising work is being done towards developing these measurements as diagnostic tools. Strategies for processing these data have been developed in order to refine the raw BOLD time course such that it best represents neural activations. This work seeks to show that the same resting state fMRI acquisition can be made sensitive to multiple clinically relevant group differences through manipulation of processing strategies, increasing the diagnostic capability of a single acquisition.

Methods: Resting state fMRI scans from a cohort of well-characterized Iraq and Afghanistan Veterans (n = 209, 2 6-minute runs per participant) were processed using a seed-based correlation to the superior third of the isthmus of the cingulate (a DMN seed) on the cortical surface using a variety of processing strategies (e.g. with and without global signal regression, varied temporal filtering and smoothing). Group-level comparisons to close-range blast exposure, post-traumatic stress disorder (PTSD), traumatic brain injury (TBI) were compared across processing strategies.

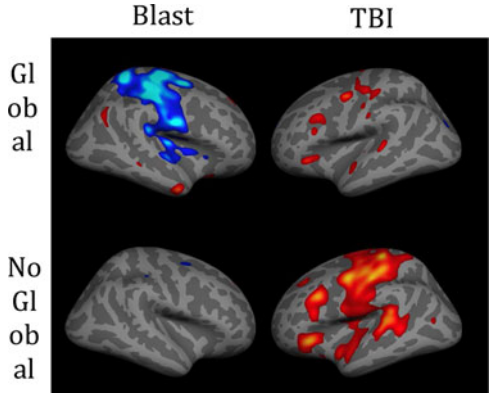

FIG. 1. Group differences ($p = 0.05$, uncorrected) due to (Left) close-range blast exposure (n = 209), and (Right) Comorbid TBI and PTSD vs PTSD only (n = 112). Analyzed with (Top) and without (Bottom) inclusion of the global signal regression.

Results: Different processing strategies revealed different group differences; the most salient example (shown in Fig 1) is the effect of global signal regression on comparisons of close-range blast and TBI. These comparisons also differed in their sensitivity to smoothing, regression of white matter and ventricular CSF time courses, and temporal filtering. Correlation to PTSD severity was improved by changing the low-pass filtering from 0.10 to 0.20 Hz.

Conclusions: These results demonstrate that the diagnostic capability of a single resting state fMRI acquisition can be expanded by incorporating multiple processing strategies including ones that deviate from those designed to maximize sensitivity to neuronal signal contribution, as they reveal materially different information. This presents the possibility of increasing the specificity of resting state BOLD clinical biomarkers through their comparison. At present, the physiological underpinnings of these observations are unknown, however, likely candidates include regional changes in hemodynamic coupling and speed of vascular reactivity.

P93B Anterior hippocampal-cortical resting-state fMRI dysconnectivity is a psychosis biomarker

N. Samudra[1], E.I. Ivleva[1], N. Hubbard[2], B. Rypma[1,2], C.A. Tamminga[1]

[1]UT Southwestern Medical Center, Dallas, TX, United States; [2]Center for BrainHealth, UT Dallas, Dallas, TX, United States

Background: Hippocampal (Hipp) activity increases in schizophrenia psychosis, based on both functional and molecular evidence. This increase potentially alters functional Hipp-cortical networks, pathologically disrupting limbic connectivity. Further, schizophrenia and psychotic bipolar patients share clinical and cognitive characteristics, implying that psychosis as a whole, beyond categorical DSM diagnoses, may represent a clinical dimension associated with unique biomarkers. Here, our aim is to identify alterations in Hipp-cortical networks using resting state fMRI (rsfMRI) in individuals with psychosis (PS) vs. healthy controls (HC). More specifically, given functional and anatomic distinctions between anterior/ventral and posterior/dorsal Hipp, we examine whether Hipp dysconnectivity along hippocampal long axis contributes differentially to the biology of psychosis.

Methods: 87 PS (23 schizophrenic, 38 schizoaffective disorder, and 26 psychotic bipolar I disorder patients) and 66 HC were included. rsfMRI scans were acquired on a 3 Tesla Philips scanner. Whole Hipp, anterior Hipp, and posterior Hipp seeds and respective bilateral connectivity networks were defined in the AFNI fMRI analysis package. Results are presented at a threshold of $p < .01$, $k = 32$ contiguous voxels.

Results: Compared to HC, PS showed reduced regional connectivity, most notably between anterior Hipp and superior temporal gyrus, anterior cingulate, thalamus, and medial frontal gyrus, as well as cerebellum and caudate, with a large number of ROIs and an anterior distribution. Whole Hipp seed connectivity resembled anterior Hipp connectivity, with a decrease in total number of ROIs with reduced connectivity. Posterior Hipp seed connectivity also demonstrated decreased connectivity in PS, but with fewer ROIs and a posterior distribution (i.e., cerebellum). Significant differences in connectivity from Hipp seeds were not noted across DSM diagnostic categories.

Conclusions: Overall Hipp-neocortical connectivity is reduced in psychosis, without respect to DSM diagnoses. Strongest

connectivity changes are localized to limbic structures, consistent with a limbic dysconnectivity model of psychosis. Anterior Hipp appears to be most involved in pathophysiology of psychosis, as it is strongly dysconnected with frontal and limbic regions associated with psychosis. This is consistent with literature implicating these regions in the pathogenesis of psychotic and affective disorders. Future analyses include testing associations between these network connectivity changes and clinical and cognitive characteristics, including psychosis severity, lifetime psychosis burden and medication effects. Improved understanding of psychosis biomarkers, including, functional dysconnectivity, may facilitate better treatment for psychotic disorders.

P94B State-dependent functional connectivity disturbance within and between brain networks in children with ADHD

A. Schläpfer[1,2], T. Koenig[3], D. Brandeis[1,2,4,5]

[1]University Clinics for Child and Adolescent Psychiatry (UCCAP), University of Zurich, Zürich, Switzerland
[2]Neuroscience Center Zurich, University of Zurich and ETH Zurich, Zürich, Switzerland
[3]University Hospital of Psychiatry Bern, Department of Psychiatric Neurophysiology, Bern, Switzerland
[4]Zurich Center for Integrative Human Physiology, University of Zurich, Zürich, Switzerland
[5]Department of Child and Adolescent Psychiatry and Psychotherapy, Central Institute of Mental Health, Medical Faculty Mannheim/ Heidelberg University, Mannheim, Germany

Background: Attention deficit hyperactivity disorder (ADHD) is one of the most common childhood neuropsychiatric disorders. Recent approaches examined brain connectivity for dysfunction in functional network organization. We hypothesize that connectivity within the default mode network (DMN), and the anticorrelation between the DMN and the cognitive control network (CCN) is reduced in ADHD, especially when switching from rest to task states. We thus examined altered state-dependent functional connectivity (FC) within and between two brain networks (DMN, CCN) in children with ADHD.
Methods: We recorded fMRI (3T, with simultaneous EEG) data to compare functional brain network differences between resting and task (tracking Stop task) states in children with ADHD and a control group. A high model order ICA was used for functional segmentation (75 components) of both tasks and groups before calculating FC within and between different networks, and compare them among tasks and groups. We only report on differences between the Stop task and the resting state.
Results: Preliminary results (n = 5 per group, study ongoing) suggest that within the DMN, children with ADHD showed less negative FC in the long-range connections between anterior and posterior cingulate cortex (ACC-PCC) and between ACC and precuneus. Within the CCN, FC tended to be weaker in children with ADHD. Several brain regions showed less FC with the right superior parietal lobule (SPL). The FC group comparison between states and networks (DMN – CCN) indicated that the ADHD group had less negative correlations between CCN and DMN particularly in PCC, and more negative connections between the two networks in SPL.
Conclusions: These findings suggest that children with ADHD may display disturbed FC differences between task and resting states both within and between the DMN and CCN networks. They show generally less pronounced negative FC differences within the DMN and less positive FC differences in the CCN. The long-range connections within the DMN may be particularly impaired in the ADHD group. These results suggest that children with ADHD may have specific difficulties while switching between rest and task. The PCC seems to play an important functional role in such state switching. Further analyses will include other brain networks like motor network and subcortical network and also include structural connectivity.

P95B Functional connectivity in multiple cortical networks is associated with cognition during aging

E.E. Shaw[1], A. Schultz[1], R.A. Sperling[1,2,3], R.L. Buckner[1,2,4], T. Hedden[1,2]

[1]Massachusetts General Hospital, Boston, MA, USA, [2]Harvard Medical School, Boston, MA, USA, [3]Brigham and Women's Hospital, Boston, MA, USA, [4]Harvard University

Background: Resting state functional connectivity magnetic resonance imaging has become a widely used tool for measuring the integrity of large-scale cortical networks (Andrews-Hanna et al., 2007; Damoiseaux et al., 2008). In this study we used a novel method for defining *a priori* cortical networks in a reference dataset that were then applied to our test dataset. We examined the relationships between four association cortex networks and three domains of cognition in a group of cognitively healthy older adults. We predicted that individuals with greater network integrity would exhibit higher cognitive scores.
Methods: We examined multiple cortical networks using Template-Based Rotation (TBR), a method that applies a priori network and nuisance component templates defined from an independent dataset to test datasets of interest. We applied a priori templates to a test dataset of 66 younger (ages 18–34) and 276 older adults (ages 65–90) from the Harvard Aging Brain Study to examine the relationship between multiple large-scale cortical networks and cognition. Cognition was assessed with factor scores derived from a neuropsychological battery, representing processing speed, executive function, and episodic memory. Resting-state BOLD data were acquired in two six-minute acquisitions on a 3-Telsa scanner, screened for data quality metrics including motion, and processed using the TBR procedure to extract individual-level metrics of network integrity in multiple cortical networks.
Results: Age differences between younger and older adults were observed in the integrity of multiple cortical networks and in cognition. Within the older adults, integrity in multiple large-scale cortical networks was positively related to all cognitive domains. Controlling for the correlations between networks, only a positive relation between the fronto-parietal control network and executive function was significant, suggesting specificity in this relationship. An exploratory analysis of cluster-level relationships with cognition found that both within-network and across-network connections were related to cognition.
Conclusions: These results extend prior work (e.g., Andrews-Hanna et al., 2007), demonstrating that functional connectivity metrics in multiple cortical networks are associated with individual variation in cognition, and further suggesting that TBR may be a useful tool for measuring relationships between reduced network integrity and cognition during aging.

P96B Lesion topography and functional connectivity disruption influence different domains of post-stroke deficit

J. S. Siegel[1], L. E. Ramsey[1], A. Z. Snyder[1,2], Ravi V. Chacko[3], K.Q. Weinberger[5], G. L. Shulman[1], M. Corbetta[1,2,4]

Background: Deficits in stoke patients have classically been attributed to focal damage to particular parts of the brain (eg. expressive language, Broca's area). More recent evidence suggests that functionality is represented in widely distributed networks. We asked whether domain specific deficit (motor, language, spatial attention, spatial memory) is better predicted by lesion location or by functional disruption to specific networks.
Methods: We recruited a heterogeneous cohort of 132 patients within 1–2 weeks following a first-time stroke. We acquired MRI, 35 min of resting state functional connectivity fMRI (FC), and an extensive behavioral battery spanning aforementioned domains. Lesions were manually segmented on the structural scans and FC correlations were calculated for each pair of 169 predefined ROIs. These measures of anatomical damage and FC correlations were entered into a leave-one-out ridge regression model to determine the percent of variance that could be explained in each behavioral domain. We mapped the most predictive weights back on to the cortex to visualize the locations and connections that are relevant to each of the domains tested.
Results: We found that some deficits corresponded better to lesion location while others corresponded better to long-range functional connections. Left motor deficit was better predicted by lesion location than FC (FC = 31.7%, lesion = 54.4% $p = 0.0045$), language deficit was better predicted by lesion location than FC (FC = 26.0%, lesion = 44.2%, $p = 0.035$), spatial memory deficit was better predicted by FC than lesion location (FC = 38.5%, lesion = 14.0%, $p = 0.0042$), visual field neglect did not show a significant difference in predictive power of FC and lesion location (FC = 31.4%, lesion = 20.4%, $p = 0.3875$).
Conclusions: These results shed light on the value of resting state functional connectivity in understanding the pathophysiology of stroke, and suggest that the relative merits of the localizationist view versus network view may depend on the domain of brain function.

P97B The Responsive Amygdala: Treatment-induced Alterations in Functional Connectivity in Pediatric Complex Regional Pain Syndrome

Simons L.E.[1,2,3], Pielech M.[1], Erpelding N.[1,2], Linnman C.[1,2], Moulton E.[1,2], Sava S.[1], Lebel A.[1,2], Serrano P.[1], Sethna N.[1,2], Berde C.[1,2], Becerra L.[1,2], Borsook D.[1,2]

[1]P.A.I.N. Group, Department of Anesthesia, Boston Children's Hospital and Center for Pain and the Brain, [2]Harvard Medical School, [3]Department of Psychiatry

Background: The amygdala is a key brain region with efferent and afferent neural connections that involve complex behaviors such as pain, reward, fear and anxiety. A role for the amygdala in pain processing has been derived from a number of preclinical and clinical investigations that include: (i) a relay station for afferent nociceptive information from the parabrachial nucleus; (ii) negative affective states; (iii) increased excitability and plasticity in chronic pain; and (iv) lesions inhibiting the development of chronic pain.
Methods: This study evaluated resting state functional connectivity of the amygdala with cortical and subcortical regions in a cohort of pediatric chronic pain patients with complex regional pain syndrome (CRPS; n = 12) with age-gender matched controls (n = 12) before (Time 1) and after (Time 2) intensive physical, occupational, and psychological pain treatment. To our knowledge, this is the first study to investigate amygdala resting state functional connectivity in children with CRPS and the first to examine brain circuit responsiveness associated with brief, intensive pain rehabilitation treatment.
Results: (1) Disease state. We observed enhanced functional connectivity between the amygdala and cognitive/emotional (prefrontal, cingulate cortex, basal ganglia), sensorimotor (thalamus, somatosensory cortex) and integrative processing (cerebellum, parietal lobe, thalamus) areas, with differences predominantly in the left amygdala in the pre-treated condition; (2) Treatment effects. Mean average pain ratings significantly decreased from 5.65 ± 0.54(SE) to 4.07 ± 0.67(SE) ($t(10) = 3.49$, $p < .01$). For pain-related fear, average fear of pain scores significantly decreased from 43.8 ± 4.2(SE) to 22.9 ± 3.3(SE) ($t(9) = 3.58$, $p < .01$). Dampened hyperconnectivity between the left amygdala and prefrontal cortex (inferior, middle), motor cortex, parietal lobe, and cingulate cortex after intensive pain rehabilitation treatment within patients with nominal differences observed among healthy controls from Time 1 to Time 2; (3) Pediatric CRPS and pain-related fear. Functional connectivity to several regions key to fear circuitry (prefrontal cortex, bilateral middle temporal lobe, bilateral cingulate, hippocampus) correlated with higher patient reported pain-related fear scores controlling for the influence of pain level; (4) Pain-related fear and treatment effects. Decreases in functional connectivity between the motor cortex, cingulate, insula, frontal areas and the left amygdala were associated with less fear at the end of treatment (after controlling for changes in pain level), suggesting that several changes in intrinsic brain functional connectivity can be linked to pain-related fear symptom improvement and maps closely to the broad changes in connectivity that were observed in patients after treatment.
Conclusions: Our data suggest that there are rapid changes in amygdala connectivity following an aggressive treatment program in children with chronic pain. Fear of pain is an important component of the behavioral consequences of the disease and is associated with alterations in brain circuitry. Implementing targeted treatment that affects specific components of the chronic pain state, such as elevated fear, can in turn impact brain pathways. Lastly, measures of intrinsic amygdala functional connectivity may serve as a potential indicator of treatment response.

P98B Resting state auditory network strength is related to age, brain structure and familial risk for developmental dyslexia in infants

Danielle D. Sliva[1], Barbara Peysakhovich[1], Yingying Wang[1,2], P. Ellen Grant[1,2,4], Nadine Gaab[1,2,3], Mathieu Dehaes[5]

[1]Boston Children's Hospital, MA, USA, [2]Harvard Medical School, Boston, MA, USA, [3]Harvard Graduate School of Education, Cambridge, MA, USA, [4]Athinoula A. Martinos Center, Charlestown, MA, USA, [5]University of Montréal, Canada

Background: Developmental dyslexia (DD) is a brain-based learning disability that affects 5–17% of children. DD is diagnosed after reading onset, despite a strong familial basis with

genetic factors likely involved in brain development[1]. Disruptions in resting state networks have been reported in children with DD[2], however it is unknown whether they are present earlier in life. We investigate factors related to functional connectivity strength, and its relationship with structural connectivity, within the auditory network in infants with (FHD+) and without (FHD-) a family history of DD to explore the potential of intrinsic functional network organization as an early precursor of DD.

Methods: Resting state functional, structural and diffusion imaging was performed on a 3T Siemens scanner with 17 FHD+ and 23 FHD− infants (4.6–17.7 months, mean 9.6 ± 3.3) during natural sleep. Pre-processing included removal of outliers (ART, www.nitrc.org/projects/artifact_detect/), slice-timing correction, realignment, co-registration to an age-appropriate anatomical template[3], and regression of signal from motion, CSF and white matter. Independent component analysis[4] was used to estimate intrinsic resting state networks ($p > 0.5$), spatial network maps ($z > 3$) were co-registered to each individual's anatomy and the auditory network component was visually identified. Diffusion processing included removal of artifactual gradients and automatic fiber-tract quantification[5]. The mean z value of each auditory map was used to assess relationships of network strength with age, family history status, gender, and mean fractional anisotropy (FA) of the inferior longitudinal fasciculus (ILF).

Results: Mean auditory network strength (z-stat) differed between FHD+ and FHD− groups ($p < 0.05$), and age and FHD status together predicted a significant amount of the variability in auditory network strength ($p < 0.001$). Moreover, FHD status ($p < 0.5$), age ($p < 0.01$), and mean FA of the ILF ($p < 0.05$) significantly correlated with auditory network strength, and higher auditory network strength was linearly associated with age ($p < 0.01$) and higher mean FA of the ILF ($p < 0.01$), after accounting for FHD status.

Conclusions: Results suggest that auditory network strength at rest is significantly related to family history, age and brain structure in infants, and therefore may be a useful early precursor of DD preceding reading and language development. Further investigation of intrinsic network organization in infants at risk may help identify brain processes and developmental trajectories associated with DD, allowing for early identification and remediation strategies prior to final network pruning and myelination.

References: [1] Peterson, R.L. & Pennington, B.F. (2012). Lancet 379(9830):1997–2007. [2] Koyama, M.S., et al. (2013). PLos One 8(2):e55454. [3] Shi, F. et al. (2011). PLoS One 6(4):e18746. [4] Beckmann, C.F. et al. (2005). Philos. Trans. R. Soc. B. Biol. Sci. 360(1457):1001–13. [5] Yeatman, J.D. et al. (2012). PLoS One 7(11):e49790.

P99B Identifying possible subtypes in depression by whole brain data mining - a strategy to refine future diagnostic classification

B. Sundermann[1], S. Feder[1], H. Wersching[2], A. Teuber[2], H. Kugel[1], W. Heindel[1], K. Berger[2], B. Pfleiderer[1]

[1]University Hospital Münster, Department of Clinical Radiology, Münster, NRW, Germany, [2]University of Münster, Institute for Epidemiology and Social Medicine, Münster, NRW, Germany

Background: Resting state fMRI (rs-fMRI) in combination with supervised learning has been introduced as a candidate diagnostic tool in major depressive disorder (MDD). Positive results have been reported from small patient samples in optimized laboratory settings. Purpose of this analysis was to explore the inherent structure of a large dataset of MDD patients recruited in clinical routine settings to guide such diagnostic approaches.

Methods: This study is based on the MDD cohort of the BiDirect Study (funded by the German Ministry of Education and Research, BMBF, grants 01ER0816 and 01ER1205). fMRI data at rest were acquired using a brief acquisition protocol at 3.0 T following varied familiarization periods. Patients without definitely unipolar MDD or with structural lesions or artefacts potentially corrupting image analyses were excluded. The resulting dataset was partitioned into multiple subsets with comparable sample characteristics to serve exploration and independent validation of potential supervised classification. Analyses reported here were carried out on a subset of 180 MDD patients (50.84 ± SD 7.13 y). Atlas-based whole brain functional connectivity (FC) of 200 regions of interest (Craddock 2012, Hum Brain Mapp 33:1914–28) was calculated. Z-transformed correlation coefficients were subjected to hierarchical clustering. Cluster stability was assessed by k-means-clustering. FC in the clusters was compared by t-tests.

Results: In a first step, three clusters were identified. One of these clusters encompassed mainly subjects with low scores for current depressive symptoms. After excluding subjects without definite MDD symptoms on the date of scanning (n = 21), two distinct highly stable clusters (92% agreement of results from hierarchical and k-means clustering) were identified. They did not differ significantly regarding demographical, protocol, clinical (including comorbidity) or treatment variables incorporated. In univariate analyses significant differences were observed between these two clusters (k-means result) in 94.7% of all pairwise FC coefficients, suggesting rather global effects.

Conclusions: Explorative unsupervised analyses of FC in MDD indicate the existence of two subgroups not defined by typical clinical phenotype, demographics, treatment or circumstances of data acquisition. Therefore, considering a potential heterogeneity of rs-fMRI datasets in MDD as well as a measure of current symptom severity seem to be useful to improve conceivable diagnostic approaches based on rs-fMRI. However, it remains unclear if subgroups identified here represent biological correlates of true subtypes in the clinically defined entity MDD or potentially confounding factors nonetheless important in diagnostic classification.

P100B Evaluating global connectivity in schizophrenia patients

S. F. Taylor[1], Y. Fang[1], D. Kessler[1], R. C. Welsh[1,2], C. Sripada[1,3]

[1]Department of Psychiatry, [2]Department of Radiology, [3]Department of Philosophy, University of Michigan, Ann Arbor, Michigan, USA

Background: Schizophrenia has long been recognized as a disorder of impaired integration and association, and recent developments in connectomics have enabled investigators to address this question through low frequency BOLD fluctuations. Using a variety of connectomic methods, recent work has identified both decreased as well as increased connectivity in schizophrenia.

Methods: Resting state fMRI scans (spiral acquisitions, TR = 2 sec, 6–8 min) were performed on 39 chronic, medicated schizophrenia (SCZ) patients (age = 40.8 ± 11.5 yrs; 29 M) and 42 healthy control (HC) subjects (age = 36.6 ± 12.1 yrs; 29 M). Pre-processing included scrubbing of high displacement frames, removal of physiological noise with CSF&WM regressions, but

no global signal regression. Three SCZ subjects (from 42) were excluded for excessive movement. Time courses from 264 spherical regions of interest from Power et al [1] were extracted and cross-correlation matrices were obtained between all regions (Pearson r, Z-transformed). For each region, we computed the global average of the correlation strength (CS-avg), average positive correlation strength (CS-pos) and average of the absolute value of the correlation strength (CS-abs). CS was averaged across the brain and within each of 13 sub-networks (within network and with whole brain) defined by Power [1].
Results: SCZ showed greater global CS-pos ($p = 0.04$) and CS-avg ($p = 0.02$) across the entire brain, but no significant difference in CS-abs. For the 13 sub-networks, there were no differences for within-network connectivity except the dorsal attention network (SCZ > HC for CS-pos & CS-avg, $p < 0.05$), but multiple SCZ > HC differences for network-to-whole brain connectivity (CS-avg, $p < 0.01$: visual, memory retrieval, salience, cerebellar; $p < 0.05$: sensori-motor hand, cingulo-opercular, fronto-parietal, dorsal attention; CS-pos, $p < 0.01$: cerebellar; $p < 0.05$: visual, memory retrieval, salience, sensori-motor hand, cingulo-opercular, dorsal attention). Analysis of movement revealed no significant group difference in mean frame displacement pre- or post-scrubbing ($p > 0.3$), and no change in results when high and low moving subjects were excluded to match groups on mean frame displacement. Exploratory analyses revealed no significant correlations between CS measures and clinical and demographic measures. However, significant positive correlation occurred between antipsychotic dosage and global CS-avg ($p = 0.04$) and CS-pos ($p = 0.13$). Antipsychotic dosage also correlated at trend or greater levels ($p < 0.2$) for every sub-network showing a significant group difference except the salience, fronto-parietal and cerebellar networks.
Conclusions: A complex picture emerges for global connectivity strength in schizophrenia, with medication a potential confound. However, given that other groups report *reduced* connectivity, these results suggest that other factors besides medication drive the heterogeneous findings.
[1] Power JD, et al, Neuron. 2011, 72(4):665–78.

P101B Fluctuations of attention network activation during the resting state reflect fluctuations in subjective attentional state

L. Van Calster[1], A. D'Argembeau[1], E. Salmon[2], F. Péters[1], S. Majerus[1]

[1]Université de Liège, Liège, Belgium, [2]Cyclotron Research Centre, Liège, Belgium

Background: While at rest, a range of cognitive processes are likely to occur in an individual's mind. These processes have received increasing interest by studies revealing the recruitment of a range of neural networks activated during the resting state. The aim of this study was to explore the function of one of these resting state networks, the dorsal attention network (dAN). We hypothesized that activation of this network during the resting state is not merely the result of neurophysiological homeostatic processes, but reflects the active recruitment of controlled attentional processes during spontaneous cognition.
Methods: The spontaneous neural activity of 16 adult participants was measured via fMRI and a novel experience-sampling technique for cognitive experiences and associated attentional state during the resting state was implemented. We determined the neural activity associated with different attentional states, by focusing on neural events shortly preceding the report of a given cognitive experience and its associated attentional state.
Results: We observed fluctuating activation of the superior frontal part of the dAN. Importantly, this activation was stronger when participants reported being in a state of controlled attention.
Conclusions: This is the first study highlighting a direct relationship between attentional network activation and individual subjective experience of attentional control, which may reflect one of the core phenomenological features of the resting state.

P102B The Idiosyncratic brain: Spatial distortion of spontaneous connectivity patterns in adults with Autism Spectrum Disorder

A. Hahamy[1], M. Behrmann[2], R. Malach[1]

[1]Department of Neurobiology, Weizmann Institute of Science, Rehovot, Israel, [2]Department of Psychology, Carnegie Mellon University, Pittsburgh, USA

Autism Spectrum Disorder (ASD) has been associated with a reduction in resting-state functional-connectivity (Just et al., 2004), though this assertion has recently been challenged by reports of increased connectivity in ASD (Lynch et al., 2013; Muller et al., 2011; Uddin et al., 2013). To address these contradictory findings, we examined whole-brain inter- and intra-hemispheric functional-connectivity in several resting-state datasets acquired from adults with high-functioning ASD and matched controls. In all analyzed datasets, we revealed consistent sets of regions of increased and decreased connectivity in ASD groups compared to controls. Importantly, we show that this heterogeneity stems from a novel ASD characteristic: idiosyncratic distortions of the functional-connectivity pattern relative to the typical "canonical" template. The magnitude of the individual pattern-distortion in homotopic inter-hemispheric connectivity was significantly correlated with behavioral symptoms of ASD. We propose that individualized alterations of the functional-connectivity organization is a core characteristic of high-functioning ASD. This result not only accounts for existing discrepant findings but offers a potential signature of altered functional brain organization in ASD.

Just, M.A., Cherkassky, V.L., Keller, T.A., and Minshew, N.J. (2004). Cortical activation and synchronization during sentence comprehension in high-functioning autism: evidence of underconnectivity. Brain 127, 1811–1821.

Lynch, C.J., Uddin, L.Q., Supekar, K., Khouzam, A., Phillips, J., and Menon, V. (2013). Default mode network in childhood autism: posteromedial cortex heterogeneity and relationship with social deficits. Biol Psychiatry 74, 212–219.

Muller, R.A., Shih, P., Keehn, B., Deyoe, J.R., Leyden, K.M., and Shukla, D.K. (2011). Underconnected, but how? A survey of functional connectivity MRI studies in autism spectrum disorders. Cereb Cortex 21, 2233–2243.

Uddin, L.Q., Supekar, K., Lynch, C.J., Khouzam, A., Phillips, J., Feinstein, C., Ryali, S., and Menon, V. (2013). Salience network-based classification and prediction of symptom severity in children with autism. JAMA Psychiatry 70, 869–879.

P103B Acute increases in functional connectivity following physical exercise are associated with cerebrovascular reactivity

T.B. Weng[1], G.L. Pierce[2], W.G. Darling[2], D. Falk[3], V.A. Magnotta[4], M.W. Voss[1]

[1]The University of Iowa, Department of Psychology, Iowa City, Iowa, USA, [2]The University of Iowa, Department of Health and

Human Physiology, Iowa City, Iowa, USA, [3]The University of Iowa, Department of Internal Medicine, Iowa City, Iowa, USA, [4]The University of Iowa, Department of Radiology, Iowa City, Iowa, USA

Background: Physical exercise has been shown to attenuate age-related cognitive decline, and reduce risk for dementia. However, the mechanisms through which regular physical exercise benefits brain function have not been fully characterized in humans. We have previously reported that a one-year exercise intervention modifies the functional connectivity of resting state networks (RSNs) in healthy older adults. In order to more directly probe the process through which repeated bouts of exercise benefit brain function, this study sought to examine the acute effects of physical exercise on RSNs in healthy younger and older adults. Additionally, we investigated whether baseline cerebrovascular reactivity (CVR) would predict responsiveness of RSNs to an acute exercise manipulation. We hypothesized that greater CVR would be associated with a greater capacity for exercise-induced change, especially in older adults.
Methods: A sample of younger (N = 12, mean age = 26) and older adults (N = 8, mean age = 67) received resting-state functional magnetic resonance imaging scans immediately before and after a 30-minute session of exercise. On separate occasions, each participant engaged in one of two conditions: 1) active cycling at 65% of maximum heart rate and 2) passive cycling in which a motor within the exercise machine mechanically moved participants' legs with minimal effect on heart rate or muscle tone. Prior to each pre-exercise resting-state scan, participants also performed a breath-holding task in the scanner. Change in functional connectivity (ΔFC) was derived for both exercise conditions by subtracting pre-exercise FC from post-exercise FC. CVR was expressed as the blood-oxygen-level dependent (BOLD) signal response to breath-holding and submitted to a linear regression as a predictor variable for exercise-induced ΔFC.
Results: Within several cognitively relevant networks, regional increases in FC were observed and were significantly greater following the active cycling compared to the passive cycling. These increases were not seen in sensory networks suggesting specificity in the effects of the exercise. Results also indicated differential effects of age where older adults showed greater ΔFC. Finally, greater CVR predicted greater ΔFC independent of age.
Conclusions: These results are the first documentation of acute exercise effects on functional brain networks in humans and are consistent with animal studies that demonstrate immediate effects of exercise on the brain. Further, the results suggest that CVR predicts responsiveness of RSNs to exercise. Long-term goals aim to identify the mechanisms by which physical exercise induces acute changes in network connectivity.

P104B How Hypothalamic Hamartoma Induces Multifocal Epilepsy and Global Encephalopathy – As Seen By Resting State Connectivity

V.L. Wolf[1], A.M. Shetty M.E.[3], A.A. Wilfong[1], and D.J. Curry[2]

[1]Department of Pediatric Neurology, Texas Children's Hospital, Baylor College of Medicine, Houston, TX, USA; [2]Department of Pediatric Neurosurgery, Texas Children's Hospital, Baylor College of Medicine, Houston, TX, USA; [3]Visualase Inc., 8058 El Rio St., Houston, Texas, 77054

Background: Epileptic encephalopathy (EE) mechanism is not well understood, as it is confounded by variability of the causative location and detectability of the underlying primary epileptogenic focus, and the downstream networks involved. Understanding the pathway from initial focus to EE holds the potential information in reversing the effect of the primary epileptogenic spread and downstream secondary epileptogic foci and EE. Children with hypothalamic hamartomas, associated with intractable epilepsy and EE, present uniquely uniform initial seizure localization, increasing the potential to more confidently identify the gap in knowledge for transformation of seizure focus to EE. We aim to define the pathway of network derangement responsible for this phenomenon using a clinically applicable, noninvasive, low risk measure - resting-state-fMRI (rs-fMRI).
Methods: Sedated rs-fMRI in 12 children with HH and 6 controls was used to determine the entire brain's rs-networks, identifying all areas of significant difference between those with HH. The severity of the derangement between these identified areas and the hypothalamus was determined using seed based partial connectivity analysis, thus, establishing the disrupted connectivity pattern between the hypothalamus and each target area. Lastly, the target areas with significant connectivity derangement with the hypothalamus were compared against prior reported areas of dysfunction detected by other modalities.
Results: The left amygdala-parahippocampal gyrus area and cingulate gyrus demonstrated the highest derangement in connectivity with the hypothalamus. These findings mirror the prior reports demonstrated by multiple other modalities - PET, electrode, and EEG-fMRI.
Conclusions: The disrupted connectivity of the neocortical networks extends far beyond the areas with direct anatomical connection to the hypothalamus. The initial spread of dysfunction is likely through direct anatomical connections. The subsequent areas disrupted are components of emotion-related networks. The cognitive and psychiatric disorders manifest as symptoms consistent with disruption of these emotion networks and provide an explanation of the epileptic encephalopathy.

P105B Childhood maltreatment affects spontaneous brain activity in young adults

D Yan[1], C.M. Anderson[2], E. Bolger[2], H. McCormack[2], C.E. McGreenery[2], K. Ohashi[2], M.H. Teicher[2]

[1]Massachusetts General Hospital, Harvard Medical School, Boston, MA, USA, [2]Brain Imaging Ctr. & Developmental Biopsychiatry Research Program., McLean Hospital, Belmont, MA, USA

Background: Childhood maltreatment is a prevalent problem and is risk factor for several psychiatric disorders. The studies of Teicher et al reported reduced hippocampal subfield volumes and altered network centrality associated with childhood maltreatment. In addition to the structural abnormality, the present study aimed to investigate the abnormality in spontaneous brain activity.
Methods: Resting state fMRI data of195 subjects who had provided self-report information about childhood maltreatment through the Adverse Childhood Experience (ACE) scale, childhood trauma questionnaire (CTQ) and Maltreatment and Abuse Chronology of Exposure (MACE) scale. Magnitudes of spontaneous brain activityin the low frequency band of resting state fMRI were analyzed in a voxelwise manner.Regression analysis was conducted to investigate the neural correlates of ACE score, MACE sum score and CTQ with demographic information as covariates (age, gender and years of education of the father, mother and the subject, as well as perceived financial sufficiency during childhood). Two groups of subjects were selected (ACE > = 3, N = 66 vs. ACE = 0, N = 68) and two sample t-test

was conducted to compare maps of magnitudes of spontaneous activity between subjects with significant childhood adversity with those with no reported adversity with the same covariates as in regression analyses.
Results: Higher levels of childhood adversity was associated with higher spontaneous activity in the precuneus, lower spontaneous activity in the dorsal medial prefrontal cortex and the insula, which is reflected from both group comparison and regression analysis with the ACE, CTQ and MACE total score as indicators of childhood adversity respectively.
Conclusions: These results suggest that childhood maltreatment affects the spontaneous brain activity of young adults in a dose-dependent manner, which implies that childhood maltreatment has long lasting impacts not only on brain structure, but also on its function.
References: Teicher, M.H. Anderson, C.M. Polcari, A. (2012) Childhood maltreatment is associated with reducedvolume in the hippocampal subfields CA3, dentate gyrus, and subiculum. PNAS. 109(9): E563–572.

Teicher MH, Anderson CM, Ohashi K, Polcari A. (2013) Childhood Maltreatment: Altered Network Centrality of Cingulate, Precuneus, Temporal Pole and Insula. Biol Psychiatry. pii: S0006-3223(13)00857-3.

P106B Neurovascular and Functional Connectivity Changes in Mild Traumatic Brain Injury (mTBI): from Acute Stage to Recovery

J. Yang[1], R. D. Welch[2], Z. Kou[3], R. Gattu[3], E. M. Haacke[3]

[1]Massachussette General Hospital Institute of Health Professions, Boston, MA, USA, [2]Emergency Medicine, Wayne State University School of Medicine, Detroit, MI, USA, [3]Radiology, Wayne State University School of Medicine, Detroit, MI, USA

Background: In the United States, about 1.7 million people sustain a Traumatic Brain Injury (TBI) each year and 75% of TBIs are concussions or mild TBI (mTBI) (Faul, Xu, Wald, Coronado, & Dellinger, 2010). Patients with mTBI are largely reported to develop post-concussion symptoms (PCS) and cognitive sequelae at one month post injury (Bazarian et al., 2005; 2008). However, most symptomatic mTBI patients have normal findings in clinical computed tomography (CT) and conventional magnetic resonance imaging (MRI) (Belanger et al., 2007). Few studies identified imaging biomarkers that are sensitive enough to detect mTBI and predict its recovery in the acute setting (within 24 hours). The objective of this study was to evaluate whether application of two advanced MRI methods, Susceptibility Weighted Imaging (SWI) and resting-state functional connectivity MRI (rs-fcMRI), will reveal acute changes in neurovascular structure and neural functions in association with clinical outcomes in mTBI patients.
Methods: 10 mTBI adult patients (mean age ± SD = 31.8 ± 10.2 years, 6 females) with GCS (Glasgow Coma Scale) score 15 treated at Detroit Receiving Hospital ER and 18 healthy age-matched controls were enrolled in the study. Patients received evaluation in acute setting (within 26 hours) and were followed up sub-acutely (within one to three months). Standardized Assessment of Concussion (SAC) and Advanced MRI scans (SWI and rs-fcMRI) were performed in the patient group for both visits. The control group received the same MRI scans for one visit. Data analysis was carried out using SPM8 (http://www.fil.ion.ucl.ac.uk/spm) and DPARSF V2.0 (Yan and Zang, 2010). The seed ROI was selected in the PCC to identify Default Mode Network (DMN). FC between other brain regions and the seed region was calculated and mapped. The cross correlation between 90 brain regions, defined by AAL Atlas, was calculated. The one-sample t-test connectivity maps of the patient and control group, as well as the two-sample t-test comparison between these groups were performed.
Results: Four of ten patients were lost to follow-up. All patients had a GCS score of 15 and normal CT results. The average SAC score was 24.8 at acute stage and 27.3 at follow-up stage (Total score = 30). Patients were significantly better over the two time points ($p < .05$), which is consistent with MRI results. The brain function connectivity increased from acute stage (26 hours) to sub-acute stage (one to three months). Patients demonstrated different FC within DMN in middle temporal gyrus, middle frontal gyrus, superior temporal gyrus, cuneus, inferior parietal lobule, superior frontal gyrus, inferior frontal gyrus compared to controls. No visible lesions or microbleeds were observed in anatomical images (SWI and T1 MPRAGE) in patients. However, SWI indicated involvement of subtle medullary veins in one patient and T1 images indicated frontal medullary vein damage post injury.
Conclusions: Taken together, both clinical outcome and advanced MRI findings indicated a recovery process post injury. mTBI patients demonstrated a distinctive FC pattern compared to the controls and started to approximate the normal level overtime. The neurovascular and FC changes open the door to understanding recovery in mTBI.

P107B Real-time fMRI neurofeedback training of amygdala modulates resting-state functional connectivity in depression

Han Yuan[1], Kymberly D. Young[1], Raquel Phillips[1], Vadim Zotev[1], Masaya Misaki[1], Jerzy Bodurka[1,2,3]

[1]Laureate Institute for Brain Research, Tulsa, Oklahoma, United States, [2]Center for Biomedical Engineering, The University of Oklahoma, Norman, Oklahoma, United States, [3]College of Engineering, The University of Oklahoma, Norman, Oklahoma, United States

Background: Amygdala hemodynamic responses to positive stimuli are attenuated in major depressive disorder (MDD), and normalize with remission. Real-time fMRI neurofeedback (rtfMRI-NF) amygdala training has been suggested as a potential therapeutic approach [1]. A recent rtfMRI-NF study reported that MDD subjects were able to increase their amygdala activity while recalling happy autobiographical memories, and this procedure resulted in improvements in self-reported mood [2]. In the present study we measured the resting state functional connectivity (RSFC) before and after rtfMRI-NF in MDD, as well as RSFC in matched healthy subjects, to investigate possibility of lasting neuromodulatory effect of rtfMRI-NF training of the amygdala in MDD.
Methods: 27 unmedicated individuals with MDD in a current major depressive episode (HDRS ≥ 17, mean ± SD: 22.11 ± 4.95) and 27 age/gender-matched, medically and psychiatrically healthy subjects (HDRS ≤ 7, mean ± SD: 1.04 ± 1.82) participated in the IRB approved study. All MDD participants underwent rtfMRI-NF in a protocol described in [2], in which they were instructed to feel happy by evoking positive autobiographical memories while trying to raise the activation level of the targeted ROI. 14 of the MDD subjects received active NF from the left amygdala (LA), and the other 13 MDD were in the control group with NF from a region putatively not involved in emotion regulation, i.e. the horizontal segment of intraparietal

sulcus. All imaging was done on a GE MR750 3T MRI scanner equipped with custom real-time fMRI system [3]. The whole brain resting-state fMRI scans (EPI, 8 min 40 sec, eyes-open, TR = 2s) were acquired before NF and on a separate visit more than one week after neurofeedback. The healthy subjects participated in a similar rtfMRI-NF protocol and a pre-NF resting-state scan was acquired. After preprocessing, RSFC was computed with the seed located in the active NF target, i.e. LA.

Results: Before NF, amygdala RSFC at the pregenual cingulate cortex (pgACC) and the precuneus in MDD differed from healthy subjects and covaried with HDRS scores ($p_{corrected} < 0.01$). ROI analysis further revealed that pre-RSFC between amygdala and pgACC and precuneus was decreased in MDDs relative to controls, and post-RSFC in MDD was partially normalized in both the active and control groups. Examining post-pre amygdala RSFC revealed that MDDs who received active NF, relative to those receiving control NF, showed increased connectivity between amygdala and left parahippocampal gyrus and bilateral middle frontal gyrus ($p_{corrected} < 0.01$).

Conclusions: The rtfMRI-NF amygdala training during happy autobiographic memory recall induces plastic, and lasting brain changes. The rtfMRI-NF enhances abnormal low amygdala-pgACC connectivity in MDD patients. Additionally, active neurofeedback enhances amygdala-hippocampus connectivity. These results suggest the importance of reinforcement learning in rehabilitating emotion regulation in depression.

References: [1] Zotev V et al. (2011) PLoS One 6: e24522. [2] Young KD et al. (2014) PLoS One 9:e88785. [3] Bodurka J & Bandettini P (2008) Neuroimage 41: S85.

P108B Resting State Functional Connectivity in non-demented Parkinson's disease

L. Zhang[1], E-Y. Lee[1], Y. Truong[7], M. Wang[6], G. Du[1], M. Lewis[1,2], and X. Huang[1,2,3,4,5]

[1]Departments of Neurology, [2]Pharmacology, [3]Neurosurgery, [4]Radiology, and [5]Kinesiology, [6]Public Health Sciences, Pennsylvania State University, Milton S. Hershey Medical Center, Hershey, PA 17033, USA; [7]Department of Biostatistics, University of North Carolina at Chapel Hill, NC 27599, USA

Background and Purpose: Parkinson's disease (PD) is a progressive neurodegenerative disorder that presents with resting tremor, bradykinesia, rigidity, and/or postural instability symptoms. Cognitive deficits in non-demented patients with PD are frequent and can be found even in the early stages of the disease. Functional connectivity studies in PD may provide more valuable information in understanding brain functional changes and the underlying pathophysiology of any deficits. In this study, we investigated the resting state functional connectivity in PD, with special focus on the sensorimotor, executive function, and default mode network (DMN).

Methods: Resting-state fMRI sequences and comprehensive cognitive function scores were acquired from 46 non-demented PD and 40 control subjects matched for age, gender, handeness and education. Cognitive measures were analyzed using model selection with adjustment for age and depression score. Resting-state functional networks were identified using the group ICA method in GIFT. The executive function, sensorimotor, and DMN networks were selected as networks of interest. Independent components (ICs) and ICs temporal correlation networks were then compared between PD and control groups.

Results: Cognitive tests showed that PD subjects demonstrated significantly lower performance in fine motor (grooved pegboard test; $p < 0.001$), executive function (spontaneous flexibility: $p = 0.02$, set-shifting: $p = 0.005$), and attention ($p = 0.03$). ICA (thresholded at $Z > 3.5$) revealed that PD subjects had significantly lower connectivity in the three networks of interest compared to controls in the following regions: bilateral precentral, inferior parietal, superior temporal and right postcentral gyri in the sensorimotor network; bilateral middle and superior frontal gyri in the executive function network; and bilateral posterior cingulate cortex, precuneus, and middle occipital gyri in the DMN. Analysis of temporal components associated with the spatial ICs within networks also showed a significant reduction of temporal lagged correlations in the sensorimotor and executive networks in PD compared to controls (shown in the Figure as arrows).

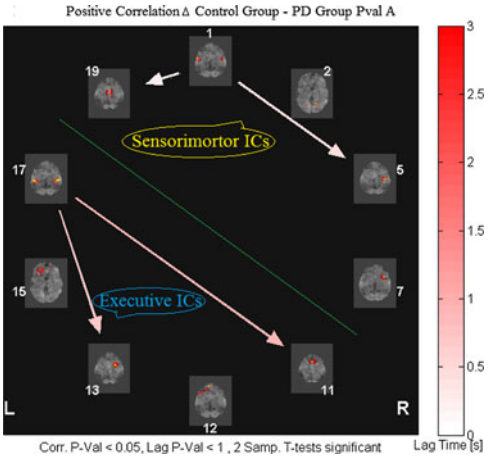

FIG. 1. Component correlation changes between PD and Control group.

Conclusions: Our study demonstrates that brain resting state functional networks (ICA) are abnormal in PD. The ICs temporal networks connectivity changes appear to be concentrated more in sensorimotor and executive function networks than in the DMN. The cognitive test results also suggested the same relationship. We hypothesize that the functional connectivity dysfunction may have a role in the development of cognitive impairment in PD.

P109B Limbic system connectivity in children with ASD in relation to emotional lability

R.H. Bennett[1], K. Somandepalli[2], A. Atasuntseva[1], A.K. Roy[1], A. Di Martino[2,3]

[1]Fordham University, Bronx, NY, USA, [2]Phyllis Green and Randolph Cowen Institute for Pediatric Neuroscience at the NYU Child Study Center of the Langone Medical Center, New York, NY, USA, [3]Autism Research and Clinical Program at the NYU Child Study Center, of the Langone Medical Center, New York, NY, USA

Background: Autism Spectrum Disorder (ASD) is a neurodevelopmental disorder characterized by deficits in social reciprocity and restricted and repetitive interests/behaviors (DSM 5, 2013). Accompanying these core features, many children with ASD tend to also display increased emotional lability (evidenced by irritability, aggression, and impulsivity often manifesting in severe temper tantrums; Mazefsky et al., 2013). At the neural level, brain structures in the limbic system, such as hippocampus and amygdala, have been shown to play a key role in emotion

processing and regulation (Vink et al., 2014). The limbic system has also been implicated in the pathophysiology of ASD. Therefore, we aimed to explore limbic system neural circuitry and examine its relation with emotional lability in children with ASD relative to typically developing controls (TDC).
Methods: We collected a 6 minutes resting-state fMRI (R-fMRI) scan in 69 (64 male) 7–12 year-old children diagnosed with ASD and 67 (43 male) TDCs, group-matched for age and performance IQ. ASD diagnosis was determined using parent report (ADI-R) and child clinical evaluation (ADOS). Parents completed questionnaires assessing social and emotional skills (e.g., Conners' Parent Rating Scale and Social Responsiveness Scale). R-fMRI data were analyzed using an alpha version of the Configurable Pipeline for the Analysis of Connectomes (C-PAC). Following standard preprocessing, single subject nuisance regression included Friston-24 motion parameters, signals from CSF and WM masks, and compcor. As a first step to investigate limbic circuitry, we conducted seed-based analyses of the hippocampus (based on Harvard Oxford Atlas 50% probability). Group comparisons used a random-effects, ordinary least-squares model (GRF corrected at $p < 0.05$, $Z > 2.3$) including age, micromovement, and IQ, as nuisance covariates. Further analyses sampling amygdala circuitry and their relationship with emotional lability severity ratings are currently ongoing.
Results: Initial group comparisons showed a mixed pattern of hypo and hyper-hippocampal connectivity in children with ASD vs. TDC. Specifically, children with ASD showed decreased bilateral hippocampal connectivity to bilateral superior temporal gyrus and to inferior frontal gyrus as well as increased right hippocampal connectivity to mid anterior cingulate cortex.
Conclusions: Children with ASD show dysfunctional hippocampal connectivity within social and emotional brain regions. These findings provide insight into the possible interconnection between social and emotion regulation deficits often seen in children with ASD. Additional neural and phenotypic variable analyses are ongoing.

Poster Session 3: Saturday, 13 September 2014

Theme 1: Technical Advances and Methodological Issues

P1C A new metric to quantify functional and effective connectivity for individual brains

C.A. Bagne

DataSpeaks Health Solutions, Troy, Michigan, USA

Background: BOLD fMRI collects vast amounts of raw and preprocessed time series data. Correlation coefficients have become a ''default mode'' for processing such data to quantify functional connectivity. Granger causality has been used to help investigate effective connectivity. DataSpeaks Health Solutions, an emerging software and services company actively seeking partnerships, offers a fundamentally new metric, embodied in DataSpeaks Interactions (DSI) Software, for processing such data. DSI Software quantifies network interactions over time, which for DataSpeaks includes functional connectivity, effective connectivity, brain responses to time varying inputs, and brain/behavior relationships as with nested time series. A recent search of ClinicalTrials.gov for fMRI identified 1110 studies. Most of these used fMRI as a tool to help optimize brain drug development.
Methods: We will compare capabilities of two methods, a statistical measure of correlation initially developed for groups versus DSI Software for individuals, for quantifying functional and effective connectivity using BOLD fMRI data for a small number of seeds for one brain. These capabilities will be identified, for presentation purposes here, starting with levels of brain activity for two seeds, S1 and S2.
Results: Unlike correlations, DSI Software is capable of: (1) Providing internally standardized (mean = 0, standard deviation = 1) scores that quantify the amount of evidence for excitatory and inhibitory Interactions-over-Time (IoT) as between S1 and S2; (2) Quantifying IoTs as functions of activity levels for S1 and S2 themselves without assuming that these relationships are linear; (3) Quantifying IoTs as functions of delay of response of S1 on S2 and persistence of response of S1 on S2 as well as for up to four additional temporal analysis parameters used to identify episodes of independent events defined on S1 and episodes of dependent events defined on S2; (4) Elucidating evidence for causality by investigating asymmetries of IoT scores obtained with the temporal analysis parameters – asymmetries that typically result from switching use of S1 and S2 as independent and dependent variables; and (5) Monitoring IoT scores over time to be sensitive to how connectivity might change over time within an imaging session. DSI Software is a measurement tool for individual brains. It is well suited to stand between the preprocessed data and statistical analyses when there are two or more brains.
Conclusions: DSI Software appears to be superior to correlation coefficients for functional connectivity and to Granger causality to quantify evidence for effective connectivity. DSI Software has great potential to provide more objective, reliable, specific, mechanistic, and actionable diagnoses of many brain disorders by using time series data from many technologies, which includes BOLD fMRI, to measure order and disorder per se as distinct from signs and symptoms as with the Diagnostic and Statistical Manual for Mental Disorders. DSI Software will help achieve the promise of fMRI for drug development. ''Good therapeutics follows good diagnostics.''

P2C Revealing brief meditation brain functional connectivity remnants

C.C.C. Bauer[1,2,3], S. Whitfield-Gabrieli[2], J.A. Brewer[3], J.L. Díaz[4], E.H. Pasaye[1], F.A. Barrios[1,2]

[1]Instituto de Neurobiología, Universidad Nacional Autónoma de México, Querétaro, México; [2]Department of Brain and Cognitive Sciences, McGovern Institute for Brain Research, Massachusetts Institute of Technology, Cambridge, MA; [3]Center for Mindfulness in Medicine, Health Care, and Society, University of Massachusetts Medical School, Worcester, MA; [4]Facultad de Medicina, Universidad Nacional Autónoma de México, México D.F., México

Background: Intrinsic resting-state functional connectivity (rsFC) in the default mode network (DMN) is altered by meditation practice. However, little is known regarding direct remnants after a brief meditation (20 min) on the functional connectivity of DMN and other resting-state networks. The aim of the present study was to investigate the immediate effects of a brief meditation on resting state functional connectivity within the DMN, dorsal attention network (DAN), and central executive network (CEN).
Methods: We analyzed resting-state fMRI data of 12 experienced meditators of two 10-minute scans, one during rest before the meditation one immediately after the meditation. We used two different methods to analyze the data. (A) Independent component analysis (ICA) on the concatenated data sets to find the three functionally relevant networks (DMN, DAN, CEN) followd by a dual regression analysis. Statistical inference was done on these spatial maps using voxel-wise permutation tests (5000). (B) rsFC analysis was performed using the Conn Toolbox where a fist-level analysis for each subject condition was estimated doing voxel-to-voxel and seed-to-voxel and group results were estimated with seed-to-voxel in a second-level analysis using seeds for the three mentioned networks. Finally, to find out the intersection of both methods, we multiplied the thresholded dual regression contrast with the Conn Toolbox contrast.
Results: Post-meditation rest, as compared to normal rest, strengthened rsFC in all three networks evidenced by both methods. Although each method revealed slightly different results, common brain regions were identified: within DMN, in the inferior frontal gyrus subcallosal gyrus, caudate, premotor cortex, insula, superior parietal lobe and parahipocampal gyrus; within DAN, superior and middle frontal gyrus, medial frontal gyrus, caudate, premotor cortex, middle temporal lobe and cerebellum; within CEN, superior and middle frontal gyrus, medial frontal gyrus, inferior frontal gyrus, anterior cingulate cortex, superior temporal lobe, primary somatosensory cortex, superior parietal lobe, lingual gyrus and cerebelum.
Conclusions: These findings reveal, first that different methods to analyze rsFC provide corresponding results, and second that a short 20 min meditation practice devises strengthening remnants on rsFC within the DMN, DAN and CEN.

P3C Spatially coupled brain networks of neural and vascular origins

M.G. Bright[1], J. Whittaker[1], I. Driver[1], K. Murphy[1]

[1]CUBRIC, School of Psychology, Cardiff University, Cardiff, United Kingdom

Background: Intrinsic brain connectivity networks must be supported by the cerebrovasculature to maintain proper function.

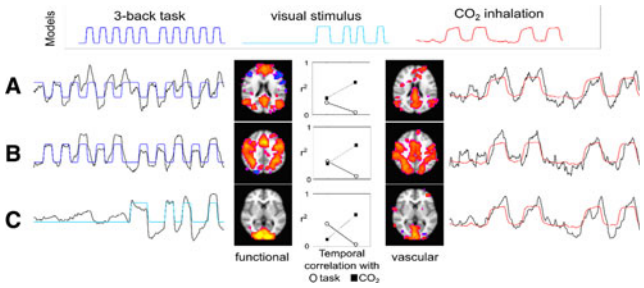

We elicit neural activity in 3 functional networks while simultaneously manipulating vascular mechanisms using hypercapnia to determine the relationships between neural and vascular networks.
Methods: Functional MRI data were acquired in 10 healthy volunteers using a 3 Tesla GE scanner and a BOLD-weighted gradient-echo EPI sequence. Three 11-minute scans were collected using a combined functional and hemodynamic paradigm. A 3-back working memory task (centrally presented digits 0–9 presented in 1.5 s intervals) was delivered in a 30-second block design. An 8 Hz flashing radial checkerboard was overlaid, also in a block design, and four 1-minute blocks of CO_2 inhalation (+5 mmHg hypercapnia) were delivered via a face mask. A high-resolution T1-weighted structural image assisted in registration to MNI template space. The 30 task datasets were motion corrected, registered, and averaged together. Because the phase of resting-state fluctuations will vary across scans, averaging the datasets minimises the influence of these signals. Using independent component analysis (MELODIC, FSL) this average dataset was decomposed into 30 components. Those demonstrating greatest positive/negative temporal correlation with the 3-back or visual stimulus paradigms were identified as neural networks. Dice's coefficient identified further components with maximal spatial overlap, and timeseries of the spatially coupled networks were examined.
Results: Task-negative Default Mode (A) and task-positive (B) networks were identified via temporal correlation with the 3-back working memory stimulus, and a visual network (C) was identified similarly using the visual stimulus model. The maximally overlapping components associated with the three neural networks demonstrated lesser correlation with the task stimuli and greater correlation with the average end-tidal CO_2 data, indicating they are dominated by vascular mechanisms.
Conclusions: Using ICA, we identified pairs of networks that are spatially similar but reflect distinct neural and vascular timeseries. Exploring both the neural and vascular structure underlying functional connectivity networks may add insight into brain development and brain health, particularly in patient populations with both neural and hemodynamic pathologies.

P4C Using Real-Time fMRI Based Neurofeedback to Probe Default Network Regulation

R.C. Craddock[1,2], A. McDonald[1], J. Lisinski[3], P. Chiu[3,4], H. Mayberg[5], S. LaConte[3,6]

[1]Nathan S. Kline Institute for Psychiatric Research, Orangeburg, VA [2]Child Mind Institute, New York, NY [3]Virginia Tech Carilion Research Institute, Roanoke, VA [4]Department of Psychology, Virginia Tech, Blacksburg, VA [5]Department of Psychiatry and Behavioral Sciences, Emory University School of Medicine, Atlanta, GA [6]Virginia Tech-Wake Forest University School of Biomedical Engineering and Sciences, Blacksburg, VA

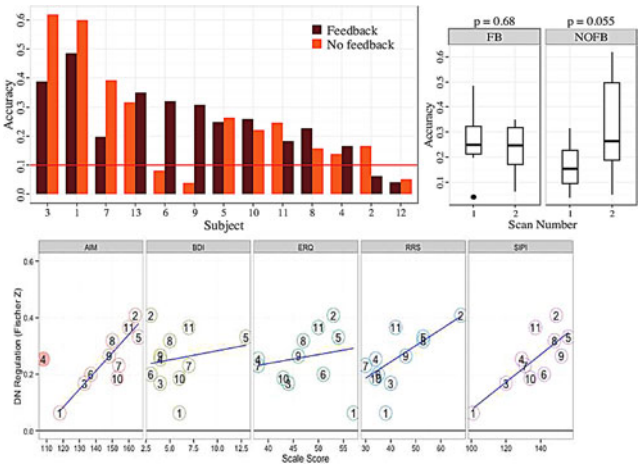

Background: The default network (DN) is consistently deactivated relative to cognitive tasks in healthy controls, leading to the hypothesis that DN interference with task positive networks can lead to psychiatric disorders such as depression, autism, and anxiety. Although intriguing, direct evaluation of DN dysregulation is challenging, and is often inferred from reduced deactivation during task performance. Emerging real-time fMRI (rtfMRI) neurofeedback techniques have the potential to probe this phenomenon with more specificity.
Methods: Thirteen healthy individuals participated in an rtfMRI neurofeedback experiment to evaluate ability to modulate DN activity. DN activity was decoded from fMRI volumes in real time using support vector regression, and was presented to participants using an analog meter display. Participants were asked to move the meter's needle by focusing their attention or mind wandering. Prior to scanning, participants were taught strategies for DN modulation, and were encouraged to optimize their strategy using the feedback. Participants also completed a ''nofeedback'' task, in which the needle was stationary.
Results: Twelve of the thirteen participants were able to modulate DN activity using biofeedback. Participants performed better at the nofeedback task when it was preceded by feedback. Ability to modulate the network correlated with phenotypic measures of rumination and mind wandering.
Conclusions: We developed a system for measuring DN regulation using realtime neurofeedback. Participants were able to modulate their DN activity and their ability to do so was correlated with phenotype. This system provides a new experimental paradigm for understanding network dysregulation and how it maps to disease states and phenotype.

P5C Task related brain networks derived from trial-by-trial variability of a slow event-related designed Flanker task

Xin Di, Bharat B. Biswal

Dept. of Biomedical Engineering, New Jersey Institute of Technology, Newark, NJ, USA

Background: Although brain network organizations have been extensively studied using resting-state fMRI (1, 2), it is still challenging to investigate brain networks that are modulated by tasks. The aim of this study was to investigate task related networks by studying correlations of trial-by-trial variability using the beta series method (3). A data-driven spatial independent component analysis (ICA) (4) was applied to these beta image series to identify task related networks.

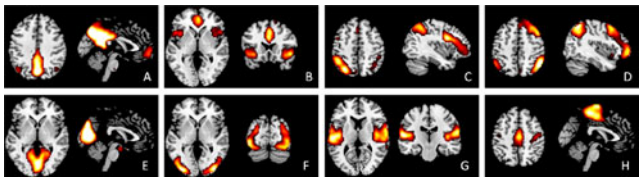

Methods: FMRI data of a slow event-related designed Flanker task were analyzed (n = 25 after removing one subject with large head motion) (5). There were totally 24 congruent and 24 incongruent trials in two separate runs. SPM8 was used for data analysis. The functional images were slice timing and motion corrected, and corregistered to subject's anatomical images. The anatomical images were segmented, and the deformation field images were used to normalize the functional images into MNI space. The functional images were smoothed using an 8 mm Gaussian kernel.

A GLM model was defined for each subject with 48 regressors representing activations of every trial, and 48 motion regressors for the two separate runs. Trial regressor was calculated by convolving a single impulse function at the trial onset with the canonical hemodynamic function (hrf). After model estimation, 48 beta maps were obtained for each subject, which represented activations of each trial. Spatial ICA (4) was performed on the concatenated beta image series across subjects. 20 components were extracted.
Results: We identified several ICs that were similar to commonly identified networks as using resting-state time series, e.g. the default mode, salience, left and right fronto-parietal, medial and lateral visual, auditory, and motor networks (Fig A through H). Mean beta values within regions of these networks were compared between the two conditions, and only the salience network regions showed higher activations in the incongruent condition compared with the congruent condition ($p < 0.05$).
Conclusions: Brain networks derived from trial-by-trial variability of a event-related task are very similar to those generally derived from resting-state data, indicating a similar underlying network structure. Further studies are needed to directly compare similarities and differences of network structures between task-related beta series networks and resting-state networks.
References: 1, Biswal et al., 1995. Magn Reson Med 34(4):537–41. 2, Biswal et al., 2010. Proc Natl Acad Sci U S A 107(10):4734–9. 3, Rissman et al., 2004. Neuroimage 23(2):752–63. 4, Calhoun et al., 2001. Hum Brain Mapp 14(3):140–51. 5, Kelly et al., 2008. Neuroimage 39(1):527–37.

P6C Sparse Connectivity Patterns in Resting State fMRI

Harini Eavani[1], Theodore D. Satterthwaite[2], Raquel E. Gur[2], Ruben C. Gur[2], Christos Davatzikos[1]

[1]Center for Biomedical Image Computing and Analytics, University of Pennsylvania, Philadelphia, Pennsylvania, USA; [2]Brain Behavior Laboratory, University of Pennsylvania, Philadelphia, Pennsylvania, USA

Background: Functional networks in the brain can be identified by grouping regions that present strongly correlated rsfMRI signals. It is now increasingly evident that neural systems use parsimonious formations to efficiently process information while minimizing redundancy. We exploit recent advances in the

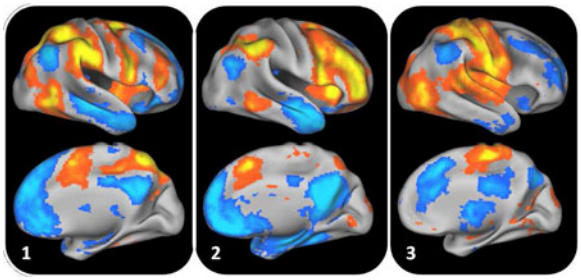

mathematics of sparse modeling to develop a methodological framework aiming to understand complex resting-state fMRI connectivity data. By favoring networks that explain the data with a relatively small number of participating brain regions, we obtain a parsimonious representation of brain function in terms of multiple ''Sparse Connectivity Patterns'' (SCPs).
Methods: Using subject-wise correlation matrices as input, and spatial sparsity as a constraint, we learn the identity of SCPs and the strength of their presence in each individual. This approach bridges the gap between discrete clustering techniques and continuous dimensionality reduction approaches, and results in SCPs that allow for spatial overlap and negatively weighted regions. To evaluate the method, we used data from 130 young adults drawn from the PNC sample [1]. Pre-processing and registration procedures are given in [1]. For reproducibility analysis, our replication data consisted of 131 subjects acquired as a part of HCP [2] and fBIRN [3], processed using the same pipeline [1]. We used a cross-validation strategy to obtain ten SCPs each for PNC and HCP + fBIRN datasets. The inner-product measure was used to quantify the comparison between the two sets of SCPs.
Results: Figure 1 shows three SCPs obtained using the PNC dataset. Opposing colors indicate anti-correlation. The reproducibility of the SCPs between the two datasets, measured using inner product was found to be 0.80 ± 0.09, comparable to that of sub-graphs obtained using InfoMap (0.86 ± 0.15) and significantly better than Temporal ICA (0.60 ± 0.12).
Conclusion: Sparse representations provide a complementary approach to ICA and graph-based approaches for network identification. These results, taken together with those from other approaches, provide a more complete picture that can help elucidate the functional organization of the brain.
References: **[1]** Satterthwaite, T.D., et al. *NeuroImage* 83(2013): 45–57. **[2]** Smith, S. M., et al. *PNAS*, 109.8(2012): 3131–3136.**[3]** Fox, M. D., et.al, Neuron 56 (1), 171(184),2007.

P7C Delineation of intrinsic connectivity networks from resting-state fNIRS signals

F.A. Fishburn[1], M.E. Norr[2], A.V. Medvedev[3], C.J. Vaidya[2,4]

[1]Interdisciplinary Program in Neuroscience, Georgetown University Medical Center; [2]Department of Psychology, Georgetown University; [3]Center for Functional and Molecular Imaging, Georgetown University Medical Center; [4]Children's Research Institute, Children's National Medical Center, Washington, DC, USA

Background: fMRI as an imaging modality for functional connectivity (FC) in young children is limited due to its sensitivity to head motion. Thus, it is important to develop alternative imaging modalities that are less sensitive to artifacts arising from head motion, such as fNIRS (functional Near-Infrared Spectroscopy). Development of an imaging modality more resilient against head motion is particularly necessary for the examination of functional connectivity networks. While some studies have used independent component analysis (ICA) on fNIRS signals, none have delineated functional networks spanning multiple brain regions. Using iterative parameter optimization and group ICA, we identified six ICNs in the resting state. All networks exhibited strong hemispheric symmetry and correspondence with known functional anatomy. Further, power spectra significantly differed between networks in the frequencies less than .10 Hz.
Methods: Sixteen subjects (6 male, 1 left-handed) were subjected to a 10-minute resting state scan. Optical data were recorded on a two-wavelength (690 and 830 nm) continuous-wave CW5 imaging system (TechEn, Inc., Milford, MA). The 40 optical channels covered: ventrolateral prefrontal cortex (vlPFC), dorsolateral prefrontal cortex (dlPFC), frontopolar cortex (FP), and parietal cortex (Par). *Resting-State Preprocessing:* Raw signals were converted to oxygenated hemoglobin concentration using Homer, then filtered to .009-.09 Hz and downsampled to 2 Hz. The 10-minute rest runs were then trimmed to the middle 6 minutes of the run. Each channel was then normalized such that its root-mean-square (i.e., quadratic mean) was equal to 1. Data from each subject was then concatenated along the time dimension to produce a 96-minute group timecourse for each channel. *Resting-State Network Delineation*: ICASSO was then used to perform ICA with FastICA 100 times for each ICA parameter: numOfIC, approach, g, and finetune. The results from the parameter set with the best quality index were then retained. The positive and negative portions of each component were separated, effectively doubling the number of components. For network visualization, the channel weights from the mixing matrix were interpolated and superimposed on a model brain using the kernels generated by NIRS-SPM. *RSN Power Spectra:* Channel spectra were produced by computing the wavelet transform of the unfiltered resting-state data and averaging across time within the 95% CI. Network spectra were computed by taking the weighted mean of channel power spectra, using the coefficients in the mixing matrix as channel weights.
Results: ICA optimization yielded 6 ICNs: 1) parietal, 2) frontopolar, 3) anterior PFC, 4) vlPFC and frontal pole, 5) lateral PFC, 6) dlPFC, parietal, and frontal pole. IC #1 had lower power than #4 and #5 in .009-.03 Hz and .015-.03 Hz bands, respectively. IC #6 had greater power than #3, #4, and #5 in the .065-.095 Hz band.
Conclusions: These results show for the first time that group ICA can be used to delineate ICNs from resting-state fNIRS signals. These networks correspond to known functional anatomy and oscillate in different frequency bands. Future research should investigate whether activation and FC analysis will benefit from being performed in network space rather than channel space.

P8C Functional integration between brain regions at rest occurs in multiple-frequency bands

S. Gohel[1,2], B. Biswal[1]

[1]New Jersey Institute of Technology, Newark, New Jersey, [2]School of Health Related Professionals, Rutgers University, Newark, New Jersey

Background: BOLD signal fluctuations during rest have been shown to be highly correlated across spatially remote functionally related brain regions predominantly in the low-frequency

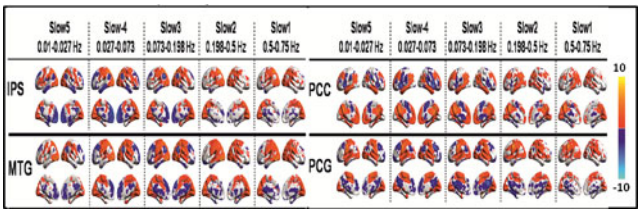

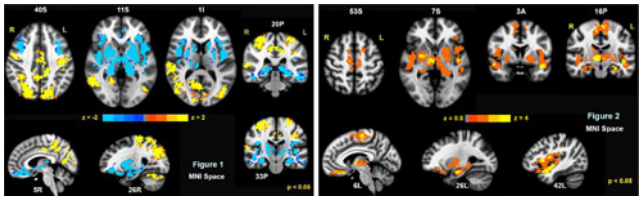

range (LFFs) (0.01–0.1 Hz) [1]. Earlier neuro-physiological studies have shown that neuronal networks show oscillations up to 500 Hz [2]. Exploration of RSFC in frequency bands higher than 0.1 Hz has been limited due to hardware limitations. In the current study, using BOLD fMRI data acquired at high sampling frequency (TR = 0.645 s), we investigate presence of RSFC for multiple frequency bands as defined by earlier neurophysiological studies [3].

Methods: 21 subjects resting state fMRI data (TR = 0.645 s, #volumes 900) and anatomical MPRAGE scan was obtained from open sharing data repository, Enhanced Nathan Kline Institute-Rockland (NKI) Sample [4]. Each of the subjects data was pre-processed using similar processing scheme as employed in [5] and temporally filtered in five different frequency bands (1) slow-5 (0.01–0.027 Hz) (2) slow-4 (0.027–0.073 Hz) (3) slow-3 (0.073–0.198 Hz) (4) Slow-2 (0.198–0.5 Hz) and (5) slow-1 (0.5–0.75 Hz). Seed based correlation was performed using four different seed regions (posterior cingulate cortex(PCC), Inferior parietal sulcus (IPS), precentral gyrus(PCG), middle temporal gyrus (MTG)). One-sample ttest ($p < 0.05$, FDR corrected) was performed to derive group level connectivity maps.

Results: Resting state networks such as, default mode network (PCC seed), motor network (PCG seed), dorsal attention network (IPS seed), temporal network (MTG seed) were consistently observed across multiple frequency bands with variation in spatial extent and connectivity strength.

Conclusions: Functional integration between brain regions at rest occurs over a wider frequency bands and RSFC is a multi-frequency band phenomenon. RSFC at these higher BOLD frequencies may represent inter-network connectivity and may provide further insight in functional integration between various neuronal processes and their roles in cognition.

References: Biswal BB, Hyde JS, 1995 MRM, 34(4), 537–541. Llinas RR, 1988 Science, 242(4886), 1654–1664. Buzsáki G Science, 304(5679), 1926–1929. Nooner KB 2012, Front Neurosci, 6:152. Biswal BB, PNAS, 2010, 107(10), 4734–4739.

P9C Anti-hubs and negative hubs in resting functional connectivity network architecture

K.S. Gopinath[1], V. Krishnamurthy[1], R. Cabanban[1]

[1]*Departments of Radiology & Imaging Sciences, Emory University, Atlanta, GA*

Background: Previous studies [1,2] have revealed a number of hubs in whole-brain resting state functional connectivity (rsFC) networks. Here, we further characterized global brain connectivity, by probing the rsFC network architecture for the presence of both anti-hubs: nodes with relatively low degree centrality (DC) based on positive cross-correlation coefficient (CC), i.e., exhibiting suppressed resting state activity; and negative hubs: nodes with relatively high degree centrality (DC) based on negative CC, i.e., hubs of anti-correlations that reflect reciprocal modulations in state dependent rsFC networks.

Methods: Normal adults (N = 12; age ~ 27 y) were scanned in a 3T MRI. Rest-state fMRI data were acquired with a whole-brain EPI sequence (TR = 2000 ms, 3 × 3 × 3 mm resolution). Preprocessing steps included a number of methodological improvements aimed at enhancing the specificity of BOLD rsFC networks. Each gray matter voxel served as a node in the high-resolution graph analysis. Two separate sets of graphs were constructed employing binarized distance matrices: one based on positive CCs and the other based on negative CCs, both thresholded to a sparsity of 0.1. The hubness of each node was determined by z-transforming the DC maps of each subject as described in [1]. Group-level hubness maps were generated from 1-sample t-test on subjects' hubness scores.

Results: Significant positive hubs of rsFC based on positive CC (Figure 1; +ve z-scores) were found in a number of areas (e.g. DMN, cerebellum, occipital and sensorimotor cortices) consistent with previous studies [1,2]. The strongest anti-hubs (Figure 1; −ve z-scores) and negative hubs (Figure 2) were found in basal ganglia, thalamus and hippocampus (Hb). Additional anti-/negative hubs were found in dorsolateral prefrontal cortex, supplementary motor area, subgenual cingulate, ventrolateral PFC, and insula.

Conclusions: Neuronal connections between regions in basal ganglia and thalamus are mostly inhibitory [3]. These could induce depression and/or reciprocal modulations of resting state activity in these areas resulting in anti-hubs and negative hubs. The presence of anti-hubs and negative hubs in frontal attention networks is consistent with reciprocal modulation of attention and DMN [4] which is strongly expressed during resting state. Results also indicate a dissociation of mood network with DMN. Anti-/negative hubs in Hb and amygdala could be due to their strong connections with basal ganglia and thalamus as well as attention and/or mood networks [5]. Further research is needed to understand the basis of these anti-hubs and negative hubs, and their role in brain function.

References: 1) Buckner et al., J. Neurosci. 29:1860–1873, 2009; 2) Cole et al., Neuroimage 49:3132–3148, 2010; 3) Crosson, Brain & Lang. 126:73–88, 2013; 4) Gusnard et al., Nat. Rev. Neurosci. 2:685–694, 2001; 5) Postuma et al., Cereb. Cort. 16:1508–1521.

P10C Comparison of peripheral NIRS to other denoising methods in resting state functional MRI

L.M. Hocke[1,2], Y. Tong[1,3], B. de B. Frederick[1,3]

[1]*McLean Hospital, Belmont, MA, USA,* [2]*Tufts Biomedical Engineering Department, Medford, MA, USA,* [3]*Harvard Medical School Department of Psychiatry, Boston, MA, USA*

Background: Functional Magnetic Resonance Imaging (fMRI) relies on blood-oxygen level dependent (BOLD) contrast to detect and quantify brain activations. BOLD signals are sensitive to changes in cerebral blood flow, blood volume and oxygenation, which result not only from neuronal activation, but also from

non-neuronal physiological processes, including cardiac effects, respiration and global low frequency oscillations (LFOs). These changes, especially in the low frequency domain (0.01–0.2 Hz), can significantly confound inferences made about neuronal processes of the BOLD signals. It is crucial to effectively identify and remove these global LFOs from BOLD fMRI.

Methods: In this study, we conducted a fMRI resting state study (TR = 0.4 s) with simultaneous physiological measurements, to thoroughly assess and compare several denoising methods on global LFOs. These methods include: 1) An optical method utilizing LFOs measured in the periphery with near-infrared spectroscopy (**NIRS**) (Tong et al., 2012), 2) the respiration volume per time (**RVT**) model (Birn et al., 2006), 3) the respiratory variation model (**RV+RRF**) and 4) the cardiac variation model (**HR+CRF**) (Chang et al., 2009). The LFO noise regressors derived from these methods were compared temporally, as were the resulting spatial patterns (correlation maps). Furthermore, the efficiency of the various methods in removing the physiological noise of resting state data was compared. An ultrafast (TR = 0.4 s) multiband EPI sequence was used in order to compare the signals in their most accurate form and to avoid effects of aliasing. Additional data with a TR of 1.5 s was acquired during the same scan for comparison of aliased data.

Results: Low temporal and spatial correlation coefficients (R < 0.3) were found between these methods. NIRS LFOs explained more than twice the amount of BOLD-fMRI variance in comparison to the other LFO methods (2–4). NIRS LFOs explained more BOLD-fMRI variance even in ROIs where other LFO methods performed well. The low correlation between methods suggests that they are detecting different components of the low frequency physiological signal.

Conclusions: NIRS LFOs of the periphery offer unique temporal information in comparison to other LFOs methods, which explains the most variance in BOLD fMRI caused by physiological low frequency noise. Our results also suggest that there is probably more than one physiological process contributing to the global LFOs.

Birn, R. M., Diamond, J. B., Smith, M. A., & Bandettini, P. A. (2006). Separating respiratory-variation-related fluctuations from neuronal-activity-related fluctuations in fMRI. Neuroimage, 31(4), 1536–1548; Chang C, Cunningham JP, Glover GH. Influence of heart rate on the BOLD signal: the cardiac response function. Neuroimage 2009;44(3):857–869; Tong, Y., Hocke, L. M., & Licata, S. C. (2012). Low-frequency oscillations measured in the periphery with near-infrared spectroscopy are strongly correlated with blood oxygen level-dependent functional magnetic resonance imaging signals. Journal of biomedical optics, 17(10), 1060041–10600410.

P11C Mapping the sleep inertia effect in the sensorimotor connectivity

Y.J Hong[1], P.J. Tsai[2], Y.T. Ko[1], Y.H. Lee[1], C.W. Wu[1]

[1]Graduate Institute of Biomedical Engineering, National Central University, Taoyuan, Taiwan, [2]Department of Biomedical Imaging and Radiological Sciences, National Yang-Ming University, Taipei, Taiwan

Background: On awakening, the brain cognitive functions do not recover from sleep swiftly but gradually, so-called 'sleep inertia' effect. According to literature, the sleep inertia effect reflects on the sluggish cognitive performance within 5 to 30 minutes immediate after sleep. We hypothesized that transient functional degradations originate from the temporary disconnections of brain networks on awakening. Therefore, we adopted the seed-correlation method to detect the sleep inertia in the motor network.

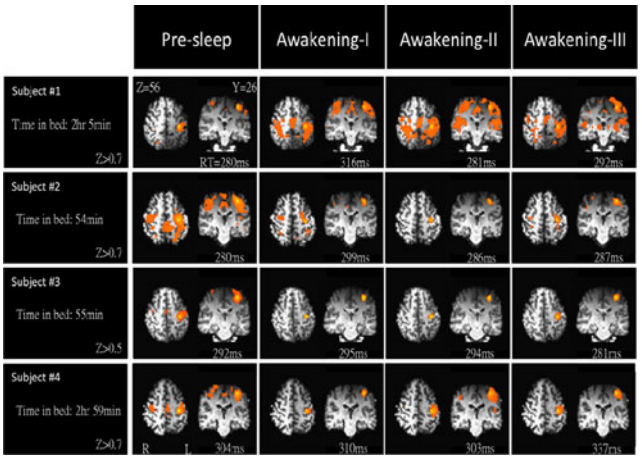

FIG. 1. Sensorimotor connectivity of 4 participants in the 4 sessions: (1) Before sleep, (2) awakening 1 (+0 min), (3) awake 2 (+20 min), and (4) awake 3 (+40 min). Time in bed of each participant and response time to the PVT task (in ms) were listed below each subject/session.

Methods: Four non-sleep-deprived healthy males (25 ± 3.4 y/o) participated this study for a nocturnal sleep in the MR environment. Simultaneous fMRI and EEG signals were recorded for 4 times: once before sleep and three times after sleep (each with 20-min gap). In each recording, a resting state (~7 min) and a psychomotor vigilance task (6 min) to investigate both brain connectivity and response time, respectively. Each fMRI dataset were preprocessed with physiological-noise removal, seed-based correlation were adopted to explore dynamic changes of the sensorimotor network before and after sleep.

Results: Figure 1 demonstrates the progressive changes of sensorimotor connectivity after sleep and also the corresponding response time. We noticed connectivity changes not only between the pre-sleep and awakening, but also between different time points following the awakening. However, strong between-subject variability was found in the 4 subjects. Although the connectivity strength did not show positive correlation with the response time, the connectivity changes were slightly correlated with the time in bed.

Conclusions: This is the first report mapping sleep inertia with functional connectivity techniques. We presented (1) dynamic recovery process of sensorimotor network along the sleep inertia period, and (2) between-subject variability dependent on the sleep duration. Such transient changes of functional connectivity may play key roles in understanding the intrinsic interactions between brain regions in the near future.

P12C Interactive game and semantic memory tasks show opposing modulation of functional connectivity in default mode networks underlying mentalizing processes

C.J. Hyatt[1], V.D. Calhoun[2,3], G.D. Pearlson[1,3], M. Assaf[1,3]

[1]Olin Neuropsychiatry Research Center, Hartford Hospital-IOL, Hartford, CT, [2]The Mind Research Network & The University of New Mexico, Albuquerque, NM, USA, [3]Dept. of Psychiatry, Yale University School of Medicine, New Haven, CT, USA

Background: Mentalizing processes are posited to subsume many sub-networks of the default mode network (DMN). We used functional MRI (fMRI), an interactive game task (domino) and a semantic memory task (semantic object retrieval task, or SORT) and spatial independent component analysis (sICA) to investigate task-related modulation of functional connectivity (FC) in sub-networks of DMN, including medial prefrontal cortex (MPFC), posterior cingulate cortex/precuneus (PCC/PrC), temporoparietal junction (TPJ) and temporal pole (TP). Our hypothesis was that Domino task events, during an event interval in which the participant learned of his/her opponent's decision to show or no-show a played chip, involved mentalizing processes and thus would show positively modulate FC in DMN sub-networks, whereas SORT task events, including memory retrieval/non-retrieval events, would negatively modulate FC in DMN sub-networks due to ''task-positive'' cognition not involving mentalizing processes.
Methods: Study participants (n = 53) were healthy and ranged in age from 17 to 60 years, (Mean ± SD: 35.1 ± 13.6 years). We performed a high order (75 components) sICA that included fMRI data from both the domino task and the SORT, and a separate high order sICA on resting state data from the same set of subjects. We evaluated task-related modulation of FC in DMN components using temporal regression of individual subject back-reconstructed ICA network time courses with each subject's modeled event regressor time courses derived from the GLM design matrix. We also compared ICA spatial maps from domino/SORT sICA with the resting state sICA using spatial regression.
Results: High order sICA split the DMN into 12 sub-network components, of which five were in the MPFC region, three were in the PCC/PrC region, and networks in TPJ and TP were split bilaterally into left and right hemisphere components. We found that domino events positively modulated FC in nine of the 12 DMN sub-networks, including MPFC(3), left/right TP, left/right TPJ and PCC/PrC(2). In contrast, SORT events negatively modulated FC in these same DMN sub-networks. Comparison of domino/SORT and resting state DMN-related ICA spatial maps showed high correlation.
Conclusions: Domino task events during the interval when the participant learns of his/her opponent's decision and strategy involve mentalizing processes that result in positive modulation of FC in a majority of DMN sub-networks, whereas SORT task events involve semantic memory recall processes that result in negative modulation of FC in these same DMN sub-networks. Our findings strongly suggest these DMN sub-networks are involved in mentalizing and social cognition.

P13C Effects of sex and handedness on the inter-hemispheric connectivity of homotopic hemispheric resting-state networks

G. Mousnier[1], P-Y. Hervé[1], M. Joliot[1]

[1]Groupe d'Imagerie Neurofonctionnelle, UMR5296 CNRS, CEA, Univ. Bordeaux

Background: Inter-hemispheric (IH) resting-state functional connectivity (RSFC) is stronger between pairs of corresponding regions of the two hemispheres, referred to as 'homotopic regions'. The resting-state networks (RSN) that result from Independent Component Analysis (ICA) of fMRI data also show a high degree of bilateral symmetry, indicating that their activity is coordinated across the two hemispheres, but no study has focused on homotopic RSFC at the RSN level yet. Furthermore,

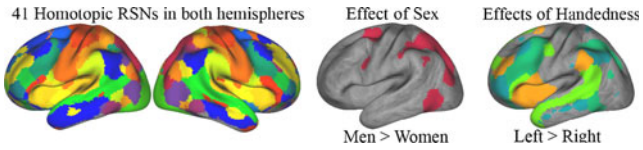

although sex has been associated with differences in terms of voxelwise IH RSFC[1], the effects of handedness, which might be expected[2], have seldom been tested. Here, we investigate the effects of sex and handedness on network-level homotopic connectivity.
Methods: We applied spatial ICA to the preprocessed resting-state 3T BOLD fMRI data of 328 healthy participants, separately in the left and right hemispheres. We then split the data into 4 groups, based on handedness and hemisphere (164 hemispheric spatial ICA[3] results in each group). In order to isolate the homotopic RSNs, defined as the neural ICs that are found reliably in all 4 groups, we applied 2 iterations of an inter-individual spatial clustering algorithm (MICCA[4]), first within groups, and second across groups. So as to exclude artefactual ICs, we inserted an IC selection step, based on anatomical and reproducibility criteria. In both hemispheres, we averaged the Z-maps of the homotopic RSNs of left- and right-handed groups. We then computed the weighted individual mean time-courses within the 2 hemispheric maps, and the IH Spearman correlation coefficient within the pairs of homotopic hemispheric RSNs. Z-transformed correlation coefficients were entered in ANCOVAs with Age and Intra-Cranial Volume as covariates and Sex and Handedness as factors ($p < 0.05$ with Bonferroni-Holm correction).
Results: A total of 41 homotopic RSN pairs were obtained. Significant main effects of Handedness on IH RSFC were found in 4 RSNs (Left > Right-handers), including the salience network[5], and covering the middle and inferior frontal gyrus, the superior temporal sulcus and inferior parietal lobule. Significant main effects of Sex were found in 1 RSN (Men > Women), which covered parieto-occipital regions.
Conclusions: Although ICAs were computed within each hemisphere, thereby removing IH correlations, many homotopic RSNs were found. Overall, the homotopic RSNs covered the whole cortical surface. This suggests that the broad intra-hemispheric network-architectures of the 2 hemispheres are very similar. In several of these homotopic RSNs, inter-hemispheric interactions were influenced by handedness or sex.
1. Zuo, 2010; 2. Cherbuin, 2006; 3. Beckmann, 2004; 4. Naveau, 2012; 5. Seeley, 2007
This work was supported by grant ANR-13-CORD-0007 BIOMIST.

P14C Separation of quasiperiodic VLF fluctuations from periodic cardiorespiratory pulses with ultra-fast MREG

V. Kiviniemi[1], X. Wang[2], V. Korhonen[1], T. Hiltunen[1], Y-F. Zang[3], P. LeVan[4], S. Keilholz[5]

[1]Radiology, Oulu Univ. Hospital, Oulu, Finland, [2]Beijing Normal Univ., Beijing, China, [3]Hanzhou Normal Univ., China, [4]Freiburg Univ., Germany [5]Emory Univ., Georgia, USA

Background: Quasiperiodic pulsations (QPP) have been shown to migrate over brain cortex in BOLD fMRI data. The undersampled classical BOLD signal has the risk of cardiorespiratory aliasing. In this study we critically sample BOLD with magnetic

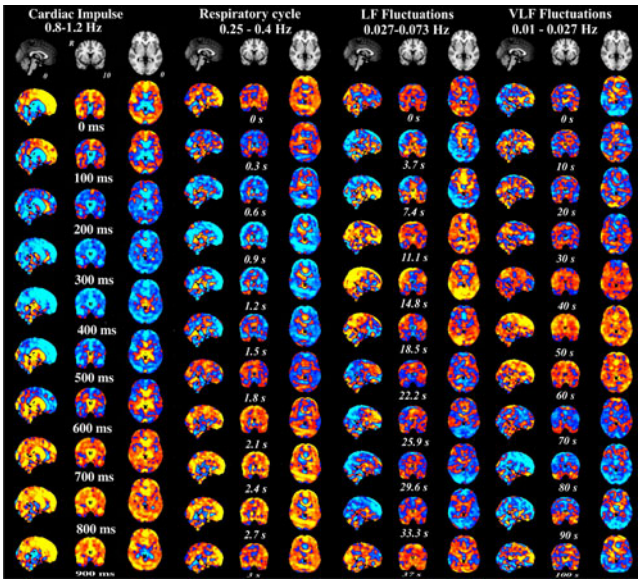

resonance encephalography (MREG, TR 100 ms) in order to explicitly separate cardiorespiratory pulsations from QPPs.

Methods: We scanned 9 subjects with MREG after informed consent and ethical approval using 3T SKYRA. We used Brain Products EEG's electrocardiogram (ECG) to identify R-peaks and scanner bellows for respiratory cycles. Onset for QPP (LF 0.027–0.073 Hz) and VLF (0.01–0.027 Hz) were derived from DMN_{vmpf} using dual regressed groupPICA temporal signal. We used QPP method in Matlab to obtain group average cardiorespiratory pulsations and QPPs in 2 mm MNI152 space.

Results: Periodic cardiac impulses, respiratory cycle can be separated from VLF/LF QPPs in the critically sampled MREG data, c.f. Fig 1 on right. Note varying time intervals running from up→down in white. Each pulsation has unique pattern of spatiotemporal spread.

Conclusions: Critically sampled MREG enables separation of periodic cardiorespiratory pulsations from QPP BOLD fluctuations. QPPs in under-sampled BOLD may have strong aliasing effects from cardiorespiratory pulsations that can be avoided in ultra-fast MREG.

P15C Emergence of the default-mode network in social interaction

R.F. Lee

Princeton University, Princeton, NJ, USA

Background: It becomes evidence that the default-mode network (DMN) (1) represents the potentials for social interaction. Although such implicit coherence has been extensively studied, its explicit activation is observed in a face-to-face eye contact study by the dyadic fMRI (dfMRI) (2). Meanwhile, the dual logic (3) model for the eye contact experiment deductively predicts the emergence of the default-state in the endogenous system. The deterministic theory and the statistical experimental data, as well as many literature, are in agreement that DMN may subserve the function of mentalization.

Methods: The BOLD response of face-to-face eye contact was observed by dfMRI (Fig. 1a) with two tasks, A and B, described in Ref. (2). It's followed by monadic fMRI in Fig. 1b where one

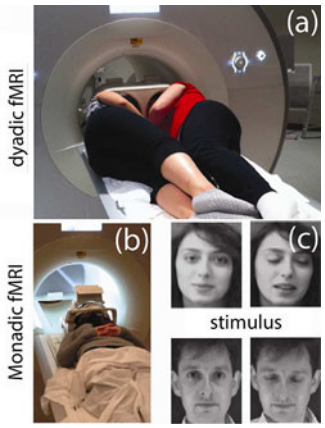

FIG. 1

Table 1	State		A-B	B-A
Exogenous system	x	y	$x \wedge \neg y$	0
	0	0	0	0
	0	1	0	0
	1	0	1	0
	1	1	0	0
Endogenous system	ξ	ψ		$\neg(\xi \wedge \psi) \wedge \neg\psi$
	0	0		i
	0	i		0
	i	0		i
	i	i		0

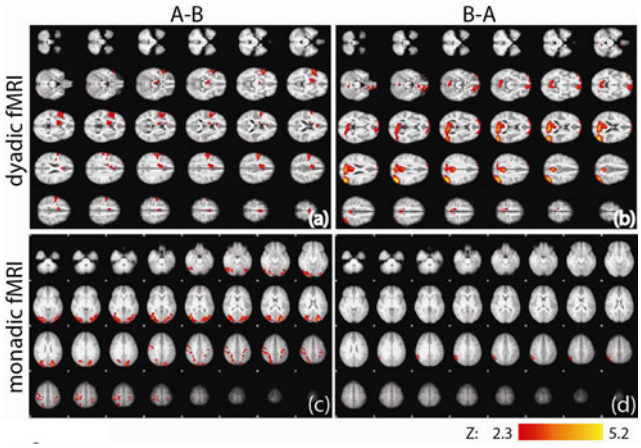

FIG. 2.

of the dyad performs the same task A and B with his/her partner's pictures (Fig. 1c). The group level GLM and their paired comparison, A-B and B-A, were calculated by FSL. Based on the dual logic (3), A-B and B-A in dfMRI correspond to the exogenous-endogenous dual system during reciprocal social interaction as shown in Tab. 1 where x and ξ are reciprocal states, y and ψ are non-reciprocal states. Note that in endogenous B-A, the default-mode ($\xi = 0$, $\psi = 0$) is superimposed with endogenous reciprocal state ($\xi = i$, $\psi = 0$).

Results: 19 pairs of dyads participated dfMRI. Their A-B and B-A responses are shown in Fig. 2a and 2b. DMN activation is

obvious in Fig. 2b. Its lateral asymmetry is an evidence of superposition between DMN and reciprocal state, as predicted in Tab. 1. Note that DMN is not activated in monadic fMRI in Fig. 2d. Here z-score > 2.3, $p < 0.05$.

Conclusions: During social interaction, DMN is no longer resting-state network any more. It's activated as endogenous system to process the discrepancy between internal and external brain states.

References: (1) Schilbach, L. et al, 2008; Consci. & Cogn. 17, p. 457; (2) Lee, R. et al, 2012, MRM, v. 68, p. 1087; (3) Lee, R. in review.

P16C Impact comparison between physiological-noise-removal and low-pass filter in resting-state functional connectivity

T.Y. Lin[1], A.L. Hsu[2], P.J. Tsai[3], S.H. Lin[4], C.W. Wu[1]

[1]Graduate Institute of Biomedical Engineering, National Central University, Taoyuan, Taiwan, [2]Institute of Biomedical Electronics and Bioinformatics, National Taiwan University, Taipei, Taiwan, [3]Department of Biomedical Imaging and Radiological Sciences, National Yang-Ming University, Taipei, Taiwan, [4]Institute of Neuroscience, National Yang-Ming University, Taipei, Taiwan

Background: Since invented in 1995, the low-pass filter (< 0.1 Hz) became a standard preprocess for the resting-state fMRI analysis. Instead, the control of physiological noise seems to be underestimated in general. Due to the non-stationarity of physiological signal, we postulated that removing the physiological noise has higher impact than applying the LPF in the resting-state fMRI signal. To strengthen this point, we controlled the participant's respiration rate to compare the impact of both analytical strategies.

Methods: Two healthy participants were scanned by a 3T Tim Trio MRI system. The resting-state fMRI signal was acquired using GE-EPI (TR = 2 s, TE = 35 ms, 30 slices, MTX = 64 × 64). We used physiologic monitoring unit to acquire respiration, pulsation and ECG signal. By visualizing a moving bar for respiration rate, the participant controlled their breathing at 6 breaths per minute and the normal breathing during the 6-min scan. After standard preprocessing, the fMRI data underwent 2 filter settings (Without filter and a typical low pass filter 0 ~ 0.08 Hz). The seed-correlation analyses were used to detect default mode network (DMN) connectivity for each breathing task.

Results: Both regression and filter did not induce significant changes in normal breath. Compared with the normal breath, the control of low respiration rate globally enhanced the DMN connectivity (Fig. 1). However, in the controlled-breath, the LPF (cut-off frequency < respiration frequency) only caused slight and local changes in the connectivity pattern; instead, after regressing out the physiological noise, the connectivity patterns was globally recovered without artificially induced correlation.

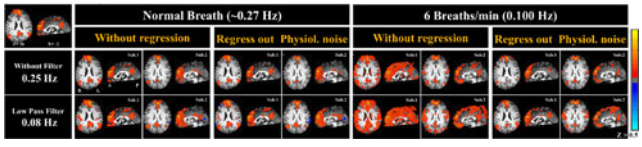

FIG. 1. Comparison of DMN connectivity patterns in both normal breathing and controlled breathing, through two types of filter and regression strategies.

Conclusions: Our result was prominent to reveal that the importance of noise removal in the resting-state fMRI analysis. Even though the low-pass filter was also regarded as an obligatory mean to exclude high-frequency noise, the non-periodic physiological noise was preserved without further noise-removal strategy. Neglecting such non-periodicity may increase the chance of imposing the artificial correlations to the outcomes and leading to the spurious interpretation.

P17C Retrieving the hemodynamic response function at rest: implication for connectivity and brain function

G. Wu[1,2], S. Laureys[3], D. Marinazzo[1]

[1]University of Gent, Belgium, [2]Southwest University, Chongqing, China, [3]University of Liège, Belgium

Background: Data-driven methods to infer directed connectivity in BOLD fMRI data are powerful and widely applicable, but may suffer of a fundamental limitation: the confounding effect of hemodynamic response function (HRF). Here we present a simple and novel blind-deconvolution technique for BOLD-fMRI signal at rest, rooted on the idea that relevant information in resting-state fMRI can be obtained by inspecting the discrete events resulting in relatively large amplitude BOLD signal peaks and extracting the HRF from these.

Methods: Neural events are detected in resting BOLD signal as point processes corresponding to signal fluctuations with a given signature. These pseudo-events are aligned so as to match the optimal delay between the cortical pseudo-events and the BOLD fluctuation. Then voxel specific HRF is retrieved. Rather than on the deconvolution (whose effectiveness has been already reported elsewhere), we concentrate here on a more general aspect, which is relevant also if no connectivity studies are planned: our method allows to retrieve the HRF at rest (named rest-HRF) for each voxel, allowing to map variations in its shape across subjects, brain locations and physiological states.

Results: We obtained the relevant HRF parameters (height, time to peak and full width at half maximum) for each voxel in resting state fMRI scans from 60 healthy subjects and mapped them on the brain surface. Then, to explore the functional changes of the HRF at rest, we first considered 3 successive fMRI scans from 48 healthy controls. During the first scan participants were instructed to rest with their eyes closed. The second and third resting state scan were randomized between resting with eyes open versus eyes closed. We report significant differences (Anova F-test, pFDR < 0.05) in the rest-HRF shape among the three conditions, mainly located in the visual areas. These clusters were different by those obtained looking at the overall signal amplitude. We then investigated how the shape of rest-HRF is modulated during propofol anesthesia. Twenty healthy right-handed volunteers were scanned in four states of consciousness: wake, mild sedation, deep sedation and recovery of consciousness. Significant differences (Anova F-test, pFDR < 0.05) were reported in the height of HRF in visual, salience and central-executive network.

Conclusions: The method presented here for blind HRF retrieval and deconvolution has two main outcomes: 1. It allows performing studies of data-driven directed connectivity without the confounding effect of the HRF across regions. 2. It allows reconstructing the HRF for every voxel in the resting brain. In

this way it is possible to map the HRF shape and its modifications onto brain function and dysfunction.

P18C Improving reliability of subject--level resting state fMRI parcellation with empirical Bayes shrinkage

A.F. Mejia[1], M.B. Nebel[2,3], H. Shou[1], C. Crainiceanu[1], J.J. Pekar[2,4], S.H. Mostofsky[2,3], B. Caffo[1], M.A. Lindquist[1]

[1]Department of Biostatistics, Johns Hopkins University, Baltimore, MD, USA, [2]Kennedy Krieger Institute, Baltimore, MD, USA, [3]Johns Hopkins School of Medicine, Baltimore, MD, USA, [4]Department of Radiology, Johns Hopkins University, Baltimore, MD, USA

Background: Recently, patterns of correlations in resting-state fMRI (rs-fMRI) data have been used to localize functionally relevant subdivisions of anatomically defined regions (van den Heuvel et al., 2008; Cohen et al. 2008; Craddock et al., 2011; Ryali et al. 2012; Blumensath et al. 2013). However, to date the scan-rescan reliability of subject-level methods remains largely unreported. We propose a method to improve scan-rescan reliability of subject-level parcellation by using empirical Bayes shrinkage towards the group average. We test our method on the precentral gyrus.
Methods: We employ a publicly available dataset that includes two 7-minute rs-fMRI sessions for each of 20 healthy adults (Landman et al., 2010). Scans were slice-time adjusted and realigned to account for motion before being transformed to MNI space. Nuisance covariates from white matter and CSF were estimated using aCompCor and regressed from the data along with absolute and differential motion estimates and linear trends. Data were spatially smoothed (6-mm kernel) and band-pass filtered (.01–0.1 Hz). The raw correlation matrix C_{ij} for each subject $i = 1, \ldots, 20$ and session $j = 1,2$ within the precentral gyrus was computed. The shrinkage estimate of the correlation matrix for subject $i = 1, \ldots, 20$ using session $j = 1,2$, is equal to $\tilde{C}_{ij} = \lambda \bar{C}_j + (1-\lambda) C_{ij}$, where $\bar{C}_j = \frac{1}{20}\sum_i C_{ij}$ and λ is the ratio of noise variance to total (signal + noise) variance. We propose methods for estimating the noise variance using both scans and when only a single scan is available for each subject. Parcellations $\Gamma(C)$ were obtained using spectral clustering as described by Ng et al. (2001) on each correlation matrix $C = C_{i1}, \tilde{C}_{i1}, C_{i2}$. C_{i2} and $\Gamma(C_{i2})$ were used as proxies for the ground truth to estimate reliability. Improvement in correlation reliability due to shrinkage was computed as the percent reduction in mean squared error MSE $(\tilde{C}_{i1}, C_{i2})$ relative to MSE (C_{i1}, C_{i2}). Improvement in parcellation reliability due to shrinkage was computed as the percent increase in Dice's coefficient of similarity Dice$\{\Gamma(\tilde{C}_{i1}), \Gamma(C_{i2})\}$ relative to Dice$\{\Gamma(C_{i1}), \Gamma(C_{i2})\}$.
Results: We report the average improvement when multiple scans are employed to estimate the noise variance, followed in parentheses with the improvement when a single scan is employed. The MSE of the shrinkage correlation estimates was 33.4% (26.5%) lower than raw estimates. The Dice similarity of parcellations obtained using shrinkage correlation estimates was 25.8% (25.5%) greater than parcellations obtained using raw correlation estimates.
Conclusions: Shrinkage correlation estimates and their corresponding parcellations show substantial improvement in the ability to accurately predict connectivity at future sessions, and the proposed methods have the potential to greatly strengthen results drawn from subject-level analysis of such parcellations.

P19C Power spectral density (PSD) of brain signal differs between genders and networks

G. Mingoia[1,2,3], I. Nenadic[2]

[1]Interdisciplinary Center for Clinical Research (IZKF), RWTH Aachen University, Aachen, Germany, [2]Department of Psychiatry and Psychotherapy, Jena University Hospital, Jena, Germany, [3]JARA-Translational Brain Medicine, Germany

Background: recent publication revealed significant functional connectivity changes in resting state networks between genders. This investigation did not provide clues about the temporal dynamics of resting state fMRI. He et al. (2011) founded that the fMRI signal consists of scale free dynamics and its power-law exponent differentiates between brain areas. Frequency power distribution was also found different in newborns compare to adult human (Fransson, 2012). Both previous studies focus their investigation on single areas and their time courses. The goal of this study is to compare the PSD in resting state fMRI networks between men and women. This investigation will be conducted directly in 11 well-known brain networks.
Methods: we obtained RS fMRI series in 83 women and 73 men, all right handed and healthy. Data were pre-processed and high-pass filtered. We applied FSL MELODIC, and an automated routine to select the components matching the anatomical definition of well-known networks (Damoiseaux et al. 2006, Seeley et al. 2007). Power spectrum of the fMRI signal was computed for each individual's networks component using the Welch method for power spectrum density estimation. The frequency spectrum functions were fitted with a power-law function $= \beta \frac{1}{x^{\alpha}}$. The power slope α was entered into ANOVA with network and gender as main factors.
Results: Anova with network as the main factor showed a significant power-law exponent dependence with network (women: $p < 0.0001$; men: $p < 0.0001$). The mean slope of frequency power spectra (α) was founded higher in men ($\alpha = 0.91$) compare to women ($\alpha = 0.76$) $p < 0.001$; following networks exhibited significant differences between genders: auditory, frontoparietal1, Sensorimotor, Visual1, Visual2, Visual3 (see figure).
Conclusions: to the best of our knowledge this study is the first comparing the PSD of well-known resting state network between gender. Results show strong differences in the frequency power distribution of spontaneous bold signal fluctuation inter gender and between networks suggesting the possibility to investigate brain networks and their rule in clinical process in frequency domain too.

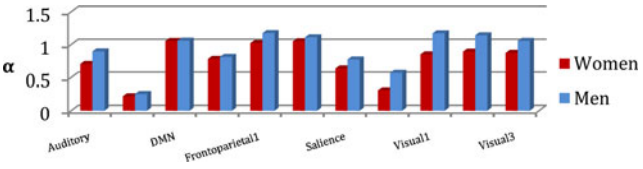

P20C How can resting brain activity help cognitive neuroscientists?

D. Papo[1]

[1]Technical University of Madrid, Madrid, Spain

Background: Resting state activity is often considered as complementary, in opposition as it were, to task-related brain activity.

Why then should cognitive neuroscientists get interested in resting brain activity, and to what extent can studying resting brain activity help characterizing the neural correlates of cognitive processes?

The different roles played by rest in functional neuroimaging and electrophysiological studies are concisely illustrated. It is shown that, in functional neuroimaging, rest is essentially equated to an energy consumption level, and used as a baseline for gauging local amplitude modulations, while in electrophysiological studies, task-independent brain activity is endowed with complex generic properties, with important implications on various operational properties of brain activity.

Results: The relationship between spontaneous and stimulus-related brain activity is understood in terms of the fluctuation-dissipation theorem (FDT)[1]. This theorem of classical physics establishes a general relationship between the (nonequilibrium) response of a system to small external perturbations and the (equilibrium) internal autocorrelation of fluctuations of some observable of the system in the absence of the perturbations. Thus, resting and task-related activities are not complementary, but two sides of the same coin: the connection between the response to external perturbations and the time correlation of the unperturbed system allows understanding the former from the latter. This in principle allows describing cognitive function in terms of generic properties of ongoing brain activity.

We first briefly illustrate various ways in which this can be done, concentrating our attention to a novel way of quantifying brain activity in terms of temperature. For equilibrium systems, the relationship between the system's relaxation after a perturbation and the correlations of the unperturbed system are expressed by temperature[2]. For non-equilibrium systems such as the brain, the FDT must be generalized, and equilibrium temperatures can be replaced by effective temperatures, which quantify the extent to which brain activity violates this theorem in its classical equilibrium form. Out-of-equilibrium systems can be at equilibrium on one scale and out of equilibrium on another, or may even be in equilibrium but show scale-dependent properties, each timescale may be associated with its own effective temperature. This allows understanding the relationship between spontaneous and stimulus-induced brain activity at various spatial and temporal scales, and the extent to which each scale of brain activity deviates from equilibrium conditions, produces entropy, etc.

Conclusions: Describing task-related with task-independent ongoing brain activity allows characterizing cognitive processes with a rich set of physically grounded descriptors e.g. in terms of convergence to the basin of attraction of given probability density functions, symmetries and symmetry breakings, universality classes, effective temperatures, degrees of FDT violation.

[1]Papo D. (2013) Why should cognitive neuroscientists study the brain's resting state? *Front. Hum. Neurosci.* **7**:45.
[2]Papo D. (2014) Measuring brain temperature without a thermometer *Front. Physiol.* **5**, 24.

P21C Augmented reality and intrinsic functional connectivity visualization application: ARiBraiN3T

G.M Rojas[1], J.A. Fuentes[1], M. Gálvez[2], D.S. Margulies[3]

[1]Advanced Medical Image Processing Lab, [2]Department of Radiology, Clínica las Condes, Santiago, Chile, [3]Max Planck Institute for Human Cognitive and Brain Sciences, Leipzig, Germany

Background: Visualization of complex neuroimaging data such as functional connectivity, tractography, functional imaging is a challenge. Different visualization solutions have been proposed. Some authors describe 2-D and 3-D advanced neuroimaging visualization methods for tractography and functional connectivity data. Others describe a stereoscopic-related method to view neuroradiological 3-D images. An Augmented Reality (AR) system generates a composite view for the user that is the combination of a real scene viewed by the user and a virtual scene generated by the computer that augments (or supplements) the scene with additional information (e.g. sound, video, graphics, etc.). Here we describe an Android AR application that shows the Default Mode, Dorsal Attention, and Ventral Attention Networks.

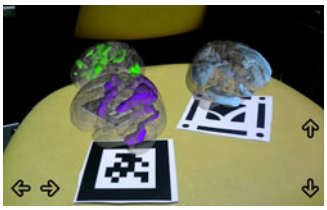

Methods: Using MNI152 2 mm standard MPRAGE image we created a mesh model using the Gray Scale Model Maker algorithm, 3DSlicer software. A 7 Yeo Network Liberal Mask (surfer.nmr.mgh.harvard.edu/fswiki/CorticalParcellation_Yeo2011) was used to create the mesh model of 7 standard Yeo Networks (Model Maker algorithm, 3D Slicer software). Laplacian HC algorithm, MeshLab was used to smooth the mesh of three Yeo networks, and brain mesh. Android application was created with javascript, and the software tools: Unity 4.02 f (graphic engine), Sublime text3 tools, Blender (mesh, materials), Gimp (textures), Qualcomm Vuforia for Unity Android & iOS (AR).

Results: ARiBraiN3T (**A**ugmented **R**eality **i**ntrinsic **Brai**n **N**etworks **3 T**argets): By focusing the three target images (Fig 1), we have produced three 3D transparent brains with the fused default mode network in light blue, dorsal attention network in blue, and ventral attention network in green (Fig 1). The user can rotate the brain using the onscreen controls, by rotating the view angle over the target image, or rotating the target image itself. The size of the brain can be changed by modifying the distance between the android based device and the target image.

Conclusions: ARiBraiN3T is an application that demonstrates the fusion of augmented reality techniques with functional connectivity data. It might be possible to further adapt this application to be used in scientific reporting and/or methodology.

P22C Non-Gaussian methods and high-pass filters in the estimation of effective connections

J.D. Ramsey[1], R. Sanchez-Romero[1], C. Glymour[1]

[1]Department of Philosophy, Carnegie Mellon University, Pittsburgh, PA, USA

Background: Low accuracy of the majority of the causal methods tested in Smith et al., (2011) shows the challenges of inferring orientations of effective connections. Here we consider causal search algorithms that exploit non-Gaussian distributional features, including some that can identify positive feedbacks and high dimensional graphs. We also report that Butterworth high-pass filters can reduce Gaussianity of the data and decrease accuracy of non-Gaussian methods.

Methods: We simulated data for 50 subjects and 28 conditions as in Smith et al. Also data for networks with feedback loops and a high dimensional 500 nodes graph. Data was generated with and

without high-pass Butterworth filter. Group data was created by standardize and concatenate 10 subjects at a time. True adjacencies of the networks were used as initial input for the procedures and only *orientation accuracy* is reported.

We consider 11 orientation methods: R1 and R2 use the idea that the distribution of summands should be closer to Gaussian than the individual summands. R3 uses entropy to decide between $x \to y$ and $y \to x$. R4 is based on ICA and finds cyclic models. These four use Anderson-Darling score for non-Gaussianity. We included methods by Hyvärinen and Smith (2013) that use LiNGAM likelihood to estimate the log of the likelihood ratio of models $x \to y$ and $y \to x$. Finally we tested Smith et al. implementation of Patel's τ (Patel et al., 2006). For the 500 nodes network we estimated adjacencies with the PC algorithm (Spirtes et al., 2000) that recursively test conditional independence and orientations with the above methods except R2 and R4.

Results: Single subject precision/recall considerably improve without the high-pass filter. In most conditions Skew/RSkew are undominated, followed by R1/R2 that are inferior in recall. R1/R2 get higher recall in larger sample size conditions. Group data improves the accuracy due to larger sample size, for filtered and unfiltered data.

In the difficult case of non-stationary connections only R4 and Patel's τ perform accurate enough with single subject data. R3, Patel's τ and R4 can be useful for this case only with group data. R1/R4 are the only that can output feedback loops. They perform much better with group data. R4 has the highest recall with good precision.

In the 500 nodes graph, for single subject data 6% of the estimated adjacencies with PC are false positives, for group data only 2%. R1, R3, Skew, RSkew, SkewE and RSkewE excel at orientation precision with group data.

Conclusions: Non-Gaussian procedures combined with methods for estimating adjacencies show promise for identifying effective connections, even in the presence of feedback loops. One lesson is to check non-Gaussianity before and after any filtering, and when necessary avoid normalizing filters. Important issues remain to be investigated. The performance on non-stationary data is not satisfactory. Further, the feedback loops we modeled are relatively simple, and accuracies with intricate loops remain to be studied. Finally, while there is some work on inference when there are latent common causes, distinguishing feedback loops from latent common causes poses a problem that is, to the best of our knowledge, unsolved either in theory or in practice.

P23C Template Based Rotation: A method for functional connectivity analysis with *a priori* templates

A.P. Schultz[1,3], J.P. Chhatwal[1,3], W. Huijbers[2,3], T. Hedden[1,3], K.R.A. van Dijk[3], D. McLaren[1,3], A. Ward[3], S. Wigman[2,3], and R.A. Sperling[2,3]

[1]Department of Neurology, Massachusetts General Hospital, Boston, MA. [2]Center for Alzheimer Research and Treatment, Department of Neurology, Brigham and Women's Hospital, Boston, MA. [3]Athinoula A. Martinos Center for Biomedical Imaging, Department of Radiology, Massachusetts General Hospital, Charlestown, MA

Background: A number of studies have demonstrated that group level functional network parcellations are highly consistent. The recent availability of large data sets with hundreds of subjects enables robust and accurate population level representations of the brain's functional organization. Taken together, we can now utilize the spatial stability of the brain's functional organization on a population level to drive individual functional connectivity analysis.

Methods: We introduce Template Based Rotation (TBR), a novel analytic approach optimized for use with *a priori* network parcellations. TBR was designed to leverage the stable spatial patterns of intrinsic connectivity derived from out-of-sample datasets by mapping data from novel sessions onto the previously defined templates. TBR is similar to dual regression, but inverts the direction of prediction such that templates are predicted from individual functional volumes. This alteration greatly reduces assumptions of spatial and temporal orthogonality implicit in dual regression. We utilize 675 subjects from the Brain Genomics Superstruct Project to create functional templates that are then applied to a test dataset from the Harvard Aging Brain Study (HABS).

Results: We demonstrate the feasibility of using *a priori* templates for connectivity analyses, and then compare the performance of TBR measures to both seed-based and dual regression measurements. Across 12 templates we find that TBR and dual regression are approximately equivalent and superior to seed based methods in detecting young vs. old differences, and for within session reliability all three methods were approximately equivalent. However, when performing inter-network and sub-network connectivity analyses, TBR offered greater flexibility, larger group differences, and more stable connectivity estimates as compared to dual regression or seed based methods.

Conclusions: We conclude that the use of *a priori* templates is feasible and that TBR is well suited to this application. Employing *a priori* network parcellations brings a number of advantages, including (1) the ability to compare small samples to a known reference group, (2) the ability to compare groups with unequal sample sizes, (3) the ability to retain a high number of components to study sub-network architecture and connectivity; (4) ease in performing interim analyses and, perhaps most importantly, (5) a higher degree of reproducibility and comparability across studies that utilize the same *a priori* network descriptions. Finally these advantages are particularly important in the context of clinical trials, where regulatory approval requires the use of pre-defined network descriptions and outcome measures.

P24C Measuring the quality of resting state fMRI data

Z. Shehzad[1,2,3], Q. Li[1], Y. Benhajali[4,5], C.G. Yan[2,6], Z. Yang[1,2], M. Milham[1,2], P. Bellec[4], and R.C. Craddock[1,2]

[1]Center for the Developing Brain, Child Mind Institute, New York, NY, USA, [2]Nathan S. Kline Institute for Psychiatric Research, Orangeburg, NY, USA, [3]Department of Psychology, Yale University, New Haven, CT, USA, [4]Département d'anthropologie, Université de Montréal, Montréal, CA, [5]Centre de recherche de l'institut de gériatrie de Montréal, Montréal, CA, [6]The Phyllis Green and Randolph Cowen Institute for Pediatric Neuroscience, New York University Child Study Center, New York, NY, [7]Département d'informatique et de recherche opérationnelle, Université de Montréal, Montréal, CA

Background: Although several measures have been proposed for assessing the quality of structural and functional MRI data, there is no clear guidance on which of the measures are the best indicators of quality, or on the ranges of values that constitute ''good'' or ''bad'' data. This is particularly problematic for resting state fMRI (R-fMRI) data, since there is no clear means for differentiating signal from noise. In the present work, a set

of spatial and temporal measures of data quality was calculated on data from the Autism Brain Imaging Data Exchange (ABIDE; Di Martino 2013). The resulting measures were compared to one another to determine their collinearity and evaluated with respect to expert-assigned quality labels assigned by visual inspection.
Methods: Three temporal and three spatial quality metrics were calculated from the unprocessed R-fMRI scans of 1098 individuals in ABIDE (14 participants were removed due to missing data). Temporal metrics were calculated for each volume in a time series and then averaged. These included: the standardized root mean squared change in fMRI signal between volumes (DVARS; Nichols 2013), mean root mean square deviation (Jenkinson 2003), and the temporal mean of AFNI's 3dTqual metric (1 minus the Spearman correlation between each fMRI volume and the median volume; Cox 1995). Spatial quality metrics were calculated on the mean EPI for each dataset and included: ghost-to-signal ratio (GSR; Giannelli 2010), spatial smoothness (FWHM; Friedman 2008), and foreground to background energy ratio (FBER).
Results: Each of the measures showed a good bit of variability between imaging sites. Ranks calculated from the geometric mean of standardized quality metrics indicated that Carnegie Mellon University (CMU) was the worst performing site and New York University (NYU) was the best. There was very little correlation between the measures except for a moderate negative correlation between GSR and FBER ($r = -.58$), which isn't surprising given the similarity in their calculation. In a multiple regression analysis, GSR and FWHM were the best predictors of expert labels ($p < 0.0001$), which reflect the fact that the visual inspection relied heavily on spatial qualities of the data.
Conclusions: We have assembled a diverse set of QC metrics for assessing the quality of R-fMRI data and have applied them to the ABIDE dataset. The measures were uncorrelated for the most part, indicating that they each capture non-overlapping information. Spatial QC measures were the most predictive of labels obtained from visual inspection. Future work will systematically assess the quality of the INDI data, with the goal of building normative distributions of various QC measures.

P25C Graph theoretic general linear model: a MATLAB toolbox

J.M. Spielberg

VA Boston Healthcare System, Boston, MA, Boston University Medical School, Boston, MA

Background: Graph theoretic methods are at the cutting edge of recent attempts to map the human connectome, but a tool to systematically and flexibly test between- and within-participant hypotheses about graph-theoretic properties of brain networks has been lacking.
Methods: To address this methodological gap, we developed a MATLAB toolbox that runs a GLM on graph theoretic properties derived from brain networks. In essence, the toolbox allows the user to test whether fundamental organizational properties of brain networks (e.g., segregation, centrality) are related to variables of interest (e.g., age).
Results: The toolbox accepts assortativity (connectivity) matrices from any type of network data (e.g., resting-state or task fMRI, DTI) and computes graph properties for each matrix to be used as dependent variables in a GLM. The GLM is quite flexible, accepting continuous & categorical between-participant predictors and categorical within-participant factors (e.g., repeated measures across time, task conditions). Tests can be for a single predictor, a contrast of predictors, or an F-test across any (sub)set of predictors. Significance is determined via non-parametric permutation tests using the method of Freedman and Lane (1983; Winkler et al., 2014), allowing valid testing with any number of nuisance predictors. The toolbox can calculate properties for both fully connected and thresholded networks. Calculation of properties for thresholded matrices is accomplished by (1) computing properties for a range of densities, and then (2) calculating the area under the curve across densities, thus decreasing the impact of threshold choice.

The toolbox also includes a processing stream for resting state and block-design task fMRI. The processing stream is quite flexible. For example, several options for partialing nuisance signals are available, including local and total white matter signal (Jo et al., 2013), calculation of Saad et al. (2013)'s GCOR, and the use of Chen et al. (2012) GNI method to determine whether global signal partialing is needed. In addition, Power et al. (2014)'s motion scrubbing method is available. For block-design task fMRI, the toolbox includes an option to deconvolve the signal (using SPM's method), split the resulting timeseries by condition, and calculate assortativity matrices for each condition (which can be used as a repeated factor in the GLM).
Conclusions: The toolbox is freely available for download at: http://www.nitrc.org/projects/metalab_gtg/

P26C Resting connectivity of the Bed Nucleus of the Stria Terminalis

S. Torrisi[1], R. Reynolds[2], N. Balderston[1], M. Ernst[1], C. Grillon[1]

[1]Section on the Neurobiology of Fear and Anxiety, National Institute of Mental Health, Bethesda, MD, USA, [2]Scientific and Statistical Computing Core, National Institute of Mental Health, Bethesda, MD, USA

Background: Dissociating the neural pathways underlying the expression of human fear vs. anxiety has been difficult given the limited spatial resolution of standard 3 Tesla (3T) MRI scanners. Animal studies point to critical roles of small, contiguous structures (Davis et al., 2010). Magnetic fields stronger than 3T offer greater signal and higher resolution so many of these structures and their broader connectivity patterns are now accessible to human research. This project uses 7T rs-fMRI to focus on functional connectivity of the Bed Nucleus of the Stria Terminalis (BNST), a small structure of the ''extended amygdala'' highly implicated in sustained states of anxiety.
Methods: We collected 10 minutes of resting fMRI on a 7 Tesla Siemens Magnetom. Whole-brain anatomical MPRAGEs were collected at 0.7 mm isotropic resolution and a resting-state EPI sequence at 1.3 mm isotropic with a TR of 2.5 seconds and smoothed with a 2.6 mm kernel. Cardiac and respiration measures were also collected. Preprocessing and analysis was performed in AFNI using ANATICOR noise removal (Jo et al., 2010). BNST masks were drawn on each subject's MPRAGE by three trained researchers and then averaged and binarized. Inter-rater reliability was assessed to establish consistency of mask creation (Lim et al., 2013). Resting state functional connectivity was calculated at both seed-to-ROI and seed-to-voxel levels. Subject specific anatomical ROIs were performed using FreeSurfer (Fischl et al., 2002) and supplemented with additional probabilistic subcortical ROIs (Keuken et al., 2014).
Results: Proof-of-concept analyses on one subject showed expected and strong BNST connectivity with dorsal amygdala and dmPFC.

Conclusions: This is the first study to assess BNST connectivity with ultra high resolution functional data. Mapping a BNST-centric network has implications for future treatment and diagnosis of anxiety disorders.

Davis, M., et al., 2010. Neuropsychopharm 35, 105–135; Fischl, B., et al., 2002. Neuron 33, 341–355; Jo, H.J., et al., 2010. NeuroImage 52, 571–582; Keuken, M.C., et al., 2014. NeuroImage 94, 40–46; Lim, I.A.L., et al., 2013. NeuroImage 82, 449–469.

P27C Changes of default mode network connectivity in subjects under different sleep pressure can be demonstrated both with BOLD- and ASL-fMRI

L. Tüshaus[1,2], A. Schläpfer[2,3], D. Brandeis[2,3], P. Achermann[1,2]

[1]University of Zurich, Institute of Pharmacology and Toxicology, Zurich, Switzerland, [2]University of Zurich and ETH Zurich, Neuroscience Center Zurich, Zurich, Switzerland, [3]University of Zurich, University Clinics for Child and Adolescent Psychiatry (UCCAP), Zurich, Switzerland

Background: Previous studies examined resting state networks (RSNs) during various vigilance states with BOLD-fMRI. Only few studies investigated RSNs with arterial spin labeling (ASL)-fMRI that provides absolute measures of cerebral blood flow (CBF) with comparable temporal and spatial resolution to BOLD-fMRI. Therefore, we conducted RSN analyses on both BOLD and CBF data, recorded in subjects under normal and increased sleep pressure.

Methods: Group 1: 21 healthy subjects (20–29 y, 12 f) with normal sleep pressure were recorded in an afternoon fMRI session. Group 2: Sleep of 21 healthy males (19–26 y) was restricted to 4 h the night before fMRI data were recorded. BOLD resting state (2 times eyes open/closed 2 min each; EPI, TR/TE 1.96 s/30 ms, 35 slices, voxels $3\times3\times3\,mm^3$) was recorded after ~8–9 h of wakefulness (Group 1) and ~18.5 h of prolonged wakefulness (Group 2), ASL resting state (5 min eyes open/closed each in Group 1, 10 min eyes open Group 2; pCASL, TR/TE 4.4 s/20 ms, label duration/post label delay 1.65 s/1.525 s, 20 slices, voxels $3\times3\times7\,mm^3$) approx. 1 h later on a 3 T Philips scanner. Between these recordings, subjects performed cognitive tasks. The fMRI data were realigned to the first image in SPM8, CBF images were quantified with in-house MATLAB scripts (see [1]). BOLD and CBF images were coregistered to individuals' T1 images, normalized to standard space, and smoothed (Gaussian kernel spatial smoothing, full width half maximum $10\times10\times10\,mm^3$). RSNs analyses of BOLD/CBF data (eyes open conditions) was performed with the GIFT toolbox, with 20 independent components (ICs).

Results: Among the identified 20 ICs of the BOLD data analysis, one IC represented the DMN (spatial sorting with established template). This IC was binarized (z-score > 1) and used as a spatial sorting mask for the 20 ICs of the CBF images. We found 3 ICs that together comprised the CBF DMN. The division of the DMN into different ICs was reported in previous studies and might in our case be due to the different measurement techniques applied. Contrast of Group 1 and Group 2 showed most pronounced differences in lateral nodes of the BOLD DMN (right/left inferior parietal lobes), whereas with the contrast of Group 2 and Group 1 differences were observed in the frontal midline node of the CBF.

Conclusions: We demonstrated that the analysis of an exemplary RSN, the DMN, was successfully identified with both BOLD and CBF data. The differences observed in the contrasts may be explained by the different level of sleep pressure in the two groups. This is likely to have influenced connectivity of the DMN along midline nodes as shown previously [2]. The spatial differences of the changes in the DMN in the BOLD/CBF data could on the one hand result from the different signal-to-noise ratio of the two techniques as well as the different signals (BOLD/CBF) used for the ICA analyses.

[1] Wang J et al., Magn Reson Med, 2003, 49:796, [2] Sämann et al., Mag Reson Mater Phy, 2010, 23:375.

Supported by a Sinergia Grant (CRSII3-136249) of the Swiss National Science Foundation.

P28C Lifespan developmental trajectories of temporal dynamics in intrinsic regional activity

C.G. Yan[1,2], S. Colcombe[1], Z. Yang[1,3], R.C. Craddock[1,3], C.E. Schroeder[1], F. X. Castellanos[1,2], M.P. Milham[1,3]

[1]Nathan Kline Institute for Psychiatric Research, Orangeburg, NY, USA; [2]New York University Child Study Center, New York, NY, USA; [3]Child Mind Institute, New York, NY, USA

Background: Resting-state fMRI methodologies are evolving to provide dynamic perspectives of the intrinsic brain. In particular, a growing number of studies have demonstrated time-varying patterns of intrinsic functional connectivity (iFC) that can be observed within, as well as between networks. However, these studies have primarily focused on the temporal variations in traditional bivariate correlation measures, rather than regional measures of intrinsic brain function (e.g., fractional amplitude of low frequency fluctuations [fALFF], regional homogeneity [ReHo], degree centrality [DC], or voxel-matched homotopic connectivity [VMHC]). Here we examined temporal dynamics for these regional measures, and explore their potential age-related variations.

Methods: Analyses were performed on 173 healthy participants (8 ~ 86 years old; 117 females) from the Enhanced Nathan Kline Institute - Rockland Sample (TR = 0.645 s, 10 minutes). Preprocessing including slice timing, realignment, and nuisance correction was performed with SPM8 and DPARSF. DARTEL was used to transform data into MNI space. To evaluate temporal variations in regional measures, sliding hamming windows (length of 100 TRs, overlapping of 3 TRs) were applied to the time series. Within each window, we calculated fALFF, ReHo, VMHC and DC. Coefficient of variation (CV) was calculated across windows for each measure. We examined age-related linear and quadratic changes in CV for each measure using a general linear model, with sex and motion as covariates.

Results: Overall, regional metrics appeared to show less temporal variation in higher-level cognitive regions, e.g., the default mode network, dorsolateral prefrontal cortex, while fluctuating more in lower-level primary regions and subcortical regions (Fig. A). Significant age effects in temporal variation were observed,

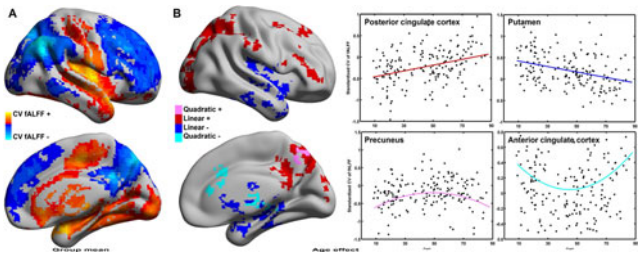

particularly for fALFF, which exhibited U-shaped quadratic age-trajectories centered around ages 45–55 depending on region (Fig B).

Conclusions: Consistent with studies of correlation-based iFC, we found that regional measures exhibit time-related variations. In particular, lower order sensorimotor and subcortical regions were characterized by relatively larger variations across measures. Initial evidence of potential age-related differences in the magnitude of temporal variations was observed for fALFF, though less for other metrics. Future work will establish approaches for optimizing the analysis and testing reliability.

P29C Characterizing Dynamic Brain Graphs in fMRI Data: Application to Schizophrenia

Qingbao Yu[1], Erik B. Erhardt[2], Vince D. Calhoun[1,3]

[1]The Mind Research Network, Albuquerque, NM, USA; [2]Department of Mathematics and Statistics, University of New Mexico, Albuquerque, NM, USA; [3]Department of Electrical and Computer Engineering, University of New Mexico, Albuquerque, NM, USA

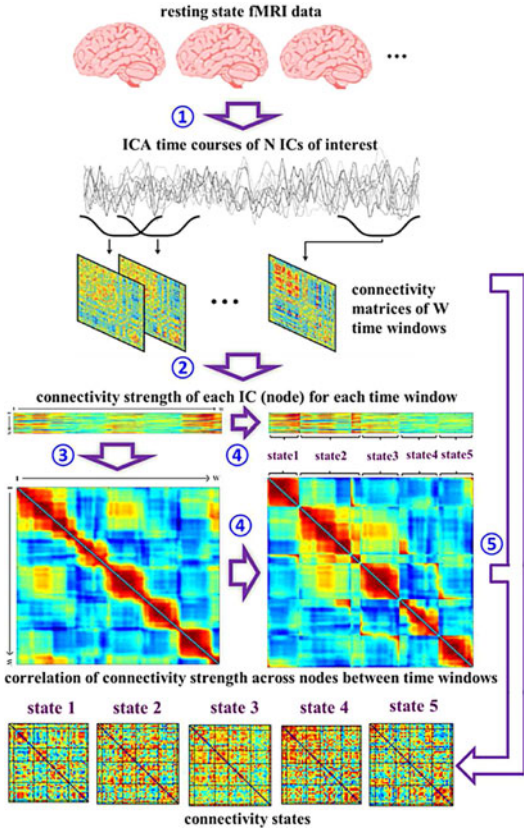

FIG. 1. Flowchart of the algorithmic pipeline for the analysis. group ICA, segment ICA time courses, and calculate the correlation between any pair of (N = 48) independent components (ICs) for each time-window; compute nodal connectivity strength of the weighted brain graph for each time-window; calculate the correlation of nodal connectivity strength between any pair of time-windows (W = 131) across (N = 48) ICs; reorder the time-windows based on the modular organization of the correlation matrix; compute the brain connectivity states by averaging the connectivity matrices of the time windows belong to the same module.

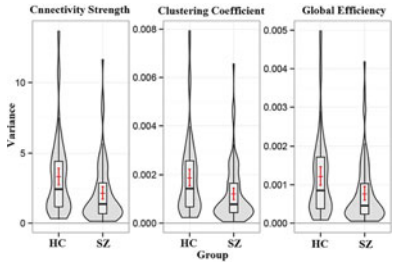

FIG. 2. Variances of the graph metrics of time-varying brain connectivity (over 131 time-windows). The mean and bootstrapped 95% confidence interval are in red, as well as a boxplot and smoothed density histogram. HCs show higher variances (Wilcoxon and permutation tests, $P < 0.001$ for all three metrics).

Background: Here we develop a novel approach to characterize dynamic graph properties of time-varying brain connectivity over time in resting state fMRI data and apply it to data collected from healthy controls (HCs) and patients with schizophrenia (SZs).

Methods: Participants include 82 HCs and 82 SZs, who complete a five-minute resting state fMRI scan (150 volumes). Time-varying brain graphs are built by group ICA, and a sliding time-window method. Connectivity states are identified using modular analysis. See Figure 1 for a pipeline of the analysis. Graph metrics including connectivity strength, clustering coefficient, and global efficiency of the time varying brain connectivity are computed.

Results: HCs show higher variances in graph metrics over 131 time-windows (see Figure 2). 276 and 278 connectivity states are identified in HCs and SZs respectively. HCs show higher graph measures across the connectivity states (each two-sample t-test, $P < 0.001$).

Conclusions: Dynamic graph properties of time-varying brain connectivity are altered in schizophrenia. This study provides a novel framework which is generalizable to many other areas including the study of different disease groups and cognitive measures.

P30C Brain Network Reconfiguration and Perceptual Decoupling during Shamanic Trance

M.J. Hove*[,1,2], J. Stelzer*[,1,3], T. Nierhaus[1], S.D. Thiel[1], C. Gundlach[1], D.S. Margulies[1], K.R.A. Van Dijk[4], R. Turner[1], P.E. Keller[1,5], B. Merker[6]

[1]Max Planck Institute for Human Cognitive and Brain Sciences, Leipzig, Germany [2]Harvard Medical School, Massachusetts General Hospital, Boston, MA, USA, [3]Danish Research Centre for Magnetic Resonance, Copenhagen, Denmark, [4]Harvard University, Cambridge, MA, USA, [5]The MARCS Institute, University of Western Sydney, Australia, [6]Kristianstad, Sweden
**equal contribution*

Background: Trance is a state of consciousness characterized by narrowed awareness of external surroundings and has long been used by shamans to gain valued insight. Shamans across cultures often induce trance by listening to rhythmic drumming. Using fMRI, we examined the brain network configuration associated with trance.

Methods: Participants were 15 experienced shamanic practitioners (mean age = 50.2 ± 8.3 y) from Germany and Austria. They had been involved with shamanic practices for an average

of 9.3 years (SD = 5.0). In the experiment, participants listened to rhythmic drumming, and either entered a trance state or remained in a non-trance state. We collected 8-minute scans on a Siemens Verio 3T scanner. We analyzed changes in network connectivity between trance and non-trance scans using Eigenvector Centrality Mapping, as well as seed-based analyses from a PCC seed. We also analyzed functional connectivity of seeds in the auditory pathway (auditory brainstem, inferior colliculus, medial geniculate nucleus, and primary auditory cortex).
Results: Trance was associated with higher eigenvector centrality (i.e., stronger hubs) in three distinct regions: posterior cingulate cortex (PCC), anterior cingulate cortex (ACC), and left insula/operculum. Seed-based analysis revealed co-activation of the PCC seed (a default network hub involved in internally-oriented cognitive states) with the ACC and insula (control network regions involved in maintaining relevant neural streams). This co-activation may indicate that an internally-oriented neural stream was amplified by the modulatory control network. Additionally, during trance, seeds within the auditory pathway were less connected, suggesting perceptual decoupling and suppression of the monotonous rhythmic drumming.
Conclusions: In sum, trance involved co-activation between default and control networks, and decoupled auditory processing. This network reconfiguration may promote an extended internal train of thought wherein integration and moments of insight can occur.

Theme 2: Structural Brain Connectivity/Multi-modal Approaches/Animal Models

P31C Choice of optimal quantitative anisotropy threshold for clinical HARDI reconstruction

C.M. Bauer[1], L. Zajac[2], B.B. Koo[2], G. Heidary[3], L.B. Merabet[1]

[1]Massachusetts Eye and Ear Infirmary, Boston, MA, USA, [2]Boston University School of Medicine – Center for Biomedical Imaging, Boston, MA, USA, [3]Boston Children's Hospital, Boston, MA, USA

Background: In studies comparing multiple clinical populations, the choice of optimal quantitative anisotropy (QA) threshold for diffusion reconstruction can drastically influence the results and may potentially lead to erroneous conclusions. This study examines the differences in whole brain neural networks in individuals with periventricular leukomalacia (PVL) compared to controls under two QA thresholds, the first being consistent across all subjects, and the second optimized to only capture white matter.
Methods: A HARDI MRI protocol was used to acquire data from 2 PVL subjects and 4 controls for comparison. HARDI images were acquired using an 8-channel head coil on a 3 Tesla Philips Achieva system using a single shot EPI sequence (64 diffusion directions, B_{max} 3000 s/mm^2, B_{min} 0 s/mm^2). HARDI volumes were corrected for eddy current artifacts and were skull-stripped prior to orientation distribution function (ODF) calculation and subsequent white matter fiber tracking and reconstruction. The brain was parcellated into 68 discrete regions in HARDI space. In house MATLAB software was used to generate connectivity matrices using tractography criteria of angle change $< 45°$, min/max length = 5/300 mm, 100,000 seeds, random fiber orientation, and Gaussian radial interpolation. The first set was calculated with QA threshold = 0.055, while the second set was calculated with QA threshold optimized within each subject (0.06–0.155).
Results: Connectivity matrices between the optimized and predetermined QA thresholds show significant differences (see Figure 1 for a representative subject from the PVL and control group). This may lead to difficulties making accurate and meaningful conclusions regarding clinical outcomes and correlations, particularly as having a set threshold can lead to artificially inflated or deflated values.
Conclusions: The choice of a predetermined QA threshold across all subject groups may lead to difficulties making accurate and meaningful conclusions regarding clinical outcomes and correlations, particularly as having a set threshold can lead to artificially inflated or deflated values.

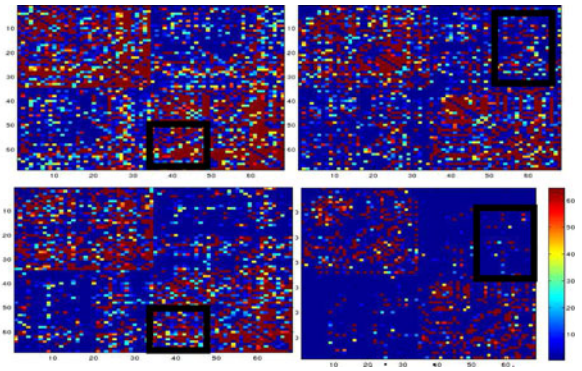

FIG. 1. Whole brain connectivity matrices from controls (left) and PVL subjects (right). The top row shows a fixed QA threshold of 0.055, while the bottom row shows the matrix generated with a QA threshold optimized on for each subject (0.06–0.155). The black boxes highlight examples where the number of fibres between ROIs is significantly different in the two QA threshold conditions.

P32C In vivo delineation of human brainstem grey matter with Diffusion Tensor Imaging at 7 Tesla

M. Bianciardi[1], N. Toschi[1,2], C. Eichner[1], B. Edlow[3], J.R. Polimeni[1], K. Setsompop[1], D. Boas[1], L.L. Wald[1]

[1]Department of Radiology, Athinoula A. Martinos Center for Biomedical Imaging, Massachusetts General Hospital and

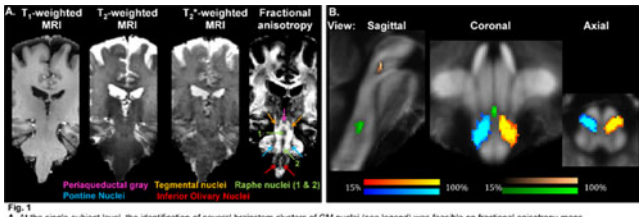

Fig. 1
A. At the single-subject level, the identification of several brainstem clusters of GM nuclei (see legend) was feasible on fractional anisotropy maps.
B. Probabilistic atlas (n. subjects = 8, % overlap) in MNI space of four brainstem GM structures (cyan/yellow: left/right inferior olivary nuclei; brown/green: raphe nuclei cluster 1/2) overlaid on fractional anisotropy maps.

Harvard Medical School, Boston, MA, United States, [2]Medical Physics Section, Department of Biomedicine and Prevention, Faculty of Medicine, University of Rome ''Tor Vergata'', Rome, Italy, [3]Department of Neurology, Athinoula A. Martinos Center for Biomedical Imaging, Massachusetts General Hospital, Boston, MA

Background: The human brainstem plays an important role in several vital functions, including arousal, nociception, autonomic homeostasis, and sensory functions. Our current knowledge of grey matter (GM) structure within the brainstem mostly derives from ex vivo studies [Paxinos and Huang, 1995; Naidich et al., 2009]. Aim of this work was to develop a novel in vivo MRI tool to identify brainstem GM structures.
Methods: Eight subjects (6 m/2 f, age 28 ± 2) participated in this IRB approved study. We employed in vivo high spatial-resolution (1.1 mm isotropic) diffusion tensor imaging (DTI) at 7 Tesla (60 directions, b $\sim$ 1000 s/mm^2, 7 interspersed b0 images, TE/TR = 60.8/5600 ms, 4 repetitions), and scrutinized the contrast in DTI-maps, including fractional-anisotropy (FA), computed after eddy-current correction and tensor estimation. We also acquired distortion- and resolution-matched T_2-, T_2*-weighted images and a 1 mm^3 T_1-weighted MPRAGE. On a single-subject basis, FA maps were automatically segmented by k-means clustering. Labels of 4 brainstem GM structures (raphe nuclei cluster 1 and 2, left and right inferior olivary nuclei clusters) were mapped and normalized to MNI space through high dimensional non-linear transformations, and a probabilistic atlas for these structures was created.
Results: In single subject FA maps, major clusters of brainstem GM structures were visible with higher contrast compared to T_1-, T_2-, and T_2*-weighted MRI (Fig. 1A). The raphe nuclei cluster 1 and the inferior olivary nuclei displayed higher overlap across subjects than the raphe nuclei cluster 2.
Conclusions: High spatial resolution DTI at 7 Tesla enabled the delineation of brainstem GM structures on a single subject basis. Our results also demonstrate the feasibility of developing a probabilistic atlas of brainstem GM structures, which coud be used as a tool to perform functional and structural connectivity studies of human brainstem GM in health and disease.

P33C Corticostriatal connectivity in children and adolescents with autism spectrum disorder

R.A Carper, S. Solders, I. Fishman, R.-A. Müller

San Diego State University, San Diego, CA

Background: Brain development is altered in children with Autism Spectrum Disorder (ASD), with accelerated brain growth in the earliest years, but atypically slow rates of growth later in childhood. Altered growth rates likely contribute to findings of abnormal structural and functional connectivity. Possible effects on striatal connectivity in ASD are not fully understood. The striatum is important for initiation and modulation of motor actions, response inhibition, and reward processing. In ASD, motor deficits such as incoordination, dyspraxia, and atypical gait are frequently reported, and rates of obsessive-compulsive disorder and attention deficit hyperactivity disorder are increased, suggesting that striatal function and connectivity may be altered. Our goal was to examine the distribution and integrity of connections between striatum and cerebral cortex in children and adolescents diagnosed with ASD.
Methods: 36 children and adolescents with ASD and 34 typically developing (TD) children ages 7–18 years were examined with diffusion weighted imaging and resting-state functional magnetic resonance imaging. Groups were matched on age, IQ, and total brain volume. (a) Probabilistic tractography was conducted with striatum as seed region and cortical ROIs as targets (frontal, parietal, temporal, occipital and insular lobes, hemispheres run separately, 3000 streamlines per seed voxel). Each voxel of the striatum was classified based on the target ROI to which it had the greatest likelihood of connecting. Volumes of these parcels were divided by total striatum volume to reflect the proportion of striatum connected to each target. (b) The 'frontal' parcel of the striatum was used to create a new seed region and tractography was repeated to subregions of the frontal lobe (precentral, orbital, medial, dorsolateral). Measures of white matter microstructure were derived from the diffusion tensor and extracted for each tract.
Results: (a) Repeated measures ANCOVA on the relative volumes of striatal parcels (covarying for subject age and head motion) found a significant interaction between target and diagnosis ($p < 0.05$) which was due to a significantly lower relative volume of frontally-connected striatum in the ASD group ($p < 0.05$). There were no group differences with regard to relative proportions devoted to sub-regions of the frontal lobe (orbital, medial, dorsolateral, precentral). (b) Microstructure (FA, MD, AD, RD) of corticostriatal tracts did not differ between groups for any of the identified tracts although there was a slight trend toward higher RD in the ASD group ($p = .08$).
Conclusions: Results suggest reduced structural connectivity of the striatum specifically with the frontal lobe. Corticostriatal pathways are involved in motor actions, response inhibition, reward processing, and goal directed behavior. A reduction in striatal regions with frontal connectivity may relate to impairments in these modulatory functions in individuals with ASD.

P34C Inter-regional resting state MRI functional connectivity covaries with correlations between Delta band local field potentials in primary somatosensory cortex of monkeys

George Wilson[1,2], Pai-Feng Wang[1,2], John C. Gore[1,2], Li Min Chen[1,2]

[1]Vanderbilt University Institute of Imaging Science, Nashville, TN, USA, [2]Department of Radiology and Radiological Sciences, Vanderbilt University Medical Center, Nashville, TN, USA

Background: The goal of this study is to better understand the origins and characteristics of resting state neural fMRI (rsfMRI) signals and their relationship to underlying electrical activity. Our previous analyses of rsfMRI signals revealed distinct and robust inter-regional correlation patterns among sub-regions of primary somatesnsory cortex (S1) in monkeys (Wang et al. Neuron 2013). Using the same experimental model, here we examined the inter-regional correlation differences in simultaneously recorded local field potentials from S1 subregions areas

3a, 3b, 1/2 and a control (face) region. We hypothesized that specific components of the local field potential (LFP) may underlie the fluctuation of rsfMRI signals.
Methods: Multi-site simultaneous microelectrode recordings were performed repeatedly in separate sessions in two anesthetized monkeys. Broadband electrophysiological signals, including spiking and LFP, were recorded simultaneously as 10 min long trials from areas 3a, 3b, 1/2 and a face control region within S1 cortex using a Plexon multi-channel recording system. Over 15 recording trials were included in the analysis. LFP signals were filtered into seven frequency bands (Delta, Theta, Alpha, Beta, Gamma low, Gamma high, and Gamma very high) for pair-wise inter-areal cross correlation analyses. Instantaneous amplitudes for the LFPs were acquired via previously published methods (Adhikari et al. 2010) using a Hilbert transform of the recorded signals.
Results: Cross-correlation analyses of the instantaneous amplitudes show differences in the strength, directionality, and lag of signals between S1 areas. The differences in signal amplitude and lag between areas were most prominent in the Delta band (1–4 Hz). The strengths of these Delta band correlations parallel the covariations of rsfMRI signals between areas. In Alpha band (9–14 Hz), the correlation between areas 3b-1 was statistically stronger than that between areas 3a-1. Furthermore, lags of rsfMRI signals between areas varied in directionality, with both areas 3a and area 1 leading area 3b, but control regions leading areas 3b and area 1.
Conclusions: Cross-correlation analyses of different components of LFP signals demonstrate that S1 areas (3a, 3b and 1/2) exhibit strong rsfMRI connectivity and also show strong interregional correlations in the 1–4 Hz Delta band of electrical activity. Relatively slow Delta range LFP oscillations may underlie the fluctuations of rsfMRI signals within SI cortex. LFP lag analyses provide insight into the direction of information processing flow among S1 areas.

P35C Functional connectivity of the ventral striatum during a reward/no-reward task in awake unrestrained domestic dogs

G. Berns[1], P. Cook[1], M. Spivak[2]

[1]*Center for Neuropolicy, Atlanta, GA, USA,*
[2]*Comprehensive Pet Therapy, Atlanta, GA, USA*

Background: The advent of cooperative canine neuroimaging (i.e., imaging dogs under behavioral, not chemical or physical restraint) has opened new avenues for understanding the mind of the domestic dog. Our group published the first fMRI findings in this new field (Berns, Brooks, & Spivak, 2012), showing differential activation of the ventral caudate nucleus to a hand signal signifying incipient reward vs a hand signal signifying no reward. Here, we report results from a psychophysiological interaction (PPI) analysis of BOLD data from the same task in a larger sample of dogs. This allowed us to localize brain areas that showed increased functional coupling with the caudate during reward prediction, providing insight into canine reward networks.
Methods: We imaged 10 dogs from the Atlanta area in a 3T MRI scanner at Emory University's FERN imaging center. Participation in the project was on a volunteer basis, and the dogs' owners conducted all training for the task under project staff guidance. Dogs each took part in six ~5 minute scans, two with their owner, two with a stranger, and two with a computer in a balanced ABCCBA order. In each scan, the dogs were presented with reward and no-reward signals in equal portion in a semi-random event design. The (reward)-(no-reward) contrast was computed for each dog across all six scan sessions. The voxels in the caudate showing maximum differential activation for this contrast were then used to generate bilateral functional 3 mm seeds. Time course of these seeds and their interaction with the experimental conditions were then used in a standard PPI connectivity analysis for each subject. Average maps were computed at the group level.
Results: Regions in right anterior thalamus and the right parietal lobe around the suprasylvian gyrus showed increased functional coupling with the caudate ($p < 0.01$) at the group level.
Conclusions: Suprasylvian cortex is essential for visual motion processing in other carnivores, and has been shown to connect with the ventral striatum through the thalamus. Notably, the ventral anterior thalamic nucleus projects directly to the basal ganglia. Our findings likely represent the basic components of a visual reward prediction network in dogs. Although holding still for the time required to conduct a resting state fMRI scan is still beyond most dogs, the results reported here indicate task-specific functional connectivity analysis is achievable. Such network-based approaches may serve as a useful compliment to the burgeoning brain and behavior literature featuring domestic dogs.

This work was supported by a grant from the Office of Naval Research.

P36C High b-value multi-shell diffusion MRI for the Human Connectome Project

M.K. Drews[1,2], Q. Fan[1], A. Nummenmaa[1], R. Zanzonico[1], A. Fotros[1], T. Witzel[1], B. Kiel[1], J.R. Polimeni[1], K. Setsempop[1], V. Renvall[1], T.G. Reese[1], S.M. Stufflebeam[1], B. Fischl[1], V.J. Wedeen[1], L.L. Wald[1], B.R. Rosen[1], R.L. Buckner[1,2], K.R.A. Van Dijk[1,2]

[1]*A.A. Martinos Center for Biomedical Imaging, MGH, Charlestown, MA, USA,* [2]*Center for Brain Science, Harvard University, Cambridge, MA, USA*

Background: Recent advances in diffusion imaging (dMRI) hardware, such as the Connectom scanner at the Martinos Center for Biomedical Imaging have allowed us to push our acquisition of dMRI data for structural connectivity analysis further than ever before (Setsempop et al., 2013). In particular, this scanner makes it possible to acquire data at higher b-values than previously feasible. However, given that there is limited time to acquire data in a typical clinical or research session, finding the optimal acquisition scheme is important. The goal of this study was to evaluate the benefits of a multi-shell acquisition scheme as compared to a high b-value single shell acquisition.
Methods: 33 healthy adults were scanned using a 64-channel helmet receive array head coil on the 3T Connectom scanner at the Martinos Center. Four sets of diffusion weighted images were acquired over five separate runs at $b = 1{,}000$ s/mm^2 (64 directions), $b = 3{,}000$ s/mm^2 (64 directions), $b = 5{,}000$ s/mm^2 (128 directions), and $b = 10{,}000$ s/mm^2 (256 directions) using the following DW-EPI protocol: TR = 8800 ms, TE = 57 ms, $\delta = 12.9$ ms, $\Delta = 21.8$ ms, iPAT = 3, max gradient strength = 243 mT/m. These data sets are publically available as part of the NIH Human Connectome Project. We applied geometric distortion correction and motion/eddy current correction algorithms (FSL) and co-registered all data from a single session to the first $b = 0$ volume. Diffusion orientation density functions (ODFs) were computed using DSI Studio (Yeh et al., 2011). The $b = 10{,}000$ single shell dataset was processed using the q-ball method (Descoteaux et al., 2007), while the multi-shell datasets were processed using generalized q-sampling

(GQI) (Yeh et al., 2011). Using these reconstructions, the datasets were evaluated on the basis of ODF shape, quantitative anisotropy (QA0, QA1, QA2), general fractional anisotropy, and tractography, both in individuals and group averages.
Results: In single shell b = 10,000 images, ODFs are sharper than in multi-shell images in the centrum semiovale (CSO), and in areas where there are crossing fibers, the second and third peaks become more prominent. These sharper ODFs facilitate tractography through areas of crossing fibers. However, other areas, such as the center of the brain or areas outside the major white matter tracts, have better signal and are more defined in a multi-shell scheme. ODFs from multi-shell sets are not quite as sharp as b = 10,000 in the CSO, however by including the lower shells, the multi-shell acquisition retains the ability to resolve fiber bundles in areas that are problematic for b = 10,000 on its own.
Conclusions: There are advantages of using high b-values such as b = 10,000, but there are also drawbacks. Multi-shell diffusion imaging becomes advantageous in a high b-value diffusion imaging scheme, allowing benefits of the higher b-value, but also compensating for some of the costs.

P37C Cortical parcellation based on DTI connectivity using classification methods – validation in the squirrel monkey

Y. Gao[1,2], B.A. Landman[1,2,5], A. J. Plassard[3], K. Shillings[1], A.S. Choe[1,2], I. Stepniewska[1,4], X. Li[1], Z. Ding[1,5], A.W. Anderson[1,2,4]

[1]Institute of Imaging Science, [2]Department of Biomedical Engineering, [3]Department of Computer Science, [4]Department of Psychology [5]Department of Electrical Engineering, [6]Department of Radiology and Radiological Science, Vanderbilt University, Nashville, TN, US

Background: Our previous study[1] shows that the DTI-derived structure-connectivity could be used as clustering features to divide the cortex into reasonable parcels. In the following study, the connectivity from the histological parcels was added into a number of supervised learning machines to parcellate the interface of gray and white matter. The accuracy of DTI-connectivity-based parcellation was calculated.
Methods: A fixed squirrel monkey brain was scanned in a 9.4 Tesla scanner (PGSE, TR = 4.6 s, TE = 42 ms, number of gradient directions = 31, b = 1020 s/mm^2). The probabilistic tractography was seeded from each voxel right underneath the cortex. The brain tissue was sectioned and stained with Nissl. 18 cortical parcels were identified based on Nissl-revealed cytoarchitecture as the ''truth''. Supervised machine learning methods included support vector machine (SVM), naïve bayes (NB), K nearest neighborhood (KNN) and decision tree (DT). Each feature vector was the fiber density from one seed point. The feature vectors from randomly selected 50% of seeds were used as training data and the remaining was the test data. The accuracy of the parcellation was the overlap of calculated parcels and the truth out of the truth.

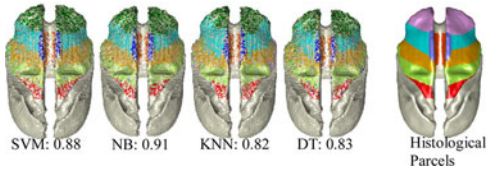

FIG. 1.

Results: Figure 1 shows the classification results and the accuracy of the parcellations.
Conclusions and discussions: With the histological parcels of the same monkey as prior, the DTI-derived structure connectivity parcellates the cortex with good accuracy.
Reference: Y Gao, ISMRM, 2014.

P38C Dynamic BOLD correlates of infraslow EEG

J.K. Grooms[1,2], G.J. Thompson[1,2], E. Schumacher[1], C. Epstein[3], S.D. Keilholz[1,2]

[1]Georgia Institute of Technology, Atlanta, GA, USA, [2]Emory University, Atlanta, GA, USA, [3]Emory University School of Medicine, Atlanta, GA, USA

Background: Recent experiments have demonstrated significant correlations between infraslow electrophysiologic and hemodynamic signals under an assumption of wide-sense temporal stationarity in both rats[1] and humans*. However, stationary methods are inadequate for capturing brief periods of variable correlation between signals[2,3]. Therefore, some investigators analyze data over timespans shorter than the acquisition period and have found evidence of time-varying relationships between different brain areas[3,4,5]. This study investigates dynamic relationships between infraslow (< 0.1 Hz) electroencephalographic (EEG) and blood-oxygen level dependent (BOLD) signals in humans.
Methods: 68 channels of infraslow EEG and BOLD data were simultaneously recorded from 8 human subjects in a resting state. Signals from both modalities were filtered to a passband of 0.01 – 0.08 Hz. Correlation between EEG signals was calculated in sliding window segments to assess dynamic activity synchronization. The dynamic relationship between modalities was also examined using sliding window correlation. FPz was chosen for this analysis because of its strong stationary correlation with BOLD signals. For both analyses, three different window lengths (12 s, 20 s, 50 s) were used that correspond to three consistently observed peaks (0.02 Hz, 0.05 Hz, 0.09 Hz) in EEG power spectra and coherence spectra with BOLD data.
Results: Infraslow EEG signals oscillated between periods of nearly global synchronous activity and periods of desynchronization in all participants and every window length tested. Dynamic spatial patterns of correlation resembling known resting state networks were consistently observed in sliding window analyses between FPz and BOLD.
Conclusions: The oscillating infraslow EEG synchronization may be related to EEG microstates and hypersynchrony found in

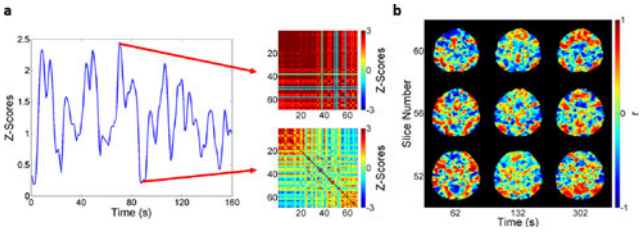

FIG. 1. **A**: Average inter-electrode EEG correlation using a window length of 20 s representing synchronization over time from a typical scan. Correlation matrices for the global maximum and minimum are shown right. **B**: Three time points of sliding window correlation between FPz and BOLD from a typical scan using a window length of 20 s.(*) Results currently in preparation for publication.

BOLD data[4]. Time-varying patterns of correlation between modalities may be related to quasi-periodic patterns in humans[6] and similar findings in rats[7]. Further work is needed to elucidate these relationships, but these results show that infraslow electrophysiology plays a role in the dynamic configuration of functional networks.

P39C Spectral Signatures of Brain Network Development in Resting State MEG

J. A. Hashmi[1,4,5]*, S. Khan[2,4,5]*, R. L. Gollub[1,4,5], J. Kong[1,4,5], M. S. Hamalainen[3,4,5], S. S. Stufflebeam[3,4,5], T. Kenet[2,4,5]

[1]Department of Psychiatry, [2]Neurology and [3]Radiology, [4]Massachusetts General Hospital, [5]Harvard Medical School, Boston, Massachusetts, United States

Background: Understanding the intricate connectivity changes in brain networks that occur over the lifespan will not only help to define what constitutes normal brain development and aging, but also provide benchmarks against which to assess what goes awry in developmental and psychiatric disorders. Existing knowledge on the development of brain networks is based on fMRI studies that demonstrate that brain networks show a higher level of local processing in children. With maturation, the processing shifts into a globally distributed network (Fair et al., 2009; Supekar et al., 2009). However, the neurophysiological underpinnings of large scale brain networks and how they change with development are not clearly known. Oscillations in specific frequency bands are a putative means for synchronizing neuronal activity between spatially segregated neuronal populations, thus forming global communication networks of the brain (Siegel et al., 2012). Here we aimed to understand how cortical oscillations contribute to developmental changes in brain networks by using direct brain signals measured with magnetoencephalography (MEG).
Methods: We used network analysis in resting state MEG data from 71 healthy subjects divided in to three groups (8–12 years, $n=23$; 13–17 years, $n=19$; 18–47 years, $n=29$) to investigate how oscillations in different frequency bands (Khan et al., 2013) contribute to developmental changes in brain networks. Connectivity was measured between 450 cortical regions by measuring temporal correlation in amplitude of MEG signals (Hipp et al., 2012) and analyzed with network theory and Graph Analysis (Hashmi et al., 2014).
Results: The slow envelope signals ($\sim$0.01–0.25 Hz) temporally synchronized the fluctuations in magnitude of neural activity resulting in globally connected networks with distinct spatial patterns for different oscillatory bands. Developmentally, our grouping showed an age related decrease in efficiency of local networks connected by gamma ($F=8.44$, $p=0.001$), alpha ($F=3.9$, $p=0.026$), delta ($F=9.6$, $p<0.0001$) and theta bands ($F=6.7$, $p<0.0001$). In contrast, efficiency of globally distributed brain networks increased for gamma ($F=4.25$, $p=0.02$) and delta ($F=5.7$, $p=0.05$) bands (Main effect: $F=7.1$, $p<0.0001$; network density = 10%). For Figure see http://martinos.org/~sheraz/rest.jpeg
Conclusions: This is the first evidence to show that networks derived from slow signals that modulate delta and gamma amplitudes are inextricably linked with developmental changes in brain network topology. Consistent with fMRI findings, our results demonstrate that younger brains have adapted to more efficiently utilize low cost local networks. As the brain develops, global high cost networks are incrementally recruited which may be linked with changes in cognitive and intellectual maturation (Basset et al., 2009). These findings not only have significant implications for fMRI based findings, they can also help to better characterize the normative range for brain network maturation. These benchmarks will have utility in early detection of several neurodevelopmental disorders such as autism and ADHD.

P40C Cortical myelination and structural brain network changes during childhood and adolescence: comparing with cortical thickness network

Seun Jeon[1], Jong-Min Lee[1]* and Brain Development Cooperative Group

[1]Department of Biomedical Engineering, Hanyang University, Seoul, South Korea

Background: Recent neuroimaging studies have characterized the development of cortical thickness network changes in childhood and adolescence. Cortical myelin contrast offers a unique understanding of brain development, and, to the best of our knowledge, has not been previously used in analysis of structural brain networks.
Methods: Data were collected from the Pediatric MRI Data Repository created for the NIH MRI Study of Normal Brain Development. The population sample consisted of 199 subjects (one scan per subject) has been categorized into 2 age groups (childhood: $n=100$, age range = 4.8–11.3 years; adolescence: $n=99$, age range = 11.4–18.3 years).

All T1-weighted MRI scan data were submitted to fully-automated CIVET pipeline. Cortical thickness was measured as the Euclidean distance between inner and outer cortical surface on 81,924 vertices. Enhanced myelin contrast (T1w/T2w ratio) was calculated after sampling MRI intensities at a depth of 50% through cortical thickness.

Average cortical thickness and myelin contrast were obtained on the 78 regions using the AAL template after regressing out the gender effect. Interregional partial correlation matrix (78×78) was obtained for each group and measure. Graph theoretical metrics (small-worldness, clustering coefficient, global efficiency and shortest pathlength) of structural brain network were calculated using cortical thickness and myelin contrast as features separately.
Results: In figure, network properties are displayed between 6% and 39% network sparsity in 3% increments. Red arrows indicate the differences in network property between childhood and adolescence group (shown at the 15% network sparsity only for an example). The group differences of graph theoretical metrics in cortical myelin network were prominently higher (more sensitive) than cortical thickness network.
Conclusions: This work represents the first examination of the cortical myelin network of healthy children and adolescents

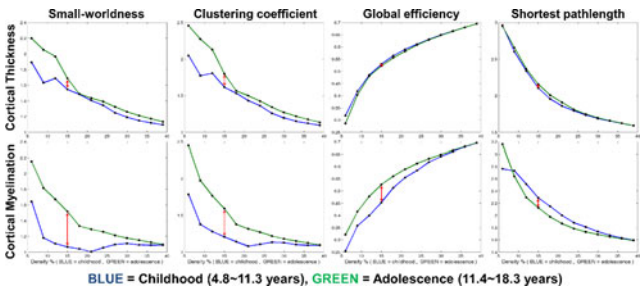

FIG. 1.

using a large cohort database. The present study indicates that with specifically designed informative developmental neuroimaging marker, myelin network measurement can serve as a most promising tool for advanced techniques to identify early wiring alterations such as autism, schizophrenia and bipolar disorder.

P41C Classifying two major axes in non-demented aging from structural and resting-functional brain connectivity

B.-B Koo[1], Y. Zhao[2], P. Shultz[1], L. Zajac[1], D. Rosene[1], R.J. Killiany[1]

[1]Boston University, Boston, MA, USA, [2]Philips Healthcare, Cleveland, Ohio, USA

Background: Since the brain operates as a large-scale complex system, it is expected that if alterations in neural connections occur during the aging process they would be detectable by multivariate and multi-site analyses. In this study, we applied a multivariate classification (Random Forest, *RF*) scheme to diffusion spectrum imaging (*DSI*) data in order to identify structural brain connectional elements associated with the process of aging in a non-human primate model of normal human aging. The features that were extracted were also compared to the resting functional (*rsfMRI*) network derived from the same subjects.
Methods: Eighteen monkeys (6 young/12 old) were used in this study. Cognition was measured and the identical imaging protocol from our previous study [*Koo et al., hippocampus, 2013*] was used: *DSI*-128 half Q-scheme with 2 mm iso-cubic voxel/ *rsfMRI*-155 volumes, 2 sec-30 msec (TR-TE) with 1-1-2 mm voxel/ T1-3D TFE with 0.6 mm iso-cubic voxel from 3T *Philips Achiva* scanner. To extract structural features, *DSI* connectivity matrix (for detailed descriptions, please see *Koo et al., 2013*) were directly embedded in *RF* (1st level). Second-level classifications were then iteratively performed to select the best subset of features, by applying different thresholds on feature importance weights obtained from the 1st level. The same process was applied to the *rsfMRI*.
Results: In *RF* structural network analysis, 346 subsets among 6921 total connections revealed the best young/old classification (~10% out-of-bag over 950 trees). By applying univariate statistics in each features, weaker structural connections were found in selected features. Significant age-related structural features mostly represented inter-lobular long-range connections, with top-ranked features representing medial parietal connections (fig.*A*). Interestingly gray matter (*GM*) projections of feature weightings, revealed 2 major axes: '*medial anterior-to-posterior*' and '*superior parietal-to-superior temporal*' (fig.*B*). The aging effects of *GM* indicate alterations to long-range connections and position relative to the axes (fig.*B, graph*). Although it was minor feature to aging, intra-lobular connections in frontal and temporal explained cognitive differences within the old (fig.C). Those 2 intra-lobular modules were connected through subcortical connections (fig.*C, graph*). *rsfMRI (446 subsets)* also revealed significant aging features mostly in its long-range connections. Selected features were mostly anterior-posterior connections with weaker strength patterns in the old (fig.*D, left*), but stronger connections in the old were also confirmed in some prefrontal inter-hemispheric prefrontal and temporal-prefrontal features (fig.*D, right*). Only one third of features overlapped between structural and function domains, but structural-functional proximities were significant in their *GM* projections (fig.*E*).
Conclusions: Our multivariate/multimodal imaging scheme consistently confirmed 2 major axes for non-demented aging. In addition, relative intactness on cognition within the old was described by the minor features outside the 2 axes. Mismatch between the features found in structural and functional networks demonstrate the complexity of network analyses. However, robust links between the two networks were confirmed by the *GM* projection patterns, namely network nodes. Importantly, cortices near major vessels (known as high energy demanding regions) were consistently found along the 2 major axes from the network node representations. This suggests that greater understanding is needed as to cerebrovascular support of brain networks in order to better understandings the neurobiology of aging.

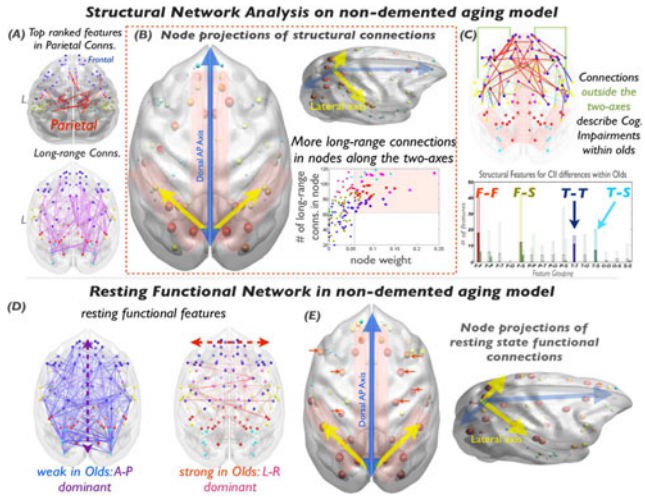

P42C Spontaneous fluctuations in low frequency local field potential correlate with resting state MRI signal in rat whisker barrel cortex

H. B. Lu, L. Wang, W. Rea, E.A. Stein, Y. Yang

Neuroimaging Research Branch, National Institute on Drug Abuse, NIH, Baltimore, MD, USA

Background: The mechanisms of resting state MRI (rsMRI) signal remain poorly understood despite widespread applications of this technique. Several lines of evidence suggest the important role of spontaneous slow and infraslow EEG oscillation underlying the low-frequency blood oxygenation level dependent (BOLD) fluctuation. However, contrasting hypotheses emphasize the roles of higher frequency (gamma) activity. This issue is fundamental in conceptualizing the roles of ongoing spontaneous activity in human brain function given that high frequency such as alpha and gamma and low frequency such as delta are involved in different brain operations. This study aims to address this question using a whisker barrel cortex (WBC) stimulation model.
Methods: A computer-controlled MRI-compatible apparatus was developed to move rat whiskers rostral-caudally with a comb. fMRI experiments were performed on a Bruker 9.4T scanner. Anesthetized rats (n = 9) received fMRI scans with and without ***continuous*** whisker stimulation (TR/TE = 1000/15 ms, 11 slices, 300 repetitions). A block design paradigm was also applied to identify the WBC. **Electrophysiological study**: Under identical anesthetic conditions, epidural EEG signals from bilateral WBC were recorded from a separate cohort of rats (n = 10) with semi-micro electrodes. EEG power synchrony between electrode pairs was computed using the complex Morlet Wavelet method.
Results: BOLD activation and functional connectivity maps are shown in Figs. 1**A-B**. In comparison to the resting condition,

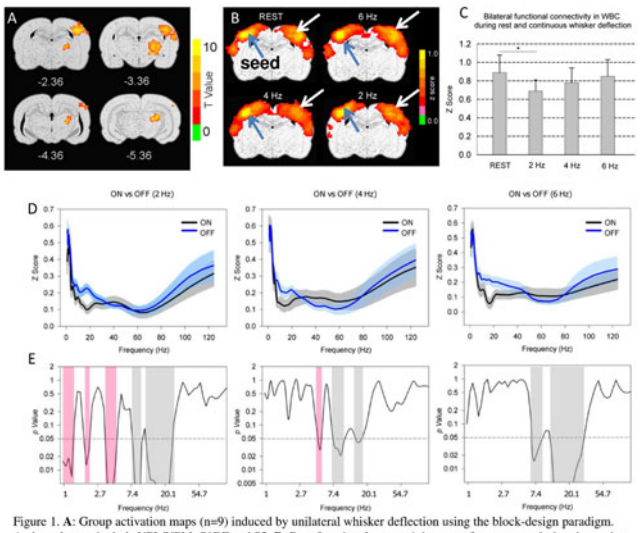

Figure 1. **A:** Group activation maps (n=9) induced by unilateral whisker deflection using the block-design paradigm. Activated areas include VPL/VPM, S1BF and S2. **B:** Raw functional connectivity maps from one rat during the resting condition and during continuous unilateral whisker stimulation (2, 4 and 6Hz); Blue arrows indicate seed voxels. **C:** Continuous unilateral whisker stimulation at 2 Hz, but not at 4 or 6 Hz, significantly reduces functional connectivity in bilateral whisker barrel cortex (N=9; *, p=0.001). **D:** Plots of power correlation (n=10) between bilateral WBC as a function of LFP frequency for each of the 3 whisker stimulations. **E:** Unilateral whisker stimulation significantly reduces power correlations in low frequency range (≤ 4Hz, pink shading) under the 2 and 4 Hz stimulus conditions. Power correlation at higher frequency ranges (>4 Hz, gray shading) was reduced across all 3 stimulus condition.

continuous unilateral whisker stimulation significantly modulated bilateral functional connectivity only at the 2 Hz, but not the 4 or 6 Hz condition (**C**). Epidural EEG data reveal that, *only* in the delta frequency range was the power correlation significantly modulated at 2 Hz, but not at 6 Hz stimulus condition, *paralleling the fMRI findings*. Power correlation in other frequency ranges were similarly modulated irrespective of the stimulus conditions.
Conclusions: We reasoned that if LFP signal in the high frequency bands were the major contributors to the rsMRI signal, then by modulating brain electrical activity within these bands, one should expect modulations in corresponding fMRI functional connectivity. This is not supported by our data: significant changes in *high frequency* EEG power synchrony were observed across all three stimulation conditions (2, 4 and 6 Hz), but only at the 2 Hz stimulation condition did we observed significant changes in functional connectivity, in which, the delta band EEG synchrony was reduced. These findings support the view that spontaneous activity in the delta band drives the rsMRI signal.
Acknowledgement: This work was supported by the Intramural Research Program of the NIH, NIDA.

P43C Altered white matter integrity and structural connectivity in adults born preterm

C. Meng[1,4,5], J. Bäuml[1,4], C. Zimmer[1], A.M. Wohlschläger[1,3,4,5], C. Sorg[1,2,4]

Departments of [1]Neuroradiology, [2]Psychiatry, [3]Neurology, [4]TUM-Neuroimaging Center of Klinikum rechts der Isar, Technische Universität München, Munich, Germany; [5]Graduate School of Systemic Neurosciences GSN, Ludwig-Maximilians-Universität, Munich, Germany

Background: Adverse neurobehavioral outcome has been well documented in preterm born population. It is assumed that atypical white matter maturation plays a crucial role for understanding neural mechanisms related to preterm birth. Diffusion tensor imaging (DTI) is a structural magnetic resonance imaging technique allowing reconstruction and assessment of three dimensional white matter tracts. Here, we focused on potential differences in white matter integrity and structural connectivity associated with preterm birth, to uncover the long-term developmental consequences in adults.
Methods: The present study is part of the prospective Bavarian Longitudinal Study (BLS) in which geographically defined whole-population sample of children born in 1985/1986 are longitudinally tracked (Wolke and Meyer, 1999). DTI scans for 154 adults were acquired by 3T Philips MRI for 85 preterm born adults (mean age, 26.45 years; 47 male; ranged in gestational age from 25 to 36 weeks), and 69 age- and gender-matched full-term born adults (mean age, 26.35 years; 44 male; ranged in gestational age from 37 to 42 weeks). Diffusion tensor and fractional anisotropy (FA) was computed by FSL's FDT toolbox. Tract-based spatial statistics was used to reconstruct whole brain white matter pathway. Determinative tractography was employed to compute structural connectivity of regions of interest. Nonparametric permutation-based tests were employed for group comparisons and assessing relationships between white matter alterations and preterm birth indexed by gestational age, birth weight, and neonatal optimality.
Results: Widespread microstructural changes were identified in adults born preterm compared with full-term born adults ($p < 0.05$, TFCE corrected). In preterm group, major white matter tracts showed reduced FA and reconfigured fiber connection, particularly in corpus callosum, thalamic radiation, right cingulum, corticospinal tract, superior and inferior longitudinal fasciculus, and inferior fronto-occipital fasciculus. Decreasing FA in corpus callosum was positively correlated with decreasing gestational age and negatively correlated with neonatal optimality (0 means best state; the higher the worst).
Conclusions: This study revealed altered white matter in adult brain, supporting long-term impact of preterm birth which continues into adulthood. These findings extended our knowledge about neurologic sequelae of preterm birth. Moreover, affected long-range structural connectivity may imply prominent whole brain reorganization underlying very early perturbation and long-term neurodevelopment.

P44C Simultaneous recording of slow hemodynamic signals from the brain and periphery

Wen-Ju Pan[1], Jacob Billings[1] and Shella Keilholz[1]

[1]BME, Emory University/ Georgia Tech, Atlanta, GA, United State

Background: Resting-state fMRI relies on slow BOLD fluctuations, assuming regional neurovascular coupling at ~0.1 Hz[1]. However, slow fluctuations have also been observed in the peripheral vasculature as well[2]. These non-neuronally-driven vascular variations that overlap in frequency with the BOLD fluctuations are a potential confound for the hypothesis that resting state fMRI reflects neural activity. To examine the relationship between slow hemodynamic fluctuations in the brain and in non-brain areas, hemodynamic signals from somatosensory cortex (S1), visual cortex (V1), and the peripheral vasculature in hind paws of rats were simultaneously examined using an optical method.
Methods: Five SD rats (male, 300–400 g) were used in this study. The hemodynamic signals of 3 cortical sites (left and right S1 and left V1), and 2 peripheral sites (bilateral hind paws) were obtained by functional near-infrared recording. The optic probes were custom-made source-detector pairs for fitting small brain sites (< 3 mm) and paw skin recordings, which detect Hb/dHb changes in light absorption at 940 nm. A thinned bone window in the skull was prepared at each cortical site, and the probe

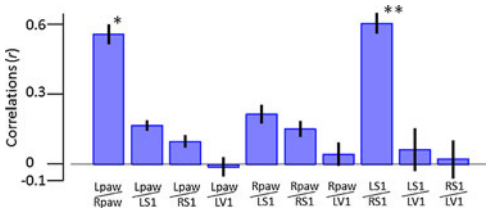

FIG. 1. Cross correlations between channel pairs. Significant higher correlations for bilateral hide paws or bilateral S1s than other pairs on 0.05–0.15 Hz signals (One-way *ANOVA*, $n=25$, $p=0.00$, *, **; no significant different between pairs of Lpaw/Rpaw and LS1/RS1). Bars indicate mean +/− SEM.

contacted the bone closely, pointing vertically to cortex. The photo-detector signals were amplified in DC amplifiers (0–100 Hz filtered, A-M Systems, model 3000), and digitalized with 1200 sampling rate (NI, PCI-6281). Signals from all 3 brain sites and 2 paw areas were simultaneously recorded for 7 minutes in each resting run under isoflurane anesthesia (2% or 1–1.5%). Data was also recorded from the euthanized rat at the end of the study. The signals from each site were compared based on frequency components and power spectra, and cross-site correlations between 0.05–0.15 Hz were calculated.

Results: signals from all sites showed prominent slow fluctuations as well as clear cardiac high frequency pulses. The paired correlations between the signals from the 5 sites summarized from 25 runs are shown in Fig. 1, and indicate robust correlations within bilateral S1 sites and bilateral paws, which are significantly higher than other pairs though certain correlations exist between brain and peripheral signals.

Conclusions: The ~0.1 Hz BOLD fluctuations may be intrinsic to the vasculature, whether in the brain or outside the brain, but the coordinated activities seem to be restricted to functional systems, and suggest that neural modulation coordinates the BOLD fluctuations underlying the basic resting fMRI signal mechanism[1].

(References: [1]. Pan, W.-J., et al., *Neuroimage* 74,288–297, 2013; [2]. Mayhew, J.E.W. et al, *Neuroimage* 4, 183–193,1996)

P45C Efficiency of Diffusion Tensor Imaging in the Estimation of Brain Connectivity; A Simulation Study

M.H A'arabi[1], A. Fathi Kazerooni[1], N. Mohammadi[1] and H. Saligheh Rad[1]

[1]*Quantitative MR Imaging and Spectroscopy Group, Research Center for Molecular and Cellular Imaging, Tehran University of Medical Sciences, Tehran, Tehran, Iran*

Background: Diffusion tensor imaging (DTI) and tractography are potent MRI tools for providing essential information about the structural networks associated with functional connectivity of the brain. This could be helpful for reliable pre-surgical planning of many brain disorders **[1]**. However, selecting suitable imaging parameters for generating fibers and assessing the brain connectivity imposes constraints in their clinical implementations: (1) higher *b*-values could provide better contrast for high cellular structures while it compromises signal-to-noise ratio (SNR); (2) SNR could be improved by increasing the number of excitations (NEX) in the acquisition and the number of diffusion gradient direction (NDGD), which both make the acquisition rather longer and not feasible for a routine clinical setting. The aim of this study is to assess the effects of using different values of NDGD, NEX and *b*-values on the fiber tracts and brain connectivity in a simulation scheme, to obtain guidelines for optimizing them for a reliable DTI quantification.

Methods: A total of 50 brain DWI (DTI) simulation data with size of $107\times79\times60$ and voxel size of $2\times2\times2\,mm^3$ were generated based on **[2]** with different NDGD, various NEX and *b*-values. Firstly, 25 data were created with *b*-values of 500, 700, 1000, 1200, 1500 s/*m*m^2, in 6, 12, 20, 30, and 64 directions for each *b*-value and NEX = 1. Then, at a *b*-value of 1200 s/*m*m^2, another 25 data were generated with NEX = 1, 2, 3, 4, 5 in 6, 12, 20, 30, and 64 directions for each NEX. The fibers were constructed using *ExploreDTI* software **[3]** and streamline algorithm with tensors estimated by linear least-squares fitting, with the fractional anisotropy (FA) threshold range of 0.2–1 and minimum angle of 30°. After fiber tracking, the brain connectivity matrix was calculated by ε-neighbor construction **[4]**.

Results: The relative errors (RE) in the number of fibers and the size of connectivity matrix (representing brain connectivity) were evaluated by changing *b*-values and NEX. It is indicated that the number of estimated fibers in lower NDGD (6–12) is sensitive to *b*-values and the growth rate of RE changes rapidly. However, higher NDGD (20–64) are less sensitive to *b*-values and RE increases in high *b*-values: in higher NDGD (20–64), RE is approximately uniform (6.8–11.7%). At a fixed *b*-value (1200 s/mm^2), by increasing NEX, the number of fibers increases by varying NDGD; but, the differences in the size of connectivity matrices are small, meaning that brain connectivity has not enhanced. By increasing the NEX in the range of 1–3, RE in number of fibers decreases rapidly; although in the range of 4–5, no notable change was observed (7.6–14.1%). Increasing the NEX could lead to significant improvement of brain connectivity (21.1-4.4%) in lower NDGD (6–12). But in higher NDGD (20–64) it did not improve significantly (7.1-2.4%).

Conclusions: Our results demonstrated that the number of fibers in the brain could vary to a desirable amount by optimizing NDGD, *b*-value and NEX parameters. These findings demonstrated that brain connectivity in DTI is sensitive to changing *b*-values but less sensitive to NEX, suggesting that reliable analysis is achieved in a routine clinical setting.

References: **[1]** Camchong J et al., Schizophrenia Bulletin, January 1, 2009. **[2]** Van Hecke W et al., Neuroimage, vol. 46, pp. 692–707, 2009. **[3]** Leemans A et al., ISMRM 2009, p. 3537. **[4]** Chung MK et al., SPIE Medical Imaging, 2011.

P46C Parallel systems in the control of speech

A.J. Simmonds[1], R.J.S. Wise[1], C. Collins[1], O. Redjep[1], D.J. Sharp[1], P. Iverson[2], R. Leech[1]

[1]*Division of Brain Sciences, Imperial College London, UK,* [2]*Division of Psychology and Language Sciences, University College London, UK*

Background: Modern neuroimaging techniques have advanced our understanding of the distributed anatomy of speech production, beyond that inferred from clinico-pathological correlations. However, much remains unknown about functional interactions between anatomically distinct components of this speech production network. One reason for this is the need to separate spatially overlapping neural signals supporting diverse cortical functions.

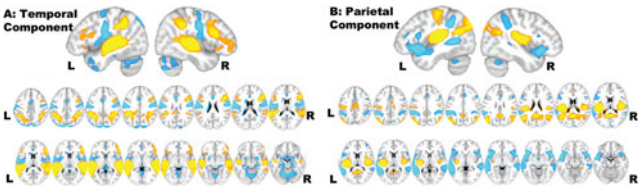

FIG. Whole-brain functional connectivity maps for the two components: *(A)* temporal (pSTG); *(B)* parietal (vAPL), positive shown in warm colors and negative (anti-correlation) in cold colors. Sagittal ($x = -44$ and 44 mm), and two rows of axial slices (upper, $z = 43$ to 15 mm, in 4 mm decrements, and lower, $z = 11$ to -17 mm). The statistical threshold for the overlays was set at $P < 0.01$, corrected for multiple comparisons using a correction for familywise error rate.

Methods: We took three separate human functional magnetic resonance imaging (fMRI) datasets (two speech production, one 'rest'). In each we decomposed the neural activity within the left posterior perisylvian speech region into discrete components.
Results: This decomposition robustly identified two overlapping spatio-temporal components, one centered on the left posterior superior temporal gyrus (pSTG), the other on the adjacent ventral anterior parietal lobe (vAPL). The pSTG was functionally connected with bilateral superior temporal and inferior frontal regions, whereas the vAPL was connected with other parietal regions, lateral and medial. Surprisingly, the components displayed spatial anti-correlation, in which the negative functional connectivity of each component overlapped with the other component's positive functional connectivity, suggesting that these two systems operate separately and possibly in competition. The speech tasks reliably modulated activity in both pSTG and vAPL, but their activity patterns dissociate in response to different speech demands. These components were also identified in subjects at ''rest'' and not engaged in overt speech production.
Conclusions: These findings indicate that the neural architecture underlying speech production involves parallel distinct components that converge within posterior peri-sylvian cortex, explaining, in part, why this region is so important for speech production.

P47C Dynamic cortical connectivity underlies the brain's default mode network

W. Tang[1], H. Liu[1], L. Douw[1,2], U.T. Eden[3], M.A. Kramer[3], M.S. Hamalainen[1], S.M. Stufflebeam[1]

[1]Athinoula A. Martinos Center for Biomedical Imaging, Massachusetts General Hospital, Charlestown, MA, USA, [2]Department of Anatomy and Neurosciences, VU University Medical Center, Amsterdam, The Netherlands, [3]Department of Mathematics and Statistics, Boston University, Boston, MA, USA

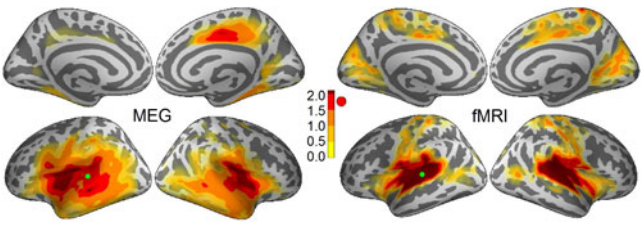

FIG. 1. Time-averaged MEG map vs. fcMRI map. Dot near the colorbar shows the minimal size of a significant cluster. Seed is in green.

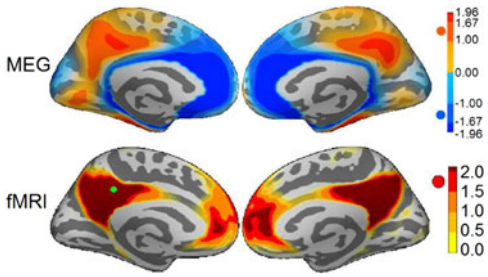

FIG. 2. Frequentness pattern of MEG connectivity shows similarity to fcMRI along the cingulate regions.

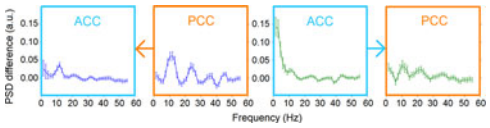

FIG. 3. Difference of the power spectral density (PSD) by contrasting time periods where connectivity was strong/weak.

Background: The neural mechanisms that result in the brain's Default-Mode Network (DMN), a cortical network first observed with hemodynamic signals, remain a puzzle for the neuroimaging field. We explore the DMN-related electrophysiology using a novel connectivity method with resting-state magnetoencephalography (MEG).
Methods: We computed MEG connectivity maps within second-long time periods with a measure adapted from Granger causality. Six seeds were chosen from primary sensory, associative and higher cognitive regions. About 300 maps were created for each seed, measuring over $\sim$300 time points the connectivity between the seed and $\sim$8000 target locations on the cortical surface.
Results: The time-average of MEG maps showed similarity to functional connectivity Magnetic Resonance Imaging (fcMRI) maps in the primary sensory areas (Fig. 1). The frequentness of strong connectivity showed a pattern that encompasses the cingulate components of the DMN (Fig. 2). Strong connectivity corresponded with high power spectral density in the delta band for the Anterior Cingulate Cortex (ACC) and in the alpha band for the Posterior Cingulate Cortex (PCC) (Fig. 3).
Conclusions: The spatial temporal patterns of the dynamic connectivity differentiate the role of ACC and PCC in the DMN according to their delta and alpha activities.

P48C FMRI of hippocampal deep brain stimulation in the rodent brain

N. Van Den Berge[1], I. Dauwe[2], P. van Mierlo[1], K. Vonck[2], C. Vanhove[1], R. Van Holen[1]

[1]Medical Image and Signal Processing Group, Ghent University-iMinds Medical IT department, Ghent, Belgium, [2]Laboratory for Clinical and Experimental Neurophysiology, Neurobiology and Neuropsychology, Ghent University Hospital, Ghent, Belgium

Background: Deep Brain Stimulation (DBS) is a promising treatment for neurological and psychiatric disorders. However, the underlying mechanism of action of DBS remains unknown. The effect of DBS has been studied primarily by direct neural recording

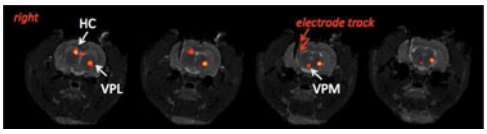

FIG. 1. Findings of one rat in whole-brain BOLD fMRI during hippocampal DBS. The statistical map is thresholded at $p < 0.05$. Activation occurs in hippocam-pal (HC) and thalamic (VPM/VPL) structures.

studies, which lack the ability to elucidate DBS related responses on a whole-brain scale. Functional Magnetic Resonance Imaging (fMRI) reflects changes in neural activity throughout the entire brain volume and may thus reveal neuroanatomical connectivity of the targeted structure in vivo. In order to visualize the whole-brain blood oxygen level dependent (BOLD) responses to DBS, we have developed an MR-compatible electrode and an acquisition protocol for simultaneous DBS and BOLD fMRI. With this study, we aimed to demonstrate that DBS during fMRI is a valuable technique to investigate the whole-brain effect of DBS.

Methods: Three adult male Sprague-Dawley rats were stereotactically implanted with a custom-made MR-compatible PtIr DBS-electrode in the right hippocampus. Electrical on-and-off Poisson distributed stimulation was applied (amplitude 75 mA, pulse duration 100 μs, frequency 130 Hz) using a block-design paradigm (20 s on/40 s off). MR images were acquired on a Pharmascan 7T (Bruker) using a rat brain volume coil. Rats were sedated with medetomidine during all fMRI acquisitions. Each fMRI run consisted of 150 repetitions with TR = 2 s, TE = 20 ms. Data were processed by means of independent component analysis. Clusters were accepted as significant if p-values were 0.05 or less after correction for multiple comparisons. Each resultant statistical map was co-registered onto a structural MR image for anatomical correlation.

Results: Hippocampal DBS evokes a bilateral BOLD response in hippocampal and thalamic substructures, as shown in fig. 1. Activation not only occurs near the electrode, but also contralateral to the electrode. Results were consistent among rats.

Conclusions: Our data indicate that real-time hippocampal DBS evokes a bilateral BOLD response in hippocampal and thalamic substructures. We demonstrated that simultaneous DBS and fMRI can be used to explore the whole-brain effect of modulating neural circuitry, making this technique potentially powerful for exploration of cerebral changes of DBS in animal models of neurological or psychiatric disorders.

P49C Structural connectivity à la mode: complementing conventional indices of white matter microstructure disorganization in ADHD

Y. Yoncheva[1], K. Somandepalli[1], P. T. Reiss[1,2,3], C. Kelly[1,3], A. Di Martino[1], M. Lazar[4], M. P. Milham[3,5], F. X. Castellanos[1,3,4]

[1]NYU Dept. of Child & Adolescent Psychiatry, NY, NY, [2]NYU Dept. of Population Health, NY, NY, [3]Nathan Kline Institute for Psychiatric Research, Orangeburg, NY, [4]NYU Dept. of Radiology, NY, NY, [5]Child Mind Institute, NY, NY, USA

Background: Diffusion tensor imaging (DTI) studies typically focus on measuring fractional anisotropy (FA) and axial diffusivity (AD). These indices may be deficient in capturing the complex white matter (WM) fiber architecture in disorders [1] or development. In contrast, the mode of anisotropy (MA) separates planar from linear diffusivity and is sensitive to subtle differences in regions with crossing fibers [2]. Yet, MA has not been examined in Attention-Deficit/Hyperactivity Disorder (ADHD).

Methods: Diffusion-weighted images (3T, $3 \times 3 \times 3$ mm voxels, 64 diffusion directions) were acquired in adults and children with and without ADHD. The adult dataset comprised 42 ADHD patients and 67 controls (age: M = 31.4, SD = 9.4 years; 43 F); the children dataset - 82 ADHD and 82 controls (age: M = 10.8, SD = 2.8 years; 44 F). Within each dataset, ADHD and healthy controls did not differ (all $p > 0.21$) in age, sex, or head motion, which can elicit spurious group WM differences [3]. Corresponding resting state scans were collected for each subject (analyses in progress). Following standard tensor fitting, FA, AD, and MA were derived and analyzed via tract-based spatial statistics. Conventional voxel-level ADHD vs. control group permutation tests on FA, AD and MA within each dataset produced p-values adjusted for family-wise error rate (FWER). Global FA, AD, and MA effects (averaged over the entire FA skeleton) were also assessed [4]. Effects of diagnosis are reported after co-varying for age, sex, and motion.

Results: In adults, voxel-level differences ($p < 0.05$ FWER-adjusted) were found in MA and AD but not FA. In children, whole-brain effects ($p < 0.05$ FWER-adjusted) manifested in MA only. Global differences in all diffusivity indices emerged in adults (p's < 0.013, all means smaller in ADHD) with largest effect for MA (Cohen's d = 1.28). ADHD children had lower MA than controls ($p < 0.00005$) while FA and AD were comparable.

Conclusions: Across both adults and children with ADHD, the strongest group differences, voxel-wise and globally, were observed in MA. We speculate this reflects diffusely decreased organization of WM structure in ADHD. Present findings confirm the involvement of structural connectivity in ADHD, yet the specific nature of this abnormality remains unclear. We anticipate also reporting on the relationship between regional decreases in MA and alterations in resting state indices in the same individuals, to mutually constrain the interpretation of structural and functional differences in ADHD.

[1] Douaud *et al.*, (2011) *NeuroImage*; [2] Ennis & Kindlmann (2006) *Magn Reson Med*
[3] Yendiki *et al.*, (2014) *NeuroImage*; [4] Reiss *et al.*, (2012) *NeuroImage*.

P50C Altered inter-subregion connectivity of the default mode network in relapsing remitting multiple sclerosis: a functional and structural connectivity study

F.Q Zhou[1,2], Y. Zhuang[3], H.H Gong[1,2], B. Wang[1], Q. Chen[1], L. Wu[1]

[1]Department of Radiology, The First Affiliated Hospital, Nanchang University, Nanchang, Jiangxi Province, China; [2]Jiangxi Province Medical Imaging Research Institute, Nanchang, Jiangxi Province, China; [3]Department of Oncology, The Second Hospital of Nanchang, Nanchang, Jiangxi Province, China

Background: Little is known about the interactions between the default mode network (DMN) subregions in relapsing-remitting multiple sclerosis (RRMS). This study used diffusion tensor imaging (DTI) and resting-state functional MRI (rs-fMRI) to examine alterations of long white matter tracts in paired DMN subregions and their functional connectivity in RRMS patients.

Methods: Twenty-four RRMS patients and 24 healthy subjects participated in this study. The fiber connections derived from DTI probabilistic tractography and the temporal correlation coefficient derived from rs-fMRI were combined to examine the inter-subregion structural-functional connectivity (SC-FC) within the DMN and its correlations with clinical markers.
Results: Compared with healthy subjects, the RRMS patients showed the following: 1) significantly decreased SC and increased FC in the pair-wise subregions; 2) two significant correlations in SC-FC coupling patterns, including the positive correlation between slightly increased FC value and long white matter tract damage in the PCC/PCUN-MPFC connection, and the negative correlations between significantly increased FC values and long white matter tract damage in the PCC/PCUN-bilateral mTL connections; 3) SC alterations [log(N track) of the PCC/PCUN-left IPL, RD value of the MPFC-left IPL, FA value of the PCC/PCUN-left mTL connections] correlated with EDSS, increases in the RD value of MPFC-left IPL connection was positively correlated to the MFIS; and decreases in the FA value of PCC/PCUN-right IPL connection was negatively correlated with the PASAT; 4) decreased SC (FA value of the MPFC-left IPL, track volume of the PCC/PCUN-MPFC, and log(N track) of PCC/PCUN-left mTL connections) was positively correlated with brain atrophy; and 5) the FC value of the PCC/PCUN-right mTL connection was negativity correlated with the PASAT.
Conclusions: In the connections of paired DMN subregions, we observed decreased SC and increased FC in RRMS patients. The relationship between MS-related structural abnormalities and clinical markers suggests that the disruption of this long-distance ''inter-subregion'' connectivity (white matter) may significantly impact the integrity of the network's function.

Theme 3: Applications in Neurological and Psychiatric Diseases

P52C Connectivity dynamics during hypnosis without target suggestion

Pablo G. Vázquez[1], Susan Whitfield-Gabrieli[2], Clemens C.C. Bauer[1], Fernando A. Barrios[1,2]

[1]Universidad Nacional Autónoma de México, Instituto de Neurobiología, Querétaro QRO. 76230, Mexico; [2]Department of Brain and Cognitive Sciences, McGovern Institute for Brain Research, Massachusetts Institute of Technology, Cambridge, 02139, MA

Background: During hypnosis, significant changes in BOLD signal associated to the anterior default mode network (DMN) and prefrontal attentional systems have been reported. However, it remains uncertain whether those changes are exclusively attributable to the hypnotic state *per se* or to the target suggestions used as control conditions. The aim of the present study is to explore the connectivity dynamics between DMN, executive control network (ECN) and salience network (SaN) by contrasting the normal alert state versus the hypnotic state in the absence of targeted suggestions.
Methods: After signing an informed consent, 23 healthy right handed volunteers (28.3 y.o, 12 females) participated in a rs-fMRI study, all were rated as mid to high hypnotic suggestible (rated 9 over 12 items of the Stanford Hypnotic Suggestibility Scale Form C). Two 6 min, resting state fMRI series with with $4\times4\times4\,mm^3$ resolution and anatomical images, were acquired using a G.E. 3.0 T scanner. One of the resting state acquisitions the subjects were in hypnotic state and the other in alert state. Functional data were corrected using ART (Artifact detection toolbox) followed by a functional connectivity analysis using Conn. Functional data was slice-timed, realigned normalized and smoothed, temporal preprocess was executed to estimate the BOLD residual signal in the gray matter model and fist-level analysis for each subject condition was estimated doing seed-to-voxel analyses. Group results were estimated with seed-to-voxel in a second-level analyses using seeds for the default mode (DMN), the executive control (ECN) and the salience (SaN) networks. Hypnotic and alert state contrast was estimated for each network.
Results: For the hypnotic state contrasted with the alert state differences in the DMN cluster were localized in the right lingual gyrus, at the left Brodmann Area 22, at the posterior cingulate gyrus and the superior frontal gyrus. ECN presented differences at the right fusiform gyrus, the cingulate gyrus and the left inferior parietal lobe. For the SaN differences were located at the left insula, the right superior temporal gyrus, the anterior cingulum and the middle frontal gyrus.
Conclusions: The DMN resulted positively augmented inferring an overload of its updating out of awareness resting state functions. The ECN showed only negative BOLD signal differences presumably evoking the anticorrelated function of the DMN. And the switching function of the SaN between non-conscious and awareness demanding conditions could have been stocked in order to maintain the lack of the ECN and the overload on the DMN since it appeared significantly connected, giving as a result a deep and maintained resting state which could define the hypnotic state *per se*.
Contrast Images between hypnotic and alert state, positive and negative low frequency BOLD signal shows functional connectivity of DMN, ECN and SaN seeds above cero in yellow-red palette and below cero in blue-green palette.

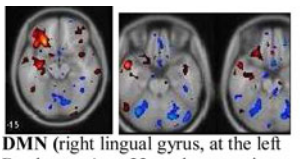

DMN (right lingual gyrus, at the left Brodmann Area 22, at the posterior cingulate gyrus and the superior frontal gyrus).

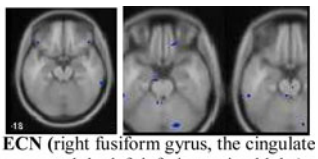

ECN (right fusiform gyrus, the cingulate gyrus and the left inferior parietal lobe).

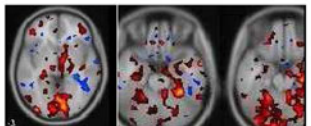

SaN (left insula, the right superior emporal gyrus, the anterior cingulum and themiddle frontal gyrus).

P53C Intrinsic Brain Networks normalize with Treatment in Pediatric Complex Regional Pain Syndrome

L. Becerra[1,2,3], L.E. Simons[1,2], A.A. Lebel[1,2], D. Borsook[1,2,3]

[1]Pain/Analgesia Imaging Neuroscience Group, Departments of Anesthesiology[2] and Radiology[3], Boston Children's Hospital; Waltham, MA USA

Background: Complex regional pain syndrome (CRPS) is a neuropathic pain condition affecting the peripheral and central nervous system characterized by the continuing presence of pain that is disproportionate to the inciting event and it is not curable in adults. Pediatric patients with CRPS typically recover with standard medical treatment. In this study, we evaluated intrinsic brain networks measures in the CRPS disease state and after an intensive multidisciplinary pain treatment program to delineate (a) network abnormalities in the disease state and (b) changes induced by treatment.
Methods: The study was approved by Boston Children's Hospital IRB. Twelve patients with unilateral lower extremity CRPS were recruited (n = 12; 14.1 ± 0.7 yrs.) and 12 age/sex matched controls (n = 12; 14.2 ± 0.8 yrs.). Patients and Healthy Controls were scanned twice, before treatment (patients-Visit 1) and at discharge (3 weeks later: Visit 2). Healthy Control scans were 3–4 weeks apart. Psychophysical: Patients' pain functional disability, and lower extremity function were evaluated pre/post treatment. Imaging: A 3T Siemens Tim Trio was used. Subjects underwent a structural scan (MPRAGE, 256 × 256 mm 192-1.33 mm slices) and a RSN scan (EPI, 41 slices isotropic 3.5 mm^3 voxels, TR/TE = 3 s/30 ms 200 volumes). Imaging Analysis: fsl tools were used for preprocessing (motion correction, brain extraction, HPF-100 s, and spatial smoothing 5 mm). A model-free approach was used utilizing fsl ICA tool (melodic). Group ICA (temporal concatenation) were first calculated and then dual regression was applied to determine differences. The main contrasts of interest were: (i) Patients vs. Controls visit 1 (*Disease Effect*); (ii) Patients visit 1 vs. Patients visit 2 (*Treatment Effect*) (iii) Patients vs. Controls Visit 2 (*Residual Effects*).
Results: Patients indicated a reduction of pain symptoms and functional disability. *Disease Effect*: Intrinsic networks associated with chronic pain in adults displayed abnormal connectivity: salience network: increased connectivity with prefrontal (PFC), cingulate and insula cortices. Default mode network: increased connectivity with frontal, postcentral and precuneus. Central executive network: increased connectivity with PFC, post central and temporal areas. Sensorimotor network: increased connectivity with frontal and parietal areas, decreased connectivity with cingulate and cerebellum. Following treatment, abnormalities in most of these networks tended to be non-significant, however, in some networks (sensorimotor network), they still persisted (Residual Effects).
Conclusions: Pediatric pain imaging studies are very sparse and difficult to perform. This is one the first studies of a chronic pain condition in children. We detected changes in intrinsic brain networks in children suffering from CRPS. After a relatively short treatment of 3 weeks, most of the observed changes were diminished. The plasticity of a young brain could be a significant factor in the recovery, as it does not occur in adults.
Acknowledgments: Support from NINDS R01 (DB), K24 (DB), NICHD K23 (LS)

P54C Graph-theoretic analysis of resting state brain networks in post-stroke aphasia

J.W. Bohland[1,2], K. Kapse[2], S. Kiran[2]

[1]Dept. of Health Sciences, Boston University, Boston, MA, USA; [2]Dept. of Speech, Language, & Hearing Sciences, Boston University, Boston, MA, USA

Background: There is recent evidence that suggests that resting-state abnormalities in chronic stroke likely influence recovery patterns. In this study, we examined resting state networks in 11 patients with post-stroke aphasia (PWA) in comparison to a database of typical resting state-connectivity patterns to identify the impact of lesions leading to aphasia on network structure, and ultimately to relate network measures to post-stroke language impairment and recovery.
Methods: 11 PWA with left hemisphere strokes and at least 4 months post onset participated. 3D anatomical images and a resting-state fMRI (rs-fMRI) series containing 140 images with TR = 3 s, and with 3.3125 mm isotropic voxel size, were acquired in each patient. A group of control subjects over the age of 50 were selected from the 1000 Functional Connectomes database [1]. The rs-fMRI series were pre-processed using standard procedures in SPM8. Reduction of non-neural noise was performed using the CompCor method [2], removing signals related to the leading principal components of voxels from the white matter and CSF. The residual signals were bandpass filtered between 0.01 and 0.08 Hz to isolate the low frequency fluctuations. Voxels were masked to select those likely to be gray matter (GM), and non GM voxels were discarded from further analysis. Because the brains of PWA are likely to undergo post-stroke functional reorganization, we used a data-driven method to cluster voxels that are spatially contiguous and have time series that are correlated above a threshold. The resulting clusters served as nodes in a graph theoretic analysis, with weighted edges determined based on: (i) the Pearson correlations between mean cluster time series, and (ii) partial correlations determined using an L1-regularized inverse covariance method (e.g., [3]).
Results: We hypothesized that rs-fMRI network ''hubs'' would shift due to post-stroke plasticity. We calculated the weighted node degree (sum of all edge weights impinging on a cluster) and betweenness centrality (the fraction of the shortest paths between all cluster pairs that pass through that node) for each cluster, in both PWA and controls. Our results show an increase in the average number of shortest paths that traverse each cluster in the graph in PWA relative to controls. We additionally hypothesized that rs-fMRI networks in PWA would show decreased efficiency relative to controls. We calculated the global graph efficiency, defined as the inverse of the harmonic mean of the shortest path lengths between all nodes, for each subject. Initial results show a consistent pattern of reduced global efficiency in PWA relative to controls.
Conclusions: Compared with controls, these results indicate inefficiencies in the post-stroke resting-state network, with greater shifts in network hubs in PWA dependent on the site and size of lesion. Such graph analytic results may ultimately prove informative in advancing individual-specific therapies for language recovery.
[1] Behzadi, Y., et al. (2007). Neuroimage, 37(1), 90–101; [2] Biswal, B. B., et al. (2010). PNAS, 107(10), 4734–4739; [3] Friedman, J., Hastie, T., & Tibshirani, R. (2008). Biostatistics, 9(3), 432–441.

P55C Association between integrity of white matter, cognitive deficits and spontaneous functional connectivity in multiple sclerosis

S.J. Buetof[1], D.J. Hawellek[2], S.M. Gold[3], S. Siemonsen[4], C. Heesen[5], G. Nolte[1], A.K. Engel[1]

[1]Dept. of Neurophysiology and Pathophysiology, UKE, Hamburg, Germany, [2]Center for Neural Science, New York University, New York City, NY, United States, [3]ZMNH, UKE, Hamburg, Germany, [4]Dept. of Diagnostic and Interventional Neuroradiology, UKE Hamburg, Germany, [5]Dept. of Neurology, UKE, Hamburg, Germany

Background: Multiple sclerosis (MS) has a diverse clinical picture due to widespread inflammatory damage in the white matter. Spontaneous (resting state) functional connectivity (rs-fcMRI) has been shown to be disturbed and to be associated with cognitive deficits (Hawellek et al., 2011). The concrete interplay between structural damage, rs-fcMRI and cognitive disturbance, however, remains unclear and is subject of the present study.
Methods: MRI data was acquired on a 3T Siemens scanner for 19 MS patients and pairwise matched controls. Cognitive deficits were assessed with the Verbal Learning and Memory Test (VLMT). Preprocessing of f/MRI data was conducted in SPM8 (Wellcome Dept. of Imaging Neuroscience, London, GB). Fractional anisotropy (FA) values were extracted with FSL (http:// www.fmrib.ox.ac.uk/fsl/). BOLD time series of 90 regions of the aal atlas (Tzourio-Mazoyer et al., 2002) were derived and corrected using the CONN toolbox (13o; MIT, Boston, USA). For the main analysis, rs-fcMRI maps were correlated with FA and VLMT, respectively, resulting in two association maps. We determined the global (correlation of z-transformed association maps), topographical (spatial overlap of significantly associated rs-fcMRI) and qualitative (comparison of association signs) relationships between those two maps.
Results: There was a significant positive correlation between the association maps, indicating a global correspondence between the signs of association. The spatial comparison of significant associations revealed a considerable topographical overlap, i.e. several connections were correlated significantly with both metrics. Associations of those connections were mainly positive in both maps. In contrast, connections that were significantly associated with only one of the two metrics were more often oppositely related to FA and VLMT (i.e. increased rs-fcMRI was related to higher FA but lower VLMT or vice versa), or to decreased values in both metrics.
Conclusions: The findings indicate that the main link between structural damage and cognitive disturbance in MS is a specific decrease of rs-fcMRI. Connections that are negatively correlated with structural or behavioral measures might reflect secondary compensatory mechanisms such as additional recruitment or prolonged synchronization of activity. They may have varying functional relevance in different phases of the disease and account for inter-individual differences. The in-depth exploration of those connections might contribute to the understanding of general principles of structure-function relationships and functional compensation mechanisms in response to structural damage.

P56C Brain network functional connectivity is disrupted in childhood obesity

B.A. Chodkowski[1,2], K.D. Niswender[3,4], R.L. Cowan[1,5]

[1]Vanderbilt Psychiatric Neuroimaging Program, [2]Vanderbilt Chemical and Physical Biology Program, [3]Tennessee Valley Healthcare System, [4]Vanderbilt Department of Medicine, Division of Diabetes, Endocrinology, and Metabolism, [5]Vanderbilt Department of Psychiatry, Nashville, TN, USA

Background: Little is known about differences in brain network functional connectivity in childhood obesity. We explore childhood obesity by examining an integrated brain network rather than a reductionist approach of mapping discrete regions. Ubiquitous media-driven exposure to visual images of food drives excess consumption of readily available high-calorie, highly palatable food. To maintain healthy weight, emotional drive (driving overconsumption) must be balanced by cognitive control (controlling overconsumption). We hypothesize that obesity is due to a disruption in the functional connectivity and balance within brain networks mediating emotional drive and cognitive control.

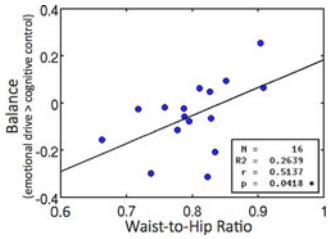

Methods: We acquired resting state fMRI data from 16 children (9 girls; mean age = 11.7 (1.5), range = [8.4, 13.9] yr; mean BMI% = 57.9 (29.1), range = [7, 96]%) from the Enhanced Nathan Kline Institute-Rockland Sample dataset. We used seed-based functional connectivity (FC) to analyze the functional organization of a feeding-related brain network. Our network includes the nucleus accumbens (NAc) as a hub that integrates inputs from the lateral orbitofrontal cortex (latOFC), associated with emotional drive, and the anterior cingulate cortex (ACC), associated with cognitive control. We quantified FC via partial correlation, and balance via an asymmetry measure computed from the partial correlation coefficients between latOFC:NAc (ρ_{drive}) and ACC:NAc ($\rho_{control}$): $balance = (\rho_{drive} - \rho_{control})/((\rho_{drive} + \rho_{control})/2)$. An increase in balance indicates an increase in emotional drive relative to cognitive control. We then determined the relationship between brain network functional connectivity and balance with waist-to-hip ratio where an increasing waist-to-hip ratio indicates increasing obesity.
Results: We discovered that increasing imbalance in network functional connectivity is associated with increasing obesity. As waist-to-hip ratio increases, the FC between latOFC:NAc (emotional drive) increases relative to the FC between ACC:NAc (cognitive control) (Figure; $p = 0.04$; $R^2 = 0.26$). This imbalance is driven by an increase in FC between latOFC:NAc ($p = 0.02$; $R^2 = 0.31$) whereas the FC between ACC:NAc does not simultaneously keep pace ($p = 0.33$; $R^2 = 0.07$; data not shown). Thus, as obesity increases, so does imbalance.
Conclusions: Our results reveal that greater functional connectivity between a network region associated with emotional drive and the NAc relative to functional connectivity between a network region associated with cognitive control and NAc is related to increasing obesity. Because intensive dieting in adults does not lead to long-lasting weight loss, understanding the neurobiological basis of childhood obesity is critical to treatment and prevention efforts.

P57C Developmental connectivity among nodes of dorsal and ventral visual networks as reflected in resting state MEG alpha oscillatory synchronization

K.R. Ciesielski[1,2], B.R. Rosen[1,4], T. Kenet[1], K.R.A. Van Dijk[1,3,4], S. Khan[1], S. Stufflebeam[1], M.S. Hämäläinen[1,4]

[1]MGH/MIT/HMS AA Martinos Center for Biomedical Imaging, Department of Radiology, Massachusetts General Hospital, Harvard Medical School, Boston, MA, USA; [2]Pediatric Neuroscience Laboratory, Department of Psychology, University of New Mexico, Albuquerque, NM, USA; [3]Center for Brain Science, Harvard University, Boston, MA; [4]Harvard-MIT Division of Health Sciences & Technology, Cambridge, MA, USA

Background: We propose that resting-state functional connectivity measures (fcMEG & fcMRI), as sensitive to developmental

changes in functional networks (Fair et al., 2007; Supecar et al., 2009), may be used with a high level of efficacy for characterization of the variability of pediatric normative control samples. The variability of brain function and behavior among healthy controls is as prominent as among those with clinical disorders, yet the fact is poorly recognized. We accept here, as a theoretical framework, the alpha-band (8–13 Hz) connectivity among nodes of two long-range attentional networks –the Dorsal Visual, (DVN, visual-spatial, frontal-parietal control) and Ventral Visual (VVN object categorization, ventral frontal-temporal control)– as a model of characterizing the normative sample. It is unclear which of the two networks develops first in ontogeny, and thus leads the developmental trajectory (Atkinson & Braddick, 2011). We hypothesize that the network that matures earlier, will display a similarity between children and adults in the pattern of alpha band synchronization and connectivity.

Methods: *Resting state fcMEG:* Males (12 aged 6–12 yrs and 12 aged 19–28 yrs) right-handed, no present or history of psychiatric disorders. *Data acquisition*: MGH MEG Unit/Vectorview TM, Elekta Neuromag with 306 sensors, 5 min fixation on a red cross with ECG/EOG monitoring. *Data Processsing:* A reliable estimate of phase alpha synchronization as a measure of connectivity between ROIs of DVN and VVN was calculated (the phase lag index or PLI; Stam et al., 2007). The PLI is a measure of asymmetry of distribution of phase differences between two time-coupled oscillating ROIs. *Resting state fcMRI Pilot Study:* Males (6 aged 6–12 yrs and 20 aged 18–28 yrs). *Data acquisition*: 3.0T Siemens Trio whole body scanner, 2D gradient echo EPI, TR 3 s, TE 30 ms, 72×72 matrix, 124 volumes, 6 min fixation on a red cross. *Data Processsing:* After standard preprocessing steps, 16 apriori defined regions of interest specific to the DVN and VVN were created and within network connectivity was computed for group analyses.

Results: The *fcMRI* pilot study shows that segregation of DVN and VVN in children is attainable, with comparable child/adult DVN parietal nodes connectivity. Increased PLIs of *fcMEG* alpha synchronization indicate significantly stronger functional connectivity between coupled oscillators in the DVN as compared to VVN in children ($p < 0.02$). The PLI values for DVN present a similar pattern of connectivity in children and adults. In the VVN the PLIs are significantly lower in children than in adults ($p < 0.03$) suggesting an incomplete development of network connectivity.

Conclusions: Functional developmental DVN connectivity, as measured by resting state *fcMEG* alpha oscillatory synchronization, displays markers of earlier maturation as compared to VVN in males aged 6–12 yrs. Earlier cognitive development of DVN has profound significance for understanding the variability of cognitive profiles in pediatric control samples and the neurobehavioral mechanisms of developmental disorders.

P58C The application of artificial neural network ensembles to autism classification using resting state functional magnetic resonance imaging data

G. Deshpande[1], J.A. Dahlen[2], W.S. Woltosz[2]

[1]AU MRI Research Center, Depts. of ECE and Psychology, Auburn University, Auburn, AL, USA, [2]Simulations Plus, Inc., Lancaster, CA, USA

Background: We have previously developed ensembles of artificial neural networks (ANNEs), powerful and commercially successful classifiers, which have been applied to problems in pharmaceutical chemistry. Using this methodology, a prototype application named ''MRIModeler™'' was created to build ANNE models to classify subjects with autism from matched healthy controls using resting state fMRI data obtained from the Autism Brain Imaging Data Exchange (ABIDE). While previous studies have reported modest accuracies using the same dataset, we report comparatively superior performance.

Methods: Resting state fMRI data from ABIDE was subjected to standard pre-processing. Subsequently, the dimensionality of the data was reduced by spatially parcellating the brain into 190 functionally homogeneous regions. Mean time series were extracted from these regions and functional connectivity between them was estimated and input as descriptors into the classifier, MRIModeler, which automates each of the following steps necessary to build high-quality predictive models: Filtering to remove descriptors that are redundant and/or highly correlated, have relatively small variance, or are underrepresented in the data set; clustering of test subjects to ensure intelligent selection of training, verification, and external test sets; ranking descriptors by their effect on the predicted property; training multiple ensembles to allow selection of the most appropriate neural network architecture; and selecting the best ensemble of neural nets to use as the final predictive model.

Results: Input filtering reduced the initial set of nearly 18000 descriptors to 416, for 423 test subjects. 43 ANN architectures (varying the number of inputs and neurons) were explored, with 165 networks trained for each architecture. A binary classification threshold was optimized for each network. From each set of 165, the best 33 were selected to form an ensemble of ANNs. The network outputs were equally weighted in voting for the classification output of the ensemble. From these ensembles, the most successful architecture was selected: 140 inputs and two neurons resulted in a sensitivity of 85% and specificity of 91%. A number of the other architectures yielded sensitivities $\geq 80\%$ and specificities $\geq 86\%$.

Conclusions: This is an early effort to apply extensive experience garnered in pharmaceutical/chemical modeling to the modeling of resting state fMRI connectivity for diagnostic purposes. Autism and its subclasses have proved particularly difficult for other groups to model. However, in this prototype effort, we have achieved sensitivity and specificity on the order of 70% to 90%. In our future work, we expect to focus on improving input selection methods, incorporating phenotypic data, and distinguishing between subclasses on the autism spectrum.

P59C Intrinsic fMRI crossmodal interaction accurately differentiates minimally responsive from unresponsive brain-damaged patients

A. Demertzi[1], G. Antonopoulos[1], H. U. Voss[2], J.S. Crone[3,4], N. D. Schiff[5,6], C. de Los Angeles[7], F. Gomez[8], M.A. Bahri[9], L. Heine[1], L. Tshibanda[10], V. Charland-Verville[1], S. Whitfield-Gabrieli[7]*, S. Laureys[1]*

[1]Coma Science Group, Cyclotron Research Center & Neurology Department, University of Liège, Belgium, [2]Department of Radiology & Citigroup Biomedical Imaging Center, Weill Cornell Medical College, NY, USA, [3]Department of Psychology & Centre for Neurocognitive Research, University of Salzburg, Austria, [4]Neuroscience Institute and Centre for Neurocognitive Research & Department of Neurology, Christian-Doppler-Clinic, Salzburg, Austria, [5]Department of Neuroscience, Weill Cornell Graduate School of Medical Sciences, NY, USA, [6]Department of Neurology & Neuroscience, Weill Cornell Medical College, NY, USA, [7]Martinos Imaging Center at

*McGovern Institute for Brain Research, MIT, Cambridge, MA, USA, [8]Computer Science Department, Universidad Central de Colombia, Bogota, Colombia, [9]Cyclotron Research Center, University of Liège, Belgium, [10]Department of Radiology, CHU University Hospital, Liège, Belgium (*equal contribution)s*

Background: We assessed the clinical relevance of the resting state fMRI in patients with disorders of consciousness, moving from group-level characterization of functional connectivity in multiple networks towards single-patient automatic classification.
Methods: Three clinical centers collected resting state fMRI data from patients in minimally conscious state (MCS), vegetative state/unresponsive wakefulness syndrome (VS/UWS), and coma. Group-level multiple-seed functional connectivity was investigated for the default mode, frontoparietal, salience, auditory, sensorimotor and visual network. Each network's anatomical correlate was investigated with the Coma Recovery Scale-Revised (CRS-R) behavioral scores regression. Between-group inferential statistics and machine learning were used to identify the network with the best discriminative capacity between patients in MCS and VS/UWS. A linear support vector machine classifier, trained on the functional connectivity of the identified network, was used to differentiate patients on an individual basis.
Results: In 51 patients, functional connectivity was partially preserved in patients in MCS (n = 26, etiology, duration), severely disrupted in patients in VS/UWS (n = 19) and absent in comatose patients (n = 6). CRS-R scores positively correlated with connectivity of key regions to conscious processing for each network. The auditory network (encompassing bilateral auditory cortices and visual areas) was selected as the most significant feature to discriminate between patients in MCS and VS/UWS; a linear support vector machine classifier confirmed this discriminant capacity in 43 out of 45 patients. In 22 patients, the automatic classification based on the auditory-visual crossmodal connectivity identified correctly 21/22 cases (95% accuracy).
Conclusions: Intrinsic fMRI audio-visual connectivity can differentiate MCS from unresponsive patients with acceptable clinical accuracy. Our findings point to the significance of preserved top-down processes in minimal consciousness and highlight the clinical utility of the resting paradigm at single-patient level diagnostics.

P61C Cannabis improves intrinsic functional brain organization of the default mode network in patients with schizophrenia and cannabis use disorder

S. Whitfield-Gabrieli[1], A.S. Fischer[2], R.M. Roth[2], A.I. Green[2]

[1]Department of Brain and Cognitive Sciences, Massachusetts Institute of Technology, Cambridge, MA [2]Department of Psychiatry, Geisel School of Medicine at Dartmouth, Lebanon, NH

Background: Up to 43% of patients with schizophrenia (SCZ) have co-occurring cannabis use disorder (CUD), which is associated with decreased treatment efficacy, increased risk of psychotic relapse, and overall poorer global functioning. Nonetheless, patients with SCZ that use cannabis show superior cognitive function. Default mode network (DMN) resting state hyperconnectivity and reduced anticorrelation with the frontal-parietal network have been implicated in symptom severity and cognitive impairment in SCZ, respectively. The underlying DMN abnormalities or the effects of cannabis on this network have not been investigated in patients with SCZ and CUD. We examined the positive correlations within the DMN as well as correlations between the (1) medial prefrontal cortex (MPFC), a component of the DMN that typically decreases during attention demanding tasks, and (2) the dorsolateral prefrontal cortex (DLPFC) a component of the frontoparietal control network that supports executive functions and typically increases in activation during attention demanding tasks.
Methods: Twelve patients with SCZ and CUD and 12 controls completed two fMRI resting scans. Prior to the second scan, patients either smoked a 3.6% THC cannabis cigarette or ingested a 15 mg THC pill. We examined the positive correlations within the DMN and the strength of the anticorrelation between the medial prefrontal cortex (MPFC) and the dorsolateral prefrontal cortex (DLPFC). We then explored the effects of cannabis and delta-9-tetrahydrocannabinol (THC) on DMN seed-to-voxel connectivity.
Results: Our findings revealed DMN hyperconnectivity, as well as reduced anti-correlation between the MPFC and DLPFC in the patient group. While cannabis and THC exerted opposing effects on positive connectivity of the DMN, both significantly increased the MPFC-to-DLPFC anticorrelation. The strength of anticorrelation significantly correlated with working memory performance in the patient group.
Conclusions: Functional pathology of DMN connectivity in SCZ may contribute to the inability to appropriately distinguish and shift attention between internally generated thoughts and external goal-oriented tasks. DMN hyperconnectivity found in cannabis-using patients with SCZ is in accordance with abnormalities found in medication naïve patients with SCZ without CUD, as well as in their first degree relatives. The presence of this abnormality in SCZ with and without CUD suggests that DMN disturbances are a core feature of the disorder not related the medications or substance use. Both smoked cannabis and THC administration significantly improved deficient anticorrelation between the MPFC and DLPFC, which may explain why patients with SCZ that use cannabis have been reported to have improved cognition as compared to non-users with SCZ. These preliminary findings suggest that low dose cannabis may improve DMN connectivity and thus may have potential as adjunctive pharmacotherapy. Future studies investigating rs-fc of the BRC in these dual diagnosis patients are needed to confirm and expand upon the present findings.

P62C Hyper connectivity in DMN and hypo connectivity in ECN in subjects exposed to High altitude

T.K. Gandhi[1], S. Chouhan[1], S. A. Anteraper[1], R. Kumar[1], K. Ray[1], U. Panjwani[1], S. Whitfield-Gabrieli[2], S. B. Singh[1]

[1]Defence Institute of Physiology and Allied Sciences, New Delhi; [2]Massachusetts Institute of Technology, USA

A large body of research on high altitude residents has reported the impairment in cognitive functions. Prolonged exposure to hypobaric hypoxia has devastating consequences to brain architecture and functions. Previous studies have reported the alternation of brain structure and consequently the functions just after the exposure to high altitude. The results are not very consistent across subject populations and the duration of exposure. Here, we have an unique opportunity to work with a group of seven subjects, who were born and brought up in sea level but were exposed to high altitude (12,000–15,000 feet) for a

period of 24–36 months and living in sea level last three years. Both neuropsychological test (WAIS IV) and the resting state functional connectivity (RSFC) was conducted during the de-induction period on experimental as well as age matched five control subjects in India. Functional connectivity analysis was performed using seed-based approaches with MATLAB based custom software package: CONN. For seed-based analysis, sources are defined as multiple seeds corresponding to the pre-defined seed regions for: (i) Default mode network (DMN) and (ii) Executive control network (ECN). Seeds for DMN and ECN were chosen to be 10-mm spheres centered on previously published foci. The cognitive performance of experimental (high altitude exposed) subjects was lower ($p < 0.01$) than the age matched controls in neuropsychological test. In RSFC analysis, we use DMN seeds (LLP, MPFC, PCC, RLP) and ECN seeds (Dorsal medial PFC, Right anterior PFC, Left superior parietal, Right superior parietal) as regions of interest (ROIs). The connectivity in executive control network is significantly higher ($p < 0.01$) in controls compared to high altitude exposed subjects group. Both the behavioral and neuroimaging studies point the impaired resting state executive network in human expose to hypobaric hypoxia condition even shorter than three years. Additional studies are underway to understand the limit of plasticity in these subject groups during de-induction stages longitudinally.

P63C Music-induced analgesia in fibromyalgia is related to lower fALFF in the pain network and higher fALFF to the posterior cingulate cortex

E.A. Garza-Villarreal[1,2,3], P. Vuust[3,6], L. Vase[7], E. Brattico[8,9,10], F.A. Barrios[11], E. Pasaye[11], T.S. Jensen[12], Z. Jiang[4,5]

[1]Faculty of Medicine and University Hospital, Universidad Autonoma de Nuevo Leon (UANL), Monterrey, Mexico, [2]Center for Research and Development in Health Sciences, UANL; [3]Center of Functionally Integrative Neuroscience, University of Aarhus, Denmark, [4]Human Performance and Performance Engineering, Kessler Foundation West Orange, NJ, USA, [5]Dept Of Biomedical Engineering, New Jersey Institute of Technology, Newark, NJ, USA, [6]The Royal Academy of Music, Aarhus/Aalborg, Denmark, [7]Department of Psychology and Behavioral Sciences, Aarhus University, Denmark, [8]Institute of Behavioral Sciences, University of Helsinki, Helsinki, Finland, [9]Finnish Center of Excellence in Interdisciplinary Music Research, University of Jyväskylä, Finland, [10]Department of Biomedical Engineering and Computational Science, Aalto University School of Science, Espoo, Finland, [11]Institute of Neurobiology, Universidad Nacional Autonoma de Mexico, Queretaro, Mexico, [12]Danish Pain Research Center, Aarhus University Hospital, Denmark

Background: Fibromyalgia (FM) is a chronic pain disease that has shown alterations in brain low-frequency fluctuations. Recent studies have shown that FM patients have alterations in the DMN, the pain network (i.e., SMA, Insula, PAG, DLPFC, Thalamus), as well as high power spectral density of low-frequency fluctuations. Listening to music reduces pain in FM, however the mechanisms of music-induced analgesia in FM are not clear. In this study we wanted to investigate the analgesic effect of music in FM by analyzing brain connectivity using the fractional amplitude of low-frequency fluctuations (fALFF). We hypothesized that brain areas related to FM pain will reduce their amplitude.
Methods: Twenty female patients with a median age of 50 (22 – 70) and confirmed diagnosis of FM were included in the study. We performed resting state fMRI before (pre) and after (pos) the patients listened to two different auditory conditions: music and control noise. The image acquisition was performed at the Institute of Neurobiology, UNAM, Mexico, using a 3.0 T scanner. To obtain fALFF maps, data were preprocessed using the AFNI FATCAT 3dRSFC program and then was analyzed using FMRIB's FSL software. We performed paired t-test between conditions Music_pos and Control_pos using thirteen 6-mm sphere ROIs (left and right hemispheres except PAG), determined from the FM literature: Insula, PAG, ACC, PCC, SMA, DLPFC and Thalamus.
Results: There was significant analgesia after listening to music in the patients. We found significant clusters related to lower fALFF in right Insula, left ACC, left SMA, right DLPFC and bilateral thalamus after the music-induced analgesia. We also found higher fALFF in left PCC.
Conclusions: In this study, music-induced analgesia decreased the fALFF in brain areas related to the spontaneous central pain in fibromyalgia, and increased the fALFF in the posterior cingulate cortex, a main part of the DMN. This suggests that music reduces pain in FM and that the analgesia may be a result of an increased power in the DMN with a consequent decrease in the FM pain network.

P64C Transcranial magnetic stimulation induced modulations of resting state motor connectivity in Writer's Cramp

R. Dawn[1], S. Gohel[2], R. Panda[1], B. Biswal[2]

[1]National Institute of Mental Health and Neurosciences, Banglore, Karntaka, India. [2]New Jersey Institute of Technology, Newark, New Jersey, US

Background: Writer's Cramp (WC) is a focal task-specific dystonia of the hand leading to involuntary contractions of arm muscles during writing [1]. Although, the pathology of WC remains unclear, it is increasingly being accepted as a motor network disorder with reduced connectivity of its various components (pre/post central gyrus, sensory motor cortex, basal ganglia and cerebellum). Repetitive transcranial magnetic stimulation (rTMS) is shown to alter cortical connectivity of the primary stimulated regions and secondarily connected areas through synaptic modulations [2]. The goal of the current study was to modulate and identify the changes in motor network connectivity as results of single rTMS simulation applied to central sulcus in WC patients.
Methods: 19 right handed male subjects (mean age: 35 years, SD: 4.9 years) with WC with no history of neurological or psychological disease were recruited. Each scanning session included an eyes closed resting state fMRI scan (TR = 3 s, no of volumes: 185) and a MPRAGE anatomical scan. WC patients underwent two session of fMRI scanning, one prior to rTMS (WC-R1) and the other immediately after the rTMS (WC-R2). Each of the subjects resting state fMRI data was pre-processed using earlier published processing scheme [3]. For each of the pre-processed BOLD fMRI data, average time-series were extracted from a total of 42 bilateral cortical and sub cortical ROIs, representing motor network. Pair-wise correlation was computed for each of these ROI pairs. Group level statistics were performed to compare connectivity differences as an effect of rTMS.
Results: Connectivity of motor network and right hemispheric connectivity was found to be modulated in R2 session (Fig 1 (B)) compared to R1 session (Fig 1(A)) as result of single rTMS session. Specifically, connectivity between the left thalamus, left

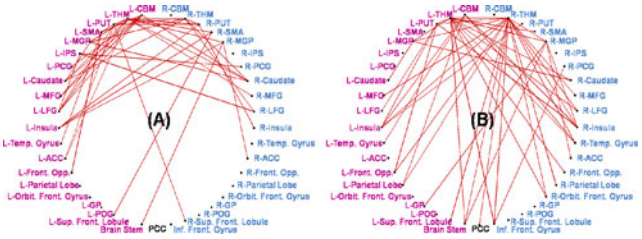

cerebellum, right globus pallidus, right thalamus and right prefrontal lobe was found to be significantly higher in session 2 compared to session 1.
Conclusions: The changes observed in motor cortex connectivity in WC patients due to a single session of rTMS are wide spread and highly affect contra-lateral hemispheric connections. These modulatory connections ns probably act through preserved hubs such as cerebellum and thalamus.
References: Ilmoniemi and Virtanen 1997. Neuroreport 8(16): 3537–3540. Hallett 2006. Human movement science 25(4): 454–463. Gohel S, Biswal (2014), Brain Connectivity doi:10.1089/brain.2013.0210.

P65C Reduced anti-correlations between cingulo-opercular and default mode networks in individuals with chronic traumatic brain injury following strategy-based reasoning training

Kihwan Han[1], Sandra B. Chapman[1], Daniel C. Krawczyk[1,2]

[1]Center for BrainHealth, The University of Texas at Dallas, Dallas, TX, USA, [2]Department of Psychiatry, University of Texas Southwestern Medical Center at Dallas, Dallas, TX, USA

Background: Several studies indicate abnormal resting-state functional connectivity in chronic Traumatic Brain Injury (TBI). We investigated potential resting-state changes in response to cognitive strategy-based rehabilitation in chronic TBI.
Methods: Fifty-two participants, age 19–65, with chronic TBI (>6 months post-injury; 5–7 on GOS-E) completed the study. Participants had no significant health-related comorbidities. Participants were randomly assigned to 8 weeks of either the Strategic Memory Advanced Reasoning Training (SMART) or the Brain Health Workshop (BHW). SMART trains strategic attention and reasoning. BHW focuses on education about the brain. A total of 115 resting-state MRI scans were acquired at pre- and post-intervention and 3 months later. Cingulo-opercular network (CON) was identified by seeding the right anterior insula and frontal operculum (R aI/fO). We then performed a linear mixed-effects modeling analysis at each voxel. Significant regions for temporal changes were identified at $p_{voxel} < 0.01$ with clusterwise multiple comparisons correction at $p_{cluster} < 0.05$.
Results: At the pre-intervention, both TBI groups had stronger anti-correlations in the Default Mode Network (DMN) areas (A). At the post- relative to the pre-intervention, SMART had reduced anti-correlations in the bilateral lateral temporal cortex (LTC, a DMN area) over BHW (B, D) At the follow-up relative to the pre-intervention, SMART had reduced anti-correlations in the bilateral LTC and left angular gyrus (DMN areas) (C, E).
Conclusions: Strategy training led to reduced anti-correlations between CON and DMN in chronic TBI. The underlying mechanisms and consequences of these phenomena are unclear. We are currently seeking to identify associations of these findings with neuropsychological measures and by comparing to healthy controls.

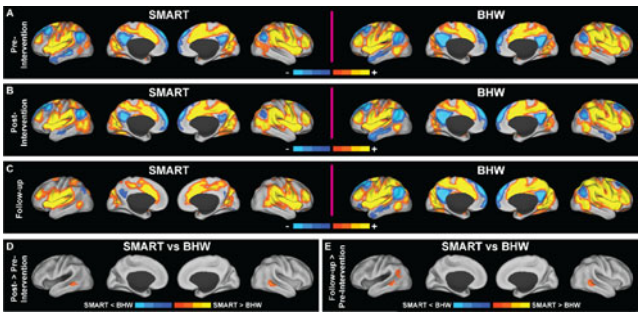

P66C Abnormal Functional Connectivity in Spinocerebellar Ataxia 2 Correlates with Clinical Measurements

C.R Hernandez-Castillo[1], R. Mercadillo[1], V. Galvez[2], L. Beltran-Parrazal[3], R. Díaz[1], J. Fernandez-Ruiz[1,2]

[1]Departamento de Fisiología, Facultad de Medicina, UNAM, Distrito Federal, México
[2]Programa Doctorado en Neuroetología, Universidad Veracruzana, Xalapa, México
[3]Centro de Investigaciones Cerebrales, Universidad Veracruzana, Xalapa, México

Background: Spinocerebellar ataxia type 2 (SCA2) is a genetic neurodegenerative disorder characterized by progressive motor impairments including coordination and balance. Earlier structural MRI SCA2 studies have shown atrophy of the pons and cerebellum, and to a lesser extent in some cortical regions. However, the impact of such structural degeneration on the functional connectivity (FC) pattern is currently unknown. The aim of this study is to examine the potential FC disruption pattern of SCA2 and its quantitative relationship with clinical measurements (SARA score).
Methods: 12 genetically confirmed SCA2 patients and their matched healthy controls (HC) participated in this study. Based on group VBM analysis, 17 regions showing atrophy in SCA2 were detected. Cluster's local maxima were used as anchor seeds in the subsequent FC analyses. After rsfMRI images were preprocessed, two-sample t-tests between SCA2 and HC were used to define FC abnormalities for each of the seed-based FC maps. Finally, Pearson's linear correlations were calculated between SARA scores and FC strength from each of the 17 significant cluster maps.
Results: SCA2 connectivity maps showed both hyper and hypoconnectivities when compared with HC for all 17 seeds used ($p > 0.05$ corrected). The highest differences were: hyperconnectivity between the seed in the right inferior frontal gyrus and the right precuneus BA7 and hypoconnectivity between the seed in the right anterior cerebellum and its own surrounding medial area. Significant correlations between the FC strength and the SARA score were found in five connections. Negative correlations include the following connections: right anterior cerebellum with middle temporal gyrus, and left precentral gyrus with the right anterior cerebellum. Positive connections' correlations include: left inferior frontal gyrus with right superior frontal gyrus, left precentral gyrus with left cingulate and right parahippocampal gyrus with left anterior cerebellum.

Conclusions: Our results delineated the abnormal functional connectivity pattern associated with areas showing structural atrophy in SCA2. The findings are characterized by both hypo and hyper synchronizations through affected areas. Further, the significant negative correlations between FC strength and the SARA score between the cerebellum and the precentral gyrus connection highlights the close relationship between physical impairment and functional connectivity abnormalities. Overall, these results provide novel and relevant information for the understanding of SCA2.
Acknowledges: This research was partially supported by DGAPA-PAPIIT IN221413 to JFR

P67C Measure of physical nicotine dependence corresponds to structural and functional alterations in the anterior cingulate-precuneus pathway

W. Huang[1], J.A. King[1], S. Ursprung[2], J.R. DiFranza[2]

[1]Center for Comparative NeuroImaging (CCNI), Department of Psychiatry, University of Massachusetts Medical School, 55 Lake Avenue North, Worcester, MA, USA, 01655
[2]Department of Family Medicine and Community Health, University of Massachusetts Medical School, 55 Lake Avenue North, Worcester, MA, USA, 01655

Background: Although the symptoms of nicotine withdrawal are primarily psychological, convention holds that drug withdrawal syndromes indicate physical dependence (PD). Perturbations in neural function provoked by a drug are thought to induce neural adaptations, which, in the absence of the drug, give rise to withdrawal symptoms. The purpose of this study is to identify neural correlates of the latent state of PD to nicotine, and the dynamic state of nicotine withdrawal.
Methods: Using functional magnetic resonance imaging, we compared 11 smokers after 11 hours of abstinence from nicotine and after satiation, with 10 nonsmoking controls, using independent component analysis (ICA) for brain network comparisons as well as a whole brain resting state functional connectivity (rsFC) analysis using the anterior cingulate cortex (ACC) as a seed.
Results: ICA demonstrated increased functional connectivity in brain networks such as the default mode network associated with the withdrawal state in multiple brain regions. In seed-based analysis, smokers in the withdrawal state showed stronger rsFC than nonsmoking controls between the ACC and the precuneus, caudate, putamen, and frontal cortex ($p < 0.05$). Among smokers, compared to the satiated state, nicotine withdrawal was associated with increased connectivity between the ACC and the precuneus, insula, orbital frontal gyrus, superior frontal gyrus, posterior cingulate cortex, superior temporal and inferior temporal lobe ($p < 0.02$). The intensity of withdrawal-induced craving correlated with the strength of connectivity between the ACC and the precuneus, insula, caudate, putamen, middle cingulate gyrus, and precentral gyrus ($r = 0.60$–0.76; $p < 0.05$).
Conclusions: In concordance with our previous report based on DTI (diffusion tensor imaging) data that structural neural connectivity between the anterior cingulate area and the precuneus increased in proportion to the progression of PD, rsFC in this pathway increases during nicotine withdrawal in correlation with the intensity of withdrawal-induced craving. These findings suggest that smoking triggers structural and functional neural adaptations in the brain that support withdrawal-induced craving.

P68C Relevance of parahippocampal - locus coeruleus functional connectivity to memory dysfunction in early Alzheimer's disease

H.I.L. Jacobs[1,2], S. Wiese[3], V. van de Ven[2], E.H.B.M. Gronenschild[1], F.R.J. Verhey[1], P.M. Matthews[4]

[1]Alzheimer Centre Limburg, School for Mental Health and Neuroscience (MHeNS), Maastricht University, Maastricht, The Netherlands, [2]Faculty of Psychology and Neuroscience, Department of Cognitive Neuroscience, Maastricht University, Maastricht, The Netherlands, [3]Faculty of Psychology and Neuroscience, Department of Neuropsychology, Maastricht University, Maastricht, The Netherlands, [4]Department of Medicine, Division of Brain Sciences, Imperial College, London, United Kingdom

Background: Neuropathology suggests an important role for the locus coeruleus (LC) in the pathophysiology of Alzheimer's disease (AD). Neuropathology and structural damage in the LC appears to be one of the earliest changes. We hypothesise that functional integration of the LC as reflected in brain connectivity also changes and that this change contributes to explaining early memory dysfunction.
Methods: To test this hypothesis, we examined fMRI resting-state functional connectivity from the left and right LC in 18 cognitively healthy older individuals and 18 amnestic, mildly cognitively impaired patients (MCI) with possible AD from the Memory Clinic (Maastricht University Medical Centre). Seed-based resting-state analyses were performed within BrainVoyager QX version 2.6.1. Grey matter atrophy was included as a covariate and also assessed by means of voxel-based-morphometry. Functional connectivity measures were correlated with performance on the word learning test for each group separately.
Results: We found that the left LC showed strong functional connectivity to the left parahippocampal gyrus (PHG) and was correlated with memory encoding and retrieval in healthy older individuals. Connectivity from the left LC was lower in patients with possible AD. Lateralisation of connectivity correlations with memory functions also was altered in these patients: greater right LC-left PHG connectivity was observed in high memory performing patients and not in patients with lower memory scores (see Figure).
Conclusions: Our results provide new evidence supporting a functionally significant role for the LC in declarative memory. They suggest early alterations and the possibility that compensatory changes contribute to preserved memory functions in patients with MCI. Structural and functional measures related to the LC may provide early markers of AD.

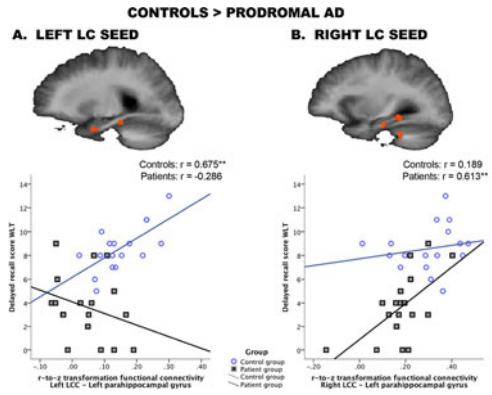

P69C Network modeling of resting state connectivity points towards the bottom up theories of schizophrenia

F. Orliac[3], N. Delcroix[5], M. Naveau[6], P. Delamillieure[1,2,3], M. Joliot[4]

[1]CHU de Caen, Service de Psychiatrie Adultes, Centre Esquirol Caen, F-14000, France; [2]Université de Caen Basse-Normandie, UFR de médecine, Caen, F-14000, France; [3]UMR 6301 CNRS-CEA-Univ. Caen, France; [4]GIN, UMR 5296 CNRS CEA Université de Bordeaux, France; [5]GIP Cyceron, UMS 3408, Caen, France; [6]Jülich Supercomputing Centre, Forschungszentrum, Jülich, Germany

Background: The dysconnectivity theory of schizophrenia proposes that schizophrenic symptoms arise from abnormalities in neuronal synchrony. Based on large-scale network functional connectivity (FC) analysis of fMRI resting state data, we search for those abnormalities and their relations to clinical variables.
Methods: We analyzed intra- and between-network FC strength of 34 resting-states networks (RNs) in 29 Schizophrenia Patients (SP) and 29 Healthy Controls (HC) using resting-state FMRI data. Each RN reference map (Naveau et al., Neuroinformatics, 2012) was used to generate subject-specific versions of the spatial maps, and associated time series, using dual regression (Beckmann et al., OHBM, 2009). For each subject FC between time series of the each RN pair was computed using Pearson's correlation; from these graphs we extracted individual subject RN degree of centrality (DC) and intra-network connectivity strength (INCS). Group differences were tested on DC, INCS (MANOVA, $p < 0.05$) and FCs (ANOVA, $p < 0.05$ Bonferonni-Holmes corrected, $N = 155$). Non-parametric Spearman test was used to assess the correlation of FC values with the 3 clinical variables: the Positive And Negative Syndrome Scale (PANSS-P and PANSS-N) and the hallucinatory status (No Hallucinations (NH), Auditory Hallucinations (AH), or Auditory and Visual Hallucinations (AVH)).
Results: Our results showed significant MANOVAs weaker DC ($p = 0.0013$) and INCS ($p = 0.0016$) in the SP group. Post-hoc analysis demonstrated that alterations affect the four RNs encompassing the occipital lobe and a right fronto-parietal RN. Among the 10 pairs showing significant lower FC in the SP compared to the HC group 7 were in between a visual RNs and one of the 3 cross-modal binding networks. Three of these pairs showed FC decrease associated with positive (PANSS-P), and one pair with negative symptoms severity (PANSS-N). Moreover, FC between one of the 4 visual networks and a multimodal sensory network was significantly lower in AVH compared to NH patients. Surprisingly, FC between a posterior component of the default mode network (described as subtending mental imaging process) and a visual associative network was found higher in SP compared to HC. FC values of this pair were positively correlated with the positive symptoms, and FC was significantly more important in AVH patient group than each of the two other groups (NH and AH).
Conclusions: Sensory networks, and more precisely visual and cross-modal binding networks seem more functionally altered than high-level cognitive networks in schizophrenia. Negative symptoms, positive symptoms and hallucinations seem related to abnormalities in visual processing and crossmodal binding, which is in line with bottom-up model of schizophrenia.

P70C Resting State Functional Connectivity Analysis of Social and Emotion Processing Neural Networks in Autism

G. Joshi, MD[1], X. J. Chai, PhD[2], Z. M. Saygin, PhD[2], J. Gabrieli, PhD[2], J. Biederman, MD[1], S. L. Furtak, BA[1], S. Whitfield-Gabrieli[2]

[1]Clinical and Research Program in Pediatric Psychopharmacology, Massachusetts General Hospital, Boston, Massachusetts, USA
[2]McGovern Institute for Brain Research, Department of Brain and Cognitive Sciences, Massachusetts Institute of Technology, Cambridge, Massachusetts, USA

Background: Autism spectrum disorder (ASD) is characterized by deficits in social and emotional reciprocity, limited introspective ability, and atypical salience. Considering the central role of social and emotional deficits in ASD examining the major brain networks engaged in social-emotion processing is of particular interest when exploring the neural basis of ASD. With this goal, we assessed the integration and segregation profiles of the default mode network (DMN) and salience network (SN) at rest in young adults with ASD by via resting state functional connectivity (RsFc) analysis.
Methods: Resting-state blood oxygen level–dependent (BOLD)-fMRI data were acquired from adolescent and young adult males with high-functioning ASD ($N = 17$; age: mean = 20.4 ± 3.5, range = 16–28 years; IQ: mean = 109.5 ± 11.8, range = 82–130) and from age-, sex-, and IQ-matched healthy controls ($N = 17$). The RsFc data were analyzed using a seed-driven whole-brain analysis approach with ***Conn*** (Whitfield-Gabrieli-Nieto Castanon, 2012). RsFc of the DMN and SN was assessed by examining the positive and negative correlations with the medial prefrontal cortex (mPFC) and the bilateral insula respectively.
Results: ASD was characterized by a divergent pattern of RsFc in the default mode and salience networks. In ASD subjects, the RsFc of the DMN, anchored around the mPFC, was characterized by reduced positive correlations with major nodes of the DMN (posterior cingulate cortex, bilateral angular gyrii), reduced negative correlations with task-positive regions (supramarginal gyrus, fusiform gyrus), and positive correlation with insula. In ASD, the RsFc of the SN, anchored around the insula, was characterized by increased positive correlation of the dorsal and ventral regions of the bilateral anterior insula with a major node of the SN (anterior cingulate cortex [dorsal and subgenual regions]), of the ventral region of bilateral posterior insula with an extended region of the SN (somatosensory cortex), and of the bilateral insula with extra-network regions (somatosensory association cortex, precuneus), and by negative correlation of the bilateral insula with an extended SN node (orbital frontal cortex). Dysregulation in RsFc activity of the DMN could be largely responsible for poor mentalizing ability in ASD. Similarly, aberrant RsFc of the insula with the ACC could account for deficits in emotional awareness, empathy, and cognitive control in ASD.
Conclusions: These findings imply atypical RsFc of the DMN and SN in ASD characterized by poor integration and segregation of the DMN and atypically greater integration of the SN in ASD. Future studies with larger sample sizes are warranted.

P71C Resting-state anticorrelations between medial and lateral prefrontal cortex: Association with working memory, aging and individual differences

Joseph B. Keller[1], Trey Hedden[3,4], Todd W. Thompson[1], Sheeba A. Anteraper[1], John D. E. Gabrieli[1,2], and Susan Whitfield-Gabrieli[1]

[1]Department of Brain and Cognitive Sciences and McGovern Institute for Brain Research, Massachusetts Institute of Technology, Cambridge, MA, USA
[2]Institute for Medical Engineering & Science, Cambridge, MA, USA

[3]Athinoula A. Martinos Center for Biomedical Imaging, Department of Radiology, Massachusetts General Hospital, Charlestown, MA, USA
[4]Department of Radiology, Massachusetts General Hospital, Harvard Medical School, Boston, MA, USA

Background: Here, we explored whether there exists shared or distinct characteristics of intrinsic brain function for age-related declines in working memory (WM) capacity and for individual differences among young adults in WM capacity. We focused on medial prefrontal cortex (MPFC) positive and negative functional connectivity because bi-directional correlations of the MPFC with different regions have been implicated across studies of aging or of individual differences among young adults in relation to executive functions and WM capacity. We examined the relation of MPFC-dorsolateral prefrontal cortex (DLPFC) anticorrelations and MPFC-posterior cingulate cortex positive correlations to WM capacity (Experiment 1) and in a separate dataset (Experiment 2).
Methods: We analyzed resting-state fMRI data of 27 older and younger adults (n = 54) and an additional cohort of younger adults (n = 70). Functional connectivity analysis was performed with a seed-driven approach using the in-house, custom software *Conn*. method, and removed together with movement-related and artifactual covariates. We also implemented methods that minimize the influence of motion artifacts and physiological noise and allow for valid interpretations of negative correlations.
Results: Relative to younger adults, older adults exhibited reductions in working memory capacity, and in MPFC-DLPFC anticorrelations. Within younger adults, greater MPFC-DLPFC anticorrelation at rest correlated with greater working memory capacity.
Conclusions: We found convergent evidence from aging and from individual differences among young adults of a relation between greater WM capacity and greater magnitude of MPFC-DLPFC anticorrelation. Older adults exhibited both reduced WM and reduced MPFC-DLPFC anticorrelation relative to younger adults. Furthermore, greater WM capacity was associated with greater MPFC-DLPFC anticorrelation in two independent cohorts of young adults with two different WM measures. These results suggest that intrinsic anticorrelations between the MPFC, a node in the default-mode network, and DLPFC, a cortical region involved in cognitive control, may serve as a shared indicator of working memory capacity both in aging and in individual differences among young adults.

P72C Functional connectivity is associated with altered brain chemistry in CPP

J. Kim[1], S. As-Sanie[2], P.C. Sundgren[3], D.J. Clauw[4], R.E. Harris[4], V. Napadow[1]

[1]Athinoula A. Martinos Center for Biomedical Imaging, Radiology, MGH, Charlestown, MA, [2]Department of Obstetrics and Gynecology, University of Michigan, Ann Arbor, MI, [3]Radiology, University of Michigan, Ann Arbor, MI, [4]Anesthesiology, Chronic Pain and Fatigue Research Center, University of Michigan Health Center, Ann Arbor, MI

Background: Endometriosis is a common gynecologic condition estimated to affect 10–15% of reproductive-aged women and up to 80% of women with chronic pelvic pain (CPP). Despite the high prevalence and often negative impact on women's lives, little is known about the mechanisms involved in the development of chronic pain in this population. We previously found that elevated levels of excitatory neurotransmitters, glutamate + glutamine (Glx), within the posterior insula and functional connectivity between the insula and default mode network (DMN) were correlated with clinical pain in fibromyalgia (Harris et al., 2009, Napadow et al., 2010). In order to better understand the underlying mechanisms of endometriosis-related CPP, we used proton magnetic resonance spectroscopy (^{1}H-MRS) and functional connectivity MRI (fcMRI) techniques to determine whether women with such pain display altered levels of excitatory neurotransmitters in the insula and how this relates with changes in brain connectivity.
Methods: Four subgroups of participants were included in this study: 17 women with endometriosis-related CPP (⊕ ENDO ⊕ CPP), 13 women with pain-free endometriosis (⊕ ENDOøCPP), 6 women with CPP but no evidence of endometriosis (øENDO ⊕ CPP) and 24 pain-free healthy controls (HC). All subjects underwent ^{1}H-MRS and fcMRI scans on a 3.0T scanner. Single voxels were placed in (1) the right anterior and (2) posterior insula (aINS and pINS) as described previously (Harris et al., 2009). Resting BOLD fcMRI data were collected for 6 minutes and seed-based connectivity analysis was performed by using seeds defined by the same voxels evaluated with ^{1}H -MRS scanning.
Results: We found elevated levels of Glx within the aINS in CPP patients groups, both ⊕ ENDO ⊕ CPP and øENDO ⊕ CPP compared to their age-matched HC. Levels of Glx did not differ between ⊕ ENDOøCPP and age-matched HC. Resting aINS connectivity to medial prefrontal cortex (MPFC) was increased in ⊕ ENDO ⊕ CPP compared to HC, but no differences were found for the other two patient subgroups compared to HC. Furthermore, for ⊕ ENDO ⊕ CPP, greater aINS connectivity to dmPFC was correlated with Glx levels in aINS, as well as pain severity and depression severity scores.
Conclusions: Consistent with our hypothesis, women with CPP (regardless of the presence of endometriosis) demonstrated elevated excitatory neurochemistry in the aINS. Patients with ⊕ ENDO ⊕ CPP had greater aINS connectivity to MPFC, which is known to be a key region of DMN. This result supports our previous findings (Napadow et al., 2010, Loggia et al., 2013) suggesting that resting DMN-insula connectivity is a potential neuroimaging maker for chronic pain. Furthermore, aINS to dMPFC connectivity was correlated with Glx levels, suggesting a linkage between enhanced excitatory neurotransmission and this extended resting connectivity between default mode and salience network brain regions. The aINS is known to also be an affective pain processing region, which is supported by our observation that increased aINS/dmPFC connectivity was associated with worse pain severity and mood-related symptomatology.

P73C Resting State Functional Networks Supporting Interoceptive Sensitivity

Ian R. Kleckner[1], Alexandra Touroutoglou[2,3], Jiahe Zhang[1], Bradford C. Dickerson[2,3,4], Karen S. Quigley[1,5], W. Kyle Simmons[6,7], Lisa Feldman Barrett[1,2,3]

[1]Northeastern University, Boston, MA, USA, [2]Martinos Center for Biomedical Imaging, Massachusetts General Hospital and Harvard Medical School, Charlestown, MA, USA, [3]Massachusetts General Hospital, Boston, MA, USA, [4]Department of Neurology, Massachusetts General Hospital and Harvard Medical School, Boston, MA, USA, [5]Edith Nourse Rogers Memorial VA Hospital, Bedford, MA, USA, [6]Laureate Institute for Brain Research, Tulsa, OK, USA, [7]Faculty of Community Medicine, The University of Tulsa, Tulsa, OK, USA

Background: Afferent feedback from the body to the brain is important in many theories of emotion, cognition, and perception. By extension, these theories highlight the role of individual differences in the ability to detect the physiological state of one's body (interoceptive sensitivity; IS). The neural correlates supporting attention to interoceptive signals, particularly from the heart, lungs, bladder, and gut, include subregions of the posterior and dorsal mid insula. In contrast, the neural correlates of IS may include additional subregions in the anterior insula, which is also involved in emotional experience and self-awareness. Although the neural correlates of IS have been studied during tasks where participants actively attend to their physiology (e.g., focusing on heartbeats), it is not known how individual differences in IS relate to individual differences in resting state functional connectivity. The present study thus examines how functional connectivity to subregions along the insula support IS.
Methods: Twenty-nine participants age 18–50 performed a heartbeat detection task outside MRI to quantify IS. One to seven days later, they performed a 6 min resting state fMRI scan. To systematically identify brain regions that exhibited functional connectivity to an insula subregion that was correlated with IS across participants, we used whole-brain connectivity analyses with seeds in four anatomically-selected subregions of the right insula: dorsal posterior, dorsal mid, dorsal anterior, and ventral anterior.
Results: From all four right insula seeds, IS was positively correlated with connectivity to medial structures including the anterior cingulate cortex and precuneus. Unique to the right dorsal posterior insula seed, IS was positively correlated with connectivity to the bilateral mid insula, precentral gyrus, and postcentral gyrus.
Conclusions: Individual subregions within the insula may support IS through different interactions across the brain: Dorsal mid posterior insula may support IS through functional connections with primary sensory and motor regions as well as with other insular subregions, whereas the mid and anterior insula may support IS through functional connections with medial brain regions related to self-referential thought.

P74C Intrinsic Functional Indices Underlying Numerical Competence in Adults

M.S. Koyama[1,2], Zarrar Shehzad[1,2], M. Milham[1,2]

[1]Nathan Kline Institute for Psychiatric Research (NKI), Orangeburg, NY, USA, [2]Child Mind Institute, New York, NY, USA

Background: Deficits in numeracy affect 5–7% of the U.S. population. Characterized by impairments in the expression and application of simple mathematic skills (e.g., addition, subtraction, multiplication, and division), affected individuals tend to suffer throughout their lifetime unless remediated. Despite its importance, our knowledge of the neural signature of numeracy remains limited to a small number of structural and task-based functional MRI studies that have implicate bilateral intraparietal sulcus (IPS) in numeracy for both children and adults. Here, using task-free resting-state fMRI (R-fMRI) data, we applied ''univariate'' and ''multivariate'' data-driven techniques to examine behavior-brain relationships with numerical competence in adults.
Methods: We examined 163 adults (18–56 years old; 62 males) without any intellectual impairment or reading deficits. Numerical competence (i.e., standardized score) was measured by WIAT Numerical Operation. Each R-fMRI data (multiband EPI: 900 volumes, TR = 645 ms, TE = 30 ms, voxel size = 3^3mm) was preprocessed via C-PAC. In univariate GLM analyses using the fractional Amplitude of Low Frequency Fluctuations (fALFF) and Regional Homogeneity (ReHo), both of which can measure local indices of intrinsic brain activity, numerical scores were entered as the covariates of interest. For our multivariate analysis, we ran Multivariate Distance Matrix Regression (MDMR: see Shehzad et al., 2014).) on voxel-wise connectivity patterns to detect regions with inter-individual variation related to numeracy. The resultant clusters from these analyses were then used as seeds for seed-based functional connectivity (FC) analysis.

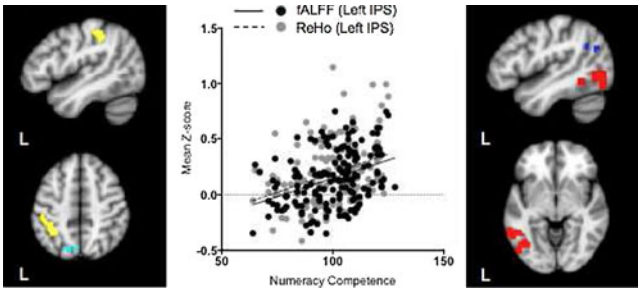

FIG. 1. Left IPS (fALFF & ReHo). **FIG. 2.** Brain-Behavior Relationships. **FIG. 3.** Left LOC (MDMR).

Results: Both fALFF and ReHo identified the left IPS as the key region associated with numerical competence (Fig 1 & 2). Seed-based FC analyses revealed that numeracy positively correlated with FC between the left IPS and the left precuneus (Fig 1). MDMR revealed that connectivity patterns in the left lateral occipital complex (LOC) significantly varied with numeracy (Fig 3). FC between the left LOC and the left angular gyrus positively correlated with numeracy (Fig 3).
Conclusions: Our results render strong support for the important role of the left IPS in numeracy in healthy adults. Additionally, the left hemisphere FC between LOC and angular gyrus (a region for retrieval of numerical facts) is associated with numeracy. This left hemisphere specialization may indicate dominant ''verbal/symbolic'' processing for numeracy in adults. Our approach can serve as a framework for examining numeracy development in children.

P75C Frequency-specific alterations of thalamuocortical connectivity in schizophrenia

Chen-Yuan Kuo[1], Tsuo-Hung Lan[1], Changwei W. Wu[2], Kun-Hsien Chou[3], Chun-Yi Lo[3], and Ching-Po Lin[3]

[1]Institution of Brain Science, National Yang-Ming University, Taipei, Taiwan, [2]Graduate Institute of Biomedical Engineering, National Central University, Taoyuan, Taiwan, [3]Institution of Neuroscience, National Yang-Ming University, Taipei, Taiwan

Background: Schizophrenia is caused by a variety of brain dysfunctions across multiple cortical networks. Because the thalamus has functional linkage with multiple cortical networks, the thalamocortical network would be the key to understand the network malfunction in schizophrenia. However, it remains unclear how the thalamocortical network is affected in schizophrenia patients. The present study aims at comparing the thalamocortical connectivity between schizophrenia patients and healthy controls.
Methods: Twenty-three schizophrenic patients and twenty-nine healthy controls participated in this study. The resting-state BOLD signal in thalamus ROI (Oxford) was retrieved for the power spectrum analysis to confirm the specific frequency band. Using

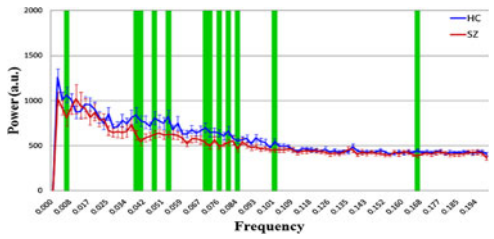

FIG. 1. Power spectrum of thalamus between HC (blue) and SZ (red), green highlights significant difference for $p < 0.05$.

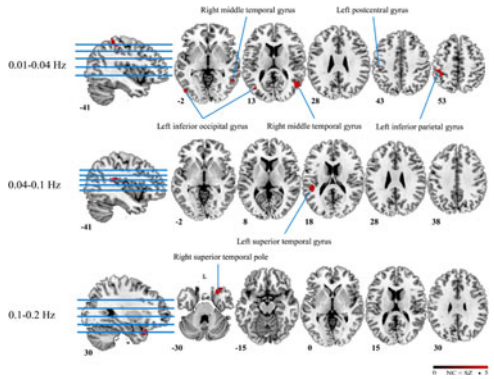

FIG. 2. Between-group functional connectivity maps in distinct frequency ranges ($P < 0.05$, FWE corrected).

three types of low-pass filter, the functional connectivity maps were generated correspondingly to detect the impact of schizophrenia.
Results: The spectral difference in thalamus between schizophrenia and healthy controls was found in the 0.04–0.1 Hz (fig. 1). Compared to controls, schizophrenia patients showed the increased functional connectivity between thalamus and left superior temporal gyrus at 0.04–0.1 Hz (fig. 2). At the other frequency bands (0.01–0.04 and 0.1–0.2 Hz), schizophrenia had increased connectivity respectively in left postcentral gyrus, left middle occipital gyrus, right middle temporal gyrus, left superior temporal gyrus, and right superior temporal pole.
Conclusions: We demonstrated that the enhanced thalamo-occipital connections in schizophrenia and the alteration of low-frequency in thalamus came with distinct thalamocortical network.

P76C Changes in Resting-State Functional Networks in Asymptomatic Welders

E-Y. Lee[1], L. Zhang[1], Y. Truong[2], G. Du[1], M. M. Lewis[1,2], X. Huang[1,2,3,4,5]

[1]Departments of Neurology, [2]Pharmacology, [3]Neurosurgery, [4]Radiology, and [5]Kinesiology, Pennsylvania State University, Milton S. Hershey Medical Center, Hershey, Pennsylvania 17033, USA; [2]Department of Biostatistics, University of North Carolina at Chapel Hill, North Carolina 27599, USA

Background: Exposure to manganese (Mn), a well-known neurotoxicant, is widespread in the general population and often associated with development of neurodegenerative disorders, such as Parkinsonism, and cognitive dysfunction. The purpose of this study was to investigate whether asymptomatic workers with chronic exposure to Mn demonstrate changes in cognitive performance and/or resting-state functional networks, which may help detect early signs of neurotoxicity.
Methods: Resting-state BOLD sequences and comprehensive cognitive function tests were acquired in 34 asymptomatic occupational welders and 30 age- and gender-matched healthy controls. Cognitive measures were analyzed using ANCOVA with adjustment for age and education, as appropriate, in SAS 9.3. Resting-state functional networks were identified using the group ICA (independent component analysis) method in GIFT. The executive function, sensorimotor and default-mode (DMN) networks were selected as networks of interest.
Results: Behavioral results revealed that welders demonstrated significantly lower performance in fine motor (grooved pegboard test; $p = 0.045$ after controlling for age) and executive function tasks (verbal fluency-letter test: $p = 0.0042$ after controlling for age and education level). Group ICA analysis (thresholded at $Z > 3.5$) revealed that welders showed significantly lower activity in the three networks of interest as compared to healthy controls in the following regions: left superior- and bilateral middle- frontal gyri in the executive function network; left pre- and post-central and paracentral gyri in the sensorymotor network; and left posterior cingulate cortex and bilateral precuneus in the DMN.
Conclusions: Asymptomatic active welders with chronic Mn exposure demonstrate reductions in both cognitive performance and resting-state functional network activity. These changes may represent early markers of Mn neurotoxicity.

P77C Task-based and Resting State Functional Connectivity Changes after Cognitive Remediation in Bipolar Disorder

K.E. Lewandowski[1,2], B.M. Cohen[1,2], M.S. Keshavan[2,3], S.H. Sperry[1], D. Ongur[1,2]

[1]McLean Hospital, Belmont, MA, USA, [2]Harvard Medical School, Boston, MA, USA, [3]Beth Israel Deaconess Medical Center, Boston, MA, USA

Background: Cognitive dysfunction is a major, lifelong feature of Bipolar Disorder (BD) and is highly associated with functional outcomes. Cognitive remediation (CR) has shown promise in improving cognitive and functional outcomes in patients with schizophrenia (SZ), and our own preliminary findings demonstrate large effects of CR on cognitive outcomes in patients with BD. Neurobiological effects of CR are poorly understood. While a handful of studies have shown neurobiological change (typically task-based activation) after CR in patients with SZ, no studies to date have examined mechanisms of change after CR in patients with BD. As a major aim of most CR programs is generalizability - both in terms of behavioral outcomes and neurobiological changes - it is hoped that CR programs might produce both focal task-based effects and generalized, task-independent effects. We aimed to examine changes in both task-based activation and resting state functional connectivity in patients with BD after CR.
Methods: BD patients (n = 16) were randomized to either a 70-session, 6-month CR paradigm (n = 8) or a dose-matched active computer control (n = 8). Note that the present findings are based on a neuroimaging study that is part of a larger clinical trial of CR in patients with BD. Cognitive outcomes were measured using the MATRICS Consensus Cognitive Battery. Neuroimaging data were collected at 3T using both task-based and resting state fMRI to examine changes in brain activation and functional connectivity after CR versus control. Task involved the Multisource

Interference Task (MSIT), and anterior cingulate activation was studied. Resting state functional connectivity of an ACC seed region examined pre- and post- intervention.
Results: Subjects in the CR group showed significantly greater improvement in most cognitive domains then control subjects, with effects in the medium to large range. Group-level analyses revealed increased ACC activation after CR during the MSIT in CR subjects butnot controls, particularly in the anterior cingulate gyrus. Resting state data suggest increased functional connectivity of the ACC to bilateral insula after CR but not control.
Conclusions: These preliminary findings suggest that CR but not an active control may increase BOLD activation in ACC during task, and may increase functional connectivity of the salience network, of which ACC is a key node. While most studies of neurobiological change after CR have focused on task-based activation changes, study of changes in resting state functional connectivity speak to the generalizability of CR-related change by examining a) more global brain changes b) in the absence of directed activity. These findings are the first of RSFC changes after CR in psychiatric illness, and suggest that some forms of CR produce generalized brain changes that may be associated with overall healthier brain function.

P78C Lesion Site Specific Intrinsic and Evoked Brain Activity After Stroke

Shang-Hua Lin[1], Po-Ting Lin[2], Si-Huei Lee[3], Shih-Ching Yeh[4], Yi-Yun Yang[3], Ching-Po Lin[1], Changwei W. Wu[2]

[1]Institute of Neuroscience, National Yang-Ming University, Taipei, Taiwan
[2]Graduate Institute of Biomedical Engineering, National Central University, Taoyuan, Taiwan; [3]Institute of Rehabilitation Medicine, Taipei Veterans General Hospital, Taipei, Taiwan; [4]Department of Computer Science and Information Engineering, National Central University, Taoyuan, Taiwan

Background: Increased recruitment of resources in the contralateral hemisphere following stroke indicated poor motor performance while moving affected limbs, whereas interhemispheric interactions are usually lateralized in normal brain. Previous studies also showed disturbed intrinsic interhemispheric connections after local damage. However, both intrinsic and task activity showed great variability depend on different lesion regions that affected motor network. Therefore, we aim to investigate the lesion specific features by comparing resting-state and task fMRI.
Methods: Three patients with stroke (Patient 1: medulla lesion, age: 46 y/o, duration to onset: 1 year; Patient 2: right thalamus and internal capsule lesion, age: 69 y/o, duration to onset: 4 months; Patient 3: Right thalamus and internal capsule lesion, age: 51 y/o, duration to onset: 1 month) and 5 healthy adults were recruited. Participants were instructed to perform grasp task and resting-state condition during MRI session. T1 and T2-FLAIR images were used to identify lesion areas and fill white matter hyperintensity regions, respectively. The fMRI data were processed by standard procedures. Structural images were coregistered to functional images followed by DARTEL normalization and smooth by SPM12b. The statistical significance for the individual analysis were set as FWE corrected $p < 0.05$ for grasp task and and $z > 0.9$ for resting-state functional connectivity (rs-FC).
Results: All patients showed left limb weakness in clinical tests. Medulla lesion patient showed increased contralesional activity using affected hand and slightly decreased FC while seeded at ipsilesional M1. Both subcortical white matter (WM) lesion patients showed no obvious contralesional activity but deminished bilateral rs-FC.
Conclusions: Corticospinal tract lesion affected task activity but leave intrinsic connections of bilateral motor cortex intact while WM lesion broke down rs-FC of interhemispheric communications without abnormal recruitment of contralesional activity.

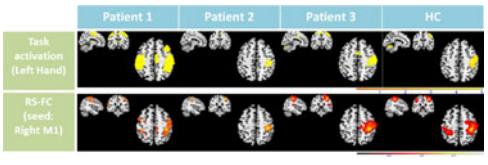

P79C BOLD variability at rest is correlated with CSF α-Synuclein in Parkinson Disease

Tara M. Madhyastha[1], Jing Zhang[2], James Leverenz[4], Shu-Ching Hu[2], Thomas J. Grabowski[1,3]

[1]Radiology, [2]Pathology, [3]Neurology, University of Washington, Seattle, WA
[4]Cleveland Clinic Lou Ruvo Center for Brain Health, Cleveland, OH

Background: α-Synuclein (α-Syn) is a major constituent of Lewy bodies, which are the hallmark of Parkinson Disease (PD) pathology. The progression of fibrillar α-Syn pathology from the brainstem to the cortex is an important neuropathological correlate of dementia.[1,2] CSF α-Syn is lower in PD and decreases longitudinally,[3] but there is no established physiological correlate of CSF α-Syn levels. It has been proposed that BOLD signal variability is a sign of physiologic health.[4] Cortical neurophysiology is affected in PD due to disruption to ascending systems and α-Syn pathology. We hypothesize that CSF α-Syn is related to regional variability of the BOLD signal in areas affected in PD.
Methods: This analysis includes 15 medicated subjects with early-stage PD (mean Hoehn&Yahr score 2) drawn from a larger study who had contributed two baseline sessions of resting state data and CSF fluid (collected within a mean of 10.2 months of imaging). Data were acquired using a Philips 3T Achieva MR System (Philips Medical Systems, Best, Netherlands, software version 3.2.2) with a 32-channel SENSE head coil. Two 12 minute resting state scans (obtained 2–3 weeks apart) and a sagittal T1-weighted 3D MPRAGE image with 1 mm isotropic voxels were used in this analysis. Functional images were preprocessed to correct for motion, remove spikes, correct for slice timing, and regress out signal from white matter and lateral ventricles. [5] Data were registered to standard space. Using the first volume of each scan as reference we computed the % change in signal of subsequent volumes, and the SD of the % change for each voxel. We quantified grey matter (GM) density using FSL FAST at the same smoothing level of the functional data. At each voxel, we calculated the partial correlation coefficient for the SD of the BOLD % signal change to CSF α-Syn,

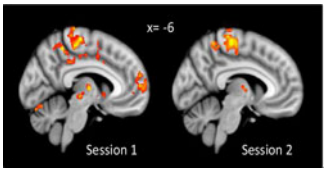

FIG. 1. Clusters where resting state BOLD variability is significantly correlated with CSF α-Syn.

controlling for GM density, using Spearman rank correlation. We corrected for multiple comparisons using cluster-based thresholding with $p = .01$ and $\alpha = .05$.
Results: Higher CSF α-Syn is reliably associated with greater variability in the precuneus, premotor cortex, central opercular cortex, thalamus and putamen, all regions known to be implicated in PD. A significant association in the ACC does not survive correction for multiple comparisons at the second session, consistent with greater motion at that timepoint. There are no regions where higher α-Syn is associated with lower BOLD variability.
Conclusions: Decreased BOLD variability may index functional disruption related to α-Syn pathology.
Acknowledgements: NIH 1RC4NS073008-01 and P50NS062 684.

P80C Decreased resting-state functional connectivity in the frontal-striatal reward system in social anxiety disorder

J. Manning[1,3], G. Reynolds[2,4], S. G. Hofmann[4], M. Pollack[5], J. D. E. Gabrieli[1,2,3], S. Whitfield-Gabrieli[1,2,3]

[1]McGovern Institute for Brain Research, Cambridge, MA, USA, [2]Poitras Center for Affective Disorders Research, Cambridge, MA, USA, [3]Department of Brain and Cognitive Sciences, Massachusetts Institute of Technology, Cambridge, MA, [4]Department of Psychology, Boston University, Boston, MA, USA, [5]Rush University Medical Center, Chicago, IL, USA

Background: We investigated differences in the intrinsic functional brain organization (functional connectivity) of the human reward system between healthy control participants and patients with social anxiety disorder. Functional connectivity was measured in the resting state via functional magnetic resonance imaging (fMRI).
Methods: 53 patients with social anxiety disorder and 33 healthy control participants underwent a 6-minute resting-state fMRI scan. Functional connectivity of the reward system was analyzed by calculating the whole-brain temporal correlations with bilateral nucleus accumbens and with ventromedial prefrontal cortex seeds. The correlations of the patients were compared to the correlations of the healthy control participants.
Results: Patients with social anxiety disorder, relative to the healthy control group, had decreased functional connectivity between the nucleus accumbens seed and the ventromedial prefrontal cortex and multiple brain regions associated with reward. Patients with social anxiety disorder, relative to the control group, had increased functional connectivity between both the nucleus accumbens seed and the ventromedial prefrontal cortex seed and more posterior brain regions, including dorsal anterior cingulate cortex. Patients with social anxiety disorder, relative to the control group, had decreased functional connectivity between the ventromedial prefrontal cortex seed and prefrontal regions, including the anterior and dorsolateral prefrontal cortices.
Conclusion: Social anxiety disorder is associated with decreased functional connectivity between regions implicated in reward anticipation and regions associated with encoding reward into value.

P81C Voxelwise eigenvector centrality mapping of the human functional connectome reveals an influence of the COMT val158met polymorphism on the default mode and somatomotor network

S. Markett[1], C. Montag[1], B. Heeren[1], R. Saryiska[1], B. Lachmann[1], B. Weber[1,2,3], M. Reuter[1]

[1]University of Bonn, Germany; [2]Life and Brain Center Bonn, Germany; [3]University Clinics Bonn, Germany

Background: Functional connections between brain regions are organized into networks and constitute the substrate of the human functional connectome, whose topography been discussed as a promising endophenotype for psychiatric disorders. Genetic influences on the entire connectome, however, have not been investigated so far. In the present study, we test for connectome-wide influences of the val158met (rs4860) polymorphism on the catechol-O-methyltransferase (COMT) gene by applying formal network analysis and eigenvector centrality mapping on the voxel level to resting state functional magnetic imaging data. COMT rs4860 is a common genetic variant of high clinical relevance, particularly with respect to schizophrenia and affective disorders.
Methods: Resting state fMRI data (245 volumes, eyes-closed) was acquired from $N = 110$ healthy participants. All participants had previously provided buccal swabs for genotyping. Genotyping of the COMT rs4680 polymorphism was performed by real time polymerase chain reaction using fluorescence melting curve detection analysis. We modeled the functional connectome as a weighted undirected graph with each voxel in the cerebrum as a node and functional connectivity between each pair of voxels as an edge. Voxelwise eigenvector centrality was computed by the matrix factorization approach and the power-iteration algorithm. Normalized eigenvector centrality maps were submitted to a second-level ANOVA model with COMT genotypes as factor levels.
Results: The COMT variant linked to high-enzyme activity increased network centrality in distributed brain areas that are known to constitute hub regions in the brain's default mode network: the medial temporal cortices and dorsomedial prefrontal cortex. Further results indicated an influence of COMT val158met on areas implicated in the somatomotor network. Here, the high-active COMT variant decreased network centrality in pre- and postcentral gyri and the paracentral lobule.
Conclusions: The present investigation is the first study to show an influence of a common genetic variant on connectivity in the entire functional connectome. The major finding of the present report is a clear influence of COMT rs4680 on connectivity of key regions in the default mode network. Disruptions of this network can be observed in schizophrenia. COMT rs4680 has been discussed as a risk factor for psychosis, thus our data suggest that eigenvector centrality in the default mode network at rest might qualify as an intermediate endophenotype for schizophrenia. Additionally, we observed an influence of COMT rs4680 on the somatomotor network. This finding is in line with the polymorphism's role in individual differences in pain perception. The present study is an important step towards understanding the molecular underpinnings of the connectome, towards the establishment of intermediate endophenotypes for psychotic disorders and towards the development of valid etiological models and informed treatment strategies.

P82C Brain differences between persistent and remitted attention-deficit/hyperactivity disorder

A.T. Mattfeld[1,2], J.D.E. Gabrieli[1,2], J. Biederman[3,4], T. Spencer[3,4], A. Brown[3,4], A. Kotte[3,4,5], E. Kagan[3,4], S. Whitfield-Gabrieli[1,2]

[1]McGovern Institute for Brain Research, Cambridge, MA, USA, [2]Department of Brain and Cognitive Sciences, Cambridge, MA, USA, [3]Clinical and Research Program in Pediatric Psychopharmacology, Boston, MA, USA, [4]Department of Psychiatry, Boston, MA, USA, [5]Department of Psychology, Honolulu, HI, USA

Background: Previous resting-state studies of attention-deficit/hyperactivity disorder (ADHD) in both adults (Castellanos et al., 2008) and children (Fair et al., 2010) have reported decreased correlations between midline regions of the default mode network (DMN). No studies have distinguished between patients who remit from childhood ADHD from those who retain a diagnosis in adulthood.
Methods: To evaluate resting state differences between persistent and remitted ADHD, we utilized resting state functional connectivity to assess the intrinsic functional brain organization in patients who had a persistent diagnosis in childhood and adulthood (n = 13), in patients who met diagnosis in childhood but not in adulthood (n = 22), and in control participants who never were diagnosed with ADHD (n = 17). We used a seed in the posterior cingulate cortex (PCC) to evaluate DMN integrity among the three groups and a seed in the medial prefrontal cortex (MPFC) to evaluate default mode and task positive network interactions.
Results: Positive functional connectivity between the posterior cingulate and medial prefrontal cortices was reduced only in patients with a persistent ADHD diagnosis into adulthood. Patients with a childhood diagnosis of ADHD who remitted as adults were not significantly different from controls. Negative functional connectivity between medial and dorsolateral prefrontal cortices were reduced in both persistent and remitted patients relative to controls
Conclusions: We identified differences and similarities in the intrinsic functional brain organization of longitudinally followed individuals who either persisted or remitted in their ADHD diagnoses in adulthood. The dissociation between PCC-MPFC and MPFC-DLPFC functional connectivities may inform the relationship between ADHD diagnoses versus variability in executive dysfunctions commonly observed.

P83C Effects of nicotine on brain network dynamics in current, former, and non-smokers

C. Mills-Finnerty[1], L.H. Sweet[2], U.S. Clark[3], C. Hanson[1], S.J. Hanson[1]

[1]Rutgers University, Newark, NJ, [2]University of Georgia, Athens, GA, [3]Icahn School of Medicine at Mount Sinai, New York, NY

Background: Characterizing brain network dynamics underlying nicotine response in current, former and non-smokers is important for determining whether nicotine affects brain networks differently for each of these groups, which has strong implications for cessation research. We quantified Bayes connectivity networks in current, former and non-smokers both on and off nicotine to examine group differences in network connectivity, and whether these differences would be impacted by nicotine administration.
Methods: Thirteen current, former, and non-smokers underwent two fMRI scans on different days, once with a nicotine patch and once with placebo patch, during which they passively viewed a crosshair baseline. Bayes network connectivity analysis was used to model connections amongst regions chosen a priori due to their implications for nicotine addiction and craving regulation, including the orbitofrontal cortex (OFC), insula, caudate, and nucleus accumbens (NA). This analysis quantifies the connectivity structure of the network and the strength of the connections (comparable to regression coefficients). Connectivity was measured separately for each group and nicotine condition, and the strengths of connections were compared across groups on vs. off nicotine, both within and between nicotine conditions.
Results: When current, former and non-smokers were on nicotine, a common network structure was observed which included: caudate-insula, caudate-NA, NA-OFC, and OFC-insula. Off nicotine, for the smokers only there was no longer a connection between caudate-NA. Former and non-smokers had stronger connections on nicotine compared to off nicotine for the OFC-NA and insula-caudate conditions. This difference was at or near significance for the OFC-NA connection only (former smokers, $t = -2.05$, $p = 0.06$; non-smokers, $t = -2.32$, $p = 0.04$). Smokers showed the opposite pattern of connection strength, with stronger connections off nicotine compared to on for OFC-NA, insula-caudate, and OFC-insula, though differences between conditions were not significant.
Conclusions: Network connectivity of former and non-smokers was affected by nicotine in a similar manner, with increases in connection strength during nicotine administration when compared to the off nicotine condition. Smokers exhibited the opposite pattern of connection strengths as former and non-smokers, with the greatest difference observed for the OFC-NA connection. The OFC is often implicated in regulation of cigarette craving, whereas NA is implicated in craving and anticipation of future reward states. Dysregulation of this corticostriatal has been proposed as one of the primary mechanisms underlying addiction. Smoker's stronger connectivity in these regions as they experience nicotine deprivation compared to satiety may reflect a feedback mechanism necessary to regulate craving states. Our results suggest that the differential effects of nicotine on current, former, and non-smokers are measureable via brain connectivity analysis. Identifying these dynamics is an important precursor for measuring factors such as long-term brain effects of nicotine exposure and risk factors related to addiction and relapse.

P84C Identification of frequencies of impaired functional connectivity related to duration of disease in temporal lobe epilepsy using wavelet coherence analysis

V.L. Morgan[1], J.C. Gore[1], B. Abou-Khalil[2], B.P. Rogers[1]

[1]Vanderbilt University Institute of Imaging Science, Nashville, TN, USA,
[2]Vanderbilt University Department of Neurology, Nashville, TN, USA

Background: In previous work we found that the resting state functional connectivity of a temporal lobe network ipsilateral to the seizure focus in temporal lobe epilepsy (TLE) linearly decreases with duration of disease [Morgan VL, et al. in review]. Here we used a wavelet coherence analysis to investigate the frequency components of the functional connectivity responsible for this relationship.
Methods: Resting functional MRI data were acquired for 20 minutes in 13 TLE patients and 13 age and gender matched healthy controls. A network ipsilateral to the seizure focus and one contralateral to the seizure focus consisting of the hippocampus, insula and thalamus were identified. Wavelet coherence analyses of each network based on the method described by Chang and Glover [2010] and algorithms by Grinsted A., et al. [2004] were implemented yielding matrices of coherence (R^2) and phase angle (θ) for each frequency at each time sample. Functional connectivity was computed as $R^2 * \mathrm{real}(e^{i\theta})$, and converted to a Z statistic using the Fisher Z transform. For each subject we calculated the time averaged functional connectivity as a function of frequency (FC_f). Then we subtracted the FC_f of the matched control from each patient. The linear correlation between each FC_f (patient-control) and duration of disease

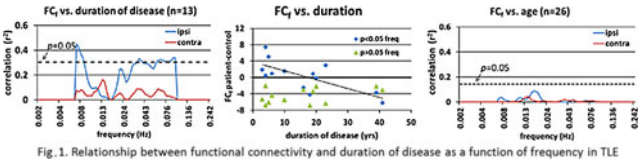

Fig. 1. Relationship between functional connectivity and duration of disease as a function of frequency in TLE

across subjects was calculated resulting in an r and p-value at each frequency.

Results: The FC_f of the ipsilateral network was correlated ($p < 0.05$) with duration of disease at approximately 0.006–0.008 Hz and 0.03–0.1 Hz, but not in the contralateral network (Figure 1, left). The FC_f averaged over the significant frequencies (blue) and the other frequencies (green) vs. duration of disease in the ipsilateral network are shown in Figure 1, middle. The correlation with age is shown for comparison (Figure 1, right).

Conclusions: The wavelet coherence analysis revealed specific frequencies of the fluctuations that decrease with duration of disease ($p = 0.005$) in the ipsilateral seizure network in these TLE patients, while the others are decreased in TLE at all durations ($p = 1.6 \times 10^{-6}$). A focused investigation of the physiological relevance of these frequencies may lead to elucidating the mechanism of how repeated seizures disrupt functional activity leading to behavioral and cognitive impairments in TLE.

P85C Neuropsychiatric symptoms and functional connectivity in mild cognitive impairment and cognitively normal elderly

C. Munro, N.J. Donovan, B. Guercio, S.E. Wigman, A.P. Schultz, R.E. Amariglio, D.M. Rentz, K.A. Johnson, R.A. Sperling, G.A. Marshall

Center for Alzheimer Research and Treatment and Department of Neurology, Brigham and Women's Hospital; Massachusetts Alzheimer's Disease Research Center and Department of Neurology, Massachusetts General Hospital, Harvard Medical School, Boston, MA, USA

Background: Neuropsychiatric symptoms, such as apathy and anxiety, commonly accompany cognitive and functional decline in early Alzheimer's disease (AD). Prior studies have shown associations between affective symptoms and medial frontal regions in mild-moderate AD dementia and the inferior temporal region primarily in mild cognitive impairment (MCI). Few studies have investigated functional connectivity changes associated with neuropsychiatric symptoms in early AD. The objective of this study was to investigate the association between functional connectivity in different brain networks and neuropsychiatric symptoms in MCI and cognitively normal (CN) elderly.

Methods: Fifty-three (39 MCI, 14 CN) subjects participated in an investigator-initiated imaging study. Neuropsychiatric symptoms were assessed using the 12-item Neuropsychiatric Inventory. Functional connectivity in 4 networks (default mode network, frontoparietal control network (FPCN), dorsal attention network, and ventral attention network) was assessed using seed-based resting-state magnetic resonance imaging. Exploratory factor analysis was used to identify 2 factors of neuropsychiatric symptoms: an Affective factor (comprised of anxiety, apathy, depression, appetite, irritability, and sleep) and a Hyperactivity factor (comprised of agitation, aberrant motor behavior, and disinhibition). Separate linear regression models with backward elimination were utilized with the neuropsychiatric factors as the dependent variable and the 4 networks as the predictors of interest. Covariates included age, sex, American National Adult Reading Test IQ (premorbid intelligence), diagnosis, processing speed and encoding memory (which have been shown to be associated with neuropsychiatric symptoms). These analyses were repeated with the individual items of the Affective factor, using the same predictors.

Results: There was a marginal association between greater Affective factor symptoms and reduced FPCN connectivity ($p = 0.06$), while greater Affective symptoms were significantly associated with a diagnosis of MCI ($p = 0.002$). There was no association between the Hyperactivity factor and any of the networks. Post-hoc analyses revealed associations between greater apathy and reduced FPCN connectivity ($p = 0.004$) and greater anxiety and reduced FPCN connectivity ($p = 0.03$).

Conclusions: These results suggest that decreased activity in the frontoparietal control network may be associated with greater affective symptoms, in particular apathy and anxiety, early in AD. These findings support prior studies using different functional imaging modalities in more impaired individuals.

P86C Graph theoretic characterization of functional MEG networks during interictal resting state in epilepsy

G. Niso[1,*], S. Carrasco[2], M. Gudín[2], F. Maestú[1], F. del-Pozo[1], E. Pereda[3]

[1]Center for Biomedical Technology, Technical University of Madrid, Madrid, Spain, [2]Hospital General Universitario, Ciudad Real, Spain, [3]Electrical Engineering and Bioengineering Group, Dept. of Basic Physics, Univ. of La Laguna, Tenerife, Spain

Background: The aim of this study is to analyze the complex network structure derived from the connectivity patterns of resting state interictal magnetoencephalography (MEG) from two different types of epileptic patients (frontal focal (FE) and idiopathic generalized (GE)) and one of healthy subjects (HS). We seek to elucidate whether epileptic brains behave differently to normal ones even in the absence of spikes.

Methods: We studied 45 subjects: 15FE, 15GE and 15HS. MEG data were recorded with a 306-channel Elekta Neuromag® system at 1 kHz (using tSSS with movement compensation) during interictal resting state with closed eyes. The analyses were performed on the 40 most stationary non-overlapping segments of 5000 ms per subject, far from recent epileptic discharges. We assess functional connectivity (FC) using two indices of phase synchronization: Phase Locking Value (PLV) and Phase Lag Index (PLI) in the frequency bands: theta [4–8]Hz, alpha [8–12]Hz, beta1 [12–20]Hz, beta2 [20–28]Hz and low-gamma [28–40]Hz. Bivariate surrogates were used to test the significance of each FC index between every two sensors. We then characterized brain network structure by estimating a list of the most commonly used network measures and later use the correlation between them to determine the minimum subset that best describe the structure of the FC networks. Statistical differences between HS and the GE/FE groups were checked using a two-sided rank sum test.

Results: Regarding the sensitivity to deep brain sources: through the sensor approach (gradiometers/magnetometers), magnetometers show higher artificial values; through the methodological approach (PLV/PLI): PLV presented higher number of links. However, to characterize differences between networks PLV gives better results, as PLI FC networks were very sparse and less consistent even intrasubject. For FC networks characterization,

four sets of measures were singled out: *Global efficiency:* differences reflect the facility of epileptic brains to ''transmit information'' or in the case of seizures straightforwardly propagate. *Algebraic connectivity:* suggests epileptic brains are more easily synchronized and have a more robust synchronized state than HS. *Betweenness:* was higher for HS in both beta bands, as was the *eccentricity.* This latter index was also higher in the FE group in the gamma-band.
Conclusions: FC network measures detect an alteration of brain interictal activity in both FE and GE, indicating that in both epilepsies, the network of neocortical sources is more prone to become (pathologically) synchronized that in HS.

P87C Complex network analysis of Hot Water Epilepsy in Drug Naïve Patients

[1]R. Panda, [1]R.D. Bharath, [2]S. Sinha, [3]A. Sahoo, [1]L. George, [2]K. Raghavendra, [3]B.B. Biswal, [1]A.K. Gupta, [2]P. Satishchandra

[1]Dept. of Neuroimaging & Interventional Radiology, National Institute of Mental Health and Neuro Science (NIMHANS), Bangalore, India; [2]Dept. Neurology, NIMHANS, Bangalore, India; [3]Dept. of Biomedical Engineering, New Jersey Institute of Technology, New Jersey, USA

Background: Hot water epilepsy (HWE) patients otherwise called ''water immersion epilepsy'' is a type of reflex epilepsy commonly presenting as a complex partial seizure. The objective of this study was to characterize the resting state functional connectivity network in drug naïve HWE patients using small world connectivity (SWC) measures.
Methodology: Twenty Drug Naïve HWE patients (seizure frequency of more than 2 per month) were scanned in this study. Twenty age and gender matched healthy controls were recruited in the control group. First the data was preprocessed using SPM (realigned, coregistered and normalized to MNI space. Subsequently the brain was parcellated into 200 ROIs (Craddock et al., 2012). The SWC measures were computed using Brain connectivity (BCT) toolbox. We computed the clustering coefficient 'C', the characteristic short path length 'L' and the small-world coefficient between controls and patients over a wide range of network density (sparsity) thresholds (10 to 50%) [1,2]. Along with the whole brain differences in SW measures ($P < 0.05$), certain regions showed significant differences ($P < 0.005$) between the patient and control group as well.
Results: We noted that the clustering coefficient and path length were decreased on a whole brain level and localized regional level as well. The patient group also had a significantly lower small world coefficient. The cortical regions which revealed decreased absolute clustering coefficient were left middle temporal gyrus, left parahippocampal gyrus, bilateral superior temporal gyrus, bilateral middle and superior frontal gyrus. Also the sub cortical regions like right posterior cingulate gyrus and right insula also showed reduced clustering coefficient.
Conclusion: The present study reveals that seizures can cause widespread decrease in the small world properties of the brain in HWE patients with frequent seizures which predominantly affect the temporal lobes bilaterally. The lower clustering coefficient and path length provide evidence for a more randomized network in HWE patients.
References: Zhang, Zhiqiang, et al. ''Altered functional–structural coupling of large-scale brain networks in idiopathic generalized epilepsy.'' *Brain* 134.10 (2011): 2912–2928; Liao, Wei, et al. ''Altered functional connectivity and small-world in mesial temporal lobe epilepsy.'' PloS one 5.1 (2010): e8525.

P88C Major Depressive Disorder Splits the Brain Network Modules Responsible for Helplessness

D.H. Peng[1,2], F. Shi[2], T. Shen[1], Z.W. Peng[2], Y.R. Fang[1], D.G. Shen[2]

[1]Division of Mood Disorders, Shanghai Mental Health Center, Shanghai Jiao Tong University School of Medicine, Shanghai, China, [2]Department of Radiology and BRIC, University of North Carolina at Chapel Hill, NC, USA

Background: Abnormal global functional connectivity (FC) network among major depressive disorder (MDD) is still poorly understood, as a pathophysiological aspect. As a novel method to investigate the global FC, few brain network modularity studies on MDD have been documented. Meanwhile, the majority of previous studies on core symptoms of depression, e.g., helplessness, were conducted only by the animal model. In this study, we first explore the underlying relationship of the helplessness symptom and the pattern of modular networks in MDD patients.
Methods: Sixteen first-episode, medication-naïve MDD patients and 16 healthy controls participated in resting-state functional magnetic resonance imaging (fMRI) scanning. After preprocessing, global FC network was constructed by using the correlations between 90 brain regions defined by the Automated Anatomical Labeling (AAL) brain atlas. Modular organization was investigated in both groups. Furthermore, using the control module as reference, the quantitative indices of inter- and intra-module connectivity were measured for each module, as well as for each brain region, to investigate its regional role.
Results: We found 4 modules in controls, while 5 atypically reorganized modules in MDD patients exhibited. Specifically, the first module in controls was separated into two different modules in MDD, showing that MDD is more functionally specialized (Fig. 1). Interestingly, a positive correlation was found among MDD patients between the helplessness factor assessed via the Hamilton Depression Scale and the intra-module connectivity of module I. Furthermore, in module I, the left superior orbitalfrontal cortex was found with increased inter-module connectivity, suggesting increased ability of cognitive decision-making. Right amygdala also demonstrated decreased intra-module connectivity, indicating impairment in emotion processing. Those two brain areas have been presumed to be involved in the process of negative cognition, e.g., helplessness in MDD.
Conclusion: We found separated modular organization in MDD and also the atypical regional roles, including the increased interconnectivity in left superior orbitalfrontal cortex and the decreased

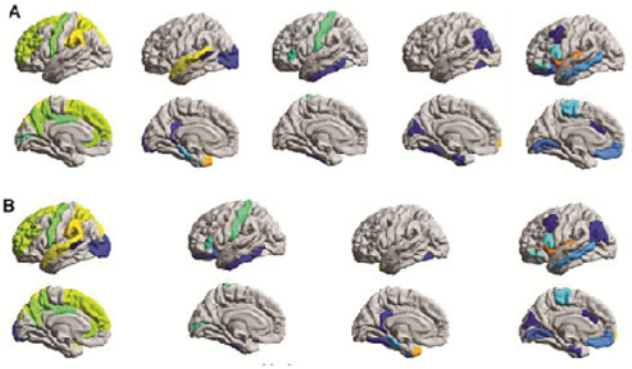

FIG. 1. Modular organizations of the global brain functional network in major depressive disorder group **(A)** with 5 modules, and in healthy control group **(B)** with 4 modules.

intra-connectivity in right amygdala. Higher intra-module connection of module I corresponds to more severe helplessness symptoms. These disrupted patterns of global module network might contribute to the cognition of helplessness in MDD.

P89C Voxel-mirrored homotopic connectivity analysis of pediatric epilepsy patients with focal cortical dysplasia

A.V. Poliakov[1]*, E.J. Novotny[2,3,4], S.L. Poliachik[1], S.D. Friedman[1], G.E. Ishak[1], J.N. Nixon[1], D.W. Shaw[1], and J.G. Ojemann[2,4]

[1]Radiology, Seattle Children's Hospital, [2]Pediatrics, [3]Neurology, [4]Neurosurgery, University of Washington, Seattle, WA, USA

Background: Disruption of connectivity in certain disease states, including epilepsy, can be demonstrated using functional connectivity MRI (fcMRI), based on task-free, resting state fMRI. In healthy controls, fcMRI reveals strong interhemispheric connectivity between homotopic (geometrically corresponding) regions across the brain. A technique to quantify functional homotopy is voxel-mirrored homotopic connectivity (VMHC), providing a voxel-wise connectivity computed between mirroring voxels in each hemisphere. Surgical resection benefits many with focal cortical dysplasia (FCD), the most common cause of medically refractory epilepsy in the pediatric population, especially with complete resection of the abnormality. Anatomical MRI imaging may not identify patients likely to benefit from surgical treatment, and lesions seen on MRI may be smaller than the seizure-generating dysplastic region. Thus, other diagnostic techniques (EEG, FDG-PET, MEG, DTI and intracranial EEG) are used to localize the seizure focus. We employed VMHC technique to evaluate a series of 7 patients with FCD in order to characterize the homotopic connectivity of dysplastic areas.
Methods: Siemens system, 3T imaging (EPIBOLD sequence, TR = 2 s, TE = 27 ms, flip angle = 90°, 4 mm isotropic voxels) obtained fcMRI scans in both awake and anesthetized patients. Awake patients were instructed to rest with eyes open. Structural T1 images linearly coregistered to standard (MNI) space, fcMRI preprocessing in standard space (1000 Functional Connectomes Project scripts; AFNI and FSL software), the VMHC analysis used Resting-State fMRI Data Analysis Toolkit (REST v. 1.8, Song et al. 2011).
Results: In 7 patients with FCD, 4 displayed dramatic reduction of homotopic connectivity in the FCD area, one showed moderate reduction and 2 did not show clear reduction.

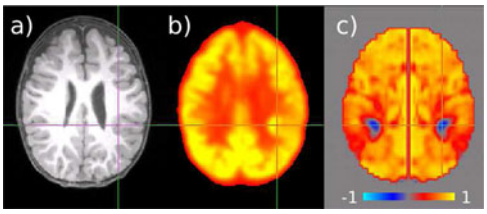

FIG. 1. Imaging result in a 3 y old male patient with FCD. a) MRI T1 revealed thickening cortex characterized by somewhat blurry grey-white boundary. b) FDG-PET showed increased metabolism and FCD location was consistent with EEG findingsc) VMHC map shows correlation coefficient of the fcMRI signals for homotopic voxels; for this case a substantial reduction of homotopic connectivity (crosshairs) compared to surrounding areas.

Conclusions: VMHC can only be used meaningfully in patients with grossly symmetric brain anatomy. Patients suffering from seizure disorders and underlying FCD that is difficult to identify using conventional imaging methods may benefit from this technique. Analysis in a small group of FCD patients revealed atypical reduction in homotopic connectivity in FCD area for most of them. Failure to detect aberrant homotopic connectivity in some patients may reflect dynamic nature of epileptogenic activity and variable VMHC patterns. This result shows promise for identifying and delineating seizure-generating dysplastic regions that may be useful for surgical planning.

P90C Importance of task positive and task negative interactions in neglect recovery

L.E. Ramsey[1], A. Baldassarre[1], G.L. Shulman[1], M. Corbetta[1,2,3]

[1]Department of Neurology, [2]Radiology, [3]Anatomy & Neurobiology, Washington University, St Louis, USA

Background: Neglect is an attention disorder, caused by lesions in the temporo-parietal or ventral frontal cortex. The deficits have been related to abnormal activation in and between regions of the dorsal attention network (DAN). Regions of the DAN, also referred to as the task-positive network, are linked to sustained attention. When using resting state fMRI, the dorsal attention network regions are highly inter-correlated and show strong negative correlations with regions of the default mode network (DMN). This task-negative network consists of regions that are more active and more highly connected during rest and has been proposed to be related to internal thought. Abnormal connectivity between regions of this network have been linked to disorders such as schizophrenia, ADHD, Parkinson's disease, TBI and generally after stroke. Recent work however suggests that reemergence of activity in the DMN regions could underlie lapses in attention and thus the interaction between regions of the DMN and DAN could be more important for attention deficits than connectivity within each of them separately. The two networks have been implicated in neglect deficits, but little is known about how this interaction is actually related to recovery. If there is indeed a relationship between the interaction of the two networks and attention this should improve for neglect patients specifically as opposed to the whole stroke group.
Methods: 18 patients with right hemisphere lesions with neglect, and 17 patients with right hemisphere lesions without neglect were included. Behavioral data and resting state fMRI was collected at 2 weeks and 3 months after stroke onset. Correlations of the low frequency fluctuations were calculated from DAN regions to all other voxels in the brain (excluding the voxels damaged by the lesion). Average maps were then created of the seeds in each network within each hemisphere and 2 by 2 ANOVA was run between the two groups and the two time-points. The significant regions are overlaid with thresholded maps of each of the networks, to classify to which network they belong. The signal is extracted for each of the groups and time-points to investigate the direction of change.
Results: The effects of time for all of the 35 stroke patients are seen between regions of the DAN. Significant interaction effects (group × time) are seen between regions of the DAN and between regions of the DAN and the DMN. The DAN-DMN connectivity is increased (less negative) in neglect patients at the sub-acute stage and this improves to close to no-deficit patients at the chronic stage. DAN-DAN connectivity is decreased (less positive) at the sub-acute stage and shows an increase towards normal levels at 3 months. Correlations between the difference in

behavior and difference in connectivity strengths are significant, indicating the behavioral relevance of these results.
Conclusions: The connectivity within the dorsal attention network seems to be related to general recovery after stroke, which might not necessarily be related to attention. An improvement in anti-correlation between the dorsal attention and default mode network regions is related to the actual recovery after neglect. This confirms the idea that the interaction between these two networks is of importance for attention.

P91C Functional connectivity MRI between the putamen and midbrain is related to striatal dopamine transporter density in patients with Lewy body disease

A. Rieckmann[1,2], S.N. Gomperts[3], K. A. Johnson[3,4], J. H. Growdon[3], K.R.A. Van Dijk[1,4]

[1]Athinoula A. Martinos Center for Biomedical Imaging, Department of Radiology, Massachusetts General Hospital, Charlestown, MA, USA, [2]Department of Radiation Sciences, Diagnostic Radiology, Umeå University, Sweden, [3]Department of Neurology, and [4]Division of Nuclear Medicine and Molecular Imaging, Massachusetts General Hospital, Boston, MA, USA, [5]Harvard University Department of Psychology, Center for Brain Science, Cambridge, MA, USA

Background: Dopamine cells of the substantia nigra heavily innervate the striatum, and their loss is a neuropathological hallmark of Lewy body disease (LBD, including Parkinson disease and dementia with Lewy bodies). Consistent with known projections, the striatum and midbrain are functionally coupled as measured with resting state fMRI in healthy young adults (e.g. Kelly et al. 2009, J Neurosci). Recent work has shown that functional connectivity between the putamen (one part of the striatum) and the midbrain is reduced in patients with Parkinson disease (Hacker et al. 2012, Brain), which suggests that individual differences in midbrain-striatal connectivity may reflect the integrity of the dopamine system in these patients. To address this question, we assessed functional connectivity of the putamen during resting state fMRI and dopamine transporter (DAT) availability in the striatum using PET in patients with LBD. We predicted that lower DAT density in the striatum would be associated with lower midbrain-putamen functional connectivity.
Methods: A total of 26 LBD subjects and 29 clinically normal age-matched control subjects underwent PET and resting state fMRI. LBD subjects were tested while on medication, and medication dose and motor and cognitive functions were recorded using standard procedures. DAT density in the striatum was assessed using 11C-Altropane PET. Partial-volume corrected distribution volume ratios for the striatum were calculated with the cerebellum as reference region. After stringent quality control of the fMRI data, 13 LBD subjects remained for analysis. Following standard fMRI pre-processing for functional connectivity analyses, connectivity strength was defined as the correlation between fMRI timeseries from the putamen and a midbrain region of interest (identified in controls).
Results: Striatal DAT was 59% lower in LBD subjects than in controls ($t(41) = 12.79$, $p < 0.01$). Of key interest, we found a significant association between DAT availability and midbrain-putamen connectivity in the LBD group ($r = 0.52$, $p = 0.03$). This association remained after controlling for medication dose, motor function, and head motion during fMRI.
Conclusions: This multi-modal neuroimaging study provides novel evidence that altered functional connectivity between midbrain and putamen reflects striatal dopamine losses in LBD. Individual differences in resting-state functional connectivity may therefore provide a useful indicator of underlying pathology in patients with LBD. These results encourage further exploration in larger samples and different disease populations.

P92C Insular and inferior frontal gyrus interhemispheric RSFC are associated to substance use disorder in a psychiatric population

R. Salas[1], H. Viswanath[1], K. Curtis[1] P.R. Baldwin[1], C.B. Frueh[1], J.C. Fowler[1]

[1]Menninger Department of Psychiatry and Behavioral Sciences, Baylor College of Medicine, Houston, TX, USA

Background: Several reports have shown that interhemispheric connectivity has been shown to be associated with substance abuse. To study the mechanisms mediating this association we used a sample of substance use disorder patients that abuse several different drugs.
Methods: We used a sample of 159 psychiatric in-patients from the Menninger Clinic in Houston. This clinic specializes in treatment of addiction, depression, anxiety and personality disorders, and houses patients for an average of about 4 weeks. Our sample is very heterogeneous and highly co-morbid, which makes results hard to interpret but ecologically relevant. We used resting state fMRI to study the functional connectivity (RSFC) of a series of frontal brain areas, including the anterior cingulated, frontal giry, and the insula, and performed correlations between the right/left RSFC among these regions and a drug-use related standardized measure taken at the clinic (WHO-A). For RSFC analysis, we use the software Conn.
Results: When we studied the different drugs assessed by the WHO-A questionnaire, we found that insular interhemispheric connectivity was associated to tobacco, alcohol, cocaine, sedatives, hallucinogens and ''other''. The inferior frontal gyrus (iFG) was associated to amphetamine and inhalant use. No associations were found for cannabis or opioid use.
Conclusions: We show here that the insula and the iFG are associated to the level of use of different drugs. Why interhemispheric insular and iFG RSFC are associated to separate and exclusive groups of drugs is an open question at this time. Efforts are ongoing to increase our sample size to be able to subdivide the population according to addiction and other co-morbidities.

P94C Resting-state connectivity changes during consolidation of delay and trace fear conditioning memory

D.H. Schultz[1], N.L. Balderston[1], L.S. Hopkins[1], F.J. Helmstetter[1,2]

[1]University of Wisconsin-Milwaukee, Milwaukee, WI, USA, [2]Medical College of Wisconsin, Milwaukee, WI, USA

Background: Resting-state functional connectivity (RSFC) is fairly stable across time, but changes can be observed in clinical populations or after performance of behavioral tasks. We hypothesized RSFC could be used to examine the time course of memory consolidation. Consolidation refers to the process of stabilizing a memory after the initial experience. Previous work has suggested that activity and plasticity is required in different regions at different times during the consolidation process. We used delay and trace fear conditioning as models of emotional memory. In both of these types of conditioning, a previously

neutral visual stimulus is paired with an aversive outcome. The brain circuitry supporting delay conditioning is well characterized with the amygdala being a critical component. Trace conditioning also relies on the amygdala, but a temporal gap between the stimuli recruits activity in several other brain areas including the hippocampus and medial prefrontal cortex.
Methods: On the first day of the experiment we collected an 8 minute baseline resting-state scan. After that scan participants were randomly assigned to one of three groups. One group underwent delay fear conditioning, the second group underwent trace fear conditioning, and a third group was exposed to the same stimuli in an explicitly unpaired manner and served as a control group. After training all participants received a second resting-state scan. Twenty-four hours later and one week following the conditioning session the participants reported back to the scanner, received a resting-state scan, and at one week they underwent a memory test. We identified several regions of interest and extracted the low frequency component of the BOLD signal from each of these regions at each time point for each participant. These correlation values were compared across groups for each of the resting-state scans.
Results: Resting-state functional connectivity was increased between the amygdala and several other regions for both the delay and the trace group twenty-four hours following acquisition. We found increased functional connectivity for the trace group relative to the delay group in several brain regions supporting trace conditioning. The most robust differences in functional connectivity were apparent twenty-four hours following acquisition and most of those increases had diminished by seven days after conditioning.
Conclusions: We believe that changes in resting-state functional connectivity following conditioning can be observed for several hours and that these changes reflect the process of memory consolidation. These results could be used to inform targets for therapeutic intervention in anxiety disorders.

P95C PACAP receptor gene polymorphism impacts resting-state functional connectivity of the amygdala among highly traumatized women

J. Shin[1], J.S. Stevens[2], N. Fani[2], T. Jovanovic[2], L.M. Almli[2], K.B. Mercer[2], K.J. Ressler[2]

[1]Georgia Institute of Technology/Georgia State University, Atlanta, GA, USA, [2]Emory University, Atlanta, GA, USA

Background: We have recently found that a single nucleotide polymorphism (SNP) in the pituitary adenylate cyclase-activating polypeptide (PACAP) receptor gene (encoded by *ADCYAP1R1*) was associated with posttraumatic stress disorder (PTSD) symptoms[1] among highly traumatized women but not men, as well as fear responses in the amygdala and hippocampus[2]. These findings suggest that amygdala reactivity is an intermediate phenotype for anxiety-related psychopathology. In the current study, we investigated individual differences in resting-state functional connectivity of the amygdala associated with *ADCYAP1R1* genotype.
Methods: Forty-nine women who had experienced moderate to high levels of lifetime trauma participated in resting state functional MRI. Twenty-two women with the CC genotype formed the risk group, and 27 women with GG or GC genotype formed the non-risk group. The datasets underwent despiking, slice-timing correction, motion correction, and smoothing. The time series were additionally processed to minimize artifacts from head motion, respiration, cardiac pulsation, and hardware using ANATICOR method[3] as well as band-pass filtering. The seed-based functional connectivity maps of the amygdala were calculated after the motions censoring (i.e., motion scrubbing[4]).
Results: Participants in the risk group did not differ from participants in the non-risk group in age, education, income, amount of trauma experienced, PTSD symptoms, depression symptoms, trait anxiety, or state anxiety immediately before the scan. However, the risk group showed decreased resting-state functional connectivity between the amygdala and ventromedial prefrontal cortex (vmPFC)($P_{corr} < 0.01$, whole-brain corrected). Furthermore, functional connectivity was significantly negatively correlated with the degree of trauma exposure during adulthood (age 18+) in the risk group ($r = -0.4$, $P < 0.03$) but not in the non-risk group ($r = -0.05$, $P < 0.4$).
Conclusions: The PACAP system impacts the amygdala-vmPFC functional connectivity at rest. Individual differences in *ADCYP1R1* genotype may contribute to dysregulated fear circuitry known to play a central role in PTSD and other anxiety disorders.

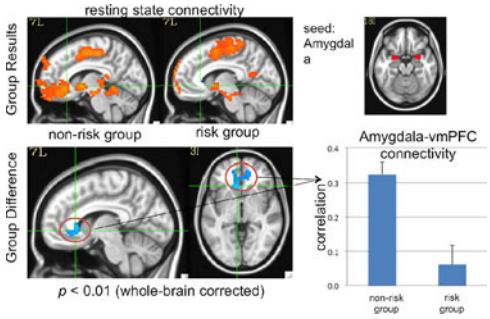

[1] Ressler KJ, et al. Nature 2011,470(7335):492–497 [2] Stevens JS, et al. PNAS 2014,111(8):3158–3163 [3] Jo HJ, et al. NeuroImage 2010,52(2):571–582 [4] Power JD, et al. NeuroImage 2012,59(3):2142–2154

P96C Effect of concussion on collegiate athletes: a resting-state fMRI study

Elif M. Sikoglu*, Suzanne M. Czerniak*[1], Ana A. Liso Navarro[1,2], Joseph McCafferty[1], Jordan Eisenstock[3], J. Herbert Stevenson[4], Jean A. King[1,5], Constance M. Moore[1,5]

[1]Center for Comparative NeuroImaging, Department of Psychiatry, University of Massachusetts Medical School, Worcester, MA; [2]Office Médico-Pédagogique, Department of Psychiatry, University of Geneva School of Medicine; [3]Department of Neurology, University of Massachusetts Medical School, Worcester, MA; [4]Department of Sports Medicine, University of Massachusetts Medical School, Worcester, MA; [5]Department of Radiology, University of Massachusetts Medical School, Worcester, MA
**Both authors contributed equally to this work*

Background: There are 1.7 million Traumatic Brain Injuries (TBI) annually in the United States, 75% of which are classified as mild, i.e. concussion. The current standard diagnosis of concussion would benefit from objective and quantitative markers, and neuroimaging techniques that go beyond the standard structural imaging techniques can be employed. To this end, we investigated resting state functional connectivity (rs-FC) in collegiate athletes to detect residual brain changes in the weeks to months following concussion.

Methods: Twenty-nine student athletes (14 concussed within 6 months of enrollment; 15 non-concussed; aged 18 to 22 years old) were recruited for this study. Neuroimaging data were acquired on a 3.0 Tesla Philips Achieva whole-body MR system (Philips Healthcare, Best, the Netherlands). Resting-state scan images were obtained using an EPI sequence (84×81 voxels, FOV: 256 mm×150 mm×256 mm, TR: 2540 msec, TE: 30 msec, flip angle: 75°, slice thickness: 3 mm, 50 slices). rs-FC analysis was performed using a hypothesis-driven seed-based approach (seed placed at anterior cingulate cortex (ACC) - neurocognitive abnormalities mediated by the ACC have been implicated in concussion). All participants also completed the Color-Word Interference Test (CWIT), a neurocognitive task mediated by the ACC.
Results: When recently concussed patients (within the past month, n=7) were compared with non-concussed patients, ACC illustrated elevated connectivity with Right Insula, Right Superior Temporal Gyrus, Left Inferior Frontal Gyrus, Left Middle Temporal Gyrus, and Right Middle Frontal Gyrus (RMFG). Similarly, when athletes who were concussed in the past 2 to 6 months (n=7) were compared with non-concussed athletes, ACC illustrated elevated connectivity with RMFG, Right Superior Temporal Gyrus, Right Transverse Temporal Gyrus, Posterior Cingulate Gyrus, Left Superior Parietal Lobule and Right Medial Frontal Gyrus. Specifically for the ACC-RMFG pair, the difference due to concussion was the most prominent ($F(1,20)=10.55$, $p<0.004$). The inhibition and inhibition/switching modules of CWIT showed impaired performance for the recently concussed patients when compared to non-concussed participants ($p=0.08$ and $p=0.023$) and also when compared to patients who were concussed in the past 2 to 6 months ($p=0.02$ and $p=0.06$).
Conclusions: Our results indicate that concussed participants had significantly increased connections between areas of the brain that underlie neurocognitive functioning, even after the neurocognitive assessments normalized. Brains of concussed athletes may have to 'work harder' than their healthy peers. Resting state brain connectivity may be able to detect prolonged brain differences in concussed athletes in a more quantitative manner than other diagnostic tools, i.e. neurocognitive testing.

P97C Progressive loss of local and global brain network efficiency in alcohol dependence

Z. Sjoerds[1,2,3], S.M. Stufflebeam[4], D.J. Veltman[2], W. van den Brink[3], B.W.J.H. Penninx[2], L. Douw[2,4]

[1]Max Planck Institute for Human Cognitive and Brain Sciences, Leipzig, Germany, [2]VU University Medical Center, Neuroscience Campus Amsterdam, Amsterdam, The Netherlands, [3]University of Amsterdam, Academic Medical Center, Department of Psychiatry, Amsterdam, The Netherlands, [4]Athinoula A. Martinos Center for Biomedical Imaging, Charlestown, Massachusetts, U.S.A

Background: Progressive alcohol dependence is characterized by altered activity in brain areas involved in addiction-related impairments in cognitive, emotional and motivational functioning. Studies have examined connectivity between these brain areas using methods like independent component analysis. However, little is known about the governing framework of the entire brain network to understand the complexity of addictive behaviors in the human brain, and the progression following chronic excessive alcohol use. We apply network theory using resting-state (RS) functional MRI (fMRI) in alcohol dependent patients to examine brain network changes associated with illness duration.
Methods: A total of 24 alcohol dependent patients and 20 matched healthy controls were scanned at a 3T Philips Intera full-body MR-system (Philips Medical Systems, Best, The Netherlands). RS data were collected for 10 minutes while participants had their eyes closed (TR/TE=2.3 s/30 ms; matrix 96×95; voxels 2.29×2.29×3 mm; 35 transverse slices). We then performed network analyses using the Brain Connectivity Toolbox. Pearson's correlations between RS fMRI time series from 114 brain regions were calculated, resulting in 114×113 connections. The 40% highest functional connections were retained for calculation of weighted global (global efficiency) and local (degree, cluster coefficient, eigenvector centrality mapping) network characteristics, which were compared between groups and within the alcohol dependent group and correlated with duration of the DSM-IV-TR diagnosis of alcohol dependence. Node-level results were corrected for multiple comparisons using the false discovery rate (FDR). Age, gender and head motion were added as covariates in all analyses.
Results: We found no significant group differences between alcohol dependent patients and controls. Regression analyses of global network characteristics with illness duration showed a decrease in efficiency ($R=-.6079$; $P=.0114$), cluster coefficient ($R=-.6204$; $P=.0060$) and degree ($R=-.6068$; $P=.0100$) with longer illness duration. Decreased node-based efficiency in the right paracingulate gyrus ($t=-4.21$) and left inferior occipital gyrus ($t=-4.46$) was related to longer alcohol dependence duration.
Conclusions: Prolonged alcohol use disorders are associated with increasing disturbances in global and local network characteristics, including losses of overall integration of information processing and local efficiency. These disturbances are likely to contribute to the behavioral impairments seen in chronic addiction patients.

P98C Hippocampal resting activity and functional connectivity predict relapse to cocaine use

Bryon Adinoff,[1,2] Hong Gu[3], Carmen Merrick,[4] Meredith McHugh,[3] Michael D. Devous,[5] Haekyung Jeon-Slaughter,[2] Hanzhang Lu,[6] Yihong Yang,[3] Elliot A. Stein[3]

[1]VA North Texas Health Care System, Dallas, Texas; [2]Department of Psychiatry, UT Southwestern Medical Center, Dallas, Texas; [3]Intramural Research Program - Neuroimaging Research Branch, National Institute on Drug Abuse, Baltimore, Maryland [4]School of Behavior and Brain Sciences, UT Dallas, Dallas, Texas; [5]Avid Pharmaceuticals, [6]Advanced Imaging Research Center, UT Southwestern Medical Center, Dallas, Texas

Background: Recidivism after treatment for cocaine dependence remains stubbornly high. There are currently no behavioral or clinical characterization biomarkers that can predict treatment outcome and only limited evidence that neurobiological alterations can successfully predict relapse in addicted individuals. This study assessed whether resting measures of regional cerebral blood flow (rCBF) and related resting state functional connectivity (rsFC), obtained in the same session, prospectively predict relapse in cocaine-dependent patients.
Methods: We assessed 40 cocaine-dependent patients who were 2- to 4-weeks abstinent following residential treatment along with 20 matched control participants. rCBF, using arterial spin labeling (ASL), and rsFC were obtained shortly prior to treatment discharge. Substance use was assessed twice-weekly following discharge. ''Relapsed'' participants were defined as those

who used stimulants within 30 days following treatment discharge (n = 22); ''Early Remission'' participants (n = 18) did not.
Results: Significant differences were seen in rCBF between Relapsed, Early Remission, and control groups only in the left posterior hippocampus (pHp) where rCBF in the Relapsed group was greater than the control group; this rCBF significantly correlated with pHp gray matter volume in controls ($r = 0.62$, $p = 0.004$), but not in either cocaine group. We then used the left pHp as a seed in a whole brain functional connectivity analysis and found that the Early Remission group had reduced connectivity strength with the posterior cingulate cortex (PCC) compared with the Relapse group. Increased pHp rCBF and strengthened pHp-PCC FC independently contributed to a survival analyses predicting days to relapse ($\chi^2 = 6.27$, df = 1, $p = .01$); the combined variables predicted relapse at 30 days intervals throughout the 24 week follow-up period with 67 to 75% accuracy.
Conclusions: In cocaine-dependent patients at risk of early relapse, increased pHp rCBF and pHp-PCC functional strength may reflect the propensity for heightened reactivity to cocaine cues or memories. Mechanisms to delink pathologically connected neural circuits may prove useful in the treatment of addicted patients prone to relapse.

P99C Regional imbalance of excitation and inhibition explains intrinsic functional brain hyper-connectivity in childhood autism

K. Supekar[1], J. Kochalka[1], V. Menon[1]

[1]*Department of Psychiatry and Behavioral Sciences, Stanford University*

Background: Autism spectrum disorder (ASD), a neurodevelopmental disorder characterized by impaired social interaction and by restricted/repetitive behavior, affects nearly 1 in 65 children. Current empirical and theoretical accounts based on studies in children posit that the underlying neurobiological disturbance causing ASD is functional brain hyper-connectivity. Remarkably, there have been no systematic attempts to characterize mechanisms underlying functional brain hyper-connectivity in children with ASD, work that is critical for understanding the etiology of this complex neurodevelopmental disorder. Here we combine rsfMRI and DTI with biophysical modeling to investigate this important, yet understudied, question.
Methods: One cohort of 40 children (ASD = 20, Typically developing (TD) = 20) was recruited at Stanford University and a second cohort of 40 children (ASD = 20, TD = 20) was recruited at Georgetown University. rsfMRI and DTI data were acquired from both cohorts. Preprocessed rsfMRI datasets were parcellated into 90 regions and wavelet analysis of the extracted regional time series was used to compute inter-regional functional connectivity across the whole brain. We first examined differences in whole-brain functional connectivity patterns between the two groups. Next, to investigate potential structural connectivity abnormalities underlying functional hyper-connectivity in children with ASD, we used DTI-based tractography and examined differences in structural connectivity measured using mean FA along the fiber tracks connecting the pair of brain regions that showed functional hyper-connectivity. Finally, to understand the neural dynamics underlying functional hyper-connectivity in ASD, we developed a biophysical computational model, comprised of multiple interacting neuronal populations, based on recently published parameters from a mouse model of autism.
Results: In both cohorts, the mean global intrinsic functional connectivity was higher in ASD, compared to TD, children. Examining structure-function relationships, we found that the functional hyper-connectivity in ASD children was not correlated with differences in structural connectivity, in both cohorts. Analyses of biophysical computational model-based simulations revealed that increasing the local neuronal coupling within each neuronal population resulted in increased intrinsic functional connectivity between neuronal populations. Importantly, these increases were observed even without any changes in structural coupling between the neuronal populations, consistent with our experimental results and highlighting the specificity of our findings.
Conclusions: Our experimental results replicated in two cohorts along with our computational modeling-based results demonstrate that aberrant local synaptic coupling similar to that observed in *in vivo* models of autism is a plausible neural mechanism of intrinsic inter-regional hyper-connectivity. More generally, our findings suggest that regional imbalance between excitation and inhibition plays a causal role contributing to the atypical brain function in ASD, providing novel mechanistic insights that have broader implications for early detection and treatment strategies.

P100C Motor network functional connectivity increases during movie-watching fMRI compared to resting-state fMRI

Y. Tie[1,2], L. Rigolo[1,2], O. Olubiyi[1,2], K. Doolin[1,2,4], A.J. Golby[1,2,3]

[1]*Harvard Medical School, Boston, MA, USA, Departments of* [2]*Neurosurgery and* [3]*Radiology, Brigham and Women's Hospital, Boston, MA, USA,* [4]*Trinity College Dublin, College Green, Dublin 2, Ireland*

Background: Pre-surgical mapping of motor and language functions is critical to avoid resection-induced deficits for patients with lesions in eloquent cortex. Functional fMRI based on motor tasks has been used to map motor areas in patients. However, patients are often unable to follow the task instruction well due to impaired movement or cognitive deficits. Resting-state fMRI has been proposed for mapping motor function based on highly correlated spontaneous fluctuations of the motor network. In this work, we explored the feasibility of using a movie-watching fMRI for mapping motor areas in individuals, by comparing functional connectivity (fc) between putative motor areas during the movie-watching and resting-state fMRI.
Methods: We enrolled 16 healthy subjects (8 males, mean age = 26.3 years, range 20–37 years). Each subject underwent a 4 min eyes-closed resting-state fMRI (rsfMRI), a 3 min 30 sec movie-watching fMRI (mwfMRI), and a 4 min blocked design hand clenching task-based fMRI. The movie clip showed the procedure of building a wardrobe, consisting of tool using, body movement, oral instruction, and voiceover. fMRI data were motion-corrected, spatially normalized to the MNI template, smoothed (6 mm FWHM Gaussian kernel), and band-pass filtered (0.01–0.08 Hz). The effect of confounds from CSF, white matter, and movement was removed by linear regression for the rsfMRI. Functional ROIs for motor areas were defined based on second-level random-effect analysis on the task-based motor fMRI, resulting in two ROIs located in the left and right pre-central gyri respectively. Then for the rsfMRI and mwfMRI of each individual subject, temporal

correlation coefficient between the average time courses within the two motor ROIs was calculated and further transformed to Fisher's *z*-score. SPM8 and REST software packages were used for data pre-processing and fc analysis.
Results: For the rsfMRI, fc between the left and right motor ROIs was 0.615 ± 0.121 (mean ± SD). For the mwfMRI, fc was 0.983 ± 0.258. Results of paired *t*-test indicated that there was significant difference between the fc measures of the rsfMRI and mwfMRI ($t = 3.59$, $p < 0.01$).
Conclusions: Our results indicate that fc between the putative motor areas in the left and right pre-central gyri increases during the movie-watching condition compared to the resting-state condition. This fact supports the feasibility of mapping motor functional areas using the movie-watching fMRI, which may provide more robust results compared to rsfMRI. This easy-to-perform paradigm can be used as a complementary approach for mapping motor areas in patients who can not perform motor tasks satisfactorily.

P101C Longitudinal brain connectivity changes in a sensorimotor network in ischaemic stroke patients

M. Veldsman[1], T. Cumming[1], A. Brodtmann[1]

[1]*The Florey Institute for Neuroscience and Mental Health, University of Melbourne, Melbourne, Australia*

Background: It has become clear that the effects of ischaemic stroke are neither confined to the lesion site nor to the acute phase of the cerebrovascular event. Recovery and reorganisation over time are likely to affect network dynamics after stroke, yet this is rarely investigated in timescales beyond a few months post-stroke. Resting state fMRI is well suited to examine the effects of stroke at a network-wide level.
Methods: Ten patients (mean age 62, 7 female) and 5 age-matched controls (mean age 60, 2 female) were scanned at 3 and 12 months post-stroke. Seven minutes of whole brain T2* echoplanar images were acquired at 3T. Lesions were manually traced on a high resolution FLAIR image. Cost function masking (with the traced lesion) was employed during unified segmentation and normalization, with an age appropriate template brain (mean 65 years). Temporal preprocessing and statistical analysis were implemented in the Conn toolbox (Whitfield-Gabrieli & Nieto-Castanon, 2012).
Results: Multivariate principal components analysis identified a region in the posterior dorsal cingulate cortex showing disruption in connectivity in patients at 3 months post-stroke compared to controls ($p < 0.05$, FDR corrected). This region served as the seed region from which bivariate correlations were carried out on a voxel-wise basis. Resting state connectivity in regions within the sensorimotor network were significantly reduced in patients 3 months after stroke compared to controls ($p < 0.05$, FDR corrected). One year after stroke, there was increased connectivity in the sensorimotor network ($p < 0.05$, FDR corrected) in regions overlapping those disrupted at the 3 month mark.
Conclusions: The pattern of abnormal connectivity in a sensorimotor network at 3 months post-stroke followed by an increase in connectivity in this same network at 1 year may be indicative of recovery of function. Resting state fMRI is well suited to examine network-level changes following stroke and to account for recovery and reorganisation beyond the acute phase.

P102C Apolipoprotein E genotype is associated with distinct resting state functional connectivity phenotypes in Alzheimer's disease

L. Wang[1], T.L. Benzinger[2,3], A. Goate[3,4], J.C. Morris[1,3], B.M. Ances[1,3]

Departments of [1]Neurology, [2]Radiology, [3]Knight Alzheimer's Disease Research Center, [4]Psychiatry, Washington University in St Louis, St Louis, MO, USA

Background: Apolipoprotein E (*APOE*) ε4 allele is the strongest genetic risk factor for developing late onset Alzheimer's disease (AD) and leads to an earlier age of onset. The presence or absence of ε4 allele is associated with distinct clinical profiles of AD. Specifically, ε4 carriers have more profound memory deficits but *APOE* ε4 non-carriers have greater impairment in executive function. Resting state functional connectivity magnetic resonance imaging (rs-fcMRI) provides a non-invasively means to study the impact of disease on multiple resting state networks (RSNs). Rs-fcMRI studies suggest that AD can be characterized by changes in multiple RSNs. The effect of *APOE* on RSNs has been primarily studied in cognitively normal people. It is unclear, among patients with symptomatic AD, whether *APOE* genotype is associated with distinct rs-fcMRI phenotypes that contribute to different clinical profiles of the disease.
Methods: Rs-fcMRI data were acquired from 69 participants with symptomatic AD [Clinical Dementia Rating (CDR) > 0]. Among them, 42 were *APOE* ε4 heterozygous and 27 were *APOE* ε3 homozygous. Rs-fcMRI data were analyzed using a seed-based approach. Functional connectivity maps of 5 RSNs were generated for each participant and were compared between *APOE* ε4 carriers and *APOE* ε3 homozygotes.
Results: *APOE* ε3 homozygotes (75.9 ± 7.7, yr) were slightly older than *APOE* ε4 carriers (74.3 ± 7.3, yr), but age difference was not statistically significant ($p = 0.37$). Disease severity was similar between *APOE* ε4 carriers (CDR sum of boxes: 3.6 ± 2.4) and *APOE* ε3 homozygotes (CDR sum of boxes: 3.2 ± 2.2) ($p = 0.57$). *APOE* ε3 homozygotes with AD had increased functional connectivity in the default mode network compared to *APOE* ε4 carriers with AD (red in the bottom row of Figure A). Conversely, *APOE* ε4 carriers with AD had greater functional connectivity in the salience network (green in the bottom row of Figure B) compared to *ApoE* ε3 homozygotes with AD.
Conclusions: *APOE* genotype may modulate rs-fcMRI phenotypes of symptomatic AD. Further work is needed to determine whether *APOE* genotype dependent rs-fcMRI phenotypes are related to different clinical manifestations of AD.

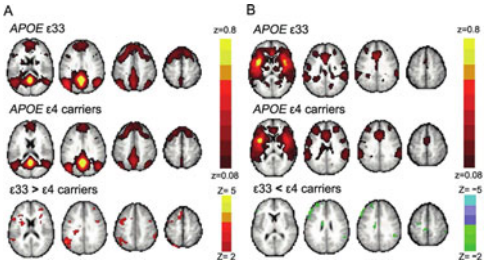

FIG. Within (top and middle) and between (bottom) group maps for the default mode network (using posterior cingulate seed) **(A)** and salience network (using left insular seed) **(B)** in *APOE* ε3 homozygotes and *APOE* ε4 carriers. Group difference maps were thresholded at a voxel-wise $p < 0.01$, uncorrected.

P103C Optimizing resting-state data analysis pipelines for early-phase drug development

E. Duff[1], B. Whitcher[2], W. Vennart[2], B.T. Wyman[2], B.L. Klaassens[3], H.C. van Gorsel[3], J.M.A. van Gerven[4], S.A.R.B. Rombouts[3], R. Sala-LLonch[5], M. Woolrich[6,1], S. Smith[1]

[1]FMRIB, University of Oxford, Oxford, United Kingdom, [2]Pfizer Inc., Groton, CT, USA, [3]Leiden University Medical Center, Leiden, The Netherlands, [4]Centre for Human Drug Research, Leiden, The Netherlands, [5]University of Barcelona, Barcelona, Spain, [6]OHBA, University of Oxford, Oxford, United Kingdom

Background: Resting-state functional magnetic resonance imaging (rfMRI) is an attractive candidate tool for early-phase drug development due to its ability to detect the effects of neuroactive compounds on the intrinsic spontaneous activity of the brain. An early assessment of functional drug effects could substantially reduce drug attrition due to lack of efficacy. However, the sensitivity of such an approach and optimal analysis strategies are unknown at this time. The present work was motivated by the need for standardized acquisition and analysis methods to transform the techniques of rfMRI into tools capable of guiding drug development.
Methods: We first defined a general resting-state drug assessment procedure; building on an existing protocol developed for task-based fMRI. This procedure involves three steps: (1) quality control, (2) quantification of pharmacodynamic effects (i.e., brain activation attributed to the drug) and (3) identification of specific effects associated with previously established signatures of efficacy. Step 2 is the focus here. A classifier was trained on resting-state acquisitions from both drug and placebo conditions with known class labels and tested in a leave-one-out framework. The ability to reliably discriminate between conditions suggests a downstream pharmacological effect. A variety of methods were combined and optimized, including seed-based and dual-regression spatial maps, network matrices using a variety of parcellation approaches, and connectivity statistics. Multiple datasets were used to produce reliable assessments, including experiments where robust modulations of the resting states were induced using common fMRI tasks and transcranial direct-current stimulation, along with a number of pharmacological datasets that varied across drug class and potency.
Results: Resting-state modulations were identified most reliably using a network matrix approach, with connectivity matrices generated using a high-dimensional spatial independent component analysis parcellation, and L1/2-regularized partial correlation as the connectivity measure. This performed well in both ''gold-standard'' datasets and most of the active-drug studies. We also found crossover designs to be crucial for the detection of effects, and acute administration of the compounds provided a good level of discrimination.
Conclusions: We have developed a procedure for drug assessment using rfMRI. The current methodology provides a useful framework to perform experiments and analyze the results, and has been shown to be effective on a modest collection of compounds. Building on this collection will further improve the data analysis pipeline.

P104C Brain activation and effective connectivity are modulated by visual-orthographic load during Chinese orthography-phonology mapping

M. Xu[1,2], L.H. Tan[1,2]

[1]State Key Laboratory of Brain and Cognitive Sciences, [2]Department of Linguistics, The University of Hong Kong, Pokfulam Road, Hong Kong, China

Background: A Chinese character, the basic unit of written Chinese, is formed with intricate strokes filled in a square configuration, as opposed to the linear structure of alphabetic words. Modern Chinese characters consist of strokes ranging from 1 (e.g., '', meaning one) to 36 strokes (e.g., '', meaning snuffling), such that visual complexity of the characters increases as stroke number increases. Furthermore, Chinese characters are defined at the monosyllabic level. Based on the properties inherent in Chinese characters, we investigated the neural systems and effective connectivity that were modulated by visual-orthographic load during orthography-phonology mapping, by varying the stroke complexity of characters in a phonological task. We hypothesized that as the stroke complexity of Chinese characters increases, the ''load'' of mapping from orthography to phonology may become heavier, and this change should be reflected in change of brain activity and connectivity.
Methods: Seventeen participants (17- to 23-year-olds) were scanned using functional MRI when they performed a tone judgment task on visually presented Chinese characters. We used SPM8 for conventional imaging data analysis and Dynamic Causal Modeling (DCM) for effective connectivity analysis. Three regions were included in connectivity analysis, i.e., left ventral occipitotemporal cortex (LvOT), left superior parietal lobule (LSPL) and left middle frontal gyrus (LMFG). Six intrinsic connections were specified and the competing models varied as to which region received driving input and which connections were modulated by high-stroke condition, resulting in 189 models for each subject. We conducted random-effect Bayesian model selection to find a winning family of models among three competing families that differed in the site of input region. We then used Bayesian model averaging across models within the winning family to make inferences on the connection parameters.
Results: High-stroke characters produced greater activation than low-stroke characters mainly in the left inferior/middle frontal gyri (BA44/BA9), bilateral superior parietal cortex (BA7), and bilateral occipitotemporal cortices (BA37/18), indicating that these regions were sensitive to the visual-orthography load during orthography-phonology mapping. DCM analyses showed that driving input more likely entered LvOT than the other two regions. Moreover, significant modulatory effects were found for high-stroke characters on the connections from LvOT to LSPL (0.15 Hz), from LSPL to LMFG (0.048 Hz), and from LMFG to LvOT (-0.46 Hz).
Conclusions: The finding shed light on the neural systems and brain connectivity that were sensitive to visual-orthographic load during Chinese orthography-phonology mapping. DCM analyses revealed that increased mapping load was associated with strengthen connectivity from LvOT to LMFG via LSPL. Moreover, LMFG exerted inhibitory top-down modulation on LvOT, which may enable more efficient information processing in LvOT.

P105C Toward Neurophenotypic Markers of Distress Tolerance

Z. Yang[1,2], N.A. Fox[3], Carl W. Lejuez[4], Z. Shehzad[2], B. Leventhal[2], F.X. Castellanos[2,5], R.C. Craddock[1,2], M.P. Milham[1,2]

[1]Child Mind Institute, New York, NY 10022, USA; [2]Nathan Kline Institute, Orangeburg, NY 10962, USA; [3]Department of Human Development and Quantitative Methodology, [4]Department of Psychology, University of Maryland, College Park, MD 20742, USA; [5]NYU Langone Medical Center Child Study Center, New York, NY 10016, USA

Background: Distress tolerance (DT), the ability to persist in goal-directed activity during emotional distress, is essential to cognitive and social function, and is deficient in various psychiatric disorders, but neuroimaging studies are rare. Inspired by RDoC, we used a recently developed behavioral task and resting state fMRI (R-fMRI) to identify the neural correlates of DT in a community-ascertained sample of individuals with and without past or current psychiatric illness. The utility of the resultant neural correlates as biomarkers for DT was evaluated using multivariate predictions.
Methods: 110 participants (12–84 y old) from the NKI-Rockland Sample were divided into high [58.2%] and low [41.8%] DT groups per the Behavior Indicator of Resiliency to Distress (BIRD) task. Groups were demographically matched. Putative intrinsic brain markers of DT were identified from univariate analyses of five common derivatives calculated from R-fMRI data and one multivariate distance matrix regression (MDMR)-based approach. Phenotypic indices included demographics, diagnosis, cognitive tests, and self-reported measures on categories such as depression, mood, risk-taking and impulsive behaviors, and personality. 28 ROI-based brain measures (clusters showing significant main effect of DT in each approach) and 51 phenotypic indices from 86 adults (high DT: n = 43) were submitted to the support vector classifier algorithm to learn a linear classifier for discriminating low and high DT. The classifier was evaluated using an inner 10-fold cross-validation recursive feature elimination (RFE) framework to reduce the feature set and an outer 10-fold cross-validation to estimate generalization error.
Results: R-fMRI results implicated DLPFC, VLPFC, ACC, cuneus, thalamus, and striatum in DT. The involvement of VLPFC, TPJ, medial temporal lobe, insula, cerebellum, and striatum in DT varied with age. MDMR was more sensitive than univariate approaches, though findings overlapped. Brain measures and phenotypic indices selected by the RFE procedure were able to predict individual DT status with an average accuracy of 90% ± 11%. Features selected by at least 8 of the 10 cross validations included 14 brain and 4 phenotypic indices. Selected brain indices consist of Degree Centrality, Dual Regression, and MDMR measures, and included portions of VLPFC, temporal cortex, insula, striatum, and amygdala. Selected phenotypic predictors included subscales of the Adult Temperament Questionnaire, Inventory of Callous-Unemotional Traits, Conners Adult ADHD Rating Scale, as well as ethnicity.
Conclusions: DT ability is reflected in intrinsic properties of regions implicated in executive control and emotional functions. Some of the identified brain-behavioral relationships depended on age. DT can be accurately classified using a small set of neurophenotypic features. The derived regions help build a foundation for studying the mechanisms by which DT contributes to psychopathology and may serve as therapeutic targets. Future work will test the currently built DT classifier on an independent sample to test its ability to generalize.

P106C Associative network desegregation in schizophrenia relates to thalamic filtering deficit

G.J. Yang[1], J.D. Murray[2], G. Repovs[3], M.W. Cole[4], D.C. Glahn[1], J.H. Krystal[1], G.D. Pearlson[1], A. Anticevic[1]

[1]Yale University, New Haven, CT, U.S.A., [2]New York University, New York, NY, U.S.A., [3]University of Ljubljana, Ljubljana, Slovenia, [4]Rutgers University, Newark, NJ, U.S.A.

Background: Schizophrenia (SCZ) is a severe mental illness characterized by disordered cognition and altered large-scale connectivity across thalamo-cortical networks [1]. Additionally, two major associative cortical networks show both increased signal variance [2] and altered functional connectivity [3] in SCZ at rest: default mode network (DMN) and fronto-parietal control network (FPN). We hypothesized that loss of associative network functional segregation may be reflected in increased co-variance between the DMN and FPN BOLD signals at rest. In turn, we hypothesized that the magnitude of this desegregation may relate to increased thalamo-sensory connectivity – perhaps reflecting a common upstream mechanism.
Methods: We conducted network analyses of DMN-FPN co-variance and thalamo-cortical over-connectivity in SCZ patients (n = 161) compared to healthy subjects (n = 164) via resting-state BOLD fMRI. For thalamo-cortical analyses, we used previously characterized cortical regions known to show over-connectivity (OC region) and under-connectivity (UC region) in SCZ. We specifically used co-variance (as opposed to correlations) as a measure of statistical dependence to avoid potentially biasing our measure by group differences in signal variance. We correlated the above measures with patient scores on the positive and negative syndrome scale (PANSS).
Results: DMN-FPN covariance was significantly elevated in SCZ compared to healthy subjects and this elevation was significantly correlated with thalamic-OC covariance in patients, but not controls. DMN-FPN covariance was positively correlated with patients' positive PANSS scores. DMN and FPN covariance in patients was also negatively correlated with thalamic-UC covariance.
Conclusions: Findings suggest reduced segregation between DMN and FPN in SCZ. This effect parallels thalamo-cortical connectivity deficits and both results may arise from a common cause, such as distributed disinhibition within select cortico-thalamic loops.
[1] Anticevic et al. (2013). ''Characterizing Thalamo-Cortical Disturbances in Schizophrenia and Bipolar Illness.'' Cerebral Cortex 2013.
[2] Yang et al. ''Altered global brain signal in schizophrenia.'' Proc Natl Acad Sci. 2014.
[3] Baker et al. ''Disruption of cortical association networks in schizophrenia and psychotic bipolar disorder.'' JAMA Psychiatry 71(2): 109–118. 2014.

P107C Impact of rTMS on resting state functional connectivity in mal de debarquement syndrome: lasting neuromodulatory effect and correlation with efficacy

Han Yuan[1], Diamond Urbano[1], Lei Ding[1,2,3], Yoon-Hee Cha[1]

[1]Laureate Institute for Brain Research, Tulsa, OK 74136, USA, [2]School of Electrical and Computer Engineering, [3]Center for Biomedical Engineering, and [4]College of Engineering, University of Oklahoma, Norman, OK 73071, USA

Background: Mal de debarquement syndrome (MdDS) is a disorder of imbalance characterized by a chronic feeling of rocking and swaying that occurs after entrainment to background motion. Best available medical treatment is only palliative and symptoms that persist beyond six months show low likelihood of remission. Repetitive transcranial magnetic stimulation (rTMS) of the dorsolateral prefrontal cortex (DLPFC) has been shown to reduce the rocking sensation in some patients. Neither predictors for treatment response nor biomarkers for treatment effect are known, however. In the present study, we measured the resting state functional connectivity (RSFC) before and after rTMS to examine its relationship with treatment response.

Methods: Ten right-handed women (age 47.6 ± 10.7 yrs) with persistent MdDS lasting from 8–91 months (mean ± STD: 40.5 ± 24.2) participated in the study with informed consent. Anatomical MPRAGE and resting-state EPI (four minutes, eyes closed, TR = 2 s) prior to rTMS and another resting-state EPI three or four hours after the last rTMS session were acquired on a GE MR750 3T scanner. Each subject underwent five sessions of rTMS on five consecutive days (1 Hz right DLPFC followed by 10 Hz left DLPFC stimulation). Subjects rated the degree of their rocking dizziness on a visual analogue scale (VAS) of 0–100 each day, where 0 was complete suppression of symptoms. Subjects were categorized into three groups in terms of their VAS difference between day 5 and day 1 (< -10: positive responder, $-10 \leq \& \leq 10$: neutral, > 10: negative responder). After preprocessing, RSFC was computed with a seed at the left entorhinal cortex (EC, MNI coordinates: −14−8−22, 1 voxel), which has been shown to be pathologically hypermetabolic in MdDS (Cha et al, 2012). To examine whether the rTMS impact on RSFC is related to the symptom changes, the post-pre difference of EC RSFC was tested for correlation with responses. Furthermore, each individual's rTMS targets in the DLPFC were identified as seeds (10-mm-radius sphere within the brain tissue mask). To examine whether the DLPFC RSFC can predict treatment responses, the pre-TMS RSFC between DLPFC and EC was tested for correlation with responses.
Results: There were three positive responders, four neutral responders and three negative responders. The whole-brain covariate analysis of post-pre EC connectivity difference and categorized response ($p < 0.01$ and cluster threshold $p < 0.05$) identified the precuneus where connectivity with EC was decreased in the positive responders and increased in negative responders (ROI correlation = −0.83, $p = 0.003$). The correlation between rTMS responses and DLPFC- EC connectivity before TMS treatment was 0.56 ($p = 0.09$).
Conclusions: Our results have demonstrated that effective rTMS treatment at the DLPFC in MdDS patients decreased the RSFC between the EC and the precuneus. The results suggest that modulation of EC-precuneus connectivity may play an important mechanistic role in alleviating MdDS symptoms. The results also suggest that DLPFC-EC connectivity may be a potential neuroimaging biomarker for predicting treatment response and can be utilized to facilitate future rTMS targeting.

P108C Altered Orbitofronto-striatal Functional Connectivity in Alcoholics using Independent Component Analysis

X. Zhu, C. Carlos, K. Marthur, D. Tomasi, R. Momenan

NIAAA, National Institutes of Health, Bethesda, MD, USA

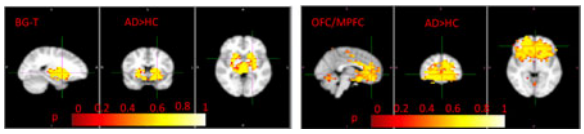

FIG. 1. BG-T (left) and OFC/MPFC (right) network showing increased functional connectivity in AD compared to HC (corrected p–value images, $p < 0.05$).

Background: Alcohol dependence (AD) is a mental disorder with both an impulsive and compulsive drive toward alcohol consumption. Dysfunction of the orbitofronto-striatal circuit (OSC) has been reported to result in compulsive behavior in addicted patients and the exaggerated motivation to obtain and use drug. Compromise in OSC connectivity has also been implicated in the craving and loss of control in alcoholism. Although functional magnetic resonance imaging (fMRI) studies have proposed dysfunction in distinct brain regions within this circuit in alcoholics, there is little information regarding the large-scale patterns of neural connectivity. The current study sought to investigate the differences in the degree of functional connectivity in the OSC between AD patients and healthy controls (HC) using resting state-fMRI and to further examine the relationship between the neuronal connectivity of AD patient and clinical characteristics.
Methods: Data were obtained from 26 AD and 26 HC. Five minutes of closed-eyes rs-fMRI images were collected. The severity of alcoholism was assessed using the alcohol-dependence scale. Impulsiveness was measured by the Barratt Impulsiveness Scale (BIS-11). Years of dependence were used to measure the chronicity of alcohol use for all subjects. Functional connectivity analysis was carried out using Independent Component Analysis (ICA).
Results: The ICA decomposition resulted in two related networks that were common to AD and HC: the basal ganglia thalamus network (BG-T), and the orbitofrontal cortex/medial PFC (OFC-MPFC) network. When compared with HC, AD showed significantly increased connectivity within the OFC-MPFC network and BG-T network (Figure 1). Functional connectivity within the BG-T was significantly positive correlated with Bis11 ($p < 0.05$, corrected) in AD. There was no significant correlation between other clinical measures of symptom severity and the strength of connectivty.
Conclusions: These findings expend literature to the abnormality hypothesis of OSC in AD patients. Specifically, our findings suggest that long-term alcohol use may result in abnormal and heightened functional connectivity of OSC in order to compensate for localized adverse effects of alcohol.